



THE PERPLEXING PHYSIOLOGY OF THE NOCICEPTIVE SYSTEM

EDITED BY: Istvan Nagy, Peter Santha and Jiri Palecek

PUBLISHED IN: Frontiers in Physiology and Frontiers in Human Neuroscience



frontiers

Frontiers eBook Copyright Statement

The copyright in the text of individual articles in this eBook is the property of their respective authors or their respective institutions or funders. The copyright in graphics and images within each article may be subject to copyright of other parties. In both cases this is subject to a license granted to Frontiers.

The compilation of articles constituting this eBook is the property of Frontiers.

Each article within this eBook, and the eBook itself, are published under the most recent version of the Creative Commons CC-BY licence.

The version current at the date of publication of this eBook is CC-BY 4.0. If the CC-BY licence is updated, the licence granted by Frontiers is automatically updated to the new version.

When exercising any right under the CC-BY licence, Frontiers must be attributed as the original publisher of the article or eBook, as applicable.

Authors have the responsibility of ensuring that any graphics or other materials which are the property of others may be included in the CC-BY licence, but this should be checked before relying on the CC-BY licence to reproduce those materials. Any copyright notices relating to those materials must be complied with.

Copyright and source acknowledgement notices may not be removed and must be displayed in any copy, derivative work or partial copy which includes the elements in question.

All copyright, and all rights therein, are protected by national and international copyright laws. The above represents a summary only. For further information please read Frontiers' Conditions for Website Use and Copyright Statement, and the applicable CC-BY licence.

ISSN 1664-8714

ISBN 978-2-88974-027-7

DOI 10.3389/978-2-88974-027-7

About Frontiers

Frontiers is more than just an open-access publisher of scholarly articles: it is a pioneering approach to the world of academia, radically improving the way scholarly research is managed. The grand vision of Frontiers is a world where all people have an equal opportunity to seek, share and generate knowledge. Frontiers provides immediate and permanent online open access to all its publications, but this alone is not enough to realize our grand goals.

Frontiers Journal Series

The Frontiers Journal Series is a multi-tier and interdisciplinary set of open-access, online journals, promising a paradigm shift from the current review, selection and dissemination processes in academic publishing. All Frontiers journals are driven by researchers for researchers; therefore, they constitute a service to the scholarly community. At the same time, the Frontiers Journal Series operates on a revolutionary invention, the tiered publishing system, initially addressing specific communities of scholars, and gradually climbing up to broader public understanding, thus serving the interests of the lay society, too.

Dedication to Quality

Each Frontiers article is a landmark of the highest quality, thanks to genuinely collaborative interactions between authors and review editors, who include some of the world's best academicians. Research must be certified by peers before entering a stream of knowledge that may eventually reach the public - and shape society; therefore, Frontiers only applies the most rigorous and unbiased reviews.

Frontiers revolutionizes research publishing by freely delivering the most outstanding research, evaluated with no bias from both the academic and social point of view. By applying the most advanced information technologies, Frontiers is catapulting scholarly publishing into a new generation.

What are Frontiers Research Topics?

Frontiers Research Topics are very popular trademarks of the Frontiers Journals Series: they are collections of at least ten articles, all centered on a particular subject. With their unique mix of varied contributions from Original Research to Review Articles, Frontiers Research Topics unify the most influential researchers, the latest key findings and historical advances in a hot research area! Find out more on how to host your own Frontiers Research Topic or contribute to one as an author by contacting the Frontiers Editorial Office: frontiersin.org/about/contact

THE PERPLEXING PHYSIOLOGY OF THE NOCICEPTIVE SYSTEM

Topic Editors:

Istvan Nagy, Imperial College London, United Kingdom

Peter Santha, University of Szeged, Hungary

Jiri Palecek, Institute of Physiology, Academy of Sciences of the Czech Republic (ASCR), Czechia

Impacts that threaten or indeed compromise the integrity of tissues trigger the development of a defence response, which through the activity of the nociceptive system includes pain. If the noxious impact does not induce tissue damage, the pain, called “nociceptive” pain, ceases within seconds after the impact is withdrawn. In contrast, if tissue damage does occur, a pain experience that usually persists until the injury is resolved and includes two major pathological sensory experiences, hypersensitivity to heat stimuli (i.e. heat hyperalgesia) and/or hypersensitivity to mechanical stimuli (i.e. mechanical allodynia) develop.

The cellular and molecular mechanisms underlying the development of nociceptive pain are fairly well understood. Our understanding of the development of pain associated with tissue injury has also significantly improved in the last decades. Hence, two fundamental mechanisms, interactions between the nervous and immune systems both within and without the central nervous system and sensitization that is a use-dependent increase in the sensitivity and activity of neurons involved in nociceptive processing have been identified being pivotal for the development of tissue injury-associated pain. However, important details of the cellular and molecular mechanisms, which account for the development of the pathological sensory experiences and those experiences becoming persistent, still await elucidation.

Citation: Nagy, I., Santha, P., Palecek, J., eds. (2021). The Perplexing Physiology of the Nociceptive System. Lausanne: Frontiers Media SA. doi: 10.3389/978-2-88974-027-7

Table of Contents

- 05 Proximal C-Terminus Serves as a Signaling Hub for TRPA1 Channel Regulation via Its Interacting Molecules and Supramolecular Complexes**
Lucie Zimova, Kristyna Barvikova, Lucie Macikova, Lenka Vyklicka, Viktor Sinica, Ivan Barvik and Viktorie Vlachova
- 15 Rating the Intensity of a Laser Stimulus, but Not Attending to Changes in Its Location or Intensity Modulates the Laser-Evoked Cortical Activity**
Diana M. E. Torta, Marco Ninghetto, Raffaella Ricci and Valéry Legrain
- 24 Longitudinal Study of Functional Reinnervation of the Denervated Skin by Collateral Sprouting of Peptidergic Nociceptive Nerves Utilizing Laser Doppler Imaging**
Szandra Lakatos, Gábor Jancsó, Ágnes Horváth, Ildikó Dobos and Péter Sántha
- 34 Peripheral Inflammatory Hyperalgesia Depends on P2X7 Receptors in Satellite Glial Cells**
Amanda Ferreira Neves, Felipe Hertzling Farias, Silviane Fernandes de Magalhães, Dionéia Araldi, Marco Pagliusi Jr., Claudia Herrera Tambeli, Cesar Renato Sartori, Celina Monteiro da Cruz Lotufo and Carlos Amílcar Parada
- 47 Tyrosine Kinase Inhibitors Reduce NMDA NR1 Subunit Expression, Nuclear Translocation, and Behavioral Pain Measures in Experimental Arthritis**
Karin N. Westlund, Ying Lu, Liping Zhang, Todd C. Pappas, Wen-Ru Zhang, Giulio Tagliabata, Sabrina L. McIlwraith and Terry A. McNearney
- 66 Chronic Pain After Spinal Cord Injury: Is There a Role for Neuron-Immune Dysregulation?**
Sílvia S. Chambel, Isaura Tavares and Célia D. Cruz
- 74 The NLRP3 Inflammasome: Role and Therapeutic Potential in Pain Treatment**
Hana Starobova, Evelyn Israel Nadar and Irina Vetter
- 86 Antinociceptive Effects of Lipid Raft Disruptors, a Novel Carboxamido-Steroid and Methyl β -Cyclodextrin, in Mice by Inhibiting Transient Receptor Potential Vanilloid 1 and Ankyrin 1 Channel Activation**
Ádám Horváth, Tünde Biró-Sütő, Boglárka Kántás, Maja Payrits, Rita Skoda-Földes, Eszter Szánti-Pintér, Zsuzsanna Helyes and Éva Szőke
- 95 IL-1 β Induced Cytokine Expression by Spinal Astrocytes Can Play a Role in the Maintenance of Chronic Inflammatory Pain**
Andrea Gajtkó, Erzsébet Bakk, Krisztina Hegedűs, László Ducza and Krisztina Holló
- 112 The Mysteries of Capsaicin-Sensitive Afferents**
Michael J. M. Fischer, Cosmin I. Ciotu and Arpad Szallasi
- 127 Projection Neuron Axon Collaterals in the Dorsal Horn: Placing a New Player in Spinal Cord Pain Processing**
Tyler J. Browne, David I. Hughes, Christopher V. Dayas, Robert J. Callister and Brett A. Graham

- 137** *Antinociceptive Effects of Sinomenine Combined With Ligustrazine or Paracetamol in Animal Models of Incisional and Inflammatory Pain*
Tianle Gao, Tao Li, Wei Jiang, Weiming Fan, Xiao-Jun Xu, Xiaoliang Zhao, Zhenming Yin, Huihui Guo, Lulu Wang, Jun Gao, Yanxing Han, Jian-Dong Jiang and Danqiao Wang
- 152** *Performance of the Surgical Pleth Index and Analgesia Nociception Index in Healthy Volunteers and Parturients*
Byung-Moon Choi, Hangsik Shin, Joo-Hyun Lee, Ji-Yeon Bang, Eun-Kyung Lee and Gyu-Jeong Noh



Proximal C-Terminus Serves as a Signaling Hub for TRPA1 Channel Regulation via Its Interacting Molecules and Supramolecular Complexes

OPEN ACCESS

Edited by:

Istvan Nagy,
Imperial College London,
United Kingdom

Reviewed by:

Merab G. Tsagareli,
Ivane Beritashvili Center
of Experimental Biomedicine, Georgia
Ari-Pekka Koivisto,
Orion Corporation, Finland
Leon D. Islas,
National Autonomous University
of Mexico, Mexico

*Correspondence:

Lucie Zimova
lucie.zimova@fgu.cas.cz
Viktorie Vlachova
viktorie.vlachova@fgu.cas.cz

Specialty section:

This article was submitted to
Integrative Physiology,
a section of the journal
Frontiers in Physiology

Received: 29 November 2019

Accepted: 18 February 2020

Published: 12 March 2020

Citation:

Zimova L, Barvikova K,
Macikova L, Vyklicka L, Sinica V,
Barvik I and Vlachova V (2020)
Proximal C-Terminus Serves as
a Signaling Hub for TRPA1 Channel
Regulation via Its Interacting
Molecules and Supramolecular
Complexes. *Front. Physiol.* 11:189.
doi: 10.3389/fphys.2020.00189

Lucie Zimova^{1*}, Kristyna Barvikova¹, Lucie Macikova^{1,2}, Lenka Vyklicka¹, Viktor Sinica^{1,3},
Ivan Barvik⁴ and Viktorie Vlachova^{1*}

¹ Department of Cellular Neurophysiology, Institute of Physiology, The Czech Academy of Sciences, Prague, Czechia,

² Department of Physiology, Faculty of Science, Charles University, Prague, Czechia, ³ Department of Physical
and Macromolecular Chemistry, Faculty of Science, Charles University, Prague, Czechia, ⁴ Division of Biomolecular Physics,
Faculty of Mathematics and Physics, Institute of Physics, Charles University, Prague, Czechia

Our understanding of the general principles of the polymodal regulation of transient receptor potential (TRP) ion channels has grown impressively in recent years as a result of intense efforts in protein structure determination by cryo-electron microscopy. In particular, the high-resolution structures of various TRP channels captured in different conformations, a number of them determined in a membrane mimetic environment, have yielded valuable insights into their architecture, gating properties and the sites of their interactions with annular and regulatory lipids. The correct repertoire of these channels is, however, organized by supramolecular complexes that involve the localization of signaling proteins to sites of action, ensuring the specificity and speed of signal transduction events. As such, TRP ankyrin 1 (TRPA1), a major player involved in various pain conditions, localizes into cholesterol-rich sensory membrane microdomains, physically interacts with calmodulin, associates with the scaffolding A-kinase anchoring protein (AKAP) and forms functional complexes with the related TRPV1 channel. This perspective will contextualize the recent biochemical and functional studies with emerging structural data with the aim of enabling a more thorough interpretation of the results, which may ultimately help to understand the roles of TRPA1 under various physiological and pathophysiological pain conditions. We demonstrate that an alteration to the putative lipid-binding site containing a residue polymorphism associated with human asthma affects the cold sensitivity of TRPA1. Moreover, we present evidence that TRPA1 can interact with AKAP to prime the channel for opening. The structural bases underlying these interactions remain unclear and are definitely worth the attention of future studies.

Keywords: TRPA1, TRP channel, calmodulin, A-kinase anchoring protein, transient receptor potential

INTRODUCTION

The Transient Receptor Potential (TRP) Ankyrin subtype 1 (TRPA1), originally called ANKTM1 (Story et al., 2003), is a cation channel expressed in a subset of dorsal root, trigeminal and visceral primary sensory neurons (Bautista et al., 2006; Kwan et al., 2006), but also in non-neuronal cells such as keratinocytes (Kwan et al., 2006), fibroblasts (Jaquemar et al., 1999), odontoblasts (El Karim et al., 2011), astroglia (Shigetomi et al., 2011), Schwann cells (De Logu et al., 2017), endothelial cells, and arterial vessels (Kwan et al., 2009). There, TRPA1 acts as a polymodal sensor of cell threats, being activated by a wide range of physical and chemical stimuli of extracellular or intracellular origin (for comprehensive reviews see (Zygmunt and Hogestatt, 2014; Chen and Hackos, 2015; Viana, 2016; Gouin et al., 2017; Koivisto et al., 2018; Wang et al., 2019) and references therein). Accumulating evidence links the physiological functions of TRPA1 to inflammation, temperature perception, mechanosensation, insulin secretion, itching, respiratory functions, regulation of the cardiovascular system, but also the homeostatic balance between the immune and nociceptive systems, as recently nicely reviewed by Talavera et al. (2019). Under certain pathological conditions such as tissue injury or inflammation, TRPA1 may undergo a wide range of posttranslational modifications that lead to various levels of functional modulation. Ca^{2+} influx through TRPA1 can release mediators such as calcitonin gene-related peptide, substance P, neurokinin A and bradykinin, which modulate the channel via G-protein-coupled receptor signaling cascades (Andrade et al., 2012; Petho and Reeh, 2012; Voolstra and Huber, 2014; Kadkova et al., 2017) and/or promote the recruitment of the channels to the cell surface (Schmidt et al., 2009; Takahashi and Ohta, 2017).

A large number (>150) of single-point mutations and chimeras of human TRPA1 have been functionally characterized in the literature (Meents et al., 2019), yet the published data do not enable us to fully understand the molecular details of the channel function, mostly because (1) the available structures of TRPA1 capture the channel in an intermediate or inactivated conformation (Paulsen et al., 2015; Suo et al., 2020) which does not allow to distinguish the functional states, (2) the structures lack information on a considerable (~50%) part of the protein, (3) the impact of the interactions of TRPA1 with various important endogenous proteins and cellular signaling mechanisms has not yet been fully characterized (Zygmunt and Hogestatt, 2014; Gouin et al., 2017; Talavera et al., 2019), and (4) the extent to which TRPA1 can be regulated by its membrane environment is still only gradually being uncovered (Hirono et al., 2004; Akopian et al., 2007; Dai et al., 2007; Karashima et al., 2008; Witschas et al., 2015; Macikova et al., 2019; Startek et al., 2019). Obviously, a better understanding of all these issues is key for a precise description of the mechanisms of TRPA1 activation, and, perhaps more importantly, for rational screening of its novel modulators as potential therapeutic agents.

The thermosensitive properties of TRPA1 are even less understood. In mammals, TRPA1 is thought to function as a cold detector (Story et al., 2003; Viswanath et al., 2003;

Bandell et al., 2004; Kwan et al., 2006; Karashima et al., 2009; Kremeyer et al., 2010), but it has been also found to play a crucial role in the detection of noxious heat (Hoffmann et al., 2013; Yarmolinsky et al., 2016; Vandewauw et al., 2018). *In vitro*, a direct cold activation of TRPA1 was demonstrated by several laboratories for mouse, rat and human orthologs (Story et al., 2003; Viswanath et al., 2003; Sawada et al., 2007; Karashima et al., 2009; del Camino et al., 2010; Moparthi et al., 2016). On the other hand, some other groups did not observe any cold activation (Jordt et al., 2004; Zurborg et al., 2007; Knowlton et al., 2010; Cordero-Morales et al., 2011; Chen et al., 2013). This is clearly not the whole story, and further intensive investigation is required to determine the specific role of mammalian TRPA1 as a temperature sensor (Sinica et al., 2019).

This article provides new evidence that the cold sensitivity of TRPA1 can be modulated by membrane phosphoinositides; specifically, by phosphatidylinositol-4,5-bisphosphate, PIP_2 . Moreover, we demonstrate that AKAP, the scaffolding A-kinase anchoring protein that is necessary for the effective phosphorylation of TRPA1 by protein kinases A and C, potentiates the channel at negative membrane potentials, suggesting the existence of basal phosphorylation or a direct effect of AKAP on TRPA1. Although these primary results provide potentially important information indicating that the membrane proximal part of the C-terminus of TRPA1 may form a hot spot contributing to a highly effective regulation of TRPA1, additional structural/functional considerations are necessary to characterize the channel in its full physiological context.

MATERIALS AND METHODS

Cell Culture, Constructs, and Transfection

Human embryonic kidney 293T (HEK293T; ATCC, Manassas, VA, United States) cells were cultured and transfected with 400 ng of cDNA plasmid encoding wild-type or mutant human TRPA1 (pCMV6-XL4 vector, OriGene Technologies, Rockville, MD, United States) and 200 ng of GFP plasmid (TaKaRa, Shiga, Japan), and, for particular experiments, 300 ng of a plasmid of wild-type TRPA1 with 300 ng of plasmid Dr-VSP (in IRES2-EGFP vector, a gift from Yasushi Okamura, Addgene plasmid #80333) or 400 ng of the plasmid of wild-type TRPA1 with 200 ng of plasmid AKAP79 (pCMV6-XL4 vector, OriGene Technologies, Rockville, MD, United States), using the magnet-assisted transfection technique (IBA GmbH, Gottingen, Germany) as described previously (Zimova et al., 2018). The mutant H1018R was generated by PCR using a QuikChange II XL Site-Directed Mutagenesis Kit (Agilent Technologies, Santa Clara, CA, United States) and confirmed by DNA sequencing (Eurofins Genomics, Ebersberg, Germany).

Electrophysiology and Cold Stimulation

All electrophysiological recordings were carried out as described previously (Zimova et al., 2018). For the experiments described in **Figure 1**, the extracellular bath solution contained: 140 mM NaCl, 5 mM KCl, 2 mM MgCl_2 , 5 mM EGTA, and 10 mM

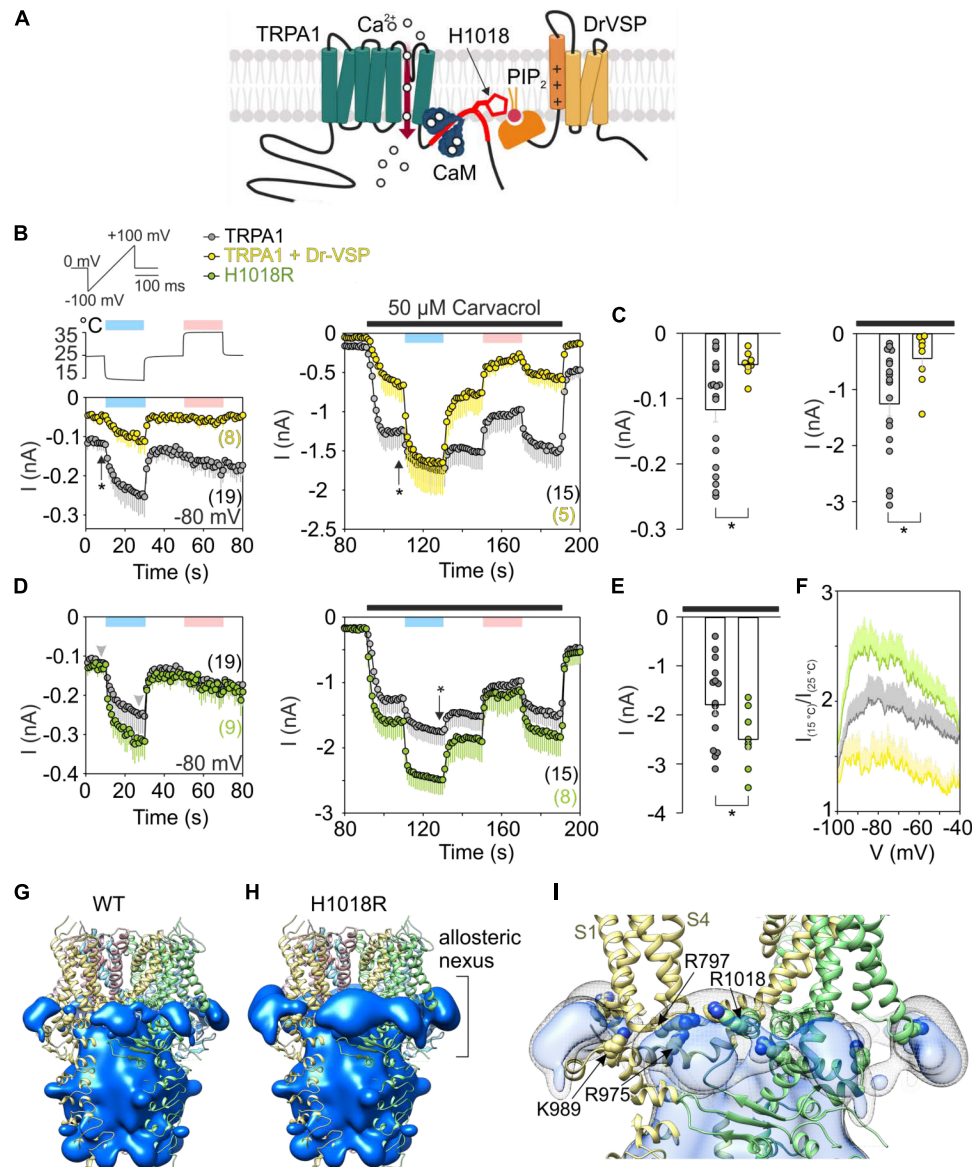


FIGURE 1 | Acute PIP₂ depletion has an opposite effect on cold-dependent gating of TRPA1 to missense histidine-to-arginine mutation at position 1018.

(A) Schematic diagram shows binding of Ca²⁺-CaM (calmodulin) to C terminus of TRPA1 (Macikova et al., 2019). The binding domain for CaM partly overlaps with the proposed binding pocket for PIP₂ (in red) which includes H1018. Voltage-sensitive phosphatase (Dr-VSP) hydrolyses PIP₂ upon depolarization greater than +50 mV. **(B)** Time course of average whole-cell currents of human TRPA1 (TRPA1, gray circles with bars indicating mean values with – SEM) and TRPA1 co-expressed with Dr-VSP (yellow circles with bars indicating mean values with – SEM), measured at –80 mV. First, the cells were exposed to a 3 s depolarizing pulse to +80 mV to activate Dr-VSP. Then, the membrane potential was linearly ramped up each second from –100 mV to +100 mV (1 V.s^{–1}). The temperature was lowered first from room temperature 25°C to 15°C (blue bar) and then raised to 35°C (pink bar); the temperature trace is shown above the first record (left). Subsequently, 50 μM carvacrol (black bar) was applied together with temperature changes (right), n is indicated in brackets. **(C)** Comparison of current amplitudes at –80 mV at times marked in **(B)** with vertical arrows. Color coding as in **(B)**. Left: The basal current through TRPA1 is significantly smaller ($P = 0.028$) when it is co-expressed with Dr-VSP that causes acute PIP₂ depletion upon voltage stimulation. Right: Responses to carvacrol are also significantly smaller ($P = 0.032$). Data are shown as single points and as mean values – SEM. **(D)** Time course of average whole-cell currents of mutant H1018R of TRPA1 (green circles with bars indicating mean value – SEM) measured at –80 mV compared with wild-type hTRPA1 as in **(B)**. **(E)** The current responses of H1018R to simultaneous exposure to 50 μM carvacrol and cold (15°C) are significantly higher ($P = 0.043$) than the currents from wild-type hTRPA1. Data are shown as single points and as mean values – SEM at times marked in **(D)** with an arrow. Color coding as in **(B,D)**. **(F)** Voltage dependence of cold activation averaged at times indicated by gray arrowheads in **(D)**. The extent of cold potentiation of TRPA1 (gray line, mean + SEM), hTRPA1 co-expressed with Dr-VSP (yellow line, mean + SEM), and H1018R (green line, as mean + SEM) at negative membrane potentials. **(G)** Areas of positive electrostatic potential (blue surface) surrounding the ligand-free structure of TRPA1 [Protein Data Bank (PDB) ID: 6PQQ] and **(H)** its mutant H1018R. **(I)** A detailed view of the region around the allosteric nexus of TRPA1 shows substantially more positive values for H1018R (side chain shown) than for TRPA1 (depicted as light gray mesh encircling light blue surface). The allosteric nexus formed by the cytoplasmic region situated below the transmembrane core has been recently proposed to be an important determinant for phospholipid binding as well as for TRPA1 gating (Zhao et al., 2019; Suo et al., 2020).

HEPES, 10 mM glucose, pH 7.4 was adjusted with TMA-OH. The intracellular solution contained 140 mM KCl, 5 mM EGTA, 2 mM MgCl₂, and 10 mM HEPES, adjusted with KOH to pH 7.4. For the experiments shown in **Figure 2**, the extracellular bath solution contained: 140 mM NaCl, 4 mM KCl, 1 mM MgCl₂, 10 mM HEPES, 5 mM glucose, pH 7.4 adjusted with NaOH. The intracellular solution contained 125 mM Cs-glucono- δ -lactone, 15 mM CsCl, 5 mM EGTA, 0.5 mM CaCl₂, 2 mM MgATP, 0.3 NaGTP, and 10 mM HEPES, adjusted to pH 7.4 with CsOH. A system for the rapid cooling and heating of solutions superfusing isolated cells under patch-clamp conditions was used as described in Dittert et al. (2006). The temperature of the flowing solution was measured with a miniature thermocouple inserted into the common outlet capillary near to its orifice, which was placed less than 100 μ m from the surface of the examined cell. Statistical significance was determined by Student's *t*-test or the analysis of variance, as appropriate; differences were considered significant at $P < 0.05$ where not stated otherwise. The data are presented as means \pm (or \pm) SEM.

RESULTS AND DISCUSSION

Predicted Role of Phosphoinositides in the Regulation of Temperature-Dependent Gating of TRPA1

The transmembrane domain of TRPA1 is composed of the voltage sensor-like domain (VSLD) formed by a bundle of four antiparallel helices, S1–S4, and the pore domain (formed by S5, S6, and two pore helices) arranged in a domain-swap manner. The proximal C terminus contains a TRP-like domain that interacts with a pre-S1 helix. There are at least two sites with separate functions from which the activity of TRPA1 can be regulated by membrane phosphatidylinositol-4,5-bisphosphate (PIP₂) or other phosphoinositides: the first, formed by the intracellular part of VSLD and contributed to by K989 from the TRP-like domain (Samad et al., 2011; Witschas et al., 2015; Zimova et al., 2018), and the second localized between adjacent subunits (T1003–P1034), capable of directly affecting the gating of the channel through the S4–S5 linker and R975 from the TRP-like domain (Macikova et al., 2019). Mutation at the highly conserved phenylalanine F1020 located in the center of the latter interacting region produced channels with faster activation kinetics and with significantly suppressed responses at negative membrane potentials. The effectiveness of PIP₂ at inhibiting or promoting the activity of TRPA1 appears to substantially depend on the conformational states of the channel (Macikova et al., 2019). Importantly, two amino acids upstream of F1020, a missense mutation of a histidine residue (rs959976) was recently found to be associated with childhood asthma (Gallo et al., 2017). The histidine-to-arginine mutation (H1018R) increased the responses of recombinant channels to insoluble coal fly ash particles by 70%, suggesting an increased sensitivity to mechanical stimuli (Deering-Rice et al., 2015). We hypothesized that arginine at

position 1018 may alter the affinity of PIP₂ to TRPA1, and thereby also influence the activation of the channel by other stimuli, particularly by heat or cold temperatures. Several structures of thermosensitive TRP channels contain lipids in the regions essentially involved in agonist binding or pore gating (Cao et al., 2013; Singh et al., 2018, 2019), and it has been proposed that the association/dissociation of lipids may be one of the underlying mechanisms of temperature sensation (Cao et al., 2013). Also, recent molecular dynamics simulations performed with the structure of the TRPA1-related channel TRPV1 at different temperatures suggest that the lipid displacement from protein binding sites may contribute to temperature-evoked actuation (Melnick and Kaviany, 2018). Because human TRPA1 is considered to be a cold-sensitive channel (Moparthy et al., 2014), we tested whether the H1018R mutation may influence the cold sensitivity of human TRPA1.

Using depolarizing voltage ramps from -100 mV to $+100$ mV under whole-cell patch clamp conditions, we measured TRPA1-mediated responses from HEK293T cells transfected with wild-type human TRPA1 or wild-type human TRPA1 together with the voltage-dependent phosphatase cloned from *Danio rerio* (Dr-VSP) to selectively deplete PIP₂ (Hossain et al., 2008; Okamura et al., 2009; Zimova et al., 2018; **Figure 1A**). We applied 20 s steps from 25°C to 15°C and to 35°C first in control extracellular solution and then in 50 μ M carvacrol, the non-electrophilic agonist of TRPA1. At positive membrane potentials the current responses were not significantly different, indicating comparable expression levels. The comparison at -80 mV indicates that an acute level of membrane PIP₂ regulates both the rate and extent of the response to individual stimuli (cold temperature or agonist) but does not affect the synergy between the stimuli (**Figures 1B,C**). Using the same voltage protocol, we measured currents from cells expressing the H1018R mutant (**Figure 1D**). Notably, the H1018R mutant exhibited significantly increased current responses at -80 mV upon the simultaneous application of agonist and cooling (**Figure 1E**). The voltage dependence of cold activation (**Figure 1F**) illustrates the opposite effects of the H1018R mutation and the acute PIP₂ depletion. To find where negatively charged PIP₂ will most likely be bound, we used the structure of human TRPA1 [Protein Data Bank (PDB) ID: 6PQQ; (Suo et al., 2020)]. By means of the “Mutate residue” plugin in VMD software (Humphrey et al., 1996), H1018 was mutated to R1018. The “PME Electrostatics” module of VMD was used to compute electrostatic maps, which were visualized with UCSF Chimera (Pettersen et al., 2004). As shown in **Figures 1G–I**, the H1018R mutation substantially extended the positive electrostatic potential surrounding the allosteric nexus formed by the cytoplasmic region situated just below the transmembrane core, indicating an increased probability of PIP₂ binding (see also the **Supplementary Material**).

These results further substantiate the previously proposed role of the proximal C-terminal linker in the PIP₂-mediated regulation of TRPA1, and also indicate that the cold sensitivity of the channel can be modulated by membrane lipids. Consistent with our results, the allosteric nexus containing this region has been recently proposed to be an important determinant for

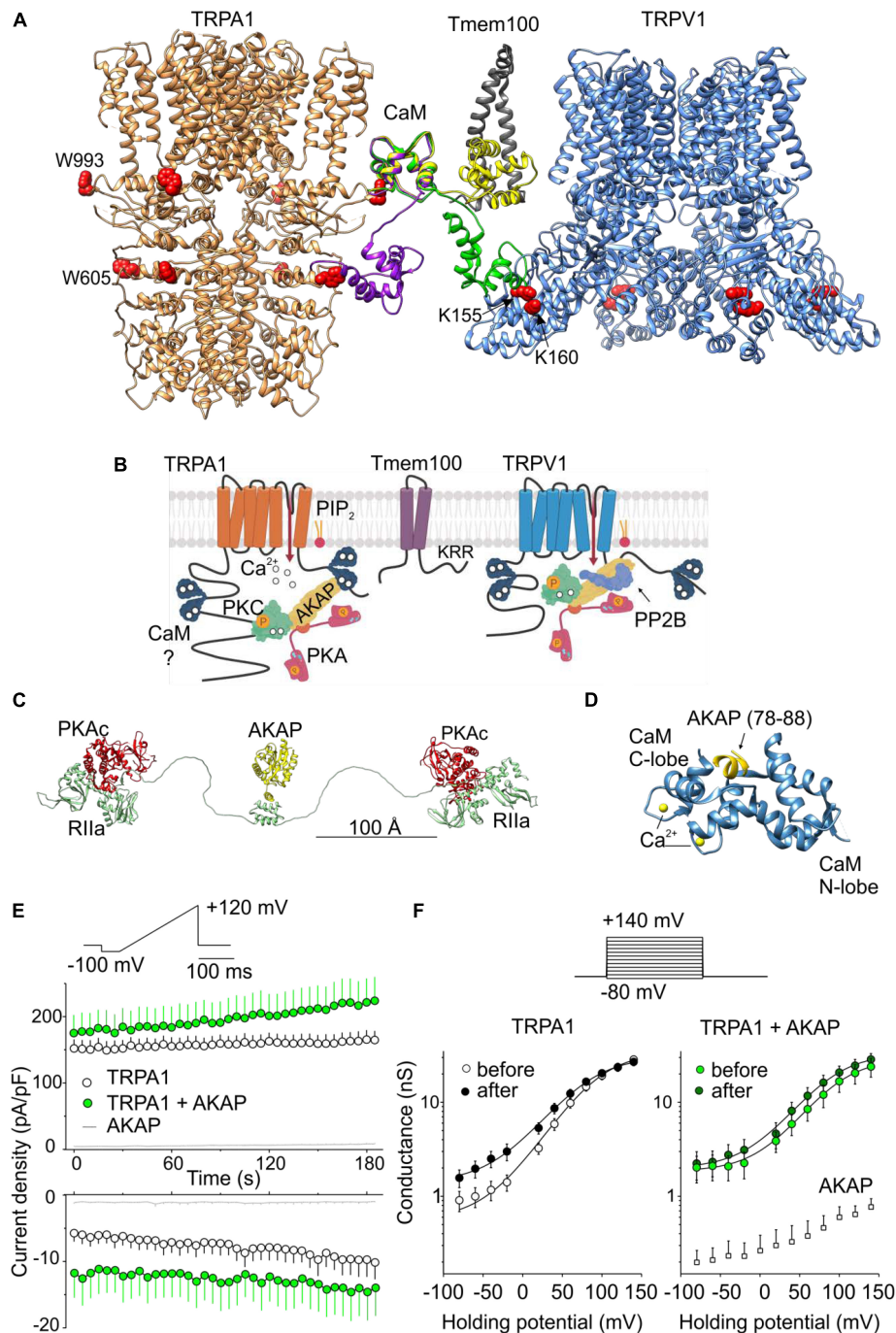


FIGURE 2 | Regulation of TRPA1 by phosphorylation and by predicted interactions with modulatory and scaffold proteins. **(A)** N- and C-lobes of Ca^{2+} /CaM (three conformers are shown in violet, green, and yellow) are capable of binding to TRPA1 but also serving as a linker binding either TRPA1 to the Tmem100 (gray ribbon) membrane protein or to the cytoplasmic binding site in the N-terminus of TRPV1. Tryptophans putatively involved in Ca^{2+} /CaM binding are shown as red side chains. **(B)** Permeating Ca^{2+} binds to calmodulin (forming a complex Ca^{2+} /CaM), phosphatidylinositol-4,5-bisphosphate (PIP₂) competes with Ca^{2+} /CaM for binding to TRPA1. A kinase anchoring protein AKAP79/150 (AKAP) binds to TRPA1 and functions as a signaling scaffold for protein kinase A (PKA) and C (PKC). The activation of PKA or PKC sensitizes TRPA1 by phosphorylation (P in orange circles). The interaction of TRPA1 with TRPV1 is regulated by the transmembrane adaptor protein Tmem100 via the amino acid KRR triplet on the C-terminus of Tmem100. AKAP also binds to TRPV1 and associates with protein phosphatase 2B (PP2B, calcineurin) to effectively dephosphorylate the channel. **(C)** Extended linear configuration (the end-to-end length ~ 385 Å) of pseudo-atomic model of pentameric protein assembly of AKAP (AKAP18γ, residues 88–317) connected to regulatory subunits (RIIα) with associated catalytic subunits (PKAc) of PKA [PDB ID: 3j4R; (Smith et al., 2013)]. **(D)** Published crystal structure of CaM (steel blue ribbon) in complex with AKAP79 peptide (yellow). Two EF hands of the C-lobe coordinate Ca^{2+} (yellow atoms). One of the two copies of the published structure is shown: PDB ID: 5NIN, chains **A** and **C**. **(E)** Average whole-cell current densities induced by depolarizing voltage measured from HEK293T cells expressing TRPA1 (white circles indicating mean \pm SEM; $n = 17$), or TRPA1 together with

(Continued)

FIGURE 2 | Continued

AKAP79 (green circles indicating mean \pm SEM; $n = 13$). Voltage ramp protocol (shown in upper trace) was applied repeatedly each 5 s for 3 min. Amplitudes were measured at -100 mV and $+100$ mV and plotted as a function of time. Mean current densities measured from HEK293T cells transfected only with AKAP79 and control plasmid are shown as light gray lines with \pm SEM ($n = 4$); absent error bars are smaller than the line thickness. **(F)** Average conductances measured at the end of pulses from currents induced by voltage-step protocol (shown above): 100-ms steps from -80 mV to $+140$ mV (increment $+20$ mV), holding potential -70 mV. Currents were measured from TRPA1 or TRPA1 together with AKAP79 before (white and light green circles) and after (black and dark green circles) the train of ramp pulses as shown in **(E)**. The data represent the mean \pm SEM ($n = 12$ and 9 , respectively). The solid lines represent the best fit to a Boltzmann function as described in (Zimova et al., 2018). Average conductances obtained from three HEK293T cells transfected with AKAP79 together with control plasmid are shown as white squares \pm SEM.

phospholipid binding as well as for TRPA1 gating (Zhao et al., 2019; Suo et al., 2020).

At present, however, it is not clear to what extent the results may reflect the situation *in vivo* and how the effects observed with the H1018R mutant may relate to human asthma. We have recently demonstrated that the cold sensitivity of human TRPA1 is similar in both HEK293T cells and also in F11 cells, which are a well characterized cellular model of peripheral sensory neurons (Sinica et al., 2019). Although the TRPA1-mediated cold responses do not differ between these two cellular models, PIP₂ signaling and H1018R expression could differ among various cell types.

Regulation of TRPA1 by Ca²⁺-Calmodulin Complex

One of the most essential modulators of TRPA1 are calcium ions, which activate the channel at low concentrations and inactivate it at higher concentrations (Jordt et al., 2004; Nagata et al., 2005; Doerner et al., 2007; Zurborg et al., 2007; Cavanaugh et al., 2008; Wang et al., 2011). Mechanistically, Ca²⁺ ions permeating through the TRPA1 channel bind the Ca²⁺-sensing protein calmodulin (CaM), which pre-associates with the membrane proximal C-terminal region of TRPA1 (L992-N1008) from where the Ca²⁺-CaM enables the channel to distinctly respond to diverse Ca²⁺ signals (Hasan et al., 2017). It does so in a bimodal manner so that it potentiates TRPA1 at low concentrations of cytosolic Ca²⁺ and inactivates the channel at higher Ca²⁺ concentrations. The proposed Ca²⁺-CaM-binding region at TRPA1 is integrated with a putative three-stranded β -sheet formed by two anti-parallel β -strands from the N-terminus and a contacting strand that follows the C-terminal TRP-like helix. The latter, peripherally exposed β -strand binds the carboxy-lobe (C-lobe) of calmodulin and even under resting concentrations of Ca²⁺ (~ 100 nM) forms a tight complex with the channel (Hasan et al., 2017). As is seen from our structural comparisons shown in **Figures 1G–I** and from our previous results (Macikova et al., 2019), this region overlaps with the interaction site for membrane PIP₂ with which Ca²⁺-CaM is likely to compete.

Whereas the C-lobe of CaM acts as an effector mediating Ca²⁺-dependent gating and a tether anchoring CaM to the binding site at TRPA1, the N-lobe of CaM is only partly involved in binding and does not affect the channel gating (Hasan et al., 2017). What could the additional role of the N-lobe in TRPA1 regulation be? CaM is a well-studied ubiquitously expressed protein involved in the regulation of a large number

of membrane and cytoplasmic proteins (Ishida and Vogel, 2006) and its role as a Ca²⁺-dependent modulator can be predicted with a relatively high degree of confidence (Yap et al., 2000; Mruk et al., 2014). Much less is known about its role as a Ca²⁺-dependent protein linker and a regulator of scaffold proteins (Villalobo et al., 2018). Structural comparisons shown in **Figure 2A** indicate that the N-lobe of CaM may either bridge different domains of TRPA1 or link the channel with some different target protein(s). This is possible due to the fact that its two independently folded Ca²⁺-binding lobes are able to interact differentially and, to some degree, separately. From the sequence analysis of human TRPA1 (Yap et al., 2000; Mruk et al., 2014), several putative CaM binding sites are predicted. Of these, the N-terminal regions K578-D606 and L488-S510, and the C-terminal region K988-K1009 have the highest score. Interestingly, the interaction of the N-lobe of CaM with the N-terminal region of TRPA1 may depend on the conformational state of the channel. Whereas the N-lobe of Ca²⁺/CaM can interact with W605 in the TRPA1 structure 3J9P obtained in the presence of allyl isothiocyanate (Paulsen et al., 2015), this tryptophan is inaccessible in the recently published structures 6PQQ, 6PQP, and 6PQO, obtained, respectively, as an apo-structure and in the presence of the reversible and irreversible electrophilic agonists BITC and JT010 (Suo et al., 2020).

Regulation of TRPA1 by Protein-Protein Interactions

In a large subset of sensory neurons, TRPA1 physically and functionally interacts with the structurally related vanilloid receptor subtype 1 channel TRPV1 (Story et al., 2003; Akopian et al., 2007; Salas et al., 2009; Staruschenko et al., 2010; Akopian, 2011; Fischer et al., 2014; Patil et al., 2020; **Figure 2B**). These two channels may desensitize or sensitize each other via the elevation of intracellular calcium ions (Jordt et al., 2004; Akopian et al., 2007). In addition, a direct association of TRPA1 with TRPV1 strongly inhibits the responses of TRPA1 to electrophilic agonists, independently of Ca²⁺ (Staruschenko et al., 2010; Fischer et al., 2014). In peptidergic neurons, the interaction of these two channels is tightly regulated by the transmembrane adaptor protein Tmem100, which loosens their association and thereby releases TRPA1 from inhibition. Structurally, the regulation of this interaction depends on a KRR amino acid triplet on the C-terminus of Tmem100 (Weng et al., 2015). Importantly, the highly positively charged C-terminus of Tmem100 also contains a putative CaM binding site predicted

with high confidence (L99–L115). Thus, the N-lobe of CaM can bind to the N-terminus of TRPA1 but can also bind to Tmem100 or TRPV1.

In **Figure 2A**, we illustrate how CaM could in principle be capable of bridging two binding sites in the TRPA1 structure or serve as a linker binding TRPA1 to the Tmem100 membrane protein or to the cytoplasmic binding site in the N-terminus of TRPV1. We used the crystal structures TRPA1 (PDB ID: 3J9P), TRPV1 (3J5P), Tmem141 (2LOR), and CaM (1MUX - a set of 30 structures determined by NMR). The C-domains of several CaM conformers from the 1MUX set were placed close to W993 in TRPA1 (red spheres), which is likely to serve as a hydrophobic anchor in the experimentally confirmed L992–N1008 binding site of CaM in the proximal C-terminal region of TRPA1 (Hasan et al., 2017). The distance between W993 and W605 (in the second putative binding site for CaM in TRPA1) roughly corresponds to the distance of the N- and C-terminal subunits in the conformer of CaM (depicted as a violet ribbon). The green conformer of CaM indicates how it could potentially bridge known binding sites in TRPA1 and TRPV1 (Lau et al., 2012). Another structure of CaM (yellow) shows the N-terminal subunit returning to the membrane, where it could be anchored by Tmem100 disturbing the TRPA1–TRPV1 complex. Interestingly, recently, the N- (amino acids 220–260) and C- (684–720) terminal domains on TRPV1 responsible for TRPA1–TRPV1 complex formation were identified (Patil et al., 2020). These domains partially overlap with the previously identified binding sites for CaM/PIP2 (189–222/682–725) (Rosenbaum et al., 2004; Ufret-Vincenty et al., 2011). This provides further support for our hypothesis that CaM could serve as linker between TRPA1 and TRPV1.

Protein Kinase A Anchoring Protein 79/150 (AKAP) Interacts With TRPA1

It has been demonstrated that TRPA1 can be sensitized by protein kinase A (PKA), protein kinase C (PKC), cyclin-dependent kinase 5, and by early signaling events linked to Ca^{2+} -dependent phosphoinositide-specific phospholipase C (PLC) enzymes that hydrolyze PIP₂ in the inner membrane leaflet (Bandell et al., 2004; Bautista et al., 2006; Dai et al., 2007; Wang et al., 2008; Hynkova et al., 2016; Brackley et al., 2017; Meents et al., 2017; Hall et al., 2018; Sulak et al., 2018; **Figure 2B**). For effective phosphorylation by PKA and PKC, TRPA1 needs the presence of a scaffolding protein, AKAP (Brackley et al., 2017), that is also required for the PKA phosphorylation of TRPV1 (Zhang et al., 2008). AKAP directly interacts with TRPA1 (Zhang et al., 2008), but it also engages in multiple protein-protein interactions including Ca^{2+} -CaM (Faux and Scott, 1997; Patel et al., 2017). Given the recently proposed importance of the AKAP-PKA pathway in TRPA1-mediated mechanical allodynia and cold hyperalgesia (Brackley et al., 2017; Miyano et al., 2019), it would be particularly important to test the hypothesis that AKAP may serve as a molecular hub that contributes to the specificity and efficiency of the cellular signaling network regulating TRPA1 under various physiological or pathophysiological conditions (**Figures 2A–D**).

Although AKAP spatially constrains phosphorylation by PKA, the regulatory subunits of PKA are capable of providing an ~16 nanometer radius of motion to the associated catalytic subunits [(Smith et al., 2013) and **Figure 2C**] and, therefore, the pathways regulating TRPA1 and TRPV1 may together form a supramolecular signaling complex.

Previous co-immunoprecipitation studies confirmed the interaction of AKAP with TRPA1 in HEK293 cells (Zhang et al., 2008) and in cultured trigeminal neurons (Brackley et al., 2017). We asked whether the overexpression of AKAP in HEK293T cells may influence the functional response of TRPA1. We measured currents induced by repeated depolarizing voltage ramps or steps from cells expressing TRPA1 or TRPA1 together with AKAP (**Figures 2E,F**). In TRPA1-expressing cells, we observed gradual current increases at negative and at positive membrane potentials ($P < 0.001$ and $P = 0.005$, respectively; $n = 17$). In cells co-expressing TRPA1 and AKAP, significant basal currents were observed at negative potentials and they did not further increase upon repeated stimulation ($P = 0.111$; $n = 13$). The expression of AKAP did not affect endogenous currents from HEK293T cells. These data can be interpreted in at least three ways: (1) AKAP may recruit TRPA1 to the plasma membrane, (2) AKAP may increase the activity of TRPA1 by increasing basal phosphorylation, and (3) the interaction with AKAP induces a conformational change that primes the channel for activation. Future, more thorough structural and functional studies that resolve the underlying mechanism may help our understanding of TRPA1 regulation and could possibly identify new targets that activate or inhibit TRPA1 for therapeutic purposes. A future direction in the search for effective treatment of asthma or mechanical and cold hyperalgesia could be to focus on a pharmacology directed toward the interacting regions of the TRPA1 channel with phospholipids and with its partner proteins, or toward the interacting proteins themselves.

DATA AVAILABILITY STATEMENT

The **Supplementary Material** contains the Particle Mesh Ewald electrostatic potential maps for the wild-type human TRPA1 (PDB ID: 6PQQ) and the R1018 mutant, visualized in UCSF Chimera 1.13. Other raw data supporting the conclusions of this article will be made available by the authors, without undue reservation, to any qualified researcher.

AUTHOR CONTRIBUTIONS

VV and LZ conceptualized the study. VS, LZ, VV, KB, and IB contributed to formal analysis. VS, LM, LZ, KB, and IB investigated the study. VV, LZ, IB, and LV supervised the study. VV contributed to writing – original draft of manuscript preparation. VV, LZ, and LV contributed to writing, reviewing, and editing. All authors contributed to manuscript revision, read, and approved the submitted version.

FUNDING

This research was funded by the Czechia Science Foundation, grant number 19-03777S. The research of LM, VS, and KB was funded by Grant Agency of Charles University (GAUK 406119).

REFERENCES

- Akopian, A. N. (2011). Regulation of nociceptive transmission at the periphery via TRPA1-TRPV1 interactions. *Curr. Pharm. Biotechnol.* 12, 89–94. doi: 10.2174/138920111793937952
- Akopian, A. N., Ruparel, N. B., Jeske, N. A., and Hargreaves, K. M. (2007). Transient receptor potential TRPA1 channel desensitization in sensory neurons is agonist dependent and regulated by TRPV1-directed internalization. *J. Physiol.* 583(Pt 1), 175–193. doi: 10.1111/jphysiol.2007.133231
- Andrade, E. L., Meotti, F. C., and Calixto, J. B. (2012). TRPA1 antagonists as potential analgesic drugs. *Pharmacol. Ther.* 133, 189–204. doi: 10.1016/j.pharmthera.2011.10.008
- Bandell, M., Story, G. M., Hwang, S. W., Viswanath, V., Eid, S. R., Petrus, M. J., et al. (2004). Noxious cold ion channel TRPA1 is activated by pungent compounds and bradykinin. *Neuron* 41, 849–857. doi: 10.1016/s0896-6273(04)00150-3
- Bautista, D. M., Jordt, S. E., Nikai, T., Tsuruda, P. R., Read, A. J., Poblete, J., et al. (2006). TRPA1 mediates the inflammatory actions of environmental irritants and proalgesic agents. *Cell* 124, 1269–1282. doi: 10.1016/j.cell.2006.02.023
- Brackley, A. D., Gomez, R., Guerrero, K. A., Akopian, A. N., Glucksman, M. J., Du, J., et al. (2017). A-Kinase anchoring protein 79/150 scaffolds transient receptor potential A1 phosphorylation and sensitization by metabotropic glutamate receptor activation. *Sci. Rep.* 7:1842. doi: 10.1038/s41598-017-01999-4
- Cao, E., Liao, M., Cheng, Y., and Julius, D. (2013). TRPV1 structures in distinct conformations reveal activation mechanisms. *Nature* 504, 113–118. doi: 10.1038/nature12823
- Cavanaugh, E. J., Simkin, D., and Kim, D. (2008). Activation of transient receptor potential A1 channels by mustard oil, tetrahydrocannabinol and Ca(2+) reveals different functional channel states. *Neuroscience* 154, 1467–1476. doi: 10.1016/j.neuroscience.2008.04.048
- Chen, J., and Hackos, D. H. (2015). TRPA1 as a drug target—promise and challenges. *Naunyn Schmiedeberg's Arch. Pharmacol.* 388, 451–463. doi: 10.1007/s00210-015-1088-3
- Chen, J., Kang, D., Xu, J., Lake, M., Hogan, J. O., Sun, C., et al. (2013). Species differences and molecular determinant of TRPA1 cold sensitivity. *Nat. Commun.* 4:2501. doi: 10.1038/ncomms3501
- Cordero-Morales, J. F., Gracheva, E. O., and Julius, D. (2011). Cytoplasmic ankyrin repeats of transient receptor potential A1 (TRPA1) dictate sensitivity to thermal and chemical stimuli. *Proc. Natl. Acad. Sci. USA* 108, E1184–E1191. doi: 10.1073/pnas.1114124108
- Dai, Y., Wang, S., Tominaga, M., Yamamoto, S., Fukuoka, T., Higashi, T., et al. (2007). Sensitization of TRPA1 by PAR2 contributes to the sensation of inflammatory pain. *J. Clin. Invest.* 117, 1979–1987. doi: 10.1172/jci30951
- De Logu, F., Nassini, R., Materazzi, S., Carvalho Goncalves, M., Nosi, D., Rossi Degl'Innocenti, D., et al. (2017). Schwann cell TRPA1 mediates neuroinflammation that sustains macrophage-dependent neuropathic pain in mice. *Nat. Commun.* 8:1887. doi: 10.1038/s41467-017-01739-2
- Deering-Rice, C. E., Shapiro, D., Romero, E. G., Stockmann, C., Bevans, T. S., Phan, Q. M., et al. (2015). Activation of transient receptor potential ankyrin-1 by insoluble particulate material and association with asthma. *Am. J. Respir. Cell Mol. Biol.* 53, 893–901. doi: 10.1165/rcmb.2015-0086OC
- del Camino, D., Murphy, S., Heiry, M., Barrett, L. B., Earley, T. J., Cook, C. A., et al. (2010). TRPA1 contributes to cold hypersensitivity. *J. Neurosci.* 30, 15165–15174. doi: 10.1523/JNEUROSCI.2580-10.2010
- Dittert, I., Benedikt, J., Vylicky, L., Zimmermann, K., Reeh, P. W., and Vlachova, V. (2006). Improved superfusion technique for rapid cooling or heating of cultured cells under patch-clamp conditions. *J. Neurosci. Methods* 151, 178–185. doi: 10.1016/j.jneumeth.2005.07.005
- Doerner, J. F., Gisselmann, G., Hatt, H., and Wetzel, C. H. (2007). Transient receptor potential channel A1 is directly gated by calcium ions. *J. Biol. Chem.* 282, 13180–13189. doi: 10.1074/jbc.m607849200
- El Karim, I. A., Linden, G. J., Curtis, T. M., About, I., McGahon, M. K., Irwin, C. R., et al. (2011). Human dental pulp fibroblasts express the “cold-sensing” transient receptor potential channels TRPA1 and TRPM8. *J. Endod.* 37, 473–478. doi: 10.1016/j.joen.2010.12.017
- Faux, M. C., and Scott, J. D. (1997). Regulation of the AKAP79-protein kinase C interaction by Ca2+/Calmodulin. *J. Biol. Chem.* 272, 17038–17044. doi: 10.1074/jbc.272.27.17038
- Fischer, M. J., Balasuriya, D., Jeggle, P., Goetze, T. A., McNaughton, P. A., Reeh, P. W., et al. (2014). Direct evidence for functional TRPV1/TRPA1 heteromers. *Pflugers Arch.* 466, 2229–2241. doi: 10.1007/s00424-014-1497-z
- Gallo, V., Dijk, F. N., Holloway, J. W., Ring, S. M., Koppelman, G. H., Postma, D. S., et al. (2017). TRPA1 gene polymorphisms and childhood asthma. *Pediatr. Allergy Immunol.* 28, 191–198. doi: 10.1111/pai.12673
- Gouin, O., L'Herondelle, K., Lebonvallet, N., Le Gall-Ianotto, C., Sakka, M., Buhe, V., et al. (2017). TRPV1 and TRPA1 in cutaneous neurogenic and chronic inflammation: pro-inflammatory response induced by their activation and their sensitization. *Protein Cell* 8, 644–661. doi: 10.1007/s12328-017-0395-5
- Hall, B. E., Prochazkova, M., Sapio, M. R., Minetos, P., Kurochkina, N., Binukumar, B. K., et al. (2018). Phosphorylation of the transient receptor potential ankyrin 1 by Cyclin-dependent Kinase 5 affects Chemo-nociception. *Sci. Rep.* 8:1177. doi: 10.1038/s41598-018-19532-6
- Hasan, R., Leeson-Payne, A. T., Jaggar, J. H., and Zhang, X. (2017). Calmodulin is responsible for Ca2+-dependent regulation of TRPA1 Channels. *Sci. Rep.* 7:45098. doi: 10.1038/srep45098
- Hirono, M., Denis, C. S., Richardson, G. P., and Gillespie, P. G. (2004). Hair cells require phosphatidylinositol 4,5-bisphosphate for mechanical transduction and adaptation. *Neuron* 44, 309–320. doi: 10.1016/j.neuron.2004.09.020
- Hoffmann, T., Kistner, K., Miermeister, F., Winkelmann, R., Wittmann, J., Fischer, M. J., et al. (2013). TRPA1 and TRPV1 are differentially involved in heat nociception of mice. *Eur. J. Pain* 17, 1472–1482. doi: 10.1002/j.1532-2149.2013.00331.x
- Hossain, M. I., Iwasaki, H., Okochi, Y., Chahine, M., Higashijima, S., Nagayama, K., et al. (2008). Enzyme domain affects the movement of the voltage sensor in ascidian and zebrafish voltage-sensing phosphatases. *J. Biol. Chem.* 283, 18248–18259. doi: 10.1074/jbc.M706184200
- Humphrey, W., Dalke, A., and Schulten, K. (1996). VMD: visual molecular dynamics. *J. Mol. Graph.* 14, 33–38. doi: 10.1016/0263-7855(96)00018-5
- Hynkova, A., Marsakova, L., Vaskova, J., and Vlachova, V. (2016). N-terminal tetrapeptide T/SPLH motifs contribute to multimodal activation of human TRPA1 channel. *Sci. Rep.* 6:28700. doi: 10.1038/srep28700
- Ishida, H., and Vogel, H. J. (2006). Protein-peptide interaction studies demonstrate the versatility of calmodulin target protein binding. *Protein Peptide Lett.* 13, 455–465. doi: 10.2174/0929866060776819600
- Jaquemar, D., Schenker, T., and Trueb, B. (1999). An ankyrin-like protein with transmembrane domains is specifically lost after oncogenic transformation of human fibroblasts. *J. Biol. Chem.* 274, 7325–7333. doi: 10.1074/jbc.274.11.7325
- Jordt, S. E., Bautista, D. M., Chuang, H. H., McKemy, D. D., Zygmunt, P. M., Hogestatt, E. D., et al. (2004). Mustard oils and cannabinoids excite sensory nerve fibres through the TRP channel ANKTM1. *Nature* 427, 260–265. doi: 10.1038/nature02282
- Kadkova, A., Synytsya, V., Krusek, J., Zimova, L., and Vlachova, V. (2017). Molecular basis of TRPA1 regulation in nociceptive neurons. A Review. *Physiol. Res.* 66, 425–439. doi: 10.33549/physiolres.933553
- Karashima, Y., Prenen, J., Meseguer, V., Owsianik, G., Voets, T., and Nilius, B. (2008). Modulation of the transient receptor potential channel TRPA1 by phosphatidylinositol 4,5-bisphosphate manipulators. *Pflugers Arch.* 457, 77–89. doi: 10.1007/s00424-008-0493-6
- Karashima, Y., Talavera, K., Everaerts, W., Janssens, A., Kwan, K. Y., Vennekens, R., et al. (2009). TRPA1 acts as a cold sensor in vitro and in vivo.

SUPPLEMENTARY MATERIAL

The Supplementary Material for this article can be found online at: <https://www.frontiersin.org/articles/10.3389/fphys.2020.00189/full#supplementary-material>

- Proc. Natl. Acad. Sci. U.S.A. 106, 1273–1278. doi: 10.1073/pnas.0808487106
- Knowlton, W. M., Bifolck-Fisher, A., Bautista, D. M., and McKemy, D. D. (2010). TRPM8, but not TRPA1, is required for neural and behavioral responses to acute noxious cold temperatures and cold-mimetics in vivo. *Pain* 150, 340–350. doi: 10.1016/j.pain.2010.05.021
- Koivisto, A., Jalava, N., Bratty, R., and Pertovaara, A. (2018). TRPA1 Antagonists for Pain Relief. *Pharmaceuticals* 11:E117. doi: 10.3390/ph11040117
- Kremeyer, B., Lopera, F., Cox, J. J., Momin, A., Rugiero, F., Marsh, S., et al. (2010). A gain-of-function mutation in TRPA1 causes familial episodic pain syndrome. *Neuron* 66, 671–680. doi: 10.1016/j.neuron.2010.04.030
- Kwan, K. Y., Allchorne, A. J., Vollrath, M. A., Christensen, A. P., Zhang, D. S., Woolf, C. J., et al. (2006). TRPA1 contributes to cold, mechanical, and chemical nociception but is not essential for hair-cell transduction. *Neuron* 50, 277–289. doi: 10.1016/j.neuron.2006.03.042
- Kwan, K. Y., Glazer, J. M., Corey, D. P., Rice, F. L., and Stucky, C. L. (2009). TRPA1 modulates mechanotransduction in cutaneous sensory neurons. *J. Neurosci.* 29, 4808–4819. doi: 10.1523/JNEUROSCI.5380-08.2009
- Lau, S. Y., Procko, E., and Gaudet, R. (2012). Distinct properties of Ca²⁺-calmodulin binding to N- and C-terminal regulatory regions of the TRPV1 channel. *J. Gen. Physiol.* 140, 541–555. doi: 10.1085/jgp.201210810
- Macikova, L., Sinica, V., Kadkova, A., Villette, S., Ciacciafava, A., Faherty, J., et al. (2019). Putative interaction site for membrane phospholipids controls activation of TRPA1 channel at physiological membrane potentials. *FEBS J.* 286, 3664–3683. doi: 10.1111/febs.14931
- Meents, J. E., Ciotu, C. I., and Fischer, M. J. M. (2019). TRPA1: a molecular view. *J. Neurophysiol.* 121, 427–443. doi: 10.1152/jn.00524.2018
- Meents, J. E., Fischer, M. J., and McNaughton, P. A. (2017). Sensitization of TRPA1 by Protein Kinase A. *PLoS One* 12:e0170097. doi: 10.1371/journal.pone.0170097
- Melnick, C., and Kaviany, M. (2018). Thermal actuation in TRPV1: role of embedded lipids and intracellular domains. *J. Theor. Biol.* 444, 38–49. doi: 10.1016/j.jtbi.2018.02.004
- Miyano, K., Shiraishi, S., Minami, K., Sudo, Y., Suzuki, M., Yokoyama, T., et al. (2019). Carboplatin enhances the activity of human transient receptor potential ankyrin 1 through the Cyclic AMP-Protein Kinase A-A-Kinase Anchoring Protein (AKAP) Pathways. *Int. J. Mo. Sci.* 20:E3271. doi: 10.3390/ijms20133271
- Moparthi, L., Kichko, T. I., Eberhardt, M., Hogestatt, E. D., Kjellbom, P., Johanson, U., et al. (2016). Human TRPA1 is a heat sensor displaying intrinsic U-shaped thermosensitivity. *Sci. Rep.* 6:28763. doi: 10.1038/srep28763
- Moparthi, L., Survery, S., Kreir, M., Simonsen, C., Kjellbom, P., Hogestatt, E. D., et al. (2014). Human TRPA1 is intrinsically cold- and chemosensitive with and without its N-terminal ankyrin repeat domain. *Proc. Natl. Acad. Sci. U.S.A.* 111, 16901–16906. doi: 10.1073/pnas.1412689111
- Mruk, K., Farley, B. M., Ritacco, A. W., and Kobertz, W. R. (2014). Calmodulation meta-analysis: predicting calmodulin binding via canonical motif clustering. *J. Gen. Physiol.* 144, 105–114. doi: 10.1085/jgp.201311140
- Nagata, K., Duggan, A., Kumar, G., and Garcia-Anoveros, J. (2005). Nociceptor and hair cell transducer properties of TRPA1, a channel for pain and hearing. *J. Neurosci.* 25, 4052–4061. doi: 10.1523/jneurosci.0013-05.2005
- Okamura, Y., Murata, Y., and Iwasaki, H. (2009). Voltage-sensing phosphatase: actions and potentials. *J. Physiol.* 587, 513–520. doi: 10.1113/jphysiol.2008.163097
- Patel, N., Stengel, F., Aebersold, R., and Gold, M. G. (2017). Molecular basis of AKAP79 regulation by calmodulin. *Nat. Commun.* 8:1681. doi: 10.1038/s41467-017-01715-w
- Patil, M. J., Salas, M., Bialuhin, S., Boyd, J. T., Jeske, N. A., and Akopian, A. N. (2020). Sensitization of small-diameter sensory neurons is controlled by TRPV1 and TRPA1 association. *FASEB J.* 34, 287–302. doi: 10.1096/fj.201902026R
- Paulsen, C. E., Armache, J. P., Gao, Y., Cheng, Y., and Julius, D. (2015). Structure of the TRPA1 ion channel suggests regulatory mechanisms. *Nature* 520, 511–517. doi: 10.1038/nature14367
- Petho, G., and Reeh, P. W. (2012). Sensory and signaling mechanisms of bradykinin, eicosanoids, platelet-activating factor, and nitric oxide in peripheral nociceptors. *Physiol. Rev.* 92, 1699–1775. doi: 10.1152/physrev.00048.2010
- Pettersen, E. F., Goddard, T. D., Huang, C. C., Couch, G. S., Greenblatt, D. M., Meng, E. C., et al. (2004). UCSF Chimera—a visualization system for exploratory research and analysis. *J. Comput. Chem.* 25, 1605–1612. doi: 10.1002/jcc.20084
- Rosenbaum, T., Gordon-Shaag, A., Munari, M., and Gordon, S. E. (2004). Ca²⁺/calmodulin modulates TRPV1 activation by capsaicin. *J. Gen. Physiol.* 123, 53–62. doi: 10.1085/jgp.200308906
- Salas, M. M., Hargreaves, K. M., and Akopian, A. N. (2009). TRPA1-mediated responses in trigeminal sensory neurons: interaction between TRPA1 and TRPV1. *Eur. J. Neurosci.* 29, 1568–1578. doi: 10.1111/j.1460-9568.2009.06702.x
- Samad, A., Sura, L., Benedikt, J., Ettrich, R., Minofar, B., Teisinger, J., et al. (2011). The C-terminal basic residues contribute to the chemical- and voltage-dependent activation of TRPA1. *Biochem. J.* 433, 197–204. doi: 10.1042/BJ20101256
- Sawada, Y., Hosokawa, H., Hori, A., Matsumura, K., and Kobayashi, S. (2007). Cold sensitivity of recombinant TRPA1 channels. *Brain Res.* 1160, 39–46. doi: 10.1016/j.brainres.2007.05.047
- Schmidt, M., Dubin, A. E., Petrus, M. J., Earley, T. J., and Patapoutian, A. (2009). Nociceptive signals induce trafficking of TRPA1 to the plasma membrane. *Neuron* 64, 498–509. doi: 10.1016/j.neuron.2009.09.030
- Shigetomi, E., Tong, X., Kwan, K. Y., Corey, D. P., and Khakh, B. S. (2011). TRPA1 channels regulate astrocyte resting calcium and inhibitory synapse efficacy through GAT-3. *Nat. Neurosci.* 15, 70–80. doi: 10.1038/nn.3000
- Singh, A. K., McGoldrick, L. L., Demirkhanyan, L., Leslie, M., Zakharian, E., and Sobolevsky, A. I. (2019). Structural basis of temperature sensation by the TRP channel TRPV3. *Nat. Struct. Mol. Biol.* 27, 221. doi: 10.1038/s41594-019-0318-7
- Singh, A. K., McGoldrick, L. L., and Sobolevsky, A. I. (2018). Structure and gating mechanism of the transient receptor potential channel TRPV3. *Nat. Struct. Mol. Biol.* 25, 805–813. doi: 10.1038/s41594-018-0108-7
- Sinica, V., Zimova, L., Barvikova, K., Macikova, L., Barvik, I., and Vlachova, V. (2019). Human and mouse TRPA1 are heat and cold sensors differentially tuned by voltage. *Cells* 9:E57. doi: 10.3390/cells9010057
- Smith, F. D., Reichow, S. L., Esseltine, J. L., Shi, D., Langeberg, L. K., Scott, J. D., et al. (2013). Intrinsic disorder within an AKAP-protein kinase A complex guides local substrate phosphorylation. *eLife* 2:e01319. doi: 10.7554/eLife.01319
- Startek, J. B., Boonen, B., Lopez-Requena, A., Talavera, A., Alpizar, Y. A., Ghosh, D., et al. (2019). Mouse TRPA1 function and membrane localization are modulated by direct interactions with cholesterol. *eLife* 8:e46084. doi: 10.7554/eLife.46084
- Staruschenko, A., Jeske, N. A., and Akopian, A. N. (2010). Contribution of TRPV1-TRPA1 interaction to the single channel properties of the TRPA1 channel. *J. Biol. Chem.* 285, 15167–15177. doi: 10.1074/jbc.M110.106153
- Story, G. M., Peier, A. M., Reeve, A. J., Eid, S. R., Mosbacher, J., Hricik, T. R., et al. (2003). ANKTM1, a TRP-like channel expressed in nociceptive neurons, is activated by cold temperatures. *Cell* 112, 819–829. doi: 10.1016/s0092-8674(03)00158-2
- Sulak, M. A., Ghosh, M., Sinharoy, P., Andrei, S. R., and Damron, D. S. (2018). Modulation of TRPA1 channel activity by Cdk5 in sensory neurons. *Channels* 12, 65–75. doi: 10.1080/19336950.2018.1424282
- Suo, Y., Wang, Z., Zubcevic, L., Hsu, A. L., He, Q., Borgnia, M. J., et al. (2020). Structural insights into Electrophile Irritant Sensing by the human TRPA1 channel. *Neuron* 105, 31009–31008. doi: 10.1016/j.neuron.2019.11.023
- Takahashi, K., and Ohta, T. (2017). Membrane translocation of transient receptor potential ankyrin 1 induced by inflammatory cytokines in lung cancer cells. *Biochem. Biophys. Res. Commun.* 490, 587–593. doi: 10.1016/j.bbrc.2017.06.082
- Talavera, K., Startek, J. B., Alvarez-Collazo, J., Boonen, B., Alpizar, Y. A., Sanchez, A., et al. (2019). Mammalian transient receptor potential TRPA1 channels: from structure to disease. *Physiol. Rev.* [Epub ahead of print].
- Ufret-Vincenty, C. A., Klein, R. M., Hua, L., Angueyra, J., and Gordon, S. E. (2011). Localization of the PIP2 sensor of TRPV1 ion channels. *J. Biol. Chem.* 286, 9688–9698. doi: 10.1074/jbc.M110.192526
- Vandewauw, I., De Clercq, K., Mulier, M., Held, K., Pinto, S., Van Ranst, N., et al. (2018). A TRP channel trio mediates acute noxious heat sensing. *Nature* 555, 662–666. doi: 10.1038/nature26137
- Viana, F. (2016). TRPA1 channels: molecular sentinels of cellular stress and tissue damage. *J. Physiol.* 594, 4151–4169. doi: 10.1113/JP270935
- Villalobo, A., Ishida, H., Vogel, H. J., and Berchtold, M. W. (2018). Calmodulin as a protein linker and a regulator of adaptor/scaffold proteins. *Biochim. Biophys. Acta Mol. Cell Res.* 1865, 507–521. doi: 10.1016/j.bbamcr.2017.12.004

- Viswanath, V., Story, G. M., Peier, A. M., Petrus, M. J., Lee, V. M., Hwang, S. W., et al. (2003). Opposite thermosensor in fruitfly and mouse. *Nature* 423, 822–823. doi: 10.1038/423822a
- Voolstra, O., and Huber, A. (2014). Post-translational modifications of TRP channels. *Cells* 3, 258–287. doi: 10.3390/cells3020258
- Wang, S., Dai, Y., Fukuoka, T., Yamanaka, H., Kobayashi, K., Obata, K., et al. (2008). Phospholipase C and protein kinase A mediate bradykinin sensitization of TRPA1: a molecular mechanism of inflammatory pain. *Brain* 131(Pt 5), 1241–1251. doi: 10.1093/brain/awn060
- Wang, Y. Y., Chang, R. B., Allgood, S. D., Silver, W. L., and Liman, E. R. (2011). A TRPA1-dependent mechanism for the pungent sensation of weak acids. *J. Gen. Physiol.* 137, 493–505. doi: 10.1085/jgp.201110615
- Wang, Z., Ye, D., Ye, J., Wang, M., Liu, J., Jiang, H., et al. (2019). The TRPA1 channel in the cardiovascular system: promising features and challenges. *Front. Pharmacol.* 10:1253. doi: 10.3389/fphar.2019.01253
- Weng, H. J., Patel, K. N., Jeske, N. A., Bierbower, S. M., Zou, W., Tiwari, V., et al. (2015). Tmem100 is a regulator of TRPA1-TRPV1 complex and contributes to persistent pain. *Neuron* 85, 833–846. doi: 10.1016/j.neuron.2014.12.065
- Witschas, K., Jobin, M. L., Korkut, D. N., Vladan, M. M., Salgado, G., Lecomte, S., et al. (2015). Interaction of a peptide derived from C-terminus of human TRPA1 channel with model membranes mimicking the inner leaflet of the plasma membrane. *Biochim. Biophys. Acta* 1848, 1147–1156. doi: 10.1016/j.bbamem.2015.02.003
- Yap, K. L., Kim, J., Truong, K., Sherman, M., Yuan, T., and Ikura, M. (2000). Calmodulin target database. *J. Struct. Funct. Genomics* 1, 8–14.
- Yarmolinsky, D. A., Peng, Y., Pogorzala, L. A., Rutlin, M., Hoon, M. A., and Zuker, C. S. (2016). Coding and Plasticity in the Mammalian Thermosensory System. *Neuron* 92, 1079–1092. doi: 10.1016/j.neuron.2016.10.021
- Zhang, X., Li, L., and McNaughton, P. A. (2008). Proinflammatory mediators modulate the heat-activated ion channel TRPV1 via the scaffolding protein AKAP79/150. *Neuron* 59, 450–461. doi: 10.1016/j.neuron.2008.05.015
- Zhao, J., King Lin, J. V., Paulsen, C. E., Cheng, Y., and Julius, D. (2019). Mechanisms governing irritant-evoked activation and calcium modulation of TRPA1. *BioRxiv* [preprint]. doi: 10.1101/2019.12.26.888982
- Zimova, L., Sinica, V., Kadkova, A., Vyklicka, L., Zima, V., Barvik, I., et al. (2018). Intracellular cavity of sensor domain controls allosteric gating of TRPA1 channel. *Sc.Signal.* 11:aan8621. doi: 10.1126/scisignal.aan8621
- Zurborg, S., Yurgionas, B., Jira, J. A., Caspani, O., and Heppenstall, P. A. (2007). Direct activation of the ion channel TRPA1 by Ca²⁺. *Nat. Neurosci.* 10, 277–279. doi: 10.1038/nn1843
- Zygmunt, P. M., and Hogestatt, E. D. (2014). Trpa1. *Handb. Exp. Pharmacol.* 222, 583–630. doi: 10.1007/978-3-642-54215-23

Conflict of Interest: The authors declare that the research was conducted in the absence of any commercial or financial relationships that could be construed as a potential conflict of interest.

Copyright © 2020 Zimova, Barvikova, Macikova, Vyklicka, Sinica, Barvik and Vlachova. This is an open-access article distributed under the terms of the Creative Commons Attribution License (CC BY). The use, distribution or reproduction in other forums is permitted, provided the original author(s) and the copyright owner(s) are credited and that the original publication in this journal is cited, in accordance with accepted academic practice. No use, distribution or reproduction is permitted which does not comply with these terms.



Rating the Intensity of a Laser Stimulus, but Not Attending to Changes in Its Location or Intensity Modulates the Laser-Evoked Cortical Activity

Diana M. E. Torta^{1,2*}, Marco Ninghetto^{1,3,4}, Raffaella Ricci³ and Valéry Legrain^{1,5}

¹Institute of Neuroscience, Université catholique de Louvain, Brussels, Belgium, ²Health Psychology Research Group, University of Leuven, Leuven, Belgium, ³Department of Psychology, University of Turin, Turin, Italy, ⁴Neuroplasticity Laboratory, Nencki Institute for Experimental Biology, Polish Academy of Science, Warsaw, Poland, ⁵Psychological Sciences Research Institute, Université catholique de Louvain, Louvain-la-Neuve, Belgium

OPEN ACCESS

Edited by:

Istvan Nagy,
Imperial College London,
United Kingdom

Reviewed by:

Li Hu,
Institute of Psychology (CAS), China
Arun Singh,
University of South Dakota,
United States

*Correspondence:

Diana M. E. Torta
diana.torta@kuleuven.be

Specialty section:

This article was submitted to Brain Imaging and Stimulation, a section of the journal *Frontiers in Human Neuroscience*

Received: 29 November 2019

Accepted: 16 March 2020

Published: 31 March 2020

Citation:

Torta DME, Ninghetto M, Ricci R and Legrain V (2020) Rating the Intensity of a Laser Stimulus, but Not Attending to Changes in Its Location or Intensity Modulates the Laser-Evoked Cortical Activity. *Front. Hum. Neurosci.* 14:120. doi: 10.3389/fnhum.2020.00120

Top-down attention towards nociceptive stimuli can be modulated by asking participants to pay attention to specific features of a stimulus, or to provide a rating about its intensity/unpleasantness. Whether and how these different top-down processes may lead to different modulations of the cortical response to nociceptive stimuli remains an open question. We recorded electroencephalographic (EEG) responses to brief nociceptive laser stimuli in 24 healthy participants while they performed a task in which they had to compare two subsequent stimuli on their Spatial location (Location task) or Intensity (Intensity Task). In two additional blocks (Location + Ratings, and Intensity + Ratings) participants had to further provide a rating of the perceived intensity of the stimulus. Such a design allowed us to investigate whether focusing on spatial or intensity features of a nociceptive stimulus and rating its intensity would exert different effects on the EEG responses. We did not find statistical evidence for an effect on the signal while participants were focusing on different features of the signal. We only observed a significant cluster difference in frontoparietal leads at approximately 300–500 ms post-stimulus between the magnitude of the signal in the Intensity and Intensity + Rating conditions, with a less negative response in the Intensity + Rating condition in frontal electrodes, and a less positive amplitude in parietal leads. We speculatively propose that activity in those electrodes and time window reflects magnitude estimation processes. Moreover, the smaller frontal amplitude in the Intensity + Rating condition can be explained by greater working memory engagement known to reduce the magnitude of the EEG signal. We conclude that different top-down attentional processes modulate responses to nociceptive laser stimuli at different electrodes and time windows depending on the underlying processes that are engaged.

Keywords: EEG, pain, laser evoked potentials (LEPs), top-down modulation, attention, ratings

INTRODUCTION

Attention can increase or decrease the magnitude of the cortical responses elicited by nociceptive stimuli depending on the processes that are involved (for reviews see Legrain et al., 2012; Torta et al., 2017). Top-down attention towards nociceptive stimuli can be incremented by asking participants to pay attention to specific features of a stimulus, or to provide a rating about its intensity and/or its unpleasantness. Whether these different top-down processes lead to different modulations of the cortical response to nociceptive stimuli remains an open question. In a previous study, Schlereth et al. (2003) asked participants to perform either an intensity or a location discrimination task, while recording the amplitude of the cortical potentials elicited by applying a laser heat stimulus (laser-evoked potentials, LEPs). The authors did not observe significant differences between the location and intensity tasks on the strength of the activity of the source of the LEPs estimated in the bilateral operculo insular cortices, the cingulate gyrus and the contralateral postcentral gyrus in the time window of the N2 and P2, the two main LEP components. In a more recent functional magnetic resonance imaging (fMRI) experiment, Lobanov et al. (2013) instructed participants to selectively attend to changes in either the spatial location or the intensity of two subsequent nociceptive stimuli. By contrasting the cortical activity during the two tasks, they showed that areas of the right posterior parietal cortex exhibited stronger and more sustained activity during the condition wherein participants were tracking spatial changes. Attention to both spatial and intensity features was associated with the activation of frontoparietal regions and the primary somatosensory cortex (S1), with a greater activation of the left dorsolateral prefrontal cortex (DLPFC) in the intensity discrimination task. One possible explanation for the discrepancy in the findings of the two studies is that the sources of the N2-P2 components of the LEPs mainly reflect activity unrelated to the specific processing of features of the stimuli such as their location or intensity. Also, the analysis of the time window of the N2-P2 components of the LEPs might have been too restrictive to identify any difference between conditions, as it implies that differences in the processing of the two features appear between 200–400 ms post-stimulus. Therefore, the first aim of this study was to investigate whether focusing on changes in the location vs. the intensity of the laser stimuli could modulate cortical activity in other post-stimulus intervals.

Previous studies have reported that rating the intensity of a laser or electrical somatosensory stimulus modulates electroencephalographic (EEG) brain activity (Becker et al., 2000; Kanda et al., 2002, see Schoedel et al., 2008 for similar findings obtained using fMRI). More in detail, it was observed that when participants rated the stimuli, an additional late positive component 350–600 ms post-stimulus appeared (Becker et al., 2000; Kanda et al., 2002). This component could not be observed in two control conditions wherein participants did not have to provide any ratings. However, no formal statistical comparison was carried out to confirm the effects, nor was it replicated in further studies. The second aim of the study was to address

statistically the question of whether being involved in a rating task during laser stimulation increased the magnitude of the LEPs as compared to conditions during which no rating was required.

Finally, the combined effects of providing a rating on the intensity of the stimulus while performing simultaneously a task on its location are unknown. Previous studies have shown that the amplitude of the LEPs is reduced when participants are engaged in a non-pain related working memory task (Legrain et al., 2013). This would suggest that non-pain related working memory load reduces cognitive resources that would be allocated to the elaboration of the nociceptive stimulus. What happens when the cognitive tasks are both pain-related and have to be shared between different features of the nociceptive stimuli remains elusive. It can be hypothesized that if the discrimination of the spatial features of the stimulus and the discrimination of its intensity require distinct and additional attentional resources, a signal of smaller amplitude in the conditions in which a rating of intensity is requested while performing a spatial task should be expected (i.e., Location + Ratings < Intensity + Ratings and/or Intensity and/or Location). On the other hand, providing a rating of intensity while discriminating the intensity of the stimulus may create a competing situation, as the two operations would share cognitive resources, i.e., discrimination of intensity. In this case, it would be expected that the amplitude of the LEPs is reduced when ratings are provided while participants have to discriminate intensity changes, but not when they have to provide a rating while they attend to the spatial features of the stimulus (e.g., Intensity + Ratings < Intensity and/or Location and/or Location + Ratings). Testing these two hypotheses was the third and final aim of this study.

MATERIALS AND METHODS

Participants

Twenty-four participants took part in this study (11 women, mean age 28.75 ± 4.29 , one left-handed). They were recruited among staff members and students of the Université catholique de Louvain and were naïve to the aims of the study. Participants with ongoing pain, history of chronic pain or neurological diseases were excluded. Before the beginning of the experiment, participants obtained information about the study and signed a written informed agreement to participate. The protocol received ethical approval from the local Ethics Committee in agreement with the convention of Helsinki.

Stimuli

Nociceptive stimuli were radiant heat stimuli applied to participants' right-hand dorsum using an Nd:YAP laser (wavelength 1.34 μm ; Stimul 1340 El.En. Firenze, Italy). The stimulus duration was 5 ms, and the laser beam diameter at the target site was 5 mm. Stimulation intensity (in Joules) was adjusted individually before the beginning of the experiment to elicit a clear pinprick sensation and a reaction time smaller than 650 ms compatible with the activation and the conduction velocity of A δ -fibers (Towell et al., 1996; Mouraux et al., 2003; Churyukanov et al., 2012). Two stimulation

intensities were defined individually based on the participant's perception using a numerical rating scale (NRS) ranging from 0 to 100, where 0 referred to *no perception* and 100 to *as intense as this stimulus could be*. High-intensity stimuli were set at an energy eliciting a percept rated around 60–70, medium intensity stimuli were set at an energy eliciting a percept rated around 40–50. The resulting intensities were of 4.03 ± 0.52 J for the medium intensity and an average of 4.27 ± 0.52 J for the high-intensity stimuli. During the experiment, the direct vision of the participant's hand, of the laser probe, and the experimenter was prevented by employing a wooden screen.

Procedure

Participants were seated in a dimly lit room with their right hand positioned on a table. The experiment consisted of four experimental blocks, one per condition, presented according to a counterbalanced and pre-defined order across participants. The predefined sequence prevented participants to receive more than three consecutive stimuli having the same intensity or location. Each block was composed of 20 stimuli, 10 high-intensity and 10 medium-intensity stimuli delivered in pseudorandom order. Ten stimuli were applied on the medial part on the right hand, and 10 on the lateral part, the two parts being dissociated by the third metacarpal bone. Stimuli were triggered manually by the experimenter using an inter-stimulus time interval ranging from 8 to 12 s. A small fixation point was positioned on the wooden screen.

During the *Location* (L) condition, participants were requested to selectively attend to changes in stimulus location and were asked to report at each trial if the stimulus was applied on the same vs. a different location as the preceding one. During the *Intensity* (I) condition, participants were requested to selectively attend to changes in stimulus intensity and were asked to report at each trial if the stimulus was applied with the same or a different intensity as the preceding one. Importantly, changes in intensity and location both occurred within the same block of stimulation, but participants were requested to focus only on changes in one of the two features. In this way, we were able to control for the relative contribution of a change in the characteristics of the stimulus and isolate the effects of feature-related selective attention (see also Lobanov et al., 2013). In the other two conditions, participants were requested to perform one of the two tasks and additionally provide, using the NRS, a rating of the intensity of each stimulus after having reported the change in location [block *Location* + *Rating* (LR)] or intensity [block *Intensity* + *Rating* (IR)].

Responses were reported verbally. Participants were encouraged to answer as accurately as possible, but they did not receive any specific instruction regarding speed. The accuracy of the task and the ratings were recorded.

See **Figure 1** for details of the experimental procedure.

Behavioral Measures

For each participant, accuracy was measured as the proportion of correct answers in each of the four conditions. Ratings of

perceived intensity of the stimuli were averaged separately for the LR and IR blocks.

Electroencephalogram

The electroencephalogram (EEG) was recorded at a 1 kHz sampling rate using a 64-channel amplifier and digitizer (ASA-LAB EEG system; Advanced Neuro Technologies, The Netherlands). Scalp signals were acquired with an average reference, using 64 shielded Ag-AgCl electrodes, positioned according to the 10–10 system (Waveguard; Advanced Neuro Technologies, The Netherlands). The ground electrode was positioned at FCz. Analysis of the EEG data was carried out using Letswave 6¹.

The continuous average-referenced EEG recordings were first band-pass filtered using 0.3–30 Hz Butterworth zero-phase (4th order filter) and then segmented in 2-s epochs extending from –0.5 to +1.5 s relative to stimulus onset. EOG artifacts were subtracted using independent component analysis (ICA; Jung et al., 2000). In all datasets, ICs related to eye movements had a large EOG channel contribution and a frontal scalp distribution. Baseline correction was performed by subtracting the –0.5 to 0 s pre-stimulus interval. Epochs exceeding ± 100 μ V were excluded. Artifact-free epochs were finally averaged for each condition (L, I, LR, IR) and each participant.

Statistical Analysis

The proportion of correct answers was analyzed using a two-way repeated-measure ANOVA with *Task* (Location vs. Intensity) and *Ratings* (presence vs. absence) as within-participant factors. Perceived intensity in the LR and IR conditions was compared with a *t*-test for paired measures. The significance level was set at $p \leq 0.05$. Effect sizes were measured using partial Eta squared for the ANOVA.

Cluster-Based Permutation Test

To explore whole scalp EEG brain activity concomitantly correcting for multiple comparisons, we performed a non-parametric temporal cluster-based permutation test on the entire duration of the epoch (–0.5 to 1.5 s). The cluster-based permutation test allows for resolving the issue of multiple comparisons of point-by-point analysis (Maris and Oostenveld, 2007; Maris, 2012). Two thousand permutations were used per comparison (L vs. LR, I vs. IR, L vs. I, LR vs. IR) to obtain a reference distribution of maximum cluster magnitude. Finally, the proportion of random partitions that resulted in a larger cluster-level statistic than the observed one (i.e., *p*-value) was calculated. Clusters in the observed data were regarded as significant if they had a magnitude exceeding the threshold of the 95th percentile of the permutation distribution (corresponding to a critical alpha-level of 0.05; see also van den Broeke et al., 2015, 2016). The critical alpha-level was lowered to 0.012 to account for the four comparisons. Nevertheless, the threshold for electrodes was deliberately left less stringent due to the exploratory nature of the study and the power characteristics of the permutation test as compared to other methods of false discovery rate (Lage-Castellanos et al., 2010).

¹<https://www.letswave.org/>

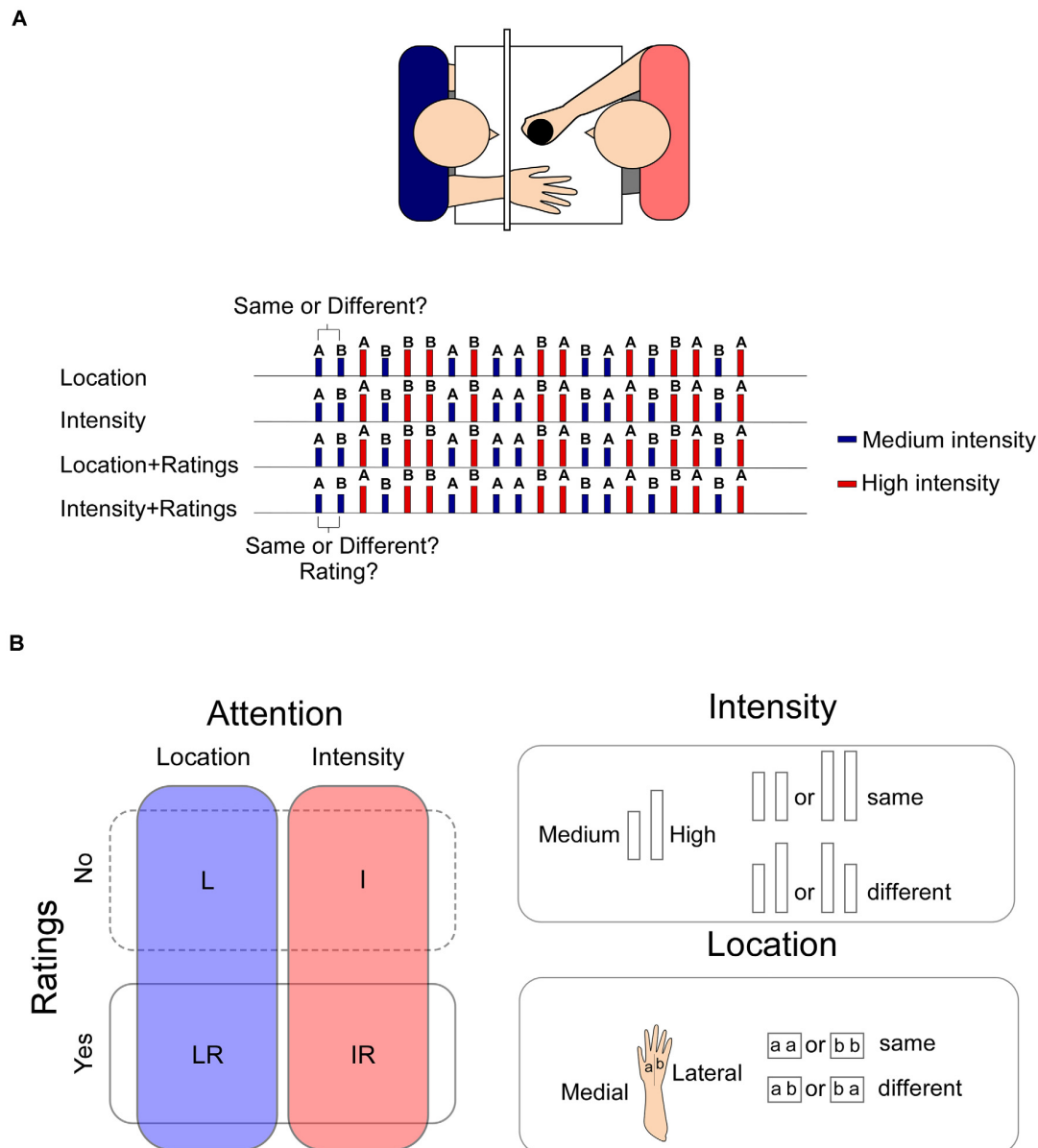


FIGURE 1 | Panel (A) upper panel: the stimuli were applied manually on the participant's right hand by one of the experimenters who was completely covered from view. The second experimenter collected the ratings and the responses. Lower panel: an example of the sequence of the stimuli. In LR and IR blocks, the response to the task was collected before the rating. Panel (B) left panel: the experiment was composed of four blocks in which participants had to focus either on changes in the location or on the intensity of the stimulus (blocks L and I). In two additional blocks, participants had also to provide a rating of the intensity of the stimulus (LR, IR). Stimuli could be of a High or a Medium intensity. Right panel: two intensities were used "High" or "Medium," which were selected at the beginning of the experiment to elicit respectively a percept of 60/70 or 40/50 out of 100. Two consecutive high intensity or low intensity stimuli were considered "same." Two consecutive stimuli of different intensities were considered "different" irrespective of the direction of the change (high-medium or medium-high). Two stimuli applied onto the same hand sector, whether medial or lateral were considered "same," whereas two consecutive stimuli applied onto the lateral or medial sector of the hand were considered "different" irrespective of the direction of the change (lateral-medial or medial-lateral).

RESULTS

Behavior

Behavioral Measures

Behavioral results are summarized in **Figure 2**. The participants' proportion of correct answers was significantly higher in the

Location conditions than in the *Intensity* ones (Main effect of *Task*: $F_{(1,23)} = 91.04$ $p < 0.001$, $\eta_p^2 = 0.80$). Moreover, the proportion of correct answers was higher when a rating was present than when it was absent (Main effect of *Rating*: $F_{(1,23)} = 5.35$ $p = 0.030$, $\eta_p^2 = 0.19$). The interaction between the two factors was not significant ($F_{(1,23)} = 1.10$ $p = 0.304$, $\eta_p^2 = 0.05$).

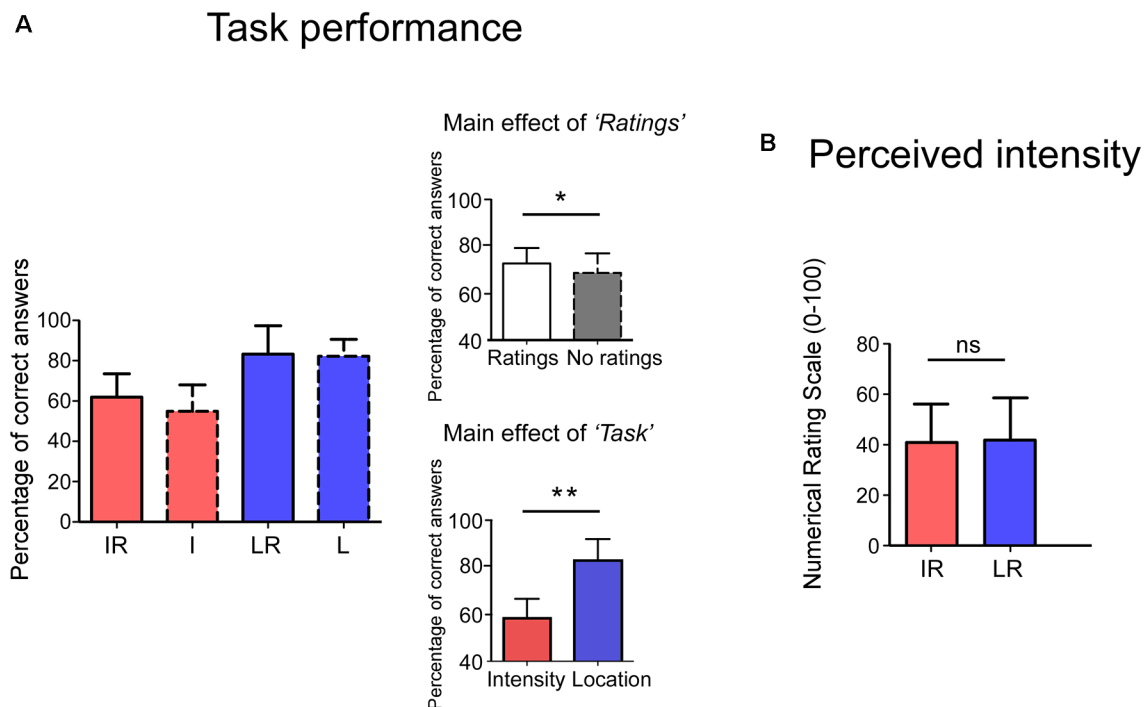


FIGURE 2 | Panel (A), the y-axis shows the percentage of correct answers. Accuracy was higher in the Rating conditions (Main effect of Rating) and in the Location Task (Main effect of Task). Interactions were not significant. Panel (B), no differences were observed in the perceived intensity for the two tasks. The y-axis represents the perceived intensity on a Numerical Rating Scale (NRS) ranging from 0 to 100. IR = Intensity + Ratings, I = Intensity LR = Location + Ratings, L = Location. * $p < 0.05$, ** $p < 0.001$, ns, not significant.

No significant difference was observed for the perceived intensity ($t_{(23)} = -0.664$ $p = 0.513$) between the IR and LR conditions.

EEG

Significant amplitude differences were observed between the I and IR conditions at a latency later than 300 ms after stimulus onset. However, only differences with a p -value smaller than 0.012 (see the statistical paragraph) were considered significant. All findings are summarized in **Table 1**, including those which resulted significant at the cluster-based permutation test, but did not survive the 0.012 cut. More specifically, the signal was more negative in frontal electrodes and more positive in parietal electrodes in the *Intensity* condition (see **Figure 3**).

We did not find any significant difference when comparing the signal of the L vs. LR, the IR vs. LR, and the L vs. I conditions.

Control Analyses

Considering that we observed a significantly better performance at the *Location* task that might have been indicative of the difficulty of the task, we investigated whether this affected the amplitude of the N2 and P2. We reasoned that a greater difficulty of the task should be associated with greater cognitive load, which in turn has been shown to reduce the amplitude of the LEP signal (Legrain et al., 2013), at least when the task was non-pain related.

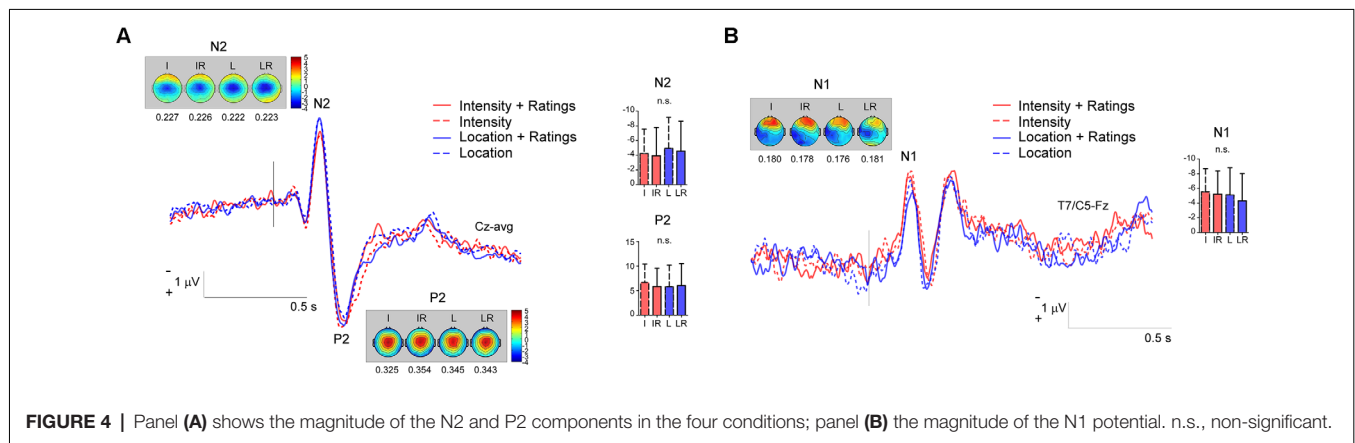
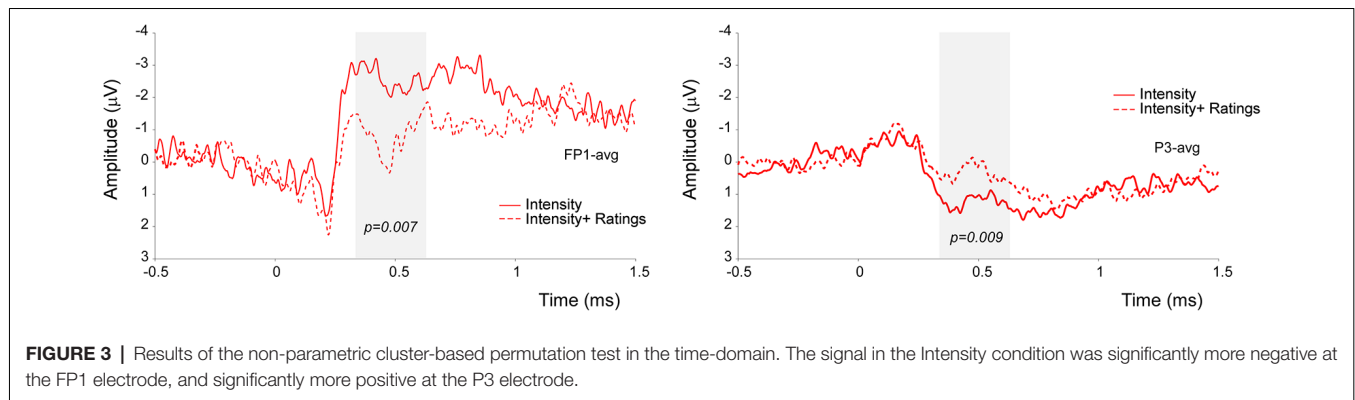
To carry out such analysis we used the same pre-processed signal that was used for the cluster based permutation test.

Individual values of the N1, N2 and P2 were extracted for each participant. The N2 was defined as the most negative deflection at Cz in the 170–250 ms interval, the P2 as the most positive deflection at Cz following the N2. The N1 was extracted by first re-referencing to Fz the averaged signal, and then extracting the average of the peaks at T7/C5 in the 120–220 ms interval. The data were then analyzed by using a two-way repeated measure ANOVA with the factors *Task* and *Rating*. The magnitude of the N1, N2 and P2 was not modulated by the tasks, indeed all p -values were >0.05 (see **Figure 4**; N2: Main effect of *Task* $F_{(1,23)} = 2.192$, $p = 0.152$ $\eta_p^2 = 0.084$, Main effect of *Rating* $F_{(1,23)} = 0.533$ $p = 0.472$ $\eta_p^2 = 0.022$, Interaction *Task* \times *Rating* $F_{(1,23)} = 0.022$ $p = 0.883$ $\eta_p^2 = 0.001$; P2: Main effect of *Task* $F_{(1,23)} = 0.535$, $p = 0.472$ $\eta_p^2 = 0.023$, Main effect of *Rating* $F_{(1,23)} = 0.394$ $p = 0.536$ $\eta_p^2 = 0.017$, Interaction *Task* \times *Rating* $F_{(1,23)} = 2.298$ $p = 0.143$ $\eta_p^2 = 0.091$; N1: Main effect of “Task” $F_{(1,23)} = 3.290$, $p = 0.083$ $\eta_p^2 = 0.125$, Main effect of “Rating” $F_{(1,23)} = 1.688$ $p = 0.207$ $\eta_p^2 = 0.068$, Interaction “Task” \times “Rating” $F_{(1,23)} = 0.170$ $p = 0.684$ $\eta_p^2 = 0.007$).

Figure 5 shows the distribution of the individual values.

DISCUSSION

This study was designed to investigate whether different top-down attentional processes led to different modulations of the cortical response to nociceptive stimuli. More specifically,



we assessed whether: (i) performing a task during which participants focused on changes either in the location or in the intensity of the laser stimuli could modulate the magnitude of the LEP responses in a time window broader than that of the N2 and P2 peaks; (ii) providing a rating of the intensity could modulate the magnitude of the brain responses; and (iii) discriminating the location or intensity of a stimulus while providing a rating of its intensity could influence the amplitude of the LEPs.

Our results provide no statistical evidence indicating that focusing on either the location or the intensity of the laser stimuli would modulate the magnitude of the induced cortical responses, not even in time intervals extending beyond that of the N2-P2 complex.

TABLE 1 | Results of the cluster-based permutation test.

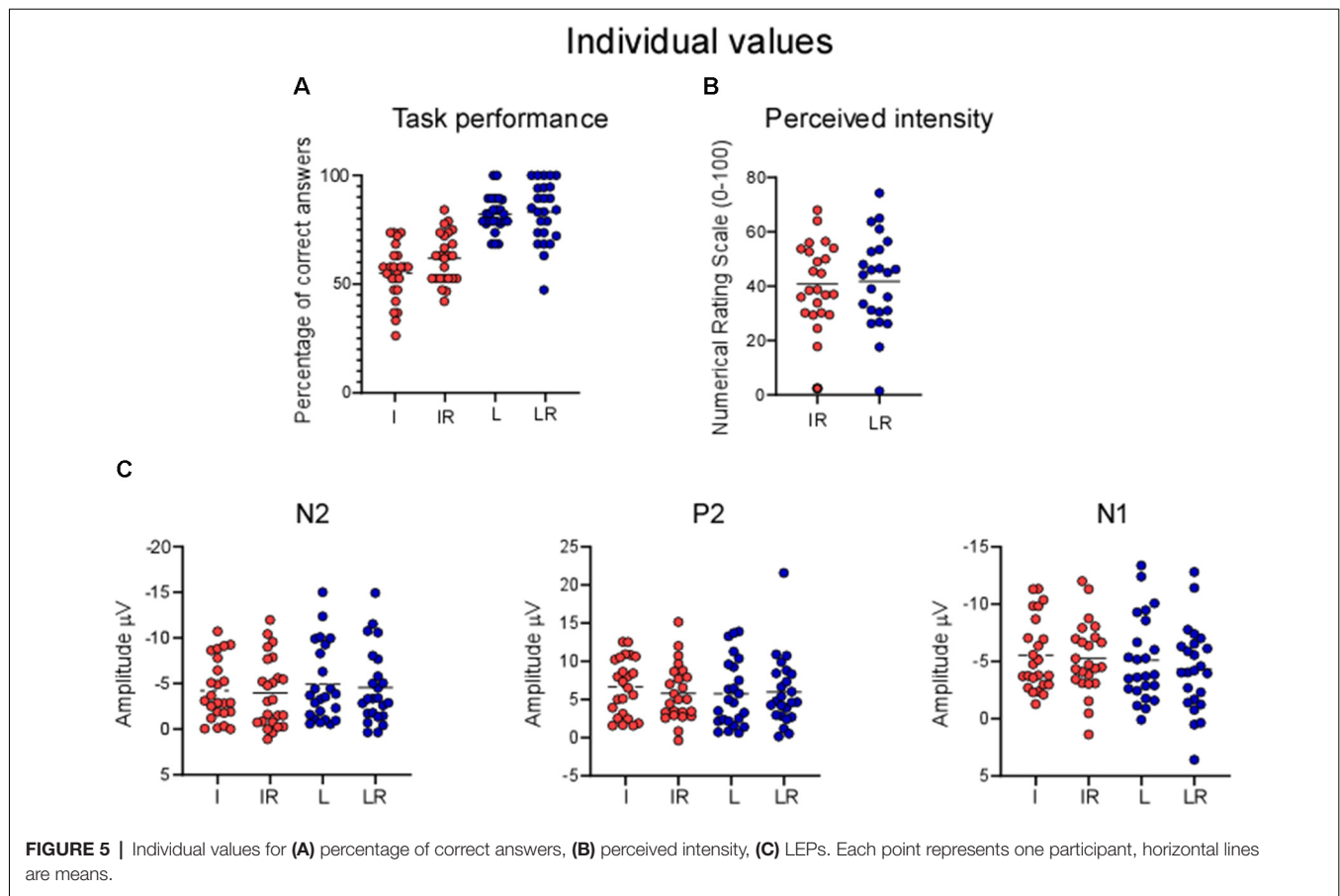
Electrode	Time window	p-value
FP1	0.34–0.54	0.007
CP5	0.80–0.90	0.039
CP1	0.40–0.54	0.028
P3	0.36–0.54	0.009
AF7	0.35–0.50	0.026
CPz	0.4–0.55	0.021
P1	0.36–0.49	0.039

Electrodes in red highlight differences still significant after setting the α cut off at 0.012. All electrodes showed differences at the $p < 0.05$ level.

Also, our findings did not disclose any statistical significance regarding the competing effect of focusing on the *location* of the stimulus while providing a rating of its intensity. However, our data indicate that a difference between the conditions in the window approximately ranging from 340 to 540 ms post-stimulus. More specifically, we observed that the signal was more negative at anterior leads (FP1) and more positive in posterior ones (P3) when no rating had to be provided.

Tracking Changes Between Location and Intensity: Behavioral and EEG Differences

Our results highlight a significantly better behavioral performance at the *Location* tasks, as compared to the *Intensity* ones. This is most likely due to the nature of the task: the two locations to be discriminated were distinguishable, being the lateral or medial side of the hand. So even if the laser beam was displaced after each stimulus, the relative distance between two consecutive stimuli applied at a *different* location (i.e., in the lateral or medial portions of the hand) was clearly above the threshold of a minimally detectable change (Frahm et al., 2018). In contrast, distinguishing the intensity of two consecutive stimuli was more challenging, due to the intrinsic variance of the perception of different laser heat stimuli. Please also note that in contrast with other studies (Schlereth et al., 2003; Mancini et al., 2016), we did not choose parameters of intensity of location that would match the participants' performance in the two



tasks, nor did we provide feedback about the quality of their performance (Mancini et al., 2016). One might argue that such a methodological difference might have reduced the possibility of observing EEG differences in the *Location* and *Intensity* blocks. Indeed, these effects could have been masked by the effects of a different cognitive load, *per se* exerting a modulation on the amplitude of the signal. While we cannot rule out this possibility, we find it is unlikely the only explanation for our findings. First, the cognitive load requested by the two tasks was not sufficiently different to affect the magnitude of the signal for the main components (see **Figures 4, 5**). Second, Schlereth et al. (2003) matched the two tasks for difficulty but observed the same findings as our present study. We, therefore, conclude that the possibility of observing differences in the modulation of cortical activity to heat stimuli due to *Intensity* or *Location* tasks strongly depends on the methodological approach that is used.

These results also challenge the possibility that the increase observed in the magnitude of the LEPs in the 100–200 ms post-stimulus, i.e., during the time windows of the negativities of the LEPs (for a review, see Legrain et al., 2002, 2012) depends on focusing on the spatial characteristics of the stimulus. Rather, we conclude that spatial attention leads to an increase in the signal only when its effects are contrasted with conditions requiring displacement of attention away from the stimulated body location (e.g., attention allocated to the other hand). *Per se*

we found no statistical evidence supporting the possibility that paying attention to spatial features of a stimulus affects the signal, neither in the N2 P2 nor in later time windows.

Effects of Rating the Stimuli

Our behavioral data also highlighted a significant, although smaller, effect of providing a rating in the accuracy of the performance. More specifically, providing a rating of intensity improved the percentage of correct answers of the discrimination tasks, irrespective of the condition (*Location* or *Intensity*). A possible interpretation is that providing the rating resulted in a greater attentional overall engagement in the task.

In line with previous reports (Becker et al., 2000; Kanda et al., 2002; van den Broeke et al., 2016, 2019), our EEG findings show that when participants were asked to provide ratings about a laser stimulus, a more positive wave appeared in parietal electrodes, at the same time window as the one observed in the present study. Therefore, we can speculate that responses occurring approximately 340–540 ms after the onset of the laser stimulus are influenced by the decisional process related to reporting the subjective perception of the stimulus. However, contrary to our present results, previous studies found an increase rather than a decrease of the amplitude in the conditions in which ratings had to be provided. We propose that this may be due to the nature of the task. Indeed, neither in Kanda et al. (2002), nor Becker et al. (2000) were participants

performing a discrimination task on the intensity characteristics of the stimulus, having to additionally provide a rating of its intensity.

Intensity vs. Intensity + Ratings

Our data also did not provide statistical evidence for significant effects of performing a spatial discrimination task while rating the intensity of the stimulus. We reasoned that focusing on the spatial location of a stimulus while providing a rating of its intensity could have an impact on the amplitude of the signal, as the two tasks might have been tapping on different cognitive resources (Lobanov et al., 2013). Alternatively that providing a rating of intensity while performing a discriminative task would result in a greater cognitive load due to competing resources. Our results support the second possibility.

Notably, the differences in the LEP magnitude were most prominent at the electrodes located on the left hemisphere (Fp1 and P3). This topographical lateralization is similar to the results obtained in fMRI by Lobanov et al., 2013 showing engagement of the left DLPFC in the discrimination of Intensity changes.

Neuroimaging and transcranial magnetic stimulation (TMS) human data and single-unit monkey recordings have consistently implicated a parietal-prefrontal network in the magnitude estimation of time, size, space, and numbers (Walsh, 2003; Lewis and Miall, 2006; Buetti and Walsh, 2009). Although a dominance of the right hemisphere has been proposed for the magnitude evaluation of numbers and space, it remains to be elucidated whether the left hemisphere becomes dominant in tasks involving motor selection (see a discussion in Buetti and Walsh, 2009). The fact that nociceptive stimuli have high behavioral relevance and can trigger motor responses to prompt defensive actions (Legrain et al., 2009; Moayed et al., 2015; Algoet et al., 2018) can explain the lateralization of the network observed in the present data.

Our findings also highlight a greater magnitude of the signal in the *Intensity* rather than the *Intensity + Rating* condition at Fp1. Previous findings have involved the same prefrontal-parietal network in working memory (Lewis and Miall, 2006) and past observations have suggested that LEPs responses are reduced when LEPs are delivered during the execution of a non-pain related working memory task (Legrain et al., 2013). Therefore we speculate that the smaller amplitude of the signal

in the *Intensity + Rating* condition may be explained by the greater working memory engagement necessary to provide the rating. We can only hypothesize why the differences between the rating and non-rating conditions did not emerge for the *Location* task. One possibility is that the greater difficulty of the *Intensity* task prompted a greater attentional engagement and therefore boosted the task effects.

To conclude, our results do not provide statistical support to the possibility that paying attention to spatial or intensity features of a stimulus affects the amplitude of EEG signals after the administration of a laser stimulus. Nevertheless, we observed that providing a rating of the intensity of a stimulus while discriminating its intensity may lead to a smaller signal. Overall, our findings also promote awareness of the importance of the control conditions in the context of top-down attentional manipulation of nociceptive stimuli.

DATA AVAILABILITY STATEMENT

The datasets generated for this study are available on request to the corresponding author.

ETHICS STATEMENT

The studies involving human participants were reviewed and approved by UC Louvain ethical commission. The participants provided their written informed consent to participate in this study.

AUTHOR CONTRIBUTIONS

DT designed research and performed data analysis. DT and MN performed data collection. All authors critically discussed the results, reviewed the article and gave their final approval.

FUNDING

DT and VL are supported by the Fund for Scientific Research of the French-speaking community of Belgium (F.R.S.-FNRS). MN was supported by a NENS grant for training stays. DT also acknowledges support from the “Asthenes” long-term structural funding—Methusalem grant (#METH/15/011) by the Flemish Government, Belgium.

REFERENCES

- Algoet, M., Duque, J., Iannetti, G. D., and Mouraux, A. (2018). Temporal profile and limb-specificity of phasic pain-evoked changes in motor excitability. *Neuroscience* 386, 240–255. doi: 10.1016/j.neuroscience.2018.06.039
- Becker, D. E., Haley, D. W., Ureña, V. M., and Yingling, C. D. (2000). Pain measurement with evoked potentials: combination of subjective ratings, randomized intensities, and long interstimulus intervals produces a P300-like confound. *Pain* 84, 37–47. doi: 10.1016/s0304-3959(99)00182-7
- Buetti, D., and Walsh, V. (2009). The parietal cortex and the representation of time, space, number and other magnitudes. *Philos. Trans. R. Soc. Lond. B Biol. Sci.* 364, 1831–1840. doi: 10.1098/rstb.2009.0028
- Churyukanov, M., Plaghki, L., Legrain, V., and Mouraux, A. (2012). Thermal detection thresholds of Aδ- and C-fibre afferents activated by brief CO₂ laser pulses applied onto the human hairy skin. *PLoS One* 7:e35817. doi: 10.1371/journal.pone.0035817
- Frahm, K. S., Mørch, C. D., and Andersen, O. K. (2018). Tempo-spatial discrimination is lower for noxious stimuli than for innocuous stimuli. *Pain* 159, 393–401. doi: 10.1097/j.pain.0000000000001095
- Jung, T. P., Makeig, S., Humphries, C., Lee, T. W., McKeown, M. J., Iragui, V., et al. (2000). Removing electroencephalographic artifacts by blind source separation. *Psychophysiology* 37, 163–178. doi: 10.1111/1469-8986.3720163
- Kanda, M., Matsushashi, M., Sawamoto, N., Oga, T., Mima, T., Nagamine, T., et al. (2002). Cortical potentials related to assessment of pain intensity with visual analogue scale (VAS). *Clin. Neurophysiol.* 113, 1013–1024. doi: 10.1016/s1388-2457(02)00125-6
- Lage-Castellanos, A., Martínez-Montes, E., Hernández-Cabrera, J. A., and Galán, L. (2010). False discovery rate and permutation test: an

- evaluation in ERP data analysis. *Stat. Med.* 29, 63–74. doi: 10.1002/sim.3784
- Legrain, V., Crombez, G., Plaghki, L., and Mouraux, A. (2013). Shielding cognition from nociception with working memory. *Cortex* 49, 1922–1934. doi: 10.1016/j.cortex.2012.08.014
- Legrain, V., Damme, S. V., Eccleston, C., Davis, K. D., Seminowicz, D. A., and Crombez, G. (2009). A neurocognitive model of attention to pain: behavioral and neuroimaging evidence. *Pain* 144, 230–232. doi: 10.1016/j.pain.2009.03.020
- Legrain, V., Guerit, J. M., Bruyer, R., and Plaghki, L. (2002). Attentional modulation of the nociceptive processing into the human brain: selective spatial attention, probability of stimulus occurrence, and target detection effects on laser evoked potentials. *Pain* 99, 21–39. doi: 10.1016/s0304-3959(02)00051-9
- Legrain, V., Mancini, F., Sambo, C. F., Torta, D. M., Ronga, I., and Valentini, E. (2012). Cognitive aspects of nociception and pain: bridging neurophysiology with cognitive psychology. *Neurophysiol. Clin.* 42, 325–336. doi: 10.1016/j.neucli.2012.06.003
- Lewis, P. A., and Miall, R. C. (2006). A right hemispheric prefrontal system for cognitive time measurement. *Behav. Processes* 71, 226–234. doi: 10.1016/j.beproc.2005.12.009
- Lobanov, O. V., Quevedo, A. S., Hadsel, M. S., Kraft, R. A., and Coghill, R. C. (2013). Frontoparietal mechanisms supporting attention to location and intensity of painful stimuli. *Pain* 154, 1758–1768. doi: 10.1016/j.pain.2013.05.030
- Mancini, F., Dolgilevica, K., Steckelmacher, J., Haggard, P., Friston, K., and Iannetti, G. D. (2016). Perceptual learning to discriminate the intensity and spatial location of nociceptive stimuli. *Sci. Rep.* 6:39104. doi: 10.1038/srep39104
- Maris, E. (2012). Statistical testing in electrophysiological studies. *Psychophysiology* 49, 549–565. doi: 10.1111/j.1469-8986.2011.01320.x
- Maris, E., and Oostenveld, R. (2007). Nonparametric statistical testing of EEG- and MEG-data. *J. Neurosci. Methods* 164, 177–190. doi: 10.1016/j.jneumeth.2007.03.024
- Moayed, M., Liang, M., Sim, A. L., Hu, L., Haggard, P., and Iannetti, G. D. (2015). Laser-evoked vertex potentials predict defensive motor actions. *Cereb. Cortex* 25, 4789–4798. doi: 10.1093/cercor/bhv149
- Mouraux, A., Guérin, J. M., and Plaghki, L. (2003). Non-phase locked electroencephalogram (EEG) responses to CO₂ laser skin stimulations may reflect central interactions between A partial- and C-fibre afferent volleys. *Clin. Neurophysiol.* 114, 710–722. doi: 10.1016/s1388-2457(03)00027-0
- Schlereth, T., Baumgartner, U., Magerl, W., Stoeter, P., and Treede, R. D. (2003). Left-hemisphere dominance in early nociceptive processing in the human parasympathetic cortex. *NeuroImage* 20, 441–454. doi: 10.1016/s1053-8119(03)00345-8
- Schoedel, A. L., Zimmermann, K., Handwerker, H. O., and Forster, C. (2008). The influence of simultaneous ratings on cortical BOLD effects during painful and non-painful stimulation. *Pain* 135, 131–141. doi: 10.1016/j.pain.2007.05.014
- Torta, D. M., Legrain, V., Mouraux, A., and Valentini, E. (2017). Attention to pain! A neurocognitive perspective on attentional modulation of pain in neuroimaging studies. *Cortex* 89, 120–134. doi: 10.1016/j.cortex.2017.01.010
- Towell, A. D., Purves, A. M., and Boyd, S. G. (1996). CO₂ laser activation of nociceptive and non-nociceptive thermal afferents from hairy and glabrous skin. *Pain* 66, 79–86. doi: 10.1016/0304-3959(96)03016-3
- van den Broeke, E. N., Hartgerink, M. D., Butler, J., Lambert, J., and Mouraux, A. (2019). Central sensitization increases the pupil dilation elicited by mechanical pinprick stimulation. *J. Neurophysiol.* 121, 1621–1632. doi: 10.1152/jn.00816.2018
- van den Broeke, E. N., Lambert, J., Huang, G., and Mouraux, A. (2016). Central sensitization of mechanical nociceptive pathways is associated with a long-lasting increase of pinprick-evoked brain potentials. *Front. Hum. Neurosci.* 10:531. doi: 10.3389/fnhum.2016.00531
- van den Broeke, E. N., Mouraux, A., Groneberg, A. H., Pfau, D. B., Treede, R. D., and Klein, T. (2015). Characterizing pinprick-evoked brain potentials before and after experimentally induced secondary hyperalgesia. *J. Neurophysiol.* 114, 2672–2681. doi: 10.1152/jn.00444.2015
- Walsh, V. (2003). A theory of magnitude: common cortical metrics of time, space and quantity. *Trends Cogn. Sci.* 7, 483–488. doi: 10.1016/j.tics.2003.09.002

Conflict of Interest: The authors declare that the research was conducted in the absence of any commercial or financial relationships that could be construed as a potential conflict of interest.

Copyright © 2020 Torta, Ninghetto, Ricci and Legrain. This is an open-access article distributed under the terms of the Creative Commons Attribution License (CC BY). The use, distribution or reproduction in other forums is permitted, provided the original author(s) and the copyright owner(s) are credited and that the original publication in this journal is cited, in accordance with accepted academic practice. No use, distribution or reproduction is permitted which does not comply with these terms.



Longitudinal Study of Functional Reinnervation of the Denervated Skin by Collateral Sprouting of Peptidergic Nociceptive Nerves Utilizing Laser Doppler Imaging

Szandra Lakatos¹, Gábor Jancsó¹, Ágnes Horváth², Ildikó Dobos¹ and Péter Sántha^{1*}

¹ Department of Physiology, University of Szeged, Szeged, Hungary, ² 1st Department of Internal Medicine, University of Szeged, Szeged, Hungary

OPEN ACCESS

Edited by:

Kate Denton,
Monash University, Australia

Reviewed by:

Alfredo Ribeiro-da-Silva,
McGill University, Canada
Arthur W. English,
Emory University School of Medicine,
United States

*Correspondence:

Péter Sántha
santha.peter@med.u-szeged.hu

Specialty section:

This article was submitted to
Integrative Physiology,
a section of the journal
Frontiers in Physiology

Received: 06 December 2019

Accepted: 08 April 2020

Published: 21 May 2020

Citation:

Lakatos S, Jancsó G, Horváth Á,
Dobos I and Sántha P (2020)
Longitudinal Study of Functional
Reinnervation of the Denervated Skin
by Collateral Sprouting of Peptidergic
Nociceptive Nerves Utilizing Laser
Doppler Imaging.
Front. Physiol. 11:439.
doi: 10.3389/fphys.2020.00439

Restitution of cutaneous sensory function is accomplished by neural regenerative processes of distinct mechanisms following peripheral nerve lesions. Although methods available for the study of functional cutaneous nerve regeneration are specific and accurate, they are unsuitable for the longitudinal follow-up of the temporal and spatial aspects of the reinnervation process. Therefore, the aim of this study was to develop a new, non-invasive approach for the longitudinal examination of cutaneous nerve regeneration utilizing the determination of changes in the sensory neurogenic vasodilatory response, a salient feature of calcitonin gene-related peptide-containing nociceptive afferent nerves, with scanning laser Doppler flowmetry. Scanning laser Doppler imaging was applied to measure the intensity and spatial extent of sensory neurogenic vasodilatation elicited by the application of mustard oil onto the dorsal skin of the rat hindpaw. Mustard oil induced reproducible and uniform increases in skin perfusion reaching maximum values at 2–4 min after application whereafter the blood flow gradually returned to control level after about 8–10 min. Transection and ligation of the saphenous nerve largely eliminated the vasodilatory response in the medial aspect of the dorsal skin of the hindpaw. In the 2nd to 4th weeks after injury, the mustard oil-induced vasodilatory reaction gradually recovered. Since regeneration of the saphenous nerve was prevented, the recovery of the vasodilatory response may be accounted for by the collateral sprouting of neighboring intact sciatic afferent nerve fibers. This was supported by the elimination of the vasodilatory response in both the saphenous and sciatic innervation territories following local treatment of the sciatic nerve with capsaicin to defunctionalize nociceptive afferent fibers. The present findings demonstrate that this novel technique utilizing scanning laser Doppler flowmetry to quantitatively measure cutaneous sensory neurogenic vasodilatation, a vascular response mediated by peptidergic nociceptive nerves, is a reliable non-invasive approach for the longitudinal study of nerve regeneration in the skin.

Keywords: sensory innervation, nociception, cutaneous vasodilatation, nerve injury, collateral sprouting, scanning laser Doppler flowmetry, TRPV1, TRPA1

Abbreviations: CGRP, calcitonin gene-related peptide; PU, perfusion unit; TRPA1, transient receptor potential ankyrin type 1 receptor; TRPV1, transient receptor potential vanilloid type 1 receptor.

INTRODUCTION

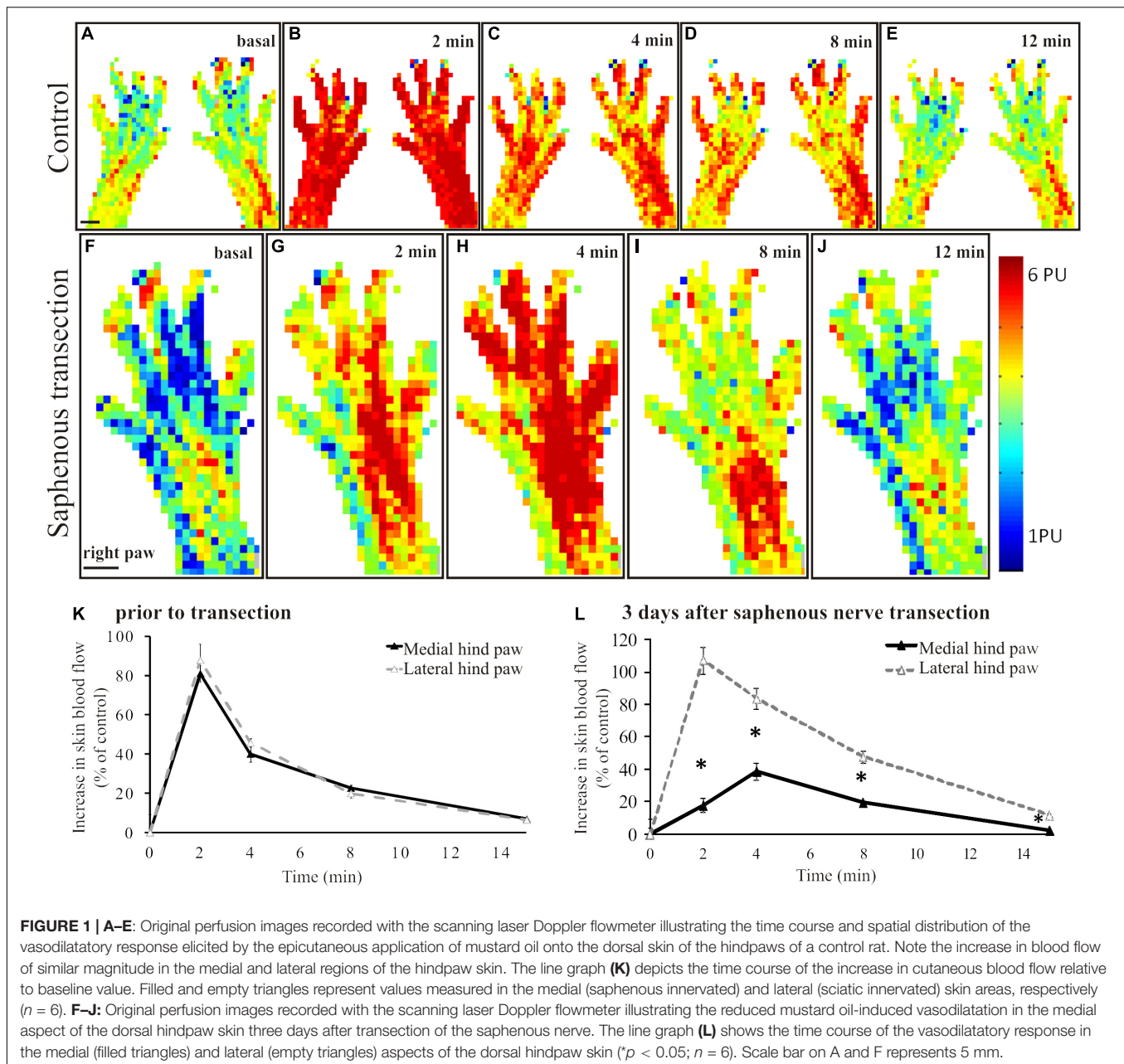
Lesions of peripheral nerves are often inflicted by common traumatic injuries or toxic agents of environmental and medicinal origins resulting in axonal degeneration and consequent loss of neural function. Restitution of cutaneous sensory functions may ensue rapidly after nerve injury. The return of sensation may be studied with various methods including measurements of changes in the thresholds to nociceptive mechanical and thermal stimuli or histological examination of skin biopsy specimens (Nolano et al., 1999; Kennedy et al., 2010; Cobianchi et al., 2014). Alternatively, reinnervation of denervated skin territories may be evaluated with the Evans blue technique by demonstrating skin areas of increased vascular permeability induced by antidromic electrical or direct chemical stimulation of nociceptive nerve endings (Jancsó and Király, 1983; Bharali and Lisney, 1988; Brennan et al., 1988; Lisney, 1989). Although these techniques are specific and accurate in determining skin areas innervated by nociceptive afferents, they have significant limitations. Techniques utilizing measurements of nociceptive thresholds and evaluation of biopsy specimens are unsuitable for the exact delineation of innervated and denervated skin regions. In contrast, the Evans blue method exactly outlines the innervated skin areas, but similarly to the biopsy technique, its use is limited in longitudinal studies.

Peptidergic chemosensitive primary sensory neurons which express the nociceptive ion channels transient receptor potential vanilloid type 1 (TRPV1) and transient receptor potential ankyrin type 1 (TRPA1) comprise a unique population of sensory neurons with dual nociceptive and secretory functions. Besides the transmission of nociceptive stimuli toward the central nervous system, chemosensitive sensory nerve endings through the release of neuropeptides such as substance P and calcitonin gene-related peptide are involved in mediation of local tissue reactions, including vascular changes (Jancsó et al., 1987; Maggi et al., 1987; Maggi and Meli, 1988; Holzer, 1998; Geppetti et al., 2008; Jancsó et al., 2009). Electrophysiological studies also disclosed that vasodilator afferent nerves are nociceptive C-fibers mostly comprised of nociceptor polymodal units in the rat (Gee et al., 1997). Ample experimental evidence indicates that sensory neurogenic plasma extravasation and sensory neurogenic vasodilatation are elicited by substance P and calcitonin gene-related peptide, respectively, released from activated chemosensitive afferent nerves (Lembeck and Holzer, 1979; Gamse et al., 1980; Brain et al., 1985; Holzer, 1998; Boros et al., 2016). Cutaneous sensory neurogenic vasodilatation can be reliably demonstrated and measured utilizing measurement of skin blood flow with laser Doppler flowmetry (Lynn et al., 1996; Gee et al., 1997).

Scanning laser Doppler flowmetry is a reliable and useful technique for the measurement of cutaneous blood flow under physiological and pathophysiological conditions including thermoregulatory vascular responses in the intact and denervated skin in both man and animals (Hu et al., 2012; Deng et al., 2016). Laser Doppler flowmetry directly measures the cutaneous blood perfusion based on the detection of frequency (“Doppler”) shift of low-power monochromatic laser light reflected from the moving

erythrocytes, but not from the stationary tissue elements in the skin (Rajan et al., 2009; Daly and Leahy, 2013; Allen and Howell, 2014). The magnitude of the intensity of shifted reflected light is proportional to the local concentration of moving erythrocytes, whereas the mean of frequency change is proportional to the average velocity of moving red blood cells (Fredriksson et al., 2009; Rajan et al., 2009). Usually an integrated value reflecting simultaneously the changes in red blood cell concentration and velocity is calculated and the tissue perfusion is expressed as an arbitrary perfusion unit (Rajan et al., 2009; Daly and Leahy, 2013). Typical laser Doppler flowmetry assesses blood flow in the microcirculation of the superficial approximately 1 mm thick layer of the skin (Fredriksson et al., 2009). Laser Doppler perfusion imaging is also based on this principle, however a point-to-point sampling on a pre-defined skin area is performed by using scanning mirrors and computerized control and processing system. The recorded perfusion map shows the local distribution of skin areas exhibiting different blood perfusion intensities. The spatial resolution of the perfusion imaging is influenced by numerous factors, but the shortest distance which could be resolved is close to the 0.1 mm range (Rajan et al., 2009; Allen and Howell, 2014). This technique is suitable not only for the measurement of changes in skin blood flow but also to determine the topographical distribution of the changes in skin perfusion. Examination of cutaneous vasodilatory responses elicited through orthodromic chemical stimulation of afferent nerve endings is a reliable technique for the demonstration of the functional innervation of the skin and the identification of innervated and denervated skin areas (Domoki et al., 2003; Illigens et al., 2013). The present experiments were initiated in an attempt to evaluate and validate scanning laser Doppler imaging as a novel non-invasive approach for the longitudinal study of the functional regeneration of cutaneous nociceptive nerves.

To support the experimental findings on degeneration and regeneration of cutaneous sensory nerves as assessed with the technique of scanning laser Doppler flowmetry, further experiments were performed using immunohistochemistry. The method of vascular labeling was utilized to identify innervated and denervated skin areas following transection of the saphenous nerve. This technique is based on the visualization of colloidal silver deposited in the basal membrane of permeable small blood vessels, mostly postcapillary venules following the epicutaneous application of mustard oil to induce neurogenic inflammation (Jancsó, 1960; Jancsó et al., 1980a). Neurogenic inflammation is a collective term for neurogenic sensory vasodilatation, mediated primarily by CGRP, and neurogenic plasma extravasation, mediated by substance P upon orthodromic or antidromic stimulation of sensory nerves (Jancsó, 1960; Jancsó et al., 1967, 2009; Lembeck and Holzer, 1979; Brain et al., 1985; Maggi and Meli, 1988; Holzer, 1998). Vascular labeling is a salient feature of increased vascular permeability (Jancsó, 1955; Majno et al., 1961). Detection of vascular labeling is a reliable measure to gather information on the functional state of sensory nerves mediating these vascular reactions, since CGRP is co-localized in almost all substance P-containing nerve fibers (Ju et al., 1987). The permeable blood vessels can be easily identified under the light microscope by the presence of colloidal silver in their walls



(Dux and Jancsó, 1994). Neurogenic inflammation and vascular labeling cannot be induced in the denervated skin (Jancsó, 1955, 1960; Jancsó et al., 1967, 1980a, 1987; Pertovaara, 1988; Sann et al., 1995; Dux et al., 1998).

MATERIALS AND METHODS

Animals

In total of eight adult male Wistar rats weighing 250–280 g at the beginning of the experiments were used in this study. The animals were maintained under a 12-h light/dark cycle with free access to food and water. The experiments were

approved by the Ethics Committee for Animal Care at the University of Szeged as per the Council Regulation of 40/2013 (II. 14.) and were carried out in full accordance with the European Communities Council Directive of 24 November 1986 (86/609/EEC). All efforts were made to minimize animal suffering. The number of experimental animals was kept as low as possible.

Surgery

For surgical interventions rats were anesthetized with a combination of ketamine (Calypsol, 70 mg/kg, i.p., Gedeon Richter, Budapest, Hungary) and xylazine (CP-Xylazin 2%, 10 mg/kg, i.p., Produlab Pharma, Raamsdonksveer, Netherlands).

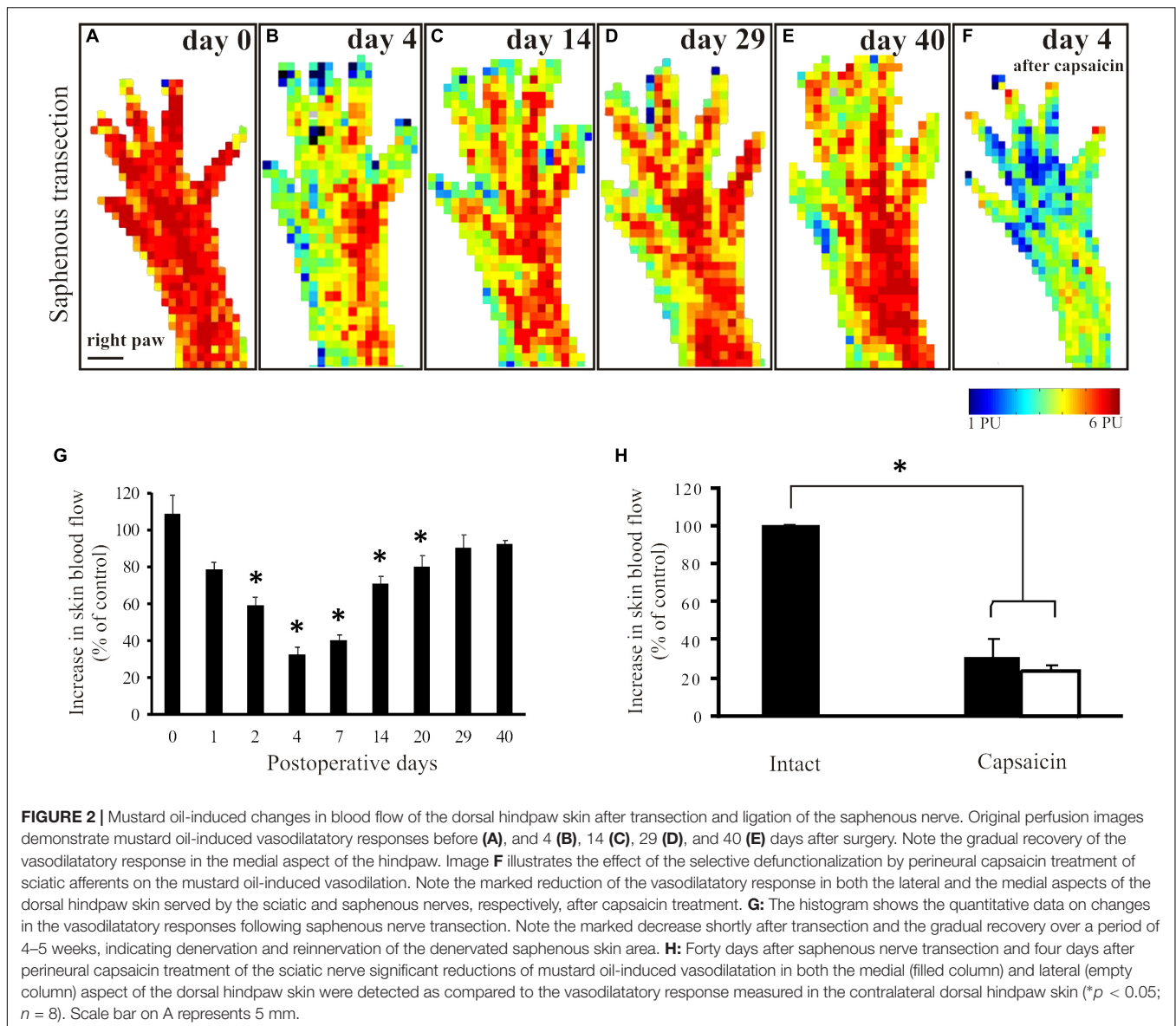


FIGURE 2 | Mustard oil-induced changes in blood flow of the dorsal hindpaw skin after transection and ligature of the saphenous nerve. Original perfusion images demonstrate mustard oil-induced vasodilatory responses before (A), and 4 (B), 14 (C), 29 (D), and 40 (E) days after surgery. Note the gradual recovery of the vasodilatory response in the medial aspect of the hindpaw. Image F illustrates the effect of the selective defunctionalization by perineural capsaicin treatment of sciatic afferents on the mustard oil-induced vasodilation. Note the marked reduction of the vasodilatory response in both the lateral and the medial aspects of the dorsal hindpaw skin served by the sciatic and saphenous nerves, respectively, after capsaicin treatment. **G:** The histogram shows the quantitative data on changes in the vasodilatory responses following saphenous nerve transection. Note the marked decrease shortly after transection and the gradual recovery over a period of 4–5 weeks, indicating denervation and reinnervation of the denervated saphenous skin area. **H:** Forty days after saphenous nerve transection and four days after perineural capsaicin treatment of the sciatic nerve significant reductions of mustard oil-induced vasodilatation in both the medial (filled column) and lateral (empty column) aspect of the dorsal hindpaw skin were detected as compared to the vasodilatory response measured in the contralateral dorsal hindpaw skin (* $p < 0.05$; $n = 8$). Scale bar on A represents 5 mm.

Peripheral Nerve Transection

The right saphenous nerve was exposed high in the thigh and transected distal to a ligature. To prevent regeneration of the nerve, a 0.5 cm long segment of the distal stump was removed. The wound was then closed and the rat was returned to the animal house.

Perineural Capsaicin Treatment

Perineural application of capsaicin was performed as described by Jancsó et al. (1980b). Briefly, the right saphenous nerve was exposed high in the thigh, isolated from the surrounding tissues with Parafilm® (Sigma-Aldrich) and wrapped with a small piece of gelfoam soaked with 0.1 ml of a 1% solution of capsaicin (Sigma, Saint Louis, United States) dissolved in saline containing 6% ethanol and 8% Tween 80. After 20 min, the gelfoam was

removed, the wound was closed, and the rat was returned to the animal house.

Measurement of Cutaneous Blood Flow With Scanning Laser Doppler Flowmetry

Scanning laser Doppler flowmetry was used to measure cutaneous blood flow in the dorsal skin of the rat hindpaw by capturing consecutive perfusion images with a PeriScan PIM3 scanning laser Doppler imager (Perimed, Järfälla, Sweden). The rats were anesthetized with a combination of ketamine and xylazine and then were placed on a heating pad to keep their body temperature at $37 \pm 0.5^\circ\text{C}$. Room temperature was kept at $22\text{--}23^\circ\text{C}$. The dorsal surface of both hindpaws was scanned by using the repeated scan mode with 52×42 pixel frame size. Distance of the scanner aperture from the skin surface was set to 19 cm and the scanner was positioned to ensure that

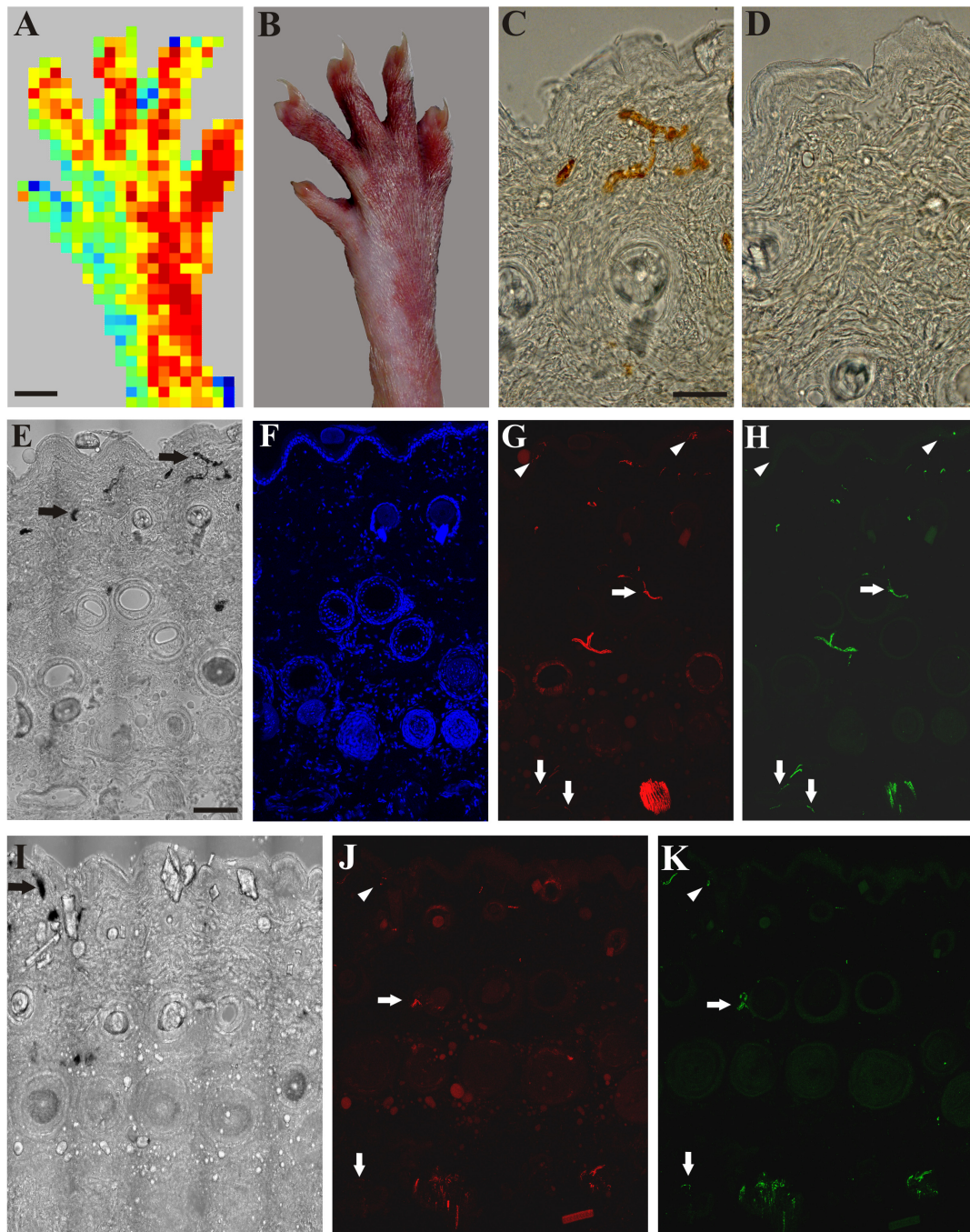


FIGURE 3 | A: Application of mustard oil increased skin blood flow in the innervated (sciatic) but not in the denervated (saphenous) skin area of the right hind paw as assessed with scanning laser Doppler imaging. **B:** Brownish coloration of the skin due to silver accumulation in the innervated (sciatic) but not in denervated (saphenous) skin area of the dorsal hind paw skin elicited by mustard oil. **C,D:** Bright field photomicrographs showing sections from the lateral intact (**C**) and medial denervated regions of the hind paw skin after transection of the saphenous nerve (**D**). Silver-labeled small venules indicate increased vascular permeability of small postcapillary venules elicited by mustard oil application in the intact dorsal hind paw skin (**C**). Silver-labeled blood vessels cannot be observed in the denervated skin 4 days after saphenous nerve transection (**D**). **E–H:** Bright field (**E**) and immunofluorescence (**F–H**) photomicrographs showing the lateral (sciatic) skin area of the dorsal hind paw skin (**E–H**) after transection of the saphenous nerve. **I–K:** Bright field (**I**) and immunofluorescence (**J,K**) photomicrographs showing the medial (saphenous) skin area of the dorsal hind paw skin of a rat 15 days after transection and ligation of the saphenous nerve. Note the localization of β -tubulin III (red) and CGRP-immunoreactive (green) nerve fibers in the epidermis (arrowheads), and around hair follicles and small arteries (arrows) in the innervated (lateral, sciatic) area of the dorsal hind paw skin identified by the presence of silver-labeled (permeable) venules (arrows in **E**). Fifteen days after transection and ligation of the saphenous nerve, some silver-labeled venules (arrow in **I**) and some β -tubulin III and CGRP-immunoreactive epidermal (arrowheads in **J,K**) and dermal (arrows in **J,K**) nerve fibers can be observed in the medial (saphenous) skin area of the dorsal hind paw skin indicative of (collateral) regeneration. Scale bars indicate 5 mm in **A** and **B** and 50 μ m in **C,E**. Scale bars in **C,E** apply for **C,D** and **E–K**, respectively.

the laser beam was perpendicular to the skin surface. Perfusion images were captured in every 2 min and measurements took 15–20 min in each animal. All flow values were expressed as means \pm S.E.M. Basal tissue perfusion and changes in blood flow induced by mustard oil (5% in liquid paraffin) were recorded in arbitrary perfusion units (PU) and expressed as per cent change relative to baseline. The value of the PU integrates the linear velocity values and the concentration of moving erythrocytes in the skin volume fraction detected by the scanner at any instances (Rajan et al., 2009). Mustard oil was applied onto the intact unshaved hairy skin of the paw. Baseline values were obtained by calculating the average of three subsequent measurements before the application of mustard oil. For quantitative evaluation, images displaying the maximum vasodilatory responses were used in each experiment.

Scanning laser Doppler images were taken before surgery and 1–40 days after saphenous nerve transection. After finishing the sequential measurement of the recovery of sensory vasodilatation (4th week post surgery) an additional measurement was made 4 days after perineural treatment of the sciatic nerve with capsaicin.

The innervation territory of the saphenous nerve was defined on the basis of perfusion images taken 4 days after transection the saphenous nerve. In each experiment the color-coded perfusion images showing the maximal vasodilatory response were selected for further processing with the ImagePro 6.2 image analysis software (MediaCybernetics, Rockville, MD, United States). After subtracting background pixel values, color segmentation was applied on the perfusion image to demarcate and separate areas showing no or minimal vasodilation from those exhibiting large (or maximal) perfusion increases. This step was followed by the generation of a binary mask representing the size and topography of denervated cutaneous areas corresponding to the innervation area of the saphenous nerve. Functional reinnervation was characterized by measuring the intensity of the vasodilatory response in the saphenous skin area as defined above.

Demonstration of Cutaneous Nerve Fibers and Permeable Blood Vessels After Induction of Neurogenic Inflammation With Mustard Oil

Rats were anesthetized with ketamine (100 mg/kg) and xylazine (10 mg/kg) and the dorsal skin of the hind paw was painted with mustard oil (allyl isothiocyanate, 5% in liquid paraffin) after an intravenous injection of a colloidal silver solution (1% in 5% glucose, 100 mg/kg). Twenty min later the animals were terminally anesthetized and perfused transcardially with a fixative containing 4% paraformaldehyde in 0.1 M phosphate buffer. The dorsal hind paw skin was removed and postfixed for another 2 h. After washing in phosphate buffer containing 30% sucrose overnight, frozen sections were cut and free-floating sections were processed for immunohistochemical staining with antibodies against tubulin and CGRP. Monoclonal mouse anti- β -tubulin III and polyclonal rabbit anti-CGRP antibodies were obtained from Sigma-Aldrich (St. Louis, Missouri, United States)

and used at a dilution of 1:4500. Sections were mounted on slides and covered with ProLong[®] Gold antifade medium (Invitrogen, Carlsbad, Calif., United States). Specimens were examined under a Zeiss LSM 700 confocal laser scanning microscope. Tile scan and z-stack maximum intensity projection images were obtained to illustrate the findings.

Statistics

Data represent means \pm S.E.M. of 5–9 independent measurements. For statistical comparisons of the mustard oil-induced vasodilatory responses one-way ANOVA was performed followed by multiple comparisons using the Dunnett's *post hoc* analysis. In all groups, normality was proved by the Shapiro-Wilk test and homogeneity of variances was confirmed by Levene's test in advance of performing ANOVA. Statistical analysis was performed by using Statistica 6.4 software (Dell Inc., Tulsa, OK, United States).

RESULTS

Scanning Laser Doppler Imaging of Cutaneous Blood Flow of the Dorsal Skin of the Rat Hindpaw: The Effect of Sensory Denervation

Scanning laser Doppler imaging revealed a largely uniform perfusion in the intact rat hindpaw skin (**Figure 1A**). The coefficients of variance of the basal perfusion values recorded on subsequent perfusion images representing the basal blood perfusion of the hind paw were 0.043 ± 0.28 (medial aspect) and 0.054 ± 0.027 (lateral aspect) with no significant difference between the two sides ($p = 0.19$). Application of mustard oil onto the skin elicited a marked increase in cutaneous blood flow with a maximum at 2–4 min (**Figures 1B,K**). The maximum increase in blood flow amounted to $87 \pm 18\%$ of the initial basal value and returned to the pre-application level after about 15–20 min (**Figures 1C–E,K**). This vasodilatory response could be repeatedly elicited by mustard oil resulting in similar perfusion patterns (data not shown). Basal blood flow measured in the denervated (saphenous) skin area was similar to that of the intact lateral (sciatic) area of the dorsal skin of the hindpaw (**Figure 1F**). However the mustard oil-induced vasodilatory response was strongly reduced in the medial aspect of the dorsal hindpaw skin 3 days after saphenous nerve denervation (**Figures 1G,H** decline of the response is shown on **Figures 1I,J**). As illustrated in **Figure 1L**, the magnitude of the vasodilatory response was reduced significantly in the medial aspect of the dorsal hindpaw skin served by the saphenous nerve, as compared with the lateral side innervated by the intact sciatic nerve.

Effect of Saphenous Nerve Transection on Mustard Oil-Induced Vasodilation in the Dorsal Hindpaw Skin

In animals to be subjected to transection and ligation of the saphenous nerve, mustard oil-induced vasodilatory responses

were measured shortly before surgery to obtain reference perfusion images (**Figure 2A**). Basal blood flow values did not differ significantly in the denervated and innervated areas of the dorsal hindpaw skin (**Figure 1F**). Four days but not one day after saphenous nerve transection mustard oil-induced increase in cutaneous blood flow was markedly reduced in the medial part of the dorsal hindpaw skin served by the saphenous nerve. Perfusion values in the skin area normally served by the saphenous nerve amounted to about $32 \pm 4\%$ of the values measured in the lateral hindpaw skin innervated by the intact sciatic nerve (**Figures 2B,G**). The vasodilatory response gradually recovered within the medial skin area of the dorsal hindpaw. The re-appearance of mustard oil-induced vasodilation first commenced in the lateral aspect of the saphenous innervation territory immediately adjacent to the skin area innervated by the intact sciatic nerve (**Figures 2C,D**). The area displaying mustard oil-induced vasodilation gradually spread toward the medial aspect of the dorsal hindpaw skin and finally, after about 4 weeks the topography of the vasodilatory response was similar to that seen before surgery (**Figure 2E**). To identify the origin of nerve fibers which reinnervated the medial part of the dorsal hindpaw skin served normally by the saphenous nerve, a second surgery was performed. The sciatic nerve was treated locally with capsaicin to defunctionalize chemosensitive afferent nerves (Jancsó et al., 1980b; Gamse et al., 1980) which mediate the sensory neurogenic vasodilatory response (Lembeck and Holzer, 1979; Lynn et al., 1996; Domoki et al., 2003). Examination of the mustard oil-induced vasodilatory response 3–4 days after perineural capsaicin revealed a marked reduction of the vasodilatory response not only in the lateral skin area, innervated by the sciatic nerve, but also in the medial skin area normally served by the saphenous nerve (**Figures 2F,H**). This finding strongly indicates that recovery of the vasodilatory response in the medial part of the dorsal hindpaw skin, normally served by the saphenous nerve, may be attributed to sciatic afferents which innervate the denervated saphenous skin area through collateral sprouting.

Immunohistochemical Demonstration of Degeneration and Regeneration of Cutaneous Nerves After Peripheral Nerve Lesions

Application of mustard oil resulted in clear-cut vascular labeling in subepidermal small blood vessels of skin areas of intact sensory innervation (perfusion image: **Figure 3A**). Silver deposits were observed in the wall of permeable small blood vessels (**Figures 3B,C**). In contrast, in the denervated skin vascular labeling could not be observed (**Figures 3B,D**). Immunohistochemistry revealed many tubulin- and/or CGRP-immunoreactive nerve fibers in the epidermis, around hair follicles and small blood vessels of the innervated skin (**Figures 3E–H**). Four days after nerve transection, nerve fibers were absent in the denervated saphenous skin areas, but the innervation of the skin area served by the intact sciatic nerve was similar to control (data are not shown). Fourteen days after saphenous nerve transection, a few silver-labeled blood vessels

could be detected in the previously denervated skin area parallel with the re-appearance of a few epidermal and subepidermal tubulin- and CGRP-immunoreactive nerve fibers indicating regeneration of the denervated skin area (**Figures 3I–K**). These nerves were completely depleted after perineural treatment of the sciatic nerve with capsaicin. Hence, these immunohistochemical findings extend and support our observations on the regeneration of the denervated skin as assessed with the aid of scanning laser Doppler flowmetry.

DISCUSSION

Longitudinal evaluation of restitution of cutaneous sensory function is essential to unravel the progress and mechanisms of nerve regeneration following peripheral nerve lesions of various origins. The findings of the present study demonstrate that repeated scanning laser Doppler imaging of cutaneous blood flow is a reliable method for the longitudinal examination of the progress of regeneration of a particular population of peptidergic nociceptive cutaneous nerves. Stimulation of cutaneous nociceptive nerve endings with mustard oil results in a marked increase of local blood flow in intact but not denervated skin areas. Previous studies have shown that mustard oil is a potent activator of the TRPA1 nociceptive ion channel (Jordt et al., 2004; Bautista et al., 2006). Although mustard oil was regarded as a selective agonist of the TRPA1 receptor, recent findings challenged this view by showing activation also of the TRPV1 receptor by this compound suggesting that besides the TRPA1 receptor, the TRPV1 receptor is also involved in the transmission of nociceptive impulses elicited by mustard oil (Everaerts et al., 2011; Gees et al., 2013). However, these studies also disclosed that mustard oil-induced inflammation is mainly mediated by the TRPA1 receptor (Everaerts et al., 2011; Gees et al., 2013). This is in accord with our previous observations showing that the vasodilatory effect of this agent is largely mediated by the activation of the TRPA1 receptor in the rat hindpaw skin (Boros et al., 2016). The vasodilation elicited by activation of the TRPA1 receptor by mustard oil is mediated by the potent vasodilatory peptide CGRP contained and released from the stimulated nociceptive nerve endings (Brain et al., 1985; Sauerstein et al., 2000; Pozsgai et al., 2010). This notion is also supported by the close spatial correlation of the distribution of CGRP-containing chemosensitive afferent nerves and vascular changes associated with neurogenic inflammation in the rat skin (Sann et al., 1995).

Denervated skin areas displayed markedly attenuated vasodilatory responses upon exposure to mustard oil. The slight mustard oil-induced increase in blood flow measured in the denervated skin areas may be attributed to possible non-neural mechanism(s) or, alternatively, to activation of TRPV1 receptors (Grant et al., 2005; Everaerts et al., 2011; Gees et al., 2013).

Mustard oil-induced vasodilation was markedly reduced in the denervated skin 3–4 days after nerve transection and was abolished completely by the 4th post-operative

day. The vasodilatory response was similar to controls 1 day after nerve transection, since at this post-lesion time cutaneous nerve endings are still functional until the onset of the rapid phase of Wallerian degeneration 1–3 days after injury (Jancsó and Király, 1983; Sta et al., 2014). Repeated measurements of mustard oil-induced vasodilatory responses revealed a gradual, time-dependent re-appearance of the vasodilatory response in the denervated skin. Following saphenous nerve transection, the size of the skin area displaying negligible vasodilatory responses after denervation gradually decreased. By the 3rd–4th post-operative week, the vasodilatory response was similar to the control in both size and intensity. To furnish independent data on the reliability of scanning laser Doppler flowmetry to examine cutaneous nerve function, immunohistochemical demonstration of tubulin- and CGRP-positive nerves were performed in intact, denervated and reinnervated skin after induction of neurogenic inflammation with mustard oil. In accord with previous findings, small blood vessels, mainly postcapillary venules were labeled with colloidal silver. No such labeled venules were seen in the denervated skin. Re-appearance of tubulin- and CGRP-immunoreactive nerve fibers in the previously denervated saphenous skin area supported our findings obtained with scanning laser Doppler flowmetry. The nerve fibers in the saphenous skin area were completely depleted after perineural treatment of the sciatic nerve with capsaicin, a treatment which induces a complete elimination of nociceptive afferent nerves (Jancsó et al., 1980b; Dux et al., 1998; Domoki et al., 2003; Kang et al., 2010). Hence, immunohistochemical findings supported our observations obtained with scanning laser Doppler flowmetry. This time-course of functional recovery observed in the previously denervated saphenous innervation area is similar to that observed in studies using behavioral testing or the Evans blue technique to examine the temporal characteristics of functional cutaneous nerve regeneration (Devor et al., 1979; Bharali and Lisney, 1988).

Previous studies have demonstrated that reinnervation of denervated skin areas may be effected by two different mechanisms: regeneration of the injured nerve and reinnervation by collateral sprouting (Devor et al., 1979; Brennan, 1986; Diamond et al., 1987; Kinnman et al., 1992). The re-innervation of the denervated skin following nerve crush occurs through regenerative sprouting of the injured nerve. The restitution of function is almost complete after nerve crush (Devor et al., 1979; Wiesenfeld-Hallin et al., 1988). If regeneration of the injured nerve is prevented by ligation of the transected nerve, as in the present study, restitution of sensory function in the denervated skin is accomplished through collateral sprouting of axons of an intact peripheral nerve serving skin areas adjacent to the denervated skin (Devor et al., 1979; Diamond et al., 1987; Pertovaara, 1988). Under the experimental conditions of the present study, intact sciatic nerve axons were expected to invade, by collateral sprouting, the denervated saphenous skin area. Our findings indicate that, indeed, this is the case. In the denervated saphenous nerve territory, the mustard oil-induced vasodilatory response gradually recovered within a period of 1–4 weeks after transection and ligation of

the saphenous nerve and, importantly, this could be largely abolished by perineural treatment of the sciatic nerve with capsaicin. Perineural capsaicin treatment was used to selectively defunctionalize sciatic nociceptive afferents (Jancsó et al., 1980a; Jancsó et al., 2008; Jancsó and Király, 1983; Petsche et al., 1983; Pini and Lynn, 1991; Domoki et al., 2003) sparing efferent autonomic and motor nerve fibers (Jancsó et al., 1987). Thus, inhibition by perineural capsaicin treatment of the mustard oil induced vasodilation not only in the lateral, but also in the medial aspect of the dorsal skin of the hindpaw, strongly indicates that reinnervation of the denervated saphenous skin area was accomplished by collateral sprouting of adjacent intact sciatic afferent fibers. This observation is in accord with previous findings which applied the Evans blue technique and behavioral testing to demonstrate the reinnervation of the denervated skin by collateral sprouting of nociceptive afferent nerves of neighboring skin areas (Devor et al., 1979; Diamond et al., 1987; Pertovaara, 1988).

In conclusion, the present observations indicate that repeated scanning laser Doppler imaging of the mustard oil-induced vasodilatory response is a reliable technique for the longitudinal study of cutaneous nerve regeneration being suitable for the follow-up of changes of both the topographical distribution and the intensity of the vasodilatory response, most probably proportional with cutaneous innervation density. An obvious limitation of this technique is that it does not provide information on the regeneration of other types of cutaneous sensory nerves, for example myelinated mechanoreceptors. Noteworthy, it has been shown that low threshold myelinated afferents lack the ability to collaterally grow into a denervated skin area (Jackson and Diamond, 1984). In addition, however, previous findings suggested that regeneration of different types of cutaneous nerves does not occur simultaneously; unmyelinated fibers regenerate more rapidly as compared to myelinated axons (Allt, 1976; Duraku et al., 2013). Human and rodent nociceptive cutaneous nerves share many functional and neurochemical traits, including the sensitivity to chemical irritants such as mustard oil and capsaicin (Jancsó, 1960; Jancsó et al., 1985; Hou et al., 2002). In the human skin mustard oil produces local and axon reflex vasodilation in the intact but not in the denervated skin (Jancsó and Janka, 1981; Jancsó et al., 1983, 1985). Demonstration of mustard oil-induced sensory neurogenic vasodilation has been used to detect the functional condition of cutaneous sensory nerves in man under physiological and pathological conditions (Jancsó and Janka, 1981; Jancsó et al., 1983; Westerman et al., 1987). Hence, with some modifications, the approach presented in this report may be applied also in human studies aimed at the examination of cutaneous nerve function affected by toxic environmental and medicinal agents, such as anticancer chemotherapeutics or by pathologies such as diabetes mellitus.

DATA AVAILABILITY STATEMENT

The data that support the findings of this study are available on request from the corresponding author, PS.

ETHICS STATEMENT

The animal study was reviewed and approved by the Ethics Committee for Animal Care at the University of Szeged as per the Council Regulation of 40/2013 (II. 14.) and were carried out in full accordance with the European Communities Council Directive of 24 November 1986 (86/609/EEC).

AUTHOR CONTRIBUTIONS

GJ, PS, and SL were responsible for the study concept and design. SL, AH, ID, GJ and PS were responsible for the data collection and analysis. SL, AH, GJ, and PS interpreted the data,

and revised the manuscript for intellectual content. All authors were involved in manuscript editing and have approved the final version for submission.

FUNDING

This work was supported by the Hungarian National Research Development and Innovation Office GINOP-2.3.2-15-2016-00034 project of the HNRDIO. PS was supported by the Szent-Györgyi Albert research grant of the Faculty of Medicine, University of Szeged. Open access publication was supported by University of Szeged Open Access Fund, grant No.: 4493.

REFERENCES

- Allen, J., and Howell, K. (2014). Microvascular imaging: techniques and opportunities for clinical physiological measurements. *Physiol. Measur.* 35, R91–R141. doi: 10.1088/0967-3334/35/7/R91
- Allt, G. (1976). "Pathology of the peripheral nerve," in *The Peripheral Nerve*, ed. D. N. Landon (London: Chapman and Hall), 666–739.
- Bautista, D. M., Jordt, S. E., Nikai, T., Tsuruda, P. R., Read, A. J., Poblete, J., et al. (2006). TRPA1 mediates the inflammatory actions of environmental irritants and proalgesic agents. *Cell* 124, 1269–1282. doi: 10.1016/j.cell.2006.02.023
- Bharali, L. A. M., and Lisney, S. J. W. (1988). Reinnervation of skin by polymodal nociceptors in rats. *Prog. Brain Res.* 74, 247–251. doi: 10.1016/S0079-6123(08)63020-63024
- Boros, K., Jancsó, G., Dux, M., Fekecs, Z., Bencsik, P., Oszlacs, O., et al. (2016). Multiple impairments of cutaneous nociceptor function induced by cardiotoxic doses of Adriamycin in the rat. *Naunyn. Schmiedeberg's Arch. Pharmacol.* 389, 1009–1020. doi: 10.1007/s00210-016-1267-x
- Brain, S. D., Williams, T. J., Tippins, J. R., Morris, H. R., and MacIntyre, I. (1985). Calcitonin gene-related peptide is a potent vasodilator. *Nature* 313, 54–56. doi: 10.1038/313054a0
- Brenan, A. (1986). Collateral reinnervation of skin by C-fibres following nerve injury in the rat. *Brain Res.* 385, 152–155. doi: 10.1016/0006-8993(86)91557-X
- Brenan, A., Jones, L., and Owain, N. R. (1988). The demonstration of the cutaneous distribution of saphenous nerve C-fibres using a plasma extravasation technique in the normal rat and following nerve injury. *J. Anat.* 157, 57–66.
- Cobianchi, S., de Cruz, J., and Navarro, X. (2014). Assessment of sensory thresholds and nociceptive fiber growth after sciatic nerve injury reveals the differential contribution of collateral reinnervation and nerve regeneration to neuropathic pain. *Exp. Neurol.* 255, 1–11. doi: 10.1016/j.expneurol.2014.02.008
- Daly, S. M., and Leahy, M. J. (2013). Go with the flow: a review of methods and advancements in blood flow imaging. *J. Biophotonics* 6, 217–255. doi: 10.1002/jbio.201200071
- Deng, A., Liu, D., Gu, C., Gu, X., Gu, J., and Hu, W. (2016). Active skin perfusion and thermoregulatory response in the hand following nerve injury and repair in human upper extremities. *Brain Res.* 1630, 38–49. doi: 10.1016/j.brainres.2015.10.045
- Devor, M., Schonfeld, D., Seltzer, Z., and Wall, P. D. (1979). Two modes of cutaneous reinnervation following peripheral nerve injury. *J. Comp. Neurol.* 185, 211–220. doi: 10.1002/cne.901850113
- Diamond, J., Coughlin, M., Macintyre, L., Holmes, M., and Visheau, B. (1987). Evidence that endogenous beta nerve growth factor is responsible for the collateral sprouting, but not the regeneration, of nociceptive axons in adult rats. *Proc. Natl. Acad. Sci. U.S.A.* 84, 6596–6600. doi: 10.1073/pnas.84.18.6596
- Domoki, F., Sántha, P., Bari, F., and Jancsó, G. (2003). Perineural capsaicin treatment attenuates reactive hyperaemia in the rat skin. *Neurosci. Lett.* 341, 127–130. doi: 10.1016/S0304-3940(03)00191-195
- Duraku, L. S., Hossaini, M., Schüttenhelm, B. N., Holstege, J. C., Baas, M., Ruigrok, T. J. H., et al. (2013). Re-innervation patterns by peptidergic Substance-P, non-peptidergic P2X3, and myelinated NF-200 nerve fibers in epidermis and dermis of rats with neuropathic pain. *Exp. Neurol.* 241, 13–24. doi: 10.1016/j.expneurol.2012.11.029
- Dux, M., and Jancsó, G. (1994). A new technique for the direct demonstration of overlapping cutaneous innervation territories of peptidergic C-fibre afferents of rat hindlimb nerves. *J. Neurosci. Methods* 55, 47–52. doi: 10.1016/0165-0270(94)90039-90036
- Dux, M., Sann, H., and Jancsó, G. (1998). Changes in fibre populations of the rat hairy skin after selective chemodenervation by capsaicin. *Eur. J. Neurosci.* 10:299.
- Everaerts, W., Gees, M., Alpizar, Y. A., Farre, R., Leten, C., Apetrei, A., et al. (2011). The capsaicin receptor TRPV1 is a crucial mediator of the noxious effects of mustard oil. *Curr. Biol.* 21, 316–321. doi: 10.1016/j.cub.2011.01.031
- Fredriksson, I., Larsson, M., and Strömberg, T. (2009). Measurement depth and volume in laser Doppler flowmetry. *Microvasc. Res.* 78, 4–13. doi: 10.1016/j.mvr.2009.02.008
- Gamse, R., Holzer, P., and Lembeck, F. (1980). Decrease of substance p in primary afferent neurones and impairment of neurogenic plasma extravasation by capsaicin. *Br. J. Pharmacol.* 68, 207–213. doi: 10.1111/j.1476-5381.1980.tb10409.x
- Gee, M. D., Lynn, B., and Cotsell, B. (1997). The relationship between cutaneous C fibre type and antidromic vasodilatation in the rabbit and the rat. *J. Physiol.* 503, 31–44. doi: 10.1111/j.1469-7793.1997.031bi.x
- Gees, M., Alpizar, Y. A., Boonen, B., Sanchez, A., Everaerts, W., Segal, A., et al. (2013). Mechanisms of transient receptor potential vanilloid 1 activation and sensitization by allyl isothiocyanate. *Mol. Pharmacol.* 84, 325–334. doi: 10.1124/mol.113.085548
- Geppetti, P., Nassini, R., Materazzi, S., and Benemei, S. (2008). The concept of neurogenic inflammation. *BJU Int. Suppl.* 101, 2–6. doi: 10.1111/j.1464-410X.2008.07493.x
- Grant, A. D., Pintér, E., Salmon, A. M. L., and Brain, S. D. (2005). An examination of neurogenic mechanisms involved in mustard oil-induced inflammation in the mouse. *Eur. J. Pharmacol.* 507, 273–280. doi: 10.1016/j.ejphar.2004.11.026
- Holzer, P. (1998). Neurogenic vasodilatation and plasma leakage in the skin. *Gen. Pharmacol.* 30, 5–11. doi: 10.1016/S0306-3623(97)00078-75
- Hou, M., Uddman, R., Tajti, J., Kanje, M., and Edvinsson, L. (2002). Capsaicin receptor immunoreactivity in the human trigeminal ganglion. *Neurosci. Lett.* 330, 223–226. doi: 10.1016/S0304-3940(02)00741-743
- Hu, W., Yang, M., Chang, J., Shen, Z., Gu, T., Deng, A., et al. (2012). Laser doppler perfusion imaging of skin territory to reflect autonomic functional recovery following sciatic nerve autografting repair in rats. *Microsurgery* 32, 136–143. doi: 10.1002/micr.20974
- Illigens, B. M. W., Siepmann, T., Roofeh, J., and Gibbons, C. H. (2013). Laser Doppler imaging in the detection of peripheral neuropathy. *Auton. Neurosci. Basic Clin.* 177, 286–290. doi: 10.1016/j.autneu.2013.06.006

- Jackson, P. C., and Diamond, J. (1984). Temporal and spatial constraints on the collateral sprouting of low-threshold mechanosensory nerves in the skin of rats. *J. Comp. Neurol.* 226, 336–345. doi: 10.1002/cne.902260304
- Jancsó, G., Dux, M., Oszlács, O., and Sántha, P. (2008). Activation of the transient receptor potential vanilloid-1 (TRPV1) channel opens the gate for pain relief. *Br. J. Pharmacol.* 155, 1139–1141. doi: 10.1038/bjp.2008.375
- Jancsó, G., Husz, S., and Simon, N. (1983). Impairment of axon reflex vasodilatation after herpes zoster. *Clin. Exp. Dermatol.* 8, 27–31. doi: 10.1111/j.1365-2230.1983.tb01740.x
- Jancsó, G., and Janka, Z. (1981). A simple test for topographical diagnosis of sensory nervous system lesions. *Eur. Neurol.* 20, 84–87. doi: 10.1159/000115212
- Jancsó, G., Katona, M., Horváth, V. J., Sántha, P., and Nagy, J. (2009). “Sensory nerves as modulators of cutaneous inflammatory reactions in health and disease,” in *NeuroImmune Biology*, ed. G. Jancso (Amsterdam: Elsevier), 3–36. doi: 10.1016/S1567-7443(08)10401-X
- Jancsó, G., and Király, E. (1983). Cutaneous nerve regeneration in the rat: reinnervation of the denervated skin by regenerative but not by collateral sprouting. *Neurosci. Lett.* 36, 133–137. doi: 10.1016/0304-3940(83)90254-90259
- Jancsó, G., Király, E., and Jancsó-Gábor, A. (1980a). Chemosensitive pain fibres and inflammation. *Int. J. Tissue React.* 2, 57–66.
- Jancsó, G., Király, E., and Jancsó-Gábor, A. (1980b). Direct evidence for an axonal site of action of capsaicin. *Naunyn. Schmiedeberg's Arch. Pharmacol.* 313, 91–94. doi: 10.1007/BF00505809
- Jancsó, G., Király, E., Such, G., Joó, F., and Nagy, A. (1987). Neurotoxic effect of capsaicin in mammals. *Acta Physiol. Hung.* 69, 295–313.
- Jancsó, G., Obál, F., Tóth-Kása, I., Katona, M., and Husz, S. (1985). The modulation of cutaneous inflammatory reactions by peptide-containing sensory nerves. *Int. J. Tissue React.* 7, 449–457.
- Jancsó, N. (1955). *Speicherung. Stoffanreicherung Im Retikuloendothel Und in Der Niere*. Budapest: Akadémiai Kiadó.
- Jancsó, N. (1960). Role of nerve terminals in the mechanism of inflammatory reactions. *Bull. Millard Fill. Hosp.* 7, 32–41.
- Jancsó, N., Jancsó-Gábor, A., and Szolcsányi, J. (1967). Direct evidence for neurogenic inflammation and its prevention by denervation and by pretreatment with capsaicin. *Br. J. Pharmacol. Chemother.* 31, 138–151. doi: 10.1111/j.1476-5381.1967.tb01984.x
- Jordt, S. E., Bautista, D. M., Chuang, H. H., McKemy, D. D., Zygmunt, P. M., Högestätt, E. D., et al. (2004). Mustard oils and cannabinoids excite sensory nerve fibres through the TRP channel ANKTM1. *Nature* 427, 260–265. doi: 10.1038/nature02282
- Ju, G., Hökfelt, T., Brodin, E., Fahrenkrug, J., Fischer, J. A., Frey, P., et al. (1987). Primary sensory neurons of the rat showing calcitonin gene-related peptide immunoreactivity and their relation to substance P-, somatostatin-, galanin-, vasoactive intestinal polypeptide- and cholecystokinin-immunoreactive ganglion cells. *Cell Tissue Res.* 247, 417–431. doi: 10.1007/bf00218323
- Kang, S., Wu, C., Banik, R. K., and Brennan, T. J. (2010). Effect of capsaicin treatment on nociceptors in rat glabrous skin one day after plantar incision. *Pain* 148, 128–140. doi: 10.1016/j.pain.2009.10.031
- Kennedy, W. R., Vanhove, G. F., Lu, S.-P., Tobias, J., Bley, K. R., Walk, D., et al. (2010). A randomized, controlled, open-label study of the long-term effects of NGX-4010, a high-concentration capsaicin patch, on epidermal nerve fiber density and sensory function in healthy volunteers. *J. Pain* 11, 579–587. doi: 10.1016/j.jpain.2009.09.019
- Kinnman, E., Aldskogius, H., Johansson, O., and Wiesenfeld-Hallin, Z. (1992). Collateral reinnervation and expansive regenerative reinnervation by sensory axons into “foreign” denervated skin: an immunohistochemical study in the rat. *Exp. Brain Res.* 91, 61–72. doi: 10.1007/BF00230013
- Lembeck, F., and Holzer, P. (1979). Substance P as neurogenic mediator of antidromic vasodilation and neurogenic plasma extravasation. *Naunyn. Schmiedeberg's Arch. Pharmacol.* 310, 175–183. doi: 10.1007/BF00500282
- Lisney, S. J. W. (1989). Regeneration of unmyelinated axons after injury of mammalian peripheral nerve. *Q. J. Exp. Physiol.* 74, 757–784. doi: 10.1113/expphysiol.1989.sp003348
- Lynn, B., Schütterle, S., and Pierau, F. K. (1996). The vasodilator component of neurogenic inflammation is caused by a special subclass of heat-sensitive nociceptors in the skin of the pig. *J. Physiol.* 494, 587–593. doi: 10.1113/jphysiol.1996.sp021516
- Maggi, C. A., Borsini, F., Santicoli, P., Geppetti, P., Abelli, L., Evangelista, S., et al. (1987). Cutaneous lesions in capsaicin-pretreated rats. A trophic role of capsaicin-sensitive afferents? *Naunyn. Schmiedeberg's Arch. Pharmacol.* 336, 538–545. doi: 10.1007/BF00169311
- Maggi, C. A., and Meli, A. (1988). The sensory-efferent function of capsaicin-sensitive sensory neurons. *Gen. Pharmacol.* 19, 1–43. doi: 10.1016/0306-3623(88)90002-X
- Majno, G., Palade, G. E., and Schoeff, G. I. (1961). Studies on inflammation. II. The site of action of histamine and serotonin along the vascular tree: a topographic study. *J. Biophys. Biochem. Cytol.* 11, 607–626. doi: 10.1083/jcb.11.3.607
- Nolano, M., Simone, D. A., Wendelschafer-Crabb, G., Johnson, T., Hazen, E., and Kennedy, W. R. (1999). Topical capsaicin in humans: parallel loss of epidermal nerve fibers and pain sensation. *Pain* 81, 135–145. doi: 10.1016/S0304-3959(99)00007-X
- Pertovaara, A. (1988). Collateral sprouting of nociceptive C-fibers after cut or capsaicin treatment of the sciatic nerve in adult rats. *Neurosci. Lett.* 90, 248–253. doi: 10.1016/0304-3940(88)90197-90198
- Petsche, U., Fleischer, E., Lembeck, F., and Handwerker, H. O. (1983). The effect of capsaicin application to a peripheral nerve on impulse conduction in functionally identified afferent nerve fibres. *Brain Res.* 265, 233–240. doi: 10.1016/0006-8993(83)90337-90332
- Pini, A., and Lynn, B. (1991). C-fibre function during the 6 weeks following brief application of capsaicin to a cutaneous nerve in the rat. *Eur. J. Neurosci.* 3, 274–284. doi: 10.1111/j.1460-9568.1991.tb00089.x
- Pozsgai, G., Bodkin, J. V., Graepel, R., Bevan, S., Andersson, D. A., and Brain, S. D. (2010). Evidence for the pathophysiological relevance of TRPA1 receptors in the cardiovascular system in vivo. *Cardiovasc. Res.* 87, 760–768. doi: 10.1093/cvr/cvq118
- Rajan, V., Varghese, B., Van Leeuwen, T. G., and Steenbergen, W. (2009). Review of methodological developments in laser Doppler flowmetry. *Lasers Med. Sci.* 24, 269–283. doi: 10.1007/s10103-007-0524-0
- Sann, H., McCarthy, P. W., Jancsó, G., and Pierau, F. K. (1995). RT97: a marker for capsaicin-insensitive sensory endings in the rat skin. *Cell Tissue Res.* 282, 155–161. doi: 10.1007/BF00319142
- Sauerstein, K., Klede, M., Hilliges, M., and Schmelz, M. (2000). Electrically evoked neuropeptide release and neurogenic inflammation differ between rat and human skin. *J. Physiol.* 529, 803–810. doi: 10.1111/j.1469-7793.2000.00803.x
- Sta, M., Cappaert, N. L. M., Ramekers, D., Baas, F., and Wadman, W. J. (2014). The functional and morphological characteristics of sciatic nerve degeneration and regeneration after crush injury in rats. *J. Neurosci. Methods* 222, 189–198. doi: 10.1016/j.jneumeth.2013.11.012
- Westerman, R. A., Low, A., Pratt, A., Hutchinson, J. S., Szolcsányi, J., Magerl, W., et al. (1987). Electrically evoked skin vasodilatation: a quantitative test of nociceptor function in man. *Clin. Exp. Neurol.* 23, 81–89.
- Wiesenfeld-Hallin, Z., Kinnman, E., and Aldskogius, H. (1988). Studies of normal and expansive cutaneous innervation territories of intact and regenerating C-fibres in the hindlimb of the rat. *Agents Actions* 25:2. doi: 10.1007/bf01965028

Conflict of Interest: The authors declare that the research was conducted in the absence of any commercial or financial relationships that could be construed as a potential conflict of interest.

Copyright © 2020 Lakatos, Jancsó, Horváth, Dobos and Sántha. This is an open-access article distributed under the terms of the Creative Commons Attribution License (CC BY). The use, distribution or reproduction in other forums is permitted, provided the original author(s) and the copyright owner(s) are credited and that the original publication in this journal is cited, in accordance with accepted academic practice. No use, distribution or reproduction is permitted which does not comply with these terms.



Peripheral Inflammatory Hyperalgesia Depends on P2X7 Receptors in Satellite Glial Cells

OPEN ACCESS

Edited by:

Peter Santha,
University of Szeged, Hungary

Reviewed by:

Parisa Gazerani,
Aalborg University, Denmark
Fumimasa Amaya,
Kyoto Prefectural University
of Medicine, Japan

*Correspondence:

Carlos Amílcar Parada
caparada@unicamp.br

† Present address:

Dionéia Araldi,
Departments of Medicine and Oral
Surgery, and Division of
Neuroscience, University of California,
San Francisco, San Francisco, CA,
United States

Specialty section:

This article was submitted to
Integrative Physiology,
a section of the journal
Frontiers in Physiology

Received: 10 January 2020

Accepted: 17 April 2020

Published: 25 May 2020

Citation:

Neves AF, Farias FH,
de Magalhães SF, Araldi D,
Pagliusi M Jr, Tambeli CH, Sartori CR,
Lotufo CMdC and Parada CA (2020)
Peripheral Inflammatory Hyperalgesia
Depends on P2X7 Receptors
in Satellite Glial Cells.
Front. Physiol. 11:473.
doi: 10.3389/fphys.2020.00473

Amanda Ferreira Neves¹, Felipe Hertzling Farias¹, Silviane Fernandes de Magalhães¹,
Dionéia Araldi[†], Marco Pagliusi Jr.¹, Claudia Herrera Tambeli¹, Cesar Renato Sartori¹,
Celina Monteiro da Cruz Lotufo² and Carlos Amílcar Parada^{1*}

¹ Department of Structural and Functional Biology, Institute of Biology, University of Campinas, Campinas, Brazil, ² Institute of Biomedical Sciences, Area of Physiological Sciences, Federal University of Uberlândia, Uberlândia, Brazil

Peripheral inflammatory hyperalgesia depends on the sensitization of primary nociceptive neurons. Inflammation drives molecular alterations not only locally but also in the dorsal root ganglion (DRG) where interleukin-1 beta (IL-1 β) and purinoceptors are upregulated. Activation of the P2X7 purinoceptors by ATP is essential for IL-1 β maturation and release. At the DRG, P2X7R are expressed by satellite glial cells (SGCs) surrounding sensory neurons soma. Although SGCs have no projections outside the sensory ganglia these cells affect pain signaling through intercellular communication. Therefore, here we investigated whether activation of P2X7R by ATP and the subsequent release of IL-1 β in DRG participate in peripheral inflammatory hyperalgesia. Immunofluorescent images confirmed the expression of P2X7R and IL-1 β in SGCs of the DRG. The function of P2X7R was then verified using a selective antagonist, A-740003, or antisense for P2X7R administered in the L5-DRG. Inflammation was induced by CFA, carrageenan, IL-1 β , or PGE₂ administered in rat's hind paw. Blockage of P2X7R at the DRG reduced the mechanical hyperalgesia induced by CFA, and prevented the mechanical hyperalgesia induced by carrageenan or IL-1 β , but not PGE₂. It was also found an increase in P2X7 mRNA expression at the DRG after peripheral inflammation. IL-1 β production was also increased by inflammatory stimuli *in vivo* and *in vitro*, using SGC-enriched cultures stimulated with LPS. In LPS-stimulated cultures, activation of P2X7R by BzATP induced the release of IL-1 β , which was blocked by A-740003. In summary, our data suggest that peripheral inflammation leads to the activation of P2X7R expressed by SGCs at the DRG. Then, ATP-induced activation of P2X7R mediates the release of IL-1 β from SGC. This evidence places the SGC as an active player in the establishment of peripheral inflammatory hyperalgesia and highlights the importance of the events in DRG for the treatment of inflammatory diseases.

Keywords: satellite glial cells, P2X7 receptors, interleukin-1beta, dorsal root ganglion, inflammatory hyperalgesia

INTRODUCTION

In the nociceptive system, primary afferent neurons transduce the injury information at its peripheral endings and transmit the resulting signal to the central nervous system (CNS). At this path, the electric signal will pass through an important structure that is often ignored, the sensory ganglia, which can be a dorsal root ganglion (DRG) or trigeminal ganglia. At the sensory ganglia resides the soma of nociceptors and other somesthetic neurons as well as specialized glial cells, the satellite glial cells (SGC). Besides the important role in metabolic support, events at DRG are known to participate in the development of pathological pain (Devor, 1999; Esposito et al., 2019). Primary afferent neurons at the DRG do not interact with one another through synaptic contact. A layer of satellite glial cells (SGCs) tightly wrap each neuronal soma, which in turn is enclosed by connective tissue to create a physically isolated unit (Devor, 1999; Hanani, 2005; Pannese, 2010; Esposito et al., 2019). This singular structure suggests active participation of SGCs in the processing of sensory information by communicating with neurons (Hanani, 2005; Costa and Moreira Neto, 2015; Fan et al., 2019). Several studies have described intercellular communication in the sensory ganglia involving gap junctions (Huang et al., 2010), calcium-dependent somatic exocytosis of transmitters (Huang and Neher, 1996), and purinergic receptors also known as purinoceptors (Gu et al., 2010; Verderio and Matteoli, 2011). Purinergic signaling through ATP release at the DRG is suggested to mediate the development of chronic pain (for review see Kobayashi et al., 2013; Magni et al., 2018).

ATP is a ubiquitous molecule found in all tissues and cells and is released into the extracellular milieu in both physiological and pathological conditions (Fitz, 2007). Receptors activated by extracellular ATP include two families of the P2 purinoceptors: the ligand-gated ionotropic channels P2X and the metabotropic G protein-coupled P2Y receptors (Burnstock, 2016). Purinoceptors have a widespread tissue distribution, including peripheral (PNS) and CNS, and they are known to partake in pain mechanisms and inflammation (North, 2016; Magni et al., 2018). For example, activation of neuronal P2X3 receptors mediates acute nociception, and the microglial P2X4 and P2X7 receptors are associated with neuropathic and inflammatory pain (Toulme et al., 2010; Inoue and Tsuda, 2012; Fabbretti, 2013; Burnstock, 2016). Increasing evidence suggest ATP as a major transmitter released in the sensory ganglia (Zhang et al., 2007; Kobayashi et al., 2013; Goto et al., 2017). Therefore, the purinoceptors in DRG may have an important role boosting intercellular communication (Gu et al., 2010; Verderio and Matteoli, 2011; Huang et al., 2013), particularly for pain signaling (Jarvis, 2010; Hanani, 2012; Kobayashi et al., 2013; Lemes et al., 2018).

After peripheral tissue injury or inflammation, molecular alterations in the DRG are involved in the development of hyperexcitability of nociceptive neurons (Krames, 2014; Berta et al., 2017). Examples of those alterations include the upregulation of P2X receptors (Kushnir et al., 2011) and upregulation of the proinflammatory cytokine interleukin-1 β (IL-1 β) (Guo et al., 2007; Araldi et al., 2013). IL-1 β was the

first proinflammatory cytokine described to be involved in inflammatory pain and hyperalgesia (Ferreira et al., 1988). Several reports emphasize that a key process for IL-1 β maturation and secretion is the ATP-induced activation of the purinergic P2X7 receptors (P2X7R), selectively expressed in macrophages and microglia (Ferrari et al., 2006; Clark et al., 2010; Stoffels et al., 2015; Giuliani et al., 2017). Within the P2X family, P2X7R has the highest threshold for ATP-induced activation and will trigger downstream mechanisms only when extracellular ATP reaches pathological concentration (North, 2002). Undoubtedly P2X7R stands out among other purinoceptors for playing a central role in several pathologic conditions (De Marchi et al., 2016), including inflammatory diseases (Savio et al., 2018) and neuropathic pain (Zhang et al., 2020). Besides, studies have reported that P2X7R are expressed in SGC within DRG (Kobayashi et al., 2005; Zhang et al., 2005), suggesting a role for visceral hyperalgesia (Liu et al., 2015) and acute nociception (Lemes et al., 2018). Therefore, in this study, we hypothesized that ATP-induced activation of P2X7R and the subsequent release of IL-1 β by SGCs could be a major process in the DRG for the establishment of inflammatory hyperalgesia in the peripheral tissue.

MATERIALS AND METHODS

Animals

Experiments were performed using 180–250 g Wistar rats obtained from the University of Campinas Multidisciplinary Center for Biological Investigation (UNICAMP-CEMIB). Animals were housed in plastic cages with soft bedding (four/cage) on a 12-h light/dark cycle (lights on at 06:00 A.M.), with controlled humidity (60–80%) and temperature (22–25°C). Food and water were available *ad libitum*. Experimental protocols were approved by the Committee on Animal Research of the University of Campinas (CEUA – UNICAMP, protocol number: 3022-1). Animal care and handling procedures were in accordance with International Association for the Study of Pain (IASP) guidelines for the use of animals in pain research (Zimmermann, 1983). A total of 90 rats (males) were used for *in vivo* experiments and molecular analysis, and other 10 animals (males and females) were used for the *in vitro* experiments. Based on previous studies from our group, in inflammatory models, pain sensitivity and cytokine expression change according to estrous cycle in females (Joseph et al., 2003; Torres-Chávez et al., 2011). However, sexual dimorphism is abolished upon removal of the hormonal factors. For this reason, we used cultures of DRG cells from both male and female rats. During the experiments, animals were simply randomized into treatments. All efforts were made to minimize animal discomfort and to reduce the number of animals used.

Hyperalgesia Induction

Complete Freund's adjuvant (CFA 50 μ L/paw, #F5881, Sigma Aldrich, St. Louis, MO, United States), λ -carrageenan (100 μ g/paw, #22049, Sigma Aldrich, St. Louis, MO, United States), Interleukin 1 beta (IL-1 β , 0.5 pg/paw, National Institute of Biological Standards and Control, South Mimms,

Hertfordshire, United Kingdom) or PGE₂ (100 ng/paw, #P5640, Sigma Aldrich, St. Louis, MO, United States) were administered subcutaneously (intraplantar) in the rat's hind paw (right side) which is within the peripheral field of the L5 DRG (Araldi et al., 2013). The mechanical stimulus was then applied to the same area to measure hyperalgesia by electronic von Frey test.

In vivo Treatments

A potent selective antagonist for P2X7R (A-740003; Tocris Bioscience, Bristol, United Kingdom) was administered in the L5 DRG (right side) immediately before intraplantar injection of the inflammatory agent (right hind paw). A-740003 was diluted in a vehicle solution of 10% dimethyl sulfoxide (DMSO) + 10% propylene glycol + 80% sterile saline (NaCl 0.9%) and administered at doses of 0.01, 0.10, and 1.00 mM. The concentrations were calculated based on the effective antihyperalgesic dose of 142 mg/kg used for systemic administration (i.p.) in similar inflammatory pain-like behaviors models by Honore et al. (2006). For intraganglionic administration, using rats with approximately 0.2 kg, we calculated concentrations 10-, 100-, and 1000-times lower (0.028, 0.28, and 2.8 mg/6 μ l), which corresponds to the doses of 0.01, 0.10, and 1.00 mM.

The antisense (AS) oligonucleotide (ODN) for P2X7R (TTTCCTTATAGTACTTGGC) or a mismatch sequence (MM, TTCCGTTAAAGAAGTAGGC) were diluted in sterile saline and administered in the L5 DRG (right side, 30 μ g/5 μ l) once a day for 4 days to allow the knockdown of the P2X7R prior to the intraplantar injection of the inflammatory agent in the right hind paw. To demonstrate the relative expression of P2X7R was not altered solely by the repeated intraganglionic injections, we also used non-treated DRG (on the contralateral side of the inflammation) in the RT-qPCR analysis as a control for basal gene expression. All ganglionic treatments in this work were administered ipsilateral to the inflammation.

Ganglionic Drug Administration

The intraganglionic injection technique was performed as previously described (Ferrari et al., 2007; Araldi et al., 2013). Briefly, rats were anesthetized by inhalation of 2–3% isoflurane and an ultra-fine needle (32 G) was inserted through a punctured skin toward the intervertebral space between L5 and L6 vertebrae. Smooth movements of the needle were performed until a paw flinch reflex was observed and 5 μ l of solution was injected. The paw-flinch reflex was used as a sign that the needle tip has reached the distal nerve insertion of the L5 DRG. This ganglionic administration is restricted to the injected L5 DRG and it does not reach the opposite ganglion, nor the spinal cord between L1–T13 segments (Oliveira et al., 2009).

Mechanical Hyperalgesia Evaluation by Electronic von Frey Test

The withdrawal threshold of the treated hind paw was measured using an electronic von Frey aesthesiometer (Insight, Ribeirão Preto, SP, Brazil) as previously described (Vivancos et al., 2004). All experiments were performed by the same experimenter blind

to all treatments, between 9:00 AM and 4:00 PM. Rats were kept in a quiet room for 1 h prior to any manipulation. Then, each animal was placed in an acrylic cage (12 cm \times 20 cm \times 17 cm) with a wire grid floor providing access to the plantar surface of the rat's hind paw. Animals were allowed to acclimate in cages for 20 min before the test. A polypropylene tip (10 μ l, #T-300, Axygen, Corning, NY, United States) adapted to a hand-held force transducer was positioned perpendicularly to the plantar surface of the rat's hind paw aiming the L5 peripheral field. Then, a gradually increasing pressure (80 g maximum) was applied until animal voluntarily withdraw its paw. This mechanical stimulus was repeated up to six times separated by a 1-min interval to prevent mechanical sensitization. The withdrawal threshold was defined as the average force (g) required to animals withdraw the stimulated paw in three consistently measurements (differences < 10%). Animals were tested before and after treatments and the results (intensity of hyperalgesia) are expressed as the variation of the mechanical threshold by subtracting the baseline values (obtained before treatment) from those obtained after the treatments (Δ mechanical threshold in grams).

Primary DRG Cultures

Dissociated DRG cell cultures were prepared as previously described (Linhart et al., 2003). Male Wistar rats (100 g) were euthanized under anesthesia and DRGs from lumbar and thoracic spine were harvested and transferred to Hank's buffered saline solution (HBSS, #H2387, Sigma Aldrich, St. Louis, MO, United States) containing 10 mM Hepes. Cells were dissociated by incubating DRGs at 37°C in 0.28 U/mL collagenase (type II; #C6885, Sigma Aldrich, St. Louis, MO, United States) for 75 min and then in 0.25% trypsin (#T4549, Sigma Aldrich, St. Louis, MO, United States) for 12 min. After three washes with DMEM (#D5523, Sigma Aldrich, St. Louis, MO, United States) containing 10% fetal bovine serum (FBS, #10100147, Thermo Fisher Scientific, Waltham, MA, United States) and penicillin 50 U/mL + streptomycin 50 mg/mL (#15140122, Thermo Fisher Scientific, Waltham, MA, United States), cells were dissociated using a fire-polished glass Pasteur pipette. Dissociated cells were then plated in dishes coated with Matrigel (#354234, Corning, Corning, NY, United States) and the cultures were maintained in a humid 5% CO₂ atmosphere at 37°C. Calcium experiments were performed after 3 days *in vitro* to allow the growth of satellite glial cells. The cultures media (DMEM + 10% FBS + 50 U/mL penicillin and 50 mg/mL streptomycin) was changed every other day.

Cell Culture Treatments for Calcium Imaging

Cultures were stimulated with 2'-(3')-O-(4-Benzoylbenzoyl)adenosine 5'-triphosphate triethylammonium salt (BzATP, #B6396, Sigma Aldrich, St. Louis, MO, United States), the main agonist for P2X7R (Donnelly-Roberts et al., 2009). BzATP was prepared 10-fold the final concentration (1 mM solution for 100 μ M final concentration) in HBSS and administered directly in the buffered solution wherein

the cultures were maintained during image acquisition. Some cultures were previously incubated with A-740003 (#3701, Tocris Bioscience, Bristol, United Kingdom), a selective antagonist of P2X7R (Honore et al., 2006) for 10 min. A-740003 was diluted at final concentrations (1 μ M) in HBSS and maintained in cultures during agonist stimulus. To confirm cellular viability in those cultures with non-responsive cells after the incubation with the P2X7R antagonist, a stimulus of capsaicin (10 μ M final concentration) was administered at the end of the experiment.

Intracellular Calcium Imaging

Calcium recordings were performed after 18–24 h of culture. Cells were loaded with the Ca^{2+} indicator Fluo-3 AM 10 μ M (#F23915, Thermo Fisher Scientific, Waltham, MA, United States) in HBSS containing 10 mM Hepes for 1 h. After loading, cells were washed three times and kept with HBSS as described. All drugs were administered directly in buffered solution during image acquisition and the Ca^{2+} dynamics was recorded for 3 min after agonist addition. Fluorescence was excited at 506 nm and images of emitted fluorescence (at 526 nm) were acquired for each second by confocal microscope (Zeiss LSM510 Meta) in the Advanced Microscopy Center of ICBIM/UFU. Data are presented as $\Delta F/F_0$, where F_0 is the baseline, to normalize for differences in cell loading. As the field of view contained 20–40 SGCs in the focal plane, recordings were made from several cells simultaneously.

SGC-Enriched Cultures

Satellite glial cells were isolated from DRG cell cultures (see section Primary DRG Cultures) using a protocol adapted from England et al. (2001), Castillo et al. (2013). DRG cell cultures were kept for 4 days *in vitro* when glial cells are numerous. To isolate SGCs, 1 mL of fresh culture media (DMEM + 10% FBS + 50 U/mL penicillin and 50 mg/mL streptomycin) was added and all cells were gently detached from the culture dishes using a fire-polished Pasteur pipette. The 1 mL of cell suspension was collected and centrifuged at 3000 g during 5 min at room temperature to remove debris. Then 250 μ L of the cell suspension was plated again on new uncoated 24-well plates (1 DRG culture was split into 4 SGC-enriched cultures). The absence of coating prevents the attachment of neurons and does not affect attachment or growth of the glial cells (Capuano et al., 2009). Also, the culture media was changed 2 h after the cells plating to remove any cell (mostly neurons) in suspension. The SGC-enriched cultures were then maintained in a humid 5% CO_2 atmosphere at 37°C for 5–7 days *in vitro* or until the SGCs have proliferated at a confluence up to 70%. Media was changed every other day.

Cell Culture Treatments for Cytokine Measurement

For the IL-1 β synthesis and release experiments, SGCs were cultured in 24-well plates and an adapted protocol from Colomar et al. (2003), Rampe et al. (2004) was used to induce IL-1 β synthesis in SGC-enriched cultures. Cultures were maintained with fresh medium (DMEM supplemented as previously

described) or stimulated with lipopolysaccharides (LPS, 1 μ g/mL; #L8274, Sigma Aldrich, St. Louis, MO, United States) for 24 h kept in a humid 5% CO_2 atmosphere at 37°C. Some cultures were then incubated for 15 min with A74000 (1 μ M) that was prepared 10-fold the final concentration and administered directly in cultures medium. After incubation, cultures were treated for 30 min with BzATP (100 μ M) also prepared 10-fold the final concentration. All drugs were diluted in the culture medium. After treatments, the supernatant was collected and mixed with protease inhibitors (10 mM EDTA and 20 μ l/ml aprotinin; Sigma Aldrich, St. Louis, MO, United States). Forthwith the cells were lysed with an ice-cold solution of Phosphate Buffer Saline (PBS) containing 0.1% Triton X-100 and protease inhibitors to obtain the cell lysates.

Enzyme-Linked Immunosorbent Assay (ELISA)

An adaptation of ELISA (Teixeira et al., 2010) was used to determine whether P2X7R was able to regulate the synthesis and releasing of IL-1 β by SGCs. The cells lysates or the supernatant were centrifuged at 10,000 rpm for 15 min at 4°C, and the supernatants were stored at –80°C for posterior use to evaluate the protein levels of IL-1 β . IL-1 β was quantified by Rat IL-1 β /IL-1F2 DuoSet ELISA Kit (#DY501, R&D Systems, Minneapolis, MN, United States) and all procedures followed the instructions of the manufacturer. All samples were running in duplicates and procedures were repeated at least twice.

DRG Immunohistochemistry

Animals were terminally anesthetized with ketamine (i.p. 85 mg/kg)/xylazine (i.p. 10 mg/kg) and perfused through the ascending aorta with saline solution followed by 4% paraformaldehyde (PFA, pH 7.4, 4°C). After perfusion, L5 DRG were removed and post-fixed in 4% PFA for 2 h, which was then replaced with 30% sucrose for 48 h at 4°C. Each DRG were embedded in optimum cutting temperature and sections of 14 μ m were made in a cryostat using gelatinized slides. The sections were processed for immunofluorescence, first incubated in 0.1 M glycine for 30 min at room temperature, to inactivate free aldehydes, and then blocked with 2% BSA in 0.2% Triton X-100 for 1 h at room temperature. The mixture of rabbit polyclonal anti-P2X7R (1:200, #APR-004, Alomone Labs, Jerusalem, ISR), goat polyclonal anti-TRPV1 (1:100, #AF3066, R&D Systems, Minneapolis, MN, United States) and mouse monoclonal anti-glutamine synthetase (1:200, #MAB302, EMD Millipore, Darmstadt, DEU) were incubated for 2 h at room temperature. A mixture of mouse monoclonal anti-GFAP (1:100, #G3893, Sigma Aldrich, St. Louis, MO, United States) and goat polyclonal anti-IL-1 β (1:100, #AF-501-NA, R&D Systems, Minneapolis, MN, United States) was incubated overnight at 4°C. Finally, a mixture of Alexa 488 (A21206), Alexa 546 (A11058) and Alexa 594 (A11058) conjugated secondary antibodies (1:1000 each, Thermo Fisher Scientific, Waltham, MA, United States) were incubated for 1 h at room temperature and then nuclei were stained with DAPI 0.25 μ g/mL (#D9542, Sigma Aldrich, St. Louis, MO, United States) for 10 min. Sections were examined

in the National Institute of Science and Technology in Photonics Applied to Cell Biology (INFABIC/UNICAMP) using a confocal laser-scanning microscope (Zeiss LSM780-NLO).

RNA Extraction, cDNA Synthesis, and qPCR Experiment

RNA was extracted from whole DRG tissue by TRIZOL® Reagent (#15596026, Thermo Fisher Scientific, Waltham, MA, United States) according to manufacturer instructions. Subsequently, total RNA was quantified by ultra-low volume spectrophotometer (Epoch Microplate Spectrometer, BioTek Instruments, Winooski, VT, United States) and 500 ng of RNA were used to perform cDNA synthesis (SuperScript® VILO cDNA Synthesis Kit, #11755, Thermo Fisher Scientific, Waltham, MA, United States). Real-Time PCR (RT-qPCR) experiment was performed for relative quantification of P2X7R and IL-1 β to an index of endogenous control genes (Arfgef1, G3bp2, Mtm8, Ppp1cc, Serpinb6) by $2^{-\Delta\Delta C_T}$ method (see Table 1 for the primer sequences). The RT-qPCR reactions were conducted using SYBR Green as a fluorescent signal (SYBR Power Up Master Mix, #4367659, Thermo Fisher Scientific, Waltham, MA, United States). Primers were designed using Primer3 software available at NCBI's Pick Primer tool¹ between exons when possible and its specificity to the gene of interest was validated by comparison with the rat genome using BLAST tool from NCBI webpage¹. Technical triplicates for all samples as well as negative controls were used for each gene.

Statistical Analysis

The statistical analysis was performed using Prism v.6 (GraphPad Software Inc., La Jolla, CA, United States). Statistical significance between groups (defined as $P < 0.05$) was calculated by one-way ANOVA and Bonferroni *post hoc* test, otherwise by using the two-tailed Student's *t*-test between two groups. Sample sizes are indicated in the figure legends and in the text. Data in the figures are expressed as mean \pm S.E.M. The long line above two or more data sets indicates no statistical difference between those groups. The symbol (#) indicates statistical difference in comparison to saline-treated group (hind paw treatments). The symbol (*) indicates statistical difference in comparison to vehicle-treated group (DRG treatments; * $P < 0.05$; ** $P < 0.01$; *** $P < 0.001$).

¹www.ncbi.nlm.nih.gov/tools/primer-blast

TABLE 1 | Primer Sequences used for RT-qPCR.

Gene	Forward sequence 5' - 3'	Reverse sequence 5' - 3'
P2rx7	AGTCCCTGTTCCCTGGCTACAAC	GGATGTCAAACGCACGCCG AAGG
Il1b	TGCTAGTGTGTGATTTCC	AGCACGAGGCATTTTGTG
Arfgef1	CAACAGGTTTAAAGCTCACGCA	TCCTGTTGAGGTGGTTGTGA
G3bp2	ACCACAAGCGGAGGAGAAAC	CATCAACCTTGGCTTTGGC
Mtm8	GTGCATTGACAGGGAAGGTG	GCCACTCTCGCTCTATCAGG
Ppp1cc	GAGACCCTCATGTGCTCCTTC	AGGCCTGATCCAACCGTG
Serpinb6	GAGTCTAGGCTACGTTCTGCTG	TCCATGATGGTGAACCTGCC

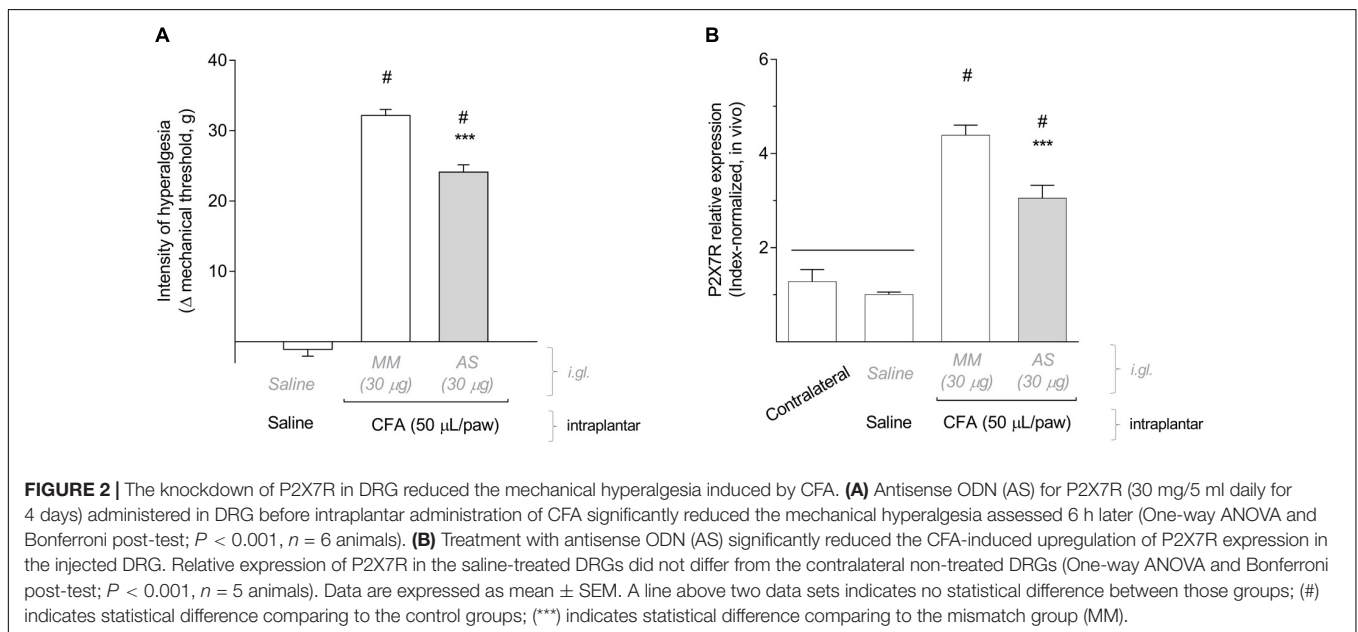
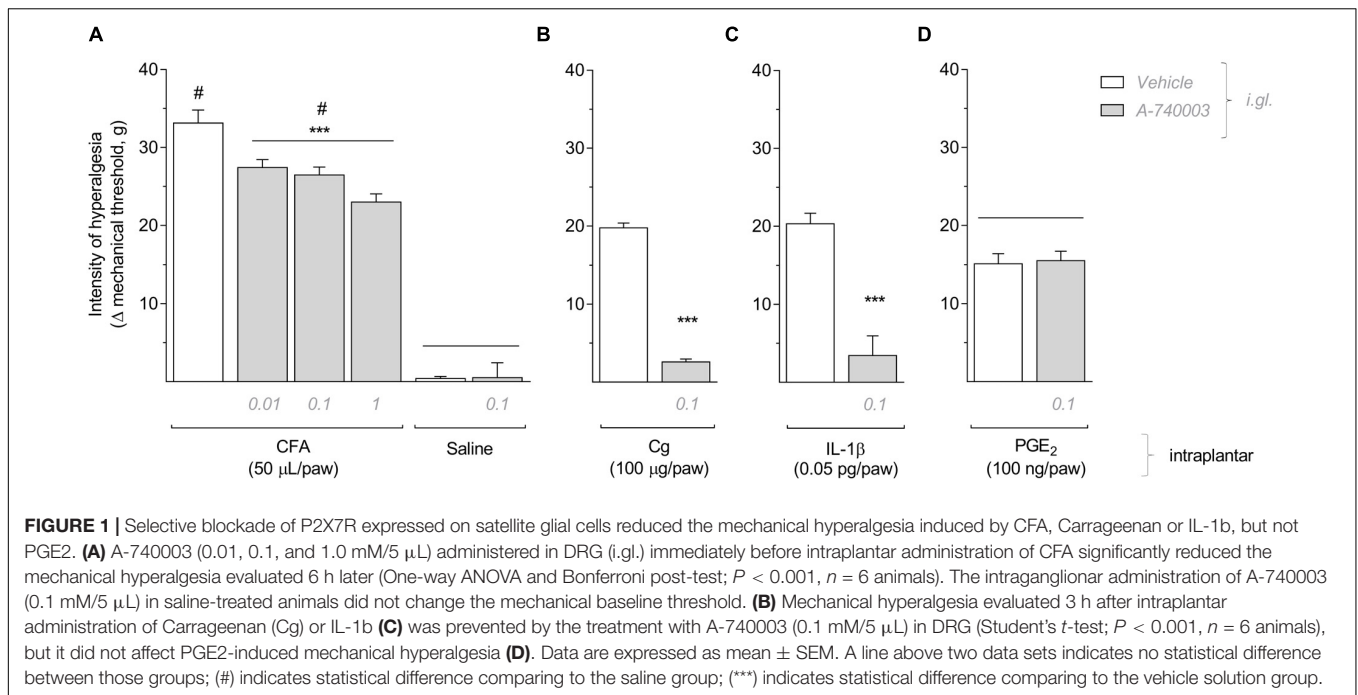
RESULTS

The Selective Blockade of P2X7R in DRG Reduces the Mechanical Hyperalgesia Induced by CFA, Carrageenan, and IL-1 β , but Not PGE₂

To evaluate the participation of P2X7R expressed in DRG during the development of peripheral inflammatory hyperalgesia, different doses of the selective P2X7R antagonist A-740003 (0.01 mM, 0.1 mM or 1.0 mM/5 μ L) were administered in the right L5 DRG immediately before intraplantar administration of CFA (50 μ L/paw) in the ipsilateral hind paw. The electronic von Frey test was conducted 6 h later to measure the mechanical hyperalgesia. As shown in Figure 1A, A-740003 decreased the CFA-induced mechanical hyperalgesia compared to vehicle-treated group (One-way ANOVA and Bonferroni post-test; $F = 11.84$, $P < 0.001$, $n = 6$). Also, the intraganglionic administration of A-740003 (0.1 mM/5 μ L) in animals treated with saline intraplantar did not change the mechanical nociceptive threshold, which excludes any alterations in the mechanical baseline. Thus, this dose was used in the following experiments. To confirm the selective effect of A-740003 (0.1 mM) on other models of inflammatory hyperalgesia, we administered carrageenan (100 μ g/paw), IL-1 β (0.5 pg/paw) or PGE₂ (100 ng/paw) in the right hind paw and measured the mechanical hyperalgesia 3 h later. A-740003 (0.1 mM/5 μ L) administered in the ipsilateral L5 DRG immediately before the inflammatory stimuli prevented the hyperalgesia induced by carrageenan and IL-1 β (Figures 1B,C; Unpaired *t*-test; $t = 23.35$ and $t = 5.89$ respectively, $P < 0.001$, $n = 6$), but did not affect the hyperalgesia induced by PGE₂ (Figure 1D; Unpaired Student's *t*-test; $t = 0.23$, $P = 0.816$, $n = 6$).

Knockdown of the P2X7R in DRG Reduces the Mechanical Hyperalgesia Induced by CFA

To knock down the expression of P2X7R in the DRG, we administered an antisense ODN for P2X7R or a mismatch sequence (MM), as control, in the right L5 DRG (30 μ g/5 μ L) once a day for 4 days before CFA injection (50 μ L/paw) in the ipsilateral hind paw. Similarly to the selective blockade with A-740003, the P2X7R knockdown using the antisense (AS) also significantly reduced the mechanical hyperalgesia, assessed 6 h after CFA injection, when compared to the MM treatment (Figure 2A; One-way ANOVA and Bonferroni post-test; $F = 331.9$, $P < 0.001$, $n = 6$). To confirm the P2X7R knockdown, we analyzed the levels of P2X7R expression by RT-qPCR in all treated DRG (AS, MM, or saline) and in non-treated DRG (contralateral) as a control for basal expression (Figure 2B). For this $2^{-\Delta\Delta C_T}$ analysis, we used an index of endogenous controls (Serpinb6, Mtm9, Arfgef1, and G3bp2). The relative expression of P2X7R in the AS-treated DRG was significantly reduced compared to the MM treatment. However, in the MM-treated DRG the expression of P2X7R was already 4-fold increased after 6 h of the CFA inflammation (One-way ANOVA and Bonferroni post-test; $F = 58.14$, $P < 0.001$, $n = 5$).



The expression of P2X7R in the saline-treated DRG did not differ from the basal expression in the contralateral DRG. This result demonstrates the P2X7R expression was not altered solely by the repeated intraganglionic injections.

P2X7R Are Expressed by Satellite Glial Cells in DRG and Can Be Functionally Activated and Blocked *in vitro*

As shown in **Figure 3A**, the immunohistochemistry co-staining P2X7R and glutamine synthetase (GS, a glial-specific enzyme)

in paraformaldehyde-fixed rat DRG sections confirmed that P2X7R are expressed on SGCs, but not on DRG neurons, after CFA inflammation. Expression of P2X7R in non-inflammatory conditions is very low (as shown in **Figure 2B**) and hardly detected by immunohistochemistry of the DRG (data not shown). To check P2X7R activation and blockade in SGCs, we evaluated changes in intracellular calcium concentration by confocal microscopy using mixed DRG cell cultures from adult rats. The P2X7R was activated by its agonist BzATP (100 μM) which increased the intracellular calcium concentration in SGCs but not in neurons (**Figure 3B**). The incubation with

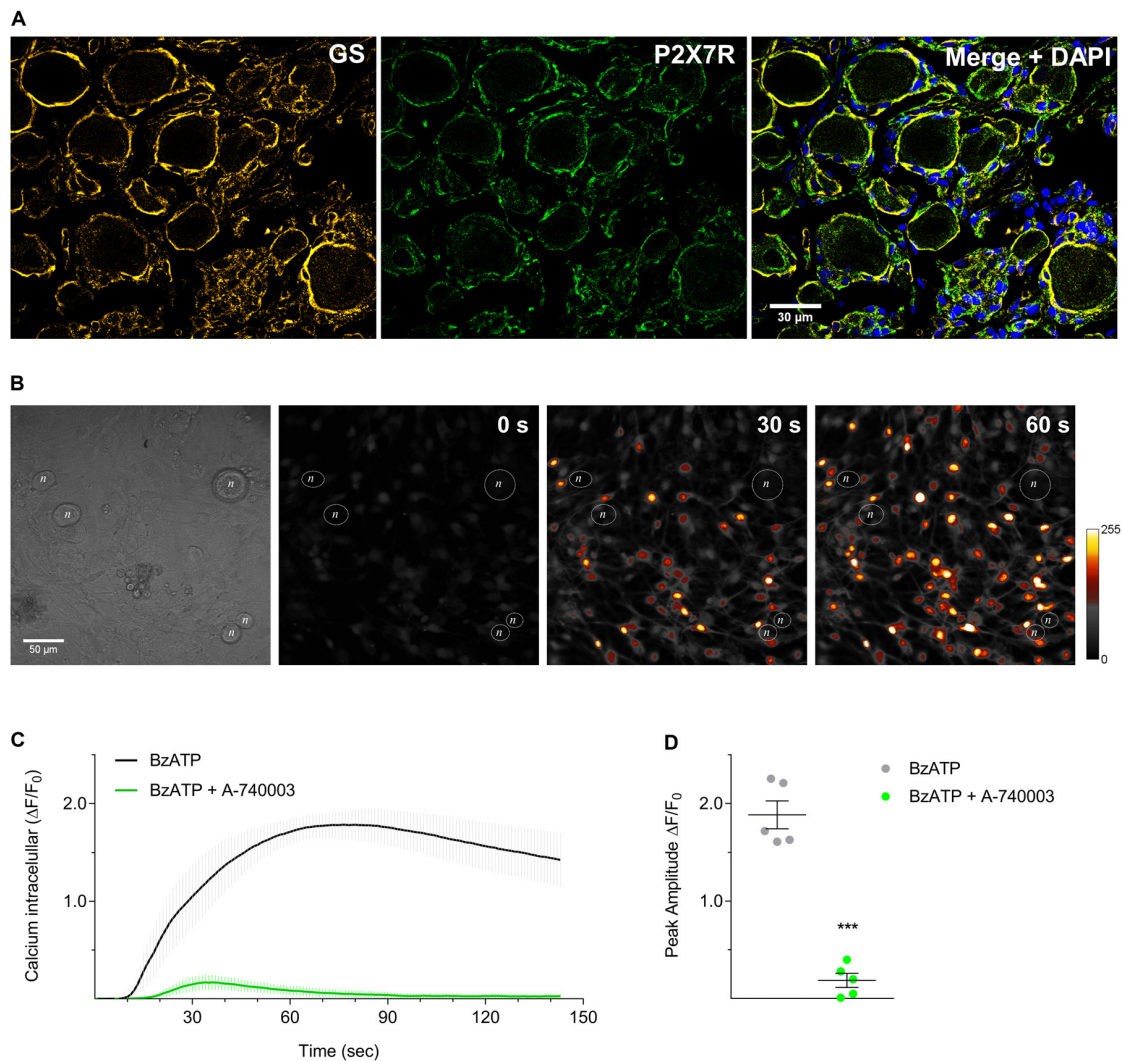


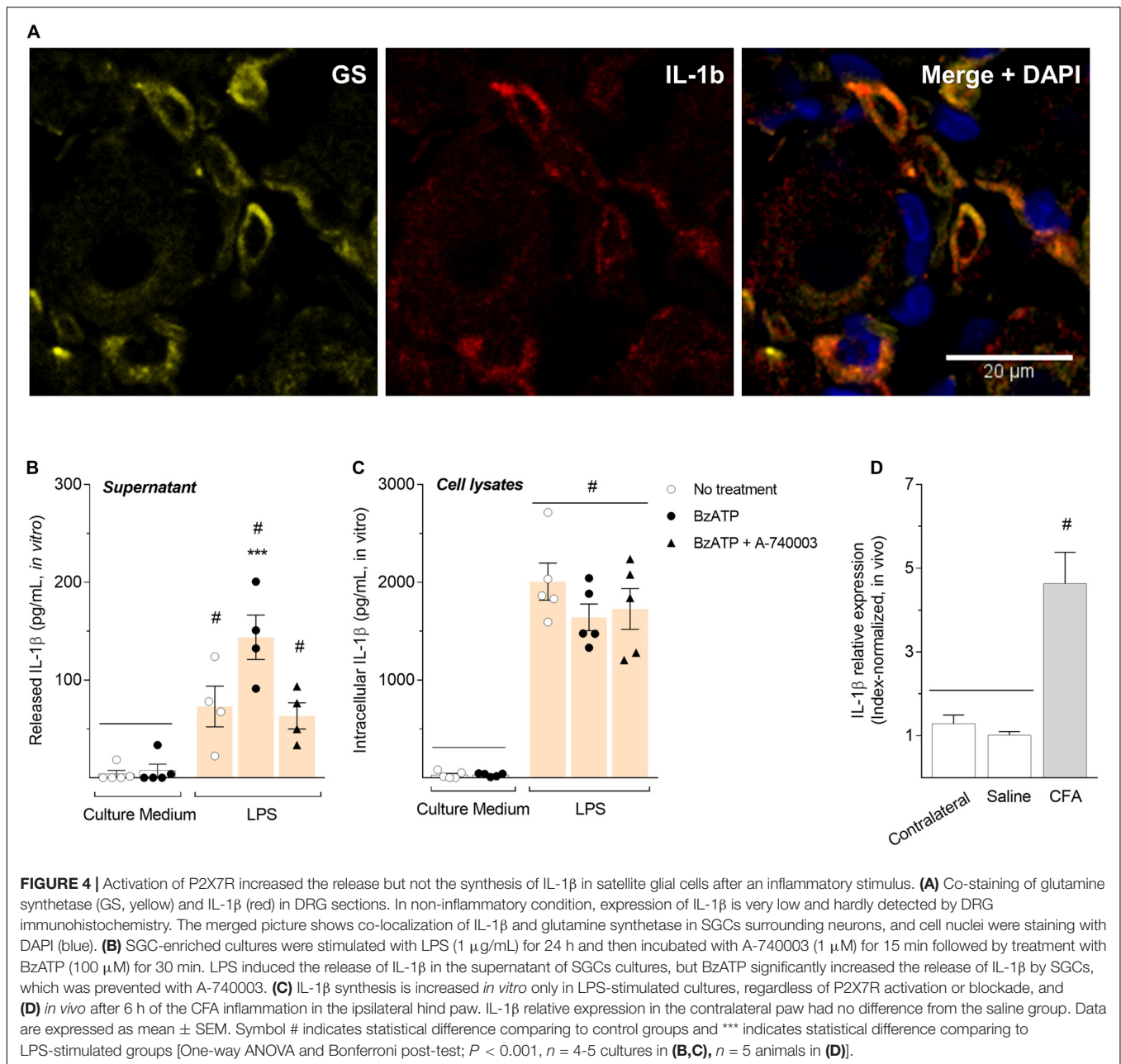
FIGURE 3 | P2X7R are expressed by SGCs in DRG and can be functionally activated and blocked in culture. **(A)** Co-staining of glutamine synthetase (GS, yellow) and P2X7R (green) in DRG sections of CFA-treated animals. In non-inflammatory condition, expression of P2X7R is very low and hardly detected by DRG immunohistochemistry. The merged picture shows co-localization of P2X7R and glutamine synthetase in SGCs surrounding neurons, and cell nuclei were staining with DAPI (blue). **(B)** BzATP (100 μ M) induced intracellular calcium surge in cultured SGCs (colored artificially) but not in neurons (n). **(C)** Pretreatment with A-740003 (1 μ M, green line) blocked the BzATP-induced intracellular calcium surge (gray line). **(D)** Maximum values of $\Delta F/F_0$ for both response curves showed in **(C)**. Data are expressed as mean \pm SEM for $n = 5$ cultures/group, 20–40 SGCs sampled per culture. Symbol *** indicates statistical difference between the response peaks (Unpaired t -test; $P < 0.001$).

P2X7R selective antagonist A-740003 (1 μ M), added to cultures 5 min before BzATP, blocked the BzATP-induced intracellular calcium surge in SGCs (**Figures 3C,D**; Unpaired Student's t -test; $t = 10.70$, $P < 0.001$, $n = 5$ cultures/group, 20–40 SGCs sampled per culture).

Activation of P2X7R Increases the Release but Not the Synthesis of IL-1 β in Satellite Glial Cells After an Inflammatory Stimulus

To confirm SGCs express IL-1 β , we performed an immunohistochemistry co-staining IL-1 β (both precursor

and mature forms) and glutamine synthetase (GS) in paraformaldehyde-fixed rat DRG sections. Our results showed that IL-1 β is expressed on SGCs after CFA-induced inflammation (**Figure 4A**), in addition to P2X7R (**Figure 3A**). To evaluate whether the release of IL-1 β in DRG is regulated by activation of P2X7R during the peripheral inflammation, we used an *in vitro* approach. SGC-enriched cultures isolated from DRG were maintained with fresh culture medium (controls) or stimulated with LPS (1 μ g/mL) for 24 h. Cultures were then incubated with A-740003 (1 μ M) for 15 min followed by treatment with BzATP (100 μ M) for 30 min. Supernatant and cell lysates were collected and the levels of IL-1 β were measured by ELISA. Our data show P2X7R activation by BzATP without an inflammatory stimulus



did not induce IL-1 β release by SGCs (**Figure 4B**, white bars). However, after the LPS inflammatory stimulation, the release of IL-1 β was induced into the supernatant of SGCs cultures. Then, P2X7R activation by BzATP significantly increased the release of IL-1 β by LPS-stimulated SGCs cultures, which was prevented by the P2X7R blockade with A-740003 (**Figure 4B**, colored bars; One-way ANOVA and Bonferroni post-test; $F = 16.60$; $P < 0.001$, $n = 5$).

Further, we investigated the intracellular levels of IL-1 β in the SGCs cultures, to test whether activation of P2X7R is relevant also for IL-1 β synthesis. Our results show that intracellular levels of IL-1 β were only increased with the

LPS inflammatory stimulation, regardless of P2X7R activation or blockade (**Figure 4C**; One-way ANOVA and Bonferroni post-test; $F = 48.12$, $P < 0.001$, $n = 5$). We also analyzed the expression of IL-1 β by RT-qPCR in the L5-DRG of rats treated with CFA (50 μ L/paw) or saline, along with non-treated DRG (contralateral) as a control for basal expression. The relative expression of IL-1 β was also increased *in vivo* after 6 h of the CFA inflammation (**Figure 4D**; One-way ANOVA and Bonferroni post-test; $F = 20.05$, $P < 0.001$, $n = 5$). The expression of IL-1 β in the saline-treated DRG did not differ from the basal expression in the contralateral DRG; both levels were very low and hardly detected also by DRG immunohistochemistry (data not shown).

DISCUSSION

Although satellite glial cells (SGCs) have no projections outside the sensory ganglia, in this study, we detected a major process occurring at the dorsal root ganglion (DRG) involving the active participation of SGCs in the development of peripheral inflammatory hyperalgesia. Peripheral inflammatory hyperalgesia is the sensitization of the peripheral terminals of nociceptors due to inflammation. It has been established that administration of inflammatory agents such as the complete Freund's adjuvant (CFA), carrageenan, or lipopolysaccharide (LPS), leads to an upregulation of proinflammatory mediators, including interleukin-1 beta (IL-1 β), in the local tissue (Cunha et al., 2000; Verri et al., 2006; Ren and Torres, 2009). IL-1 β as a mediator of the inflammatory hyperalgesia induces the upregulation of cyclooxygenase-2 (COX-2) and stimulates the subsequent release of COX products, such as prostaglandin E2 (PGE₂). PGE₂ is the main mediator responsible for nociceptive sensitization that causes inflammatory hyperalgesia in both peripheral (Ferreira, 1981; Verri et al., 2006) and the CNS (Samad et al., 2001).

Using a technique to administer drugs directly into the DRG (right L5), we selectively inhibited P2X7R activation in SGC by injecting the selective P2X7R antagonist A-740003 (Honore et al., 2006) or the antisense oligonucleotides knocking down P2X7R expression. The selective blockade of P2X7R expressed on SGCs prevented the mechanical hyperalgesia induced by carrageenan or IL-1 β . Also, P2X7R blockade or knockdown significantly reduced the mechanical hyperalgesia assessed 6 h after the CFA administration. Undoubtedly, P2X7R stands out among other purinergic receptors for playing a central role in inflammatory and neuropathic pain-like behavior (Dell'Antonio et al., 2002; Chessell et al., 2005; McGaraughty et al., 2007; Carroll et al., 2009; Honore et al., 2009; Arulkumaran et al., 2011; Luchting et al., 2016; and for review see Savio et al., 2018; Zhang et al., 2020). Besides, studies suggest that P2X7R expressed particularly in DRG have a role for the neuropathic pain-like behavior associated with HIV glycoprotein 120 (Wu et al., 2017), visceral hyperalgesia (Liu et al., 2015), and acute nociception (Lemes et al., 2018). In the present study, we describe for the first time the active participation of P2X7R expressed on SGCs on the establishment of peripheral inflammatory hyperalgesia.

However, we have shown that the selective blockade of P2X7R in DRG did not affect the PGE₂-induced hyperalgesia. As a final inflammatory mediator, PGE₂ acts on EP receptors and directly stimulates primary afferent neurons. Thus, the administration of PGE₂ at a pharmacological dose of 100 ng/paw induces hyperalgesia (Prado et al., 2013). But the model of PGE₂ inducing hyperalgesia lacks important upstream events, such as the IL-1 β signaling, which is a shared event between the other models of hyperalgesia we used – CFA, carrageenan, and IL-1 β (Cunha et al., 2000; Ren and Torres, 2009). In addition to inducing the synthesis of PGE₂, IL-1 β can also play as a final inflammatory mediator acting at nociceptors, a mechanism that substantially increases neuronal excitability in pain signaling (Cunha et al., 2000; Binshtok et al., 2008; Dinarello, 2018). Therefore, we suggest that a mechanism dependent on IL-1 β , but

not prostaglandins, could be promoting the somatic release of ATP in DRG and leading to the activation of P2X7R on SGCs.

Our results revealed the constitutive expression of P2X7R in DRG, and the immunofluorescence confirmed the expression of P2X7R in SGCs. However, P2X7R expression was considerably increased (4-fold) after the intraplantar administration of CFA. Other studies, mostly in neuropathic pain-like behavior models, also detected upregulation of P2X receptors in trigeminal SGCs (Kushnir et al., 2011) and specifically upregulation of P2X7R in spinal microglia (Kobayashi et al., 2011; He et al., 2012; Li et al., 2017), and Schwann cells (Song et al., 2015). ATP-induced purinergic signaling is used by glial cells for intercellular communication in both central (Butt, 2011; Verderio and Matteoli, 2011; Puerto et al., 2013) and peripheral nervous system (Gu et al., 2010; Hanani, 2012; Huang et al., 2013). In neurons, ATP accumulates in vesicles near the presynaptic membrane and is released by exocytosis as a neurotransmitter (Burnstock, 2006; Lazarowski, 2012). Particularly in the sensory ganglia, studies have already suggested that vesicles holding ATP can be released by the cell body of sensory neurons following activation with capsaicin (Matsuka et al., 2001) or electrical stimulation (Zhang et al., 2007). Increasing evidence show ATP as a major transmitter released in the sensory ganglia (for review see Kobayashi et al., 2013; Goto et al., 2017); and intercellular communication via purinergic signaling appears to be an essential mechanism for pain (Ding et al., 2000; Toulme et al., 2010; Kobayashi et al., 2013; Burnstock, 2016; Lemes et al., 2018; Magni et al., 2018). Therefore, the upregulation of P2X7R in SGCs could be relevant for boosting intercellular communication in DRG during inflammatory hyperalgesia.

A potential role for P2X7R from SGCs during inflammatory hyperalgesia is the regulation of IL-1 β release in DRG. IL-1 β is produced from an inactive precursor protein, pro-IL-1 β (31 kDa), that remains accumulated at the intracellular compartment. For the IL-1 β maturation, a multiprotein complex called inflammasomes is recruited by mechanisms yet not fully understood to cleave the pro-IL-1 β into the active form (17 kDa) and ensure its following secretion (Brough and Rothwell, 2007; Garlanda et al., 2013; Malik and Kanneganti, 2017). Several reports emphasize that ATP-mediated P2X7R activation is essential for rapid maturation and release of IL-1 β from activated immune cells, including macrophages and microglial cells (Ferrari et al., 2006; Clark et al., 2010; Stoffels et al., 2015; Giuliani et al., 2017). In the present study, we also verified a connection between P2X7R activation and IL-1 β release from SGCs after inflammatory stimulation. In SGC-enriched cultures treated with LPS, the activation of P2X7R by BzATP induced the release of IL-1 β in the supernatant, which was blocked by A-740003. However, the activation of P2X7R without the inflammatory stimulus did not provoke the release of IL-1 β or the synthesis of the pro-IL-1 β . These results might indicate the involvement of caspases proteins which participates in the IL-1 β maturation (Maelfait et al., 2008).

We found that SGCs activated by the inflammatory stimuli show an increased expression of IL-1 β both *in vivo* and

in vitro through a mechanism independent of P2X7R activation. Likewise, other studies have also reported the upregulation of IL-1 β in SGCs in consequence of peripheral inflammation or nerve injury (Guo et al., 2007; Takeda et al., 2007; Araldi et al., 2013). Although P2X7R activation has a critical role on IL-1 β release, there is no evidence on P2X7R modulation on the expression of the IL-1 β precursor (Chessell et al., 2005; Clark et al., 2010; Giuliani et al., 2017). The synthesis of pro-IL-1 β is primarily induced by pathological conditions and normally involves activation of toll-like receptors (TLRs) (Dinarello, 2018). In our *in vitro* approach, LPS itself could be triggering the synthesis of the IL-1 β precursor in SGCs through direct stimulation of the toll-like receptors 4 (TLR4) (Tse et al., 2014). However, further investigation is required to understand the mechanism underlying the increase of pro-IL-1 β synthesis in DRG *in vivo*. Possibly, different neuronal mediators might be involved to induce IL-1 β synthesis in SGC. Sensory neurons in response to electrical or chemical stimulation can release substance P or glutamate concurrent with ATP (Matsuka et al., 2001; Dissing-Olesen et al., 2014). Also, trigeminal cells in culture stimulated with IL-1 β release calcitonin gene-related peptide (CGRP) through a mechanism dependent on COX-2-induced PGE₂ synthesis (Neeb et al., 2011). Because SGCs have receptors for CGRP (De Corato et al., 2011), substance P (Matsuka et al., 2001) and NMDA (Ferrari et al., 2014), these neuronal mediators could also participate in neuron-glia signaling in the DRG.

In summary, our study has provided evidence for a specific role of P2X7R in neuronal soma-glia communication associated with the regulation of the IL-1 β release in DRG during peripheral hyperalgesia. Our data suggest that inflammatory mediators released at the peripheral level lead to ATP release at the DRG, activating P2X7R at SGC and triggering the release of IL-1 β . At the DRG, IL-1 β was shown to upregulate cyclooxygenase activity and thus inducing prostaglandin production (Araldi et al., 2013). Prostaglandins are responsible for neuronal sensitization, contributing to the development and maintenance of the inflammatory hyperalgesia. Therefore, peripheral inflammation appears to induce a further inflammatory response at the sensory ganglia that might maintain or amplify neuronal sensitization, increasing pain-like behavior.

This study draws attention to the sensory ganglia as an important pharmacological target and can be used to support the development of new treatments for inflammatory diseases. We have described a pharmacological mechanism of analgesia that is independent of COX inhibition and targets structures outside the CNS. Also, the ganglionic injection is a technique, *per se*, translational. In humans, it has been used to treat mainly patients with chronic pain (Sapunar et al., 2012). Here we used this technique as a methodological tool to investigate hyperalgesia-related mechanisms restrict to the DRG. It's noteworthy that the

DRG is only partially covered by the dura mater, thus showing good bioavailability to drugs acting in the peripheral nervous system (Esposito et al., 2019). Therefore, DRG could be targeted by the systemic administration of drugs that do not cross the blood-brain barrier. Treatments using those classes of drugs would have reduced side effects without the limitations of using ganglionic injections.

DATA AVAILABILITY STATEMENT

All datasets generated for this study are included in the manuscript.

ETHICS STATEMENT

The animal study was reviewed and approved by Committee on Animal Research of the University of Campinas (3022-1).

AUTHOR CONTRIBUTIONS

AN, CL, and CP conceived the project and designed the study. AN, FF, and SM acquired the data. AN, DA, CT, CS, and CL analyzed and interpreted the data. AN, MP, CL, and CP drafted the manuscript. AN, FF, SM, DA, MP, CT, CS, CL, and CP approved the final version to be submitted.

FUNDING

This study was supported by São Paulo Research Foundation (FAPESP) grant #2013/08678-6 and by the Coordination for the Improvement of Higher Education Personnel (CAPES – Brazil), Finance Code 001.

ACKNOWLEDGMENTS

We thank the access to equipment and assistance provided by the Advanced Microscopy Center at the Institute of Biomedical Sciences (ICBIM), Federal University of Uberlândia, and by the National Institute of Science and Technology on Photonics Applied to Cell Biology (INFABIC) at the State University of Campinas (INFABIC is co-funded by FAPESP #08/57906-3 and CNPq 573913/2008-0). We also thank Willians F. Vieira, Ph.D. and Catarine M. Nishijima, Ph.D. for their expertise and assistance throughout our study.

REFERENCES

- Araldi, D., Ferrari, L. F., Lotufo, C. M., Vieira, A. S., Athie, M. C., Figueiredo, J. G., et al. (2013). Peripheral inflammatory hyperalgesia depends on the COX increase in the dorsal root ganglion. *Proc. Natl. Acad. Sci. U.S.A.* 110, 3603–3608. doi: 10.1073/pnas.1220668110
- Arulkumaran, N., Unwin, R. J., and Tam, F. W. (2011). A potential therapeutic role for P2X7 receptor (P2X7R) antagonists in the treatment of inflammatory diseases. *Expert Opin. Investig. Drugs* 20, 897–915. doi: 10.1517/13543784.2011.578068
- Berta, T., Qadri, Y., Tan, P.-H., and Ji, R.-R. (2017). Targeting dorsal root ganglia and primary sensory neurons for the treatment of chronic pain.

- Expert Opin. Ther. Targets* 21, 695–703. doi: 10.1080/14728222.2017.1328057
- Binshtok, A. M., Wang, H., Zimmermann, K., Amaya, F., Vardeh, D., Shi, L., et al. (2008). Nociceptors are interleukin-1 sensors. *J. Neurosci.* 28, 14062–14073. doi: 10.1523/JNEUROSCI.3795-08.2008
- Brough, D., and Rothwell, N. J. (2007). Caspase-1-dependent processing of pro-interleukin-1 β is cytosolic and precedes cell death. *J. Cell Sci.* 120, 772–781. doi: 10.1242/jcs.03377
- Burnstock, G. (2006). Historical review: ATP as a neurotransmitter. *Trends Pharmacol. Sci.* 27, 166–176. doi: 10.1016/j.tips.2006.01.005
- Burnstock, G. (2016). “Purinergic Mechanisms and Pain,” in *Advances in Pharmacology*, Vol. 75, ed. J. E. Barrett (Cambridge, MA: Academic Press), 91–137. doi: 10.1016/bs.apha.2015.09.001
- Butt, A. M. (2011). ATP: a ubiquitous gliotransmitter integrating neuron-glia networks. *Semin. Cell Dev. Biol.* 22, 205–213. doi: 10.1016/j.semcdb.2011.02.023
- Capuano, A., De Corato, A., Lisi, L., Tringali, G., Navarra, P., and Dello Russo, C. (2009). Proinflammatory-activated trigeminal satellite cells promote neuronal sensitization: relevance for migraine pathology. *Mol. Pain* 5:43. doi: 10.1186/1744-8069-5-43
- Carroll, W. A., Donnelly-Roberts, D., and Jarvis, M. F. (2009). Selective P2X7 receptor antagonists for chronic inflammation and pain. *Purinergic Signal.* 5, 63–73. doi: 10.1007/s11302-008-9110-6
- Castillo, C., Norcini, M., Martin Hernandez, L. A., Correa, G., Blanck, T. J. J., and Recio-Pinto, E. (2013). Satellite glia cells in dorsal root ganglia express functional NMDA receptors. *Neuroscience* 240, 135–146. doi: 10.1016/j.neuroscience.2013.02.031
- Chessell, I. P., Hatcher, J. P., Bountra, C., Michel, A. D., Hughes, J. P., Green, P., et al. (2005). Disruption of the P2X7 purinoceptor gene abolishes chronic inflammatory and neuropathic pain. *Pain* 114, 386–396. doi: 10.1016/j.pain.2005.01.002
- Clark, A. K., Staniland, A. A., Marchand, F., Kaan, T. K. Y., McMahon, S. B., and Malcangio, M. (2010). P2X7-dependent release of interleukin-1 and nociceptin in the spinal cord following lipopolysaccharide. *J. Neurosci.* 30, 573–582. doi: 10.1523/JNEUROSCI.3295-09.2010
- Colomar, A., Marty, V., Médina, C., Combe, C., Parnet, P., Amédée, T., et al. (2003). Maturation and release of interleukin-1 β by lipopolysaccharide-primed mouse Schwann cells require the stimulation of P2X7 receptors. *J. Biol. Chem.* 278, 30732–30740. doi: 10.1074/jbc.M304534200
- Costa, F. A. L., and Moreira Neto, F. L. (2015). Satellite glial cells in sensory ganglia: its role in pain. *Braz. J. Anesthesiol.* 65, 73–81. doi: 10.1016/j.bjan.2013.07.013
- Cunha, J. M., Cunha, F. Q., Poole, S., and Ferreira, S. H. (2000). Cytokine-mediated inflammatory hyperalgesia limited by interleukin-1 receptor antagonist. *Br. J. Pharmacol.* 130, 1418–1424. doi: 10.1038/sj.bjp.0703434
- De Corato, A., Lisi, L., Capuano, A., Tringali, G., Tramutola, A., Navarra, P., et al. (2011). Trigeminal satellite cells express functional calcitonin gene-related peptide receptors, whose activation enhances interleukin-1 β pro-inflammatory effects. *J. Neuroimmunol.* 237, 39–46. doi: 10.1016/j.jneuroim.2011.05.013
- De Marchi, E., Orioli, E., Dal Ben, D., and Adinolfi, E. (2016). “P2X7 Receptor as a Therapeutic Target,” in *Advances in Protein Chemistry and Structural Biology*, ed. R. Donev (Cambridge, MA: Academic Press Inc), 39–79.
- Dell’Antonio, G., Quattrini, A., Cin, E. D., Fulgenzi, A., and Ferrero, M. E. (2002). Relief of inflammatory pain in rats by local use of the selective P2X7 ATP receptor inhibitor, oxidized ATP. *Arthritis Rheumatism* 46, 3378–3385. doi: 10.1002/art.10678
- Devor, M. (1999). Unexplained peculiarities of the dorsal root ganglion. *Pain* 82, S27–S35. doi: 10.1016/S0304-3959(99)00135-9
- Dinarello, C. A. (2018). Overview of the IL-1 family in innate inflammation and acquired immunity. *Immunol. Rev.* 281, 8–27. doi: 10.1111/imr.12621
- Ding, Y., Cesare, P., Drew, L., Nikitaki, D., and Wood, J. N. (2000). J. ATP, P2X receptors and pain pathways. *J. Auton. Nervous Syst.* 81, 289–294. doi: 10.1016/S0165-1838(00)00131-4
- Dissing-Olesen, L., LeDue, J. M., Rungta, R. L., Hefendehl, J. K., Choi, H. B., and MacVicar, B. A. (2014). Activation of neuronal NMDA receptors triggers transient ATP-mediated microglial process outgrowth. *J. Neurosci.* 34, 10511–10527. doi: 10.1523/JNEUROSCI.0405-14.2014
- Donnelly-Roberts, D. L., Namovic, M. T., Han, P., and Jarvis, M. F. (2009). Mammalian P2X7 receptor pharmacology: comparison of recombinant mouse, rat and human P2X7 receptors. *Br. J. Pharmacol.* 157, 1203–1214. doi: 10.1111/j.1476-5381.2009.00233.x
- England, S., Hebllich, F., James, I. F., Robbins, J., and Docherty, R. J. (2001). Bradykinin evokes a Ca²⁺-activated chloride current in non-neuronal cells isolated from neonatal rat dorsal root ganglia. *J. Physiol.* 530, 395–403. doi: 10.1111/j.1469-7793.2001.0395k.x
- Esposito, M. F., Malayil, R., Hanes, M., and Deer, T. (2019). Unique characteristics of the dorsal root ganglion as a target for neuromodulation. *Pain Med.* 20, S23–S30. doi: 10.1093/pm/pnz012
- Fabbretti, E. (2013). ATP P2X3 receptors and neuronal sensitization. *Front. Cell. Neurosci.* 7:236. doi: 10.3389/fncel.2013.00236
- Fan, W., Zhu, X., He, Y., Zhu, M., Wu, Z., Huang, F., et al. (2019). The role of satellite glial cells in orofacial pain. *J. Neurosci. Res.* 97, 393–401. doi: 10.1002/jnr.24341
- Ferrari, D., Pizzirani, C., Adinolfi, E., Lemoli, R. M., Curti, A., Idzko, M., et al. (2006). The P2X 7 receptor: a key player in IL-1 processing and release. *J. Immunol.* 176, 3877–3883. doi: 10.4049/jimmunol.176.7.3877
- Ferrari, L. F., Cunha, F. Q., Parada, C. A., and Ferreira, S. H. (2007). A novel technique to perform direct intraganglionic injections in rats. *J. Neurosci. Methods* 159, 236–243. doi: 10.1016/j.jneumeth.2006.07.025
- Ferrari, L. F., Lotufo, C. M., Araldi, D., Rodrigues, M. A., Macedo, L. P., Ferreira, S. H., et al. (2014). Inflammatory sensitization of nociceptors depends on activation of NMDA receptors in DRG satellite cells. *Proc. Natl. Acad. Sci. U.S.A.* 111, 18363–18368. doi: 10.1073/pnas.1420601111
- Ferreira, S. H. (1981). Inflammatory pain, prostaglandin hyperalgesia and the development of peripheral analgesics. *Trends Pharmacol. Sci.* 2, 183–186. doi: 10.1016/0165-6147(81)90306-0
- Ferreira, S. H., Lorenzetti, B. B., Bristow, A. F., and Poole, S. (1988). Interleukin-1 β as a potent hyperalgesic agent antagonized by a tripeptide analogue. *Nature* 334, 698–700. doi: 10.1038/334698a0
- Fitz, J. G. (2007). Regulation of cellular ATP release. *Trans. Am. Clin. Climatol. Assoc.* 118, 199–208.
- Garlanda, C., Dinarello, C. A., and Mantovani, A. (2013). The interleukin-1 family: back to the future. *Immunity* 39, 1003–1018. doi: 10.1016/j.immuni.2013.11.010
- Giuliani, A. L., Sarti, A. C., Falzoni, S., and Di Virgilio, F. (2017). The P2X7 receptor-interleukin-1 liaison. *Front. Pharmacol.* 8:123. doi: 10.3389/fphar.2017.00123
- Goto, T., Iwai, H., Kuramoto, E., and Yamanaka, A. (2017). Neuropeptides and ATP signaling in the trigeminal ganglion. *Jap. Dental Sci. Rev.* 53, 117–124. doi: 10.1016/j.jdsr.2017.01.003
- Gu, Y., Chen, Y., Zhang, X., Li, G.-W., Wang, C., and Huang, L.-Y. M. (2010). Neuronal soma-satellite glial cell interactions in sensory ganglia and the participation of purinergic receptors. *Neuron Glia Biol.* 6, 53–62. doi: 10.1017/S1740925X10000116
- Guo, W., Wang, H., Watanabe, M., Shimizu, K., Zou, S., LaGraize, S. C., et al. (2007). Glial-cytokine-neuronal interactions underlying the mechanisms of persistent pain. *J. Neurosci.* 27, 6006–6018. doi: 10.1523/JNEUROSCI.0176-07.2007
- Hanani, M. (2005). Satellite glial cells in sensory ganglia: from form to function. *Brain Res. Brain Res. Rev.* 48, 457–476. doi: 10.1016/j.brainresrev.2004.09.001
- Hanani, M. (2012). Intercellular communication in sensory ganglia by purinergic receptors and gap junctions: implications for chronic pain. *Brain Res.* 1487, 183–191. doi: 10.1016/j.brainres.2012.03.070
- He, W. J., Cui, J., Du, L., Zhao, Y. D., Burnstock, G., Zhou, H. D., et al. (2012). Spinal P2X 7 receptor mediates microglia activation-induced neuropathic pain in the sciatic nerve injury rat model. *Behav. Brain Res.* 226, 163–170. doi: 10.1016/j.bbr.2011.09.015
- Honore, P., Donnelly-Roberts, D., Namovic, M., Zhong, C., Wade, C., Chandran, P., et al. (2009). The antihyperalgesic activity of a selective P2X7 receptor antagonist, A-839977, is lost in IL-1 $\alpha\beta$ knockout mice. *Behav. Brain Res.* 204, 77–81. doi: 10.1016/j.bbr.2009.05.018
- Honore, P., Donnelly-Roberts, D., Namovic, M. T., Hsieh, G., Zhu, C. Z., Mikusa, J. P., et al. (2006). A-740003 [N-(1-[(cyanoinimino)(5-quinolinylamino)methyl]amino)-2,2-dimethylpropyl)-2-(3,4-dimethoxyphenyl)acetamide], a novel and selective P2X7 receptor antagonist, dose-dependently reduces neuropathic pain in the rat. *J. Pharmacol. Exp. Ther.* 319, 1376–1385. doi: 10.1124/jpet.106.111559

- Huang, L.-Y., and Neher, E. (1996). Ca²⁺-dependent exocytosis in the somata of dorsal root ganglion neurons. *Neuron* 17, 135–145. doi: 10.1016/S0896-6273(00)80287-1
- Huang, L.-Y. M., Gu, Y., and Chen, Y. (2013). Communication between neuronal somata and satellite glial cells in sensory ganglia. *Glia* 61, 1571–1581. doi: 10.1002/glia.22541
- Huang, T.-Y. Y., Belzer, V., and Hanani, M. (2010). Gap junctions in dorsal root ganglia: possible contribution to visceral pain. *Eur. J. Pain* 14, e1–e11. doi: 10.1016/j.ejpain.2009.02.005
- Inoue, K., and Tsuda, M. (2012). Purinergic systems, neuropathic pain and the role of microglia. *Exp. Neurol.* 234, 293–301. doi: 10.1016/j.expneurol.2011.09.016
- Jarvis, M. F. (2010). The neural-glial purinergic receptor ensemble in chronic pain states. *Trends Neurosci.* 33, 48–57. doi: 10.1016/j.tins.2009.10.003
- Joseph, E. K., Parada, C. A., and Levine, J. D. (2003). Hyperalgesic priming in the rat demonstrates marked sexual dimorphism. *Pain* 105, 143–150. doi: 10.1016/S0304-3959(03)00175-1
- Kobayashi, K., Fukuoka, T., Yamanaka, H., Dai, Y., Obata, K., Tokunaga, A., et al. (2005). Differential expression patterns of mRNAs for P2X receptor subunits in neurochemically characterized dorsal root ganglion neurons in the rat. *J. Comp. Neurol.* 481, 377–390. doi: 10.1002/cne.20393
- Kobayashi, K., Takahashi, E., Miyagawa, Y., Yamanaka, H., and Noguchi, K. (2011). Induction of the P2X7 receptor in spinal microglia in a neuropathic pain model. *Neurosci. Lett.* 504, 57–61. doi: 10.1016/j.neulet.2011.08.058
- Kobayashi, K., Yamanaka, H., and Noguchi, K. (2013). Expression of ATP receptors in the rat dorsal root ganglion and spinal cord. *Anat. Sci. Int.* 88, 10–16. doi: 10.1007/s12565-012-0163-9
- Krames, E. S. (2014). The role of the dorsal root ganglion in the development of neuropathic pain. *Pain. Med.* 15, 1669–1685. doi: 10.1111/pme.12413
- Kushnir, R., Cherkas, P. S., and Hanani, M. (2011). Peripheral inflammation upregulates P2X receptor expression in satellite glial cells of mouse trigeminal ganglia: a calcium imaging study. *Neuropharmacology* 61, 739–746. doi: 10.1016/j.neuropharm.2011.05.019
- Lazarowski, E. R. (2012). Vesicular and conductive mechanisms of nucleotide release. *Purinergic Signal.* 8, 359–373. doi: 10.1007/s11302-012-9304-9
- Lemes, J. B. P., de Campos Lima, T., Santos, D. O., Neves, A. F., de Oliveira, F. S. F. S., Parada, C. A., et al. (2018). Participation of satellite glial cells of the dorsal root ganglia in acute nociception. *Neurosci. Lett.* 676, 8–12. doi: 10.1016/j.neulet.2018.04.003
- Li, J., Li, X., Jiang, X., Yang, M., Yang, R., Burnstock, G., et al. (2017). Microvesicles shed from microglia activated by the P2X7-p38 pathway are involved in neuropathic pain induced by spinal nerve ligation in rats. *Purinergic Signal.* 13, 13–26. doi: 10.1007/s11302-016-9537-0
- Linhart, O., Obreja, O., and Kress, M. (2003). The inflammatory mediators serotonin, prostaglandin e2 and bradykinin evoke calcium influx in rat sensory neurons. *Neuroscience* 118, 69–74. doi: 10.1016/S0306-4522(02)00960-0
- Liu, S., Shi, Q., Zhu, Q., Zou, T., Li, G. G., Huang, A., et al. (2015). P2X7 receptor of rat dorsal root ganglia is involved in the effect of moxibustion on visceral hyperalgesia. *Purinergic Signal.* 11, 161–169. doi: 10.1007/s11302-014-9439-y
- Luchting, B., Heyn, J., Woehle, T., Rächinger-Adam, B., Kreth, S., Hinske, L. C., et al. (2016). Differential expression of P2X7 receptor and IL-1 β in nociceptive and neuropathic pain. *J. Neuroinflamm.* 13:100. doi: 10.1186/s12974-016-0565-z
- Maelfait, J., Vercammen, E., and Janssens, S. (2008). Stimulation of Toll-like receptor 3 and 4 induces interleukin-1 β maturation by caspase-8. *J. Exp. Med.* 205, 1967–1973. doi: 10.1084/jem.20071632
- Magni, G., Riccio, D., and Ceruti, S. (2018). Tackling chronic pain and inflammation through the purinergic system. *Curr. Med. Chem.* 25, 3830–3865. doi: 10.2174/0929867324666170710110630
- Malik, A., and Kanneganti, T.-D. (2017). Inflammasome activation and assembly at a glance. *J. Cell Sci.* 130, 3955–3963. doi: 10.1242/jcs.207365
- Matsuka, Y., Neubert, J. K., Maidment, N. T., and Spigelman, I. (2001). Concurrent release of ATP and substance P within guinea pig trigeminal ganglia in vivo. *Brain Res.* 915, 248–255. doi: 10.1016/S0006-8993(01)02888-8
- McGaraughty, S., Chu, K. L., Namovic, M. T., Donnelly-Roberts, D. L., Harris, R. R., Zhang, X.-F., et al. (2007). P2X7-related modulation of pathological nociception in rats. *Neuroscience* 146, 1817–1828. doi: 10.1016/j.neuroscience.2007.03.035
- Neeb, L., Hellen, P., Boehnke, C., Hoffmann, J., Schuh-Hofer, S., Dirnagl, U., et al. (2011). IL-1 β stimulates COX-2 dependent PGE2 synthesis and CGRP release in rat trigeminal ganglia cells. *PLoS One* 6:e17360. doi: 10.1371/journal.pone.0017360
- North, R. A. (2002). Molecular physiology of P2X receptors. *Physiol. Rev.* 82, 1013–1067. doi: 10.1152/physrev.00015.2002
- North, R. A. (2016). P2X receptors. *Philos. Trans. R. Soc. Lond. B Biol. Sci.* 371, 20150427. doi: 10.1098/rstb.2015.0427
- Oliveira, M. C., Pegregrini-da-Silva, A., Tambeli, C. H., and Parada, C. A. (2009). Peripheral mechanisms underlying the essential role of P2X3,2/3 receptors in the development of inflammatory hyperalgesia. *Pain* 141, 127–134. doi: 10.1016/j.pain.2008.10.024
- Pannese, E. (2010). The structure of the perineuronal sheath of satellite glial cells (SGCs) in sensory ganglia. *Neuron Glia Biol.* 6, 3–10. doi: 10.1017/S1740925X10000037
- Prado, F. C., Araldi, D., Vieira, A. S., Oliveira-Fusaro, M. C. G., Tambeli, C. H., and Parada, C. A. (2013). Neuronal P2X3 receptor activation is essential to the hyperalgesia induced by prostaglandins and sympathomimetic amines released during inflammation. *Neuropharmacology* 67, 252–258. doi: 10.1016/j.neuropharm.2012.11.011
- Puerto, A., Wondosell, F., and Garrido, J. J. (2013). Neuronal and glial purinergic receptors functions in neuron development and brain disease. *Front. Cell. Neurosci.* 7:197. doi: 10.3389/fncel.2013.00197
- Rampe, D., Wang, L., and Ringheim, G. E. (2004). P2X7 receptor modulation of β -amyloid- and LPS-induced cytokine secretion from human macrophages and microglia. *J. Neuroimmunol.* 147, 56–61. doi: 10.1016/j.jneuroim.2003.10.014
- Ren, K., and Torres, R. (2009). Role of interleukin-1 β during pain and inflammation. *Brain Res. Rev.* 60, 57–64. doi: 10.1016/j.brainresrev.2008.12.020
- Samad, T. A., Moore, K. A., Sapirstein, A., Billet, S., Allchorne, A., Poole, S., et al. (2001). Interleukin-1 β -mediated induction of Cox-2 in the CNS contributes to inflammatory pain hypersensitivity. *Nature* 410, 471–475. doi: 10.1038/35068566
- Sapunar, D., Kostic, S., Banozic, A., and Puljak, L. (2012). Dorsal root ganglion - a potential new therapeutic target for neuropathic pain. *J. Pain Res.* 5, 31–38. doi: 10.2147/JPR.S26603
- Savio, L. E. B., de Andrade Mello, P., da Silva, C. G., and Coutinho-Silva, R. (2018). The P2X7 receptor in inflammatory diseases: angel or demon? *Front. Pharmacol.* 9:52. doi: 10.3389/fphar.2018.00052
- Song, X. M., Xu, X. H., Zhu, J., Guo, Z., Li, J., He, C., et al. (2015). Up-regulation of P2X7 receptors mediating proliferation of Schwann cells after sciatic nerve injury. *Purinergic Signal.* 11, 203–213. doi: 10.1007/s11302-015-9445-8
- Stoffels, M., Zaal, R., Kok, N., van der Meer, J. W. M., Dinarello, C. A., and Simon, A. (2015). ATP-Induced IL-1 β specific secretion: true under stringent conditions. *Front. Immunol.* 6:54. doi: 10.3389/fimmu.2015.00054
- Takeda, M., Tanimoto, T., Kadoi, J., Nasu, M., Takahashi, M., Kitagawa, J., et al. (2007). Enhanced excitability of nociceptive trigeminal ganglion neurons by satellite glial cytokine following peripheral inflammation. *Pain* 129, 155–166. doi: 10.1016/j.pain.2006.10.007
- Teixeira, J. M., Oliveira, M. C. G., Parada, C. A., and Tambeli, C. H. (2010). Peripheral mechanisms underlying the essential role of P2X7 receptors in the development of inflammatory hyperalgesia. *Eur. J. Pharmacol.* 644, 55–60. doi: 10.1016/j.ejphar.2010.06.061
- Torres-Chávez, K. E., Fischer, L., Teixeira, J. M., Fávoro-Moreira, N. C., Obando-Pereda, G. A., Parada, C. A., et al. (2011). Sexual dimorphism on cytokines expression in the temporomandibular joint: the role of gonadal steroid hormones. *Inflammation* 34, 487–498. doi: 10.1007/s10753-010-9256-6
- Toulme, E., Tsuda, M., Khakh, B. S., and Inoue, K. (2010). “On the role of ATP-gated P2X receptors in acute,” in *Inflammatory and Neuropathic Pain*, 2010th Edn, eds L. Kruger and A. R. Light (Boca Raton, FL: CRC Press).
- Tse, K. H., Chow, K. B. S., Leung, W. K., Wong, Y. H., and Wise, H. (2014). Primary sensory neurons regulate Toll-like receptor-4-dependent activity of glial cells in dorsal root ganglia. *Neuroscience* 279, 10–22. doi: 10.1016/j.neuroscience.2014.08.033
- Verderio, C., and Matteoli, M. (2011). ATP in neuron-glia bidirectional signalling. *Brain Res. Rev.* 66, 106–114. doi: 10.1016/j.brainresrev.2010.04.007
- Verri, W. A., Cunha, T. M., Parada, C. A., Poole, S., Cunha, F. Q., and Ferreira, S. H. (2006). Hypernociceptive role of cytokines and chemokines: targets for analgesic drug development? *Pharmacol. Ther.* 112, 116–138. doi: 10.1016/j.pharmthera.2006.04.001

- Vivancos, G. G., Verri, W. A. Jr., Cunha, T. M., Schivo, R. S. I., Parada, C. A., Cunha, F. Q., et al. (2004). An electronic pressure-meter nociception paw test for rats. *Braz. J. Med. Biol. Res.* 37, 391–399. doi: 10.1590/S0100-879X2004000300017
- Wu, B., Peng, L., Xie, J., Zou, L., Zhu, Q., Jiang, H., et al. (2017). The P2X7 receptor in dorsal root ganglia is involved in HIV gp120-associated neuropathic pain. *Brain Res. Bull.* 135, 25–32. doi: 10.1016/j.brainresbull.2017.09.006
- Zhang, W., Zhu, Z., and Liu, Z. (2020). The role and pharmacological properties of the P2X7 receptor in neuropathic pain. *Brain Res. Bull.* 155, 19–28. doi: 10.1016/j.brainresbull.2019.11.006
- Zhang, X., Chen, Y., Wang, C., and Huang, L.-Y. (2007). Neuronal somatic ATP release triggers neuron-satellite glial cell communication in dorsal root ganglia. *Proc. Natl. Acad. Sci. U.S.A.* 104, 9864–9869. doi: 10.1073/pnas.0611048104
- Zhang, X.-F. F., Han, P., Faltynek, C. R., Jarvis, M. F., and Shieh, C.-C. C. (2005). Functional expression of P2X7 receptors in non-neuronal cells of rat dorsal root ganglia. *Brain Res.* 1052, 63–70. doi: 10.1016/j.brainres.2005.06.022
- Zimmermann, M. (1983). Ethical guidelines for investigations of experimental pain in conscious animals. *Pain* 16, 109–110. doi: 10.1016/0304-3959(83)90201-4

Conflict of Interest: The authors declare that the research was conducted in the absence of any commercial or financial relationships that could be construed as a potential conflict of interest.

Copyright © 2020 Neves, Farias, de Magalhães, Araldi, Pagliusi, Tambeli, Sartori, Lotufo and Parada. This is an open-access article distributed under the terms of the Creative Commons Attribution License (CC BY). The use, distribution or reproduction in other forums is permitted, provided the original author(s) and the copyright owner(s) are credited and that the original publication in this journal is cited, in accordance with accepted academic practice. No use, distribution or reproduction is permitted which does not comply with these terms.



Tyrosine Kinase Inhibitors Reduce NMDA NR1 Subunit Expression, Nuclear Translocation, and Behavioral Pain Measures in Experimental Arthritis

Karin N. Westlund^{1,2,3*}, Ying Lu³, Liping Zhang³, Todd C. Pappas^{3†}, Wen-Ru Zhang³, Giulio Tagliatela^{3,4}, Sabrina L. McIlwrath¹ and Terry A. McNearney^{3,5,6‡}

OPEN ACCESS

Edited by:

Peter Santha,
University of Szeged, Hungary

Reviewed by:

Han-Rong Weng,
Mercer University, United States
Pablo Munoz,
University of Valparaíso, Chile

*Correspondence:

Karin N. Westlund
khigh@salud.unm.edu

†Present address:

Todd C. Pappas,
Head of Clinical Research, Everlywell
Inc., Austin, TX, United States

‡Consultant, Self-employed,
Houston, TX, United States

Specialty section:

This article was submitted to
Integrative Physiology,
a section of the journal
Frontiers in Physiology

Received: 17 December 2019

Accepted: 08 April 2020

Published: 27 May 2020

Citation:

Westlund KN, Lu Y, Zhang L,
Pappas TC, Zhang W-R,
Tagliatela G, McIlwrath SL and
McNearney TA (2020) Tyrosine Kinase
Inhibitors Reduce NMDA NR1 Subunit
Expression, Nuclear Translocation,
and Behavioral Pain Measures
in Experimental Arthritis.
Front. Physiol. 11:440.
doi: 10.3389/fphys.2020.00440

¹ Research Division, New Mexico VA Health Care System, Albuquerque, NM, United States, ² Anesthesiology, University of New Mexico Health Sciences Center, Albuquerque, NM, United States, ³ Neuroscience and Cell Biology, University of Texas Medical Branch at Galveston, Galveston, TX, United States, ⁴ Neurology, University of Texas Medical Branch at Galveston, Galveston, TX, United States, ⁵ Microbiology and Immunology, University of Texas Medical Branch at Galveston, Galveston, TX, United States, ⁶ Internal Medicine, University of Texas Medical Branch at Galveston, Galveston, TX, United States

In the lumbar spinal cord dorsal horn, release of afferent nerve glutamate activates the neurons that relay information about injury pain. Here, we examined the effects of protein tyrosine kinase (PTK) inhibition on NMDA receptor NR1 subunit protein expression and subcellular localization in an acute experimental arthritis model. PTK inhibitors genistein and lavendustin A reduced cellular histological translocation of NMDA NR1 in the spinal cord occurring after the inflammatory insult and the nociceptive behavioral responses to heat. The PTK inhibitors were administered into lumbar spinal cord by microdialysis, and secondary heat hyperalgesia was determined using the Hargreaves test. NMDA NR1 cellular protein expression and nuclear translocation were determined by immunocytochemical localization with light and electron microscopy, as well as with Western blot analysis utilizing both C- and N-terminal antibodies. Genistein and lavendustin A (but not inactive lavendustin B or diadzein) effectively reduced (i) pain related behavior, (ii) NMDA NR1 subunit expression increases in spinal cord, and (iii) the shift of NR1 from a cell membrane to a nuclear localization. Genistein pre-treatment reduced these events that occur *in vivo* within 4 h after inflammatory insult to the knee joint with kaolin and carrageenan (k/c). Cycloheximide reduced glutamate activated upregulation of NR1 content confirming synthesis of new protein in response to the inflammatory insult. In addition to this *in vivo* data, genistein or staurosporin inhibited upregulation of NMDA NR1 protein and nuclear translocation *in vitro* after treatment of human neuroblastoma clonal cell cultures (SH-SY5Y) with glutamate or NMDA (4 h). These studies provide evidence that inflammatory activation of peripheral nerves initiates increase in NMDA NR1 in the spinal cord coincident with development of pain related behaviors through glutamate non-receptor, PTK dependent cascades.

Keywords: pain, membrane trafficking, inflammation, glutamate, central sensitization, genistein

INTRODUCTION

A critical and unresolved issue in activation dependent neuronal signaling is identification of the numerous signaling molecules and matching them with their specific roles. Discovery and systematic dissection of signaling networks that contribute to inflammatory pain have revealed complex interactions (Hammaker et al., 2003; Kawasaki et al., 2004; Latremoliere and Woolf, 2009), initiated after the significant rise of glutamate following an inflammatory insult (Sluka and Westlund, 1992, 1993a,b; Sorkin et al., 1992). Non-receptor Src family protein tyrosine kinase (PTK) interactions with tyrosine residues of ionotropic NMDA receptor NR2A/B subunits impact phosphorylation, channel protein insertion, and activation state, particularly in the hippocampus as it impacts long term potentiation (LTP). The NMDA receptor NR1 subunit, part of this heteromeric ion channel, has been less well studied since it was reported that immunoprecipitated NR1 is not phosphorylated on tyrosine residues in hippocampal preparations (Lau and Huganir, 1995; Huang and Hsu, 1999).

In the present study, NR1 expression increase in the lumbar spinal cord was initiated by knee joint inflammation with k/c injection. Two PTK inhibitors (genistein and lavendustin A) and their inactive analogs (diadzein and lavendustin B) were investigated to determine their influence on pain related behavior, spinal cord content and cellular localization of NR1 after inflammatory hindlimb insult. The PTK inhibitors reduced spinal cord NR1 neuronal expression and nuclear translocation in the spinal cord, as well as improved secondary heat hypersensitivity on the footpad in an experimental knee joint arthritis.

MATERIALS AND METHODS

Animals

All studies followed the Institutional Animal Care and Use Committee Guidelines, in accordance with the guidelines of the National Institutes of Health and the international Association for the Study of Pain. Eighty-eight Sprague–Dawley rats (250–300 g, Harlan) were used in these pharmacologic, biochemical, behavioral and immunocytochemistry studies. All efforts were made to minimize animal suffering, to reduce the number of animals used, and to utilize alternatives to *in vivo* techniques, when available. All animals were housed in a room with a constant ambient temperature of 22°C and 12 h light/dark cycle with free access to food and water.

Pre-treatment in Rats With Acute Monoarthritis

On Day 1, anesthetized animals received surgical implantation of a microdialysis fiber for spinal administration of PTK

inhibitors and inactive analogs. On Day 2, baseline behavioral testing was followed by pre-treatment infusion of agents for 1.5 h, prior to induction of knee joint inflammation under brief anesthesia. Behavioral testing was repeated 4 h after induction of joint inflammation. Use of a k/c knee joint injection (k/c, 3%/3%, 0.1 ml in saline) acute inflammatory pain model allows clear separation of the zone of inflammation and the sensitized hindpaw for testing responses (secondary hyperalgesia) indicative of central sensitization. Animals were anesthetized and either (i) transcardially perfused with paraformaldehyde (PFA) for light and EM immunohistochemical and immunogold studies, or (ii) fresh, frozen tissues collected for biochemical analysis.

PTK Inhibitors and Cycloheximide

Two PTK inhibitors and their inactive analogs were compared in these studies ($n = 30$). Genistein (5, 7-dihydroxy-3-(4-hydroxyphenyl)-4H-1-benzopyran-4-one; 4',5,7-trihydroxy-isoflavone, Cat # G-103, RBI, Natick, MA, United States) is a reversible PTK inhibitor that decreases NMDA currents in hippocampal patch clamp studies (Akiyama et al., 1987; Wang and Salter, 1994; Yu et al., 2016). Daidzein (4',7-Dihydroxyisoflavone), is an analog of genistein that lacks PTK inhibitory activity and had no effect on NMDA currents in patch clamp studies. Lavendustin A (5-Amino-[N-2,5-dihydroxybenzyl-N'-2-hydroxybenzyl] salicylic acid, Cat # 428150, Lot #B42143 Calbiochem, LaJolla, CA, United States), is a structurally distinct PTK inhibitor that reversibly depressed NMDA currents, and was tested along with its inactive analog, lavendustin B (5-amino-(N,N'-bis-2-hydroxybenzyl) salicylic acid, Cat # 428160, Lot # B39919 & B49301, Calbiochem). The drugs (genistein, lavendustin A & B and daidzein) were dissolved in the 50% dimethyl sulfoxide (DMSO) in aCSF vehicle.

Cycloheximide is a widely used protein synthesis inhibitor and actinomycin D, a potent transcription inhibitor. Cycloheximide [$n = 3$, 30 mg/kg, intraperitoneal (i.p.)] or actinomycin D ($n = 3$, 10 mg/kg, i.p.) were given in some *in vivo* studies to determine if the observed staining density and intracellular localization changes were due to *de novo* NR1 protein synthesis.

Spinal Microdialysis Installation for Drug Infusion

One day prior to the induction of arthritis, the microdialysis fiber was surgically implanted in anesthetized rats (sodium pentobarbital, 40 mg/kg) (Skilling et al., 1988; Sluka and Westlund, 1992). A small midline incision was made in the skin over the L1 vertebral level. The vertebrae were cleared of muscle and 1 mm holes were drilled in the lateral aspect on both sides of the L1 vertebrae to expose access to the L3–L4 spinal segment. A microdialysis fiber (200 μ m o.d., 45,000 MW cut-off, Hospal, AN69) was threaded transversely across the dorsal horn through the holes and stabilized with dental cement. The microdialysis fiber was coated with epoxy except for the 2 mm permeable portion passing through the spinal gray matter. The microdialysis fiber was connected to PE₂₀ tubing (Becton Dickinson & Co., San Diego, CA, United States) which was tunneled under the

Abbreviations: aCSF, artificial cerebrospinal fluid; DAB, diaminobenzidine; DRG, dorsal root ganglia; EM, electron microscopy; GABA, gamma amino butyric acid; k/c, kaolin/carrageenan; LPS, lipopolysaccharide; NGF, nerve growth factor; NMDA, N-methyl-D-aspartate; NR1, NMDA receptor 1; PTK, non-receptor protein tyrosine kinase; PWL, paw withdrawal latency; WGA-HRP, wheat germ agglutinin-horse radish peroxidase.

skin to the nape of the neck. In surgical control animals, the microdialysis fiber was implanted only in the subcutaneous tissue over the back muscle and similarly tunneled to the neck. This facilitated the blinded approach. The aCSF was infused (5 μ l/min) for 1.5 h and then the tube was heat sealed for use on the following day.

Dose Response and Estimate of Drug Delivered

Based on estimates for genistein concentrations measured by spectrophotometer (Beckman DU650, Beckman Coulter, Inc., Fullerton, CA, United States) after transfer across the microdialysis membrane into aCSF, a maximum of 5.6% of the drug dose in the tube crosses into the tissue. Therefore, with the diffusion barriers presented by the tissue, the neurons are likely to have been maximally exposed to <56 μ M genistein or <25 μ M lavendustin, much lower than the 1 mM concentration inside the microdialysis fiber. It has been shown that doses of genistein greater than 30 μ M can directly inhibit NMDA channel activation, while lower doses and lavendustin A inhibit PTK activation and have no direct effect on NMDA channels (Huang et al., 2010).

Dose response curves for paw withdrawal latency in response to stimulation with heat were generated for animals receiving genistein spinally at concentrations inside the microdialysis of 200 μ M ($n = 3$), 500 μ M ($n = 4$), 1 mM ($n = 9$), and 2 mM ($n = 3$). The most effective pre-treatment dose for spinally administered genistein was 1 mM. Animals received spinal lavendustin A or B as positive and negative controls for genistein, respectively. Concentrations tested were 0.1 mM ($n = 3$), 0.5 mM ($n = 3$), and 1 mM ($n = 5$). The most effective dose of lavendustin A in these pre-treatment studies was 0.5 mM. A genistein dose of 1 mM was used for the surgical control animals ($n = 3$) receiving superficial implantation of the microdialysis tubing for subcutaneous drug delivery. Daidzein was also tested at a dose of 1 mM ($n = 3$). Also, eight additional control animals received the vehicle (V), 50% DMSO in aCSF.

Induction of the Knee Joint Inflammation Model

An acute inflammatory response restricted to the knee joint was induced when 3% kaolin and 3% carrageenan (k/c; in sterile saline; 0.1 ml; pH 7.4) was injected directly into the joint cavity while animals were briefly anesthetized with sodium methohexital (Brevital, 40 mg/kg, i.p., Mettawa, IL, United States). The knee joint was flexed manually until the rat awakened (approximately 5–10 min). Behavioral testing was initiated 4 h after k/c intra-articular injection. In this k/c arthritis model, localized joint swelling, as well as limping and guarding of the limb, were well developed 4 h post-injection (Sluka and Westlund, 1993a). Surface temperature readings of both knees were obtained with a digital infrared temperature probe. Bilateral knee joint circumferences were obtained with a thin, flexible tape measure around the center of the knee joint with the limb held in extension. Measurements were collected before (baseline) and 4 h after intra-articular injection of the knee joint with k/c after

the rat was re-anesthetized with sodium pentobarbital (40 mg/kg, i.p.), just prior to perfusion with 4% paraformaldehyde (PFA).

Behavioral Assessment

Fifty-eight rats were used for the behavioral studies. The nociceptive behavioral measure documented bilaterally was decreased threshold withdrawal response to radiant heat, reflecting secondary heat hypersensitivity and central sensitization (Hargreaves et al., 1988; Sluka et al., 1994). Animals were placed in Lucite cubicles on a glass top table cooled with a fan and allowed to accommodate for 30 minutes prior to testing. A hand-held metal box focusing a high intensity light through an aperture (1 \times 0.8 cm) was used to apply radiant heat through the glass to the plantar surface of the hindpaw until the animal lifted its hindpaw. The time delay until reflexive withdrawal response was considered the paw withdrawal latency (PWL), measured in seconds (s). Both hindpaws were tested independently at 5 min intervals for a total of 5 trials. A mean of these 5 readings was used as PWL response at each time point. The same observer performed the tests for each group under blinded conditions. A 15 s duration was used as a maximum cutoff, but was never employed. In the experimental rats, the PWL was measured before (baseline) placement of the microdialysis fiber (Day 1) and after administration of drug or vehicle had been infused for 1.5 h (Day 2) at which time k/c was injected into the knee joint. The final measurement for PWL was 4 h after induction of arthritis.

Immunocytochemical Localization of NMDA Receptor Subunit NR1

Animal Preparations

Animals were anesthetized and transcardially perfused with a brief warm saline rinse followed by fixative solution (4% PFA in 0.1 M phosphate buffer, pH 7.4). The lumbar spinal cord (L4–6) was dissected and tissues were soaked overnight in 30% buffered sucrose and cut frozen at 30 μ m on a sliding microtome. Tissue sections were randomly selected from serial sets spaced at least 100 μ m apart. The tissues from some animals ($n = 8$) were briefly permeabilized with a 50% buffered ethanol treatment or Triton-X 100 added to the diluent.

Spinal Cord Immunohistochemistry for NMDA NR1 Subunit

Tissue sections from twenty one rats were stained immunocytochemically for glutamate receptors NR1, NR2A/B, NR2C, mGluR1 and mGluR5 using commercial antibodies (0.5–1 μ g/ml, Chemicon International, Temecula, CA, United States). None of these receptors had staining associated with the nucleus in unstimulated conditions. The NR1 antibody was validated with RT-PCR and immunoprecipitation (McNearney et al., 2010). The primary antibodies were diluted in phosphate buffered saline (PBS) with 0.1% BSA and 0.1% Triton-X-100 for overnight incubation on the spinal cord tissues at room temperature on a rotating shaker. After washing in PBS (pH 7.6), the tissue sections were incubated in the appropriate secondary antibody, either anti-mouse or anti-rabbit IgG (1:200, 90 min). Sections were reacted with DAB (1.5 mg/ml) solution as the chromogen and peroxide (3%, 0.5 μ l/ml) to produce a brown

reaction product. Semi-quantitative staining density measure was determined using NIH ImageJ ($n = 5$).

Spinal Cord Immunohistochemistry for PhosphoNR1 in a Rat Model of Chronic Trigeminal Nerve Pain

To validate the nuclear immunostaining, confirmation was sought in another chronic pain model, the chronic constriction injury of the infraorbital nerve (CCI-ION) (Vos et al., 2000). The unilateral chronic constriction injury (CCI) was induced on the infraorbital trigeminal nerve (ION) branch. The rat was anesthetized with isoflurane (4.0% vol in 1.0 l/min oxygen), and the left ION dissected free within the orbital cavity. Two chromic gut sutures (5-0, Ethicon 634G, Ethicon, Somerville, NJ, United States) were tied loosely around the left ION (2 mm apart) while the naive control animal did not undergo surgery or anesthesia ($n = 3$). The incision was closed using 5-0 nylon suture (Cat. # MV-661, Med-Vet International, Mettawa, IL, United States) and animals recovered in less than 15 min following surgery. Mechanical sensitivity was tested on the whiskerpad at baseline prior to CCI surgery and weekly for the following 12 weeks when animals were euthanized, transcardially perfused with 4% PFA, and cervical spinal cord excised, cryoprotected in 30% sucrose, embedded in Optimal Cutting Temperature compound (OCT, Thermo Fisher Scientific, Ottawa, Ontario, Canada) and frozen at -80°C .

Tissue sections were cut at 20 μm thickness and collected on glass slides, washed with PBS, blocked (3% normal goat serum, 0.01% Triton X-100, in PBS) and incubated overnight in anti phosphoNR1 antibody (1:2,000; Upstate, New York, NY, United States) at room temperature on a rotating shaker. Antibody staining was visualized using a goat anti-rabbit secondary antibody conjugated to Alexa Fluor 488 (Molecular Probes) and counterstained with the nuclear dye DAPI. Images were taken at 100x magnification using light optics on the Fluoview FV1200 confocal microscope (Olympus, Center Valley, PA, United States).

Immunocytochemical Method Controls

Immunocytochemical method controls included sections processed in the absence of the primary or secondary antibody or Vectastain avidin-biotin complex (ABC) kit reagents (1 h, Vector Laboratories, Burlingame, CA, United States). The specificity of the transmitter antibodies was confirmed by appearance of a single band by Western blot using the C-terminus NR1 antibody from (0.5 to 1 $\mu\text{g}/\text{ml}$; Chemicon, Cat #AB1516, Temecula, CA, United States). This antibody identified a splice variant containing a nuclear localization sequence region. An N-terminus NR1 antibody (Upstate, New York, NY, United States) provided equivalent localization in spinal cord and in cultured human clonal SH-SY5Y cells. To further intensify the reaction product, particularly for visualization of nuclear rings, some of the tissues were treated with colloidal gold conjugated IgG and reacted with a silver chloride solution to produce an intense black reaction product.

As a positive control, immunocytochemical staining for NF κ B p50 was also performed, with diluent only as negative control. Inhibition of nuclear localization with tyrosine kinase inhibitor

genistein was demonstrated in our tandem controls, as has been previously reported for I κ B p50 subunit degradation and NF κ B nuclear localization (Garcia Palacios et al., 2005). Increased staining for NR1 and nuclear translocation were also inhibited by NMDA receptor antagonist, MK-801, as a negative control in cultured cells.

Electron Microscopy

Ultrastructural analysis by EM was performed on spinal cords with pre- and post-embedding immunostaining. Two groups of rats ($n = 3$ each, control and 4 h after k/c induced arthritis) were deeply anesthetized, then perfused via ascending aorta puncture with a mixture of 2.5% glutaraldehyde and 1% PFA. The lumbar cords were removed and cut at a 30 μm thickness with a vibratome. The spinal cord sections were incubated overnight in 1% sodium borohydride, then 50% buffered ethanol (pH 7.4).

Pre-embedding immunostaining

Tissue sections were blocked and incubated with mouse anti-NMDA NR1 subunit monoclonal antibody overnight (Pharmingen, San Diego, CA, United States). After washing with PBS (pH 7.6, $\times 6$), tissue sections were incubated in secondary antibody, biotinylated horse anti-mouse IgG (1:100) for 2 hr. NMDA NR1 subunit was visualized after incubation with ABC kit reagents (1 h) and reaction with the chromogen DAB (1.5 mg/ml) and peroxide (3%, 0.5 $\mu\text{l}/\text{ml}$) to produce an electron dense product (Hsu et al., 1981). Final sections were treated with osmium, dehydrated through graded alcohols and embedded in Poly/BED 812 resin for visualization with an electron microscope (JEM-100CX, JEOL, Ltd., Tokyo, Japan).

Retrogradely labeled spinothalamic tract neurons

In 4 animals, injections were made into the ventral posterolateral thalamus with wheat germ agglutinin conjugated with horseradish peroxidase (WGA- HRP, Sigma-Aldrich, St. Louis, MO, United States) to identify spinal projection neurons prior to processing for immunocytochemical staining (Ye and Westlund, 1996). The WGA-HRP was visualized as large, dense crystals using tetramethylbenzidine stabilized with ammonium paratungstate and DAB. The crystals were clearly differentiated from the amorphous immunohistochemical staining for the NMDA NR1 subunit.

Post-embedding colloidal gold immunohistochemistry

With post-embedding immunogold histochemistry the antibody was bound to small round gold beads to identify the NMDA NR1 subunit (Westlund et al., 1992). Ultrathin sections on single-slot formvar coated nickel grids were etched sequentially in 1% solution of periodic acid for 10 min, 20% sodium meta-periodate for 15 min and 1% sodium borohydride for 10 min. The sections were washed in distilled water between solutions in 1:30 dilution for 30 min. Sections were placed on droplets containing the mouse anti-NMDA NR1 antibody (1:100; Pharmingen) overnight at 4°C . After wash in 0.05 M Tris-buffered saline (TBS) (pH 7.2) with 0.2% bovine serum album (BSA), grids were incubated in the rabbit anti-mouse IgG coupled to 10 nm gold

spheres (1.5 h TBS, pH 8.2, Janssen Pharmaceutica, Beerse, Belgium), washed twice in TBS buffer (pH 7.2) then distilled water, prior to uranyl acetate (5 min) and lead citrate (1–1.5 min) for contrast.

Immunocytochemistry for Clonal Neuronal Cells

Clonal human SH-SY5Y neuroblastoma cells (CRL2266, ATCC, Bethesda, MD, United States) were plated on poly-D-lysine (PDL) treated glass coverslips and maintained in a humidified atmosphere of 95% air and 5% CO₂ at 37°C in Neurobasal Medium (Invitrogen, Carlsbad, CA, United States). For nuclear translocation experiments, plated cells were incubated with 100 μM L-glutamate or vehicle for 4 h at 37°C. In some conditions, cells were preincubated with 50 μM genistein or 100 nM staurosporin, a broad spectrum tyrosine kinase inhibitor (Calbiochem) for 5 min at 37°C before the addition of 100 μM glutamate. After the incubation, the cells were fixed with 4% PFA for 1 h room temperature in preparation for staining. Three replicates minimum were studied.

Immunocytochemistry was performed using PBS containing Mg²⁺ and Ca²⁺ (PBSAT). All procedures were performed at 4°C. Cells were washed three times and post-fixed in ice-cold 70% methanol for 30 min. Fixed cells were incubated with the mouse anti-NMDA NR1-specific antibody (1:100, Pharmingen) in 1% BSA (Fraction V, Sigma) and 0.025% Tween-20 (1% PBSAT) for 16 h at 4°C on a rotating shaker. After the primary antibody was removed, the cells were washed 3 X in 1% PBSAT, then incubated with rabbit anti-mouse Alexa Fluor 488 green (1:100 dilution, 30 min, Molecular Probes, Inc., Eugene OR, United States). Cells were washed 3 X with 1% PBSAT, glass coverslips mounted on slides with 20% glycerol-PBS. Computer-assisted quantification was performed on images taken with a Nikon FXA confocal laser microscope equipped with a SPOT digital system (Nikon Instruments, Melville, NY, United States).

Western Blot Analysis Protocols

Preparation of Rat Spinal Cord for Western Blot

Rats were anesthetized at experiment end and perfused for 2 min with ice cold saline/heparin. Spinal cord L4-L6 laminae I and II were dissected and homogenized in Radioimmunoprecipitation assay (RIPA, Sigma) lysis buffer with protease inhibitors at 4°C. Samples from treated spinal cord (40 μg protein) and β-actin control (3 μg) were diluted with running buffer and loaded on 8% gels for electrophoresis (100 mv) separation for 2 h, 20 min. Protein was transferred (85–70 mv) for 90 min. The membranes were blocked with 5% milk in Tris-buffered saline with Tween-20 (TBST) for 1 hr prior to overnight incubation in mouse anti-NMDA NR1 antibody (1:1,000 in 2.5% milk TBST, 4°C, Pharmagen). After washing (5 × 6 min), membranes were incubated in goat anti-mouse IgG-HRP in 2.5% milk TBST (1:5,000) for 1 h after extensive wash and enhanced chemiluminescence (ECL) detection. Three replicates minimum were studied.

Preparation of Nuclear and Cytosolic Protein Extracts of Cultured Cells

SH-SY5Y cell cultures were plated at 10⁷/treatment group and grown to 80% confluence, then incubated 16 h in serum free F12:DMEM. Subsequently the cells were treated with final NMDA concentrations of 0, 0.1, 1.0, and 10 μM or control (water, 0.001%) in F12:DMEM for 6 h. All protein isolation procedures were performed at 4°C (Nuclei Isolation kit, NUC-101, Sigma). Cells were washed twice with divalent cation-free PBS and detached from tissue culture flasks using 1 mM EDTA in PBS. The cells were pelleted at 500 × g for 5 min and resuspended in 300 μl lysis buffer consisting of 10 mM Tris-HCl (pH 7.4), 2 mM MgCl₂, protease inhibitors (40 μg/ml phenyl methylsulfonylfluoride, 100 μg/ml leupeptin, 1 μg/ml aprotinin) and 1% thiodiglycol. Cells were lysed with 30 strokes of a type-B pestle and small fractions monitored with a microscope to confirm complete lysis of cells and intact nuclei. A 50 μl aliquot was reserved as total protein extract. The nuclei were pelleted at 800 × g and the supernatant (cytosolic fraction) removed and frozen at –80°C. The nuclei were washed once with lysis buffer and placed in 100 μl nuclear extraction buffer (400 mM NaCl, 20 mM HEPES pH 7.9, 1 mM EDTA, 1 mM EGTA, 1 mM dithiothreitol, protease inhibitors), resuspended by vortexing, and placed on a shaker at 1400 RPM in a 4°C room for 20 min. The non-soluble matter was pelleted at 10,000 × g for 20 min and the supernatant (nuclear fraction) removed and frozen at –80°C. Three replicates minimum were studied.

SDS–PAGE and Immunoblot Assays

For SDS–PAGE, 40 μg of each of the lysates was added to an equal volume of 2 x Laemmli Buffer (62.5 mM Tris-HCl pH 6.8, 2% [wt/vol] SDS, 20% [vol/vol] glycerol, 5% [vol/vol] 2-mercaptoethanol) and heated at 95°C for 5 min. The samples were resolved on pre-cast 7.5% polyacrylamide gels (Bio Rad, Hercules, CA, United States) and transferred to PVDF Hybond-P membranes. Protein was transferred (85–70 mv) for 90 min. The membranes were blocked with 5% milk in Tris-buffered saline with Tween-20 (TBST) Tris-HCL pH 8.3, 39 mM glycine, 20% methanol [vol/vol] at 80 V for 2 h. Primary anti-NMDA NR1 antibodies included a monoclonal recognizing the N-terminus (Pharmingen) and a polyclonal recognizing the C-terminus (1:100, Chemicon). Immunoreactive bands were visualized with enhanced chemiluminescence (Amersham). Three replicates minimum were studied.

Statistics

Data are presented as mean values plus or minus standard error (SE) Student's *t*-tests were used to assess significant differences in mean values between paired and unpaired groups in some studies. Comparative analyses among the treatment groups versus the vehicle group were performed on immunohistochemical and behavioral data collected at baseline and after 4 h of inflammation with one-way ANOVA and Newman-Keuls Multiple Comparison (behavior and

immunostaining density) or Mann-Whitney *U*-test (*in vitro* study) *post hoc* testing. A *p*-Value < 0.05 was considered significant.

RESULTS

Pretreatment With Genistein Attenuated Heat Hypersensitivity in Rats With k/c Induced Arthritis

Paw withdrawal latency (PWL) to radiant heat was significantly reduced from baseline at 4 h after induction of the k/c knee joint inflammation. As we have reported previously in this inflammatory arthritis model in rats, reduced PWL is indicative of central sensitization and secondary heat hyperalgesia (Sluka and Westlund, 1993a). **Figure 1** demonstrates behavioral responses in the vehicle and PTK inhibitor analog pretreatment groups with k/c arthritis. The decrease in PWL response occurred maximally on the side ipsilateral to the inflamed knee 4 h in control animals and was linearly correlated with the increase in joint swelling. In the present study, similar responses were demonstrated for arthritic rats intrathecally treated with vehicle (75.3% of baseline, *p* < 0.01).

Pre-treatment with genistein (1 mM) and the other related agents tested in naïve animals did not alter PWL values from baseline PWL, as demonstrated at 1.5 h. However, as shown in **Figure 1A**, all treatment groups with arthritis had PWL thresholds significantly less than baseline (*p* < 0.01). Pre-treatment with the PTK inhibitor, genistein, significantly attenuated the inflammation-induced decrease in PWL in this arthritis model (88.47% of baseline, *p* < 0.01 compared to vehicle pretreated arthritic rats).

The structurally distinct PTK inhibitor, Lavendustin A, also significantly abrogated the development of secondary hyperalgesia (92.28% of baseline) compared to vehicle. Secondary hyperalgesia typical of this model developed after administration of vehicle and the inactive analogs, daidzein and lavendustin B (75.32, 82.12, and 80.54% of baseline, respectively). Dose response curves are shown for genistein, lavendustin A, and lavendustin B (**Figures 1B,C**, respectively), and were used to derive the optimal doses for the full study.

Joint Temperature and Circumference in Arthritic Joints Were Unaffected by Intraspinal Genistein

Surface joint temperature (degrees Celsius) and circumference (cm) were measured at baseline, and at 4 h, when the animals were tested for secondary hyperalgesia. In all arthritic groups, the ipsilateral joint temperatures were significantly elevated compared to baseline levels (105 – 108% increase over baseline, *p* < 0.02). In addition, the ipsilateral joint circumferences were significantly increased compared to baseline levels (114 – 118% over baseline, *p* < 0.04). Although secondary hyperalgesia values were significantly blunted at the

4 h time point with intraspinal genistein and lavendustin A, increases in joint circumferences and surface temperatures in the arthritic joints were similar to the vehicle pretreated arthritic animals.

Increased Expression of Spinal NMDA NR1 Subunit 4 h After Induction of k/c-Induced Arthritis and Reduction by Genistein

NMDA NR1 Expression Changes in Spinal Cord Immunostaining

While NMDA NR1 immunostaining in the dorsal and ventral horns of the lumbar (L4) spinal cord was abundant in naïve non-arthritic rats (**Figure 2A**), NMDA NR1 immunostaining was visibly increased in the ipsilateral dorsal horn in rats with knee joint k/c induced monoarthritis at 4 h (**Figure 2B**). Analysis of immunostaining density demonstrated that NMDA NR1 staining in the lumbar spinal cord lamina I and II ipsilateral to the inflamed knee joint was greatly increased in dorsal horn in vehicle injected arthritic rats compared to naïve animals (216.95 ± 29% vs. 100%, respectively, *p* < 0.01) (**Figure 2E**). Arthritis induced increase in NMDA NR1 immunostaining was blunted by genistein pretreatment compared to those pretreated with vehicle (154.53 ± 26 vs 216.95 ± 29, respectively, *p* = 0.07), and was not significantly increased compared to naïve controls.

The phosphoNR1 was also identified with immunostaining and noted to be distributed uniformly in the dorsal horn of naïve rats (**Figure 2C**). Immunostaining for phosphoNR1 was visibly diminished at 4 h in rats with k/c arthritis, particularly in dorsal horn laminae I and II (**Figure 2D**). Similarly in a separate study, at 12 weeks a visible decrease in phosphoNR1 was detected in the cervical spinal cord of a rat model of chronic neuropathic trigeminal pain compared to naïve control (**Supplementary Figure S1**).

Increased Spinal NMDA NR1 Protein Expression in Knee Joint Arthritis Reduced by Pretreatment With Genistein or Lavendustin A Shown by Western Blot

Figure 2F demonstrates with Western blots and bar graphs, the relative densities of band patterns of NMDA NR1 protein lysates derived from the lumbar spinal cord from non-arthritic and arthritic rats (*n* = 5/group). In these studies, compared to naïve non-arthritic rats (N), the NMDA NR1 band densities for spinal cord of arthritic rats (V, vehicle treated) were significantly increased (100 vs. 179 ± 39%, *p* < 0.05).

Groups of rats were also intraspinally pretreated with genistein, with genistein's active (lavendustin, LA), or with inactive (lavendustin B, LB) or (daidzein, D) analogs. NMDA NR1 band densities were not increased in arthritic rats treated with PTK inhibitor genistein or its active analog lavendustin A, compared to the naïve non-arthritic rats (N, 97 ± 10.2 and 65.21 ± 8.4 respectively). Arthritic rats treated with inactive analogs daidzein or lavendustin B had increased band densities over the normal controls but were not significantly different from the vehicle treated arthritic rats (120 ± 13.6 and 145 ± 18, respectively). There were no increases in NMDA NR1

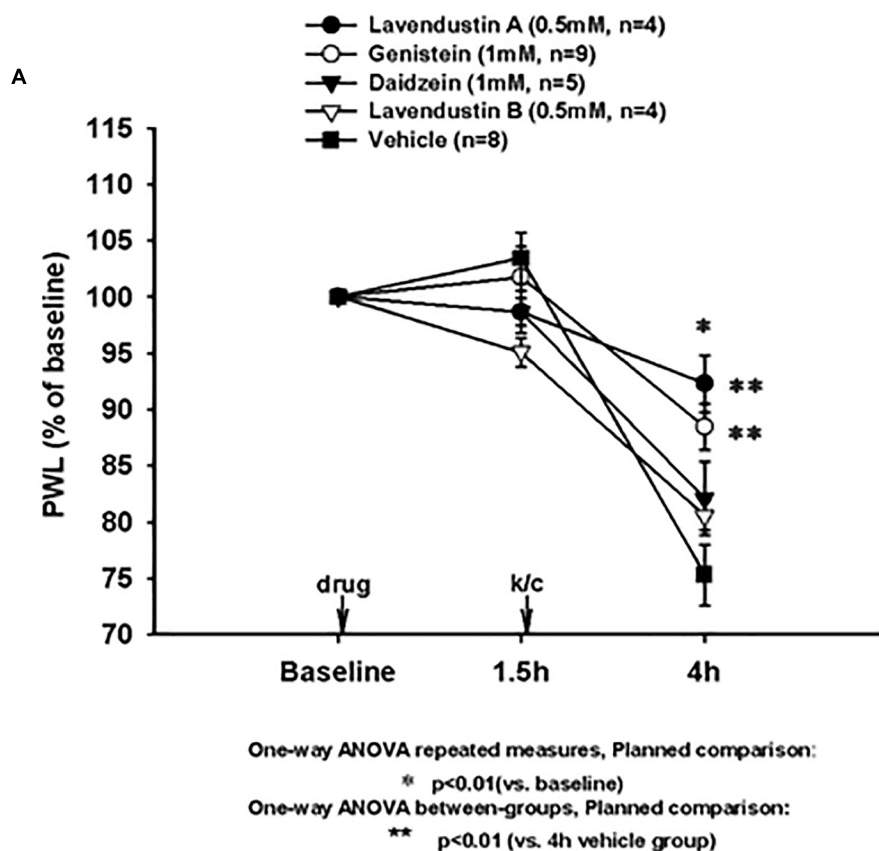
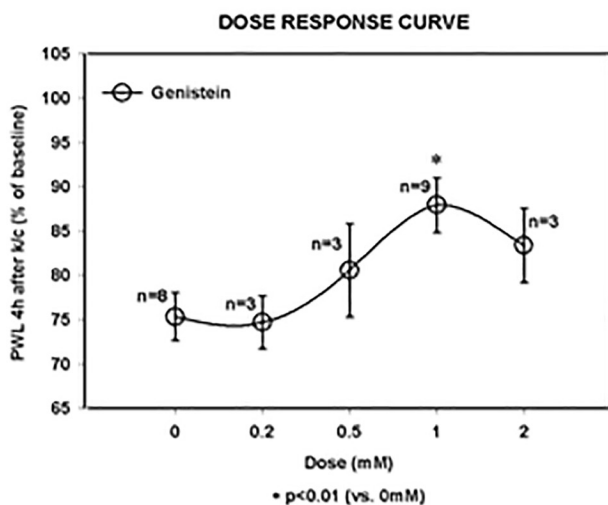
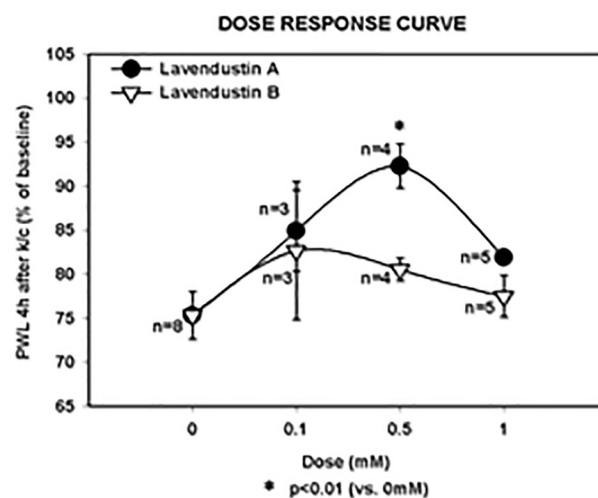
**B****C**

FIGURE 1 | Arthritis induced hypersensitivity (4 h) and effects of non-receptor tyrosine kinase inhibitor pre-treatments. **(A)** Paw withdrawal latency (PWL) decreases induced by knee joint inflammation were significant in all treatment groups (*significantly different from baseline for all groups; * $p < 0.01$). Pretreatment with genistein (Gen) and lavendustin A (Lav A) significantly (** $p < 0.01$ versus 4 h vehicle group) attenuated PWL decreases observed in animals with kaolin and carrageenan (k/c) arthritis induction 1.5 h post-drug infusion. Pretreatment with lavendustin B (Lav B) or diadzein (Dia) had no effect. **(B)** Dose response curve is shown for pretreatment with genistein and **(C)** lavendustin A and B. Lav A ($n = 4$), Gen ($n = 9$), Dia ($n = 5$), Lav B ($n = 4$), and Veh ($n = 8$). Dosing was provided intraspinally by microdialysis fiber, * $p < 0.01$ compared to 0 mM, one way ANOVA repeated measurement, planned comparison.

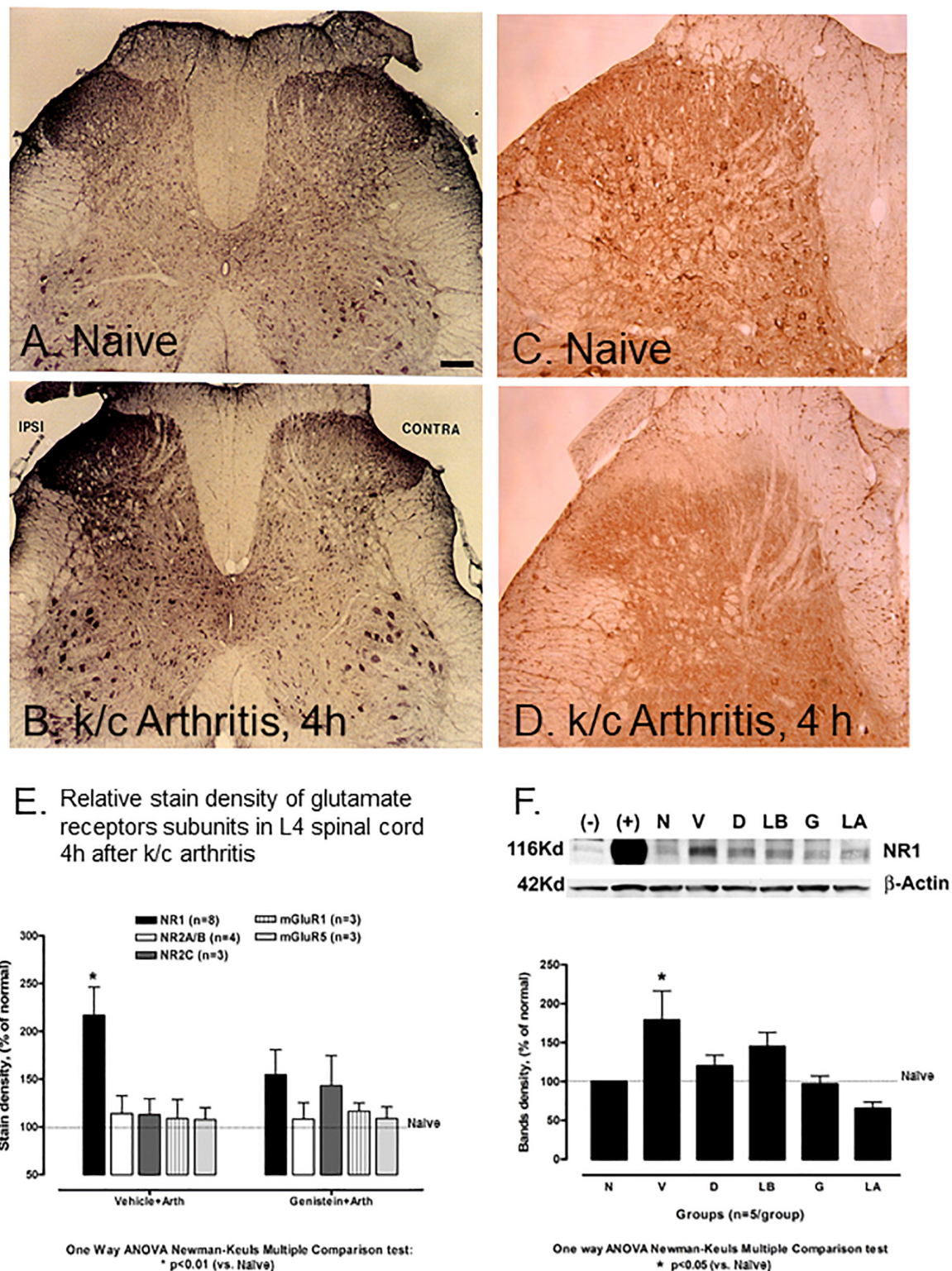


FIGURE 2 | Effect of non-receptor tyrosine kinase inhibitors on NMDA NR1 and immunostaining of NR1, pNR1, and other NMDA receptor subunits in rat L-4 spinal cord. **(A)** Representative photomicrograph of NMDA NR1 intensified immunostaining in a naïve animal. **(B)** NMDA NR1 in an arthritic rat with ipsilateral k/c knee joint inflammation at 4 h. **(C)** PhosphoNR1 immunostaining distributed uniformly in the dorsal horn of naïve rats. **(D)** PhosphoNR1 immunostaining diminished at 4 h, particularly in dorsal horn laminae I and II in rats with k/c arthritis. **(E)** Relative staining density of NMDA NR1 in animals with k/c arthritis (4 h) was significantly

(Continued)

FIGURE 2 | Continued

increased in the superficial ipsilateral dorsal horn (I-II) compared to naives when vehicle pre-treated, but not when pre-treated with genistein. Staining densities of other subunits tested did not significantly change compared to controls, with or without genistein. ($n = 3-8$) $*p < 0.01$ compared to the naive group **(F)** NMDA NR1 protein expression band density was increased significantly in spinal cord (L4-6) of animals with k/c arthritis (4 h) determined with Western blot analysis. Pretreatment with genistein, lavendustin A, and related agents successfully prevented the increase. Densities shown in the bar graph were corrected relative to β -actin. Positive (+) and negative (–) controls are provided. N, naïve; V, vehicle; D, daidzein; LB, lavendustin B; G, genistein; LA, lavendustin A pretreatments in arthritic rats. $*p < 0.05$ compared to the naive group. One way ANOVA with Newman–Keuls Multiple Comparison *post hoc* testing. Scale Bar = 100 μm in panels **(A,B)** and 50 μm in panels **(C,D)**.

receptor in any group in the contralateral dorsal horn of the spinal cord.

Other Spinal Glutamate Receptors Were Less Affected or Unchanged in k/c-Induced Arthritis

Other glutamate receptor subunits tested included ionotropic NR2A/B, NR2C, metabotropic mGluR1 and mGluR5. These subunits did not significantly increase in the spinal cord in vehicle treated animals at 4 h after k/c injection (113.98 ± 19 , 112.87 ± 16.5 , 108.81 ± 19.8 and 107.65 ± 12.31 , respectively), (**Figure 2E**, left bars) nor did they stain the nucleus. NR2A/B, mGluR1 and mGluR5, also did not significantly increase above background values in the arthritic rats pretreated with genistein (108.04 ± 17.5 , 116.46 ± 8.72 and $110.97 \pm 10.14\%$, respectively). Ionotropic NMDA NR2C was slightly elevated (**Figure 2E**, right bars) compared to the naive controls.

Parallel control studies determined that results obtained in animals with k/c induced arthritis in the absence of vehicle pretreatment or with sham surgery alone (external subcutaneous microdialysis fiber) matched those of arthritic animals with vehicle pre-treatment. Neither vehicle treated animals nor those with k/c induced arthritis demonstrated increased staining densities on the contralateral side or compared to naive, non-arthritic controls.

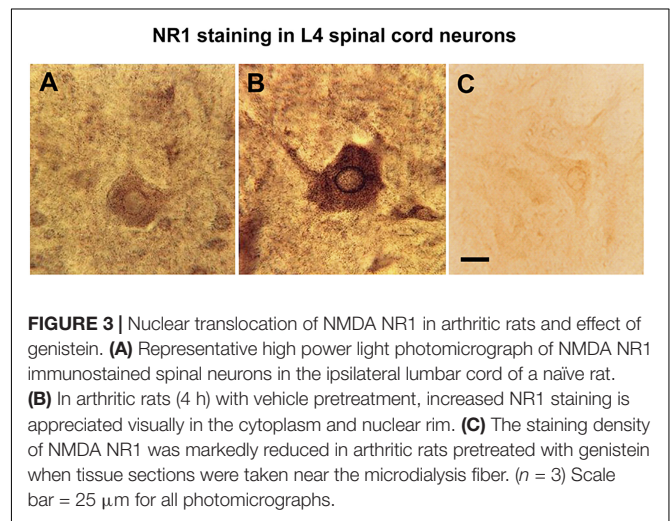
Nuclear Translocation of NMDA NR1 and Blunting by Genistein

NMDA NR1 Immunostaining Decrease by Genistein

The rapid increase in NR1 staining within 4 h of k/c joint injection included a shift in its cellular localization pattern within spinal cord neurons. Comparison of spinal cord neurons in animals with k/c-induced arthritis at 4h with neurons in naive animals (**Figure 3A**), identified markedly increased stain density, especially in the perinuclear regions and in the nucleus (**Figure 3B**). Similar staining was revealed with either C- or N-terminal NR1 specific antibodies. Pretreatment of animals with genistein effectively abrogated the increased nuclear staining density of NMDA NR1 in spinal neurons of k/c treated animals. The cell shown in **Figure 3C** was from the spinal segment near the site of genistein administration in a k/c arthritic animal and thus was nearly devoid of NR1 staining.

NMDA NR1 Subcellular Localization by Electron Microscopy (EM)

Electron microscopy images confirmed NMDA NR1 localization in the nucleus of neuronal cells from the ipsilateral spinal cord of



animals with k/c induced arthritis at 4 h (**Figure 4**). Immunogold labeling was found along the nuclear membrane (**Figures 4A,B** arrowheads). In naïve animals, immunoperoxidase labeling for NMDA NR1 was primarily localized at synaptic densities on the outer cell membrane (**Figure 4C**, large arrows) of spinothalamic tract neurons (**Figure 4C**, large dense crystals; open arrow). For better EM visualization of NMDA NR1 immunolocalization at the synaptic density in a control animal without dense counterstain, refer to Figure 13a in Petralia et al. (1994). The **Figure 4D** is the higher power image of the nuclear membrane marked as the inset in **Figure 4B**. Colloidal gold labeled NMDA NR1 was observed both in the cytoplasm and nucleus, including in proximity to the nuclear pore sites (arrows, uncolorized and colorized views). The EM images support nuclear translocation of the NR1 subunit at 4 h that is temporally concurrent to the development of the physiologic and nociceptive arthritic changes.

Partial Inhibition of NMDA NR1 by a Protein Synthesis Inhibitor

In some animals, pre-treatment with cycloheximide was given before k/c induction of arthritis to eliminate *de novo* protein synthesis. Dorsal horn (**Figures 5A,B**) and ventral horn sections (**Figures 5C,D**) from arthritic animals are shown after induction of k/c arthritis. The prominent nuclear rim staining is best appreciated in the ventral horn (**Figure 5C**). After

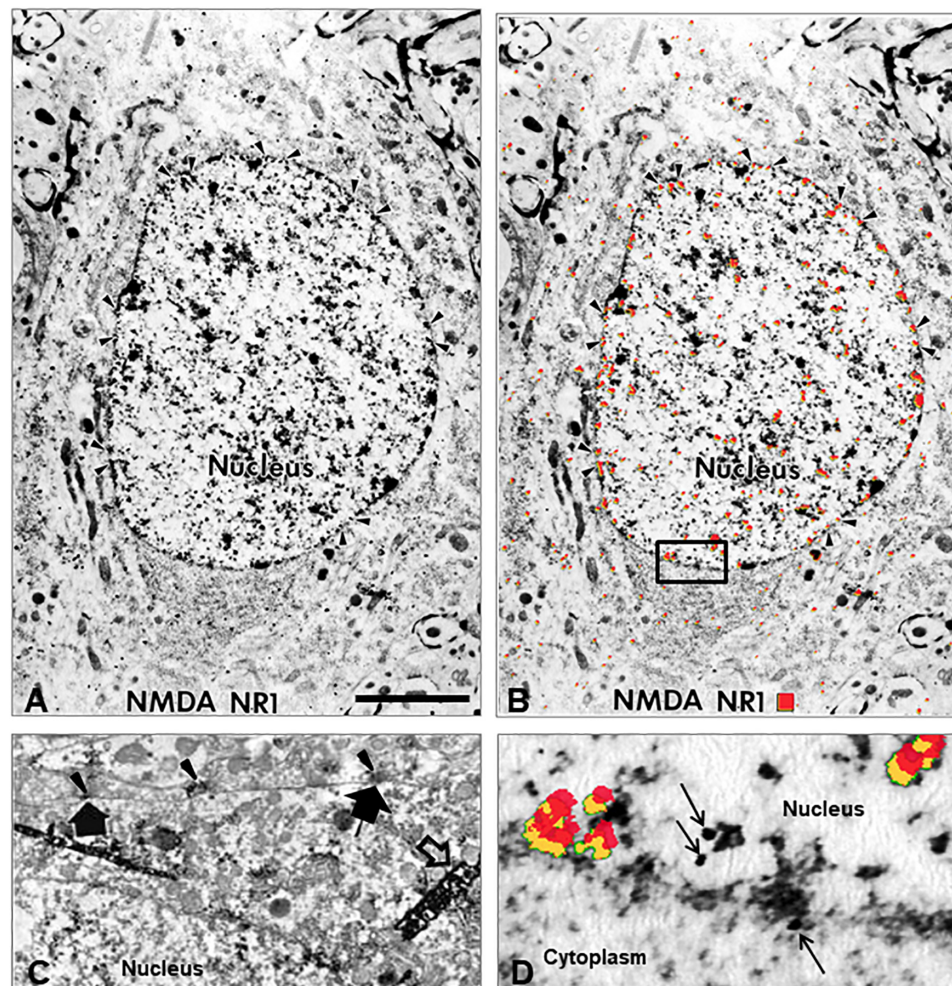


FIGURE 4 | Nuclear translocation of NMDA NR1. **(A)** Electron micrograph (EM) illustrating the intracellular distribution of NMDA glutamate receptor NR1 subunit in a spinal cord neuron 4 h after k/c induction of knee joint inflammation. The immunolocalization of the NR1 subunit is evident in the nucleus, particularly in a distribution pattern reminiscent of other receptor localizations, i.e., at the rim of nuclear pores on the nuclear membrane rather than at the post-synaptic localization typical in spinal neurons of naive rats. **(B)** The same EM image with red pseudocolor enhances the ability to observe the subcellular immunostaining of the colloidal gold particles found particularly in the nucleus, nuclear rim, and nuclear pores (arrowheads). **(C)** NMDA NR1 in naive animals is typically localized along the cell membrane. The arrowheads indicate NMDA NR1 in the pre-synaptic region of terminals and the large arrows indicate post-synaptic membrane immunolabeling with diaminobenzidine on a spinothalamic tract neuron identified by large dense crystals (open arrows) after WGA-HRP retrograde transport from thalamus (Ye and Westlund, 1996). **(D)** High power EM of the inset outlined in panel **(B)**, with red pseudocolor (yellow shadowing) or arrows to indicate immunogold labeling of NMDA NR1 at the nuclear membrane. ($n = 3$) Scale Bar in A = 3 μm in panels **(A,B)**; 1.33 μm in panel **(C)**; 0.3 μm in panel **(D)**.

intraperitoneal pretreatment with either saline (**Figures 5A,C**) or cycloheximide (30 mg/kg, **Figures 5B,D**), the increase in spinal cord NR1 staining in arthritic animals was visibly $\sim 50\%$ less with cycloheximide pretreatment. The remaining nuclear staining present in the cycloheximide treated arthritic animals indicated NR1 translocation to the nucleus was independent of *de novo* protein synthesis. Pretreatment with transcription inhibitor actinomycin D reduced some of the diffuse staining but not the nuclear translocation. Pre-treatment with leptomycin, a potent, specific nuclear export inhibitor and class II histone deacetylase inhibitor, also reduced nuclear NR1 immunostaining in animals with arthritis. These findings together suggest some of the localization

at the nucleus was *de novo* synthesis and some was from intracellular stores.

Cellular Response to Glutamate on SH-SY5Y Neuroblastoma Cells *in vitro* Increased Expression of NMDA NR1 Subunit and Nuclear Translocation in Human SH-SY5Y Neuroblastoma Cells After Glutamate and NMDA Activation

Studies performed in clonal SH-SY5Y human neuroblastoma cells further assessed cellular localization of NMDA NR1 with glutamate receptor activation as shown with immunocytochemical studies (**Figure 6**). Immunocytochemical

NR1 staining in DH and VH of spinal cord (4h)

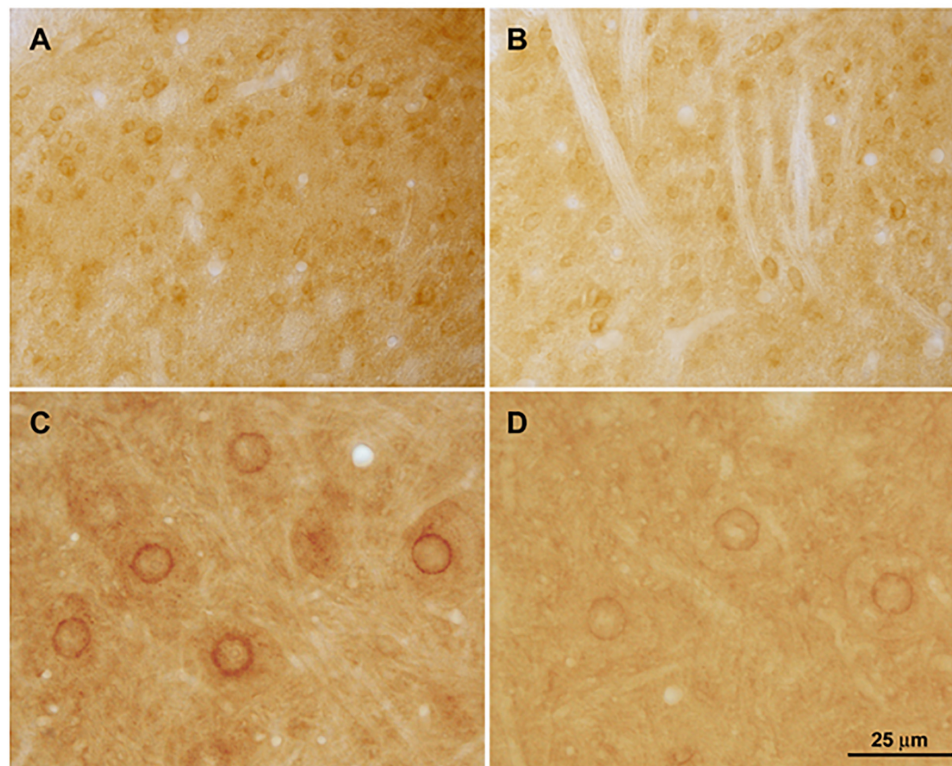


FIGURE 5 | Effect of cycloheximide protein synthesis inhibition. Arthritic rats were pretreated with saline (**A**, dorsal horn and **C**, ventral horn) or protein synthesis inhibitor cycloheximide (30 mg/kg, i.p.) (**B,D**). Relative increases in NMDA NR1 receptor nuclear rim immunostaining density in arthritic rats could potentially be attributed to newly synthesized protein. Some constitutive NR1 remains. ($n = 3$) Scale Bar = 75 μm in panels (**A,B**) and 25 μm in panels (**C,D**).

staining patterns of NMDA NR1 in SH-SY5Y cells treated with 100 μM glutamate for 4 h were compared to unstimulated cells (**Figure 6A**). Increased intensity of NMDA NR1 staining was observed, with an intracellular shift to perinuclear regions, the nuclear rim, and within the nucleus (**Figure 6B**). Similar staining was revealed with either C- or N-terminal specific antibodies.

Response to NMDA With Western Blot for Cytosolic and Nuclear Expression

Figure 6C demonstrates the same shift in cellular protein localization of NR1 with Western blots in the clonal SH-SY5Y human neuroblastoma cells after treatment with NMDA. Cells were treated with a dilution series of NMDA (0–10 μM), then extracted for cytosolic and nuclear fractions. The NMDA NR1 band densities were evident from the cytosolic fractions in the unstimulated and stimulated cells with added NMDA to a final concentration of 0, 0.5, 5.0 or 10.0 μM NMDA. A smaller but significant mean increase was also noted in the cytosolic fractions at NMDA concentrations of 0.5 and 5 μM compared to the untreated cells (110 ± 0.88 , $p = 0.03$ and 130 ± 1.09 , $p = 0.015$ vs. 100%, respectively).

Minimal or no NR1 band densities were appreciated in the nuclear fractions above the untreated control cells at

NMDA concentrations of 0, 0.1, 0.5, or 1.0 μM , respectively (**Figure 6C**). However, at 5 μM NMDA, there was a marked increase in NMDA NR1 band density in the nuclear fraction compared to the control cells (300 ± 70 vs. 100%, respectively, $p = 0.003$), indicating a shift to NR1 nuclear localization. As an additional control, human clonal SW982 synoviocytes were treated with NMDA (5 μM) and ACPD (5 μM), and their nuclei isolated. The isolated nuclei had visibly increased NMDA NR1 immunostaining compared to nuclei of untreated cultures (**Supplementary Figure S2**).

Response to Glutamate After Pretreatment With Genistein or Staurosporine

N-methyl-D-aspartate NR1 nuclear localization was further assessed in clonal SH-SY5Y human neuroblastoma cell cultures pretreated with protein kinase inhibitors, genistein or staurosporine, as shown in **Figure 7**. Compared to unstimulated cells (**Figure 7A**), cells incubated with 100 μM glutamate for 4 h (**Figures 7C,E**) had increased staining in nuclear, nuclear rim, and perinuclear regions. Pretreatment with 50 μM genistein (**Figure 7F**) or 100 nM staurosporine (**Figures 7B,D**) before glutamate incubation resulted in minimal nuclear staining of NMDA NR1. Staining at the cell border was intense, and staining in the perinuclear region

SH-SY5Y Human Clonal Neuroblastoma Cells

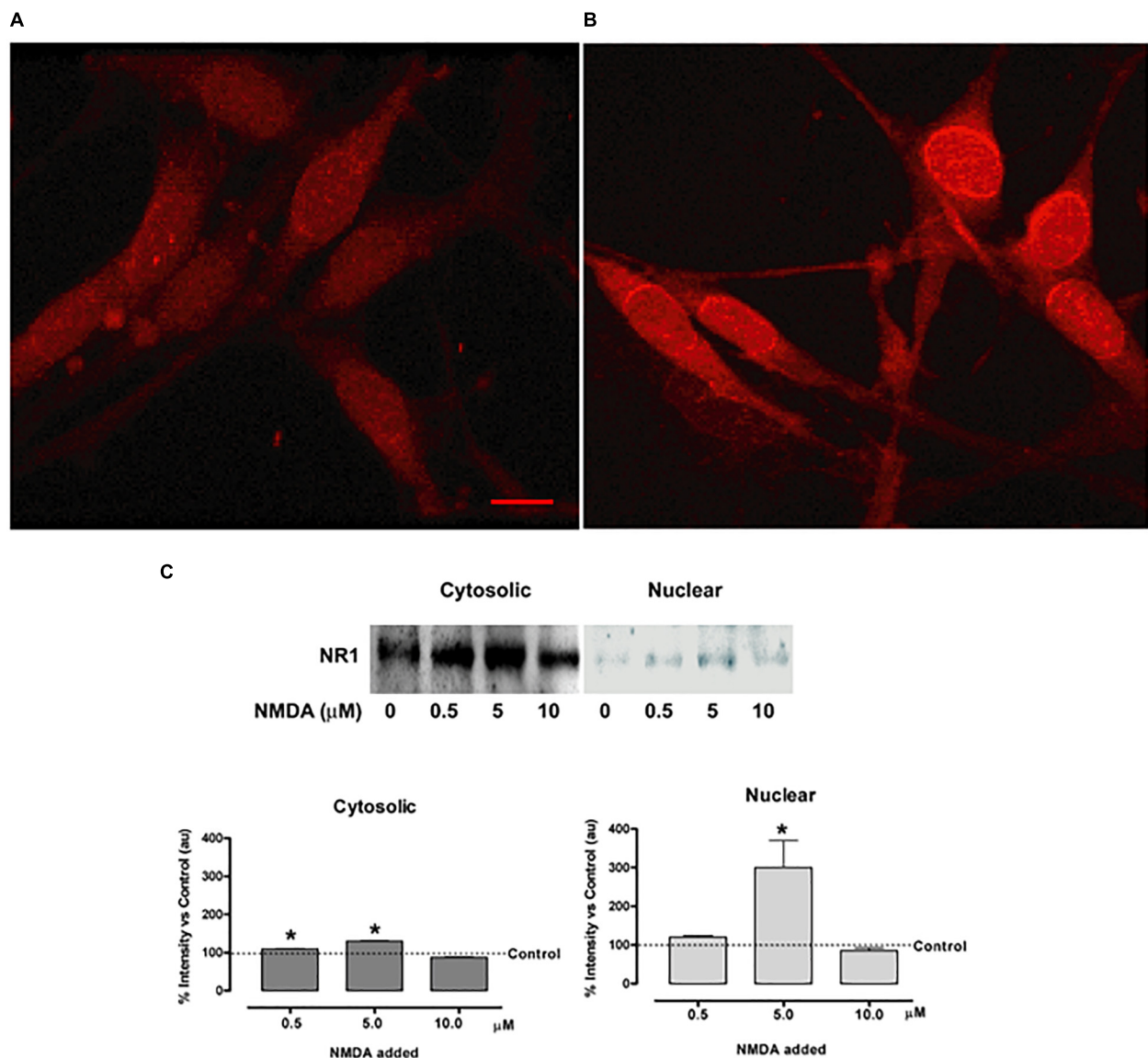


FIGURE 6 | NMDA NR1 staining and nuclear translocation in cultured SH-SY5Y human neuroblastoma cells by glutamate agonists. **(A)** Glutamate NMDA NR1 receptor staining of cultured SH-SY5Y neuroblastoma cells in unstimulated cultures. **(B)** Cells stimulated with 100 μ M L-glutamate for 4 h demonstrated increased cytoplasmic and nuclear staining for NR1 compared to control. **(C)** Bands representing one of three studies using Western blot analyses in which cultured SH-SY5Y neuroblastoma cells were stimulated with glutamate receptor agonist NMDA at 0, 0.5, 5.0, or 10.0 μ M concentrations for 4 h. NMDA NR1 subunit was detected predominantly in the cytosolic fractions at low NMDA doses and showed increased expression in the nuclear fractions at 5 μ M NMDA doses. The bar graphs demonstrate the mean \pm SE corrected band densities of cytosolic and nuclear fractions from the three studies performed. Each condition was done in triplicate and repeated 3 times. Scale Bar = 10 μ m in panels **(A,B)**. * p < 0.05 compared to unstimulated controls.

was still evident. Two insets are provided to demonstrate semi-quantitative Western blot analysis of NR1 expression in treated cells. Treatment of the cells with 100 μ M L-glutamate increased the expression of NR1 in the nuclear fraction 3-fold (**Figure 7E** inset). Pretreatment of the cells with 50 μ M genistein diminished the expected increase of NR1 seen with treatment of 5 μ M NMDA in the nuclear fraction by 40% (**Figure 7F** inset).

DISCUSSION

In an acute arthritis model, we provided evidence that NMDA NR1 subunit is increased and showed cellular redistribution that temporally corresponded with secondary thermal hypersensitivity. Direct delivery of PTK inhibitors genistein or lavendustin A to the affected spinal cord segment by microdialysis blocked both the increase in cellular NMDA

SH-SY5Y Human Clonal Neuroblastoma Cells

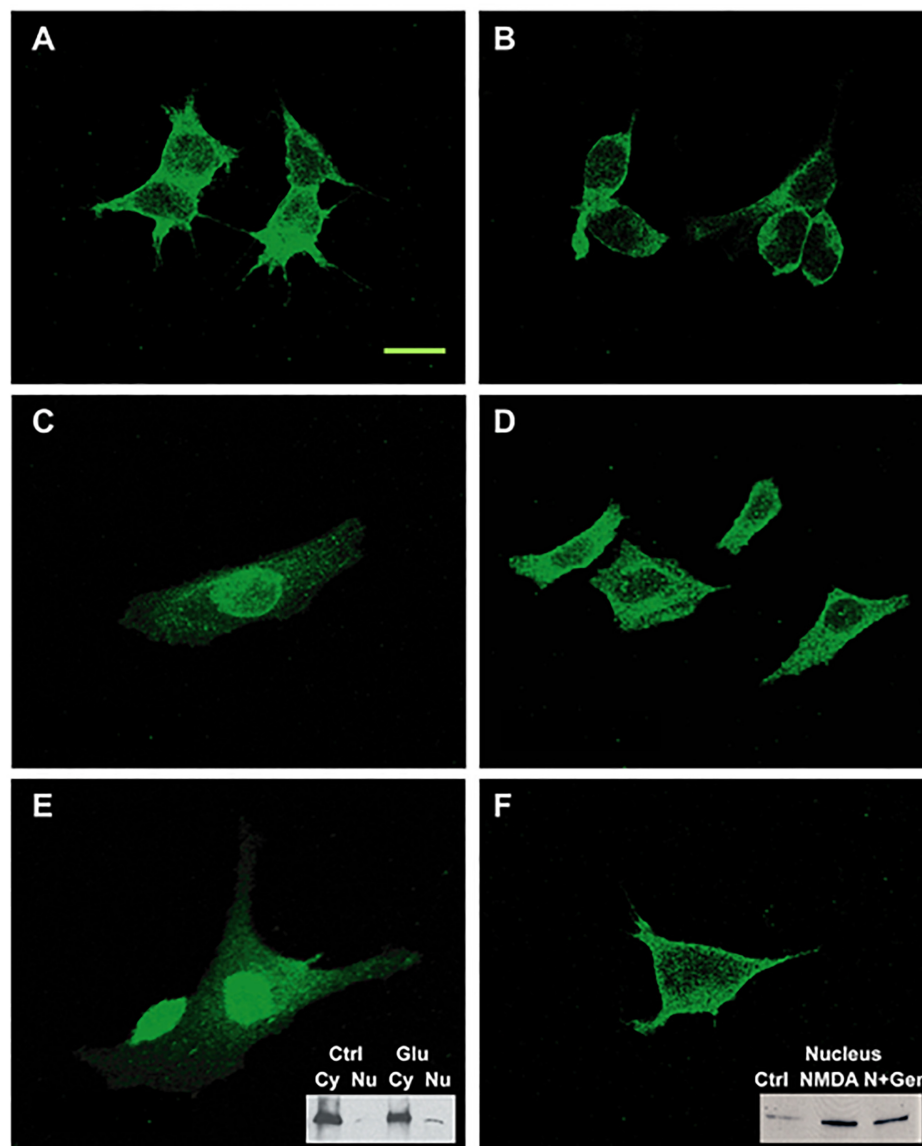


FIGURE 7 | SH-SY5Y neuroblastoma cells activated by glutamate agonists: NMDA NR1 staining and nuclear translocation blunted by PTK inhibitor pre-treatment. **(A)** NMDA NR1 staining of cultured SH-SY5Y neuroblastoma cells in untreated cells. **(C,E)** In comparison, nuclear translocation is noted in cells stimulated with L-glutamate (100 μ M) at 4 h; **(B,D)** Cells pretreated with staurosporin (100 nM), a broad spectrum kinase inhibitor, prior to stimulation with L-glutamate do not have nuclear localization. **(F)** Cells pretreated with genistein (50 μ M) then stimulated with L-glutamate also do not have nuclear localization. Two insets are provided to demonstrate expression of NR1 in treated cells by Western blot analysis. **(E inset)** Treatment of the cells with L-glutamate increased the expression of NR1 in the nuclear fraction by three-fold. **(F inset)** Pretreatment of the cells with genistein diminished the expected increase of NR1 seen with treatment of NMDA (5 μ M) in the nuclear fraction by 40%. Each condition was done in triplicate and repeated 3 times. Scale Bar = 20 μ m.

NR1 expression and its subcellular redistribution. Importantly, lumbar pretreatment with these PTK inhibitors resulted in significant blunting of the secondary hyperalgesic response in a dose dependent manner, indicated by increased paw withdrawal latency at 4 h compared to vehicle treatment. However, this *spinal* administration did not impact scores of joint circumference or surface temperature at 4 hr. Similarly, the *in vitro* studies in clonal neuronal cell cultures activated with glutamate reflected similar

increases in NMDA NR1 protein expression and subcellular redistribution that were blunted with PTK inhibitors.

The early increases in the NMDA NR1 subunit by 4 h and the shift to the nuclear compartment shown here with an *in vivo* arthritis model and the *in vitro* studies provide evidence of the importance of NMDA NR1 as an intracellular signaling molecule that likely impacts downstream cellular function directly at the nucleus. The studies with the PTK inhibitors provide

evidence that protein tyrosine phosphorylation is important in (i) modulation of nociceptive responses induced by peripheral k/c arthritis, (ii) induced NMDA NR1 subunit expression increases in the spinal cord, and (iii) NMDA NR1 subunit trafficking from the cell membrane to the nuclear membrane. The present studies add to proposed mechanisms whereby non-receptor tyrosine kinase phosphorylation events alter neuronal responsivity with resultant nociceptive hypersensitivity (Obreja et al., 2002). These data support direct involvement of NR1 nuclear translocation in modification of transcriptional responses to glutamate.

The Role of PTK in the Development of Secondary Hyperalgesia

The PTK inhibitors have been suggested as effective therapeutic interventions for inflammatory pain (Bonilla-Hernán et al., 2011). Our current study and previous studies by others support the hypothesis that NMDA activation initiates tyrosine kinase mediated events that generate hyperalgesic behavioral responses (Obreja et al., 2002; Zhu et al., 2012). Persistent enhancement of glutamate release in spinal cord contributes to altered neuronal responsiveness precipitating hypersensitivity. The intra-articular k/c model utilized here inflamed the knee joint allowing nociceptive testing of the ipsilateral uninjured footpad and a clear secondary heat hypersensitivity response. This model of acute joint injury was used to demonstrate the onset of acute nociceptive changes that will occur with joint trauma, and how this can be blunted with one temporally related pretreatment dosing of a PTK inhibitor such as genistein.

Spinal cord increase in NMDA NR1 protein and its nuclear translocation within 4 h after k/c arthritis induction are coincident in time with development of peripheral inflammation and secondary hyperalgesia. Tyrosine phosphorylation of the NR2B, but not the NR2A, is also associated with the development of persistent pain after inflammation (Guo et al., 2002). Our previous studies have supported a pivotal role for spinal cord excitatory amino acid release and its role in activation of spinothalamic pain pathway neurons and central sensitization (Dougherty et al., 1992a,b; Sorkin et al., 1992; Sluka and Westlund, 1993a). Others have demonstrated subsequent activation of NMDA NR1 in the dorsal horn initiated by peripheral injury, including arthritis (reviewed in Dubner and Ruda, 1992; Woolf and Costigan, 1999; Guo et al., 2002; South et al., 2003). Alternatively, depletion of NMDA NR1 in the dorsal horn or its targeted blockade with use of NMDA antagonists or antisense mRNA produces a spectrum of response blunting, through attenuation of injury-initiated responses (Sluka and Westlund, 1992, 1993b; Woolf and Salter, 2000; South et al., 2003; Inturrisi, 2005).

Arthritis-Induced Spinal Cord NMDA NR1 Elevations Are Blocked by Pretreatment With Genistein

These NMDA mediated events in the spinal cord facilitate neuronal plasticity events and ultimately induce complex inflammatory and neural contributors to central sensitization. The NMDA NR1 increases in the spinal cord are consistent with

long-term potentiation in other parts of the neuraxis, such as the hippocampus (Abe and Saito, 1993; Bartanusz et al., 1995; Yu et al., 1997). This involves phosphorylation of NR1 and NR2B subunits and can be prevented by activation and interactions with G protein-coupled mGluR and NK1 tachykinin receptors that increase intracellular Ca^{2+} (Guo et al., 2002; Zhang et al., 2002; Caudle et al., 2005). Previous *in vitro* studies have shown that genistein inhibits nociceptive trigeminal neuron excitability through a non-specific inhibition of voltage dependent sodium channels (Liu et al., 2004). Selective deletion of 80% of NMDA NR1 subunit in lumbar spinal cord by injection of adeno-associated virus expressing Cre recombinase into floxed NR1 mice results in functional loss of NMDA, but not AMPA currents (Inturrisi, 2005). In contrast to the present study, phosphorylated NR1 has been shown to be increased in spinal cord after brief intense activation of peripheral afferent nerves with capsaicin and in the streptozotocin induced rodent diabetes model (Zou et al., 2002; Daulhac et al., 2011; Wang et al., 2017). The visibly reduced spinal cord phosphoNR1 in a chronic neuropathic pain model may reflect long term depletion (**Supplementary Figure S1**). Less phosphoNR1 in Lamina I and II in the arthritic animals at 4 h may reflect maximal utilization (**Figure 3**). Intense afferent activation would result in increased new translational expression of NMDA NR1 and membrane insertion from intracellular stores by 4 h. Meanwhile, phosphoNR1 utilization would be maximal. In any event the data here is quite different and may simply reflect antibody binding to different phosphoNR1 variants.

Nuclear Localization of NMDA NR1

Nuclear translocation of the NMDA NR1 subunit was evident by light and electron microscopy in both dorsal and ventral horn neurons and in glial cells using both N- and C-terminal antibodies directed against NMDA NR1, indicating that the NR1 subunit was intact.

The NMDA NR1 subunit has a putative nuclear localization signal (NLS) region required for this translocation (Acc Number NM_007327 Human NMDA NR1 nucleotide sequence, GenBank, NCBI). Holmes et al. (2002a,b) have reported functional NLS sequences for NR1-1 and NR1-4 splice variants located equally in both the cytoplasm and nucleus, suggesting their small size allows ready passage through nuclear pores (Holmes et al., 2002a,b). Involvement of released serine and the inter-organelle signaling modulator/chaperone, Sigma-1 receptor, are proposed as functional mediators in NMDA NR1 upregulation, translocation, phosphorylation, central sensitization, and nociceptive hypersensitivity (Sluka and Westlund, 1993a,b; Zou et al., 2000; Kim et al., 2008; Roh et al., 2008; Su et al., 2010; Azkona et al., 2016; Choi et al., 2018). The EM photographs provided here support an easy passage through nuclear pores for NMDA NR1 (**Figures 4A,B,D**).

Subcellular localization in the nucleus has been characterized for transfected cell cultures in molecular studies (Marsh et al., 2001; Holmes et al., 2002a,b). In the k/c inflammatory arthritis model, NMDA NR1 was the only glutamate receptor subunit of those tested whose expression significantly increased in the gray matter, although NR2 upregulation has been reported in more intense formalin-induced and CFA inflammation models

(Gaunitz et al., 2002; Azkona et al., 2016). NMDA NR1 localization in control animals more typically is shown with EM to represent post-synaptic membrane localization (Liu et al., 1994; Petralia et al., 1994; Ye et al., 1999). Previous reports have also implicated NR1 cellular membrane associated translocations for subunit recycling.

The numerous present studies support nuclear translocation as one responsibility for the glutamate NMDA NR1-1 not shared by other glutamate NR1-4 subunits in initial hours after persisting afferent nerve activation, though it is not clear at this point which of the glutamate NR1-1 and NR1-4 subunits might be responsible.

The nuclear translocation of the NR1 subunit after glutamate activation suggests NR1 protein also plays a direct role in the fast intracellular signaling responses to glutamate activation. The histological data demonstrating a shift in the subcellular location of the NR1 subunit supports NR1's role as a rapid intracellular mediator acting through direct communication with the nucleus. The findings indicate activated NMDA could produce rapid downstream events resulting in increased NR1 subunit protein potentially required to mobilize the shift in NR2 subunit composition and numbers that promote hypersensitivity in this acute arthritis model.

The modulation of trafficking to the cell nucleus promoting transcriptional changes that impact NMDA ion channel function impacts the well characterized mechanisms generating LTP that extends activation for days and weeks in the hippocampus (Abe and Saito, 1993; Wang and Salter, 1994; Fadool et al., 1997; Yu et al., 1997; Lu et al., 1998). Activation of NMDA NR1 signaling pathway is correlated with miRNA219 levels, long-term potentiation (LTP), and hippocampal pyramidal cell number (Zhang et al., 2019).

Activation of membrane associated NMDA channels modulates trafficking of signaling mediators to the cell nucleus, such as MAPK, NF κ B, PKA, NFAT and calmodulin (reviewed in Thompson et al., 2004). Activity dependent binding and phosphorylation of importin α to the NLS present in the cytoplasmic tail of NR1-1a provides translocation from the synapse to the nucleus during transcription-dependent forms of neuronal plasticity (Jeffrey et al., 2009). Diversity of NMDA receptor configurations providing a variety of resultant physiological and pharmacological properties and functions is based on differential RNA splicing (Zukin and Bennett, 1995). Differing results in expression after injury is reported depending on timing after injury, location of the injury, and the splice variant recognized by the particular antibodies utilized (Zou et al., 2000, 2002; Gaunitz et al., 2002; Guo et al., 2002; Caudle et al., 2003, 2005; Brenner et al., 2004). The persisting hypothesis is that alternatively spliced cassettes of the NR1 protein play differing roles in the functional characteristics of the NMDA receptors adjusting to specific physiological or injury states (Prybylowski et al., 2001). It is clear that the timing of migration to the nucleus is rapid and coincides with the development of hypersensitivity.

Central sensitization, however, is a highly complex and interactive process involving numerous neurotransmitter events. Phosphorylation of NMDA NR1 after intradermal capsaicin

injection is increased at 30 and 60 min in the spinal cord dorsal horn (Zou et al., 2000). In that study, there was no difference from naïve at subsequent 120 and 180 min time points as hypersensitivity resolved. Other studies have also found that phosphoNR1 is increased after temporomandibular joint inflammation is induced with carrageenan (Cavalcante et al., 2013). The present data indicate that at 4 h, there is decreased staining density in lumbar spinal cord phosphoNR1 in animals with k/c arthritis compared to naïve animals. Likewise, in a chronic trigeminal neuropathic pain model with persisting hypersensitivity, staining density for phosphoNR1 in C1 spinal cord was less than in naïve animals at 10 weeks (see **Supplementary Figure S1**). The significance of this variability in different pain models captured at various time points is not entirely known. Likely, variability is due to the timing of different molecular signaling mechanisms along with rapid versus slow gearing up and also likely entailing depletions with long term persistence. The present study supports NMDA NR1 presence in the nucleus corresponding to molecular events occurring in the initial 2–4 h after intense knee joint afferent activation and central sensitization resulting in secondary hypersensitivity on the footpad. Taken together, considering many other studies the timing of molecular signaling events producing hypersensitivity depends on whether the study is done in the acute or chronic pain setting, which model is studied, what time point is selected (hours, days, months), and the nature of the stimulus.

The lack of effect on swelling of the isolated joint space itself in the present study is not surprising. We have previously shown a spinal NMDA antagonist does not reduce joint swelling, while a non-NMDA antagonist does reduce joint swelling (Sluka et al., 1994). Numerous studies have reported inflammatory cytokines in synovial fluids obtained from knees after direct trauma (Hooshmand et al., 2007; Liu et al., 2019). Elevated levels of synovial fluid excitatory amino acids glutamate (Glu) and aspartate (Asp) from traumatic joints in humans have been reported (McNearney et al., 2000). The addition of NMDA has been shown to increase NMDA NR1 and inflammatory cytokines in primary and clonal human synoviocyte cultures (Flood et al., 2007; McNearney et al., 2010). NMDA and ACPD induced increase in tumor necrosis factor alpha (TNF α) is also blunted by genistein pretreatment (**Supplementary Figure S3**). Other reports have found physiologic relevance to glutamate and NMDA receptors and elevated glutamate levels in other peripheral tissues, including bone (Chenu et al., 1998; Gu and Publicover, 2000; Gu et al., 2002) and tendons (Kader et al., 2002; Svedman et al., 2018). Knee joint glutamate increases have been reported in patients with Achilles tendinitis (Alfredson and Lorentzon, 2003).

Block of NMDA NR1 Nuclear Localization With Genistein

Transport of NR1 subunit to the nucleus was markedly reduced after pretreatment with various tyrosine kinase inhibitors in both spinal cord and clonal neuroblastoma cell cultures, indicating the importance of tyrosine kinase phosphorylation events to cellular transport in injury responses. The concentration of genistein

used (50 μ M) can also directly block glutamate activation of NMDA channels (Huang et al., 2010). Genistein does not inhibit all nuclear translocation events (Htun et al., 1998), but anti-inflammatory effects are reportedly efficacious in disorders related to steroid receptors (Garcia Palacios et al., 2005) and especially protein kinase mediated cell signaling events involved in translocation. Inhibition of protein synthesis by pretreatment with cycloheximide reduced neuronal NR1 staining by about 50% in spinal neurons but did not abrogate all nuclear staining. Thus, nuclear translocation of constitutive NR1 occurs after glutamate activation prior to *de novo* synthesis of NMDA NR1. In a previous *in vitro* study assessing the consequence of NMDA NR1 activation in human cultured synoviocytes, we reported that nuclear translocation after NMDA addition is evident within 1–2 h (McNearney et al., 2010). In that study, nuclear translocation of NMDA NR1 in activated synoviocytes was blocked by pre-treatment with MK-801.

Genistein Improves Viability and Has Neuroprotective Effects

Emerging clinical studies are reporting improvements in pain, systemic inflammatory, and cancer symptoms with genistein treatment (Gupta et al., 2011; Liu et al., 2019). Genistein inhibits reactive oxygen species production and aggregation of platelets in rats (Schoene and Guidry, 1999). Other studies report the peripheral use of genistein, related agents and isoflavones have local anti-inflammatory activity (by PTK inhibition) *in vitro* and in animal models, including arthritis (Orlicek et al., 1999; Verdrengh et al., 2003; Dijsselbloem et al., 2004; McNearney et al., 2010; Mohammad-Shahi et al., 2011; Li et al., 2014; Liu et al., 2019). For example, genistein blocks thermal hypersensitivity in inflammatory pain models (Lu et al., 2000; Guo et al., 2002). Genistein reduced serum granulocyte, monocyte, and lymphocyte inflammatory response to collagen-induced arthritis as either pretreatment or post-treatment (Verdrengh et al., 2003). In addition to its ability to inhibit PTK, genistein blocks NMDA receptors via a rapid, voltage-dependent, PTK-independent mode of action at an extracellular site (Huang et al., 2010). In that study, Lavendustin A is a specific PTK inhibitor analog with no direct effect on NMDA activated current. With continuous subcutaneous administration of genistein, reductions in sciatic nerve expression of NF- κ B, IL-1 β and IL-6 mRNAs, neuronal and inducible nitric oxide synthase in DRG, spinal cord and thalamus were reported in a sciatic nerve ligation model (Valsecchi et al., 2008). Genistein also reduced NGE, oxidative stress, inflammation, and nociceptive hypersensitivity in a time- and dose-dependent manner, and vascular dysfunction that follow streptozotocin induced diabetes in mice (Valsecchi et al., 2011). Genistein, but not inactive daidzein, reduced the rise in serum TNF alpha levels caused by systemic LPS (Ruetten and Thiernemann, 1997) (see also **Supplementary Figure S3**).

Genistein's neuroprotective effects were demonstrated *in vitro* in neurodegeneration models with both pre- and post-treatment protocols. Pre-treated PC-12 or post-treated SH-SY5Y cells exposed to β -amyloid or β -amyloid fragment ($A\beta_{25-35}$) are protected from apoptotic events (Tan and Kim, 2016; Xu et al.,

2019). Genistein post-treatment reduces Bax mRNA increase and Bcl-2 mRNA expression decrease to $A\beta_{25-35}$ exposure (Xu et al., 2019). $A\beta_{25-35}$ induced increases in Ca^{2+} concentration decreased in response to genistein shown with intracellular fluorescent dye indicator response (Xu et al., 2019). Genistein increased expression of the GluR2 and decreased NR2B subunit (Guo et al., 2002; Xu et al., 2019). A commonality in these effects may be related to genistein's reported ability to directly block glutamate activation of NMDA channels (Huang et al., 2010).

Limitations of the Study

Limitations noted in the study and considerations of the related literature include the necessity to determine the dynamics of PTK phosphorylation in other inflammatory models. Differences here compared to other literature reports appear to be related more to the nature of the models under study, mechanisms involved in different insults whether inflammatory or neurogenic, and the timing involved for development of insult response. Likewise, consideration of whether the treatments are pre- or post-model induction is necessary to establish the relationship of inflammatory or neurogenic events to secondary hypersensitivity and the mechanisms that might limit central sensitization. Our study is limited to one time point, during maximal arthritic injury in an acute arthritis model. A time course might be necessary to assess the timing and dosing of PTK inhibitors in arthritis models, to identify the protocol that reflects minimal joint injury or trauma. Another consideration is to question if systemic, intra-articular or oral ingestion of genistein would best mitigate secondary hypersensitivity. Or would systemic administration be more efficacious for extra-articular structures of the joint. Since many variations and models are examined, our study with direct spinal administration is but one to consider.

CONCLUSION

The development of secondary thermal hyperalgesia and upregulation of NR1 protein in response to peripheral tissue injury requires phosphorylation events mediated by non-receptor, protein tyrosine kinase. The increased expression and shift of the NMDA NR1 subunit to the nuclear compartment occurring in response to induction of arthritis (4 h) is concomitant with the development of spinal level sensitization indicated by secondary thermal hyperalgesia. Combined with the *in vitro* data, we have provided evidence that glutamate NMDA NR1 subunit plays a pivotal role as a rapidly responsive intracellular signaling mediator of NMDA-mediated glutamate activation mediated by protein tyrosine kinase. This pretreatment protocol with a PTK inhibitor that blunts neuronal NMDA NR1 increases, and translocation initiated changes has generated speculation that currently available PTK inhibitors, such as genistein, might offer clinical efficacy with pretreatment, "on-demand" dosing. Future studies will determine if this can be translated to a preemptive or prophylactic dosing strategy to benefit from the analgesic and possibly chondroprotective functions of PTK inhibitors in the immediate phase of acute joint trauma in humans, as shown here in a rat arthritis model.

DATA AVAILABILITY STATEMENT

The datasets generated for this study are available on request to the corresponding author.

ETHICS STATEMENT

The animal studies were reviewed and approved by the University of Texas Medical Center Galveston IACUC and the New Mexico Veterans Administration Health Care System (NMVAHCS) IACUC review committees.

AUTHOR CONTRIBUTIONS

KW, TM, and TP conceived the study and designed the experiments. YL, W-RZ, GT, TP, SM, and LZ performed the experiments. TM, YL, TP, and LZ analyzed the data. KW and TM wrote the manuscript. All authors read and approved the final version of the manuscript.

FUNDING

These studies were funded by the Merit Review Award BX002695, Office of Research and Development, Medical Research Service, United States Department of Veterans Affairs. This communication does not necessarily reflect the views of the Department of Veterans Affairs or the U.S. government. These studies were also supported by grants from the Sealy Endowment; NIH NS32778 to KW; NIH P01NS11255 to KW, TM, and GT. NIH R21 AR48371 to KW and TM; the Dana Foundation; and a UTMB endowment award to KW and TM.

REFERENCES

- Abe, K., and Saito, H. (1993). Tyrosine kinase inhibitors, herbimycin A and lavendustinA, block formation of long-term potentiation in the dentate gyrus in vivo. *Brain Res.* 621, 167–170.
- Akiyama, T., Ishida, J., Nakagawa, S., Ogawara, H., Watanabe, S., Itoh, N., et al. (1987). Genistein, a specific inhibitor of tyrosine-specific protein kinases. *J. Biol. Chem.* 262, 5592–5595.
- Alfredson, H., and Lorentzon, R. (2003). Intratendinous glutamate levels and eccentric training in chronic *Achilles tendinosis*: a prospective study using microdialysis technique. *Knee Surg. Sports Traumatol. Arthrosc.* 11, 196–199.
- Azkona, G., Saavedra, A., Aira, Z., Aluja, D., Xifró, X., Baguley, T., et al. (2016). Striatal-enriched protein tyrosine phosphatase modulates nociception: evidence from genetic deletion and pharmacological inhibition. *Pain* 157, 377–386.
- Bartanusz, V., Aubry, J. M., Pagliusi, S., Jezova, D., Baffi, J., and Kiss, J. Z. (1995). Stress-induced changes in messenger RNA levels of N-methyl-D-aspartate and AMPA receptor subunits in selected regions of the rat hippocampus and hypothalamus. *Neuroscience* 66, 247–252.
- Bonilla-Hernán, M. G., Miranda-Carús, M. E., and Martín-Mola, E. (2011). New drugs beyond biologics in rheumatoid arthritis: the kinase inhibitors. *Rheumatology* 50, 1542–1550.
- Brenner, G. J., Ji, R. R., Shaffer, S., and Woolf, C. J. (2004). Peripheral noxious stimulation induces phosphorylation of the NMDA receptor NR1 subunit at the PKC-dependent site, serine-896, in spinal cord dorsal horn neurons. *Eur. J. Neurosci.* 20, 375–384.

SUPPLEMENTARY MATERIAL

The Supplementary Material for this article can be found online at: <https://www.frontiersin.org/articles/10.3389/fphys.2020.00440/full#supplementary-material>

FIGURE S1 | Expression of phosphorylated NR1 subunit is decreased in a chronic pain model. Expression of phosphorylated NR1 (pNR1) subunit is decreased in a model of chronic trigeminal neuropathic pain (CCI-ION) in rat cervical spinal cord. Immunostaining for pNR1 (green) in cervical spinal cord section from naïve control rat (A) and 12 weeks after unilateral chronic constriction injury of the infraorbital branch of the trigeminal nerve (B) was more intense in the uninjured sample. Tissue samples were counter stained with DAPI (blue) ($n = 3$).

FIGURE S2 | NMDA NR1 in isolated SW892 human clonal synoviocyte nuclei. Nuclei isolated from treated and untreated cultures of SW892 human clonal synoviocytes were immunostained for NMDA NR1. Cultures were treated with NMDA and ACPD (5 μ M each, 12 h) the nuclei were isolated from cytoplasm and FAC sorted. Three replicates minimum were studied. Scale Bar = 50 μ m. A. NMDA NR1 staining of untreated isolated SW892 human clonal synoviocyte nuclei. B. NMDANR1 staining of isolated SW892 human clonal synoviocyte nuclei from cell cultures treated with NMDA + ACPD.

FIGURE S3 | NMDA and ACPD stimulated TNF-alpha release from SW892 human clonal synoviocytes is blunted following preincubation with PTK inhibitor genistein. Human clonal SW892 synovial cells were cultured to 2×10^6 million cells/well. Cell were pre-incubated with genistein 5 μ M, or vehicle for 1 hour at 37°C. After 1 hour, 5 μ M NMDA and 5 μ M ACPD or vehicle was added to assigned wells. The plates were incubated at 37°C for 24 hours. At 24 hours, cell culture supernatant was harvested from each well and TNF-alpha levels were ascertained by immunoassay (R&D Systems, MN, USA). Cells were also evaluated for viability with trypan blue exclusion and LDH release. Each condition was done in triplicate and repeated 3 times. This graph demonstrates low levels of supernatant TNF-alpha in untreated cells. When cells were incubated with NMDA and ACPD, there was a robust increase in supernatant TNF-alpha. Cells incubated with genistein alone showed a slight increase over baseline levels seen in the untreated cells. Cells preincubated with genistein before additions of NMDA and ACPD demonstrated a marked decrease in supernatant TNF alpha at 24 hours. This figure demonstrates that genistein incubation with synoviocyte cultures can impact cytokine response to neurotransmitter stimulation. Genistein has been reported to blunt arthritic response in other experimental studies (Mohammad-Shahi et al., 2011; Li et al., 2014; Liu et al., 2019).

- Caudle, R. M., Perez, F. M., Del Valle-Pinero, A. Y., and Iadarola, M. J. (2005). Spinal cord NR1 serine phosphorylation and NR2B subunit suppression following peripheral inflammation. *Mol. Pain* 1:25.
- Caudle, R. M., Perez, F. M., King, C., Yu, C. G., and Yezierski, R. P. (2003). N-methyl-D-aspartate receptor subunit expression and phosphorylation following excitotoxic spinal cord injury in rats. *Neurosci. Lett.* 349, 37–40.
- Cavalcante, A. L., Siqueira, R. M., Araujo, J. C., Gondim, D. V., Ribeiro, R. A., Quetz, J. S., et al. (2013). Role of NMDA receptors in the trigeminal pathway, and the modulatory effect of magnesium in a model of rat temporomandibular joint arthritis. *Eur. J. Oral Sci.* 121, 573–583.
- Chenu, C., Serre, C. M., Raynal, C., Burt-Pichat, B., and Delmas, P. D. (1998). Glutamate receptors are expressed by bone cells and are involved in bone resorption. *Bone* 22, 295–299.
- Choi, H. S., Lee, M. J., Choi, S. R., Smeester, B. A., Beitz, A. J., and Lee, J. H. (2018). Spinal Sigma-1 receptor-mediated dephosphorylation of astrocytic aromatase plays a key role in formalin-induced inflammatory nociception. *Neuroscience* 372, 181–191. doi: 10.1016/j.neuroscience.2017.12.031
- Daulhac, L., Maffre, V., Mallet, C., Etienne, M., Privat, A. M., Kowalski-Chauvel, A., et al. (2011). Phosphorylation of spinal N-methyl-d-aspartate receptor NR1 subunits by extracellular signal-regulated kinase in dorsal horn neurons and microglia contributes to diabetes-induced painful neuropathy. *Eur. J. Pain* 15, 169–169.
- Dijsselbloem, N., Vanden Berghe, W., De Naeyer, A., and Haegeman, G. (2004). Soy isoflavone phyto-pharmaceuticals in interleukin-6 affections. Multi-purpose

- nutraceuticals at the crossroad of hormone replacement, anti-cancer and anti-inflammatory therapy. *Biochem. Pharmacol.* 68, 1171–1185.
- Dougherty, P. M., Palecek, J., Paleckova, V., Sorkin, L. S., and Willis, W. D. (1992a). The role of NMDA and non-NMDA excitatory amino acid receptors in the excitation of primate spinothalamic tract neurons by mechanical, chemical, thermal, and electrical stimuli. *J. Neurosci.* 12, 3025–3041.
- Dougherty, P. M., Sluka, K. A., Sorkin, L. S., Westlund, K. N., and Willis, W. D. (1992b). Neural changes in acute arthritis in monkeys. I. Parallel enhancement of responses of spinothalamic tract neurons to mechanical stimulation and excitatory amino acids. *Brain Res. Brain Res. Rev.* 17, 1–13.
- Dubner, R., and Ruda, M. A. (1992). Activity-dependent neuronal plasticity following tissue injury and inflammation. *Trends Neurosci.* 15, 96–103.
- Fadool, D. A., Holmes, T. C., Berman, K., Dagan, D., and Levitan, I. B. (1997). Tyrosine phosphorylation modulates current amplitude and kinetics of a neuronal voltage-gated potassium channel. *Neurophysiology* 78, 1563–1573.
- Flood, S., Parri, R., Williams, A., Duance, V., and Mason, D. (2007). Modulation of interleukin-6 and matrix metalloproteinase 2 expression in human fibroblast-like synoviocytes by functional ionotropic glutamate receptors. *Arthritis Rheum.* 56, 2523–2534.
- Garcia Palacios, V., Robinson, L. J., Borysenko, C. W., Lehmann, T., Kalla, S. E., and Blair, H. (2005). Negative regulation of RANKL-induced osteoclastic differentiation in RAW264.7 Cells by estrogen and phytoestrogens. *J. Biol. Chem.* 280, 13720–13727.
- Gaunitz, C., Schüttler, A., Gillen, C., and Allgaier, C. (2002). Formalin-induced changes of NMDA receptor subunit expression in the spinal cord of the rat. *Amino Acids* 23, 177–182.
- Gu, Y., Genever, P. G., Skerry, T. M., and Publicover, S. J. (2002). The NMDA type glutamate receptors expressed by primary rat osteoblasts have the same electrophysiological characteristics as neuronal receptors. *Calcif. Tissue Int.* 70, 194–203.
- Gu, Y., and Publicover, S. J. (2000). Expression of functional metabotropic glutamate receptors in primary cultured rat osteoblasts. Cross-talk with N-methyl-D-aspartate receptors. *J. Biol. Chem.* 275, 34252–34259.
- Guo, W., Zou, S., Guan, Y., Ikeda, T., Tal, M., Dubner, R., et al. (2002). Tyrosine phosphorylation of the NR2B subunit of the NMDA receptor in the spinal cord during the development and maintenance of inflammatory hyperalgesia. *J. Neurosci.* 22, 6208–6217.
- Gupta, S. C., Kim, J. H., Kannappan, R., Reuter, S., Dougherty, P. M., and Aggarwal, B. B. (2011). Role of nuclear factor κ B-mediated inflammatory pathways in cancer-related symptoms and their regulation by nutritional agents. *Exp. Biol. Med.* 236, 658–671.
- Hall, R. A., and Soderling, T. R. (1997). Differential surface expression and phosphorylation of the N-methyl-D-aspartate receptor subunits NR1 and NR2 in cultured hippocampal neurons. *J. Biol. Chem.* 272, 4135–4140.
- Hammaker, D., Sweeney, S., and Firestein, G. S. (2003). Signal transduction networks in rheumatoid arthritis. *Ann. Rheum. Dis.* 62(Suppl. 2), 86–89.
- Hargreaves, K., Dubner, R., Brown, F., Flores, C., and Joris, J. (1988). A new and sensitive method for measuring thermal nociception in cutaneous hyperalgesia. *Pain* 32, 77–88.
- Holmes, K. D., Mattar, P., Marsh, D. R., Jordan, V., Weaver, L. C., and Dekaban, G. A. (2002a). The C-terminal C1 cassette of the N-methyl-D-aspartate receptor 1 subunit contains a bi-partite nuclear localization sequence. *J. Neurochem.* 81, 1152–1165.
- Holmes, K. D., Mattar, P. A., Marsh, D. R., Weaver, L. C., and Dekaban, G. A. (2002b). The N-methyl-D-aspartate receptor splice variant NR1-4 C-terminal domain. Deletion analysis and role in subcellular distribution. *J. Biol. Chem.* 277, 1457–1468.
- Hooshmand, S., Soung, do, Y., Lucas, E. A., Madhally, S. V., Levenson, C. W., et al. (2007). Genistein reduces the production of proinflammatory molecules in human chondrocytes. *J. Nutr. Biochem.* 18, 609–614.
- Hsu, S. M., Raine, L., and Fanger, H. (1981). Use of avidin-biotin-peroxidase complex (ABC) in immunoperoxidase techniques: a comparison between ABC and unlabeled unlabeled antibody (PAP) procedures. *J. Histochem. Cytochem.* 29, 577–580.
- Htun, P., Ito, W. D., Hoefer, I. E., Schaper, J., and Schaper, W. (1998). Intramyocardial infusion of FGF-1 mimics ischemic preconditioning in pig myocardium. *J. Mol. Cell Cardiol.* 30, 867–877.
- Huang, C. C., and Hsu, K. S. (1999). Protein tyrosine kinase is required for the induction of long-term potentiation in the rat hippocampus. *J. Physiol.* 520(Pt 3), 783–796.
- Huang, R., Singh, M., and Dillon, G. H. (2010). Genistein directly inhibits native and recombinant NMDA receptors. *Neuropharmacology* 58, 1246–1251.
- Inturrisi, C. E. (2005). The role of N-methyl-D-aspartate (n.d.) receptors in pain and morphine tolerance. *Minerva Anesthesiol.* 71, 401–403.
- Jeffrey, R. A., Ch'ng, T. H., O'Dell, T. J., and Martin, K. C. (2009). Activity-dependent anchoring of importin alpha at the synapse involves regulated binding to the cytoplasmic tail of the NR1-1a subunit of the NMDA receptor. *J. Neurosci.* 29:15613.
- Kader, D., Saxena, A., Movin, T., and Maffulli, N. (2002). Achilles tendinopathy: some aspects of basic science and clinical management. *Br. J. Sports Med.* 36, 239–249.
- Kawasaki, Y., Kohno, T., Zhuang, Z. Y., Brenner, G. J., Wang, H., Van Der Meer, C., et al. (2004). Ionotropic and metabotropic receptors, protein kinase A, protein kinase C, and Src contribute to C-fiber-induced ERK activation and cAMP response element-binding protein phosphorylation in dorsal horn neurons, leading to central sensitization. *J. Neurosci.* 24, 8310–8321.
- Kim, H. W., Roh, D. H., Yoon, S. Y., Seo, H. S., Kwon, Y. B., Han, H. J., et al. (2008). Activation of the spinal sigma-1 receptor enhances NMDA-induced pain via PKC- and PKA-dependent phosphorylation of the NR1 subunit in mice. *Br. J. Pharmacol.* 154, 1125–1134.
- Latremoliere, A., and Woolf, C. J. (2009). Central sensitization: a generator of pain hypersensitivity by central neural plasticity. *J. Pain* 10, 895–926.
- Lau, L. F., and Haganir, R. L. (1995). Differential tyrosine phosphorylation of N-methyl-D-aspartate receptor subunits. *J. Biol. Chem.* 270, 20036–20041.
- Li, J., Li, J., Yue, Y., Hu, Y., Cheng, W., Liu, R., et al. (2014). Genistein suppresses tumor necrosis factor α -induced inflammation via modulating reactive oxygen species/Akt/nuclear factor κ B and adenosine monophosphate-activated protein kinase signal pathways in human synovial cells. *Drug Des. Devel. Ther.* 8, 315–323.
- Liu, F.-C., Wang, C. C., Lu, J. W., Lee, C. H., Chen, S. C., Ho, Y. J., et al. (2019). Chondroprotective Effects of Genistein against Osteoarthritis Induced Joint Inflammation. *Nutrients* 11:E1180.
- Liu, H., Wang, H., Sheng, M., Jan, L. Y., Jan, Y. N., and Basbaum, A. I. (1994). Evidence for presynaptic N-methyl-D-aspartate autoreceptors in the spinal cord dorsal horn. *Proc. Natl. Acad. Sci. U.S.A.* 91, 8383–8387. doi: 10.1073/pnas.91.18.8383
- Liu, L., Yang, T., and Simon, S. A. (2004). The protein tyrosine kinase inhibitor, genistein, decreases excitability of nociceptive neurons. *Pain* 112, 131–141.
- Lu, W. Y., Zhang, L. P., Salter, M. W., and Westlund, K. N. (2000). Tyrosine kinase inhibitors prevent development of secondary hyperalgesia in carrageenan-induced arthritic rats. *Soc. Neurosci. Abstr.* 26:1692.
- Lu, Y. M., Roder, J. C., Davidow, J., and Salter, M. W. (1998). Src activation in the induction of long-term potentiation in CA1 hippocampal neurons. *Science* 279, 1363–1367.
- Marsh, D. R., Holmes, K. D., Dekaban, G. A., and Weaver, L. C. (2001). Distribution of an NMDA receptor:GFP fusion protein in sensory neurons is altered by a C-terminal construct. *J. Neurochem.* 77, 23–33.
- McNairney, T., Speegle, D., Lawand, N., Lisse, J., and Westlund, K. N. (2000). Excitatory amino acid profiles of synovial fluid from patients with arthritis. *J. Rheumatol.* 27, 739–745.
- McNairney, T. A., Ma, Y., Chen, Y., Taghialatela, G., Yin, H., Zhang, W. R., et al. (2010). A peripheral neuroimmune link: glutamate agonists upregulate NMDA NR1 receptor mRNA and protein, vimentin, TNF-alpha, and RANTES in cultured human synoviocytes. *Am. J. Physiol. Regul. Integr. Comp. Physiol.* 298, R584–R598.
- Mohammad-Shahi, M., Haidari, F., Rashidi, B., Saei, A. A., Mahboob, S., and Rashidi, M.-R. (2011). Comparison of the Effects of Genistein and Daidzein with Dexamethasone and Soy Protein on Rheumatoid Arthritis in Rats. *Bioimpacts. Science* 1, 161–170.
- Obreja, O., Schmeltz, M., Poole, S., and Kress, M. (2002). Interleukin-6 in combination with its soluble IL-6 receptor sensitizes rat skin nociceptors to heat, in vivo. *Pain* 96, 57–62.
- Orlicke, S. L., Hanke, J. H., and English, B. K. (1999). The src family-selective tyrosine kinase inhibitor PP1 blocks LPS and IFN-gamma-mediated TNF and iNOS production in murine macrophages. *Shock* 12, 350–354.

- Petralia, R. S., Yokotani, N., and Wenthold, R. J. (1994). Light and electron microscope distribution of the NMDA receptor subunit NMDAR1 in the rat nervous system using a selective anti-peptide antibody. *J. Neurosci.* 14, 667–696.
- Prybylowski, K. L., Grossman, S. D., Wrathall, J. R., and Wolfe, B. B. (2001). Expression of splice variants of the NR1 subunit of the N-methyl-D-aspartate receptor in the normal and injured rat spinal cord. *J. Neurochem.* 76, 797–805.
- Roh, D. H., Kim, H. W., Yoon, S. Y., Seo, H. S., Kwon, Y. B., Kim, K. W., et al. (2008). Intrathecal injection of the sigma(1) receptor antagonist BD1047 blocks both mechanical allodynia and increases in spinal NR1 expression during the induction phase of rodent neuropathic pain. *Anesthesiology* 109, 879–889.
- Ruetten, H., and Thiernemann, C. (1997). Effects of typhostins and genistein on the circulatory failure and organ dysfunction caused by endotoxin in the rat: a possible role for protein tyrosine kinase. *Br. J. Pharmacol.* 122, 59–70.
- Schoene, N. W., and Guidry, C. A. (1999). Dietary soy isoflavones inhibit activation of rat platelets. *J. Nutr. Biochem.* 10, 421–426.
- Skilling, S. R., Smullin, D. H., Beitz, A. J., and Larson, A. A. (1988). Extracellular amino acid concentrations in the dorsal spinal cord of freely moving rats following veratridine and nociceptive stimulation. *J. Neurochem.* 51, 127–132.
- Sluka, K. A., Jordan, H. H., Willis, W. D., and Westlund, K. N. (1994). Differential effects of N-methyl-D-aspartate (n.d.) and non-NMDA receptor antagonists on spinal release of amino acids after development of acute arthritis in rats. *Brain Res.* 664, 77–84.
- Sluka, K. A., and Westlund, K. N. (1992). An experimental arthritis in rats: dorsal horn aspartate and glutamate increases. *Neurosci. Lett.* 145, 141–144. doi: 10.1016/0304-3940(92)90006-s
- Sluka, K. A., and Westlund, K. N. (1993a). Spinal cord amino acid release and content in an arthritis model: the effects of pretreatment with no-NMDA, NMDA and NK1 receptor antagonists. *Brain Res.* 627, 89–103.
- Sluka, K. A., and Westlund, K. N. (1993b). Centrally administered non-NMDA but not NMDA receptor antagonists block peripheral knee joint inflammation. *Pain* 55, 217–225.
- Sorkin, L. S., Westlund, K. N., Sluka, K. A., Dougherty, P. M., and Willis, W. D. (1992). Neural changes in acute arthritis in monkeys. IV. Time-course of amino acid release into the lumbar dorsal horn. *Brain Res. Brain Res. Rev.* 17, 39–50.
- South, S. M., Kohno, T., Kaspar, B. K., Hegarty, D., Vissel, B., Drake, C. T., et al. (2003). A conditional deletion of the NR1 subunit of the NMDA receptor in adult spinal cord dorsal horn reduces NMDA currents and injury-induced pain. *J. Neurosci.* 23, 5031–5040.
- Su, T.-P., Hayashi, T., Maurice, T., Buch, S., and Ruoho, A. E. (2010). The sigma-1 receptor chaperone as an inter-organellar signaling modulator. *Trends Pharmacol. Sci.* 31, 557–566.
- Svedman, S., Westin, O., Aufwerber, S., Edman, G., Nilsson-Helander, K., Carmont, M. R., et al. (2018). Longer duration of operative time enhances healing metabolites and improves patient outcome after Achilles tendon rupture surgery. *Knee Surg. Sports Traumatol. Arthrosc.* 26, 2011–2020.
- Tan, J. W., and Kim, M. K. (2016). Neuroprotective effects of biochanin A against β -amyloid-induced neurotoxicity in PC12 Cells via a mitochondrial-dependent apoptosis pathway. *Molecules* 21:E548. doi: 10.3390/molecules21050548
- Thompson, K. R., Otis, K. O., Chen, D. Y., Zhao, Y., O'Dell, T. J., and Martin, K. C. (2004). Synapse to nucleus signaling during long-term synaptic plasticity: a role for the classical active nuclear import pathway. *Neuron* 44, 997–1009.
- Valsecchi, A. E., Franchi, S., Panerai, A. E., Rossi, A., Sacerdote, P., and Colleoni, M. (2011). The soy isoflavone genistein reverses oxidative and inflammatory state, neuropathic pain, neurotrophic and vasculature deficits in diabetes mouse model. *Eur. J. Pharmacol.* 650:694.
- Valsecchi, A. E., Franchi, S., Panerai, A. E., Sacerdote, P., Trovato, A. E., and Colleoni, M. (2008). Genistein, a natural phytoestrogen from soy, relieves neuropathic pain following chronic constriction sciatic nerve injury in mice: anti-inflammatory and antioxidant activity. *J. Neurochem.* 107, 230–240.
- Verdrengh, M., Jonsson, I. M., Holmdahl, R., and Tarkowski, A. (2003). Genistein as an anti-inflammatory agent. *Inflamm. Res.* 52, 341–346.
- Vos, B. P., Benoist, J. M., Gautron, M., and Guilbaud, G. (2000). Changes in neuronal activities in the two ventral posterior medial thalamic nuclei in an experimental model of trigeminal pain in the rat by constriction of one infraorbital nerve. *Somatosens Mot. Res.* 17, 109–122.
- Wang, J., Sun, Z., Wang, Y., Wang, H., and Guo, Y. (2017). The role and mechanism of glutamic NMDA receptor in the mechanical hyperalgesia in diabetic rats. *Neurol. Res.* 39, 1006–1013.
- Wang, Y. T., and Salter, M. W. (1994). Regulation of NMDA receptors by tyrosine kinases and phosphatases. *Nature* 369, 233–235.
- Westlund, K. N., Sun, Y. C., Sluka, K. A., Dougherty, P. M., Sorkin, L. S., and Willis, W. D. (1992). Neural changes in acute arthritis in monkeys. II. Increased glutamate immunoreactivity in the medial articular nerve. *Brain Res. Brain Res. Rev.* 17, 15–27.
- Woolf, C. J., and Costigan, M. (1999). Transcriptional and posttranslational plasticity and the generation of inflammatory pain. *Proc. Natl. Acad. Sci. U.S.A.* 96, 7723–7730.
- Woolf, C. J., and Salter, M. W. (2000). Neuronal plasticity: increasing the gain in pain. *Science* 288, 1765–1769.
- Xu, H. N., Li, L. X., Wang, Y. X., Wang, H. G., An, D., Heng, B., et al. (2019). Genistein inhibits A β 25–35-induced SH-SY5Y cell damage by modulating the expression of apoptosis-related proteins and Ca²⁺ influx through ionotropic glutamate receptors. *Phytother. Res.* 33, 431–441.
- Ye, Z., and Westlund, K. N. (1996). Ultrastructural localization of glutamate receptor subunits (NMDAR1, AMPA GluR1 and GluR2/3) and spinothalamic tract cells. *Neuroreport* 7, 2581–2585.
- Ye, Z., Wimalawansa, S. J., and Westlund, K. N. (1999). Receptor for calcitonin gene-related peptide: localization in the dorsal and ventral spinal cord. *Neuroscience* 92, 1389–1397.
- Yu, J., Bi, X., Yu, B., and Chen, D. (2016). Isoflavones: anti-inflammatory benefit and possible caveats. *Nutrients* 8:E361. doi: 10.3390/nu8060361
- Yu, X. M., Askalan, R., Keil, G. J. II, and Salter, M. W. (1997). NMDA channel regulation by channel-associated protein tyrosine kinase Src. *Science* 275, 674–678.
- Zhang, L., Chen, Z. W., Yang, S. F., Shaer, M., Wang, Y., Dong, J. J., et al. (2019). MicroRNA-219 decreases hippocampal long-term potentiation inhibition and hippocampal neuronal cell apoptosis in type 2 diabetes mellitus mice by suppressing the NMDAR signaling pathway. *CNS Neurosci. Ther.* 25, 69–77.
- Zhang, L., Lu, Y., Chen, Y., and Westlund, K. N. (2002). Group I metabotropic glutamate receptor antagonists block secondary thermal hyperalgesia in rats with knee joint inflammation. *J. Pharmacol. Exp. Ther.* 300, 149–156.
- Zhu, Y., Dua, S., and Gold, M. S. (2012). Inflammation-induced shift in spinal GABA(A) signaling is associated with a tyrosine kinase-dependent increase in GABA(A) current density in nociceptive afferents. *J. Neurophysiol.* 108, 2581–2593.
- Zou, X., Lin, Q., and Willis, W. D. (2000). Enhanced phosphorylation of NMDA receptor 1 subunits in spinal cord dorsal horn and spinothalamic tract neurons after intradermal injection of capsaicin in rats. *J. Neurosci.* 20, 6989–6997.
- Zou, X., Lin, Q., and Willis, W. D. (2002). Role of protein kinase A in phosphorylation of NMDA receptor 1 subunits in dorsal horn and spinothalamic tract neurons after intradermal injection of capsaicin in rats. *Neuroscience* 115, 775–786.
- Zukin, R. S., and Bennett, M. V. (1995). Alternatively spliced isoforms of the NMDAR1 receptor subunit. *Trends Neurosci.* 18, 306–313.

Conflict of Interest: TP was currently employed by the Everlywell Inc., Austin, TX, United States though not at the time that these studies were performed.

The remaining authors declare that the research was conducted in the absence of any commercial or financial relationships that could be construed as a potential conflict of interest.

Copyright © 2020 Westlund, Lu, Zhang, Pappas, Zhang, Taglialetta, McIlwrath and McNearney. This is an open-access article distributed under the terms of the Creative Commons Attribution License (CC BY). The use, distribution or reproduction in other forums is permitted, provided the original author(s) and the copyright owner(s) are credited and that the original publication in this journal is cited, in accordance with accepted academic practice. No use, distribution or reproduction is permitted which does not comply with these terms.



Chronic Pain After Spinal Cord Injury: Is There a Role for Neuron-Immune Dysregulation?

Sílvia S. Chambel^{1,2}, Isaura Tavares^{1,3} and Célia D. Cruz^{1,2*}

¹ Department of Biomedicine, Experimental Biology Unit, Faculty of Medicine, University of Porto, Porto, Portugal,

² Translational NeuroUrology Group, Instituto de Investigação e Inovação em Saúde - i3S, Universidade do Porto, Porto, Portugal, ³ Pain Research Group, Instituto de Investigação e Inovação em Saúde - i3S, Universidade do Porto, Porto, Portugal

OPEN ACCESS

Edited by:

Istvan Nagy,
Imperial College London,
United Kingdom

Reviewed by:

Paul McCulloch,
Midwestern University, United States
Carlos Wilson,
University Institute of Biomedical
Sciences of Córdoba (IUCBC),
Argentina
Elizabeth Bradbury,
King's College London, United
Kingdom

*Correspondence:

Célia D. Cruz
ccruz@med.up.pt

Specialty section:

This article was submitted to
Integrative Physiology,
a section of the journal
Frontiers in Physiology

Received: 11 March 2020

Accepted: 08 June 2020

Published: 07 July 2020

Citation:

Chambel SS, Tavares I and
Cruz CD (2020) Chronic Pain After
Spinal Cord Injury: Is There a Role
for Neuron-Immune Dysregulation?
Front. Physiol. 11:748.
doi: 10.3389/fphys.2020.00748

Spinal cord injury (SCI) is a devastating event with a tremendous impact in the life of the affected individual and family. Traumatic injuries related to motor vehicle accidents, falls, sports, and violence are the most common causes. The majority of spinal lesions is incomplete and occurs at cervical levels of the cord, causing a disruption of several ascending and descending neuronal pathways. Additionally, many patients develop chronic pain and describe it as burning, stabbing, shooting, or shocking and often arising with no stimulus. Less frequently, people with SCI also experience pain out of context with the stimulus (e.g., light touch). While abolishment of the endogenous descending inhibitory circuits is a recognized cause for chronic pain, an increasing number of studies suggest that uncontrolled release of pro- and anti-inflammatory mediators by neurons, glial, and immune cells is also important in the emergence and maintenance of SCI-induced chronic pain. This constitutes the topic of the present mini-review, which will focus on the importance of neuro-immune dysregulation for pain after SCI.

Keywords: spinal cord injury, pain, glia, immune, astrocyte, microglia

INTRODUCTION – SPINAL CORD INJURY

Spinal cord injury (SCI) causes major disturbances in sensory, motor, and autonomic function, leading to permanent loss of function and strongly impacting the physical, psychological, and social well-being of patients and caregivers (Braaf et al., 2017). It is estimated that 27 million people live worldwide with life-long consequences of SCI (James et al., 2019). Loss of function reflects the spinal level of the injury, with a high prevalence of injuries at the cervical and thoracic segments; the type of injury (compression, laceration, contusion, or ischemic insult); and the extent of the damage (Silva et al., 2014). Although life expectancy has greatly increased due to improved medical care, patients' quality of life is severely compromised by several factors, including chronic pain (Yang et al., 2014; Kjell and Olson, 2016).

CELLULAR ACTIVATION IN SCI AT THE LESION SITE

Tissue remodeling begins immediately after SCI and continues for extended periods of time. SCI-induced alterations in the spinal cord occur in four steps (Rust and Kaiser, 2017). The (1) *primary*

injury comprises the initial mechanical trauma (Rossignol et al., 2007). Within the first hours after injury, tissue damage initiates a series of destructive events that disrupt the spinal cord vasculature and blood-spinal cord barrier (BSCB). During *secondary injury* (2), platelets begin to invade the injury site and cause vasospasm, resulting in ischemia, glutamate release and oxidative stress (Park et al., 2004). The lesion extends and neuronal and glial cells undergo apoptosis and necrosis. Endogenous molecules, such as interleukin (IL)-1 α , IL-33, ATP, and danger-associated molecular patterns (DAMPs) (Didangelos et al., 2016; Yang et al., 2017; Tran et al., 2018), are released by dying neurons and glial cells. This initiates a neuroinflammatory response, mediated by CNS astrocytes, microglia, and blood-borne neutrophils (Alizadeh et al., 2019).

Astrocytes are the first responders after a CNS injury (Pineau et al., 2010). Immediately after SCI, astrocytes become reactive (Xu et al., 1999; Bradbury and Burnside, 2019). Reactive astrocytes increase cytokine [e.g., IL-1 β , IL-6, IL-12, tumor necrosis factor alpha (TNF- α) and interferon gamma (IFN- γ)] and chemokine (e.g., CCL2, CXCL1, and CXCL2) release in response to injury, which trigger recruitment of neutrophil and pro-inflammatory macrophages (Pineau et al., 2010; Alizadeh et al., 2019). Reactive astrocytes also release TGF- β and IL-10 that harness inflammation and avoid spreading of apoptotic and necrotic cells (Alizadeh et al., 2019) (**Table 1**).

Neutrophils are the first immune cells to respond to SCI, peaking at 24 h post-injury (Dusart and Schwab, 1994) but mostly disappear following the acute inflammatory phase (Neirinx et al., 2014). Neutrophils are most likely attracted by CXCL1 and leukotriene-B $_4$ (LTB $_4$) secreted at the injury site. Invading neutrophils release pro-inflammatory molecules that exacerbate astrocytes and microglia activation at the lesion (Perkins and Tracey, 2000; Schomberg and Olson, 2012) (**Table 1**).

CNS resident *microglia* polarize within 5–15 min in response to injury, extending their processes toward the injury site. Once activated, microglia assume an amoeboid shape, proliferate and migrate to the lesion site (Popovich and Hickey, 2001; Sroga et al., 2003). There they play a crucial role in clearing cellular debris and aiding in wound sealing and glial scar maturation (Vilhardt, 2005; Loane and Byrnes, 2010). Microglia also express receptors to DAMPs released by injured neurons (Block et al., 2007; Loane and Byrnes, 2010). They are also responsible for releasing TNF- α , IL-1 β , and C1q, which induce the activation of a subtype of astrocytes responsible for neuronal and oligodendrocyte cell death (Liddelow et al., 2017), an event linked to the emergence of neuropathic pain (**Table 1**).

While SCI-related microglial activation used to be perceived as an exclusively harmful event, it is now recognized that microglia also exert a neuroprotective role. Studies have shown cavity enlargement after early microglia ablation following SCI (Hines et al., 2009). More recently, using a *Cx3cr1*^{creER} mouse model, researchers demonstrated that eliminating microglia results in enhanced glial scar formation and neuronal and oligodendrocyte death, accompanied by poor locomotor performance (Bellver-Landete et al., 2019).

Twenty-four hours post-injury, circulating *monocytes* are recruited to the site of injury, where they differentiate into

macrophages. Macrophages can be broadly divided into pro-inflammatory M1 or anti-inflammatory M2 macrophages. M1 macrophages are activated via toll-like receptors (TLRs) and IFN- γ , upregulating the expression of pro-inflammatory cytokines such as IL-6, IL-1 β , IL-12, and TNF- α , and causing axonal retraction. Conversely, the M2 phenotype is activated by IL-13 or IL-4 (Gensel and Zhang, 2015). The shift from M1 to M2 macrophages is known to contribute to tissue healing (Deonarain et al., 2007; Nahrendorf et al., 2007) but does not occur, or is strongly impaired, in the lesioned spinal tissue (Kigerl et al., 2009). Kigerl et al. (2009) have demonstrated that, in a mouse model of midthoracic spinal contusion, M1 macrophage turnover is exacerbated in response to SCI, dominating the lesion site and nearby spared tissue, while M2 macrophages are short-lived, dissipating within 3–7 days post-SCI (**Table 1**).

Adaptive immune response also plays an important role in inflammatory response after SCI. After being activated in the spleen and bone marrow within 24 h post-SCI, *T- and B-lymphocytes* infiltrate the injured spinal cord, their numbers peaking at 7 days post-injury and remaining elevated in chronic stages of disease (Sroga et al., 2003; Jones, 2014). Activated T cells are particularly important on the modulation of inflammation following SCI as they can affect neuronal and glial survival via release of pro-inflammatory cytokines and chemokines (Jones, 2014), thus impairing recovery following SCI. Further information on the role of lymphocytes following SCI can be found elsewhere (Jones, 2014; Noble et al., 2018) (**Table 1**).







The third step comprises (3) *formation and maturation of the glial scar* by activated astrocytes. Recent studies revealed that microglia are also important players in glial scar formation, by accumulating around the scar and modulating astrocyte proliferation during scar formation via insulin-like growth factor 1 (IGF-1) (Bellver-Landete et al., 2019). Moreover, Zhou et al. (2020) have also demonstrated that microglia form a concentric physical barrier between the center of the lesion and its border, promoting wound compaction and recovery.

The final step in spinal cord remodeling after SCI consists of restricted (4) *structural tissue regeneration* occurring in the weeks and months after SCI (Shechter and Schwartz, 2013; Rust and Kaiser, 2017). However, the environment surrounding the scar is highly inhibitory axonal regrowth and reconnection. Thus, recovery of function is rarely achieved after a CNS injury, prompting the emergence of subsequent pathologies, including chronic neuropathic pain.

PAIN

Pain is defined by the International Association for the Study of Pain (IASP) as an unpleasant sensory and emotional experience, associated with actual or potential tissue damage, or described in terms of such damage (Loeser and Treede, 2008). While acute pain is usually well managed by patients and clinicians and resolved within a short period of time, chronic pain loses its protective role and becomes a disease in itself, even after resolving the triggering cause.

TABLE 1 | Innate and adaptive cells involved in the release of immune molecules at the injury site following spinal cord injury.

	Type of cell	Function at the injury site	Pro-inflammatory molecules released at the injury site	Anti-inflammatory molecules released at the injury site
<i>Innate immune cells</i>	Astrocytes	– Switch from quiescent to reactive following SCI – Recruit neutrophils and M1-macrophages – Involved in glial scar formation	IL-1 β , IL-6, IL-12, TNF- α , IFN- γ , TGF- β CCL2, CXCL1, CXCL2	TGF- β , IL-10
	 Microglia	– Clear cellular debris from neuronal and glial cell apoptosis – Aid in wound sealing	IL-1 β , IL-2, IL-6, IL-12, IL-18, TNF- α , IFN- γ , C1q NO, ROS	TGF- β , IL-10, IGF-1
	 Neutrophils	– Attracted by CXCL1 and LTB4 – Clear debris from the injury site – Recruit monocytes/macrophages	IL-1 β , IL-8, IL-12, TNF- α , IFN- γ MPO, MMP-9	Unknown
	 Monocytes Macrophages	– Polarization from M1-M2 subtypes	IL-1 β , IL-6, IL-12, IL-18, TNF- α , IFN- γ NO, ROS	IL-10, TGF- β
				
<i>Adaptive immune cells</i>	T-lymphocytes	– Promote CNS fibrosis and autoimmunity	IL-1 β , IL-12, TNF- α CCL2, CCL5, CXCL10	IL-2, IL-4, IL-5, IL-6, TGF- β
	 B-lymphocytes	– Promote autoimmunity and demyelination	Unknown	Unknown
				

Pain perception is often initiated by the activation of nociceptors by noxious chemical, mechanical, or thermal stimuli in the periphery. These sensory neurons fall into two categories: medium-sized myelinated A δ fibers and small-diameter, unmyelinated C-fibers. In the spinal cord, they synapse with relaying second-order neurons (either specific nociceptive neurons (NS) or wide-dynamic range neurons (WDR) or with inhibitory/excitatory spinal interneurons. Axons originated in these spinal cord neurons transmit ascending input to several supraspinal areas, namely the brainstem areas and the thalamus, the latter of which relays nociceptive information to cortical areas (Fenton et al., 2015; Boadas-Vaello et al., 2016). Nociceptive input is then processed and perceived, resulting in the activation of top-down descending modulation. These pathways may recruit higher brain centers, such as the prefrontal cortex and the amygdala, linked to cognitive and emotional aspects of pain. Top-down modulation also involves several supraspinal nuclei, including a midline relay circuit centered at the periaqueductal gray and rostral ventromedial medulla (PAG-RVM) (Heinricher et al., 2009; Boadas-Vaello et al., 2016). This key PAG-RVM circuit is connected with several brainstem regions, such as the locus coeruleus, the caudal ventrolateral medulla (VLM), and the dorsal reticular nucleus (DRt). The VLM and the DRt are reciprocally linked with the spinal cord, in circuits that may decrease or increase nociceptive information (Martins and Tavares, 2017). Descending pathways operate via release

of serotonin, norepinephrine, and dopamine at supraspinal and spinal levels (Bourne et al., 2014). Considering the complexity of ascending and descending nociceptive neurotransmission, described in detail elsewhere (Boadas-Vaello et al., 2016; Martins and Tavares, 2017), it comes as no surprise that SCI strongly compromises these circuits and jeopardizes endogenous pain control circuits.

Pain Following Spinal Cord Injury

Pain arising after SCI has life-long consequences, strongly impairing patients' quality of life and often exceeding the impact of other functional disabilities. Pain manifests itself in several ways after SCI. While acute pain accompanies the injury and the recovery period, receding with tissue scarring, chronic pain emerges due to maladaptive neuroplasticity. More than 50% of SCI patients report chronic pain within a year of spinal lesion (Dijkers et al., 2009; Finnerup, 2013; Burke et al., 2017). Gabapentin, opioids and pregabalin remain gold standard for SCI-associated pain treatment, but are often ineffective and do not prevent pain worsening (Widerström-Noga, 2017).

Classically, SCI-related chronic pain can be divided into three major groups: nociceptive, neuropathic, or other/unknown pain (Bryce et al., 2012). Nociceptive SCI-derived pain includes musculoskeletal and visceral pain (Bryce et al., 2012; Shiao and Lee-Kubli, 2018). Neuropathic pain reflects SCI-induced

damages in the somatosensory system and is divided into at-level, below-level, and above-level neuropathic pain. At-level pain usually emerges at early time points after SCI. It refers to pain felt in the dermatomes at the level of injury and includes central and peripheral components. Below-level pain is typically of central origin, felt diffusely below the level of injury and appearing when chronicity has set (Siddall et al., 2003; Finnerup, 2013). Finally, above-level neuropathic pain is now described as “other neuropathic pain” (Finnerup, 2013), relating to injury management, such as wheelchair pulling or pain following surgery.

Neuropathic Pain Emergence Following Peripheral Nerve Injury

Spatial and temporal activation of glial cells in the spinal cord in several animal models of peripheral nerve injury has been vastly studied, but fewer data are available regarding SCI-induced neuropathic pain. This surely reflects the difficulties of reporting pain levels in animals with impaired mobility, as classical tests evaluate evoked responses to peripheral stimuli (Silva et al., 2014; Kramer et al., 2017). Therefore, much of our present knowledge on SCI-induced neuropathic pain stems from studies using models of peripheral nerve injury. Early studies in peripheral neuropathic pain reported increased GFAP immunostaining, an established marker for astrocytes, in the spinal dorsal horn (SDH) that correlated with emergence of hyperalgesia after sciatic nerve constriction injury (Garrison et al., 1991). Wagner and Myers demonstrated the role of TNF- α in hyperalgesia arising after sciatic nerve compression (Wagner and Myers, 1996), which has been proved to induce activity in primary nociceptors, hyperalgesia, and inflammation in rats (Sorkin et al., 1997; Junger and Sorkin, 2000), a process resulting from glial activation (Colburn et al., 1999; Zhuang et al., 2005). Macrophages are also involved in the emergence of neuropathic pain in models of peripheral nerve injury. Blockade of macrophage-colony stimulating factor signaling in a mouse model of partial sciatic nerve ligation prevented the development of injury-associated neuropathic pain (Lee et al., 2018). Further data on the role of neuroimmune interactions in peripheral nerve injury models can be found elsewhere (Malcangio, 2019; Tozaki-Saitoh and Tsuda, 2019).

Neuropathic Pain Emergence Following Spinal Injury

The Role of Microglia and Astrocytes

Fewer studies have focused on the contribution of immune and glial cells to the emergence of neuropathic pain after SCI. Early studies by Peng et al. (2006) have demonstrated that a T13 unilateral hemisection produces bilateral microglia activation and TNF- α expression below the lesion level, correlating with hindpaw mechanical allodynia in SCI rats. Treating a T13 rat hemisection with etanercept, a TNF- α blocker, resulted in decreased mechanical allodynia and microglial activation. Treatment with minocycline, a microglial inhibitor, also improved pain-associated behaviors, demonstrating that TNF- α is critical in the establishment of neuropathic pain after

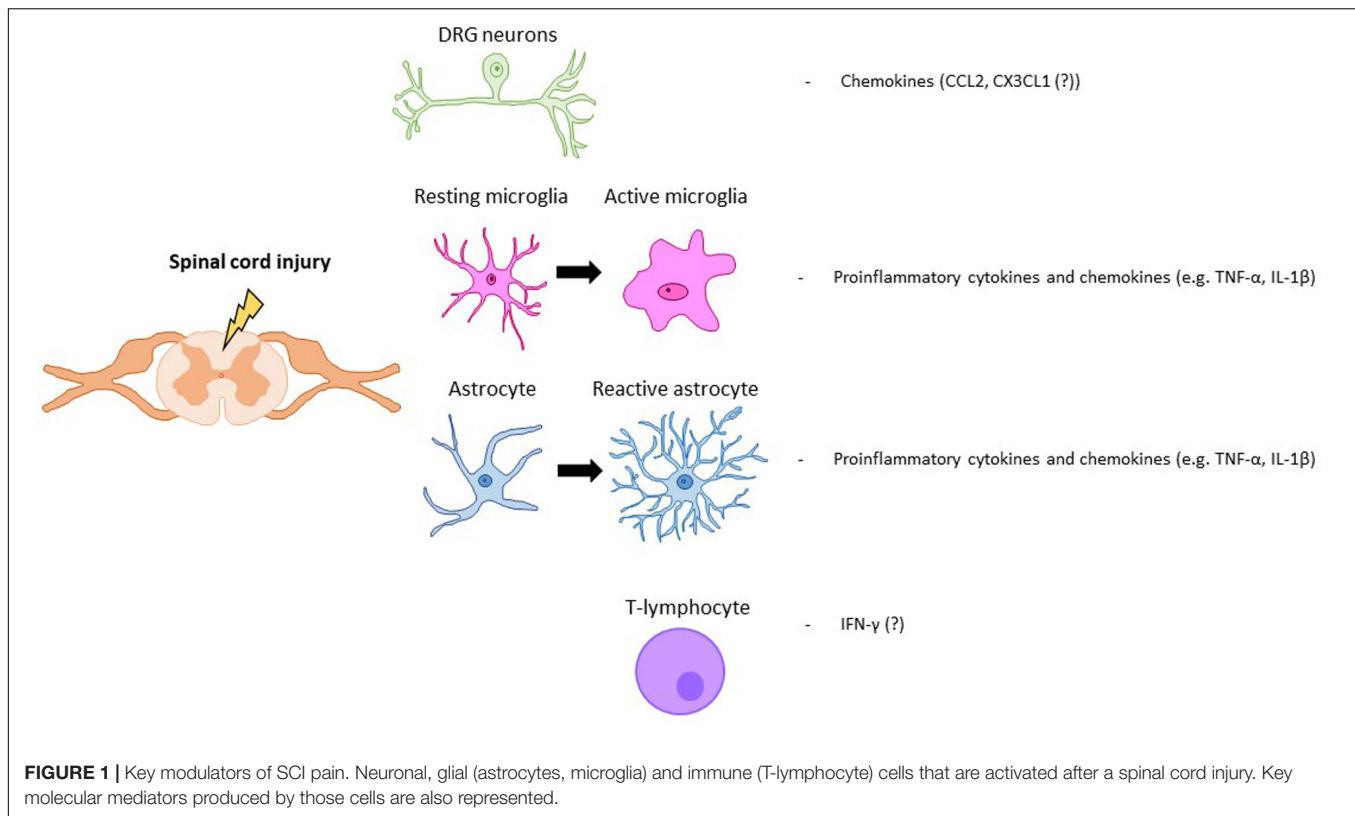
SCI and dependent on microglial activation (Marchand et al., 2009). Thoracic spinal contusion also causes chronic activation of microglia as far as the lumbar spinal cord (Hains et al., 2003; Zai and Wrathall, 2005). When microglia activation is reversed by intrathecal administration of minocycline, lumbar SDH neurons hyperexcitability and pain-related behaviors decrease (Hains and Waxman, 2006; Tan et al., 2009). Early intrathecal administration of carbenoxolone, a gap junction decoupler, to T13 hemisected rats prevents astrocyte activation distant from the injury site and attenuates the development of thermal hyperalgesia and mechanical allodynia (Roh et al., 2010). Intrathecal administration of propentofylline (PPF), that prevents astrocytic and microglial activation and regulates the release of pro-inflammatory cytokines (Raghavendra et al., 2003; Arriagada et al., 2007), after a T13 transverse hemisection attenuates the development of mechanical allodynia and thermal hyperalgesia in the rat. Additionally, PPF reduces astrocyte and microglia activation away from the lesion site, thus decreasing hyperexcitability of lumbar WDR neurons and reducing below-level neuropathic pain in the rat (Gwak et al., 2008; Gwak and Hulsebosch, 2009).

At-level central neuropathic pain depends on p38-MAPK signaling. Following a thoracic contusion injury, p38 α -MAPK is activated in neurons and microglia, but not in astrocytes, contributing to neuronal hyperexcitability (Crown et al., 2006, 2008; Gwak et al., 2009). Several other studies have identified microglial and astrocytic activation as key events for the development of below-level neuropathic pain (Detloff et al., 2008; Carlton et al., 2009; Gwak et al., 2012).

The Role of Immune Mediators

Following a SCI, interactions between nociceptive neurons, SDH neurons and glial cells are severely altered. After SCI, nociceptors become hyperactive and, upon stimulation, secrete increased amounts of glial modulators such as ATP, colony-stimulating factor-1 (CSF1), chemokines or caspase-6 (CASP6) (Ji et al., 2016). These molecules activate spinal microglia in the SDH, which respond by increasing the expression ATP and CX3CL1 receptors. Microglial cells increase secretion of TNF- α and IL-1 β , responsible for enhancing excitatory and suppressing inhibitory synaptic transmissions in spinal cord lamina II neurons (Kawasaki et al., 2008). In the SDH, activated astrocytes are also able to potentiate excitatory synaptic transmission Nerve growth factor (NGF) release, which facilitates nociceptive neurotransmission, leads to neuropathic pain (Chen et al., 2014). In addition, NGF, which is also produced by infiltrating immune cells, may induce spinal expansion of the central terminals of nociceptors, amplifying synaptic input and further contributing to central neuropathic pain (Stroman et al., 2016; Gwak et al., 2017). SCI-induced dysregulation of neuron-glia crosstalk is not restricted to the spinal cord but has also been reported within dorsal root ganglia (DRG), affecting the interaction between Schwann cells within DRG neurons (Lee-Kubli et al., 2016) (**Figure 1**).

Chemokines are vital players in neuropathic pain development and maintenance following peripheral nerve injury (Zhang et al., 2017). They are likely involved in the



mechanism of SCI-induced chronic neuropathic pain but the number of studies using SCI models to detail the contribution of specific chemokines is lacking.

The Role of Neurons

SCI-induced neuropathic pain also reflects neuronal hyperexcitability and increased spontaneous activity, observed both in DRG and spinal neurons, associated with behavioral responses to mechanical and thermal stimuli. This is concomitant with persistently activated microglia and astrocytes in SDH segments distant from the lesion site, the primary target of pro-inflammatory mediators released by those cells (Bedi et al., 2010). Therefore, there has been interest in developing strategies to control and reduce neuronal hyperexcitability, particularly at the spinal level. In a recent rodent SCI study, mouse cortical GABAergic interneurons, derived from the embryonic medial ganglionic eminence (MGE), have been transplanted into the spinal cord. This has resulted in a reduction in hyperexcitability associated with neuropathic pain (Braz et al., 2017). Efforts to translate these preclinical transplantation studies to the clinic are still ongoing.

CLINICAL TRIALS ON SCI-ASSOCIATED PAIN

Neuroimmune interactions on pain emergence after SCI are still rarely addressed on clinical trials. Kwon et al. (2009) found increased levels of TNF- α receptor 1 in

cerebrospinal fluid (CSF), which correlated with the emergence of neuropathic pain. A phase II trial on the effects of minocycline administration after traumatic SCI revealed, at 1-year follow-up, improved motor recovery but effects on pain improvement were not fully satisfactory (Casha et al., 2012; Badhiwala et al., 2018b).

DISCUSSION AND CONCLUSION

Alleviation of neuropathic pain arising after SCI is still an unmet need for most SCI patients. Current pharmacological pain treatments are unsatisfactory and there is an urgent need to develop more effective strategies. Therefore, neuroimmune dysregulation in the context of CNS injuries has emerged as a putative target for improved treatment of SCI-induced neuropathic pain. Accumulating evidence supports a role for neuro-immune dysregulation, often reflecting altered crosstalk between neurons, activated glial cells and invading immune cells (macrophages and T-cells). Dysregulation occurs as a consequence of the inflammatory response to SCI. This response is necessary in the early post-SCI stages to close the injury site but the resulting scar prevents full tissue regeneration and leads to maladaptive neuroplasticity and chronic pain. The challenge is, therefore, to control the inflammatory response and promote tissue repair, both at a structural and functional levels. Presently, methylprednisolone, a potent anti-inflammatory

drug, is the only medication in clinical practice used to treat SCI in early stages. Methylprednisolone has a widespread activity and is able to reduce cytokine release (Uldreda et al., 2016) but reported side effects, and lack of positive outcomes in pain control, among other chronic problems, has led investigators to question its use (Evaniew et al., 2016; Monteiro et al., 2018). The identification of glial cells as important sources of pro- and anti-inflammatory neuromodulators allowed the identification of carbenoxolone, minocycline, and PPF as eventual therapeutic tools (Shultz and Zhong, 2017; Badhiwala et al., 2018a). Although these drugs have produced interesting results in pre-clinical and early clinical trials, dosages and timing for intervention need to be critically defined in the future for effective pain management.

REFERENCES

- Alizadeh, A., Dyck, S. M., and Karimi-Abdolrezaee, S. (2019). Traumatic spinal cord injury: an overview of pathophysiology, models and acute injury mechanisms. *Front. Neurol.* 10:282. doi: 10.3389/fneur.2019.00282
- Arriagada, O., Constandil, L., Hernández, A., Barra, R., Soto-Moyano, R., and Laurido, C. (2007). Effects of interleukin-1 β on spinal cord nociceptive transmission in intact and propentofylline-treated rats. *Int. J. Neurosci.* 117, 617–625. doi: 10.1080/00207450600773806
- Badhiwala, J. H., Ahuja, C. S., and Fehlings, M. G. (2018a). Time is spine: a review of translational advances in spinal cord injury. *J. Neurosurg. Spine* 30, 1–18. doi: 10.3171/2018.9.spine18682
- Badhiwala, J. H., Wilson, J. R., Kwon, B. K., Casha, S., and Fehlings, M. G. (2018b). A review of clinical trials in spinal cord injury including biomarkers. *J. Neurotr.* 35, 1906–1917.
- Bedi, S. S., Yang, Q., Crook, R. J., Du, J., Wu, Z., Fishman, H. M., et al. (2010). Chronic spontaneous activity generated in the somata of primary nociceptors is associated with pain-related behavior after spinal cord injury. *J. Neurosci.* 30, 14870–14882. doi: 10.1523/jneurosci.2428-10.2010
- Bellver-Landete, V., Bretheau, F., Mailhot, B., Vallières, N., Lessard, M., Janelle, M. E., et al. (2019). Microglia are an essential component of the neuroprotective scar that forms after spinal cord injury. *Nat. Commun.* 10:518.
- Block, M. L., Zecca, L., and Hong, J.-S. (2007). Microglia-mediated neurotoxicity: uncovering the molecular mechanisms. *Nat. Rev. Neurosci.* 8, 57–69. doi: 10.1038/nrn2038
- Boadas-Vaello, P., Castany, S., Homs, J., Álvarez-Pérez, B., Deulofeu, M., and Verdú, E. (2016). Neuroplasticity of ascending and descending pathways after somatosensory system injury: reviewing knowledge to identify neuropathic pain therapeutic targets. *Spinal Cord* 54, 330–340. doi: 10.1038/sc.2015.225
- Bourne, S., Machado, A. G., and Nagel, S. J. (2014). Basic anatomy and physiology of pain pathways. *Neurosurg. Clin. N. Am.* 25, 629–638. doi: 10.1016/j.nec.2014.06.001
- Braaf, S., Lennox, A., Nunn, A., and Gabbe, B. (2017). Social activity and relationship changes experienced by people with bowel and bladder dysfunction following spinal cord injury. *Spinal Cord* 55, 679–686. doi: 10.1038/sc.2017.19
- Bradbury, E. J., and Burnside, E. R. (2019). Moving beyond the glial scar for spinal cord repair. *Nat. Commun.* 10, 3879–3879.
- Braz, J. M., Etlin, A., Juarez-Salinas, D., Llewellyn-Smith, I. J., and Basbaum, A. I. (2017). Rebuilding CNS inhibitory circuits to control chronic neuropathic pain and itch. *Progress Brain Res.* 231, 87–105. doi: 10.1016/bs.pbr.2016.10.001
- Bryce, T. N., Biering-Sørensen, F., Finnerup, N. B., Cardenas, D. D., Defrin, R., Lundeberg, T., et al. (2012). International spinal cord injury pain classification: part I. Background and description. March 6–7, 2009. *Spinal Cord* 50, 413–417. doi: 10.1038/sc.2011.156
- Burke, D., Fullen, B. M., Stokes, D., and Lennon, O. (2017). Neuropathic pain prevalence following spinal cord injury: a systematic review and meta-analysis. *Eur. J. Pain* 21, 29–44. doi: 10.1002/ejp.905
- Carlton, S. M., Du, J., Tan, H. Y., Nesic, O., Hargett, G. L., Bopp, A. C., et al. (2009). Peripheral and central sensitization in remote spinal cord regions contribute to central neuropathic pain after spinal cord injury. *Pain* 147, 265–276. doi: 10.1016/j.pain.2009.09.030
- Casha, S., Zygun, D., McGowan, M. D., Bains, I., Yong, V. W., and Hurlbert, R. J. (2012). Results of a phase II placebo-controlled randomized trial of minocycline in acute spinal cord injury. *Brain* 135, 1224–1236. doi: 10.1093/brain/aww072
- Chen, G., Park, C. K., Xie, R. G., Berta, T., Nedergaard, M., and Ji, R. R. (2014). Connexin-43 induces chemokine release from spinal cord astrocytes to maintain late-phase neuropathic pain in mice. *Brain* 137, 2193–2209. doi: 10.1093/brain/awu140
- Colburn, R. W., Rickman, A. J., and DeLeo, J. A. (1999). The effect of site and type of nerve injury on spinal glial activation and neuropathic pain behavior. *Exp. Neurol.* 157, 289–304. doi: 10.1006/exnr.1999.7065
- Crown, E. D., Gwak, Y. S., Ye, Z., Johnson, K. M., and Hulsebosch, C. E. (2008). Activation of p38 MAP kinase is involved in central neuropathic pain following spinal cord injury. *Exp. Neurol.* 213, 257–267. doi: 10.1016/j.expneurol.2008.05.025
- Crown, E. D., Ye, Z., Johnson, K. M., Xu, G.-Y., McAdoo, D. J., and Hulsebosch, C. E. (2006). Increases in the activated forms of ERK 1/2, p38 MAPK, and CREB are correlated with the expression of allodynia following spinal cord injury. *Exp. Neurol.* 199, 397–407. doi: 10.1016/j.expneurol.2006.01.003
- Deonarine, K., Panelli, M. C., Stashower, M. E., Jin, P., Smith, K., Slade, H. B., et al. (2007). Gene expression profiling of cutaneous wound healing. *J. Transl. Med.* 5, 11–11.
- Detloff, M. R., Fisher, L. C., McGaughy, V., Longbrake, E. E., Popovich, P. G., and Basso, D. M. (2008). Remote activation of microglia and pro-inflammatory cytokines predict the onset and severity of below-level neuropathic pain after spinal cord injury in rats. *Exp. Neurol.* 212, 337–347. doi: 10.1016/j.expneurol.2008.04.009
- Didangelos, A., Puglia, M., Iberl, M., Sanchez-Bellot, C., Roschitzki, B., and Bradbury, E. J. (2016). High-throughput proteomics reveal alarmins as amplifiers of tissue pathology and inflammation after spinal cord injury. *Sci. Rep.* 6:21607.
- Dijkers, M., Bryce, T., and Zanca, J. (2009). Prevalence of chronic pain after traumatic spinal cord injury: a systematic review. *J. Rehabil. Res. Dev.* 46, 13–29.
- Dusart, I., and Schwab, M. E. (1994). Secondary cell death and the inflammatory reaction after dorsal hemisection of the rat spinal cord. *Eur. J. Neurosci.* 6, 712–724. doi: 10.1111/j.1460-9568.1994.tb00983.x
- Evaniew, N., Belley-Côté, E. P., Fallah, N., Noonan, V. K., Rivers, C. S., and Dvorak, M. F. (2016). Methylprednisolone for the treatment of patients with acute spinal cord injuries: a systematic review and meta-analysis. *J. Neurotr.* 33, 468–481. doi: 10.1089/neu.2015.4192
- Fenton, B. W., Shih, E., and Zolton, J. (2015). The neurobiology of pain perception in normal and persistent pain. *Pain Manag.* 5, 297–317. doi: 10.2217/pmt.15.27
- Finnerup, N. B. (2013). Pain in patients with spinal cord injury. *Pain* 154(Suppl. 1), S71–S76.
- Garrison, C. J., Dougherty, P. M., Kajander, K. C., and Carlton, S. M. (1991). Staining of glial fibrillary acidic protein (GFAP) in lumbar spinal cord increases

AUTHOR CONTRIBUTIONS

SC wrote the first version of the manuscript and edited the subsequent versions. IT and CC corrected and edited the original manuscript and subsequent versions. All authors contributed to the article and approved the submitted version.

FUNDING

Funding came from Prémio Melo e Castro 2016 – Santa Casa da Misericórdia de Lisboa. SC was supported by Fundação para a Ciência e Tecnologia (Ph.D. Scholarship SFRH/BD/135868/2018).

- following a sciatic nerve constriction injury. *Brain Res.* 565, 1–7. doi: 10.1016/0006-8993(91)91729-k
- Gensel, J. C., and Zhang, B. (2015). Macrophage activation and its role in repair and pathology after spinal cord injury. *Brain Res.* 1619, 1–11. doi: 10.1016/j.brainres.2014.12.045
- Gwak, Y. S., Crown, E. D., Unabia, G. C., and Hulsebosch, C. E. (2008). Propentofylline attenuates allodynia, glial activation and modulates GABAergic tone after spinal cord injury in the rat. *Pain* 138, 410–422. doi: 10.1016/j.pain.2008.01.021
- Gwak, Y. S., and Hulsebosch, C. E. (2009). Remote astrocytic and microglial activation modulates neuronal hyperexcitability and below-level neuropathic pain after spinal injury in rat. *Neuroscience* 161, 895–903. doi: 10.1016/j.neuroscience.2009.03.055
- Gwak, Y. S., Hulsebosch, C. E., and Leem, J. W. (2017). Neuronal-glial interactions maintain chronic neuropathic pain after spinal cord injury. *Neural Plast.* 2017:2480689.
- Gwak, Y. S., Kang, J., Unabia, G. C., and Hulsebosch, C. E. (2012). Spatial and temporal activation of spinal glial cells: role of gliopathy in central neuropathic pain following spinal cord injury in rats. *Exp. Neurol.* 234, 362–372. doi: 10.1016/j.expneurol.2011.10.010
- Gwak, Y. S., Unabia, G. C., and Hulsebosch, C. E. (2009). Activation of p-38alpha MAPK contributes to neuronal hyperexcitability in caudal regions remote from spinal cord injury. *Exp. Neurol.* 220, 154–161. doi: 10.1016/j.expneurol.2009.08.012
- Hains, B. C., Klein, J. P., Saab, C. Y., Craner, M. J., Black, J. A., and Waxman, S. G. (2003). Upregulation of sodium channel Nav1.3 and functional involvement in neuronal hyperexcitability associated with central neuropathic pain after spinal cord injury. *J. Neurosci.* 23, 8881–8892. doi: 10.1523/jneurosci.23-26-08881.2003
- Hains, B. C., and Waxman, S. G. (2006). Activated microglia contribute to the maintenance of chronic pain after spinal cord injury. *J. Neurosci.* 26, 4308–4317. doi: 10.1523/jneurosci.0003-06.2006
- Heinricher, M. M., Tavares, I., Leith, J. L., and Lumb, B. M. (2009). Descending control of nociception: specificity, recruitment and plasticity. *Brain Res. Rev.* 60, 214–225. doi: 10.1016/j.brainresrev.2008.12.009
- Hines, D. J., Hines, R. M., Mulligan, S. J., and Macvicar, B. A. (2009). Microglia processes block the spread of damage in the brain and require functional chloride channels. *Glia* 57, 1610–1618. doi: 10.1002/glia.20874
- James, S. L., Theadom, A., Ellenbogen, R. G., Bannick, M. S., Montjoy-Venning, W., Lucchesi, L. R., et al. (2019). Global, regional, and national burden of traumatic brain injury and spinal cord injury, 1990–2016: a systematic analysis for the Global Burden of Disease Study 2016. *Lancet Neurol.* 18, 56–87.
- Ji, R. R., Chamesian, A., and Zhang, Y. Q. (2016). Pain regulation by non-neuronal cells and inflammation. *Science* 354, 572–577. doi: 10.1126/science.aaf8924
- Jones, T. B. (2014). Lymphocytes and autoimmunity after spinal cord injury. *Exp. Neurol.* 258, 78–90. doi: 10.1016/j.expneurol.2014.03.003
- Junger, H., and Sorkin, L. S. (2000). Nociceptive and inflammatory effects of subcutaneous TNFalpha. *Pain* 85, 145–151. doi: 10.1016/s0304-3959(99)00262-6
- Kawasaki, Y., Zhang, L., Cheng, J.-K., and Ji, R.-R. (2008). Cytokine mechanisms of central sensitization: distinct and overlapping role of interleukin-1beta, interleukin-6, and tumor necrosis factor-alpha in regulating synaptic and neuronal activity in the superficial spinal cord. *J. Neurosci.* 28, 5189–5194. doi: 10.1523/jneurosci.3338-07.2008
- Kigerl, K. A., Gensel, J. C., Ankeny, D. P., Alexander, J. K., Donnelly, D. J., and Popovich, P. G. (2009). Identification of two distinct macrophage subsets with divergent effects causing either neurotoxicity or regeneration in the injured mouse spinal cord. *J. Neurosci.* 29, 13435–13444. doi: 10.1523/jneurosci.3257-09.2009
- Kjell, J., and Olson, L. (2016). Rat models of spinal cord injury: from pathology to potential therapies. *Dis. Model Mech.* 9, 1125–1137. doi: 10.1242/dmm.025833
- Kramer, J. L. K., Minhas, N. K., Jutzeler, C. R., Erskine, E. L. K. S., Liu, L. J. W., and Ramer, M. S. (2017). Neuropathic pain following traumatic spinal cord injury: models, measurement, and mechanisms. *J. Neurosci. Res.* 95, 1295–1306. doi: 10.1002/jnr.23881
- Kwon, B. K., Curt, A., Belanger, L. M., Bernardo, A., Chan, D., Markez, J. A., et al. (2009). Intrathecal pressure monitoring and cerebrospinal fluid drainage in acute spinal cord injury: a prospective randomized trial. *J. Neurosurg. Spine* 10, 181–193. doi: 10.3171/2008.10.spine08217
- Lee, S., Shi, X. Q., Fan, A., West, B., and Zhang, J. (2018). Targeting macrophage and microglia activation with colony stimulating factor 1 receptor inhibitor is an effective strategy to treat injury-triggered neuropathic pain. *Mol. Pain* 14:1744806918764979.
- Lee-Kubli, C. A., Ingves, M., Henry, K. W., Shiao, R., Collyer, E., Tuszyński, M. H., et al. (2016). Analysis of the behavioral, cellular and molecular characteristics of pain in severe rodent spinal cord injury. *Exp. Neurol.* 278, 91–104. doi: 10.1016/j.expneurol.2016.01.009
- Liddel, S. A., Gattenplan, K. A., Clarke, L. E., Bennett, F. C., Bohlen, C. J., Schirmer, L., et al. (2017). Neurotoxic reactive astrocytes are induced by activated microglia. *Nature* 541, 481–487.
- Loane, D. J., and Byrnes, K. R. (2010). Role of microglia in neurotrauma. *Neurotherapeutics* 7, 366–377. doi: 10.1016/j.nurt.2010.07.002
- Loeser, J. D., and Treede, R.-D. (2008). The Kyoto protocol of IASP basic pain terminology. *Pain* 137, 473–477. doi: 10.1016/j.pain.2008.04.025
- Malcangio, M. (2019). Role of the immune system in neuropathic pain. *Scand. J. Pain* 20, 33–37. doi: 10.1515/sjpain-2019-0138
- Marchand, F., Tsantoulas, C., Singh, D., Grist, J., Clark, A. K., Bradbury, E. J., et al. (2009). Effects of Etanercept and Minocycline in a rat model of spinal cord injury. *Eur. J. Pain* 13, 673–681. doi: 10.1016/j.ejpain.2008.08.001
- Martins, I., and Tavares, I. (2017). Reticular formation and pain: the past and the future. *Front. Neuroanat.* 11:51. doi: 10.3389/fnana.2017.00051
- Monteiro, S., Salgado, A. J., and Silva, N. A. (2018). Immunomodulation as a neuroprotective strategy after spinal cord injury. *Neural Regen. Res.* 13, 423–424.
- Nahrendorf, M., Swirski, F. K., Aikawa, E., Stangenberg, L., Wurdinger, T., Figueiredo, J.-L., et al. (2007). The healing myocardium sequentially mobilizes two monocyte subsets with divergent and complementary functions. *J. Exp. Med.* 204, 3037–3047. doi: 10.1084/jem.20070885
- Neirinx, V., Coste, C., Franzen, R., Gothot, A., Rogister, B., and Wislet, S. (2014). Neutrophil contribution to spinal cord injury and repair. *J. Neuroinflamm.* 11:150.
- Noble, B. T., Brennan, F. H., and Popovich, P. G. (2018). The spleen as a neuroimmune interface after spinal cord injury. *J. Neuroimmunol.* 321, 1–11. doi: 10.1016/j.jneuroim.2018.05.007
- Park, E., Velumian, A. A., and Fehlings, M. G. (2004). The role of excitotoxicity in secondary mechanisms of spinal cord injury: a review with an emphasis on the implications for white matter degeneration. *J. Neurotr.* 21, 754–774. doi: 10.1089/0897715041269641
- Peng, X.-M., Zhou, Z.-G., Glorioso, J. C., Fink, D. J., and Mata, M. (2006). Tumor necrosis factor-alpha contributes to below-level neuropathic pain after spinal cord injury. *Ann. Neurol.* 59, 843–851. doi: 10.1002/ana.20855
- Perkins, N. M., and Tracey, D. J. (2000). Hyperalgesia due to nerve injury: role of neutrophils. *Neuroscience* 101, 745–757. doi: 10.1016/s0306-4522(00)00396-1
- Pineau, I., Sun, L., Bastien, D., and Lacroix, S. (2010). Astrocytes initiate inflammation in the injured mouse spinal cord by promoting the entry of neutrophils and inflammatory monocytes in an IL-1 receptor/MyD88-dependent fashion. *Brain Behav. Immun.* 24, 540–553. doi: 10.1016/j.bbi.2009.11.007
- Popovich, P. G., and Hickey, W. F. (2001). Bone marrow chimeric rats reveal the unique distribution of resident and recruited macrophages in the contused rat spinal cord. *J. Neuropathol. Exp. Neurol.* 60, 676–685. doi: 10.1093/jnen/60.7.676
- Raghavendra, V., Tanga, F., and DeLeo, J. A. (2003). Inhibition of microglial activation attenuates the development but not existing hypersensitivity in a rat model of neuropathy. *J. Pharmacol. Exp. Ther.* 306, 624–630. doi: 10.1124/jpet.103.052407
- Roh, D.-H., Yoon, S.-Y., Seo, H.-S., Kang, S.-Y., Han, H.-J., Beitz, A. J., et al. (2010). Intrathecal injection of carbenoxolone, a gap junction decoupler, attenuates the induction of below-level neuropathic pain after spinal cord injury in rats. *Exp. Neurol.* 224, 123–132. doi: 10.1016/j.expneurol.2010.03.002
- Rossignol, S., Schwab, M., Schwartz, M., and Fehlings, M. G. (2007). Spinal cord injury: time to move? *J. Neurosci.* 27, 11782–11792.

- Rust, R., and Kaiser, J. (2017). Insights into the dual role of inflammation after spinal cord injury. *J. Neurosci.* 37, 4658–4660. doi: 10.1523/jneurosci.0498-17.2017
- Schomberg, D., and Olson, J. K. (2012). Immune responses of microglia in the spinal cord: contribution to pain states. *Exp. Neurol.* 234, 262–270. doi: 10.1016/j.expneurol.2011.12.021
- Shechter, R., and Schwartz, M. (2013). CNS sterile injury: just another wound healing? *Trends Mol. Med.* 19, 135–143. doi: 10.1016/j.molmed.2012.11.007
- Shiao, R., and Lee-Kubli, C. A. (2018). Neuropathic pain after spinal cord injury: challenges and research perspectives. *Neurotherapeutics* 15, 635–653. doi: 10.1007/s13311-018-0633-4
- Shultz, R. B., and Zhong, Y. (2017). Minocycline targets multiple secondary injury mechanisms in traumatic spinal cord injury. *Neural Regen. Res.* 12, 702–713.
- Siddall, P. J., McClelland, J. M., Rutkowski, S. B., and Cousins, M. J. (2003). A longitudinal study of the prevalence and characteristics of pain in the first 5 years following spinal cord injury. *Pain* 103, 249–257. doi: 10.1016/s0304-3959(02)00452-9
- Silva, N. A., Sousa, N., Reis, R. L., and Salgado, A. J. (2014). From basics to clinical: a comprehensive review on spinal cord injury. *Prog. Neurobiol.* 114, 25–57. doi: 10.1016/j.pneurobio.2013.11.002
- Sorkin, L. S., Xiao, W. H., Wagner, R., and Myers, R. R. (1997). Tumour necrosis factor- α induces ectopic activity in nociceptive primary afferent fibres. *Neuroscience* 81, 255–262. doi: 10.1016/s0306-4522(97)00147-4
- Sroga, J. M., Jones, T. B., Kigerl, K. A., McGaughy, V. M., and Popovich, P. G. (2003). Rats and mice exhibit distinct inflammatory reactions after spinal cord injury. *J. Comp. Neurol.* 462, 223–240. doi: 10.1002/cne.10736
- Stroman, P. W., Khan, H. S., Bosma, R. L., Cotoi, A. I., Leung, R., Cadotte, D. W., et al. (2016). Changes in pain processing in the spinal cord and brainstem after spinal cord injury characterized by functional magnetic resonance imaging. *J. Neurotr.* 33, 1450–1460. doi: 10.1089/neu.2015.4257
- Tan, A. M., Zhao, P., Waxman, S. G., and Hains, B. C. (2009). Early microglial inhibition preemptively mitigates chronic pain development after experimental spinal cord injury. *J. Rehabil. Res. Dev.* 46, 123–133.
- Tozaki-Saitoh, H., and Tsuda, M. (2019). Microglia-neuron interactions in the models of neuropathic pain. *Biochem. Pharmacol.* 169:113614. doi: 10.1016/j.bcp.2019.08.016
- Tran, A. P., Warren, P. M., and Silver, J. (2018). The biology of regeneration failure and success after spinal cord injury. *Physiol. Rev.* 98, 881–917. doi: 10.1152/physrev.00017.2017
- Ulfendraj, A., Chio, J. C., Ahuja, C. S., and Fehlings, M. G. (2016). Modulating the immune response in spinal cord injury. *Expert. Rev. Neurother.* 16, 1127–1129. doi: 10.1080/14737175.2016.1207532
- Vilhardt, F. (2005). Microglia: phagocyte and glia cell. *Int. J. Biochem. Cell Biol.* 37, 17–21. doi: 10.1016/j.biocel.2004.06.010
- Wagner, R., and Myers, R. R. (1996). Schwann cells produce tumor necrosis factor α : expression in injured and non-injured nerves. *Neuroscience* 73, 625–629. doi: 10.1016/0306-4522(96)00127-3
- Widerström-Noga, E. (2017). Neuropathic pain and spinal cord injury: phenotypes and pharmacological management. *Drugs* 77, 967–984. doi: 10.1007/s40265-017-0747-8
- Xu, K., Malouf, A. T., Messing, A., and Silver, J. (1999). Glial fibrillary acidic protein is necessary for mature astrocytes to react to beta-amyloid. *Glia* 25, 390–403. doi: 10.1002/(sici)1098-1136(19990215)25:4<390::aid-glia8>3.0.co;2-7
- Yang, D., Han, Z., and Oppenheim, J. J. (2017). Alarmins and immunity. *Immunol. Rev.* 280, 41–56. doi: 10.1111/immr.12577
- Yang, Q., Wu, Z., Hadden, J. K., Odem, M. A., Zuo, Y., Crook, R. J., et al. (2014). Persistent pain after spinal cord injury is maintained by primary afferent activity. *J. Neurosci.* 34, 10765–10769. doi: 10.1523/jneurosci.5316-13.2014
- Zai, L. J., and Wrathall, J. R. (2005). Cell proliferation and replacement following contusive spinal cord injury. *Glia* 50, 247–257. doi: 10.1002/glia.20176
- Zhang, Z.-J., Jiang, B.-C., and Gao, Y.-J. (2017). Chemokines in neuron-glia cell interaction and pathogenesis of neuropathic pain. *Cell Mol. Life Sci.* 74, 3275–3291. doi: 10.1007/s00018-017-2513-1
- Zhou, X., Wahane, S., Friedl, M. S., Kluge, M., Friedel, C. C., Avramopoulos, K., et al. (2020). Microglia and macrophages promote corraling, wound compaction and recovery after spinal cord injury via Plexin-B2. *Nat. Neurosci.* 23, 337–350. doi: 10.1038/s41593-020-0597-7
- Zhuang, Z.-Y., Gerner, P., Woolf, C. J., and Ji, R.-R. (2005). ERK is sequentially activated in neurons, microglia, and astrocytes by spinal nerve ligation and contributes to mechanical allodynia in this neuropathic pain model. *Pain* 114, 149–159. doi: 10.1016/j.pain.2004.12.022

Conflict of Interest: The authors declare that the research was conducted in the absence of any commercial or financial relationships that could be construed as a potential conflict of interest.

Copyright © 2020 Chambel, Tavares and Cruz. This is an open-access article distributed under the terms of the Creative Commons Attribution License (CC BY). The use, distribution or reproduction in other forums is permitted, provided the original author(s) and the copyright owner(s) are credited and that the original publication in this journal is cited, in accordance with accepted academic practice. No use, distribution or reproduction is permitted which does not comply with these terms.



The NLRP3 Inflammasome: Role and Therapeutic Potential in Pain Treatment

Hana Starobova¹, Evelyn Israel Nadar¹ and Irina Vetter^{1,2*}

¹ Centre for Pain Research, Institute for Molecular Bioscience, University of Queensland, St Lucia, QLD, Australia, ² School of Pharmacy, The University of Queensland, St Lucia, QLD, Australia

Pain is a fundamental feature of inflammation. The immune system plays a critical role in the activation of sensory neurons and there is increasing evidence of neuro-inflammatory mechanisms contributing to painful pathologies. The inflammasomes are signaling multiprotein complexes that are key components of the innate immune system. They are intimately involved in inflammatory responses and their activation leads to production of inflammatory cytokines that in turn can affect sensory neuron function. Accordingly, the contribution of inflammasome activation to pain signaling has attracted considerable attention in recent years. NLRP3 is the best characterized inflammasome and there is emerging evidence of its role in a variety of inflammatory pain conditions. In vitro and in vivo studies have reported the activation and upregulation of NLRP3 in painful conditions including gout and rheumatoid arthritis, while inhibition of NLRP3 function or expression can mediate analgesia. In this review, we discuss painful conditions in which NLRP3 inflammasome signaling has been pathophysiologically implicated, as well as NLRP3 inflammasome-mediated mechanisms and signaling pathways that may lead to the activation of sensory neurons.

Keywords: NOD, LRR and PYD domains-containing protein 3, neuro-inflammation, MCC950, interleukin-1 β , sensory neurons, inflammatory diseases, interleukin-1 receptor

OPEN ACCESS

Edited by:

Istvan Nagy,
Imperial College London,
United Kingdom

Reviewed by:

Arpeeta Sharma,
Baker Heart and Diabetes Institute,
Australia
Debora Lo Furno,
Università di Catania, Italy

*Correspondence:

Irina Vetter
i.vetter@imb.uq.edu.au

Specialty section:

This article was submitted to
Integrative Physiology,
a section of the journal
Frontiers in Physiology

Received: 17 March 2020

Accepted: 24 July 2020

Published: 19 August 2020

Citation:

Starobova H, Nadar EI and Vetter I
(2020) The NLRP3 Inflammasome:
Role and Therapeutic Potential in Pain
Treatment. *Front. Physiol.* 11:1016.
doi: 10.3389/fphys.2020.01016

INTRODUCTION

Chronic pain is a dynamic process involving ongoing changes and adaption within the peripheral and central nervous systems and accompanies a vast number of inflammatory and non-inflammatory pathological states such as cancer, diabetes or rheumatoid arthritis.

Sensory neurons, including nociceptors, express a variety of ion channels and receptors involved in transformation of external stimuli into electrical signals, such the Transient Receptor Potential channels TRPV1, TRPV2, TRPV3, TRPA1, and TRPM8; purine receptor 3 (P2X₃); voltage-gated sodium channel (Na_v) subtypes Na_v1.7, Na_v1.8, and Na_v1.9 and voltage-gated potassium channels (K_v). The activation of these channels and receptors by thermal, mechanical or chemical nociceptive stimuli generate an action potential that is transmitted along the axons to the central nervous system. The immune system and neuro-inflammation play a crucial role in sensitization of the peripheral and central nervous systems, including activation of nociceptors. Specifically, microglia, satellite glia cells, Schwann cells, oligodendrocytes, keratinocytes, macrophages or T-cells releasing pro-inflammatory signaling molecules, such as interleukin-1 β (IL-1 β) or adenosine-triphosphate (ATP), are implicated in the pathology of various painful conditions (Ji et al., 2016;

Inoue and Tsuda, 2018). Moreover, the depletion of macrophages reduces hyperalgesia in different rodent models of neuropathic pain (Barclay et al., 2007; Mert et al., 2009; Kobayashi et al., 2015; Zhang et al., 2016) and macrophages were shown to directly regulate the peristaltic activity of the colon via interaction with the enteric neurons and to release a variety of pain mediators such as nerve growth factor, tumor necrosis factor or IL-1 β (Muller et al., 2014; McMahon et al., 2015).

Inflammasomes are a group of pattern recognition receptors (PRR) that detect pathogen- or damage-associated molecular patterns (PAMPs and DAMPs) and activate inflammatory responses. To date, there are six known inflammasome multi-protein complexes: NACHT, LRR and PYD/CARD domains-containing proteins - NLRP1, NLRP3, NLRP6, NLRP12, and NLRC4, and AIM2 (absent in melanoma 2) (Strowig et al., 2012). While the NLR family of the inflammasomes are fundamental component of the innate immune system, recognizing a broad spectrum of viral and bacterial stimuli, such as bacterial or viral RNA, lipopolysaccharides or uric acid crystals (Franchi et al., 2009b), AIM2 recognizes double stranded DNA released during various bacterial and viral infections (Sharma et al., 2019). Out of all the NLR inflammasomes, the NLRP3 inflammasome is amongst the best characterized, being predominantly expressed by immune cells such as macrophages and neutrophils and to a lesser extent by dendritic cells, microglia and dorsal root ganglia (Guarda et al., 2011b; Gustin et al., 2015; Fann et al., 2018). The activation of NLRP3 leads to release of IL-1 β , a cytokine that is known to directly sensitize nociceptors and to cause pain (Binshtok et al., 2008). Increased NLRP3 expression and activation, together with the release of IL-1 β , has been linked to pathogenesis of several painful inflammatory and non-inflammatory conditions such as rheumatoid arthritis, gout, neuropathic pain and diabetic wound healing (**Table 1**). In this review, we discuss the mechanisms leading to NLRP3 inflammasome activation in painful conditions, the resulting signaling pathways that can lead to the sensitization or activation of sensory neurons, as well as the therapeutic potential of NLRP3 inflammasome inhibition to mediate analgesia.

ACTIVATION OF THE NLRP3 INFLAMMASOME

The activation of the NLRP3 inflammasome requires, with some exceptions, two signals. The first signal leads to priming of the NLRP3 inflammasome by endogenous molecules (e.g., tumor necrosis factor (TNF) and IL-1 β) or microbial components such as lipopolysaccharides. These compounds activate their cognate receptors, leading to nuclear factor- κ B-dependent increase of NLRP3 and pro-IL-1 β expression (**Figure 1A**) (Bauernfeind et al., 2009; Franchi et al., 2009a). The second signal causes the direct activation of NLRP3 and can involve several cellular signaling events such as potassium ion efflux, changes in calcium signaling, increase in production of reactive oxygen species by mitochondria or lysosomal leakage and release of cathepsin-B (**Figure 1A**; Brough et al., 2003; Bauernfeind et al., 2011; Munoz-Planillo et al., 2013; Orlowski et al., 2015). In the canonical

NLRP3 signaling pathway, the activation of NLRP3 leads to assembly of a multi-protein complex that recruits caspase-1 via caspase activation and recruitment domain (CARD) interactions to promote caspase activation. Activated caspase-1 then cleaves pro-IL-1 β and pro-interleukin-18 (pro-IL-18) into their active forms (Hu et al., 2013; Lu et al., 2014, 2015, 2016). Additionally, active caspase-1 cleaves the pore former pro-gasdermin D into its active form, inducing pyroptosis, a form of inflammatory cell death (Sagulenko et al., 2013).

The NLRP3 inflammasome can also be activated via non-canonical signaling pathways that were observed as a preferable response to gram-negative bacteria in mice, and are independent of toll-like receptor 4-dependent priming (TLR4) (Kayagaki et al., 2013). The non-canonical pathway involves the activation of caspase-11 by lipopolysaccharides, which leads to ATP efflux via pannexin-1 and subsequent activation of P2X-purinoreceptor-7 (P2X7), efflux of intracellular potassium and activation of NLRP3. Caspase-11 also directly cleaves pro-gasdermin-D, inducing pyroptosis (Kayagaki et al., 2011; Shi et al., 2015; Yang et al., 2015).

Recently, another NLRP3 activation pathway, the so-called alternative inflammasome pathway, was discovered in human monocytes. This pathway is dependent on priming, independent of K⁺ efflux, involves caspase-8 activation and does not induce apoptosis-inducing speck-like protein containing CARD (ASC-speck) formation or pyroptosis (Gaidt et al., 2016).

IL-1 β -INDUCED ACTIVATION OF SENSORY NEURONS

Activation of the NLRP3 inflammasome leads to release of active IL-1 β , an inflammatory cytokine that regulates the function of various cells, such as immune and neuronal cells (Strowig et al., 2012; **Figure 1B**). IL-1 β is released at the site of inflammation and is a well-known pain-inducing molecule. Several rodent studies have shown that intraplantar or intraperitoneal injection of IL-1 β causes severe hyperalgesia (Ferreira et al., 1988; Amaya et al., 2006). IL-1 β likely increases the excitability of nociceptors by altering the function of several neuronal ion channels and receptors, including transient receptor potential channels (TRPA1 and TRPV1), N-methyl-D-aspartate (NMDA) and gamma-aminobutyric acid (GABA) receptors, as well as voltage-gated K⁺, Na⁺, and Ca²⁺ channels (Binshtok et al., 2008; Schafers and Sorkin, 2008; Ren and Torres, 2009; Malsch et al., 2014; Stemkowski et al., 2015; Zanos et al., 2018). In this context, IL-1 β can be considered to be a direct neuromodulator, and although the molecular signaling pathways leading to enhanced excitability have not been studied extensively, signaling via neuronal IL-1 receptors and activation of p38-mitogen-activated protein kinase appear to contribute mechanistically. Specifically, IL-1 β alters the voltage-dependence of slow inactivation of tetrodotoxin (TTX)-resistant Na_v current in sensory neurons and also enhances persistent TTX-resistant current (Binshtok et al., 2008). Importantly, IL-1 β -induced mechanical allodynia is also relieved in mice lacking the TTX-resistant isoform Na_v1.9 (Amaya et al., 2006), supporting an important contribution of

TABLE 1 | NLRP3 in pain pathology.

Disease / Condition	Description	Study description	Species	NLRP3 involvement	References
Bladder pain syndrome/ interstitial cystitis	Persistent pain or discomfort in bladder often caused by urinary tract infection.	Expression of Neurokinin-1 receptor and Substance P in nerve cells and bladder epithelial cells of the urinary bladder mucosa; examination of bladder pathology in knockout animals.	M (C57BL6/J, <i>Tlr4</i> ^{-/-} , <i>Il1b</i> ^{-/-} , <i>Asc</i> ^{-/-} , <i>Nlrp3</i> ^{-/-})	Deteriorated bladder pathology in <i>Asc</i> ^{-/-} and <i>Nlrp3</i> ^{-/-} mice.	Butler et al., 2018
Burns pain	Pain caused by burn trauma associated with severe acute or chronic pain.	Assessment of burn-induced mechanical allodynia, thermal allodynia, edema and weight bearing in <i>Nlrp3</i> ^{-/-} and <i>Ice</i> ^{-/-} mice, and in C57BL6/J after administration of MCC950.	M (C57BL6/J, <i>Nlrp3</i> ^{-/-} , <i>Ice</i> ^{-/-})	Attenuated weight bearing changes in <i>Nlrp3</i> ^{-/-} and mice treated with MCC950. No effect on mechanical or thermal allodynia.	Deuis et al., 2017
Metastatic cancer-induced bone pain (CIBP)	Bone pain caused by tumor metastasis associated with inflammation, hypercalcemia, skeletal fractures, compression of the spinal cord or nerves.	Assessment of CIBP induced mechanical allodynia (von Frey) and expression of NLRP3, ASC, Casp1 and IL-1 β in spinal cord.	R	MCC950 treatment attenuated CIBP-related mechanical allodynia. MCC950 administration restored increased expression of NLRP3, ASC, Casp1 and IL-1 β in spinal cord.	Chen et al., 2019
Chemo-therapy induced peripheral neuro-pathy	Neuropathy induced by damage of peripheral nerves by chemotherapy agents, manifested by pain, numbness, tingling, gait disturbances and loss of sensory discrimination.	Investigation of NLRP3 expression in spinal cord of oxaliplatin- and paclitaxel-induced peripheral neuropathy model.	M	No increased expression of NLRP3 after oxaliplatin or paclitaxel administration in spinal cord.	Tonkin et al., 2018
		Assessment of expression of NLRP3, Casp1 and IL-1 β in DRG and SN. Assessment of mechanical allodynia after administration of phenyl-N-tert-butyl nitrone (PNB) in paclitaxel-induced neuropathic pain model.	R	Increased expression of NLRP3, Casp1 and IL-1 β in macrophages infiltrating in dorsal root ganglia and sciatic nerve. PNB attenuated mechanical allodynia and decreased NLRP3 expression in dorsal root ganglia and sciatic nerve.	Jia et al., 2017
		Investigation of paclitaxel effect on priming of the NLRP3 inflammasome.	M (C57BL6, <i>Nlrp3</i> ^{-/-})	Paclitaxel primes the NLRP3 inflammasome via TLR4	Son et al., 2019
		Assessment of mechanical allodynia of mice in a bortezomid-induced peripheral neuropathy model and the intrathecal treatment with NLRP3 siRNA.	M	NLRP3 siRNA significantly prevented mechanical allodynia induced by bortezomib treatment.	Liu C. C. et al., 2018
		Assessment of the NLRP3 activation in oxaliplatin induced peripheral neuropathy model in rats treated with MCC950.	R	Increased activation of NLRP3 in astrocytes. MCC950 significantly reduces mechanical hyperalgesia following oxaliplatin treatment.	Wahlman et al., 2018
Cryopyrin associated periodic syndrome (CAPS)	Inherited autosomal dominant autoinflammatory disorder involving mutation in NLRP3; manifested by neurological symptoms such as headache and myalgia. Vast evidence of NLRP3 involvement in CAPS pathology, however no direct link of NLRP3 to pain pathology.	Case study of 13-year-old female with high fever, pericarditis, arthralgia, arthritis of the knees, abdominal pain and marked increase in inflammatory markers.	H	Mutation of the CIAS1/NLRP3 gene. No direct link of NLRP3 to pain symptoms.	Insalaco et al., 2014

(Continued)

TABLE 1 | Continued

Disease / Condition	Description	Study description	Species	NLRP3 involvement	References
		Forty-seven adult patients with CAPS with mutations in NLRP3 (CIAS1) gene and pathognomonic symptoms. Weekly subcutaneous injections of rilonacept (160 mg).	H	Rilonacept decreased the severity of key symptoms including joint pain and eye redness/pain.	Hoffman et al., 2008
		Case study of three family members with CAPS carrying mutation in NLRP3 (CIAS1) gene and treatment with anakinra.	H	Improved symptomatology after anakinra treatment including pain severity.	Maksimovic et al., 2008
		Case study of male patient with mutation of NLRP3 (CIAS1) gene treated with anakinra.	H	Improved pain scores and symptomatology following anakinra treatment.	Gerard et al., 2007
		Two siblings with mutation in NLRP3 (CIAS1) treated with anakinra.	H	Increased activity of Casp1 and levels of IL-1 β . Improved symptomatology following anakinra treatment.	Verma et al., 2010
Fibro-myalgia	Inherited autosomal dominant disease characterized by severe pain in the extremities.	Investigation of the role of coenzyme Q10 (CoQ10) and mitochondrial dysfunction in NLRP3 inflammasome activation in patients and rodent CoQ10 deficiency model.	H M	Increased expression of NLRP3 and IL-1 β in blood of patients with fibromyalgia that was reduced by treatment with CoQ10 treatment. Reduced NLRP3 inflammasome expression and activation in mice, accompanied with increased latencies in hot plate and tail flick test.	Cordero et al., 2014
Gout	Inflammatory arthropathy, associated with pain, caused by deposition of monosodium urate in the joints. Vast evidence of NLRP3 involvement in gout, however, no direct link of NLRP3 to pain pathology.	Investigation of uric acid crystals activation of NLRP3.	M (<i>Asc</i> ^{-/-} , <i>Casp1</i> ^{-/-} , <i>IL-1R</i> ^{-/-})	Uric acid activates the NLRP3 and increases the production of IL-1 β and IL-18. Deficient release of IL-1 β in macrophages from <i>Asc</i> ^{-/-} and <i>Casp1</i> ^{-/-} mice following uric acid treatment.	Martinon et al., 2006
		Assessment of the effect of procyanidins on Monosodium Urate Crystals (MSU) treated Raw 264.7 cells and in rodent model of Gout in CD-1 mice.	CD-1 mice	Procyanidins attenuated gout pain and suppressed ankle swelling and inhibited MSU-induced activation of the NLRP3 inflammasome and increase of IL-1 β .	Liu et al., 2017
Migraine	Chronic painful disorder characterized by attacks of severe headache and neurological symptoms.	Ten patients with chronic active gouty arthritis treated with rilonacept.	H	Decrease of the pain score following rilonacept treatment.	Terkeltaub et al., 2009
		Investigation of NLRP3 and IL-1 β expression and mechanical hyperalgesia in nitroglycerin induced chronic migraine model in mice treated with MCC950.	M	MCC950 reduced periorbital and hind paw mechanical hypersensitivity and restored increased expression of IL-1 β in trigeminal ganglia of nitroglycerin treated mice.	He et al., 2019
Neuro-pathic pain	Pain due to damage or disease affecting the peripheral or central nervous system; manifested as spontaneous pain (stimulus-independent pain) or pain hypersensitivity (stimulus-evoked pain).	Investigation of NLRP3 expression and mechanical hyperalgesia in spinal cord after chronic constriction injury (CCI) of the sciatic nerve and following the treatment with the adenosine triphosphate (ATP) release inhibitor Peptide5 (connexin-43 mimetic peptide).	M	Peptide5 restores the expression levels of NLRP3, ASC and cleaved CASP1 in spinal cord and attenuates mechanical allodynia following CCI of the sciatic nerve.	Tonkin et al., 2018

(Continued)

TABLE 1 | Continued

Disease / Condition	Description	Study description	Species	NLRP3 involvement	References
		Investigation of NLRP3, Casp1 and IL-1 β involvement and expression in spinal cord following partial sciatic nerve ligation (PSNL). Assessment of mechanical and thermal hyperalgesia.	M	PSNL induces overexpression of NLRP3, activation of Casp1 and release of IL-1 β in spinal cord.	Pan et al., 2018
		Investigation of the effect of MCC950 on heat and mechanical hyperalgesia in relapsing-remitting experimental encephalomyelitis (RR-EAE)-mouse model of MS-associated neuropathic pain.	M	MCC950 attenuates mechanical hyperalgesia of mice in RR-EAE-mouse model of MS-associated neuropathic pain.	Khan et al., 2018
		Investigation of the role of NLRP3 expression and IL-1 β production in spared nerve injury (SNI).	M (C57BL6, <i>Nlrp3</i> ^{-/-})	No increased expression of NLRP3 inflammasome components in the spinal cord at mRNA level. No difference in mechanical or thermal responses of C57BL6 or <i>Nlrp3</i> ^{-/-} mice after SNI.	Curto-Reyes et al., 2015
		Assessment of the effect of dexmedetomidine on NLRP3 expression, Casp1 activation and levels of IL-1 β and mechanical allodynia in model of osteoarthritis induced by papain.	M	Dexmedetomidine reduces knee inflammation, gait abnormalities, mechanical and heat hyperalgesia and the expression levels of NLRP3, activated Casp1 and IL-1 β .	Cheng et al., 2019
Post-operative pain	Tissue trauma caused by surgery, involving peripheral and/or central nervous system, manifested by acute or chronic pain, neuropathic pain and hypersensitivity.	Investigation of NLRP3 inflammasome contribution to postoperative pain and assessment of mechanical sensitization.	M (C57BL6/J, <i>Nlrp3</i> ^{-/-})	Only male, but not female, <i>Nlrp3</i> ^{-/-} recover from surgery-induced mechanical sensitization faster than male and female C57BL6/J mice. Immune-mediated sex differences in postoperative pain.	Cowie et al., 2019
Rheuma-toid arthritis (RA)	Autoimmune chronic progressive disease resulting in deformity and pain of the joints of hands, feet, wrists and elbows. Vast evidence of NLRP3 involvement in rheumatoid arthritis pathology, however, no direct link of NLRP3 to pain pathology.	Investigation of NLRP3 activation in synovial tissues from RA and osteoarthritis patients and in rodent model of collagen-induced arthritis treated with MCC950.	M H	NLRP3 inflammasome pathway was activated in synovia of RA patients. MCC950 reduced joints inflammation, bone destruction, NLRP3 activation in the synovia and production of IL-1 β .	Guo et al., 2018
		Investigation of A20 deficiency on NLRP3 activation in rodent RA model.	M (<i>A20</i> ^{myel-KO} , <i>Nlrp3</i> ^{-/-} , <i>Casp1</i> ^{-/-} , <i>IL-1R</i> ^{-/-})	A20 deficiency enhanced NLRP3 activation, pyroptosis and IL-1 β secretion. Inflammation and cartilage destruction were reduced in <i>Nlrp3</i> ^{-/-} and <i>Casp1</i> ^{-/-} mice.	Vande Walle et al., 2014
		Assessment of expression levels of NLRP3, ASC, pro- and active Casp1, pro- and active IL-1 β in blood of RA patients.	H	Increased expression of NLRP3, ASC, active – Casp1 and pro-IL-1 β .	Choulaki et al., 2015

(Continued)

TABLE 1 | Continued

Disease / Condition	Description	Study description	Species	NLRP3 involvement	Ref
Schnitzler syndrome	Rare autoimmune disease that involves inflammation, fever, muscle, bone, and/or joint pain.	Six male patients diagnosed with Schnitzler syndrome and treated with anakinra.	H	Pain regression following anakinra treatment.	Szturz et al., 2014
Diabetes mellitus (DM) wound	Delayed wound healing, painful foot ulcers affecting quality of life in DM patients. Evidence of NLRP3 and IL-1 β expression in DM wound pathology but no direct link to pain pathology.	Skin defects of 2 \times 2 cm ² on the back of the rats. Quantification of ROS and NLRP3 in wound tissue.	R	Increased expression of NLRP3, IL-1 β and ASC mRNA in wounds of diabetic rats.	Dai et al., 2017
		Assessment of mRNA and protein expression from chronic wound tissues from diabetic and non-diabetic patients of size >2 cm ² and <25 cm ²	H DM patients Non DM subjects	Upregulation of NLRP3, caspase1 and IL-1 β mRNA and protein levels in DM patient wounds.	Zhang et al., 2017

R: rat, M: mouse, H: human, TLR4: toll-like receptor 4, IL-1 β : interleukin-1 β , ASC: apoptosis speck-like protein, NLRP3: NOD, LRR, and PYD domains-containing protein 3, Casp1: caspase-1, DRG: dorsal root ganglia, SN: sciatic nerve, DM: diabetes mellitus.

altered ion channel function to the neuromodulatory effects of IL-1 β . Additionally, IL-1 β also mediates production of endogenous molecules such as nerve growth factor, prostaglandin E₂, cyclooxygenase-2 and calcitonin-gene related peptide that may further contribute to peripheral sensitization (Zucali et al., 1986; Safieh-Garabedian et al., 1995; Reinold et al., 2005; **Figure 1B**).

Increased levels of IL-1 β accompany a vast number of inflammatory and non-inflammatory diseases and pathological states such as Alzheimer's disease, cancer or rheumatoid arthritis (RA) (Mrak and Griffin, 2000; Lewis et al., 2006; Lo Gullo et al., 2014; Ruscitti et al., 2015). There is accumulating evidence for NLRP3 and cytokine expression in gout pathology as well, which is evidenced by studies conducted in animal models and human clinical studies (Martinon et al., 2006). A human monoclonal antibody targeting IL-1 β that was used in randomized control trials showed significant reduction in risk of developing first gout flares as well as the prevention of recurring gout flares (Schlesinger et al., 2011). Several studies have shown increased expression of IL-1 β in tissue and blood in rodent animal models of, for example, metastatic cancer-induced bone pain, chemotherapy induced peripheral neuropathy, cryopyrin associated periodic syndrome, fibromyalgia, migraine and many other painful conditions (Verma et al., 2010; Cordero et al., 2014; Jia et al., 2017; Chen et al., 2019; He et al., 2019; **Table 1**). Additionally, IL-1 β was found to be upregulated in the blood of patients suffering from painful conditions, and in tissues of rodents in various models of inflammatory or non-inflammatory pain (Ren and Torres, 2009; Gui et al., 2016), underpinning the importance of IL-1 β in disease pathology. Only few studies used the global knockout of the IL-1 β or IL1R, however, some of the studies did not assess pain behavior (**Table 1**). For example, a study investigating bladder pain syndrome in *Il1b*^{-/-} mice showed no improvement in bladder pathology and pain (Butler et al., 2018) while studies in *IL-1R*^{-/-} mice assessing gout and rheumatoid arthritis did not investigate pathology or pain improvement (Martinon et al., 2006; Vande Walle et al., 2014). Moreover, increased levels of IL-1 β do not necessarily involve activation of NLRP3 as IL-1 β can also be released

via alternative mechanisms, including activation of the NLRP1, NLRC4, and AIM2 inflammasomes (Martinon et al., 2002; Strowig et al., 2012).

Activation of NLRP3 also leads to release of active interleukin-18 (IL-18), which has been found to mediate painful conditions such as muscle pain, cancer-induced bone pain and neuropathic pain (Liu S. et al., 2018; Vasudeva et al., 2015; Yoshida et al., 2018). However, it is currently unclear whether IL-18 can also directly contribute to nociceptor sensitization, or whether these effects are secondary to other IL-18-induced signaling events.

NLRP3 IN PAIN PATHOLOGY

The NLRP3 inflammasome has been implicated in the pathology of many painful diseases and conditions such as bladder pain, neuropathic pain, rheumatoid arthritis, gout, migraine and many more (**Table 1**). With increasing insight into the role of the immune system in the pathology of multiple diseases, it is perhaps not surprising that NLRP3 has also been suggested as a driving factor in the development of many painful diseases. However, despite the clear links between inflammation and pain, as well as NLRP3 and inflammation, relatively few studies have directly assessed the contribution of NLRP3 signaling to pain.

A prototypical NLRP3-linked condition is cryopyrin-associated periodic syndrome (CAPS), an inherited autosomal dominant autoinflammatory disorder characterized by recurrent episodes of inflammation and fever. CAPS patients carry mutations in the NLRP3 (CIAS1) gene leading to activation of the NLRP3 inflammasome and overproduction of IL-1 β . Accordingly, treatment with riloncept, a soluble IL-1 decoy receptor, or anakinra, an IL-1 receptor antagonist, improve the symptomatology of those patients. However, there is only limited – though promising – evidence regarding efficacy of these treatments against painful symptoms often reported by CAPS patients, such as headaches and myalgia (Gerard et al., 2007; Hoffman et al., 2008; Maksimovic et al., 2008; Verma et al., 2010).

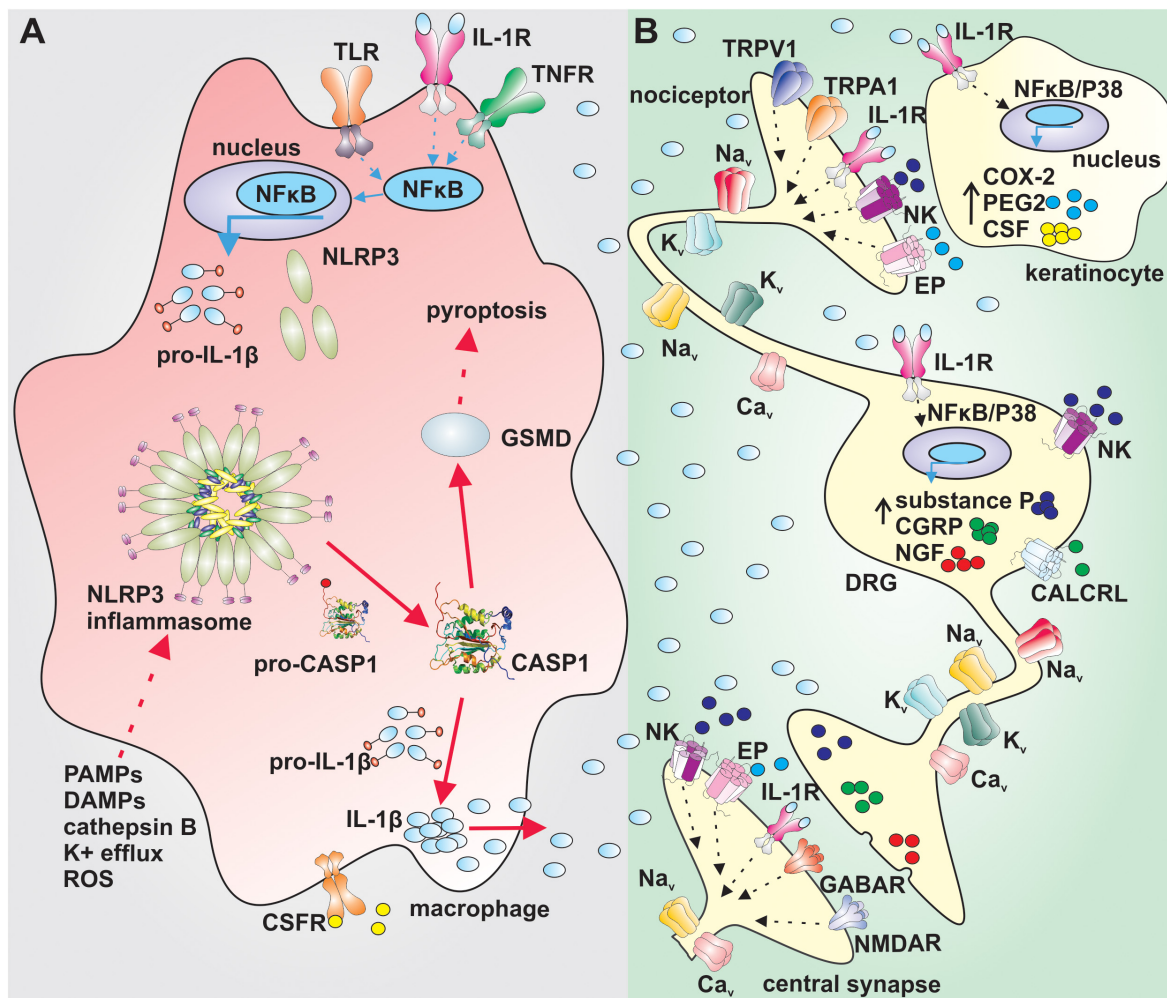


FIGURE 1 | Putative mechanism of sensory nerve sensitization by IL-1 β . **(A)** Priming of the NLRP3 inflammasome via activation of TLRs, IL-1R or TNFR in NF κ B dependent manner in macrophages leads to increased expression of NLRP3 and pro-IL-1 β (blue arrows). The canonical activation of the NLRP3 (red arrows) by PAMPs, DAMPs, cathepsin B, K⁺ efflux or ROS leads to assembly of the NLRP3 inflammasome complex, activation of CASP1 and cleavage of pro-IL-1 β and GSMD. Active IL-1 β is released by macrophages and exerts its effect via IL-1R on sensory nerves and surrounding cells. Active GSMD initiates pyroptosis. **(B)** IL-1 β increases the gene expression of COX-2, PEG2, and CSF in keratinocytes in a NF κ B/P38 mitogen kinase dependent manner. PEG2 sensitize peripheral nerves and CSF regulates differentiation, proliferation and survival of macrophages. IL-1 β increases excitability of nociceptors by altering the function of tetrodotoxin-resistant voltage-gated sodium channels via IL-1R and increases the gene expression in dorsal root ganglia in a NF κ B/P38 mitogen kinase dependent manner. Substance P, CGRP, and NGF sensitize further peripheral nerves. IL-1 β : interleukin 1 β ; TLR: toll-like receptor; IL-1R: interleukin-1 receptor; TNFR: tumor necrosis factor α receptor; NF κ B: nuclear factor κ B; NLRP3: NACHT, LRR, and PYD domains-containing protein 3; PAMPs: pathogen-associated molecular pattern; DAMPs: damage-associated molecular pattern; ROS: reactive oxygen species; CASP1: caspase 1; CSFR: colony-stimulating factor receptor; GSMD: gasdermin D; Na_v: voltage gated sodium channel; EP: prostaglandin E receptor; NK: neurokinin receptor; CGRP: calcitonin gene-related peptide; CALCRL: calcitonin gene-related peptide receptor; NGF: nerve growth factor; COX-2: cyclooxygenase type 2; PEG2: prostaglandin E2; CSF: colony stimulating factor; NMDAR: N-methyl-D-aspartate receptor; K_v: voltage gated potassium channel; Ca_v: voltage gated calcium channel; TRPV1: transient receptor potential channel vanilloid; TRPA1: transient receptor potential channel ankyrin; GABAR: gamma-aminobutyric acid receptor.

Increased expression of NLRP3 and IL-1 β was also found in blood of patients suffering from fibromyalgia, and treatment with coenzyme Q10 decreased both overexpression of NLRP3 as well serum IL-1 β and IL-18 levels (Cordero et al., 2014). Similar mechanisms were also observed in a rodent model of fibromyalgia, where coenzyme Q10 decreased pain behaviors in the hot plate and tail flick tests (Cordero et al., 2014).

In common inflammatory disorders characterized by pain as a predominant symptom, such as rheumatoid arthritis,

osteoarthritis and gout, release of cytokines including IL-1 β is well-known to contribute to pathology. Accordingly, treatments aimed at inhibiting IL-1 β effects – including with biologics such as anakinra, canakinumab and rilonacept – is a common therapeutic approach that shows some promise in alleviating painful symptoms (Martinon et al., 2006; Terkeltaub et al., 2009; Vande Walle et al., 2014; Choulaki et al., 2015; Liu et al., 2017; Guo et al., 2018; Cheng et al., 2019). However, these studies provide only limited evidence about the analgesic

effect of these substances. Similarly, Schnitzler syndrome, a rare autoimmune disease characterized by joint pain and arthritis, was linked to rare NLRP3 gene mutations and increased IL-1 β release, and treatment with anakinra caused pain regression in six male patients (Szturcz et al., 2014; Pathak et al., 2019). However, while NLRP3 has been implicated in the pathology of these conditions, IL-1 β can also be released upon activation of NLRP1, NLRC4, and AIM2 inflammasomes (Martinon et al., 2002; Terkeltaub et al., 2009; Strowig et al., 2012; Liu et al., 2017; Cheng et al., 2019). Thus, the direct contribution of NLRP3 to IL-1 β release, and pain, in these conditions remains to be unequivocally demonstrated. Illustrating this point is the observation that burns pain – which is accompanied by severe inflammation, including increased levels of IL-1 β (Ono et al., 1995; Vindenes et al., 1998) – developed normally in animals lacking NLRP3 (*Nlrp3*^{-/-}) or caspase-1/caspase11 (*Ice*^{-/-}) (Deuis et al., 2017).

Varied outcomes were also reported in studies assessing the contribution of NLRP3 to neuropathic pain, which may be accompanied by significant neuro-inflammation. Increased expression and activation of NLRP3 as well as increased production of IL-1 β were reported in several rodent models of nerve injury and chemotherapy-induced neuropathic pain (Jia et al., 2017; Khan et al., 2018; Liu C. C. et al., 2018; Pan et al., 2018; Tonkin et al., 2018; Wahlman et al., 2018; Son et al., 2019). However, while NLRP3 expression and activation was increased after chronic constriction injury of the sciatic nerve and partial sciatic nerve ligation, spared nerve injury did not result in elevated expression of NLRP3 inflammasome components, and pain behaviors of *Nlrp3*^{-/-} mice were unaltered (Curtoreyes et al., 2015; Pan et al., 2018; Tonkin et al., 2018). Similarly, investigations of the expression and activation of NLRP3 in models of oxaliplatin-induced neuropathy resulted in seemingly contradictory findings (Tonkin et al., 2018; Wahlman et al., 2018). These studies highlight the need for careful consideration of experimental procedures – including the type of injury, cell types included in analysis and methods used to assess expression and activity of NLRP3 – in preclinical studies addressing the contributions of the NLRP3 inflammasome to painful conditions.

While publications claiming direct or indirect NLRP3-modulating effects by analgesic compounds are plentiful, relatively few studies have assessed the contribution of NLRP3 signaling to pain using highly selective NLRP3 modulators or *Nlrp3*^{-/-} animals. These approaches have revealed a key contribution of NLRP3 to migraine, with MCC950, a specific NLRP3 antagonist, reducing periorbital and hind paw mechanical hypersensitivity and reversing increased expression of IL-1 β in trigeminal ganglia (He et al., 2019). Similarly, treatment with MCC950 attenuated mechanical allodynia in a rodent model of cancer-induced bone pain, and in oxaliplatin-induced peripheral neuropathy model and restored the increased expression levels of NLRP3, ASC, caspase-1 and IL-1 β in spinal cord to basal levels (Wahlman et al., 2018; Chen et al., 2019). Interestingly, Cowie et al. showed that the deletion of the NLRP3 gene causes immune-mediated sex differences in pain behavior, as male *Nlrp3*^{-/-} mice recovered from surgery-induced behavioral

and mechanical sensitization faster than female *Nlrp3*^{-/-} mice (Cowie et al., 2019).

THERAPEUTIC POTENTIAL OF NLRP3 MODULATORS FOR PAIN TREATMENT

The complex signaling cascades associated with NLRP3 activation lend themselves to pharmacological intervention at multiple points, including direct inhibition of NLRP3 activation, inhibition of inflammasome assembly, inhibition of caspase-1 or gasdermin-D, or inhibition of the biological effects of downstream effectors such as IL-1 β . For the latter, a number of approved modulators – including IL-1 receptor antagonists or inhibitory antibodies – are clinically available, as outlined above. However, as IL-1 β production is the result of several convergent signaling pathways, inhibition of the biological activities of IL-1 β may result in unintended immunosuppressive effects. Accordingly, a number of specific NLRP3 inhibitors with various mechanisms of NLRP3 inhibition have been reported, some of which are currently in clinical development [for review see Zahid et al. (2019); Jiang et al. (2020); Olcum et al. (2020); Zhang et al. (2020)].

The small molecule MCC950 inhibits the canonical and non-canonical activation of the NLRP3 inflammasome (Coll et al., 2015) while the ketone metabolite β -hydroxybutyrate inhibits only canonical activation of the NLRP3 inflammasome via inhibition of potassium efflux (Youm et al., 2015). The type I interferons, including IFN- α and IFN- β , inhibit the NLRP3-dependent production of IL-1 β and IL-18 through a yet unknown mechanism (Guarda et al., 2011a) and IFN- β therapy of multiple sclerosis in patients reduces IL-1 β levels and NLRP3 protein expression (Malhotra et al., 2015). Additionally, the induction of autophagy by resveratrol, or the inhibition of NLRP3 expression by microRNA-223, inhibits NLRP3 activation and the production of IL-1 β (Bauernfeind et al., 2012; Chang et al., 2015).

However, despite overwhelming evidence linking the NLRP3 inflammasome to IL-1 β and IL-18 production and inflammation, and convincing evidence that these cytokines can in turn mediate pain, the therapeutic potential of compounds targeting NLRP3 inflammasome signaling pathways remain to be assessed. Certainly, for some painful conditions such as cancer-induced bone pain, chemotherapy- or multiple sclerosis-induced neuropathy, migraine and fibromyalgia, inhibition of NLRP3 signaling appears to be a promising pain treatment strategy. However, only few clinical studies using selective NLRP3 inhibitors are in progress, and additional preclinical studies are required to increase our understanding of the NLRP3-dependent mechanisms contributing to peripheral or central sensitization and pain. Additionally, as activation of the NLRP3 inflammasome regulates immune responses, it is important to consider putative side effect that could arise from NLRP3 inhibition. For example, NLRP3 activation is a first defensive response to bacterial infections, suggesting that NLRP3 inhibitors could be associated with an increased susceptibility to infections. Moreover, inhibition of NLRP3-dependent IL-1 β release may affect tumor progression. For

example, tumor progression and metastasis of melanoma, gastric and colon cancer were shown to be driven by IL-1 β (Krelin et al., 2007; Okamoto et al., 2010; Dunn et al., 2012; Li et al., 2012), whereas the inhibition of IL-1 β delayed the regression of the murine B16 melanoma hepatic metastases (Vidal-Vanaclocha et al., 1994). Moreover, the treatment of patients or mice, with metastatic breast cancer, with anakinra, a specific IL-1R inhibitor, significantly reduced the tumor growth (Holen et al., 2016; Wu et al., 2018). Therefore, use of NLRP3 or IL-1 β inhibitors for cancer- or chemotherapy-associated pain requires careful investigation and consideration.

In summary, our understanding of the therapeutic potential of NLRP3 inhibition for the treatment of various painful disorders remains limited, despite emerging evidence that these targeted anti-inflammatory approaches may provide benefit. It is likely that analgesic effects will be realized for selected pain types, or subgroups of patients. Undoubtedly, with an increasing number of NLRP3 inhibitors entering clinical trials, significant insights into the therapeutic potential of these treatment approaches will be gained from additional pre-clinical and clinical studies.

CONCLUSION

NLRP3 inflammasome activation is increasingly recognized as a key molecular event underpinning numerous

inflammatory conditions, including those associated with significant pain. However, our understanding of molecular mechanisms leading to activation of the NLRP3 inflammasome, and subsequent effects on sensory systems, remains limited. Accordingly, the involvement of NLRP3 in the development of specific painful conditions, and the positive as well as negative effects of NLRP3 inhibition on human health remain to be determined in future studies.

AUTHOR CONTRIBUTIONS

HS and EN wrote the manuscript. IV edited the manuscript. HS designed figures and tables. All authors contributed to the article and approved the submitted version.

FUNDING

HS was supported by the University of Queensland International Scholarship. IV was supported by a the National Health and Medical Research Council of Australia fellowship (APP1162503) and project grant (APP1186835).

REFERENCES

- Amaya, F., Wang, H., Costigan, M., Allchorne, A. J., Hatcher, J. P., Egerton, J., et al. (2006). The voltage-gated sodium channel Na(v)1.9 is an effector of peripheral inflammatory pain hypersensitivity. *J. Neurosci.* 26, 12852–12860. doi: 10.1523/jneurosci.4015-06.2006
- Barclay, J., Clark, A. K., Ganju, P., Gentry, C., Patel, S., Wotherspoon, G., et al. (2007). Role of the cysteine protease cathepsin S in neuropathic hyperalgesia. *Pain* 130, 225–234. doi: 10.1016/j.pain.2006.11.017
- Bauernfeind, F., Bartok, E., Rieger, A., Franchi, L., Nunez, G., and Hornung, V. (2011). Cutting edge: reactive oxygen species inhibitors block priming, but not activation, of the NLRP3 inflammasome. *J. Immunol.* 187, 613–617. doi: 10.4049/jimmunol.1100613
- Bauernfeind, F., Rieger, A., Schildberg, F. A., Knolle, P. A., Schmid-Burgk, J. L., and Hornung, V. (2012). NLRP3 inflammasome activity is negatively controlled by miR-223. *J. Immunol.* 189, 4175–4181. doi: 10.4049/jimmunol.1201516
- Bauernfeind, F. G., Horvath, G., Stutz, A., Alnemri, E. S., MacDonald, K., Speert, D., et al. (2009). Cutting edge: NF-kappaB activating pattern recognition and cytokine receptors license NLRP3 inflammasome activation by regulating NLRP3 expression. *J. Immunol.* 183, 787–791. doi: 10.4049/jimmunol.0901363
- Binshtok, A. M., Wang, H., Zimmermann, K., Amaya, F., Vardeh, D., Shi, L., et al. (2008). Nociceptors are interleukin-1beta sensors. *J. Neurosci.* 28, 14062–14073.
- Brough, D., Le Feuvre, R. A., Wheeler, R. D., Solovyova, N., Hilfiker, S., Rothwell, N. J., et al. (2003). Ca²⁺ stores and Ca²⁺ entry differentially contribute to the release of IL-1 beta and IL-1 alpha from murine macrophages. *J. Immunol.* 170, 3029–3036. doi: 10.4049/jimmunol.170.6.3029
- Butler, D. S. C., Ambite, I., Nagy, K., Cafaro, C., Ahmed, A., Nadeem, A., et al. (2018). Neuroepithelial control of mucosal inflammation in acute cystitis. *Sci. Rep.* 8:11015.
- Chang, Y. P., Ka, S. M., Hsu, W. H., Chen, A., Chao, L. K., Lin, C. C., et al. (2015). Resveratrol inhibits NLRP3 inflammasome activation by preserving mitochondrial integrity and augmenting autophagy. *J. Cell Physiol.* 230, 1567–1579. doi: 10.1002/jcp.24903
- Chen, S. P., Zhou, Y. Q., Wang, X. M., Sun, J., Cao, F., HaiSam, S., et al. (2019). Pharmacological inhibition of the NLRP3 in fl ammasome as a potential target for cancer-induced bone pain. *Pharmacol. Res.* 147:104339. doi: 10.1016/j.phrs.2019.104339
- Cheng, F., Yan, F. F., Liu, Y. P., Cong, Y., Sun, K. F., and He, X. M. (2019). Dexmedetomidine inhibits the NF-kappaB pathway and NLRP3 inflammasome to attenuate papain-induced osteoarthritis in rats. *Pharm. Biol.* 57, 649–659. doi: 10.1080/13880209.2019.1651874
- Choulaki, C., Papadaki, G., Repa, A., Kampouraki, E., Kambas, K., Ritis, K., et al. (2015). Enhanced activity of NLRP3 inflammasome in peripheral blood cells of patients with active rheumatoid arthritis. *Arthritis Res. Ther.* 17:257.
- Coll, R. C., Robertson, A. A., Chae, J. J., Higgins, S. C., Munoz-Planillo, R., Inserra, M. C., et al. (2015). A small-molecule inhibitor of the NLRP3 inflammasome for the treatment of inflammatory diseases. *Nat. Med.* 21, 248–255.
- Cordero, M. D., Alcocer-Gomez, E., Culic, O., Carrion, A. M., de Miguel, M., Diaz-Parrado, E., et al. (2014). NLRP3 inflammasome is activated in fibromyalgia: the effect of coenzyme Q10. *Antioxid. Redox. Signal.* 20, 1169–1180. doi: 10.1089/ars.2013.5198
- Cowie, A. M., Menzel, A. D., O'Hara, C., Lawlor, M. W., and Stucky, C. L. (2019). NOD-like receptor protein 3 inflammasome drives postoperative mechanical pain in a sex-dependent manner. *Pain* 160, 1794–1816. doi: 10.1097/j.pain.0000000000001555
- Curto-Reyes, V., Kirschmann, G., Pertin, M., Drexler, S. K., Decosterd, I., and Suter, M. R. (2015). Neuropathic pain phenotype does not involve the NLRP3 inflammasome and its end product interleukin-1beta in the mice spared nerve injury model. *PLoS One* 10:e0133707. doi: 10.1371/journal.pone.0133707
- Dai, J., Zhang, X., Wang, Y., Chen, H., and Chai, Y. (2017). ROS-activated NLRP3 inflammasome initiates inflammation in delayed wound healing in diabetic rats. *Int. J. Clin. Exp. Pathol.* 10:9902.
- Deuis, J. R., Yin, K., Cooper, M. A., Schroder, K., and Vetter, I. (2017). Role of the NLRP3 inflammasome in a model of acute burn-induced pain. *Burns* 43, 304–309. doi: 10.1016/j.burns.2016.09.001

- Dunn, J. H., Ellis, L. Z., and Fujita, M. (2012). Inflammasomes as molecular mediators of inflammation and cancer: potential role in melanoma. *Cancer Lett.* 314, 24–33. doi: 10.1016/j.canlet.2011.10.001
- Fann, D. Y., Lim, Y. A., Cheng, Y. L., Lok, K. Z., Chunduri, P., Baik, S. H., et al. (2018). Evidence that NF-kappaB and MAPK signaling promotes NLRP3 inflammasome activation in neurons following ischemic stroke. *Mol. Neurobiol.* 55, 1082–1096. doi: 10.1007/s12035-017-0394-9
- Ferreira, S., Lorenzetti, B., Bristow, A., and Poole, S. J. N. (1988). Interleukin-1 β as a potent hyperalgesic agent antagonized by a tripeptide analogue. *Nature* 334:698. doi: 10.1038/334698a0
- Franchi, L., Eigenbrod, T., and Nunez, G. (2009a). Cutting edge: TNF- α mediates sensitization to ATP and silica via the NLRP3 inflammasome in the absence of microbial stimulation. *J. Immunol.* 183, 792–796. doi: 10.4049/jimmunol.0900173
- Franchi, L., Warner, N., Viani, K., and Nunez, G. (2009b). Function of Nod-like receptors in microbial recognition and host defense. *Immunol. Rev.* 227, 106–128. doi: 10.1111/j.1600-065x.2008.00734.x
- Gaidt, M. M., Ebert, T. S., Chauhan, D., Schmidt, T., Schmid-Burgk, J. L., Rapino, F., et al. (2016). Human monocytes engage an alternative inflammasome pathway. *Immunity* 44, 833–846. doi: 10.1016/j.immuni.2016.01.012
- Gerard, S., le Goff, B., Maugars, Y., Berthelot, J. M., and Malard, O. (2007). Lasting remission of a Muckle-Wells syndrome with CIAS-1 mutation using half-dose anakinra. *Joint Bone Spine* 74:659. doi: 10.1016/j.jbspin.2007.01.032
- Guarda, G., Braun, M., Staehli, F., Tardivel, A., Mattmann, C., Forster, I., et al. (2011a). Type I interferon inhibits interleukin-1 production and inflammasome activation. *Immunity* 34, 213–223. doi: 10.1016/j.immuni.2011.02.006
- Guarda, G., Zenger, M., Yazdi, A. S., Schroder, K., Ferrero, I., Menu, P., et al. (2011b). Differential expression of NLRP3 among hematopoietic cells. *J. Immunol.* 186, 2529–2534. doi: 10.4049/jimmunol.1002720
- Gui, W. S., Wei, X., Mai, C. L., Murugan, M., Wu, L. J., Xin, W. J., et al. (2016). Interleukin-1 β overproduction is a common cause for neuropathic pain, memory deficit, and depression following peripheral nerve injury in rodents. *Mol. Pain* 12:1744806916646784.
- Guo, C., Fu, R., Wang, S., Huang, Y., Li, X., Zhou, M., et al. (2018). NLRP3 inflammasome activation contributes to the pathogenesis of rheumatoid arthritis. *Clin. Exp. Immunol.* 194, 231–243. doi: 10.1111/cei.13167
- Gustin, A., Kirchmeyer, M., Koncina, E., Felten, P., Losciuto, S., Heurtaux, T., et al. (2015). NLRP3 inflammasome is expressed and functional in mouse brain microglia but not in astrocytes. *PLoS One* 10:e0130624. doi: 10.1371/journal.pone.0130624
- He, W., Long, T., Pan, Q., Zhang, S., Zhang, Y., Zhang, D., et al. (2019). Microglial NLRP3 inflammasome activation mediates IL-1 β release and contributes to central sensitization in a recurrent nitroglycerin-induced migraine model. *J. Neuroinflamm.* 16:78.
- Hoffman, H. M., Throne, M. L., Amar, N. J., Sebai, M., Kivitz, A. J., Kavanaugh, A., et al. (2008). Efficacy and safety of rilonacept (interleukin-1 Trap) in patients with cryopyrin-associated periodic syndromes: results from two sequential placebo-controlled studies. *Arthritis Rheum.* 58, 2443–2452. doi: 10.1002/art.23687
- Holen, I., Lefley, D. V., Francis, S. E., Rennicks, S., Bradbury, S., Coleman, R. E., et al. (2016). IL-1 drives breast cancer growth and bone metastasis in vivo. *Oncotarget* 7, 75571–75584. doi: 10.18632/oncotarget.12289
- Hu, Z., Yan, C., Liu, P., Huang, Z., Ma, R., Zhang, C., et al. (2013). Crystal structure of NLRC4 reveals its autoinhibition mechanism. *Science* 341, 172–175. doi: 10.1126/science.1236381
- Inoue, K., and Tsuda, M. (2018). Microglia in neuropathic pain: cellular and molecular mechanisms and therapeutic potential. *Nat. Rev. Neurosci.* 19, 138–152. doi: 10.1038/nrn.2018.2
- Insalaco, A., Prencipe, G., Buonomo, P. S., Ceccherini, I., Bracaglia, C., Pardeo, M., et al. (2014). A novel mutation in the CIAS1/NLRP3 gene associated with an unexpected phenotype of cryopyrin-associated periodic syndromes. *Clin. Exp. Rheumatol.* 32, 123–125.
- Ji, R. R., Chamesian, A., and Zhang, Y. Q. (2016). Pain regulation by non-neuronal cells and inflammation. *Science* 354, 572–577. doi: 10.1126/science.aaf8924
- Jia, M., Wu, C., Gao, F., Xiang, H., Sun, N., Peng, P., et al. (2017). Activation of NLRP3 inflammasome in peripheral nerve contributes to paclitaxel-induced neuropathic pain. *Mol. Pain* 13:1744806917719804.
- Jiang, H., Gong, T., and Zhou, R. (2020). The strategies of targeting the NLRP3 inflammasome to treat inflammatory diseases. *Adv. Immunol.* 145, 55–93. doi: 10.1016/bs.ai.2019.11.003
- Kayagaki, N., Warming, S., Lamkanfi, M., Vande Walle, L., Louie, S., Dong, J., et al. (2011). Non-canonical inflammasome activation targets caspase-11. *Nature* 479, 117–121.
- Kayagaki, N., Wong, M. T., Stowe, I. B., Ramani, S. R., Gonzalez, L. C., Akashi-Takamura, S., et al. (2013). Noncanonical inflammasome activation by intracellular LPS independent of TLR4. *Science* 341, 1246–1249. doi: 10.1126/science.1240248
- Khan, N., Kuo, A., Brockman, D. A., Cooper, M. A., and Smith, M. T. (2018). Pharmacological inhibition of the NLRP3 inflammasome as a potential target for multiple sclerosis induced central neuropathic pain. *Inflammopharmacology* 26, 77–86. doi: 10.1007/s10787-017-0401-9
- Kobayashi, Y., Kiguchi, N., Fukazawa, Y., Saika, F., Maeda, T., and Kishioka, S. (2015). Macrophage-T cell interactions mediate neuropathic pain through the glucocorticoid-induced tumor necrosis factor ligand system. *J. Biol. Chem.* 290, 12603–12613. doi: 10.1074/jbc.m115.636506
- Krelin, Y., Voronov, E., Dotan, S., Elkabets, M., Reich, E., Fogel, M., et al. (2007). Interleukin-1 β -driven inflammation promotes the development and invasiveness of chemical carcinogen-induced tumors. *Cancer Res.* 67, 1062–1071. doi: 10.1158/0008-5472.can-06-2956
- Lewis, A. M., Varghese, S., Xu, H., and Alexander, H. R. (2006). Interleukin-1 and cancer progression: the emerging role of interleukin-1 receptor antagonist as a novel therapeutic agent in cancer treatment. *J. Transl. Med.* 4:48.
- Li, Y., Wang, L., Pappan, L., Galliher-Beckley, A., and Shi, J. (2012). IL-1 β promotes stemness and invasiveness of colon cancer cells through Zeb1 activation. *Mol. Cancer* 11:87. doi: 10.1186/1476-4598-11-87
- Liu, C. C., Huang, Z. X., Li, X., Shen, K. F., Liu, M., Ouyang, H. D., et al. (2018). Upregulation of NLRP3 via STAT3-dependent histone acetylation contributes to painful neuropathy induced by bortezomib. *Exp. Neurol.* 302, 104–111. doi: 10.1016/j.expneurol.2018.01.011
- Liu, H. J., Pan, X. X., Liu, B. Q., Gui, X., Hu, L., Jiang, C. Y., et al. (2017). Grape seed-derived procyanidins alleviate gout pain via NLRP3 inflammasome suppression. *J. Neuroinflamm.* 14:74.
- Liu, S., Liu, Y. P., Lv, Y., Yao, J. L., Yue, D. M., Zhang, M. Y., et al. (2018). IL-18 contributes to bone cancer pain by regulating glia cells and neuron interaction. *J. Pain* 19, 186–195. doi: 10.1016/j.jpain.2017.10.003
- Lo Gullo, A., Mandraffino, G., Imbalzano, E., Mamone, F., Aragona, C. O., D'Ascola, A., et al. (2014). Toll-like receptor 3 and interleukin 1 β expression in CD34+ cells from patients with rheumatoid arthritis: association with inflammation and vascular involvement. *Clin. Exp. Rheumatol.* 32, 922–929.
- Lu, A., Li, Y., Schmidt, F. I., Yin, Q., Chen, S., Fu, T. M., et al. (2016). Molecular basis of caspase-1 polymerization and its inhibition by a new capping mechanism. *Nat. Struct. Mol. Biol.* 23, 416–425. doi: 10.1038/nsmb.3199
- Lu, A., Li, Y., Yin, Q., Ruan, J., Yu, X., Egelman, E., et al. (2015). Plasticity in PYD assembly revealed by cryo-EM structure of the PYD filament of AIM2. *Cell Discov.* 1:15013.
- Lu, A., Magupalli, V. G., Ruan, J., Yin, Q., Atianand, M. K., Vos, M. R., et al. (2014). Unified polymerization mechanism for the assembly of ASC-dependent inflammasomes. *Cell* 156, 1193–1206. doi: 10.1016/j.cell.2014.02.008
- Maksimovic, L., Stirnemann, J., Caux, F., Ravet, N., Rouaghe, S., Cuisset, L., et al. (2008). New CIAS1 mutation and anakinra efficacy in overlapping of Muckle-Wells and familial cold autoinflammatory syndromes. *Rheumatology (Oxford)* 47, 309–310. doi: 10.1093/rheumatology/kem318
- Malhotra, S., Rio, J., Urcelay, E., Nurtdinov, R., Bustamante, M. F., Fernandez, O., et al. (2015). NLRP3 inflammasome is associated with the response to IFN- β in patients with multiple sclerosis. *Brain* 138, 644–652. doi: 10.1093/brain/awu388
- Malsch, P., Andratsch, M., Vogl, C., Link, A. S., Alzheimer, C., Brierley, S. M., et al. (2014). Deletion of interleukin-6 signal transducer gp130 in small sensory neurons attenuates mechanonociception and down-regulates TRPA1 expression. *J. Neurosci.* 34, 9845–9856. doi: 10.1523/jneurosci.5161-13.2014
- Martinon, F., Burns, K., and Tschopp, J. (2002). The inflammasome: a molecular platform triggering activation of inflammatory caspases and processing of proIL-1 β . *Mol. Cell* 10, 417–426.

- Martinon, F., Petrilli, V., Mayor, A., Tardivel, A., and Tschopp, J. (2006). Gout-associated uric acid crystals activate the NALP3 inflammasome. *Nature* 440, 237–241.
- McMahon, S. B., La Russa, F., and Bennett, D. L. (2015). Crosstalk between the nociceptive and immune systems in host defence and disease. *Nat. Rev. Neurosci.* 16, 389–402.
- Mert, T., Gunay, I., Ocal, I., Guzel, A. I., Inal, T. C., Sencar, L., et al. (2009). Macrophage depletion delays progression of neuropathic pain in diabetic animals. *Naunyn. Schmiedeberg's Arch. Pharmacol.* 379, 445–452.
- Mrak, R. E., and Griffin, W. S. (2000). Interleukin-1 and the immunogenetics of Alzheimer disease. *J. Neuropathol. Exp. Neurol.* 59, 471–476.
- Muller, P. A., Kosco, B., Rajani, G. M., Stevanovic, K., Berres, M. L., Hashimoto, D., et al. (2014). Crosstalk between muscularis macrophages and enteric neurons regulates gastrointestinal motility. *Cell* 158, 300–313.
- Munoz-Planillo, R., Kuffa, P., Martinez-Colon, G., Smith, B. L., Rajendiran, T. M., and Nunez, G. (2013). K(+) efflux is the common trigger of NLRP3 inflammasome activation by bacterial toxins and particulate matter. *Immunity* 38, 1142–1153.
- Okamoto, M., Liu, W., Luo, Y., Tanaka, A., Cai, X., Norris, D. A., et al. (2010). Constitutively active inflammasome in human melanoma cells mediating autoinflammation via caspase-1 processing and secretion of interleukin-1beta. *J. Biol. Chem.* 285, 6477–6488.
- Olum, M., Tastan, B., Ercan, I., Eltutan, I. B., and Genc, S. (2020). Inhibitory effects of phytochemicals on NLRP3 inflammasome activation: a review. *Phytomedicine* 75:153238.
- Ono, I., Gunji, H., Zhang, J. Z., Maruyama, K., and Kaneko, F. (1995). A study of cytokines in burn blister fluid related to wound healing. *Burns* 21, 352–355.
- Orlowski, G. M., Colbert, J. D., Sharma, S., Bogoy, M., Robertson, S. A., and Rock, K. L. (2015). Multiple cathepsins promote Pro-IL-1beta synthesis and NLRP3-mediated IL-1beta activation. *J. Immunol.* 195, 1685–1697.
- Pan, Z., Shan, Q., Gu, P., Wang, X. M., Tai, L. W., Sun, M., et al. (2018). miRNA-23a/CXCR4 regulates neuropathic pain via directly targeting TXNIP/NLRP3 inflammasome axis. *J. Neuroinflamm.* 15:29.
- Pathak, S., Rowczenio, D. M., Owen, R. G., Doody, G. M., Newton, D. J., Taylor, C., et al. (2019). Exploratory study of MYD88 L265P, rare NLRP3 variants, and clonal hematopoiesis prevalence in patients with schnitzler syndrome. *Arthritis Rheumatol.* 71, 2121–2125.
- Reinold, H., Ahmadi, S., Depner, U. B., Layh, B., Heindl, C., Hamza, M., et al. (2005). Spinal inflammatory hyperalgesia is mediated by prostaglandin E receptors of the EP2 subtype. *J. Clin. Invest.* 115, 673–679.
- Ren, K., and Torres, R. (2009). Role of interleukin-1beta during pain and inflammation. *Brain Res. Rev.* 60, 57–64.
- Ruscitti, P., Cipriani, P., Di Benedetto, P., Liakouli, V., Berardicurti, O., Carubbi, F., et al. (2015). Monocytes from patients with rheumatoid arthritis and type 2 diabetes mellitus display an increased production of interleukin (IL)-1beta via the nucleotide-binding domain and leucine-rich repeat containing family pyrin 3 (NLRP3)-inflammasome activation: a possible implication for therapeutic decision in these patients. *Clin. Exp. Immunol.* 182, 35–44.
- Safieh-Garabedian, B., Poole, S., Allchorne, A., Winter, J., and Woolf, C. J. (1995). Contribution of interleukin-1 beta to the inflammation-induced increase in nerve growth factor levels and inflammatory hyperalgesia. *Br. J. Pharmacol.* 115, 1265–1275.
- Sagulenko, V., Thygesen, S. J., Sester, D. P., Idris, A., Cridland, J. A., Vajjhala, P. R., et al. (2013). AIM2 and NLRP3 inflammasomes activate both apoptotic and pyroptotic death pathways via ASC. *Cell Death Differ.* 20, 1149–1160.
- Schafers, M., and Sorkin, L. (2008). Effect of cytokines on neuronal excitability. *Neurosci. Lett.* 437, 188–193.
- Schlesinger, N., Mysler, E., Lin, H. Y., De Meulemeester, M., Rovinsky, J., Arulmani, U., et al. (2011). Canakinumab reduces the risk of acute gouty arthritis flares during initiation of allopurinol treatment: results of a double-blind, randomised study. *Ann. Rheum. Dis.* 70, 1264–1271.
- Sharma, B. R., Karki, R., and Kanneganti, T. D. (2019). Role of AIM2 inflammasome in inflammatory diseases, cancer and infection. *Eur. J. Immunol.* 49, 1998–2011.
- Shi, J., Zhao, Y., Wang, K., Shi, X., Wang, Y., Huang, H., et al. (2015). Cleavage of GSDMD by inflammatory caspases determines pyroptotic cell death. *Nature* 526, 660–665.
- Son, S., Shim, D. W., Hwang, I., Park, J. H., and Yu, J. W. (2019). Chemotherapeutic agent paclitaxel mediates priming of NLRP3 inflammasome activation. *Front. Immunol.* 10:1108. doi: 10.3389/fimmu.2019.01108
- Stemkowski, P. L., Noh, M. C., Chen, Y., and Smith, P. A. (2015). Increased excitability of medium-sized dorsal root ganglion neurons by prolonged interleukin-1beta exposure is K(+) channel dependent and reversible. *J. Physiol.* 593, 3739–3755.
- Strowig, T., Henao-Mejia, J., Elinav, E., and Flavell, R. (2012). Inflammasomes in health and disease. *Nature* 481, 278–286.
- Szturcz, P., Sediva, A., Zurek, M., Adam, Z., Stork, J., Cermakova, Z., et al. (2014). Anakinra treatment in Schnitzler syndrome - results of the first retrospective multicenter study in six patients from the Czech Republic. *Klin. Onkol.* 27, 111–126.
- Terkeltaub, R., Sundry, J. S., Schumacher, H. R., Murphy, F., Bookbinder, S., Biedermann, S., et al. (2009). The interleukin 1 inhibitor rilonacept in treatment of chronic gouty arthritis: results of a placebo-controlled, monosequence crossover, non-randomised, single-blind pilot study. *Ann. Rheum. Dis.* 68, 1613–1617.
- Tonkin, R. S., Bowles, C., Perera, C. J., Keating, B. A., Makker, P. G. S., Duffy, S. S., et al. (2018). Attenuation of mechanical pain hypersensitivity by treatment with Peptide5, a connexin-43 mimetic peptide, involves inhibition of NLRP3 inflammasome in nerve-injured mice. *Exp. Neurol.* 300, 1–12.
- Vande Walle, L., Van Opdenbosch, N., Jacques, P., Fossoul, A., Verheugen, E., Vogel, P., et al. (2014). Negative regulation of the NLRP3 inflammasome by A20 protects against arthritis. *Nature* 512, 69–73.
- Vasudeva, K., Vodovotz, Y., Azhar, N., Barclay, D., Janjic, J. M., and Pollock, J. A. (2015). In vivo and systems biology studies implicate IL-18 as a central mediator in chronic pain. *J. Neuroimmunol.* 283, 43–49.
- Verma, D., Eriksson, P., Sahdo, B., Persson, A., Ejdebäck, M., Sarndahl, E., et al. (2010). Two adult siblings with atypical cryopyrin-associated periodic syndrome due to a novel M299V mutation in NLRP3. *Arthritis Rheum.* 62, 2138–2143.
- Vidal-Vanaclocha, F., Amezcua, C., Asumendi, A., Kaplanski, G., and Dinarello, C. A. (1994). Interleukin-1 receptor blockade reduces the number and size of murine B16 melanoma hepatic metastases. *Cancer Res.* 54, 2667–2672.
- Vindenes, H. A., Ulvestad, E., and Bjerknes, R. (1998). Concentrations of cytokines in plasma of patients with large burns: their relation to time after injury, burn size, inflammatory variables, infection, and outcome. *Eur. J. Surg.* 164, 647–656.
- Wahlman, C., Doyle, T. M., Little, J. W., Luongo, L., Janes, K., Chen, Z., et al. (2018). Chemotherapy-induced pain is promoted by enhanced spinal adenosine kinase levels through astrocyte-dependent mechanisms. *Pain* 159, 1025–1034.
- Wu, T. C., Xu, K., Martinek, J., Young, R. R., Banchereau, R., George, J., et al. (2018). IL1 receptor antagonist controls transcriptional signature of inflammation in patients with metastatic breast cancer. *Cancer Res.* 78, 5243–5258.
- Yang, D., He, Y., Munoz-Planillo, R., Liu, Q., and Nunez, G. (2015). Caspase-11 requires the pannexin-1 channel and the purinergic P2X7 pore to mediate pyroptosis and endotoxin shock. *Immunity* 43, 923–932.
- Yoshida, S., Hagiwara, Y., Tsuchiya, M., Shinoda, M., Koide, M., Hatakeyama, H., et al. (2018). Involvement of neutrophils and interleukin-18 in nociception in a mouse model of muscle pain. *Mol. Pain* 14:1744806918757286.
- Youn, Y. H., Nguyen, K. Y., Grant, R. W., Goldberg, E. L., Bodogai, M., Kim, D., et al. (2015). The ketone metabolite beta-hydroxybutyrate blocks NLRP3 inflammasome-mediated inflammatory disease. *Nat. Med.* 21, 263–269.
- Zahid, A., Li, B., Kombe, A. J. K., Jin, T., and Tao, J. (2019). Pharmacological inhibitors of the NLRP3 inflammasome. *Front. Immunol.* 10:2538. doi: 10.3389/fimmu.2019.02538
- Zanos, T. P., Silverman, H. A., Levy, T., Tsaava, T., Battinelli, E., Lorraine, P. W., et al. (2018). Identification of cytokine-specific sensory neural signals by decoding murine vagus nerve activity. *Proc. Natl. Acad. Sci. U.S.A.* 115, E4843–E4852.
- Zhang, H., Li, Y., de Carvalho-Barbosa, M., Kavelaars, A., Heijnen, C. J., Albrecht, P. J., et al. (2016). Dorsal Root ganglion infiltration by macrophages contributes to paclitaxel chemotherapy-induced peripheral neuropathy. *J. Pain* 17, 775–786.

- Zhang, X., Dai, J., Li, L., Chen, H., and Chai, Y. (2017). NLRP3 inflammasome expression and signaling in human diabetic wounds and in high glucose induced macrophages. *J. Diab. Res.* 2017:5281358.
- Zhang, X., Xu, A., Lv, J., Zhang, Q., Ran, Y., Wei, C., et al. (2020). Development of small molecule inhibitors targeting NLRP3 inflammasome pathway for inflammatory diseases. *Eur. J. Med. Chem.* 185:111822.
- Zucali, J. R., Dinarello, C. A., Oblon, D. J., Gross, M. A., Anderson, L., and Weiner, R. S. (1986). Interleukin 1 stimulates fibroblasts to produce granulocyte-macrophage colony-stimulating activity and prostaglandin E2. *J. Clin. Invest.* 77, 1857–1863.

Conflict of Interest: The authors declare that the research was conducted in the absence of any commercial or financial relationships that could be construed as a potential conflict of interest.

Copyright © 2020 Starobova, Nadar and Vetter. This is an open-access article distributed under the terms of the Creative Commons Attribution License (CC BY). The use, distribution or reproduction in other forums is permitted, provided the original author(s) and the copyright owner(s) are credited and that the original publication in this journal is cited, in accordance with accepted academic practice. No use, distribution or reproduction is permitted which does not comply with these terms.



Antinociceptive Effects of Lipid Raft Disruptors, a Novel Carboxamido-Steroid and Methyl β -Cyclodextrin, in Mice by Inhibiting Transient Receptor Potential Vanilloid 1 and Ankyrin 1 Channel Activation

OPEN ACCESS

Edited by:

Peter Santha,
University of Szeged, Hungary

Reviewed by:

Janos Paloczi,
National Institutes of Health (NIH),
United States
Vincenzo Barrese,
University of Naples Federico II, Italy

*Correspondence:

Ádám Horváth
horvatadam7@gmail.com

[†] These authors have contributed
equally to this work

Specialty section:

This article was submitted to
Clinical and Translational Physiology,
a section of the journal
Frontiers in Physiology

Received: 05 May 2020

Accepted: 18 August 2020

Published: 23 September 2020

Citation:

Horváth Á, Biró-Sütő T, Kántás B,
Payrits M, Skoda-Földes R,
Szánti-Pintér E, Helyes Z and Szőke É
(2020) Antinociceptive Effects of Lipid
Raft Disruptors, a Novel
Carboxamido-Steroid and Methyl
 β -Cyclodextrin, in Mice by Inhibiting
Transient Receptor Potential Vanilloid
1 and Ankyrin 1 Channel Activation.
Front. Physiol. 11:559109.
doi: 10.3389/fphys.2020.559109

Ádám Horváth^{1,2*}, Tünde Biró-Sütő^{1,2†}, Boglárka Kántás^{1,2}, Maja Payrits^{1,2},
Rita Skoda-Földes³, Eszter Szánti-Pintér³, Zsuzsanna Helyes^{1,2} and Éva Szőke^{1,2}

¹ Department of Pharmacology and Pharmacotherapy, Medical School, University of Pécs, Pécs, Hungary, ² János Szentágothai Research Centre and Centre for Neuroscience, University of Pécs, Pécs, Hungary, ³ Department of Organic Chemistry, Institute of Chemistry, University of Pannonia, Veszprém, Hungary

Transient Receptor Potential Vanilloid 1 and Ankyrin 1 (TRPV1, TRPA1) cation channels are expressed in nociceptive primary sensory neurons, and play an integrative role in pain processing and inflammatory functions. Lipid rafts are liquid-ordered plasma membrane microdomains rich in cholesterol, sphingomyelin, and gangliosides. We earlier proved that lipid raft disintegration by cholesterol depletion using a novel carboxamido-steroid compound (C1) and methyl β -cyclodextrin (MCD) significantly and concentration-dependently inhibit TRPV1 and TRPA1 activation in primary sensory neurons and receptor-expressing cell lines. Here we investigated the effects of C1 compared to MCD in mouse pain models of different mechanisms. Both C1 and MCD significantly decreased the number of the TRPV1 activation (capsaicin)-induced nocifensive eye-wiping movements in the first hour by 45% and 32%, respectively, and C1 also in the second hour by 26%. Furthermore, C1 significantly decreased the TRPV1 stimulation (resiniferatoxin)-evoked mechanical hyperalgesia involving central sensitization processes, while its inhibitory effect on thermal allodynia was not statistically significant. In contrast, MCD did not affect these resiniferatoxin-evoked nocifensive responses. Both C1 and MCD had inhibitory action on TRPA1 activation (formalin)-induced acute nocifensive reactions (paw liftings, lickings, holdings, and shakings) in the second, neurogenic inflammatory phase by 36% and 51%, respectively. These are the first *in vivo* data showing that our novel lipid raft disruptor carboxamido-steroid compound exerts antinociceptive and antihyperalgesic effects by inhibiting

TRPV1 and TRPA1 ion channel activation similarly to MCD, but in 150-fold lower concentrations. It is concluded that C1 is a useful experimental tool to investigate the effects of cholesterol depletion in animal models, and it also might open novel analgesic drug developmental perspectives.

Keywords: inflammation, lipid rafts, methyl β -cyclodextrin, nerve terminal, pain, sensory neuron, steroid, Transient Receptor Potential channel

INTRODUCTION

Transient Receptor Potential (TRP) Vanilloid 1 and Ankyrin 1 (TRPV1 and TRPA1) cation channels are multimeric receptors activated by a variety of inflammatory mediators and tissue irritants, temperature changes and mechanical stimuli besides the classical exogenous agonists such as capsaicin (CAPS), resiniferatoxin (RTX) and formaldehyde, allyl-isothiocyanate (in mustard oil), respectively (McKemy et al., 2002; Peier et al., 2002; Reid and Flonta, 2002; Grimm et al., 2003, 2005; Lee et al., 2003; Bandell et al., 2004; Corey et al., 2004; Jordt et al., 2004; Macpherson et al., 2005, 2007; McNamara et al., 2007; Trevisani et al., 2007; Wagner et al., 2008; Majeed et al., 2010; Vilceanu and Stucky, 2010; Vriens et al., 2011, 2014; Bautista et al., 2013; Drews et al., 2014; Oberwinkler and Philipp, 2014). TRPV1 and TRPA1 are often co-localized on the CAPS-sensitive peptidergic sensory neurons and play key regulatory roles in pain and inflammation (Szolcsányi, 2004; Salas et al., 2009). Pro-inflammatory neuropeptides such as Substance P and calcitonin gene-related peptide released from the activated CAPS-sensitive sensory nerve fibers evoke vasodilation, plasma protein extravasation and inflammatory cells activation in the innervated area called neurogenic inflammation, as well as nociceptor sensitization (Helyes et al., 2003a, 2009; Szolcsányi, 2004). Therefore, both TRPV1 and TRPA1 have been in the focus of analgesic and anti-inflammatory drug development, especially for the treatment of chronic neuropathic pain and inflammatory diseases with neurogenic inflammatory components (chronic obstructive pulmonary diseases, psoriasis, arthritis, inflammatory bowel diseases) (Moran et al., 2011; Kaneko and Szallasi, 2014; Nilius and Szallasi, 2014). The presently available drugs do not provide satisfactory pain relief in most cases or induce severe side effects after long-term use (Botz et al., 2017). Great efforts have been put into the development of TRPV1 antagonists which proved to be very effective in both preclinical and phase II and III clinical trials, but due to their hyperthermic side effects they could not be registered in the clinical practice (Helyes et al., 2003b; Lee et al., 2015). TRPA1 is also considered to

be a promising analgesic target based on experimental and human studies which seem to be free of severe side effects (Romanovsky et al., 2009; Botz et al., 2017). These data clearly suggest the drug developmental potential of TRPV1 and TRPA1 blockade, therefore alternative mechanisms in addition to the direct antagonism have been proposed as promising inhibitors options (Ferrari and Levine, 2015; Sághy et al., 2015, 2018; Lin et al., 2019).

Recent results of extensive lipid raft research in the last two decades have had a great impact on cell biology and pharmacology. Lipid rafts are specialized microdomains in the plasma membrane rich in cholesterol, sphingomyelins and gangliosides (Simons and Ikonen, 1997). Several receptors, ion channels and signaling molecules including TRPV1 and TRPA1 ion channels are located in lipid rafts and disruption of these membrane regions affects their functions (Liu et al., 2006; Morenilla-Palao et al., 2009; Szöke et al., 2010; Sághy et al., 2015). However, data are controversial about the outcomes of lipid raft modulation on TRP channels. Although several *in vitro* data show that lipid raft decomposition inhibits TRP channel opening, there are only two recent *in vivo* evidence. Methyl β -cyclodextrin (MCD)-induced membrane cholesterol depletion led to antinociception in the RTX-evoked mononeuropathy model via phosphatidylinositol 4,5-bisphosphate (PI(4,5)P₂) hydrolysis (Lin et al., 2019) and significantly attenuated the prostaglandin E₂ (PGE₂)-evoked mechanical hyperalgesia in rats (Ferrari and Levine, 2015).

Several endogenous steroids have been described to inhibit TRPV1. Dehydroepiandrosterone (DHEA) is able to decrease CAPS-evoked currents in primary sensory neurons (Chen et al., 2004). However, it is not clear if DHEA bind directly to the CAPS-binding domain or it is an allosteric modulator of TRPV1. The neurosteroid pregnenolone sulfate (PS) has a variety of neuropharmacological actions including glycinergic synaptic transmission in the pain pathway. PS, pregnanolone, pregnanolone sulfate, progesterone or dihydrotestosterone administration in extracellular way significantly inhibited TRP Canonical 5 (TRPC5) channel activation within 1–2 min, 17 β -estradiol (E₂) and dehydroepiandrosterone sulfate had weak inhibitory effects. TRPC5 channels are able to direct stereo-selective steroid modulation quickly, and it is lead to channel inhibition (Majeed et al., 2011). We published earlier that our novel synthetic carboxamido-steroid compound (C1) decreased activation of TRP channels located on primary sensory neurons, such as TRPV1, TRPA1, TRP Melastatin 3 (TRPM3), and TRP Melastatin 8 (TRPM8). Furthermore, we provided the first evidence and the presence and the position of the carboxamido group was important for this

Abbreviations: C1, carboxamido-steroid compound; CAPS, capsaicin; CRAC, Cholesterol Recognition/interaction Amino acid Consensus; DHEA, dehydroepiandrosterone; DRG, dorsal root ganglion; E₂, 17- β estradiol; MCD, methyl β -cyclodextrin; PGE₂, prostaglandin E₂; PI(4,5)P₂, phosphatidylinositol 4,5-bisphosphate; PS, pregnenolone sulfate; RAMEB, random methylated β -cyclodextrins; RTX, resiniferatoxin; TrkA, tropomyosin-related kinase A; TRP, Transient Receptor Potential; TRPA1, Transient Receptor Potential Ankyrin 1; TRPC5, Transient Receptor Potential Canonical 5; TRPM3, Transient Receptor Potential Melastatin 3; TRPM8, Transient Receptor Potential Melastatin 8; TRPV1, Transient Receptor Potential Vanilloid 1.

action mediated by cholesterol depletion from the plasma membrane. This effect was similar to that of MCD, but in a much lower, 1000-fold concentration (Szánti-Pintér et al., 2015; Sággy et al., 2018).

Based on these data obtained on primary sensory neuronal cultures here we investigated the effects of C1 compound in mouse pain models of different mechanisms related to TRPV1 and TRPA1 activation in comparison with MCD.

MATERIALS AND METHODS

Animals and Ethics

Twelve to sixteen week-old male C57BL/6 mice were used to test CAPS-evoked nocifensive reactions, and NMRI mice of the same age and sex in the formalin-, and RTX-induced models. The animals were kept in standard plastic cages at 24–25°C, under a 12–12 h light-dark cycle and provided with standard rodent chow and water *ad libitum* in the Laboratory Animal House of the Department of Pharmacology and Pharmacotherapy, University of Pécs. All experimental procedures were carried out according to the 1998/XXVIII Act of the Hungarian Parliament on Animal Protection and Consideration Decree of Scientific Procedures of Animal Experiments (243/1988). The studies were approved by the Ethics Committee on Animal Research of Pécs University according to the Ethical Codex of Animal Experiments and license was given (license No.: BAI/35/702-6/2018.).

Synthesis of Steroid Compound C1

The steroid compound C1 was synthesized by a method, which was described earlier in details (Horváth et al., 2011; Szánti-Pintér et al., 2011, 2015). In brief, the 16-keto-18-nor-13 α -steroid was obtained via an unusual Wagner–Meerwein rearrangement of 16 α ,17 α -epoxy-5 α -androstane in the presence of an imidazolium-based ionic liquid (Horváth et al., 2011). The derivatization of the unnatural steroid was performed by Barton's methodology leading to an iodoalkene mixture (Szánti-Pintér et al., 2015). The iodoalkene mixture was converted to N-(prop-2-ynyl)-carboxamides via a palladium-catalyzed aminocarbonylation reaction and after a column chromatography, C1 was obtained in pure form.

CAPS-Evoked Acute Chemonocifensive Reaction

The effects of C1 and MCD compared to the saline control were investigated on acute chemonociception, 30 μ g/ml CAPS (20 μ l) was instilled in the right eye of the mice. Local pretreatments (20 μ l) with 100 μ M C1 or 15 mM MCD were performed 30 min before the test. CAPS-induced eye-wiping movements with the forelegs were counted during 1 min, as previously described (Szolcsányi et al., 1975; Szőke et al., 2002). We counted only the one-leg movements, washing- or other two-hand movements were excluded. CAPS instillation was repeated 2 and 3 h after its first administration.

RTX-Induced Thermal Allodynia and Mechanical Hyperalgesia

Resiniferatoxin (0.1 μ g/ml, 20 μ l, ultrapotent TRPV1 agonist) was injected intraplantarly into right hindpaws. RTX induces an acute neurogenic inflammation with rapid development of thermal allodynia due to peripheral sensitization, and later mechanical hyperalgesia due to both peripheral and central mechanisms (Meyer and Campbell, 1981; Pan et al., 2003). Control thermo- and mechanonociceptive thresholds were measured on two consecutive days before the experiment, which were used for self-control comparisons. Intraplantar pretreatments (20 μ l) with 100 μ M or 500 μ M C1 and 15 mM MCD were performed 30 min before the RTX administration, which evokes a short acute nocifensive reaction of paw licking, biting, lifting or shaking. The thermonociceptive threshold was measured by an increasing temperature Hot Plate (IITC Life Science, Woodland Hills, CA, United States) 10, 20, and 30 min after RTX injection, and the mechanical hyperalgesia was investigated by Dynamic Plantar Aesthesiometer (DPA, Ugo Basile, Italy) 30, 60, and 90 min after RTX administration, as described earlier (Almási et al., 2003; Payrits et al., 2017; Kántás et al., 2019).

Formalin-Evoked Acute Nocifensive Behavior

Intraplantarly injected formalin (20 μ l, 2.5%) immediately induced nocifensive reactions. The duration of hindpaw licking, lifting, shaking and holding in an elevated position were measured between 0 and 5 min (first phase). It is related to direct chemical stimulation of nociceptors mainly via the TRPA1 receptor. After a resting period (ca. 10–15 min), the duration of the nocifensive behaviors was measured between 20 and 45 min (second phase). This is due to neurogenic inflammatory mechanisms (Tjølsen et al., 1992). Intraplantar pretreatments (20 μ l) with 100 μ M C1 or 15 mM MCD were performed 30 min before formalin administration.

Drugs and Chemicals

Methyl β -cyclodextrin (Sigma, St. Louis, MO, United States) was dissolved in saline to reach final concentration of 15 mM (500 mg/kg). C1 was dissolved in dimethyl sulfoxide to obtain a 10 mM stock solution. Further dilution was made with saline to reach final concentrations of 100 μ M (850 μ g/kg) or 500 μ M (4.25 mg/kg). CAPS from Sigma was diluted with saline from a 10 mg/ml stock solution of 10% ethanol, 10% Tween 80 in saline to reach final concentration of 30 μ g/ml. RTX (Sigma) was dissolved in ethanol to yield a 1 mg/ml stock solution, and further diluted with saline to reach final concentration of 0.1 μ g/ml. Formalin was diluted with phosphate-buffered saline from a 6% formaldehyde stock solution (Molar Inc., Hungary).

Statistical Analysis

All data are the means \pm SEM of six animals per group in the CAPS-evoked eye wiping test and formalin test, and 12–20 animals per group in the RTX-induced thermal allodynia and mechanical hyperalgesia model. Statistical analysis was

performed by Two-way ANOVA followed by Bonferroni's multiple comparisons *post hoc* test, in all cases $p < 0.05$ was considered statistically significant.

RESULTS

C1 and MCD Reduce the Number of CAPS-Evoked Eye-Wiping Movements

The number of CAPS-evoked eye-wipings in the 1st, 2nd, and 3rd h in the saline-pretreated group were 42.0 ± 1.9 ; 33.7 ± 1.8 ; 28.0 ± 3.3 , respectively. In contrast, the corresponding values in the C1-pretreated group were: 23.0 ± 4.2 ; 23.0 ± 3.8 ; 23.7 ± 3.5 (Figure 1A). In case of MCD pretreatment, the number of CAPS-evoked wiping in the saline-pretreated control animals were 32.2 ± 3.9 ; 27.2 ± 2.1 and 26.5 ± 2.2 after 1st, 2nd, and 3rd CAPS instillation. MCD-pretreated animals showed less of eye-wipings with the following results: 23.8 ± 2.7 ; 24.2 ± 3.3 ; 22.7 ± 2.7 (Figure 1B).

In both cases slightly decreasing response to CAPS was observed due to CAPS-evoked desensitization of the TRPV1 receptor. C1 significantly and gradually decreased the number of eye-wipings both in the 1st and 2nd h, while MCD exerted significant effect only in the 1st h.

C1 and MCD Do Not Influence RTX-Induced Thermal Allodynia

The baseline heat threshold values of untreated mice were between 44°C and 49°C . RTX-induced $9.5\text{--}16.3 \pm 2.3\text{--}3.1\%$; $9.1\text{--}9.6 \pm 2.3\text{--}3.2\%$ and $4.3\text{--}5.3 \pm 1.4\text{--}1.6\%$ ($39.0\text{--}41.9 \pm 1.1\text{--}1.5^\circ\text{C}$; $41.8\text{--}42.3 \pm 0.8\text{--}1.4^\circ\text{C}$; $43.9\text{--}44.5 \pm 0.6\text{--}1.0^\circ\text{C}$) drop of the thermonociceptive threshold 10, 20, and 30 min after its intraplantar injection in the saline-pretreated control groups. The corresponding values were $11.6 \pm 2.3\%$ ($40.7 \pm 1.1^\circ\text{C}$); $3.3 \pm 1.6\%$ ($43.9 \pm 0.9^\circ\text{C}$); $3.8 \pm 1.6\%$ ($47.0 \pm 0.5^\circ\text{C}$) for $100 \mu\text{M}$ C1, $14.5 \pm 1.8\%$ ($39.7 \pm 0.9^\circ\text{C}$); 6.6 ± 1.4 ($43.3 \pm 0.6^\circ\text{C}$); $0.3 \pm 1.7\%$ ($46.5 \pm 0.6^\circ\text{C}$) for $500 \mu\text{M}$ C1 and $8.3 \pm 2.0\%$ ($42.4 \pm 1.0^\circ\text{C}$); $7.8 \pm 0.9\%$ ($42.6 \pm 0.3^\circ\text{C}$); $5.8 \pm 2.1\%$ ($43.5 \pm 1.2^\circ\text{C}$) for 15 mM MCD.

Neither C1 nor MCD altered the RTX-induced thermal allodynia (Figures 2A,B).

C1 Diminishes RTX-Induced Mechanical Hyperalgesia

The basal mechanonociceptive thresholds of the intact mouse paw were between 8 and 10 g. RTX-evoked drop of the mechanonociceptive threshold values were $43.9\text{--}44.5 \pm 3.2\text{--}6.2\%$; $37.3\text{--}37.9 \pm 3.9\text{--}8.1\%$ and $26.9\text{--}39.5 \pm 3.0\text{--}4.2\%$ ($5.0\text{--}5.4 \pm 0.3\text{--}0.6 \text{ g}$; $5.6\text{--}6.0 \pm 0.4\text{--}0.7 \text{ g}$; $5.5\text{--}7.0 \pm 0.2\text{--}0.4 \text{ g}$) 30, 60, and 90 min after the injection in the saline pretreated control groups. The corresponding values were $30.0 \pm 5.2\%$ ($6.5 \pm 0.4 \text{ g}$); $20.1 \pm 5.0\%$ ($7.4 \pm 0.4 \text{ g}$); $10.4 \pm 4.8\%$ ($8.3 \pm 0.4 \text{ g}$) for $100 \mu\text{M}$ C1, $19.0 \pm 3.1\%$ ($7.8 \pm 0.3 \text{ g}$); $16.6 \pm 2.9\%$ ($8.0 \pm 0.3 \text{ g}$); $14.3 \pm 3.0\%$ ($8.2 \pm 0.8 \text{ g}$) for $500 \mu\text{M}$ C1 and $36.6 \pm 6.4\%$ ($5.4 \pm 0.5 \text{ g}$); $43.4 \pm 3.4\%$ ($4.9 \pm 0.3 \text{ g}$); $29.7 \pm 6.4\%$ ($6.0 \pm 0.5 \text{ g}$) for 15 mM MCD.

Both $100 \mu\text{M}$ and $500 \mu\text{M}$ of C1 alleviated the RTX-induced mechanical hyperalgesia, but MCD had no effect (Figures 3A,B).

C1 and MCD Alleviate Formalin-Evoked Acute Nocifensive Behaviors

The durations of formalin-evoked acute nocifensive behaviors in the saline-pretreated control group were $179.5 \pm 16.0 \text{ s}$ and $331.5 \pm 45.0 \text{ s}$ in the first and second phases, respectively. In the C1 pretreated animals these values were $144.2 \pm 18.5 \text{ s}$ and $212.2 \pm 31.5 \text{ s}$ (Figure 4A). In case of MCD pretreatment, the nocifensive behaviors durations in the saline control group were $173.9 \pm 17.6 \text{ s}$ and $330.5 \pm 49.2 \text{ s}$ in the two phases, respectively. Compared to the MCD-pretreated group, the corresponding values were $155.9 \pm 5.1 \text{ s}$ and $163.2 \pm 31.3 \text{ s}$ (Figure 4B).

Neither C1 nor MCD modified the nocifensive behaviors in the first phase related to direct chemical activation of TRPA1 receptors, but both compounds significantly decreased the pain reactions in the second phase resulting from acute neurogenic inflammation.

DISCUSSION

We present here the analgesic effect of lipid raft decomposition depleting cholesterol by C1 and MCD (Szánti-Pintér et al., 2015; Sággy et al., 2018). We demonstrated that C1 and MCD diminished TRPV1 and TRPA1 activation-induced acute nocifensive behaviors, furthermore, C1 inhibited the development of TRPV1 stimulation-evoked mechanical hyperalgesia.

Both C1 and MCD significantly diminished the number of CAPS instillation-induced eye-wiping movements in the 1st h by 45 and 32%, respectively, and C1 also in the 2nd h by 26%. We observed a slightly decreasing response in the 2nd and 3rd h to CAPS due to desensitization of TRPV1 receptor (Sharma et al., 2013). Furthermore, C1 significantly decreased RTX-induced mechanical hyperalgesia involving central sensitization processes as well, while its inhibitory effect on thermal allodynia induced predominantly by peripheral sensitization mechanisms (Pan et al., 2003) was not statistically significant. In contrast MCD did not affect these RTX-induced nocifensive responses. Both compounds had inhibitory action on formalin-evoked acute neurogenic inflammatory nocifensive reactions (paw liftings, lickings, holdings, and shakings) in the second, neurogenic inflammatory phase by 36 and 51%, respectively.

These novel *in vivo* results are well supported by our previous *in vitro* findings showing that C1 and MCD significantly and concentration-dependently inhibit TRPV1 and TRPA1 receptor activation both on primary sensory neuronal cultures and receptor-expressing cell line (Szöke et al., 2010; Szánti-Pintér et al., 2015; Sággy et al., 2015, 2018). We have previously proved by filipin staining and fluorescence spectroscopy that C1 similarly to MCD depleted cholesterol from the plasma membrane of sensory neurons, and therefore, they are both considered to be lipid raft disruptors (Sággy et al., 2018). Furthermore, we described that the presence and the

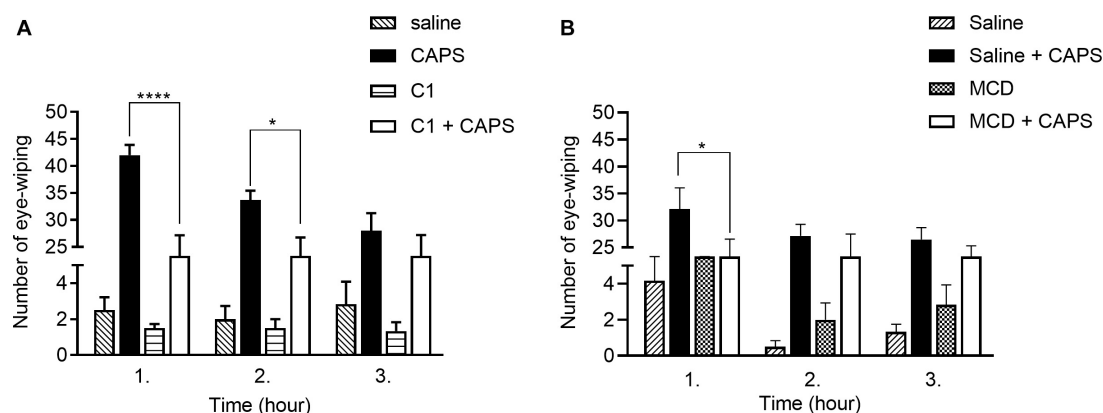


FIGURE 1 | Effect of 100 μ M C1 (A) and 15 mM MCD (B) in the CAPS-evoked acute chemonociceptive reaction. Both compounds reduced the number of eye-wipings. Data are means \pm SEM of $n = 6$ animals/group. Two-way ANOVA with Bonferroni *post hoc* test was used for statistical analysis ($*p < 0.05$; **** $p < 0.0001$ C1/MCD pretreatment vs. saline pretreatment).

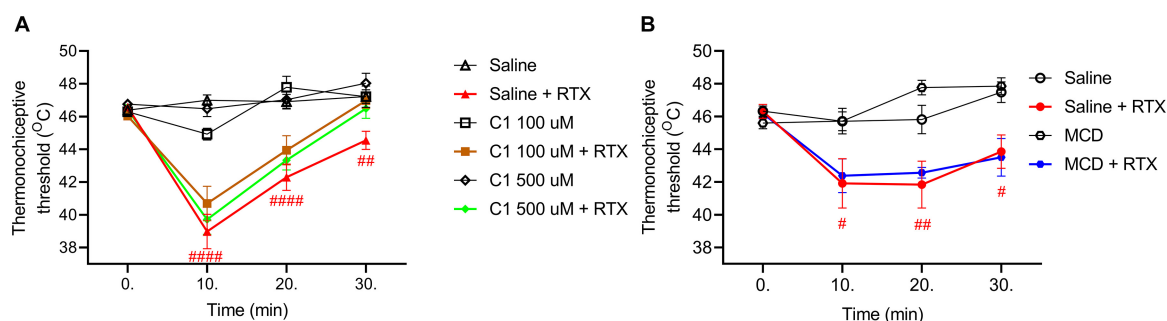


FIGURE 2 | Effect of 100 μ M or 500 μ M (A) and 15 mM MCD (B) on the RTX-induced thermal allodynia. Neither lower or higher concentration of C1, nor MCD did influence the thermonociceptive threshold changing. Red lines represent the saline pretreatment, brown or green lines the 100 μ M or 500 μ M C1 pretreatment and blue line the 15 MCD pretreatment, respectively. Data are means \pm SEM of $n = 12$ –20 animals/group. Red hashes represent the significance in the saline-pretreated group (values after RTX-injection compared to control). Two-way ANOVA with Bonferroni *post hoc* test was used for statistical analysis.

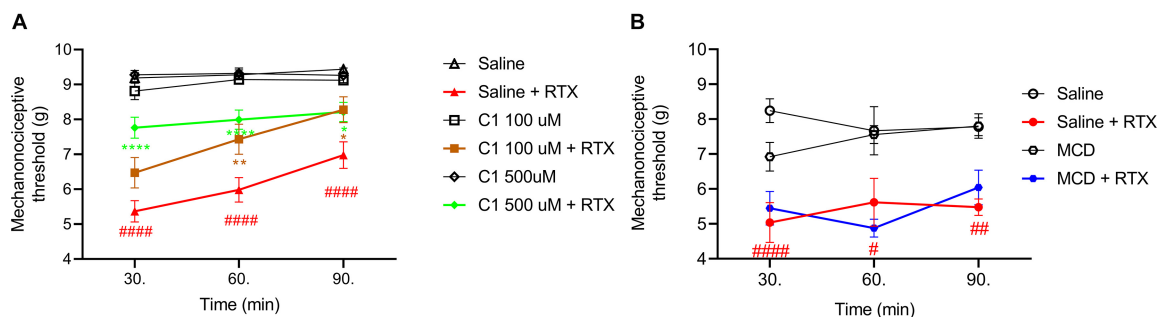


FIGURE 3 | Effect of 100 μ M or 500 μ M (A) and 15 mM MCD (B) on the RTX-induced mechanical hyperalgesia. Both 100 μ M and 500 μ M C1 alleviated, while MCD did not alter the mechanonociceptive threshold changing. Red lines represent the saline pretreatment, brown or green lines the 100 μ M or 500 μ M C1 pretreatment and blue line the 15 MCD pretreatment, respectively. Data are means \pm SEM of $n = 12$ –20 animals/group. Red hashes represent the significance in the saline-pretreated group (values after RTX-injection compared to control). Two-way ANOVA with Bonferroni *post hoc* test was used for statistical analysis ($*p < 0.05$; ** $p < 0.01$; **** $p < 0.0001$ C1 pretreatment vs. saline pretreatment).

position of the carboxamido group on the steroidal skeleton are substantial for TRP channel inhibition. The importance of stereoselectivity was emphasized for the inhibitory effects of steroids on the TRPC5 cation channel. Progesterone and

pregnanolone diminished TRPC5 channel function, while the stereo-isomer of pregnanolone, pregnenolone and a progesterone metabolite allopregnanolone had no inhibitory effects. It is suggested, that stereo-isomerism due to a minimal

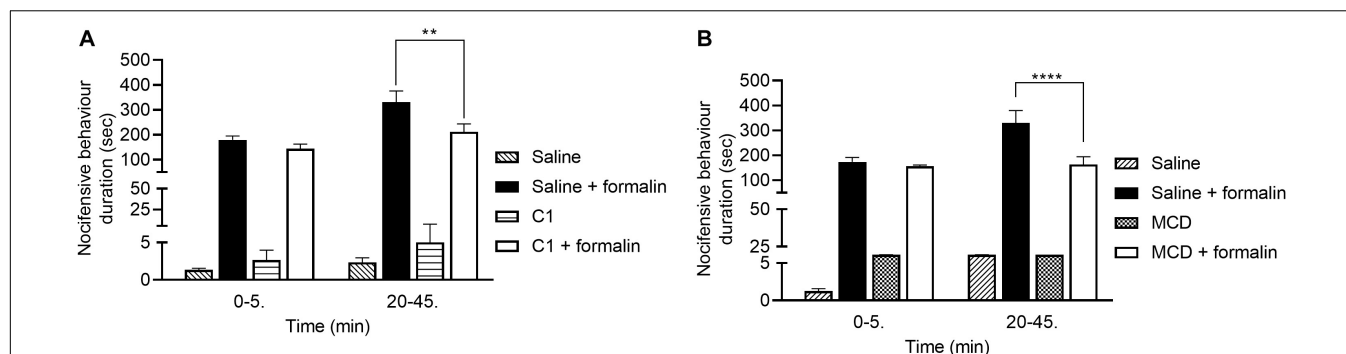


FIGURE 4 | Effect of 100 μ M C1 (**B**) and 15 mM MCD (**A**) in the formalin-evoked acute nociceptive behaviors. Both C1 and MCD altered the second, neurogenic inflammatory phase. Data are means \pm SEM of $n = 6$ animals/group. Two-way ANOVA with Bonferroni *post hoc* test was used for statistical analysis (** $p < 0.01$; **** $p < 0.0001$ C1/MCD pretreatment vs. saline pretreatment).

structural change might be sufficient to alter the biological effect (Majeed et al., 2011). CAPS-induced currents in sensory neurons were decreased by DHEA, but the molecular mechanism is unclear. Although the authors suggested its direct effects on the CAPS-binding domain or an allosteric modulation its action on the lipid rafts surrounding the TRPV1 is also possible (Chen et al., 2004). In a previous study we demonstrated that E2 incubation anticipated the TRPV1 desensitization via the tropomyosin-related kinase A (TrkA) receptor. We provided *in vivo* and *in vitro* evidence for E2-induced TRPV1 receptor sensitization mediated by TrkA via E2-evoked genomic and non-genomic mechanisms (Payrits et al., 2017). Cholesterol depletion by MCD decreased the CAPS-evoked currents in dorsal root ganglion (DRG) primary sensory neurons (Liu et al., 2006). In contrast, MCD did not influence the heat-evoked responses on TRPV1-transfected *Xenopus laevis* oocytes (Liu et al., 2003) or 3 H-RTX binding to TRPV1 receptors on rat C6 glioma cells (Bari et al., 2005). Cholesterol enrichment in isolated membrane segments can modulate the temperature threshold for TRPV1 activation through specific Cholesterol Recognition/interaction Amino acid Consensus (CRAC) motifs (Morales-Lázaro and Rosenbaum, 2019). Increased membrane cholesterol, but not its diastereoisomer epicholesterol addition, inhibited CAPS-, heat- and voltage-induced TRPV1 currents (Picazo-Juárez et al., 2011). These results were also supported by structural studies of CRACs (Levitan et al., 2014; Saha et al., 2017).

Although there are several *in vitro* evidence that lipid raft disruption affected TRP channel activation (Szöke et al., 2010; Sághy et al., 2015), there are only sporadic, recent *in vivo* reports. MCD-related cholesterol depletion induced antinociception in RTX-induced mononeuropathy through PI(4,5)P₂ hydrolysis in mice (Lin et al., 2019). Intraplantar injection of MCD attenuated the PGE₂-, but not cyclopentyladenosine-evoked mechanical hyperalgesia. It is suggest that the development of PGE₂-evoked hyperalgesia is closely related to lipid raft integrity (Ferrari and Levine, 2015). Both local and systemic administration of random methylated β -cyclodextrins (RAMEB) attenuated complete Freund's adjuvant-induced thermal allodynia and mechanical hyperalgesia in rats. RAMEB might

capture the prostaglandin content and then decrease the inflammatory pain which might be a novel anti-inflammatory and analgesic tool (Sauer et al., 2017). Intraplantar injection of another components of lipid rafts, the ganglioside GT1b, produced nociceptive responses and enhanced formalin-induced nociceptive reactions. On the other hand, intraplantar injection of sialidase, which cleaves sialyl residues from gangliosides, attenuated these responses (Watanabe et al., 2011; Sántha et al., 2020). The flavanone isosakuranetin blocked PS-induced Ca²⁺-influx in DRG neurons and significantly attenuated the noxious heat- and PS-induced pain sensation in mice (Straub et al., 2013).

The present *in vivo* data provide the first evidence that the novel C1 compound modifying lipid rafts surrounding the TRPV1 and TRPA1 ion channels exerts antinociceptive and antihyperalgesic effects. The maximal inhibitory effect observed in both TRPV1 and TRPA1 activation-induced nociceptive tests were similar to that of MCD, but in 150-fold lower concentrations. Furthermore, C1 proved to be effective also on RTX-evoked mechanical hyperalgesia that was not affected by MCD. However, despite the well-established lipid rafts disrupting abilities of both C1 and MCD (Szöke et al., 2010; Sághy et al., 2015, 2018), their direct inhibitory actions on the TRPV1 and TRPA1 ion channel activation cannot be excluded.

We conclude that the novel C1 compound is a useful experimental tool to investigate the effects of cholesterol depletion in animal models, and it also might open novel opportunities for analgesic drug development.

DATA AVAILABILITY STATEMENT

All datasets presented in this study are included in the article/supplementary material.

ETHICS STATEMENT

The animal study was reviewed and approved by the Ethics Committee on Animal Research, University of Pécs.

AUTHOR CONTRIBUTIONS

ÉS and JSz contributed to the conceptualization. MP, ÁH, BK, TB-S, ESP, and RS-F contributed to the methodology. ÁH and TB-S contributed to the formal analysis, writing – original draft preparation, visualization, and project administration. ÁH, BK, TB-S, and MP contributed to the investigation. ZH and ÉS contributed to the resources, writing – review and editing, supervision, and funding acquisition. All authors contributed to the article and approved the submitted version.

FUNDING

This work was supported by the National Brain Research Program 2017-1.2.1-NKP -2017-00002 (NAP-2; Chronic Pain Research Group), the Hungarian National Research, Development and Innovation Office (OTKA K120014), Hungarian National Grants GINOP-2.3.2-15-2016-00050,

EFOP-3.6.2-16-2017-00006, and EFOP-3.6.2-16-2017-00008), as well as 17886-4/23018/FEKUTSTRAT excellence grant. MP was supported by the New National Excellence Program of the Ministry of Human Capacities ÚNKP-18-4, ÉS by the János Bolyai Research Scholarship of the Hungarian Academy of Sciences and by the New National Excellence Program of the Ministry of Human Capacities ÚNKP-18-4, and ÚNKP-19-4 New National Excellence Program of the Ministry for Innovation and Technology grant.

ACKNOWLEDGMENTS

The authors thank Dóra Ömböli for her expert technical assistance, and the Late Prof. János Szolcsányi for his expert advices during the experimental procedures. Prof. Szolcsányi passed away during the course of this study, and this paper is dedicated to his memory.

REFERENCES

- Almási, R., Pethő, G., Bölskei, K., and Szolcsányi, J. (2003). Effect of resiniferatoxin on the noxious heat threshold temperature in the rat: a novel heat allodynia model sensitive to analgesics. *Br. J. Pharmacol.* 139, 49–58. doi: 10.1038/sj.bjp.0705234
- Bandell, M., Story, G. M., Hwang, S. W., Viswanath, V., Eid, S. R., Petrus, M. J., et al. (2004). Noxious cold ion channel TRPA1 is activated by pungent compounds and bradykinin. *Neuron* 41, 849–857. doi: 10.1016/S0896-6273(04)00150-3
- Bari, M., Battista, N., Fezza, F., Finazzi-Agrò, A., and Maccarrone, M. (2005). Lipid rafts control signaling of type-1 cannabinoid receptors in neuronal cells: implications for anandamide-induced apoptosis. *J. Biol. Chem.* 280, 12212–12220. doi: 10.1074/jbc.M411642200
- Bautista, D. M., Pellegrino, M., and Tsunozaki, M. (2013). TRPA1: a gatekeeper for inflammation. *Annu. Rev. Physiol.* 75, 181–200. doi: 10.1146/annurev-physiol-030212-183811
- Botz, B., Bölskei, K., and Helyes, Z. (2017). Challenges to develop novel anti-inflammatory and analgesic drugs: novel anti-inflammatory and analgesic drugs. *Wiley Interdiscip. Rev. Nanomed. Nanobiotechnol.* 9:e1427. doi: 10.1002/wnan.1427
- Chen, S.-C., Chang, T.-J., and Wu, F.-S. (2004). Competitive inhibition of the capsaicin receptor-mediated current by dehydroepiandrosterone in rat dorsal root ganglion neurons. *J. Pharmacol. Exp. Ther.* 311, 529–536. doi: 10.1124/jpet.104.069096
- Corey, D. P., García-Añoveros, J., Holt, J. R., Kwan, K. Y., Lin, S.-Y., Vollrath, M. A., et al. (2004). TRPA1 is a candidate for the mechanosensitive transduction channel of vertebrate hair cells. *Nature* 432, 723–730. doi: 10.1038/nature03066
- Drews, A., Mohr, F., Rizun, O., Wagner, T. F. J., Dembla, S., Rudolph, S., et al. (2014). Structural requirements of steroidal agonists of transient receptor potential melastatin 3 (TRPM3) cation channels: structural requirements of TRPM3 agonists. *Br. J. Pharmacol.* 171, 1019–1032. doi: 10.1111/bph.12521
- Ferrari, L. F., and Levine, J. D. (2015). Plasma membrane mechanisms in a preclinical rat model of chronic pain. *J. Pain* 16, 60–66. doi: 10.1016/j.jpain.2014.10.007
- Grimm, C., Kraft, R., Sauerbruch, S., Schultz, G., and Harteneck, C. (2003). Molecular and functional characterization of the melastatin-related cation channel TRPM3. *J. Biol. Chem.* 278, 21493–21501. doi: 10.1074/jbc.M300945200
- Grimm, C., Kraft, R., Schultz, G., and Harteneck, C. (2005). Activation of the melastatin-related cation channel TRPM3 by d-erythro-Sphingosine. *Mol. Pharmacol.* 67, 798–805. doi: 10.1124/mol.104.006734
- Helyes, Z., Németh, J., Thán, M., Bölskei, K., Pintér, E., and Szolcsányi, J. (2003a). Inhibitory effect of anandamide on resiniferatoxin-induced sensory neuropeptide release in vivo and neuropathic hyperalgesia in the rat. *Life Sci.* 73, 2345–2353. doi: 10.1016/S0024-3205(03)00651-9
- Helyes, Z., Pinter, E., Németh, J., and Szolcsányi, J. (2003b). Pharmacological targets for the inhibition of neurogenic inflammation. *Curr. Med. Chem.* 2, 191–218. doi: 10.2174/1568014033483806
- Helyes, Z., Pinter, E., Sandor, K., Elekes, K., Banvolgyi, A., Keszthelyi, D., et al. (2009). Impaired defense mechanism against inflammation, hyperalgesia, and airway hyperreactivity in somatostatin 4 receptor gene-deleted mice. *Proc. Natl. Acad. Sci. U.S.A.* 106, 13088–13093. doi: 10.1073/pnas.0900681106
- Horváth, A., Szájli, Á., Kiss, R., Kóti, J., Mahó, S., and Skoda-Földes, R. (2011). Ionic liquid-promoted wagner-meerwein rearrangement of 16 α ,17 α -Epoxyandrostanes and 16 α ,17 α -Epoxyestrans. *J. Org. Chem.* 76, 6048–6056. doi: 10.1021/jo2006285
- Jordt, S.-E., Bautista, D. M., Chuang, H., McKemy, D. D., Zygmunt, P. M., Högestätt, E. D., et al. (2004). Mustard oils and cannabinoids excite sensory nerve fibres through the TRP channel ANKTM1. *Nature* 427, 260–265. doi: 10.1038/nature02282
- Kaneko, Y., and Szallasi, A. (2014). Transient receptor potential (TRP) channels: a clinical perspective: clinical perspective on TRPs. *Br. J. Pharmacol.* 171, 2474–2507. doi: 10.1111/bph.12414
- Kántás, B., Börzsei, R., Szőke, É., Bánhegyi, P., Horváth, Á., Hunyady, Á., et al. (2019). Novel drug-like somatostatin receptor 4 agonists are potential analgesics for neuropathic pain. *Int. J. Mol. Sci.* 20:6245. doi: 10.3390/ijms20246245
- Lee, N., Chen, J., Sun, L., Wu, S., Gray, K. R., Rich, A., et al. (2003). Expression and characterization of human transient receptor potential melastatin 3 (hTRPM3). *J. Biol. Chem.* 278, 20890–20897. doi: 10.1074/jbc.M211232200
- Lee, Y., Hong, S., Cui, M., Sharma, P. K., Lee, J., and Choi, S. (2015). Transient receptor potential vanilloid type 1 antagonists: a patent review (2011 – 2014). *Expert Opin. Ther. Pat.* 25, 291–318. doi: 10.1517/13543776.2015.1008449
- Levitán, I., Singh, D. K., and Rosenhouse-Dantsker, A. (2014). Cholesterol binding to ion channels. *Front. Physiol.* 5:65. doi: 10.3389/fphys.2014.00065
- Lin, C.-L., Chang, C.-H., Chang, Y.-S., Lu, S.-C., and Hsieh, Y.-L. (2019). Treatment with methyl- β -cyclodextrin prevents mechanical allodynia in resiniferatoxin neuropathy in a mouse model. *Biol. Open* 8:bio039511. doi: 10.1242/bio.039511
- Liu, B., Hui, K., and Qin, F. (2003). Thermodynamics of heat activation of single capsaicin ion channels VR1. *Biophys. J.* 85, 2988–3006. doi: 10.1016/S0006-3495(03)74719-5
- Liu, M., Huang, W., Wu, D., and Priestley, J. V. (2006). TRPV1, but not P2X₃, requires cholesterol for its function and membrane expression in rat nociceptors. *Eur. J. Neurosci.* 24, 1–6. doi: 10.1111/j.1460-9568.2006.04889.x

- Macpherson, L. J., Dubin, A. E., Evans, M. J., Marr, F., Schultz, P. G., Cravatt, B. F., et al. (2007). Noxious compounds activate TRPA1 ion channels through covalent modification of cysteines. *Nature* 445, 541–545. doi: 10.1038/nature05544
- Macpherson, L. J., Geierstanger, B. H., Viswanath, V., Bandell, M., Eid, S. R., Hwang, S., et al. (2005). The pungency of garlic: activation of TRPA1 and TRPV1 in response to Allicin. *Curr. Biol.* 15, 929–934. doi: 10.1016/j.cub.2005.04.018
- Majeed, Y., Agarwal, A., Naylor, J., Seymour, V., Jiang, S., Muraki, K., et al. (2010). Cis-isomerism and other chemical requirements of steroidal agonists and partial agonists acting at TRPM3 channels: TRPM3 steroid stereo-selectivity. *Br. J. Pharmacol.* 161, 430–441. doi: 10.1111/j.1476-5381.2010.00892.x
- Majeed, Y., Amer, M., Agarwal, A., McKeown, L., Porter, K., O'Regan, D., et al. (2011). Stereoselective inhibition of transient receptor potential TRPC5 cation channels by neuroactive steroids: TRPC5 inhibition by steroids. *Br. J. Pharmacol.* 162, 1509–1520. doi: 10.1111/j.1476-5381.2010.01136.x
- McKemy, D. D., Neuhauser, W. M., and Julius, D. (2002). Identification of a cold receptor reveals a general role for TRP channels in thermosensation. *Nature* 416, 52–58. doi: 10.1038/nature719
- McNamara, C. R., Mandel-Brehm, J., Bautista, D. M., Siemens, J., Deranian, K. L., Zhao, M., et al. (2007). TRPA1 mediates formalin-induced pain. *Proc. Natl. Acad. Sci. U.S.A.* 104, 13525–13530. doi: 10.1073/pnas.0705924104
- Meyer, R. A., and Campbell, J. N. (1981). Myelinated nociceptive afferents account for the hyperalgesia that follows a burn to the hand. *Science* 213, 1527–1529. doi: 10.1126/science.7280675
- Morales-Lázaro, S. L., and Rosenbaum, T. (2019). “Cholesterol as a key molecule that regulates TRPV1 channel function,” in *Direct Mechanisms in Cholesterol Modulation of Protein Function Advances in Experimental Medicine and Biology*, eds A. Rosenhouse-Dantsker and A. N. Bukiya (Cham: Springer International Publishing), 105–117. doi: 10.1007/978-3-030-14265-0_6
- Moran, M. M., McAlexander, M. A., Biró, T., and Szallasi, A. (2011). Transient receptor potential channels as therapeutic targets. *Nat. Rev. Drug Discov.* 10, 601–620. doi: 10.1038/nrd3456
- Morenilla-Palao, C., Pertusa, M., Meseguer, V., Cabedo, H., and Viana, F. (2009). Lipid raft segregation modulates TRPM8 channel activity. *J. Biol. Chem.* 284, 9215–9224. doi: 10.1074/jbc.M807228200
- Nilius, B., and Szallasi, A. (2014). Transient receptor potential channels as drug targets: from the science of basic research to the art of medicine. *Pharmacol. Rev.* 66, 676–814. doi: 10.1124/pr.113.008268
- Oberwinkler, J., and Philipp, S. E. (2014). “TRPM3,” in *Mammalian Transient Receptor Potential (TRP) Cation Channels Handbook of Experimental Pharmacology*, eds B. Nilius and V. Flockerzi (Berlin: Springer Berlin Heidelberg), 427–459. doi: 10.1007/978-3-642-54215-2_17
- Pan, H.-L., Khan, G. M., Alloway, K. D., and Chen, S.-R. (2003). Resiniferatoxin induces paradoxical changes in thermal and mechanical sensitivities in rats: mechanism of action. *J. Neurosci.* 23, 2911–2919. doi: 10.1523/JNEUROSCI.23-07-02911.2003
- Payrits, M., Sághy, É., Cseko, K., Pohóczy, K., Bölskei, K., Ernsts, D., et al. (2017). Estradiol sensitizes the transient receptor potential Vanilloid 1 receptor in pain responses. *Endocrinology* 158, 3249–3258. doi: 10.1210/en.2017-00101
- Peier, A. M., Moqrich, A., Hergarden, A. C., Reeve, A. J., Andersson, D. A., Story, G. M., et al. (2002). A TRP channel that senses cold stimuli and menthol. *Cell* 108, 705–715. doi: 10.1016/S0092-8674(02)00652-9
- Picazo-Juárez, G., Romero-Suárez, S., Nieto-Posadas, A., Llorente, I., Jara-Oseguera, A., Briggs, M., et al. (2011). Identification of a binding motif in the S5 helix that confers cholesterol sensitivity to the TRPV1 ion channel. *J. Biol. Chem.* 286, 24966–24976. doi: 10.1074/jbc.M111.237537
- Reid, G., and Flonta, M.-L. (2002). Ion channels activated by cold and menthol in cultured rat dorsal root ganglion neurones. *Neurosci. Lett.* 324, 164–168. doi: 10.1016/S0304-3940(02)00181-7
- Romanovsky, A. A., Almeida, M. C., Garami, A., Steiner, A. A., Norman, M. H., Morrison, S. F., et al. (2009). The transient receptor potential Vanilloid-1 channel in thermoregulation: a thermosensor it is not. *Pharmacol. Rev.* 61, 228–261. doi: 10.1124/pr.109.001263
- Sághy, É., Payrits, M., Biró-Sütő, T., Skoda-Földes, R., Szánti-Pintér, E., Erotyák, J., et al. (2018). Carboxamido steroids inhibit the opening properties of transient receptor potential ion channels by lipid raft modulation. *J. Lipid Res.* 59, 1851–1863. doi: 10.1194/jlr.M084723
- Sághy, É., Szőke, É., Payrits, M., Helyes, Z., Börzsei, R., Erotyák, J., et al. (2015). Evidence for the role of lipid rafts and sphingomyelin in Ca²⁺-gating of transient receptor potential channels in trigeminal sensory neurons and peripheral nerve terminals. *Pharmacol. Res.* 100, 101–116. doi: 10.1016/j.phrs.2015.07.028
- Saha, S., Ghosh, A., Tiwari, N., Kumar, A., Kumar, A., and Goswami, C. (2017). Preferential selection of Arginine at the lipid-water-interface of TRPV1 during vertebrate evolution correlates with its snorkeling behaviour and cholesterol interaction. *Sci. Rep.* 7:16808. doi: 10.1038/s41598-017-16780-w
- Salas, M. M., Hargreaves, K. M., and Akopian, A. N. (2009). TRPA1-mediated responses in trigeminal sensory neurons: interaction between TRPA1 and TRPV1. *Eur. J. Neurosci.* 29, 1568–1578. doi: 10.1111/j.1460-9568.2009.06702.x
- Sántha, P., Dobos, I., Kis, G., and Jancsó, G. (2020). Role of gangliosides in peripheral pain mechanisms. *Int. J. Mol. Sci.* 21:1005. doi: 10.3390/ijms21031005
- Sauer, R.-S., Rittner, H. L., Roewer, N., Sohajda, T., Shityakov, S., Brack, A., et al. (2017). A novel approach for the control of inflammatory pain: prostaglandin E2 complexation by randomly methylated β -Cyclodextrins. *Anesth. Analg.* 124, 675–685. doi: 10.1213/ANE.0000000000001674
- Sharma, S. K., Vij, A. S., and Sharma, M. (2013). Mechanisms and clinical uses of capsaicin. *Eur. J. Pharmacol.* 720, 55–62. doi: 10.1016/j.ejphar.2013.10.053
- Simons, K., and Ikonen, E. (1997). Functional rafts in cell membranes. *Nature* 387, 569–572. doi: 10.1038/42408
- Straub, I., Krügel, U., Mohr, F., Teichert, J., Rizun, O., Konrad, M., et al. (2013). Flavanones that selectively inhibit TRPM3 attenuate thermal nociception in vivo. *Mol. Pharmacol.* 84, 736–750. doi: 10.1124/mol.113.086843
- Szánti-Pintér, E., Balogh, J., Csók, Z., Kollár, L., Gömöry, Á., and Skoda-Földes, R. (2011). Synthesis of steroid-ferrocene conjugates of steroidal 17-carboxamides via a palladium-catalyzed aminocarbonylation – Copper-catalyzed azide-alkyne cycloaddition reaction sequence. *Steroids* 76, 1377–1382. doi: 10.1016/j.steroids.2011.07.006
- Szánti-Pintér, E., Wouters, J., Gömöry, Á., Sághy, É., Szőke, É., Helyes, Z., et al. (2015). Synthesis of novel 13 α -18-norandrostane-ferrocene conjugates via homogeneous catalytic methods and their investigation on TRPV1 receptor activation. *Steroids* 104, 284–293. doi: 10.1016/j.steroids.2015.10.016
- Szőke, E., Seress, L., and Szolcsányi, J. (2002). Neonatal capsaicin treatment results in prolonged mitochondrial damage and delayed cell death of B cells in the rat trigeminal ganglia. *Neuroscience* 113, 925–937. doi: 10.1016/s0306-4522(02)00208-7
- Szőke, É., Börzsei, R., Tóth, D. M., Lengel, O., Helyes, Z., Sándor, Z., et al. (2010). Effect of lipid raft disruption on TRPV1 receptor activation of trigeminal sensory neurons and transfected cell line. *Eur. J. Pharmacol.* 628, 67–74. doi: 10.1016/j.ejphar.2009.11.052
- Szolcsányi, J. (2004). Forty years in capsaicin research for sensory pharmacology and physiology. *Neuropeptides* 38, 377–384. doi: 10.1016/j.npep.2004.07.005
- Szolcsányi, J., Jancsó-Gábor, A., and Joó, F. (1975). Functional and fine structural characteristics of the sensory neuron blocking effect of capsaicin. *Naunyn Schmiedeberg's Arch. Pharmacol.* 287, 157–169. doi: 10.1007/BF00510447
- Tjølsen, A., Berge, O. G., Hunskaar, S., Rosland, J. H., and Hole, K. (1992). The formalin test: an evaluation of the method. *Pain* 51, 5–17. doi: 10.1016/0304-3959(92)90003-t
- Trevisani, M., Siemens, J., Materazzi, S., Bautista, D. M., Nassini, R., Campi, B., et al. (2007). 4-Hydroxynonenal, an endogenous aldehyde, causes pain and neurogenic inflammation through activation of the irritant receptor TRPA1. *Proc. Natl. Acad. Sci. U.S.A.* 104, 13519–13524. doi: 10.1073/pnas.0705923104
- Vilceanu, D., and Stucky, C. L. (2010). TRPA1 mediates mechanical currents in the plasma membrane of mouse sensory neurons. *PLoS One* 5:e12177. doi: 10.1371/journal.pone.0012177
- Vriens, J., Held, K., Janssens, A., Tóth, B. I., Kerselaers, S., Nilius, B., et al. (2014). Opening of an alternative ion permeation pathway in a nociceptor TRP channel. *Nat. Chem. Biol.* 10, 188–195. doi: 10.1038/nchembio.1428

- Vriens, J., Owsianik, G., Hofmann, T., Philipp, S. E., Stab, J., Chen, X., et al. (2011). TRPM3 is a nociceptor channel involved in the detection of noxious heat. *Neuron* 70, 482–494. doi: 10.1016/j.neuron.2011.02.051
- Wagner, T. F. J., Loch, S., Lambert, S., Straub, I., Mannebach, S., Mathar, I., et al. (2008). Transient receptor potential M3 channels are ionotropic steroid receptors in pancreatic β cells. *Nat. Cell Biol.* 10, 1421–1430. doi: 10.1038/ncb1801
- Watanabe, S., Tan-No, K., Tadano, T., and Higashi, H. (2011). Intraplantar injection of gangliosides produces nociceptive behavior and hyperalgesia via a glutamate signaling mechanism. *Pain* 152, 327–334. doi: 10.1016/j.pain.2010.10.036

Conflict of Interest: The authors declare that the research was conducted in the absence of any commercial or financial relationships that could be construed as a potential conflict of interest.

Copyright © 2020 Horváth, Biró-Sütő, Kántás, Payrits, Skoda-Földes, Szánti-Pintér, Helyes and Szőke. This is an open-access article distributed under the terms of the Creative Commons Attribution License (CC BY). The use, distribution or reproduction in other forums is permitted, provided the original author(s) and the copyright owner(s) are credited and that the original publication in this journal is cited, in accordance with accepted academic practice. No use, distribution or reproduction is permitted which does not comply with these terms.



IL-1 β Induced Cytokine Expression by Spinal Astrocytes Can Play a Role in the Maintenance of Chronic Inflammatory Pain

Andrea Gajtkó, Erzsébet Bakk, Krisztina Hegedűs, László Ducza and Krisztina Holló*

Department of Anatomy, Histology and Embryology, Faculty of Medicine, University of Debrecen, Debrecen, Hungary

OPEN ACCESS

Edited by:

Istvan Nagy,
Imperial College London,
United Kingdom

Reviewed by:

Livio Luongo,
University of Campania Luigi Vanvitelli,
Italy
Gábor Jancsó,
University of Szeged, Hungary

*Correspondence:

Krisztina Holló
krisztina.hollo@med.unideb.hu;
hollo.krisztina@med.unideb.hu

Specialty section:

This article was submitted to
Integrative Physiology,
a section of the journal
Frontiers in Physiology

Received: 16 March 2020

Accepted: 23 October 2020

Published: 16 November 2020

Citation:

Gajtkó A, Bakk E, Hegedűs K,
Ducza L and Holló K (2020) IL-1 β
Induced Cytokine Expression by
Spinal Astrocytes Can Play a Role
in the Maintenance of Chronic
Inflammatory Pain.
Front. Physiol. 11:543331.
doi: 10.3389/fphys.2020.543331

It is now widely accepted that the glial cells of the central nervous system (CNS) are key players in many processes, especially when they are activated via neuron-glia or glia-glia interactions. In turn, many of the glia-derived pro-inflammatory cytokines contribute to central sensitization during inflammation or nerve injury-evoked pathological pain conditions. The prototype of pro-inflammatory cytokines is interleukin-1 β (IL-1 β) which has widespread functions in inflammatory processes. Our earlier findings showed that in the spinal cord (besides neurons) astrocytes express the ligand binding interleukin-1 receptor type 1 (IL-1R1) subunit of the IL-1 receptor in the spinal dorsal horn in the chronic phase of inflammatory pain. Interestingly, spinal astrocytes are also the main source of the IL-1 β itself which in turn acts on its neuronal and astrocytic IL-1R1 leading to cell-type specific responses. In the initial experiments we measured the IL-1 β concentration in the spinal cord of C57BL/6 mice during the course of complete Freund adjuvant (CFA)-induced inflammatory pain and observed a peak of IL-1 β level at the time of highest mechanical sensitivity. In order to further study astrocytic activation, primary astrocyte cultures from spinal cords of C57BL/6 wild type and IL-1R1 deficient mice were exposed to IL-1 β in concentrations corresponding to the spinal levels in the CFA-induced pain model. By using cytokine array method we observed significant increase in the expressional level of three cytokines: interleukin-6 (IL-6), granulocyte-macrophage colony stimulating factor (GM-CSF) and chemokine (C-C motif) ligand 5 (CCL5 or RANTES). We also observed that the secretion of the three cytokines is mediated by the NF κ B signaling pathway. Our data completes the picture of the IL-1 β -triggered cytokine cascade in spinal astrocytes, which may lead to enhanced activation of the local cells (neurons and glia as well) and can lead to the prolonged maintenance of chronic pain. All these cytokines and the NF κ B pathway can be possible targets of pain therapy.

Keywords: IL-1 β , astrocyte, spinal cord, chronic pain, inflammatory cytokines and chemokines

INTRODUCTION

Astrocytes are the most abundant glial cells in the CNS, they are responsible for many functions as supporting cells in the central nervous system (CNS) e.g., maintenance of the ionic milieu, induction of the blood brain barrier, removal of excess neurotransmitters etc. (Verkhratsky and Nedergaard, 2018). However, it is clear now, that astrocytes are not merely supporting cells in

the CNS, but they are capable to modulate neuronal excitability (Suter et al., 2007; Milligan and Watkins, 2009; Kuner, 2010; Ji et al., 2019) and in this way contribute to the onset and maintenance of numerous CNS pathologies including chronic pain (Gao and Ji, 2010; Chiang et al., 2012; Liddelow and Barres, 2015). One possible way of modulating neuronal activity is the astroglial production of cytokines and chemokines which can act on their neuronal receptors (Zhang and An, 2007) thus contribute to neuron-glia interactions. Such enhanced cytokine expression was observed in neuropathic and inflammatory pain as well (Calvo et al., 2012; Jayaraj et al., 2019). Some of these cytokines and chemokines are also means of glia-glia communication as their receptors are expressed by glial cells (Conti et al., 2008; Trettel et al., 2019).

In this study we focused on the role of interleukin-1 β (IL-1 β) which is the prototype of pro-inflammatory cytokines, it is a regulator of many immunological functions (Sims and Smith, 2010). It was shown to be involved in the pathomechanism of several inflammatory disorders which are also associated with pain (Dinarello et al., 2012). In the CNS its receptor (IL-1R1) was found to be expressed by neurons (Niederberger et al., 2007; Cao and Zhang, 2008; Zhu et al., 2008) and glial cells (Wang et al., 2006; Zhu et al., 2008; Liao et al., 2011; Gruber-Schoffnegger et al., 2013). It has been reported that IL-1 β can induce astrocytic activation and astrogliosis (Herx and Yong, 2001). Our earlier findings (Holló et al., 2017) also suggest that during inflammatory pain IL-1 β can act on spinal neurons and astrocytes. It has been revealed that IL-1 β induce cell type-specific response in the cells of the CNS due to a neuron specific isoform of the IL-1 receptor accessory protein (IL-1RAcP), which is a required receptor partner in IL-1 signaling (Huang et al., 2011). In nerve cells IL-1 β modulates neuronal excitability by e.g., potentiation of NMDA-mediated intracellular calcium signaling (Viviani et al., 2003; Cao and Zhang, 2008), while IL-1 β activated astrocytes produce a cascade of inflammatory mediators which can further enhance and possibly prolong neuroinflammation-induced chronic pain (Zhang and An, 2007).

In this study we intended to identify those cytokines and chemokines which are secreted by IL-1 β -stimulated spinal astrocytes. We also intended to investigate the activation of the NF- κ B signaling pathway which is associated with astrocyte-specific IL-1 β signaling.

MATERIALS AND METHODS

Animals

The study protocol was reviewed and approved by the recommendations of the Animal Care Committee of the University of Debrecen, Hungary according to national laws and European Union regulations [European Communities Council Directive of 24 November 1986 (86/609/EEC)], and was properly conducted under the supervision of the University's Guidelines for Animal Experimentation. All animals were kept under standard conditions with chow and water *ad libitum*. The experiments were performed on male C57BL/6 mice (Gödöllő, Hungary). The animals were divided into experimental groups.

Experimental group 1 (6 control mice) and experimental group 2 (21 CFA treated animals). In animals within the treated group chronic inflammation was induced by intraplantar injection of 50 μ l 1:1 mixture of physiological saline solution and complete Freund-adjutant (CFA) (Sigma, St Louis, United States) into the right hindpaw of mice according to the method described earlier (Hylden et al., 1989).

Nociceptive Behavioral Test

Control and CFA-treated animals were tested for paw withdrawal responses to noxious mechanical stimuli. Mechanical sensitivity of the animals was detected by a modified von Frey test (Dynamic Plantar Aesthesiometer, Ugo Basile, Gemonio, Italy). Animals were placed into a cage with acrylic sidewalls and mesh floor. After 15 min of habituation, a flexible, von Frey-type filament (diameter = 0.5 mm) exerted increasing force on the plantar surface of the hindpaw, until the animal withdrew it. The mechanical withdrawal threshold (MWT) for both hind paws were measured before CFA injection and the tests were repeated daily after CFA injection. The MWT was detected automatically. The test was repeated five times for each paw with 2 min intervals alternating between the right and the left paw. From the experimental data mean value and standard error of mean (SEM) were calculated. Statistical differences among the data were calculated according to the One Way ANOVA test.

IL-1 β Quantitative ELISA

Mouse IL-1 β /IL-1F2 Quantikine ELISA kit (RnD Systems, Minneapolis, United States, cat. no. MLB00C) was applied for the measurement of total IL-1 β amount in spinal cord tissue homogenates. Briefly, control animals ($n = 3$) and CFA-treated animals ($n = 3$ /day) on experimental days 1–5 were sacrificed (after measuring the mechanical pain sensitivity levels), the spinal cord was dissected and the dorsal horn of the L4–L5 segments was removed, the treated (right side) and the non-treated (left side) of the tissue was handled separately. After measuring their weight, the tissue samples were mechanically homogenized in ice cold RIPA buffer supplemented with protease inhibitors (Pierce Protease Inhibitor Mini tablet, Thermo Scientific, Rockford, United States). After 20 min. of gentle rocking on ice the samples were centrifuged (10 min, 15000 rpm, at 4°C) to remove insoluble tissue debris. 50 μ l of supernatant was used in triplicates to determine the IL-1 β content of the tissue homogenates. Then the experiments were performed according to the instructions by the manufacturer. Finally, the IL-1 β content was calculated for 1 mg of spinal cord tissue.

Primary Astrocyte Cultures

For the production of spinal cord astrocyte cultures we basically followed the procedure already described (Hegyi et al., 2018) with slight modifications. Briefly, the whole spinal cord was removed from 2 to 4 day old C57BL/6 and IL-1 receptor type-1 (IL-1R1) deficient/(B6.129S7-Il1r1 tm1/mx./J stock #003245) created by Labow et al. (1997) and purchased from Jackson Laboratories (Bar Harbor, ME, United States)/pups after decapitation and placed into ice-cold dissecting buffer (136 mM NaCl, 5.2 mM KCl, 0.64 mM Na₂HPO₄, 0.22 mM KH₂PO₄, 16.6 mM glucose,

22 mM sucrose, 10 mM HEPES supplemented with 0.06 U/ml penicillin and 0.06 U/ml streptomycin). The isolated spinal cords were carefully cleaned to remove meninges then placed into fresh dissecting solution containing 0.025 g/ml bovine trypsin (Sigma, St Louis, United States) and were incubated at 37°C for 30 min. Then the solution was replaced by Minimum Essential Medium (MEM, Gibco, Life Technologies Ltd., Parsippany, United Kingdom) supplemented with 10% Fetal Bovine Serum (FBS, Hyclone, GE Healthcare Bio-Sciences, Pittsburgh, United States). After 5 min. incubation at room temperature the tissue pieces were gently suspended by a Pasteur pipette and the cell suspension was filtered through a nylon mesh (Cell Strainer, Sigma, pore size: 100 μ m), the cell number was identified and the suspension was diluted to a cell density of 1×10^6 /ml, the cells were placed into 24 well tissue culture plates (0.5 ml/well). The cell cultures were kept at 37°C in a 5% CO₂ atmosphere, the medium was replaced the following day and every second day thereafter.

3-[4,5-Dimethylthiazole-2-yl]-2,5-Diphenyltetrazolium Bromide (MTT) Assay

Astrocyte cultures prepared from spinal cords of C57/BL6 wild type and IL-1R1-deficient mice were used to test the mitochondrial activity of the MTT assay. Briefly, after 24 h stimulation with increasing concentrations (0.1, 1, 10, 25, and 100 pg/ml) of recombinant murine IL-1 β protein (cat. no. 211-11B, PeproTech, Rocky Hill, United States) the culture media was replaced by PBS containing 0.1 mg/ml MTT. After 4 h incubation the supernatants were removed and the formazan product was dissolved in isopropyl alcohol. Finally, the absorbance was measured at $\lambda = 570$ nm by microplate reader (Titertek Uniscan, Flow Laboratories, Helsinki, Finland) in duplicates. Absorbance values were averaged and statistical differences were calculated by ANOVA statistical probe.

Proteome Profiler Assay

The Proteome Profiler Mouse Cytokine Array Kit, Panel A (R&D Systems, cat. no. ARY006) was utilized for the parallel determination of the relative levels of selected mouse cytokines and chemokines produced by the primary astrocyte cultures. Prior to the assay, cells were stimulated by 10 pg/ml recombinant murine IL-1 β protein (PeproTech) for 24 h. Then the supernatants were pooled from 12 well non-treated, control and 12 well IL-1 β -stimulated cultures. After centrifugation (10 min, 800 rpm at 4°C) 1 ml of the supernatants were mixed with Array Buffer and the Antibody Detection Cocktail and were added to the nitrocellulose membranes pre-coated with the capture antibodies. Then we followed the instructions by the manufacturer. The signal was developed by DuoLux Chemiluminescent Substrate Kit (Vector Laboratories, Burlingame, United States, cat. no. SK-6604) and the image was captured by FluorChem E (Protein Simple, San Jose, United States).

The developed membranes were analyzed by the Image-J software. First, pixel densities were determined for each spot on the membranes, then the background signal was subtracted from

each value. Finally, we compared the corresponding signals on different arrays to determine the relative change (fold change) in cytokine levels between samples. Statistical differences among the data were calculated according to the ANOVA test, the difference between groups was considered significant if $p \leq 0.05$.

Immunohistochemistry

Immunohistochemistry was performed on astrocyte cultures which were kept on coverslips placed into 24 well culture dishes. After 7–10 days of culturing the coverslips were removed and the cells were fixed with 4% paraformaldehyde (15 min.). Then the cells were washed in PBS containing 100 mM glycine followed by 10 min. incubation in PBS. Aspecific labeling was blocked by PBS containing 10% normal serum for 50 min. Then the cells were incubated with the primary antibodies (anti-IL-6, anti-GM-CSF, anti-CCL5, PeproTech, produced in rabbit); anti-NF- κ B p65/Thermo Fisher-Invitrogen, Waltham, United States, produced in rabbit/, GFAP/Synaptic Systems, Göttingen, Germany, produced in mouse/) overnight at 4°C. The following day the cells were incubated with the appropriate secondary antibodies (120 min. RT). Finally, the cell nuclei were stained with DAPI. Immunofluorescent images were acquired by an Olympus FV3000 confocal microscope with a 60 \times oil-immersion lens (NA: 1.4). Single 1- μ m-thick optical sections were scanned from the cell cultures, the confocal settings (laser power, confocal aperture and gain) were identical for all methods. The scanned images were processed by Adobe Photoshop CS5 software.

Fluorescent Double Immunostaining of Spinal Cord Sections

Non-treated C57BL/6 mice ($n = 3$) and CFA-treated mice on post-injection day 1 ($n = 3$) and on post-injection day 4 ($n = 3$) were deeply anesthetized with sodium pentobarbital intraperitoneally (50 mg / kg.) and transcardially perfused with Tyrod's solution (oxygenated with a mixture of 95% O₂, 5% CO₂), followed by a fixative (4% paraformaldehyde dissolved in 0.1 M phosphate buffer/PB, pH 7.4/). After transcardial fixation the lumbar segments of the spinal cord were removed and placed into the same fixative for an additional 4–5 h, and immersed in 10 and 20% sucrose dissolved in 0.1 M PB until they sank. In order to aid reagent penetration the spinal cord was freeze-thawed in liquid nitrogen. After cryoprotection tissue pieces were embedded into agarose, and the L4–L5 segments of the spinal cords were sectioned at 50 μ m on a vibratome, followed by extensive washing in 0.1 M PB.

In order to study the co-localization of GFAP with the cytokine markers double immunolabelings were performed. Before staining with the primary antibodies tissue sections were kept in 10% normal donkey serum (Vector Labs) for 50 min. Free-floating sections were then incubated with a mixture of antibodies that contained (a) GFAP (diluted 1: 2000, Synaptic Systems, produced in mouse) and one of the following antibodies: (b) anti-IL-6 (1:500, Peprotech, produced in rabbit), (c) anti-GM-CSF (1:500, Peprotech, produced in rabbit), (d) anti-CCL5 (1:500, Peprotech, produced in rabbit). The sections were kept in the

primary antibody mixtures at 4°C for 2 days and then they were placed into the solution of secondary antibodies for 2 h (goat anti-mouse IgG conjugated with Alexa Fluor 488/diluted 1:2000, Invitrogen/and goat-anti-rabbit IgG conjugated with Alexa Fluor 555/diluted 1:2000, Invitrogen/). Finally, sections were mounted on glass slides and covered with Vectashield mounting medium (Vector Labs).

Single 1- μ m-thick optical sections were scanned with an Olympus FV3000 confocal microscope. Scannings were performed with a 10 \times objective lens (NA: 0.4). All the setting (laser power, confocal aperture) were the same for all scans. Images obtained from three non-treated, and six CFA-injected animals (3 on post-injection day 1 and 4, respectively) were processed with Adobe Photoshop CS5 software. By filtering the background staining, basal threshold values were set for both GFAP and the other markers.

Quantitative Analysis of the Spinal Cord Sections

The confocal fluorescent z-stack sections of spinal dorsal horn specimen were captured with 60 \times oil-immersion lens (NA: 1.4) of an Olympus FV3000 confocal laser microscope. All confocal settings were adjusted with the same parameters (confocal aperture, laser aperture- and intensity). The obtained image stacks were further analyzed with IMARIS software (Bitplane), which evaluated the co-localization data between the immunoreactive spots of IL-6, GM-CSF, CCL5 cytokines and the GFAP labeled astrocyte profiles rendered by the algorithm based on the staining in a standard way. The co-localization was validated if the detected spots and astrocyte surfaces were within the distance of 0.3 μ m from each other. The analysis was carried out on five randomly selected images at each marker taken from control and treated superficial spinal dorsal horn sections of day 1 and 4 following CFA injection, respectively. The co-localization numbers for each cytokine and time point were averaged and standard error of means were calculated. Statistical differences between groups was analyzed by the Kruskal-Wallis statistical probe followed by Mann-Whitney pairwise comparison.

Cell Treatment and Western Blotting

10–12-day-old astrocyte cultures were stimulated with different concentrations of IL-1 β (ranging between 0.1 and 100 pg/ml) for variable durations (between 2 and 24 h). For NF- κ B inhibition the cultures were treated with BAY-11-7082 for 4 h together with 10 ng/ml IL-1 β in PBS. The SN50 peptide was used as a pretreatment for 1 h which was followed by 4, 8 or 16 h of IL-1 β application. After the treatments the culture supernatants were removed and the proteins of 200 μ l of supernatant was precipitated with two-times amount of ice cold acetone. The precipitated proteins were separated by centrifugation (10 min, 3000 rpm 4°C). Cells attaching the culture plates were lysed and cytosol and nuclear fractions were separated as it has been already described. Supernatants and cytosol/nuclear fractions were kept in aliquots at –70°C until they are used for western blotting.

Briefly, the supernatants or cellular fractions were mixed with reducing sample buffer (1:1 ratio) and run on 12%

SDS-polyacrylamide gels. The separated proteins were electroblotted onto PVDF membranes. After blocking the unspecific labeling with 10% BSA solution, the membranes were treated with anti-primary antibody (anti-IL-6, anti-GM-CSF, anti-CCL5/Peptotech, produced in rabbit/; anti-p50, anti-ikB/Santa Cruz, produced in mouse/; anti-p65/Invitrogen, produced in mouse/GFAP/Synaptic Systems, produced in mouse/) followed by incubation with the corresponding goat-anti-rabbit-HRP or goat-anti-mouse-HRP (DAKO, Glostrup, Denmark) secondary antibody. Finally, the labeled bands were visualized by 3, 3'-diaminobenzidine.

Enzyme Linked Immunosorbent Assay (ELISA)

ELISA was performed as already described (Holló et al., 2000). Briefly, (after titration in increasing dilutions) the astrocyte culture supernatants were diluted in 1:1 ratio by ELISA coating buffer (15 mM Na₂CO₃, 35 mM NaHCO₃, pH 9.6) and used for coating of 96 well polystyrol ELISA plates (Maxisorp, NUNC Intermed, Copenhagen, Denmark). Free binding capacity of the wells was blocked by 1% gelatin (Reanal, Budapest, Hungary) in PBS. After washing with PBS anti-IL-6, anti-GM-CSF or anti-CCL-5 primary antibodies were added (1:1000, 2 h, 37°C), followed by goat-anti-rabbit-HRP secondary antibody (1:500, DAKO). Color reaction was developed by o-phenylenediamine and the optical density was measured at λ = 492 nm by ELISA plate reader (Titertek, Uniscan). Graphs represent results of three independent experiments.

Antibody Controls

The cytokine antibody specificity was tested on control spinal cord sections by antibody depletion as it has been described earlier (Holló et al., 2017). Briefly, the diluted anti-IL-6, anti-GM-CSF, anti-CCL5 antibodies were mixed with recombinant murine IL-6, GM-CSF and CCL5 peptides (PeproTech), respectively. The mixtures and also diluted primary antibodies alone, were incubated at 4°C for 18 h and then centrifuged (4°C, 30,000g, 30 min). Thereafter the spinal cord sections were treated with one of the cytokine antibodies or with one of the pre-incubated mixtures for 48 h at 4°C, then placed into biotinylated goat anti-rabbit IgG dissolved in TPBS (diluted 1:200, Vector Labs, Burlingame, United States) for 4 h at room temperature. The color reactions were developed by 3,3'-diaminobenzidine. Photomicrographs were taken by Olympus CX-31 epifluorescent microscope with fixed settings. The pre-adsorption of cytokine antibodies with the appropriate cytokine proteins abolished the specific immunostaining (**Supplementary Material**).

RESULTS

Mechanical Pain Sensitivity of C57/BL6 Mice During the Course of CFA-Induced Inflammatory Pain

The mechanical withdrawal threshold (MWT) was very similar in all animals before CFA injection (4.91 ± 0.039 g).

On the treated, right (ipsi-lateral) hind paw, the CFA-treatment induced a highly significant increase in pain sensitivity on the first experimental day, MWT dropped to 2.96 ± 0.052 g ($p = 0.000101$). The reduction of the MWT values continued until day 3 and 4 when MWT values decreased to 2.03 ± 0.117 and 1.99 ± 0.065 g, respectively. There was no statistically significant difference between MWT values on day 3 and day 4. We followed the measurement for an additional day and we found that on day 5 the nociceptive sensitivity significantly attenuated ($p = 0.000381$), MWT values reached 2.43 ± 0.118 g. However, this significant change was not observed on the left (contra-lateral) side and the MWT levels were stable through the course of the experiment (Figure 1A).

According to other authors (Hylden et al., 1989; Pitzer et al., 2016) the drop in MWT values peaks on the third day after CFA administration, which is in accord with our observations.

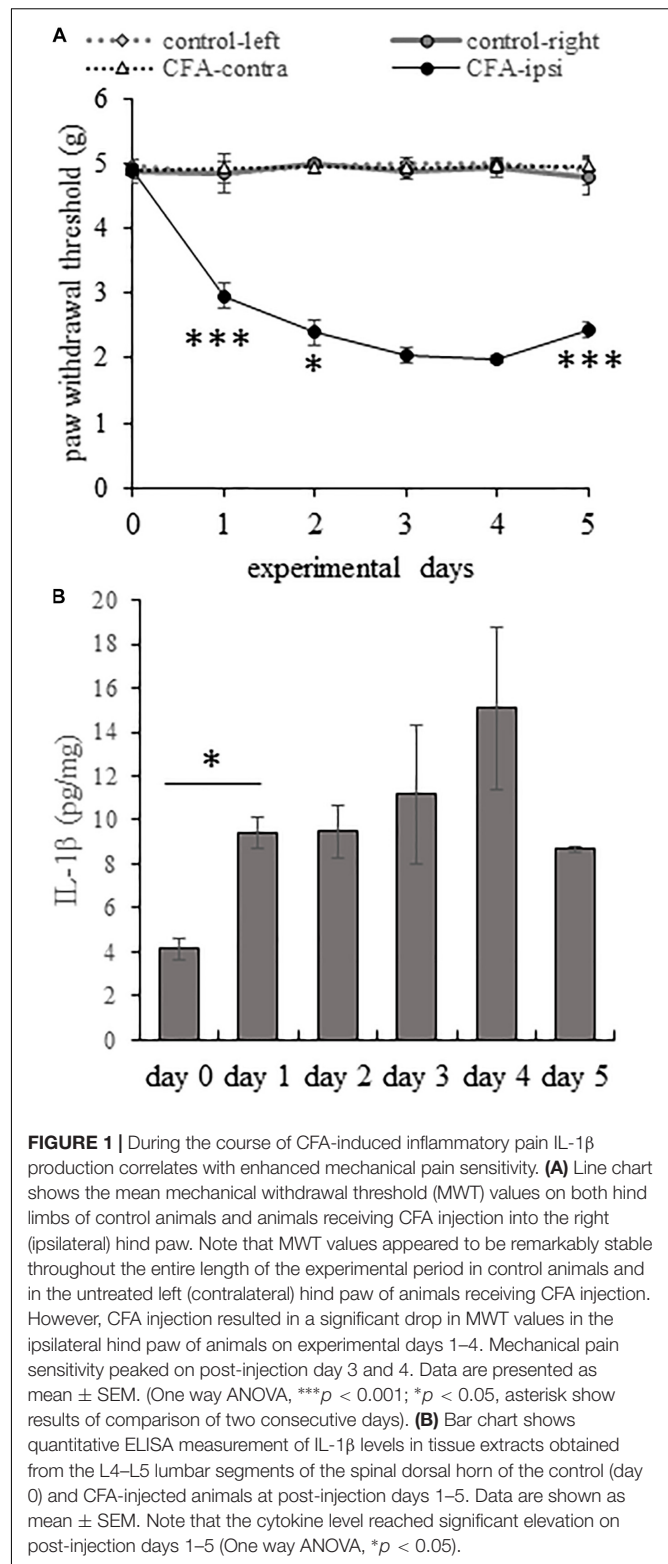
Peripheral Inflammation Evoked by CFA Injection Induced Elevation of Spinal IL-1 β Expression

Although the expression of IL-1 β has already been demonstrated in the spinal cord (Raghavendra et al., 2004; Liu et al., 2008), there has been no data in the literature to follow the time dependent changes in the expression of the cytokine in inflammatory pain. Thus, we intended to explore how the expression of IL-1 β changes in CFA-induced inflammatory pain at the protein level (Figure 1B) in the spinal dorsal horn tissue extract of the L4–L5 spinal segments, which is known to receive primary afferent inputs from the plantar surface of the hind paw (Molander and Grant, 1985).

Measuring the quantity of IL-1 β protein with the quantitative ELISA method we found that CFA-evoked plantar inflammation induced a significant elevation in the expression of IL-1 β . The basal level of the cytokine was 4.15 ± 0.43 pg/mg in the spinal dorsal horn tissue extract of the L4–L5 spinal segments which significantly ($p = 0.049$) increased to 9.43 ± 0.73 pg/mg on experimental day 1, correlating the significant drop of MWT measured on the ipsi-lateral hindpaw of the CFA injected animals on the same day. Highest cytokine level was measured on day 4 (15.08 ± 3.66 pg/mg) corresponding the highest mechanical pain sensitivity. We followed the cytokine level for an additional day and observed that on day 5 of the experiment the IL-1 β concentration dropped to 8.69 ± 0.12 pg/mg. Our earlier experiments showed that the mechanical pain sensitivity gradually attenuates after day 5 and finally returns to the basal level on post-injection day 11 (Holló et al., 2017).

We found in the literature only one paper where the IL-1 β content of spinal cord is given to the weight of the tissue. Wang et al. (1997) found lower level of the cytokine in the control rat spinal cord. This difference can be due several reasons e.g., species differences between rats and mice, or due to the different sample collection as they used the entire spinal cord for the measurement while we extracted only the dorsal horn tissue.

Significant changes in the nociceptive behavior and robust elevation of the IL-1 β production in the spinal cord suggest that



the first 24 h is a very critical period during the course of the CFA-evoked pain. Thus, in the further experiments we detected the activation and cytokine/chemokine secretion of spinal astrocyte cultures in this period.

Cultured Spinal Astrocytes Express the Ligand Binding Unit of the IL-1 Receptor (IL-1R1) and They Are Activated by IL-1 β in a Concentration-Dependent Way

Astrocytic activation is increasingly accepted as a factor which contributes to chronic pain states through its contribution to central sensitization. Thus we wanted to investigate astrocytic activation using IL-1 β as a stimulating agent which is upregulated in the spinal cord during inflammatory pain and its upregulation correlates with the nociceptive sensitivity during the course of CFA-evoked pain.

Although we and others (Wang et al., 2006; Holló et al., 2017) already showed that the spinal astrocytes express IL-1R1, we confirmed its expression on the cultured astrocytes (Figure 2A).

As a next step, cell activity (MTT) assay was performed to identify the lowest IL-1 β concentration which is suitable to increase astrocytic activity significantly. We used serial dilutions (1–100 ng/ml) of the recombinant IL-1 β protein and found that 24 h stimulation with 10 ng/ml of the protein increased significantly the cellular activity to $167 \pm 12.23\%$ ($p = 0.02815$) of the control level (Figure 2B). Thus, we used this concentration of the cytokine in the further stimulation experiments. As a negative control, we also tested the IL-1 β responsiveness of spinal astrocyte cultures isolated from IL-1R1 knock-out mice and

we found no significant upregulation of mitochondrial activity (data not shown).

Spinal Astrocytic Secretome Profile Reveals IL-1 β -Induced Overexpression of 3 Cytokines and Chemokines Out of the 24 Produced by Non-treated Astrocyte Cultures

We detected the secretion of 24 cytokines/chemokines in the supernatant of spinal astrocyte cultures out of the 40 molecules included into the assay (Figure 3A). When comparing the cytokine levels in culture supernatants obtained from control and IL-1 β -treated spinal astrocytes, we observed the production of the same cytokines/chemokines, we have not detected any newly synthesized molecules. We, however, found significant upregulation of three molecules: CCL5 (RANTES), GM-CSF, IL-6. Highest, approximately seven fold change was measured for the production of CCL5 (RANTES), which was also highly significant ($p = 0.0002$) if compared with the control level of the chemokine. GM-CSF levels exceeded approximately four fold ($p = 0.0025$) and IL-6 levels approximately 2 fold ($p = 0.0022$) the control levels of the cytokines, respectively (Figure 3B).

We followed the time-dependent changes of the three chemokine/cytokine levels during the critical 24 h as we observed in the spinal cord the significant enhancement of IL-1 β secretion

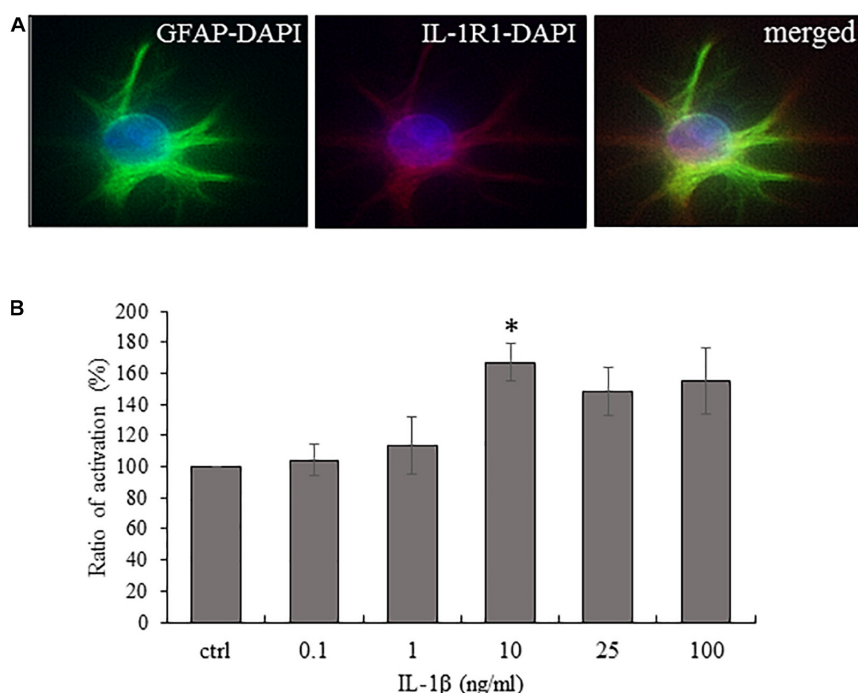


FIGURE 2 | Cultured spinal astrocytes express IL-1R1 and their activity is significantly increased upon IL-1 β stimulation. **(A)** Cultured spinal astrocytes express the ligand binding unit or IL-1 receptor (IL-1R1). Micrographs of fluorescent images illustrating co-localization between GFAP astrocytic marker (a,c; green) and IL-1R1 (b,c; red). Panel a–c represent control cultures. Mixed colors (yellow) on the superimposed image (c) indicate double labeled structures. On all images DAPI was used to label cell nuclei (blue). **(B)** Dose-dependent (1–100 ng/ml) enhancement of astrocytic activity by IL-1 β was determined by MTT assay after 24 h of treatment. Quantification of MTT activity is presented as fold change over the control cells in percentage. Data are shown as mean \pm SEM of three independent experiments in duplicate assay (ANOVA Repeated Measures, followed by Tukey's pairwise comparison * $p < 0.05$ versus control group).

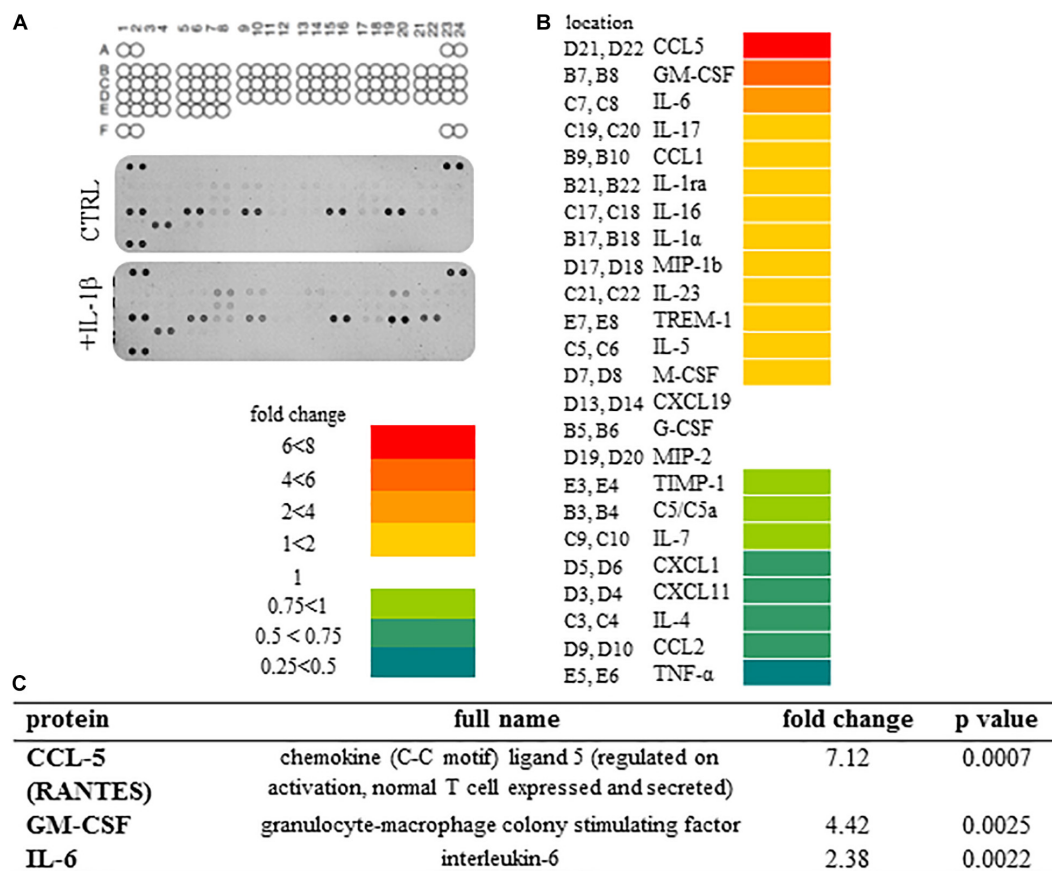


FIGURE 3 | Secretome profile of IL-1 β treated spinal astrocytes reveals the expression of 24 cytokines and chemokines. **(A)** Coordinates of cytokines on array membranes and developed membranes. The Proteome Profiler array used in the experiments allowed the detection of 40 cytokines, chemokines and other soluble factors. Upper panel shows array coordinates. Middle panel shows expression of cytokines/chemokines in the supernatant of unstimulated spinal astrocytes, and lower panel shows expression of cytokines/chemokines by IL-1 β stimulated astrocytes. **(B)** Heat map analysis of spinal astrocytic cytokine profile after 24 h of IL-1 β stimulus. Left column shows array coordinates of cytokines/chemokines in the middle column and right column shows the fold change of their amount. **(C)** List of cytokines/chemokines which are significantly overexpressed in the supernatant of spinal astrocyte cultures upon IL-1 β stimulation.

during this period. The time-course experiments showed slightly different secretion pattern of the three molecules. Early activation of CCL5 secretion, was observed even after 2 h of IL-1 β treatment it considerably elevated level ($179.0 \pm 2.59\%$) and it reached its peak after 8 h of stimulation ($253.4 \pm 0.5.6\%$, $p = 0.006272$). While the IL-6 and GM-CSF activation was slower, increased gradually until the end-point of the experiment. At this time the two cytokine levels were significantly elevated if compared with the control level (IL-6: $189.5 \pm 1.74\%$, $p = 0.002369$; GM-CSF: $219.3 \pm 2.35\%$, $p = 0.000209$), in accordance with the Protein Profiler data (Figure 4A).

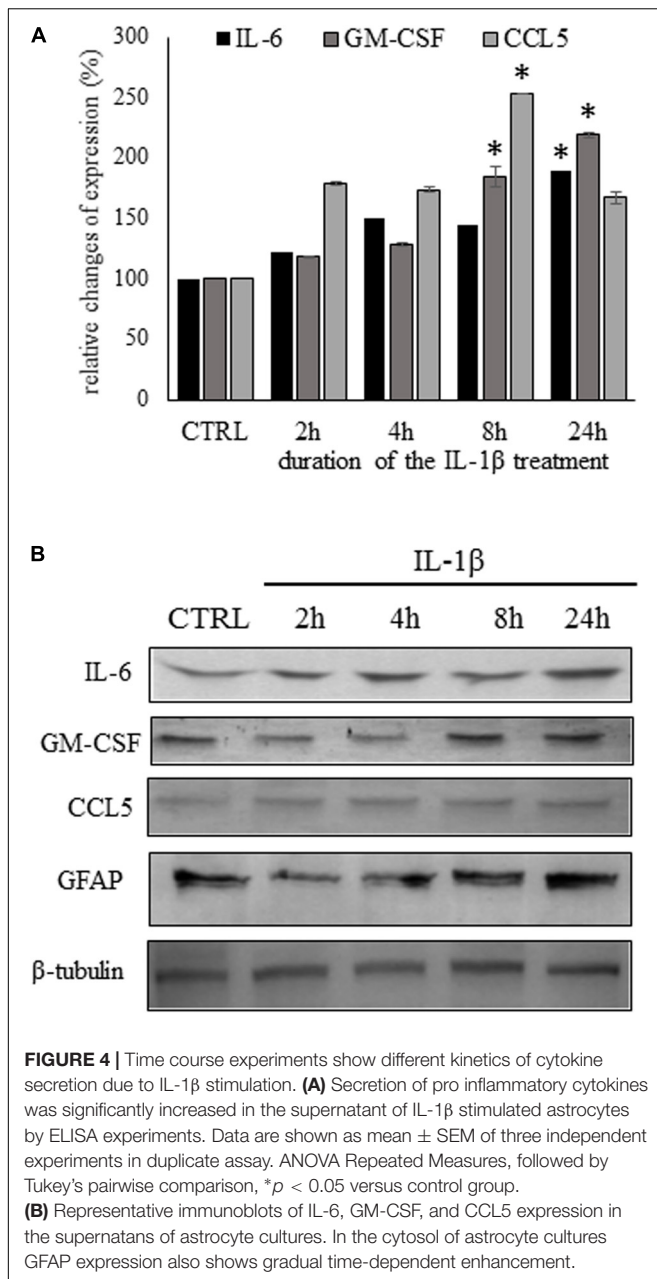
We also carried out western blot analysis from the supernatants of the control and IL-1 β -stimulated cultures for the detection of the three significantly upregulated cytokines. We observed immunoreactive bands at the expected molecular weight of each cytokine/chemokine. The changes in cytokine levels, observed on the western blots, were comparable of the data received by the ELISA experiments. In the cell lysates of the cultures IL-1 β -induced gradual increase of GFAP expression, similarly as it has been described previously

by other authors (Liddelow et al., 2017; Yang et al., 2019; Figure 4B).

To further demonstrate the astrocytic expression of the cytokines, we also performed double immunostainings on control astrocytes and on cultures which received 24 h of IL-1 β -treatment. The 1 μ m thick optical images showed co-localization of the three cytokines/chemokines with the GFAP marker in the control cultures and enhanced expression of the cytokines and GFAP in the IL-1 β -stimulated astrocytes (Figure 5).

Spinal Expression of IL-6, GM-CSF and CCL5 Is Increased During the Course of CFA-Evoked Inflammatory Pain

To determine if the three selected cytokines were also overexpressed in the spinal dorsal horn upon peripheral CFA-injection, spinal cord sections were prepared from the L4–L5 segments which receive primary afferent fibers from the hindpaws. In control sections low levels of cytokines were



detected which was mostly restricted to the superficial laminae (corresponding to Rexed laminae I and II, **Figures 6.1–6.3, 6.10–6.12, 6.19–6.21**). To follow the time-dependent changes of the selected cytokines during the course of the pain model we obtained confocal images from the initial phase of the model (post-injection day 1) and at the time of highest mechanical sensitivity (post-injection day 4). Interestingly, in case of IL-6 and GM-CSF we could observe considerable elevation of cytokine expression on both sides of the spinal cord, on the first post-injection day. The intensity of the immunoreactivity was increased further on post-injection day 4 and was more pronounced on the ipsi-lateral (right) side (**Figures 6.4–6.9, 6.13–6.18**). The CCL5 chemokine showed different time course:

on the first post-injection day just a moderate enhancement of the CCL5 + signal was visible (**Figures 6.22–6.24**), and it was only on post-injection day 4 (**Figures 6.25–6.27**) when the pronounced elevation of the chemokine was detected in the superficial layers of the ipsi-lateral (right side) spinal dorsal horn.

Quantitative Analysis of Spinal IL-6, GM-CSF and CCL5 Expression and Co-localization With GFAP Marker During the Course of CFA-Induced Pain Model

IMARIS software analysis shows that peripheral CFA injection significantly enhanced the number of IL-6, GM-CSF and CCL5 immunoreactive spots on experimental day 1 and 4 in spinal dorsal horn. Changes in the absolute numbers of immunoreactive puncta (**Figures 7A–C**) was in all cases highly significant ($p < 0.001$). Similarly, the number of co-localized cytokine spots on astrocytes was found to be significantly higher in the CFA-treated animals compared to control animals (**Figures 7D–F**). The co-localization between GFAP and IL-6, GM-CSF and CCL5 was quite similar in control conditions ($6.25 \pm 1.03\%$, $5.04 \pm 0.64\%$, and $6.79 \pm 0.48\%$, respectively). However, after the CFA-treatment the ratio of co-localization was highest between IL-6 cytokine and GFAP marker both on day 1 ($11.65 \pm 1.33\%$, $p = 0.00085$) and on day 4 ($21.10 \pm 1.21\%$, $p = 0.00019$). The enhancement in co-localization values for the other two cytokines were more moderate, but still significant. On experimental day one the co-localization with GFAP profiles increased to $7.33 \pm 0.69\%$ ($p = 0.002$) in case of GM-CSF and to $8.93 \pm 0.77\%$ ($p = 0.012$) in case of CCL5. The co-localization values for the latter two cytokines significantly elevated further on experimental day 4 (GM-CSF: $14.57 \pm 0.064\%$, $p = 0.00019$; CCL5: $17.53 \pm 1.26\%$, $p = 0.00012$).

We also demonstrated on high magnification confocal images the co-localization between the three studied cytokines and the GFAP+ astrocytic profiles (**Figures 7G 1–9**).

IL-1 β Activates the NF- κ B Pathway in Spinal Astrocytes

IL-1 β signaling is associated with the NF- κ B and MAPK pathways (Medzhitov, 2001). As astrocyte-specific activation of the NF- κ B pathway upon IL-1 β stimulation has already been reported by Srinivasan et al. (2004) in the hippocampus, we intended to explore the role of the pathway in the spinal astrocyte cultures.

To reveal the effect of IL-1 β on the NF- κ B signaling we studied several members of the pathway in the astrocyte cell lysates (Oeckinghaus et al., 2011). We detected the cytosolic and nuclear levels of the p65 (RelA) and the inhibitory κ B. When following the time course of these IL-1 β -induced NF- κ B activation we found the elevation of the NF- κ B p65 protein in the cytosol of astrocytes within 2 h. The translocation of p65 protein to the nucleus occurred after 4 h of stimulation and it was paralleled by the decrease of the inhibitory κ B unit in the cytosol (**Figure 8A**). The nuclear translocation of the p65

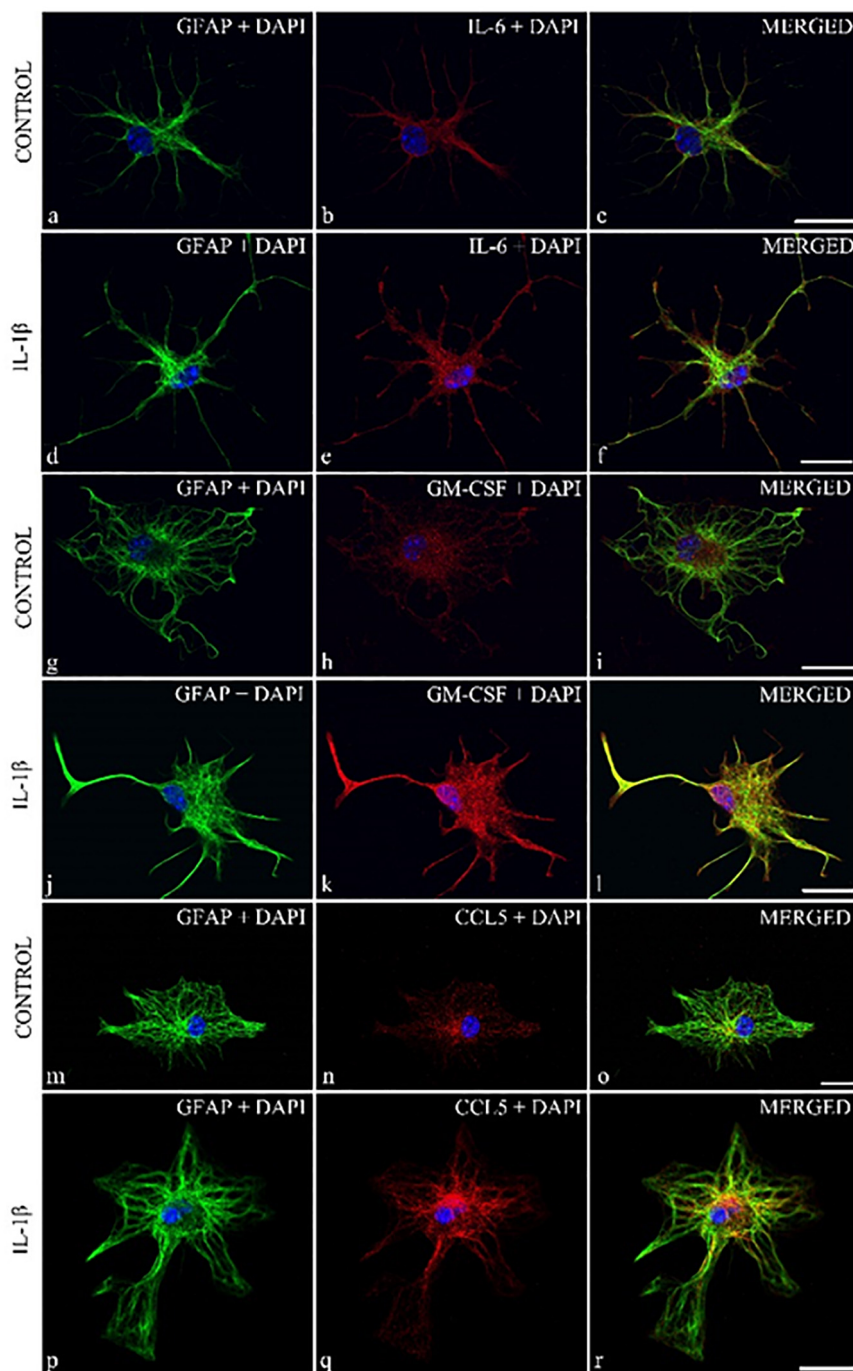


FIGURE 5 | Localization of cytokines in cytoplasmic compartment of GFAP + spinal astrocyte cultures: enhanced cytokine expression was observed in IL-1 β stimulated spinal astrocytes. Micrographs of single 1 μ m thick laser scanning confocal optical sections illustrating co-localization between GFAP astrocytic marker (green) and IL-6, GM-CSF, CCL5 cytokines (red). Panels (a–c, g, h, l–n) represent control, while (d–f, i–k, o–q) show cultures which received 24 h of IL-1 β treatment. Mixed colors (yellow) on the superimposed images (c, f, h, k, n, r) indicate double labeled structures. On all images DAPI was used to label cell nuclei (blue). Scale bar 10 μ m.

protein was also demonstrated by immunohistological staining of astrocyte cultures, which showed the presence of the protein after 2 h of IL-1 β stimulation (Figures 8B e–h) and increased further

after 2 additional hours of treatment (Figure 8Bi–l). These data demonstrate the IL-1 β -induced activation of the NF- κ B pathway in the spinal astrocytes.

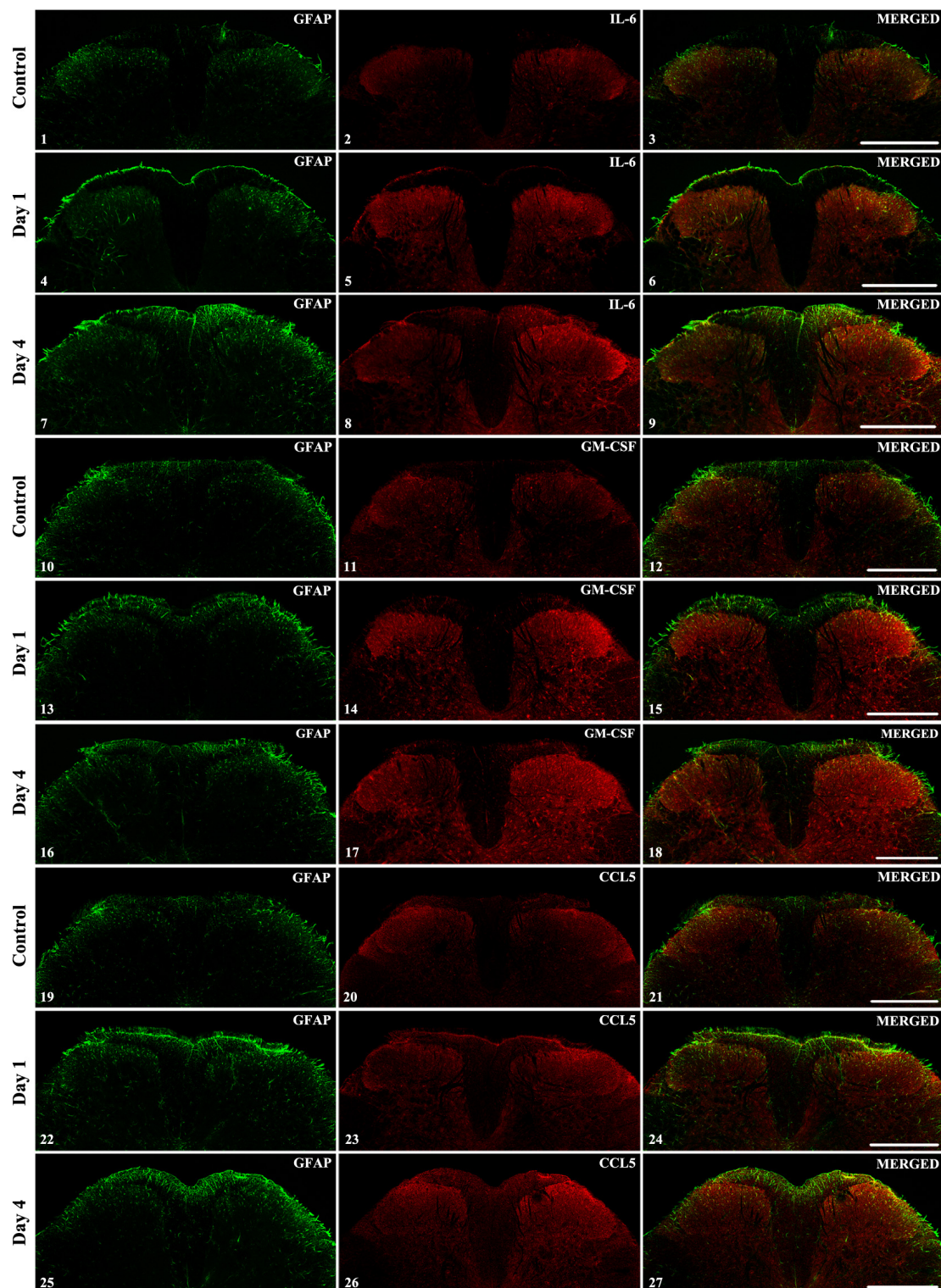


FIGURE 6 | The spinal expression of IL-6, GM-CSF, and CCL5 cytokines during the course of CFA-evoked pain. Representative 1 μ m thick confocal images illustrating the co-localization between immunolabeling for IL-6 (red; 6.2, 6.5, 6.8), GM-CSF (red; 6.11, 6.14, 6.17) CCL5 (red; 6.20, 6.23, 6.26) and the immunoreactivity of astrocytes (GFAP, green; first column of the figures) in the superficial spinal dorsal horn. Mixed colors (yellow) on the superimposed images (last column of the figures) indicate double-labeled structures. For each cytokine the first row of the images are taken from control samples, whereas the second row of images represents the first day after CFA injection and the third row shows the spinal expression of the cytokines on post-injection day 4. Increased labeling of the cytokines was apparent on the ipsi-lateral (right side) of the spinal cords on post-injection day 4 (panels 6.8, 6.17, and 6.26). In each case scale bars: 500 μ m.

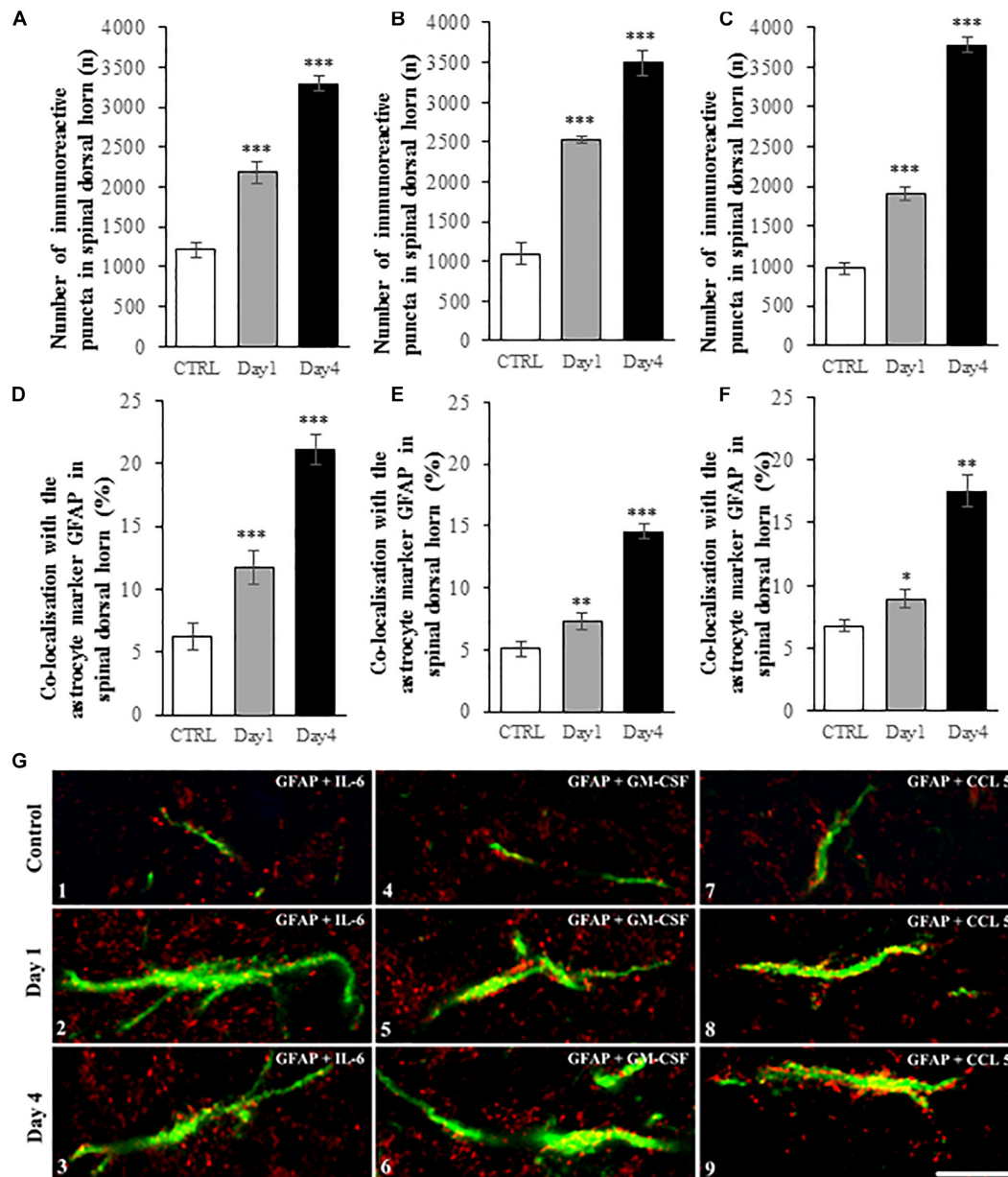


FIGURE 7 | IMARIS analysis of spinal cord sections show enhanced expression IL-6, GM-CSF, and CCL5 and increased co-localization of the cytokines with GFAP astrocyte marker during the course of CFA-evoked inflammatory pain. **(A–C)** Histograms show significant elevation of IL-6 **(A)**, GM-CSF **(B)** and CCL5 **(C)** immunoreactive puncta in spinal dorsal horn on post-injection days 1 and 4. Data are shown as mean \pm SEM of five randomly selected spinal cord specimen (ANOVA, followed by Tukey's pairwise comparison $***p < 0.001$ versus control group). **(D–F)** Bar charts represent the ratio of co-localization between the IL-6 **(D)**, GM-CSF **(E)** and CCL5 **(F)** cytokine and GFAP in control and treated (on post-injection day 1 and 4) spinal cord specimen. Data are shown as mean \pm SEM of five randomly selected spinal cord specimen. (Kruskal-Wallis statistical probe, followed by Mann-Whitney pairwise comparison $*p < 0.05$, $**p < 0.01$, $***p < 0.001$ versus control group). **(G)** Representative high magnification superimposed confocal images of GFAP + astrocyte profiles (green) and IL-6 (red, G.1–3), GM-CSF (red, G.4–6) and CCL5 (red, G.7–9) immunoreactive puncta. First row of images (G.1, G.4, G.7) represents control specimen. Second (G.2, G.5, G.8) and third (G.3, G.6, G.9) rows show specimen on post-injection day 1 and 4, respectively. Mixed color (yellow) indicates co-localization of the markers. Scale bar: 10 μ m.

IL-1 β -Induced IL-6 Secretion Is Significantly Suppressed by the NF- κ B Inhibitor BAY 11-7082

To confirm the role to NF- κ B activation in the IL-1 β induced cytokine/chemokine secretion we utilized the NF- κ B inhibitor

BAY 11-7082, which is an irreversible inhibitor of $\text{I}\kappa\text{B}-\alpha$ phosphorylation resulting in the inactivation of NF- κ B pathway (Pierce et al., 1997; Phulwani et al., 2008). As in the previous experiments we detected the nuclear translocation of the p50 protein after this time period, the cultures were treated for 4 h

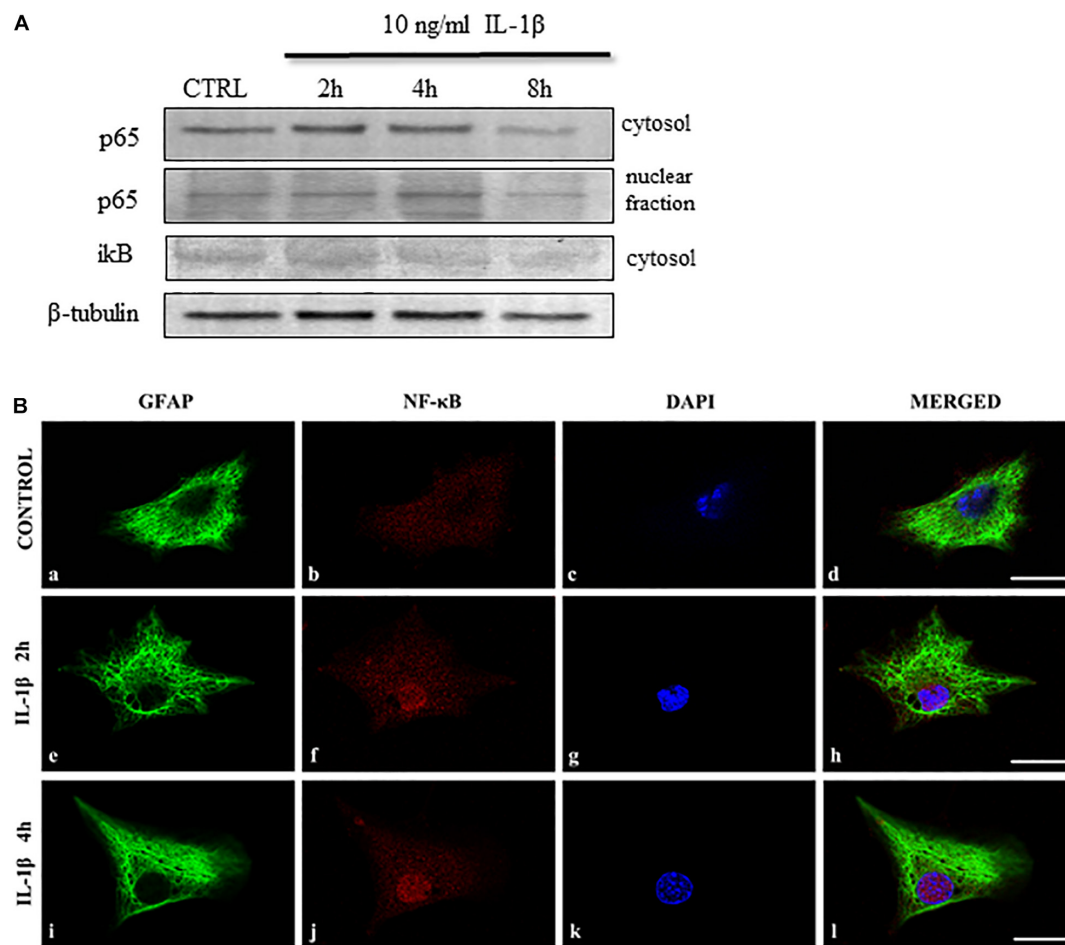


FIGURE 8 | IL-1 β activates the NF- κ B signaling pathway in spinal astrocyte cultures. **(A)** Representative immunoblots show time-dependent changes of the NF- κ B signaling pathway upon IL-1 β stimulation of spinal astrocyte cultures. NF- κ B p65 expression increase after 2 h of stimulation in the cytosol and the p65 protein appears in the nuclear fraction after 2 h of treatment. The inhibitory ikB unit is downregulated in the cytosol of the cultures upon 4 h of stimulation. **(B)** Micrographs of single 1 μ m thick laser scanning confocal optical sections illustrating cytoplasmic expression [GFAP astrocytic marker (green)] of p65 protein in control cultures (panels **a–d**). The nuclear translocation of the p65 protein was observed after 2 (panels **e–h**) and 4 h (panels **i–l**) of IL-1 β treatment. On all images DAPI was used to label cell nuclei (blue). Mixed color (purple) on the superimposed images (**d,h,l**) indicate double labeled structures. Scale bars: 10 μ m.

with IL-1 β and different concentrations (ranging between 1 and 10 μ M) of the NF- κ B inhibitor. To validate the experimental system we confirmed that the inhibitor blocks the activation of NF- κ B and we observed decrease in the cytosolic p50 and nuclear p65 proteins upon treatment with the inhibitor (**Figure 9A**). When measuring the cytokine levels in the supernatant of the cultures we observed decreased concentrations in the BAY 11-7082-treated culture supernatants, but it reached significant level only in case of IL-6 production ($67.3 \pm 8.6\%$, $p = 0.009$) (**Figure 9B**).

IL-1 β -Induced IL-6, GM-CSF, CCL5 Secretion Is Significantly Suppressed by the NF- κ B Inhibitor SN50 at Different Time Points

As a second approach to influence NF- κ B signaling we used the SN50 peptide, which is a cell permeable inhibitor of NF- κ B

nuclear translocation (Lin et al., 1995). Its specificity for the NF- κ B pathway is confirmed in lower concentration (Boothby, 2001), thus we used the SN50 peptide for 1 h pre-treatment of the astrocyte cultures in 5 and 10 μ M concentrations, which was followed by 4, 8 or 16 h of IL- β stimulation. We could detect significant attenuation of the GM-CSF expression of the SN50 pre-treated cultures after 8 h of IL-1 β treatment if compared to the IL-1 β -treated cultures. The relative GM-CSF expression values of the IL- β -treated cultures was $141.5 \pm 16.21\%$ which dropped to $94.14 \pm 1.22\%$; ($p = 0.02$) upon 5 μ M SN50 pre-treatment (**Figure 10A**). For IL-6 and CCL5 the significant reduction of the cytokine levels was observed after 16 h of stimulation (**Figure 10B**). The IL- β -induced relative expression of IL-6 and CCL5 was $112.78 \pm 3.77\%$ and $120.24 \pm 2.38\%$, respectively. These levels were significantly reduced due to 1 h pre-treatment with 10 μ M SN50 (for IL-6 $83.22 \pm 3.57\%$; $p = 0.002$ and for CCL5 $106.16 \pm 6.03\%$; $p = 0.043$).

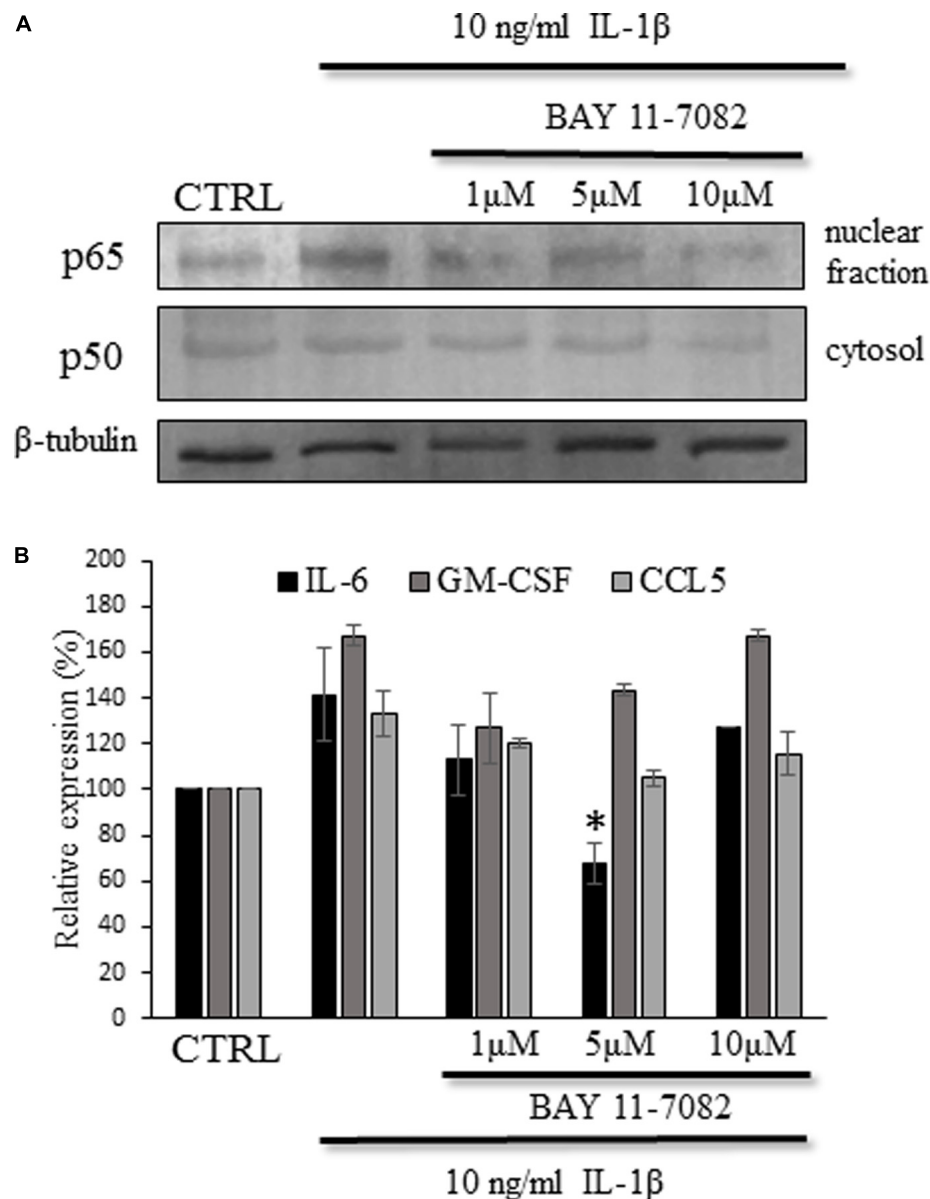


FIGURE 9 | IL-6 expression was attenuated by the BAY 11-7082 inhibitor of the NF- κ B signaling pathway. **(A)** Representative immunoblot show decreased p65 expression in the nuclear fraction upon BAY 11-7082 treatment. **(B)** Histogram shows cytokine levels determined by ELISA method. The IL-6 production of the astrocyte cultures is significantly attenuated. Data are shown as mean \pm SEM of three independent experiments in duplicate. One-way ANOVA, followed by Student-Newman-Keuls pairwise comparison, * $p < 0.05$.

DISCUSSION

In summary, we found correlation of spinal dorsal horn IL-1 β expression with the nociceptive behavior during the course of CFA-evoked inflammatory pain. We show that the stimulation of spinal astrocyte cultures by IL-1 β results in significantly enhanced secretion of three inflammatory cytokines/chemokines: IL-6, GM-CSF and CCL5 (RANTES). The overexpression of the three selected cytokines was also confirmed in the spinal dorsal horn during the CFA-induced pain model. We studied the activation of the NF- κ B signaling pathway which is associated

with astrocyte-specific IL-1 β signaling and we found its time-dependent activation during the course of IL-1 β treatment. Finally, the inhibition of the NF- κ B pathway resulted in the significant attenuation of cytokine production.

IL-1 β exerts its action through its receptor which has a ligand binding unit (IL-1R1) and an accessory protein responsible for the signal transduction (IL-1RAcP) (Ren and Torres, 2009). The IL-1R1 was shown to be expressed by neurons and glial cells in the CNS. However, the ligand binding induce cell type specific responses, which is aided by the neuron-specific isoform of the IL-1RAcPb (Huang et al., 2011).

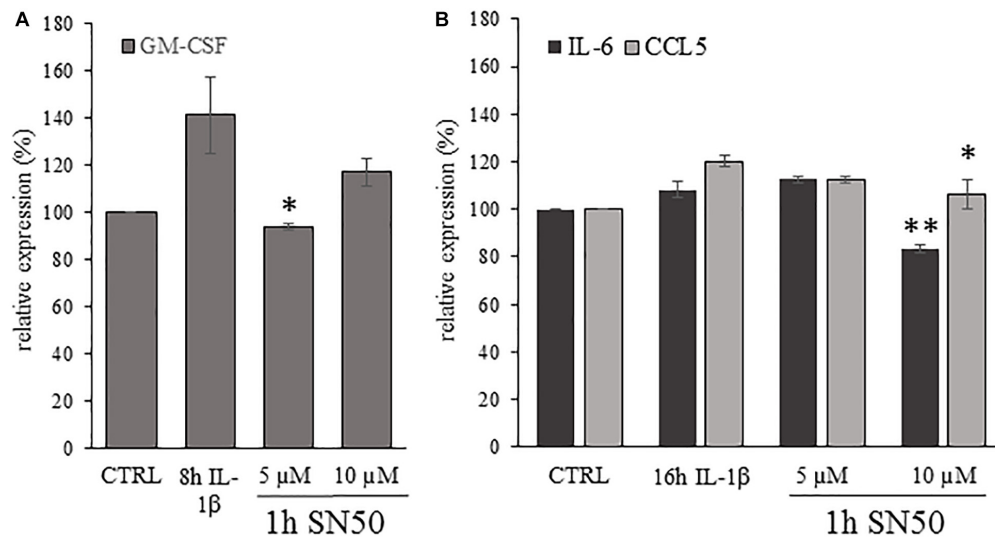


FIGURE 10 | Astrocytic cytokine expression was significantly reduced by SN50, inhibitor of NF- κ B nuclear translocation. **(A)** Histogram shows relative GM-CSF levels determined by ELISA method after 1 h of pre-treatment by SN50 and 8 h of IL-1 β stimulation. The GM-CSF secretion of the astrocyte cultures is significantly down regulated by 5 μ M SN50 if compared with the IL-1 β -treated cultures. **(B)** Histogram shows relative IL-6 and CCL5 levels in the supernatant of the astrocyte cultures measured by ELISA method after 1 h of SN50 pre-treatment and 16 h of IL-1 β stimulation. Both cytokine levels show significant reduction due to 10 μ M SN50 treatment if compared with the IL-1 β -treated cultures. Data are shown as mean \pm SEM of two independent experiments in duplicate. One-way ANOVA, followed by Student-Newman-Keuls pairwise comparison, * p < 0.05; ** p < 0.01.

Gruber-Schoffnegger et al. (2013) suggested two possible ways how cytokines can act in the CNS: directly on neurons and indirectly by activating local glial cells to secrete further neuroactive substances which in turn modulate nerve cell functions. In this study our aim was to explore the latter way of cytokine actions by detecting the IL-1 β -induced cytokine/chemokine production in spinal astrocytes.

Astrocytic activation can be induced by numerous agents including lipopolysaccharide (LPS) (Tarassishin et al., 2014), adenosine-triphosphate (ATP) (Adzic et al., 2017), glutamate (Aronica et al., 2005), cytokines etc. Upon different activation signals (or their combinations) astrocytes can turn into neurotoxic A1 or neuroprotective A2 phenotype. While in different pain states A1 astrocytes can release neurotoxins which can trigger the death of neurons and glial cells, A2 astrocytes induce cell survival and tissue regeneration (Li et al., 2019). Recently, however, it was suggested that astrocytic activation is possibly not an all-or-nothing phenomenon, but it is rather “gradated” (Matias et al., 2019). Liddelow et al. (2017) showed that in many cases the reactive astrocyte phenotype is not so polarized. Among others they showed that IL-1 β stimulation induced upregulation of A1 and A2 marker genes. In another study neuroprotective aspects of IL-1 β stimulated astrocytes was also revealed as genes encoding neurotrophic factors were upregulated in the cultures (Teh et al., 2017).

During CNS insults or injury both astrocytes and microglia are activated and their bidirectional communication can be important for their further fates and their possible role in CNS disorders. Microglia usually react faster to pathological stimuli and by their secreted molecules they can contribute to the

consecutive activation of astrocytes (Jha et al., 2019). It was shown that IL-1 β can be one of those microglia-derived factors which can lead to astrocytic activation. On the other hand, although astrocytic activation has a “lag phase,” it is more prolonged - in this way, they can have a role in the maintenance of enhanced pain states (Gao and Ji, 2010).

Interestingly, we found IL-1 β -induced significant upregulation of pro-inflammatory cytokines/chemokines and we did not detect significant downregulation of any anti-inflammatory cytokines. All three identified molecules were shown previously to be expressed in different areas of the CNS.

IL-6 is classically described as a pro-inflammatory cytokine which induce T lymphocyte population expansion and B lymphocyte differentiation, but it is well described now that in a context-dependent way IL-6 may have anti-inflammatory functions as well (Hunter and Jones, 2015). Its ligand binding receptor (mIL-6R) is expressed on very limited cell types (e.g., monocytes/macrophages, microglia). But by an alternative “trans-signaling,” using the soluble IL-6 receptor (sIL-6R), it can exert its effect on many cell types including neurons (Zhou et al., 2016). The role of IL-6 in nervous tissue is “case-sensitive” as it was reported for the immune system: the classical signaling through mIL-6R initiates anti-inflammatory signals whereas the trans-signaling pathway is more pro-inflammatory (Rothaug et al., 2016).

GM-CSF is more known of its hemopoietic function as a colony stimulating factor of the granulocyte-macrophage lineage, but it is also a pro-inflammatory cytokine with numerous functions in innate and adaptive immunity (Donatien et al., 2018). GM-CSF was already shown to play role in tumor-nerve interaction in bone cancer pain (Schweizerhof et al., 2009).

And it was found to initiate central sensitization by inducing microglial BDNF secretion in chronic post ischemic pain (Tang et al., 2018). Besides microglia its receptor (GM-CSFR) is expressed on cortical and hippocampal neurons (Krieger et al., 2012).

The chemokine CCL5 (RANTES), as other members of the chemokine family regulate leukocyte trafficking to sites of inflammation and it is a dominantly pro-inflammatory agents.

CCL5 can bind to three receptors chemokine (C-C motif) receptor 1 (CCR1), CCR3 and CCR5 and is involved in several pain states (Yin et al., 2015). The main receptor, CCR5 is expressed by microglial cells and it induces the alternatively activated M2 phenotype differentiation (Laudati et al., 2017), which is known to inhibit pro-inflammatory signals. In this way, CCL5 may have an anti-inflammatory, anti-nociceptive role when it activates the CCR5 receptor.

The NF- κ B pathway plays crucial role in the astrocyte specific response for IL-1 β stimulation. Besides its important function during inflammation in peripheral tissues, it is also a mediator of cytokine and chemokine secretion by astrocytes. Genes encoding the three selected cytokines were shown earlier to be associated with the NF- κ B signaling pathway in other cell types (Schreck and Bauerle, 1990; Wickremasinghe et al., 2004; Son et al., 2008).

In summary, the three of the selected cytokines/chemokines and also the NF- κ B pathway can all be important target molecules in inflammatory pain conditions. Specific receptors of the three molecules were shown on microglial cells. GM-CSFR is expressed on neurons and for IL-6 *trans*-signaling is available for its neuronal effect. The astrocytic production of these molecules support the theory of the indirect action of IL-1 β , by inducing astrocytic secretion of mediators which can be means of complicated networks of glia-neuron and glia-glia interactions and can contribute to the enhanced activity of the local cellular networks thus can be part of the process of central sensitization. Another interesting feature of this system is, that astrocytes themselves produce IL-1 β and it would be important to understand the consequences of this “autocrine-loop” and possibly influence its functioning to shift astrocytic activation toward the A2 “protective-type” to attenuate the activity of the local cells which may lead to the inhibition of the pro-nociceptive processes.

REFERENCES

- Adzic, M., Stevanovic, I., Josipovic, N., Laketa, D., Lavrnja, I., Bjelobaba, I. M., et al. (2017). Extracellular ATP induces graded reactive response of astrocytes and strengthens their antioxidative defense in vitro. *J. Neurosci. Res.* 95, 1053–1066. doi: 10.1002/jnr.23950
- Aronica, E., Gorter, J. A., Rozemuller, A. J., Yankaya, B., and Troost, D. (2005). Activation of metabotropic glutamate receptor 3 enhances interleukin (IL)-1 β -stimulated release of IL-6 in cultured human astrocytes. *Neuroscience* 130, 927–933. doi: 10.1016/j.neuroscience.2004.10.024
- Boothby, M. (2001). Specificity of sn50 for NF- κ B? *Nat. Immunol.* 2, 471–472. doi: 10.1038/88652
- Calvo, M., Dawes, J. M., and Bennett, D. L. (2012). The role of the immune system in the generation of neuropathic

DATA AVAILABILITY STATEMENT

The raw data supporting the conclusions of this manuscript will be made available by the authors, without undue reservation, to any qualified researcher.

ETHICS STATEMENT

The animal study was reviewed and approved by Animal Care Committee of the University of Debrecen, Hungary according to national laws and European Union regulations [European Communities Council Directive of 24 November 1986 (86/609/EEC)].

AUTHOR CONTRIBUTIONS

KHo designed the experiments, analyzed data and prepared the manuscript. AG and KHe carried out the immunocytochemical stainings on the spinal cord sections. AG, KHe, and EB conducted the behavioral experiments and prepared the astrocyte cultures. LD performed the IMARIS analysis of the sections and reviewed the manuscript. AG photographed the immunostained sections. KHo and EB carried out the Proteome Profiler, ELISA and western blot experiments. All authors read and approved the manuscript.

FUNDING

This work was supported by the Hungarian National Brain Initiative, KTIA_NAP_13-1-2003-0001. This study was also supported by the Neuroscience Ph.D. program of the University of Debrecen, Hungary.

SUPPLEMENTARY MATERIAL

The Supplementary Material for this article can be found online at: <https://www.frontiersin.org/articles/10.3389/fphys.2020.543331/full#supplementary-material>

pain. *Lancet Neurol.* 11, 629–642. doi: 10.1016/S1474-4422(12)70134-5

Cao, H., and Zhang, Y. Q. (2008). Spinal glial activation contributes to pathological pain states. *Neurosci. Biobehav. Rev.* 32, 972–983. doi: 10.1016/j.neubiorev.2008.03.009

Chiang, C. Y., Sessle, B. J., and Dostrovsky, J. O. (2012). Role of astrocytes in pain. *Neurochem. Res.* 37, 2419–2431. doi: 10.1007/s11064-012-0801-6

Conti, B., Tabarean, I., Sanchez-Alavez, M., Davis, C., Brownell, S., Behrens, M., et al. (2008). Cytokine receptors in the brain. *Neuroimmune Biol.* 6, 21–38.

Dinarello, C. A., Simon, A., and van der Meer, J. W. M. (2012). Treating inflammation by blocking interleukin-1 in a broad spectrum of diseases. *Nat. Rev. Drug Discov.* 11, 633–652. doi: 10.1038/nrd3800

Donatien, P., Anand, U., Yiangou, Y., Sinisi, M., Fox, M., MacQuillan, A., et al. (2018). Granulocyte-macrophage colony-stimulating factor receptor expression

- in clinical pain disorder tissues and role in neuronal sensitization. *Pain Reports* 3:e676. doi: 10.1097/PR9.0000000000000676
- Gao, Y. J., and Ji, R. R. (2010). Targeting astrocyte signaling in chronic pain. *Neurotherapeutics* 7, 482–493. doi: 10.1016/j.nurt.2010.05.016
- Gruber-Schoffnegger, D., Drdla-Schutting, R., Hönigsperger, C., Wunderbaldinger, G., Gassner, M., and Sandkühler, J. (2013). Induction of thermal hyperalgesia and synaptic long-term potentiation in the spinal cord lamina I by TNF- α and IL-1 β is mediated by glial cells. *J. Neurosci.* 33, 6540–6551. doi: 10.1523/jneurosci.5087-12.2013
- Hegyi, Z., Oláh, T., Kőszeghy, Á., Piscitelli, F., Holló, K., Pál, B., et al. (2018). CB1 receptor activation induces intracellular Ca²⁺ mobilization and 2-arachidonoylglycerol release in rodent spinal cord astrocytes. *Sci. Rep.* 8:10562.
- Herx, L. M., and Yong, V. W. (2001). Interleukin-1 beta is required for the early evolution of reactive astrogliosis following CNS lesion. *J. Neuropathol. Exp. Neurol.* 60, 961–971. doi: 10.1093/jnen/60.10.961
- Holló, K., Ducza, L., Hegyi, Z., Dócs, K., Hegedűs, K., Bakk, E., et al. (2017). Interleukin-1 receptor type 1 is overexpressed in neurons but not in glial cells within the rat superficial spinal dorsal horn in complete Freund adjuvant-induced inflammatory pain. *J. Neuroinflammation* 14:125. doi: 10.1186/s12974-017-0902-x
- Holló, K., Glant, T. T., Garzó, M., Finnegan, A., Mikecz, K., and Buzás, E. (2000). Complex pattern of Th1 and Th2 activation with a preferential increase of autoreactive Th1 cells in BALB/c mice with proteoglycan (aggrecan)-induced arthritis. *Clin. Exp. Immunol.* 120, 167–173. doi: 10.1046/j.1365-2249.2000.01174.x
- Huang, Y., Smith, D. E., Ibanez-Sandoval, O., Sims, J. E., and Friedman, V. J. (2011). Neuron-specific effects of interleukin-1 β are mediated by a novel isoform of the IL-1 receptor accessory protein. *J. Neurosci.* 31, 18058–18059.
- Hunter, C., and Jones, S. A. (2015). IL-6 as a keystone cytokine in health and disease. *Nat. Rev. Immunol.* 16, 448–457. doi: 10.1038/nri.3153
- Hylden, J. L. K., Nahin, R. L., Traub, R. J., and Dubner, R. (1989). Expansion of receptive fields of spinal lamina I projection neurons in rats with unilateral adjuvant-induced inflammation: the contribution of dorsal horn mechanisms. *Pain* 37, 229–243. doi: 10.1016/0304-3959(89)90135-8
- Jayaraj, R. L., Azimullah, S., Beiram, R., Jalal, F. Y., and Rosenberg, G. A. (2019). Neuroinflammation: friend and foe for ischemic stroke. *J. Neuroinflammation* 16:142. doi: 10.1186/s12974-019-1516-2
- Jha, M. K., Jo, M., Kim, J. H., and Suk, K. (2019). Microglia-astrocyte crosstalk: an intimate molecular conversation. *Neuroscientist* 25, 227–240. doi: 10.1177/1073858418783959
- Ji, R. R., Donnelly, C. R., and Nedergaard, M. (2019). Astrocytes in chronic pain and itch. *Nat. Rev. Neurosci.* 20, 667–685. doi: 10.1038/s41583-019-0218-1
- Krieger, M., Both, M., Kranig, S., Pitzer, C., Klugmann, M., Vogt, G., et al. (2012). The hematopoietic cytokine granulocyte-macrophage colony stimulating factor is important for cognitive functions. *Sci. Rep.* 2:697. doi: 10.1038/srep00697
- Kuner, R. (2010). Central mechanisms of pathological pain. *Nat. Med.* 16, 1258–1266. doi: 10.1038/nm.2231
- Labow, M., Shuster, D., Zetterstrom, M., Nunes, P., Terry, R., Cullinan, E. B., et al. (1997). Absence of IL-1 signaling and reduced inflammatory response in IL-1 type I receptor-deficient mice. *J. Immunol.* 159, 2452–2461.
- Laudati, E., Curro, D., Navarra, P., and Lisi, L. (2017). Blockade of CCR5 receptor prevents M2 microglia phenotype in a microglia-glioma paradigm. *Neurochem. Int.* 108, 100–108. doi: 10.1016/j.neuint.2017.03.002
- Li, T., Chen, X., Zhang, C., Zhang, Y., and Yao, W. (2019). An update on reactive astrocytes in chronic pain. *J. Neuroinflamm.* 16:140. doi: 10.1186/s12974-019-1524-2
- Liao, Y. H., Zhang, G. H., Jia, D., Wang, P., Qian, N. S., He, F., et al. (2011). Spinal astrocytic activation contributes to mechanical allodynia in a mouse model of type 2 diabetes. *Brain Res.* 1368, 324–335. doi: 10.1016/j.brainres.2010.10.044
- Liddelow, S., and Barres, B. (2015). SnapShot: astrocytes in health and disease. *Cell* 162, 1170–1170. doi: 10.1016/j.cell.2015.08.029
- Liddelow, S. A., Guttenplan, K. A., Clarke, L. E., Bennett, F. C., Bohlen, C. J., Schirmer, L., et al. (2017). Neurotoxic reactive astrocytes are induced by activated microglia. *Nature* 541, 481–487. doi: 10.1038/nature.21029
- Lin, Y. Z., Yao, S. Y., Veach, R. A., Torgerson, T. R., and Hawiger, J. (1995). Inhibition of nuclear translocation of transcription factor NF-kappa B by a synthetic peptide containing a cell membrane-permeable motif and nuclear localization sequence. *J. Biol. Chem.* 270, 14255–14258. doi: 10.1074/jbc.270.24.14255
- Liu, S., Xu, G. Y., Johnson, K. M., Echetebe, C., Ye, Z., Hulsebosch, C. E., et al. (2008). Regulation of interleukin-1 β by the interleukin-1 receptor antagonist in the glutamate-injured spinal cord: endogenous neuroprotection. *Brain Res.* 1231, 63–74. doi: 10.1016/j.brainres.2008.07.035
- Matias, I., Morgado, J., and Gomes, F. C. A. (2019). Astrocyte heterogeneity: impact to brain aging and disease. *Front. Aging Neurosci.* 11:59. doi: 10.3389/fnagi.2019.00059
- Medzhitov, R. (2001). Toll-like receptors and innate immunity. *Nat. Rev. Immunol.* 1, 135–145.
- Milligan, E. D., and Watkins, L. R. (2009). Pathological and protective roles of glia in chronic pain. *Nat. Rev. Neurosci.* 10, 23–36. doi: 10.1038/nrn2533
- Molander, C., and Grant, G. (1985). Cutaneous projections from the rat hindlimb foot to the substantia gelatinosa of the spinal cord studied by transganglionic transport of WGA-HRP conjugate. *J. Comp. Neurol.* 237, 476–484. doi: 10.1002/cne.902370405
- Niederberger, E., Schmidtke, A., Gao, W., Kühlein, H., Ehnert, C., and Geisslinger, G. (2007). Impaired acute and inflammatory nociception in mice lacking the p50 subunit of NF-kappaB. *Eur. J. Pharmacol.* 559, 55–60. doi: 10.1016/j.ejphar.2006.11.074
- Oeckinghaus, A., Hayden, M. S., and Ghosh, S. (2011). Crosstalk in NF- κ B signaling pathways. *Nat. Immunol.* 12, 695–708. doi: 10.1038/ni.2065
- Phulwani, N. K., Esen, N., Syed, M. M., and Kielian, T. (2008). TLR2 expression in astrocytes is induced by TNF- α and NF- κ B dependent pathways. *J. Immunol.* 181, 3841–3849. doi: 10.4049/jimmunol.181.6.3841
- Pierce, J. W., Schoenleber, R., Jesmok, G., Best, J., Moore, S. A., Collins, T., et al. (1997). Novel inhibitors of cytokine-induced ikappa balpha phosphorylation and endothelial cell adhesion molecule expression show anti-inflammatory effects in vivo. *J. Biol. Chem.* 272:21096. doi: 10.1074/jbc.272.34.21096
- Pitzer, C., Kuner, R., and Tappe-Theodor, A. (2016). Voluntary and evoked behavioral correlates in inflammatory pain conditions under different social housing conditions. *Pain Rep.* 1:e564. doi: 10.1097/PR9.0000000000000564
- Raghavendra, V., Flobert, Y., Tanga, F. Y., and DeLeo, J. A. (2004). Complete Freund's adjuvant-induced peripheral inflammation evokes glial activation and proinflammatory cytokine expression in the CNS. *Eur. J. Neurosci.* 20, 467–473. doi: 10.1111/j.1460-9568.2004.03514.x
- Ren, K., and Torres, R. (2009). Role of interleukin-1 β during pain and inflammation. *Brain Res. Rev.* 60, 57–64. doi: 10.1016/j.brainresrev.2008.12.020
- Rothaug, M., Becker-Pauly, C., and Rose-John, S. (2016). The role of interleukin-6 signaling in nervous tissue. *Biochim. Biophys. Acta* 1863(6 Pt A), 1218–1227. doi: 10.1016/j.bbamcr.2016.03.018
- Schreck, R., and Bauerle, P. A. (1990). NF-KB as inducible transcriptional activator of the granulocyte-macrophage colony-stimulating factor gene. *Mol. Cell. Biol.* 10, 1281–1286. doi: 10.1128/mcb.10.3.1281
- Schweizerhof, M., Stösser, S., Kurejova, M., Njoo, C., Gangadharan, V., Agarwal, N., et al. (2009). Hematopoietic colony-stimulating factors mediate tumor-nerve interactions and bone cancer pain. *Nat. Med.* 15, 802–807. doi: 10.1038/nm.1976
- Sims, J. E., and Smith, D. E. (2010). The IL-1 family: regulators of immunity. *Nat. Rev. Immunol.* 10, 89–102. doi: 10.1038/nri2691
- Son, Y. H., Jeong, Y. T., Lee, K. A., Choi, K. H., Kim, S. M., Rhim, B. Y., et al. (2008). Roles of MAPK and NF-kappaB in interleukin-6 induction by lipopolysaccharide in vascular smooth muscle cells. *J. Cardiovasc. Pharmacol.* 51, 71–77. doi: 10.1097/FJC.0b013e31815bd23d
- Srinivasan, D., Yen, J. H., Joseph, D. J., and Friedman, W. (2004). Cell type-specific interleukin-1beta signaling in the CNS. *J. Neurosci.* 24, 6482–6488. doi: 10.1523/jneurosci.5712-03.2004
- Suter, M. R., Wen, Y. R., Decosterd, I., and Ji, R. R. (2007). Do glial cells control pain? *Neuron Glia Biol.* 3, 255–268. doi: 10.1017/s1740925x08000100
- Tang, Y., Liu, L., Xu, D., Zhang, W., Zhang, Y., Zhou, J., et al. (2018). Interaction between astrocytic colony stimulating factor and its receptor on microglia mediates central sensitization and behavioral hypersensitivity in chronic post ischemic pain model. *Brain Behav. Immun.* 68, 248–260. doi: 10.1016/j.bbi.2017.10.023
- Tarassishin, L., Suh, H. S., and Lee, S. C. (2014). LPS and IL-1 differentially activate mouse and human astrocytes: role of CD14. *Glia* 62, 999–1013. doi: 10.1002/glia.22657

- Teh, D. B. L., Prasad, A., Jiang, W., Ariffin, M. Z., Khanna, S., Belorkar, A., et al. (2017). Transcriptome Analysis Reveals Neuroprotective aspects of Human Reactive Astrocytes induced by Interleukin 1 β . *Sci. Rep.* 7:13988. doi: 10.1038/s41598-017-13174-w
- Trettel, F., Di Castro, M. A., and Limatola, C. (2019). Chemokines: key molecules that orchestrate communication among neurons, microglia and astrocytes to preserve brain function. *J. Neurosci.* [Epub ahead of print]. doi: 10.1016/j.neuroscience.2019.07.035
- Verkhatsky, A., and Nedergaard, M. (2018). Physiology of astroglia. *Physiol. Rev.* 98, 239–289. doi: 10.1152/physrev.00042.2016
- Viviani, B., Bartesaghi, S., Gardoni, F., Vezzani, A., Behrens, M. M., Bartfai, T., et al. (2003). Interleukin-1 β enhances NMDA receptor-mediated intracellular calcium increase through activation of the Src family of kinase. *J. Neurosci.* 23, 8692–8700. doi: 10.1523/jneurosci.23-25-08692.2003
- Wang, C. X., Olschowka, J. A., and Wrathall, J. R. (1997). Increase of interleukin-1 β mRNA and protein in the spinal cord following experimental traumatic injury in the rat. *Brain Res.* 759, 190–196. doi: 10.1016/s0006-8993(97)00254-0
- Wang, X. F., Yin, L., Hu, J. G., Huang, L. D., Yu, P. P., Jiang, X. Y., et al. (2006). Expression and localization of p80 interleukin-1 receptor protein in the rat spinal cord. *J. Mol. Neurosci.* 29, 45–53. doi: 10.1385/jmn:29:1:45
- Wickremasinghe, M. I., Thomas, L. H., O’Kane, C. M., Uddin, J., and Friedland, J. S. (2004). Transcriptional mechanisms regulating alveolar epithelial cell-specific CCL5 secretion in pulmonary tuberculosis. *J. Biol. Chem.* 279, 27199–27210. doi: 10.1074/jbc.M403107200
- Yang, C. C., Lin, C. C., Jou, M. J., Hsiao, L. D., and Yang, C. M. (2019). RTA 408 inhibits interleukin-1 β -induced MMP-9 expression via suppressing protein kinase-dependent NF- κ B and AP-1 activation in rat brain astrocytes. *Int. J. Mol. Sci.* 20:E2826. doi: 10.3390/ijms20112826
- Yin, Q., Fan, Q., Zhao, Y., Cheng, M. Y., Liu, H., Li, J., et al. (2015). Spinal NF- κ B and chemokine ligand 5 expression during spinal glial cell activation in a neuropathic pain model. *PLoS One* 10:e0115120. doi: 10.1371/journal.pone.0115120
- Zhang, J. M., and An, J. (2007). Cytokines, inflammation and pain. *Int. Anesthesiol. Clin.* 45, 27–37. doi: 10.1097/AIA.0b013e318034194e
- Zhou, Y. Q., Liu, Z., Liu, Z. H., Chen, S. P., Li, M., Shahveranov, A., et al. (2016). Interleukin-6: an emerging regulator of pathological pain. *J. Neuroinflamm.* 13:141. doi: 10.1186/s12974-016-0607-6
- Zhu, J., Wei, X., Feng, X., Song, J., Hu, Y., and Xu, J. (2008). Repeated administration of mirtazapine inhibits development of hyperalgesia/allodynia and activation of NF- κ B in a rat model of neuropathic pain. *Neurosci. Lett.* 433, 33–37. doi: 10.1016/j.neulet.2007.12.037

Conflict of Interest: The authors declare that the research was conducted in the absence of any commercial or financial relationships that could be construed as a potential conflict of interest.

Copyright © 2020 Gajtkó, Bakk, Hegedűs, Ducza and Holló. This is an open-access article distributed under the terms of the Creative Commons Attribution License (CC BY). The use, distribution or reproduction in other forums is permitted, provided the original author(s) and the copyright owner(s) are credited and that the original publication in this journal is cited, in accordance with accepted academic practice. No use, distribution or reproduction is permitted which does not comply with these terms.



The Mysteries of Capsaicin-Sensitive Afferents

Michael J. M. Fischer¹, Cosmin I. Ciotu¹ and Arpad Szallasi^{2*}

¹ Center of Physiology and Pharmacology, Medical University of Vienna, Vienna, Austria, ² 1st Department of Pathology and Experimental Cancer Research, Semmelweis University, Budapest, Hungary

OPEN ACCESS

Edited by:

Istvan Nagy,
Imperial College London,
United Kingdom

Reviewed by:

Peter M. Blumberg,
Other, Frederick, United States
Livio Luongo,
University of Campania Luigi Vanvitelli,
Italy
Michael Iadarola,
National Institutes of Health Clinical
Center (NIH), United States

*Correspondence:

Arpad Szallasi
szallasiarpad@gmail.com

Specialty section:

This article was submitted to
Clinical and Translational Physiology,
a section of the journal
Frontiers in Physiology

Received: 21 April 2020

Accepted: 13 November 2020

Published: 16 December 2020

Citation:

Fischer MJM, Ciotu CI and
Szallasi A (2020) The Mysteries
of Capsaicin-Sensitive Afferents.
Front. Physiol. 11:554195.
doi: 10.3389/fphys.2020.554195

A fundamental subdivision of nociceptive sensory neurons is named after their unique sensitivity to capsaicin, the pungent ingredient in hot chili peppers: these are the capsaicin-sensitive afferents. The initial excitation by capsaicin of these neurons manifested as burning pain sensation is followed by a lasting refractory state, traditionally referred to as “capsaicin desensitization,” during which the previously excited neurons are unresponsive not only to capsaicin but a variety of unrelated stimuli including noxious heat. The long sought-after capsaicin receptor, now known as TRPV1 (transient receptor potential cation channel, subfamily V member 1), was cloned more than two decades ago. The substantial reduction of the inflammatory phenotype of *Trpv1* knockout mice has spurred extensive efforts in the pharmaceutical industry to develop small molecule TRPV1 antagonists. However, adverse effects, most importantly hyperthermia and burn injuries, have so far prevented any compounds from progressing beyond Phase 2. There is increasing evidence that these limitations can be at least partially overcome by approaches outside of the mainstream pharmaceutical development, providing novel therapeutic options through TRPV1. Although ablation of the whole TRPV1-expressing nerve population by high dose capsaicin, or more selectively by intersectional genetics, has allowed researchers to investigate the functions of capsaicin-sensitive afferents in health and disease, several “mysteries” remain unsolved to date, including the molecular underpinnings of “capsaicin desensitization,” and the exact role these nerves play in thermoregulation and heat sensation. This review tries to shed some light on these capsaicin mechanisms.

Keywords: capsaicin, TRPV1 receptor, ion channel, pain, sensory neuron, inflammation, thermoregulation

CAPSAICIN AS A TOOL BEFORE TRPV1 WAS DISCOVERED

Natural products like capsaicin afford a unique tool to dissect important physiological pathways. The recognition that consuming the fruits of capsicum plants evokes a characteristic “hot” burning sensation in the human tongue and oral mucosa is probably as old as the domestication and cultivation of these plants (going back to 8,000 years in South America) (Perry et al., 2007). And here is the first great “mystery” of capsaicin-sensitive afferents: how come that the very same pungent sensation that repels herbivores (like deer) from eating the capsicum pods is found pleasurable by so many humans? Recently, experts tried to solve this puzzle in the journal *Temperature* with such fascinating explanations like the cooling effect of spicy food (capsaicin as “natural air-conditioner”), the food-preserving, anti-microbial action of capsicum

(capsaicin as “refrigerator”), or simply the “masochism” of chili-lovers (Szallasi, 2016). Nonetheless, the human fondness of, or aversion to hot pepper is probably far more complex than these models imply (Byrnes and Hayes, 2013).

From *Capsicum*, capsaicin was first isolated in 1846 (Thresh, 1846), and its chemical structure determined in 1919 (Nelson, 1919). In 1912, Wilbur Scoville invented his human tongue-based scale to measure the “hotness” of pepper extracts (Gmyrek, 2013; Sweat et al., 2016). Ever since, capsaicin has remained a reference agonist in sensory pharmacology (Szolcsányi, 1984; O'Neill et al., 2012). The early capsaicin findings were detailed elsewhere (Szolcsányi, 1984, 2004) and only the most important milestones are listed here.

The effect of capsaicin on thermoregulation was first noted 150 years ago when hot pepper extract applied to the stomach of dogs produced a fall in rectal temperature (Högyes, 1878). With regard to pain and inflammation, Nicholas (Miklós) Jancsó made the astute observation that capsaicin evoked strong and persistent “desensitization” after exposure to the rat cornea, skin, and airways (Jancsó and Jancsó, 1949; Jancsó et al., 1967).

Capsaicin research gathered speed in the 1970s. Electrical nerve stimulation was shown to cause neurogenic inflammation, and this could be ablated by prior high dose capsaicin exposure. Similarly, responsiveness to mustard oil or cigarette smoke (both turned out to activate TRPA1) or the sodium channel modulator veratridine was reduced. Since these substances only partially cross-desensitize, this indicated a prolonged silencing of the capsaicin-sensitive neurons, and an overlap with the respective receptor populations (Szolcsányi et al., 1975). In contrast, mechanical sensitivity was largely untouched by high concentrations of capsaicin. In the 1980s, researchers acquired important new tools to study capsaicin-sensitive afferents, including ruthenium red as the first (though non-selective) capsaicin antagonist (Maggi et al., 1988), capsazepine as the first synthetic and somewhat selective capsaicin antagonist (Urban and Dray, 1991), and resiniferatoxin, an ultrapotent capsaicin analog with a unique spectrum of actions (Szallasi and Blumberg, 1989).

Much of our early knowledge of capsaicin-sensitive pathways came from the desensitization experiments. It cannot be emphasized enough that the literature uses the term “capsaicin desensitization” loosely, in an ill-defined manner. By “desensitization”, some investigators mean a fully reversible capsaicin-induced refractory state, whereas others use it more broadly to include irreversible changes due to neuronal death (Szallasi and Blumberg, 1999).

It is not clear whether the reversible and irreversible refractoriness following capsaicin (or resiniferatoxin) administration reflect quantitative or qualitative differences. For example, in the human neurogenic bladder, topical resiniferatoxin induces a long lasting (up to several months), but fully reversible, increase in the cystoscopic volume at which the voiding urge is activated (Cruz et al., 1997), without causing any noticeable changes in the bladder biopsies at the light or electron microscopic level (Silva et al., 2001). By contrast, resiniferatoxin applied to the bodies of capsaicin-sensitive neurons causes

irreversible changes by selectively ablating these cells *via* Ca^{2+} influx-mediated cytotoxicity (Karai L. et al., 2004).

Using resiniferatoxin as a “molecular scalpel” to achieve permanent analgesia has a clear therapeutic potential (Iadarola and Gonnella, 2013). Indeed, intrathecal resiniferatoxin is already undergoing clinical trials in severe osteoarthritic pain (www.clinicaltrials.gov, NCT 04044742 Sorrento Therapeutics Inc., 2020), and in cancer patients with chronic intractable pain (www.clinicaltrials.gov, NCT 00804154, 2020). Furthermore, a site-specific (intraarticular) trans-capsaicin (CNTX-4975) injection has shown promise in osteoarthritis knee pain (Stevens et al., 2019); the results of two on-going phase 3 trials are expected soon.

Calcium is clearly a key player in capsaicin actions (Wood et al., 1988; Bevan and Szolcsányi, 1990). Calcium overload also underlies both desensitization and neurotoxicity by resiniferatoxin (Olah et al., 2001). Of note, capsaicin and resiniferatoxin differ in the kinetics of the Ca^{2+} influx that they evoke: the current is fast and rapidly normalizing for capsaicin, whereas it is sustained and long-lasting for resiniferatoxin (Szallasi et al., 1999). This difference is so striking that it even led to the proposal (later discredited by the cloning of the vanilloid receptor, TRPV1) of distinct vanilloid receptors mediating capsaicin (C-type) and resiniferatoxin (R-type) actions, respectively (Bíró et al., 1998). One may argue that there is a fine and ill-defined line that separates reversible desensitization from irreversible toxicity. This may involve the route of application (peripheral nerve terminal *versus* cell body), the kinetics of Ca^{2+} influx, the phosphorylation state of the receptor protein, as well as other, as yet unidentified, mechanisms.

In rat models of chronic neuropathic pain, there appears to be a genetic reprogramming in injured nociceptive neurons in which pain-promoting mechanisms are up-regulated: it was referred to as messenger plasticity (Hökfelt et al., 1994). Interestingly, resiniferatoxin administration was found to change the phenotype of sensory neurons the opposite way, by down-regulating the expression of substances known to promote pain (e.g., substance P), and by up-regulating endogenous pain-counteracting compounds, like galanin (Szallasi, 1996). Importantly, resiniferatoxin also blocked the neuronal synthesis of its own receptor. These resiniferatoxin-induced neurochemical changes, collectively referred to as “vanilloid-induced messenger plasticity,” were fully reversible, and their recovery coincided with the return of pain sensitivity (Szallasi and Blumberg, 1999).

Early experiments already showed that acute systemic exposure to capsaicin reduced body temperature (hypothermia), and, after ablation of the sensitive neurons, it rendered animals unable of behavior saving themselves from overheating (hyperthermia) (Jancsó-Gábor et al., 1970). These observations could have served as an early warning of the thermoregulatory side-effects of TRPV1 antagonists that, somehow, had to be rediscovered later. It should be mentioned here that the undesirable effects on the body temperature have been minimized in the second generation TRPV1 antagonists (Gomtsyan et al., 2015), but whether this also reduced potential therapeutic uses

in parallel is not yet known. Site and mechanism of the body temperature regulation fall beyond the scope of this review and are discussed elsewhere (Garami et al., 2018).

In the 1970s, based on the fairly strict structure-activity-requirements for capsaicin-like activity, Szolcsányi and coworkers postulated the existence of a specific capsaicin receptor (Szolcsányi and Jancsó-Gábor, 1975). In 1990, specific binding of resiniferatoxin provided the first biochemical proof for the existence of this receptor, called the vanilloid receptor VR1 (Szallasi and Blumberg, 1990), and [^3H]resiniferatoxin autoradiography was used to visualize the expression of this receptor in several species, including man (Szallasi, 1995). In patch-clamped *Xenopus oocytes*, a capsaicin-induced current was observed following the injection of RNA extracted from rat sensory neurons (Szallasi, unpublished observations). With this, the hunt for the capsaicin receptor was on.

THE DISCOVERY OF TRPV1

In 1997, the laboratory of David Julius was the first to identify the rat capsaicin (vanilloid) receptor *via* an expression cloning strategy that took advantage of the Ca^{2+} conductance (Caterina et al., 1997). The human isoform showed largely similar properties (Hayes et al., 2000). The availability of a plasmid led to rapid characterisation of the properties of the receptor protein, including pharmacological and biophysical properties. Importantly, the capsaicin receptor turned out to be a transient receptor potential (TRP) channel. Within the TRP superfamily, the capsaicin receptor as TRPV1 is the founding member of the now populous TRPV (vanilloid) subdivision, TRPV1 to TRPV6 (Clapham, 2003).

Regarding the “transient nature” of TRP channels, it is really a misnomer explained by the history of this naming convention. In 1969, a drosophila eye mutant labeled *trp* responded to lasting light stimulation with a transient depolarizing after-potential instead of the normal prolonged response (Cosens and Manning, 1969). The respective wild-type *trp* gene was isolated and could rescue this phenotype (Montell et al., 1985). So, the wild-type channel in fact causes a persistent (and not transient) current; nevertheless, this ion channel family now bears the name “transient”. This is in contrast to many ion channels, which fully adapt when exposed to constant stimulation, and is important to continuously code pain for a persistent stimulus.

Subsequently, the Julius laboratory generated and characterized the *Trpv1* knockout mouse, which misses exon 13 that codes mainly for the pore loop and transmembrane domain 6. These animals looked normal, but lacked responses to capsaicin, showed normal responses to noxious mechanical stimuli, and expressed minimal inflammatory thermal hyperalgesia (Caterina et al., 2000). This phenotype was consistent with that of the capsaicin-desensitized rodents and rendered TRPV1 immediately as an attractive pharmacological target. In addition, which could have been an early warning of the burn injury in patients on TRPV1 antagonists, there was a reduced pain-related behavior to noxious heat, in particular at higher temperatures (Caterina et al., 2000).

A separately generated *Trpv1* knockout mouse led to similar results (Davis et al., 2000).

Moreover, the crystal structure of the TRPV1 protein was largely solved by cryo-electron microscopy (Liao et al., 2013), including an open conformation (Cao et al., 2013) and the transmembrane part in a chemically more native lipid nanodisc environment (Gao et al., 2016).

TRPV1 AS A SENSOR

TRPV1 is multimodally-gated channel, activated in concert by both physical and chemical stimuli. Importantly, from a “native state”, the channel’s sensitivity can be substantially increased by chemical modification, e.g., phosphorylation (Numazaki et al., 2002; Szallasi et al., 2007; Utreras et al., 2013; Nagy et al., 2014). Consequently, the adjustable working range of the responsiveness is surprisingly broad. Furthermore, different modes of activation can act in an additive or supraadditive fashion, and thus subthreshold stimuli acting together may reach the activation threshold.

TRPV1 is activated by heat (Caterina et al., 1997) with a threshold of just above 40 °C (Zhang et al., 2018): this is not far from the human heat pain threshold of about 40 °C (Yarnitsky et al., 1995; Rolke et al., 2006). The ion channel pore domain is responsible for the sensitivity to heat (Zhang et al., 2018). TRPV1 is also activated by acidic pH (Tominaga et al., 1998) with good concentration-dependent coding below pH 6. The biophysics of this activation along with the amino acid residues involved were detailed elsewhere (Jordt et al., 2000; Ryu et al., 2007; Aneiros et al., 2011). The proton-activation of TRPV1 is complicated by the proton-induced inhibition, which applies to most currents, including proton-activated ones (Fischer et al., 2003; Lee and Zheng, 2015).

Natural pharmacological agonists of TRPV1 include both pungent plant products (e.g., capsaicin, piperine and resiniferatoxin) and painful animal venoms and toxins (from spiders, scorpions, centipedes, snakes, and jelly fish, etc.) (Geron et al., 2017; Chu et al., 2020). In addition to capsaicin, chili peppers contain other less pungent compounds like capsiate, summarized under the term “capsinoids”. Of note, pungent compounds occur in various plant-derived spices like red and black pepper, mustard, horse radish, and wasabi. Although these spices taste similarly, their active ingredients act on different molecular targets, primarily TRPV1 and TRPA1.

The existence of endogenous TRPV1 activators (so-called “endovanilloids”) with physiological or pathophysiological relevance remains putative. Although several endogenous lipids, e.g., anandamide (Zygmunt et al., 1999) and other acylethanolamines (Brito et al., 2014), were reported to activate TRPV1 *in vitro*, this activation was observed at such high concentrations that are unlikely to occur *in vivo*. This is also true for lipid oxidation products (Hwang et al., 2000).

Voltage-dependent gating of TRP ion channels was first shown for TRPM4 (Launay et al., 2002). Voltage also seems to be a cooperative factor in the gating of TRPV1 (Voets et al., 2004). Osmotic activation of TRPV1 was also reported, but this has

not been reproduced by others (Nishihara et al., 2011). TRPV1 is regulated by phospholipids, but the details are a controversial issue which was critically reviewed elsewhere (Rohacs, 2015).

Inflammatory sensitisation of TRPV1 is an important mechanism of on-going pain (Fischer et al., 2010; Malek et al., 2015). A fast and large degree of sensitisation can be achieved by phosphorylation of the TRPV1 protein, more so *via* protein kinase C than protein kinase A (Premkumar and Ahern, 2000; Vellani et al., 2001; Bhawe et al., 2002; Mandadi et al., 2006; Fischer and Reeh, 2007; Wang et al., 2015). Furthermore, substances generated under inflammatory conditions (e.g., nerve growth factor) may either regulate TRPV1 expression (Amaya et al., 2004; Chu et al., 2011) and or act more directly (Zhang et al., 2005).

The substantial variation in the exact thermal activation threshold of TRPV1 is due to its phosphorylation state (Sugiura et al., 2002; Huang et al., 2006; Li et al., 2014). Conformational changes (sensitisation) by phosphorylation bring the channel closer to its activation state, thereby lowering the activation threshold for agonists. This concept applies not only to chemical agonists but to all modes of activation, including temperature and voltage. Protons and/or capsaicin can act with temperature in a supraadditive fashion (Jordt et al., 2000; Kichko and Reeh, 2004), and this also applies to voltage (Voets et al., 2004). The extent of channel activation by a specific agonist-binding site depends on the agonist, with a partial agonist showing less shift and acting antagonistic to a full agonist. Indeed, this expected phenomenon was demonstrated for iodo-resiniferatoxin (Shimizu et al., 2005). Less expected was the different number of agonist-bound sites for activation: using concatemers with inactivated capsaicin or proton binding sites, it was shown that one capsaicin is sufficient to activate TRPV1, but the same response needs four protons, indicating an agonist-site dependent shift toward activation (Hazan et al., 2015).

Since increased TRPV1 sensitivity might primarily occur as part of local pathology (e.g., local inflammation) (Malek et al., 2015), in contrast to addressing TRPV1 directly (Moran and Szallasi, 2018), selectively targeting sensitisation without affecting the native channel has been investigated as a novel therapeutic approach (Btresh et al., 2013; Fischer et al., 2013; Hanack et al., 2015; Sonderrmann et al., 2019). It is hoped that side effects that plagued the use of *per os* TRPV1 antagonists can be avoided by this approach.

Continuous or frequently repeated TRPV1 stimulation leads to receptor tachyphylaxis that should be clearly distinguished from capsaicin-induced defunctionalisation of the whole sensory neuron. Tachyphylaxis depends on Ca^{2+} influx, dephosphorylation (Docherty et al., 1996; Mohapatra and Nau, 2005), and association with protein complexes (Por et al., 2013); combined, these effects lead to decreased TRPV1 presence in the plasma membrane. When the Ca^{2+} influx is terminated, the channel is recycled to the plasma membrane from the intracellular depots by shuttle molecules like synaptotagmin 1 (Tian et al., 2019). Of note, a fraction of internalized TRPV1 gets degraded (Sanz-Salvador et al., 2012). Similar to cooperative activation, desensitization by different modalities is also at least partially convergent; for example,

desensitization by heat also renders TRPV1 less sensitive to capsaicin (Sánchez-Moreno et al., 2018).

TRPV1 expression is found through the animal kingdom. Species-related differences in TRPV1 function allow a molecular dissection of ion channel biophysics. The Bactrian camel (*Camelus ferus*) and the thirteen-lined ground squirrel (*Ictidomys tridecemlineatus*) both show reduced sensitivity to heat, resisting activation of TRPV1 until 46°C (Laursen et al., 2016). Similarly, chicken (*Gallus gallus*) TRPV1 has an increased activation threshold of around 46°C, but is additionally insensitive to capsaicin (Jordt and Julius, 2002). At the other end of the thermal scale, there are species that have developed a high sensitivity to thermal stimuli such as the axolotl (*Ambystoma mexicanum*) or zebrafish (*Danio rerio*) that have TRPV1 activation thresholds of ~31°C (Hori and Saitoh, 2020) and ~33 °C (Gau et al., 2013), respectively. The platypus (*Ornithorhynchus anatinus*) exhibits a lack of heat induced desensitization of TRPV1 in the context of normal heat activation thresholds (Luo et al., 2019), rendering it more susceptible than more evolved species to heat induced damage. Here, the platypus TRPV1 helped to dissect the heat-induced desensitization in mouse TRPV1, where an interaction between the C- and N-termini leads to the rearrangement of the outer pore domain (Luo et al., 2019). In contrast to other modes of activation like heat, capsaicin sensitivity is more evolutionary conserved, notable exceptions being the avian TRPV1 (Jordt and Julius, 2002) and the tree shrew (*Tupaia belangeri chinensis*), the latter with an EC_{50} of 1.9 mM (Han et al., 2018). Medicinal leech (*Hirudo medicinalis*), clawed frog (*Xenopus tropicalis*), and rabbit (*Oryctolagus cuniculus*) TRPV1 all exhibit reduced capsaicin sensitivity, with EC_{50} values of 100, 85, and 15 μM , respectively (Gavva et al., 2004; Ohkita et al., 2012; Summers et al., 2014). Taken together, these observations imply that the acquisition of capsaicin sensitivity was an early event in evolution, and that birds lost their capsaicin sensitivity.

TRPV1 exerts its primary function in the plasma membrane as noxious signal integrator, although a large fraction is always in intracellular compartments with rapid cycling. Although the presence of TRPV1 in the endoplasmic reticulum is well-established (Turner et al., 2003; Gallego-Sandín et al., 2009), the functional relevance of this observation is unclear since the sensitivity of TRPV1 to capsaicin in the endoplasmic reticulum is about ~100-fold lower than in the plasma membrane. Moreover, Ca^{2+} depletion of the endoplasmic reticulum poses substantial cellular stress which can lead to cell death, and this can be induced by higher capsaicin concentrations than required for TRPV1 activation at the plasma membrane (Karai L. J. et al., 2004).

In the mouse, two splice variants of TRPV1 (missing some exons) have been reported. These variants are not sensitive to capsaicin, but they interact with the full-length channel and act inhibitory in a concentration-dependent manner (Vos et al., 2006; Eilers et al., 2007). The physiological function of these negative variants remains unknown. Alternative splicing of TRPV1 in the trigeminal ganglia allows vampire bats (*Desmodus rotundus*) to detect infrared radiation; the respective short TRPV1 isoform has an activation threshold of about 30 °C (Gracheva et al., 2011), similar to how pit vipers and pythons use TRPA1 in their infrared sensing organs

(Gracheva et al., 2010). Similar splicing occurs in cattle (*Bos taurus*), coast moles (*Scapanus orarius*), dogs (*Canis lupus*), and all members of the *Laurasiatheria* clade (a large group of placental mammals), highlighting a mechanism for physiological tuning of thermosensory nerve fibers (Gracheva et al., 2011).

The role of TRPV1 in body weight regulation also remains a mystery. One study reported that *Trpv1* knockout mice remain lean on high-fat diet (Mottet and Ahern, 2008), another study found no difference between the body weight of wild-type and *Trpv1* knockout animals (Marshall et al., 2013), and a third study described a mouse which is lean and hyperactive when young, and lazy and fat when becomes old (Wanner et al., 2011).

THE TRPV1-POSITIVE NEURON POPULATION

TRPV1 Expression

TRPV1 is expressed in a subpopulation of sensory afferents, primarily of the small to medium diameter (Szallasi, 2016). These are mainly slow-conducting, unmyelinated C-fibers, and a subpopulation of thin myelinated A-fibers (Mitchell et al., 2010, 2014; Blivis et al., 2017). The cell bodies of the neurons that give rise to these afferents are located in sensory (e.g., dorsal root and trigeminal) ganglia. These neurons transmit sensory information from the periphery to the dorsal horn of the spinal cord.

The fraction of TRPV1-expressing neurons in sensory ganglia depends on the species, as well as on the location. Expression data are mainly based on protein, mRNA, or reporters. In a study with direct comparison, TRPV1 was expressed in 37% of mouse and 47% of rat dorsal root ganglion (DRG) neurons (Orozco et al., 2001). There are systematic differences between laboratory mouse strains (Ono et al., 2015). A similar TRPV1 expression was found in trigeminal and visceral afferents (Helliwell et al., 1998). Interestingly, TRPV1 mRNA was found in 47% of rat DRG neurons with TRPA1 expression in a subpopulation of these and a mutually exclusive TRPM8 expression (Kobayashi et al., 2005). This was somewhat unexpected since TRPV1 is a heat sensor whereas TRPA1 (at least in some studies) and TRPM8 are both cold-responsive.

If TRPV1 is co-expressed with TRPA1, one has to assume that it has functional consequences. Indeed, functional interaction between these two channels was reported (Staruschenko et al., 2010), differential for neuronal subpopulations (Patil et al., 2020), and the properties of an enforced heteroconcatamer has been described (Fischer et al., 2014).

TRPV1 reporter mice allow a sensitive analysis of TRPV1 expression without dependency on antibody specificity. Reporting expression via LacZ, PLAP, or Cre-Lox systems all showed a robust TRPV1 presence in peripheral sensory neurons with good correlation to functional responses, but the percentage responding was not quantified (Wang et al., 2017). The extent of brain and extraneuronal TRPV1 expression is a controversial issue beyond the scope of this review (capsaicin-sensitive afferents), therefore the reader is referred to the literature (Mezey et al., 2000; Kauer and Gibson, 2009; Cavanaugh et al., 2011; Fernandes et al., 2012; Bevan et al., 2014; Martins et al., 2014).

TRPV1 is a useful marker of nociceptive neurons, but it is unclear what is common in these neurons beside their TRPV1 expression. Yes, TRPV1 activation can cause pain without any doubt, but there are neurons outside the TRPV1-positive populations which can transmit pain, and, conversely, there is no proof that every TRPV1-expressing neuron is nociceptive. Indeed, afferents expressing TRPV1 seem to serve distinct functions in different organs. For example, TRPV1-positive afferents in the pancreas has been implicated in the pathomechanism of diabetes; in the gastrointestinal system they were linked to thermoregulation; in the respiratory system their activation causes cough; and in the urinary bladder they are involved in the micturition reflex (Moran et al., 2011). Another reflex pathway, the Bezold-Jarisch reflex (also known as the pulmonary chemoreflex) is also initiated by capsaicin-sensitive afferents (Harron and Kobinger, 1984). Even in the skin, TRPV1 contributes to multiple distinct sensations, as e.g., warmth and heat. The dual, sensory-afferent nature of these fibers further complicates the picture.

There is a partial overlap between TRPV1 expression and other commonly used markers in sensory pharmacology. Most, but not all, TRPV1-positive neurons are peptidergic, expressing calcitonin gene-related peptide (CGRP) and substance P (SP) (Holzer, 1988; Szallasi and Blumberg, 1999). In the mouse, peptidergic and isolectin B4-binding populations cover most sensory neurons and are mutually exclusive. However, despite clear differences in their spinal projection (Silverman and Kruger, 1990), ascribing a function to these two neurochemically distinct populations is less trivial. Therefore, these are often combined with TRPV1, which intersects differently with these populations in the mouse and rat (Dirajlal et al., 2003; Price and Flores, 2007).

With the advent of single-cell RNA sequencing, the sensory neuron populations can be clustered with high precision. Two studies analyzed mouse DRG neuron populations (Usoskin et al., 2015; Li et al., 2016) and a further study used murine trigeminal ganglia (Nguyen et al., 2017), but a synthesis of these is not trivial. Based on RNA profile, these studies described 10–17 subpopulations. In one study, TRPV1 was expressed in 6 of the 11 clusters and comprised 44% of all DRG neurons (Usoskin et al., 2015). In the second study, TRPV1 was detected in 8 of the 17 clusters, comprising 30% of all DRG neurons (Li et al., 2016). And in the third study, TRPV1 was found in 7 of the 13 clusters, comprising 50% of all trigeminal neurons (Nguyen et al., 2017). Human sensory neuron TRPV1 mRNA data have been compared to mouse (Ray et al., 2018). These data are from adult animals. In embryonic stage and in newborns, capsaicin-sensitive neurons are more widely distributed (Hjerling-Leffler et al., 2007).

Using RNA sequencing data, one may develop hypotheses about the TRPV1 responsiveness of populations which completely, partially or do not overlap with TRPV1 expression. For example, for MrgprA3 or TRPM8 there is little overlap with TRPV1, therefore at best minor changes are to be expected in response to TRPV1 activation after MrgprA3 lineage ablation. This is in line with experimental observations of an unchanged response to capsaicin (Han et al., 2013; Pogorzala et al., 2013). In contrast, NaV1.8 is largely overlapping, allowing to expect an absence of capsaicin response after NaV1.8 lineage

ablation, which fits the experimental observation (Abrahamsen et al., 2008). Potential heterogeneity of the TRPV1-sensitive population can be further addressed by an intersectional approach, which eliminates a subfraction of these neurons. Ablation of CGRP α -expressing neurons reduced the time-spent licking after capsaicin injection to half, indicating that both the remaining as well as the ablated population contribute to pain-related behavior (McCoy and Zylka, 2014). Deletion of MrgprD eliminates primarily the non-peptidergic subfraction of neurons, comprising a small subset of the TRPV1-expressing neurons. Mice with MrgprD lineage ablation have been generated, but responsiveness to capsaicin has not been reported. This or a similar approach will allow in the future addressing, whether TRPV1-expressing neurons contain subpopulations, which equip the organism with distinct sensitivities.

Finally, RNA sequencing results allow an investigation of coexpressed proteins, whether they control TRPV1 expression, membrane presence and trafficking, and thereby facilitate or repress TRPV1 function.

Activation of TRPV1 in Sensory Neurons

Activation by capsaicin of TRPV1 causes a burning pain sensation in human skin and mucosa, the intensity and duration of which can be controlled over a wide range. The discovery that TRPV1 can also be activated by noxious heat provided a mechanistic explanation for the “burning” nature of capsaicin-evoked pain. Psychophysical experimentation with capsaicin in the human oral cavity was extensively used to study desensitization and change of temperature perception (Smutzer and Devassy, 2016). In fact, Szolcsányi and coworkers used the human tongue to establish structure-activity relations for capsaicin analogs (Szolcsányi and Jancsó-Gábor, 1975). The capsaicin threshold on the tongue is 0.15–1.0 μM (Rozin et al., 1981; Sizer and Harris, 1985).

Although the use of the human tongue as experimental model went out of favor, injection of capsaicin into the skin, first described in 1987, is still a broadly used human pain model (Simone et al., 1987). The concentration-dependence of intensity and duration of capsaicin-evoked pain is well-established (Simone et al., 1989). A frequent rating, a small volume of 50 μl and a low concentration of 3.2 μM capsaicin, which is close to the threshold of the originally described model, allows a reliable pain model that lasts about one-minute (Schwarz et al., 2017). A topical capsaicin cream can also be used as a pain model, for example to test analgesic actions in humans (Lee et al., 2019).

Intraplantar capsaicin injection is an established animal pain model, with observing pain-related aversive behavior as a readout. This model was extensively used to establish target occupation and on-target analgesia by TRPV1 antagonists (Li et al., 1999; Laird et al., 2001; Massaad et al., 2004; Gavva et al., 2005). Alternatively, TRPV1 activation can also be scrutinized using the eye-wiping test (Lee et al., 2001; Bates et al., 2010).

Capsaicin-induced pain is prevented by the TRPV1 antagonists, capsazepine and BCTC. The advent of capsazepine facilitated TRPV1 research, but given inhibition of voltage-gated calcium channels (Docherty et al., 1997) and activation of

TRPA1 (Kistner et al., 2016), it cannot be considered state of the art. BCTC is a potent inhibitor of TRPV1 (Valenzano et al., 2003), but turned out also to inhibit TRPM8 (Behrendt et al., 2004). This is a more acceptable flaw for use in expression systems and also for sensory fibers, as there is little overlap in expression of TRPV1 and TRPM8, as discussed above. The use of these early compounds is supplanted by potent and highly selective TRPV1 antagonists (Aghazadeh Tabrizi et al., 2017; Moran and Szallasi, 2018).

The human capsaicin-induced pain model was used to demonstrate a local axon reflex flare, primary hyperalgesia and secondary hyperalgesia (Magerl et al., 1998; Serra et al., 1998). The cellular time course of tachyphylaxis is well reflected in responses to repetitive stimulation (Witting et al., 2000). The model appears suitable to test analgesics (Wang et al., 2008).

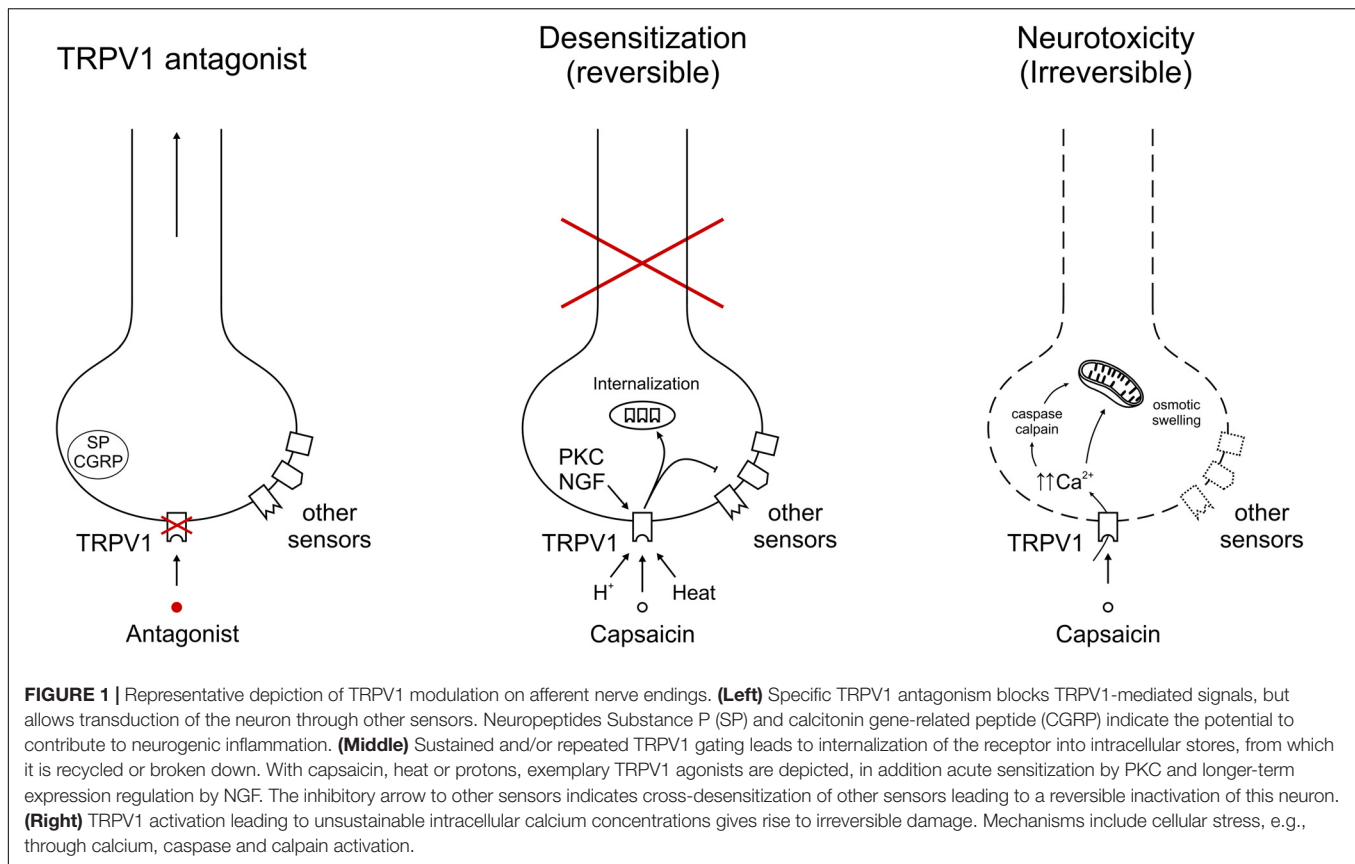
The response of human fibers to injection of capsaicin recorded by microneurography indicated the existence of two functional populations, a mechanosensitive and a mechanosensitive (Schmelz et al., 2000; Serra et al., 2004), with the mechanosensitive population further differentiated into subpopulations in primates (Wooten et al., 2014). However, it is unclear how these functional subpopulations map into the neuronal subpopulations defined by RNA sequencing.

Intravenous capsaicin in humans exceeding 0.5 $\mu\text{g/kg}$ caused a burning sensation in chest, face, rectum and extremities (Winning et al., 1986). The majority of orally consumed capsaicin is resorbed; the pharmacokinetic and further metabolism has been investigated (Chaiyasit et al., 2009). In oral consumption, the interaction with other gustatory and olfactory stimuli is interesting. The four primary taste qualities attenuated the effects of capsaicin, but capsaicin reduced only sweet, sour and bitter but not salty taste (Lawless and Stevens, 1984; Stevens and Lawless, 1986).

Ablation of the TRPV1-Sensitive Population

TRPV1 antagonists only block TRPV1, leaving the respective neurons functional and allowing these to be activated by a number of additional pain targets. By contrast, TRPV1 agonists like capsaicin desensitize the whole neuron, rendering it “silent” (Figure 1). This explains why the capsaicin desensitization experiments overestimated the analgesic potential of TRPV1 antagonists. Furthermore, as mentioned above, capsaicin “desensitization” can be reversible and permanent, with an ill-defined line between the two.

There are multiple ways to achieve “capsaicin desensitization.” The traditional approach is injection of a TRPV1 agonist, in most studies capsaicin, with incrementally increasing doses (Jancsó and Jancsó-Gábor, 1959). The dose escalation can finally reach concentrations manyfold of the LD₅₀ of naive animals. This is necessary because the therapeutic window of capsaicin is narrow, and using single doses allows only partial desensitization before respiratory depression by capsaicin kills the experimental animal (Palecek et al., 1989). Despite pulmonary dose-limiting side effects, systemic capsaicin administration leads to a critical drop of total peripheral resistance (Donnerer and Lembeck,



1982), which might be at least partially caused by the potent vasodilator CGRP released into the systemic circulation (Tang et al., 1997). The full capsaicin dose that is required for complete desensitization is usually given over a period of 5 days. In rats, desensitization can last up to 2–3 months (Jancsó et al., 1967). This is in keeping with the human experience using the topically administered high concentration capsaicin patch, Qutenza. Of note, resiniferatoxin has a much broader therapeutic window, and full desensitization can be achieved by means of a single s.c. injection (Szallasi and Blumberg, 1999).

In embryonic and in early neonatal stage, TRPV1 expression extends to a larger fraction of neurons (Hjerling-Leffler et al., 2007), therefore the fraction of capsaicin-ablated neurons is larger compared to adults (Ritter and Dinh, 1992), and there are even differences between prenatal and neonatal treatment (Perfumi and Sparapassi, 1999). The irreversible pharmacological ablation of a sensory neuronal subpopulation is still a unique and “mysterious” feature of capsaicin and its analogs.

The mechanisms underlying neurotoxicity by capsaicin remain unclear, since the so far identified mechanisms that are dependent on Ca²⁺ influx and activation of calpain and caspase are not particularly TRPV1-specific. Moreover, activation of other ion channels with high calcium conductance does not yield similar results. Adding to the confusion, neonatal capsaicin administration leads to widespread neuronal loss in the rat brain, interpreted by the investigators as hypoxic damage caused by the capsaicin-evoked respiratory arrest (Ritter and Dinh, 1992).

Ablation of the TRPV1-lineage is also possible by expressing the diphtheria toxin receptor as a cell death switch under the TRPV1 promoter. Injecting the diphtheria toxin in such animals allows ablation of the TRPV1-expressing neurons (Baral et al., 2018).

A further approach to investigate the TRPV1 lineage is a functional silencing, which has been described for the charged and membrane impermeable sodium channel blocker, QX314. Coadministration with a TRPV1 agonist allows selective uptake of QX314 through the ion channel pore of the TRPV1 channel (Brenneis et al., 2013). The treated animals showed deficits in heat and mechanical pressure, but not in pinprick and touch detection. They also showed reduced inflammatory hyperalgesia. However, QX314 also permeates the ion channel pore of TRPA1 (Stueber et al., 2016) which limits specificity.

So, what are the main differences between *Trpv1* knockout animals and those with “silenced” TRPV1 lineage? *Trpv1* knockouts show only minor defects in physiological heat sensation (Caterina et al., 2000). In contrast, ablation of the whole TRPV1 lineage by diphtheria toxin eliminated withdrawal from a 55°C hot plate within the test cutoff values (Mishra et al., 2011). Profound thermal hypoalgesia was also noted in rats following resiniferatoxin administration (Xu et al., 1997; Bölskei et al., 2010). There was also a strong effect on the thermal preference, with both extreme hot and cold temperatures largely ignored by these animals (Pogorzala et al., 2013). In humans, desensitization by capsaicin elevated the heat detection

threshold and reduced suprathreshold pain (Rosenberger et al., 2020). The difference between eliminating the TRPV1 lineage and only TRPV1 suggested the presence of further heat sensing ion channels in neurons expressing TRPV1. Based on the observations, one may argue that TRPV1 plays only a minor role in physiological heat sensation of rodents, and the additional channels involved in mice were unexpected (Vandewauw et al., 2018). In contrast, TRPV1 inhibition in human subjects clearly elevated the heat thresholds, therefore TRPV1 acts a first line of defense against acute non-damaging heat (Arendt-Nielsen et al., 2016; Maniatis et al., 2018). Interestingly, modality specific TRPV1 antagonist NEO6860, which does not block heat activation *in vitro*, did also not alter human heat thresholds (Brown et al., 2017). The behavioral response to “inflammatory soup” (that contains ATP, prostaglandins, bradykinin, histamine, and serotonin) was markedly reduced after TRPV1 lineage-ablation; however, this misses a direct comparison to the *Trpv1* knockout as a relevant fraction of inflammatory sensitization converges on TRPV1 (Caterina et al., 2000). Pain-related behavior induced by ATP was also reduced after TRPV1 lineage-ablation, indicating that the involved ATP receptors substantially overlap with TRPV1. The resting body temperature was not different after TRPV1-lineage ablation, but the counterregulation to thermal stress as well as the induction of fever by interleukin-1 β was reduced. The TRPV1 lineage was also required for ongoing inflammatory pain induced by carrageenan, but TRPV1 inhibition could not antagonize this as resiniferatoxin pretreatment (Okun et al., 2011). Comparison of RNA sequencing of TRPV1-expressing neurons and the complementary population shows the relative abundance of many established pain targets (Goswami et al., 2014).

Topical capsaicin desensitization has a clear therapeutic potential to relieve pain, but has also mysterious inconsistencies. In fact, over-the-counter capsaicin creams are broadly available for muscle and arthritic pain, though their analgesic value is only marginally better than placebo (Szallasi and Blumberg, 1999). To increase clinical efficacy, site-specific capsaicin injections and dermal patches have been developed. Qutenza is a dermal patch (capsaicin, 8% w/w), indicated for neuropathic pain (Blair, 2018). It provides a variable, but clinically meaningful improvement in neuropathic pain patients for about 3 months (Martini et al., 2012; Wagner et al., 2013; Maihöfner and Heskamp, 2014).

For decades, sensitivity to capsaicin was recognized as a functional signature of primary sensory neurons. Indeed, for concentrations of up to 1 μ M there is little evidence for non-specific, TRPV1-independent capsaicin actions. At 10 μ M and above, however, capsaicin loses its selectivity for TRPV1 and starts interacting with various enzymes, changing membrane fluidity, and blocking other receptors (Holzer, 1991; Szallasi and Blumberg, 1999; Braga Ferreira et al., 2020). Indeed, cell death evoked by capsaicin 100 μ M is well documented in *Trpv1* knockout mice (Yang et al., 2014). When the clinical experience with high concentration capsaicin preparations is puzzling, the possibility that excessive capsaicin concentrations may also have acted on targets other than TRPV1 should be considered.

First, there is the high capsaicin concentration in the Qutenza patch. Acute desensitization can be achieved by

low concentration (0.02–0.15% are common) capsaicin cremes (Derry and Moore, 2012), but a 1% dermal patch is less efficacious than the 8% patch to achieve a reversible “cutaneous nerve terminal axotomy”. The variable delivery through the skin and the systemic redistribution might only partially explain why Qutenza contains a concentration which is orders of magnitude (by about 4×10^6) higher than the EC₅₀ of capsaicin at human TRPV1. Data on transdermal delivery indicate that within one hour about 1% of the capsaicin contained in the Qutenza patch is delivered (Wohlrab et al., 2015). A potential explanation for the required high concentration might be a need to reach intracellular TRPV1 (Zhao and Tsang, 2017), about 100-fold higher capsaicin concentrations compared to the plasma membrane were required for a half-maximal effect (Gallego-Sandín et al., 2009).

Second, in Qutenza-treated patients, the density of TRPV1-positive dermal fibers was reduced with corresponding reduction in the detection of touch and pinprick stimuli, but not heat sensation, which is at odds with expectations based on animal data obtained with TRPV1 ablation (Kennedy et al., 2010).

Third, the duration of clinical pain relief clearly exceeds the recovery of skin sensitivity, which is largely normalized after 21 days (Lo Vecchio et al., 2018).

Fourth, the Qutenza effect differs between patients and healthy volunteers. The induced pain in healthy volunteers shows high variability, including subjects classified as non-responders, of which many had barely any capsaicin patch-induced pain (Gustorff et al., 2013; Papagianni et al., 2018). The capsaicin patch may affect A δ -fiber function in humans, and the extent was correlated with pain reduction by the capsaicin patch (Papagianni et al., 2018). Expression of TRPV1 in A δ -fibers during disease states, but not under physiological conditions might serve as explanation.

Finally, one has to keep in mind that for Qutenza to be clinically effective, the treated patient must have functional capsaicin-sensitive nerves, which may not be the case for some individuals. For example, patients with advanced diabetes may lose most of their TRPV1+ afferents as implied by a murine model of diabetic peripheral neuropathy (Pabbidi et al., 2008).

CONCLUDING THOUGHTS: THE MYSTERIES OF CAPSAICIN-SENSITIVE AFFERENTS

Capsaicin research has a long and rich history. In dogs, Högyes reported the hypothermic action of intragastric pepper extract in 1878 as the first indication of the role that TRPV1-positive afferents play in thermoregulation (Högyes, 1878). Yet, almost 150 years later, the exact mechanism by which TRPV1 regulates body temperature remains a mystery. Early studies with microinjection of capsaicin into brain nuclei pointed to the existence of a capsaicin-responsive thermoregulation center in the preoptic area (Jancsó-Gábor et al., 1970). By contrast, results obtained with peripherally restricted TRPV1 antagonists implicated a peripheral target (Tamayo et al., 2008). Other studies (Szolcsányi, 2015) argued that capsaicin “tricks” animals into

feeling hot, and these animals try to cool down by seeking out cold surfaces. Indeed, capsaicin-treated rodents have red ears due to vasodilation, and they spread out in their cages. Moreover, dogs pant and humans sweat in response to capsaicin. However, rats desensitized to capsaicin suffer heat stroke when moved to a heat chamber, implying that capsaicin may impair thermoregulation instead of simply causing hypothermia (Jancsó-Gábor et al., 1970).

TRPV1 agonists and antagonists induce opposite changes in body temperature, hypo- and hyperthermia, respectively. Based on these observations, it was proposed that TRPV1 has an endogenous tone (Gavva, 2008). This model located TRPV1+ afferents responsible for body temperature changes in the gastrointestinal tract. Yet, ablation by resiniferatoxin of the abdominal TRPV1-expressing afferents did not eliminate the capsaicin-sensitive thermoregulatory response (Szolcsányi, 2015). Adding to the confusion, global *Trpv1* knockout mice have normal body temperature (Szelényi et al., 2004). Though one may argue that these animals may have developed alternative thermoregulatory pathways to compensate for the missing TRPV1.

Studies with TRPV1 antagonists further clouded the picture. It turned out that some antagonists caused a febrile reaction in human volunteers whereas others did not change body temperature perceptibly or, paradoxically, they even lowered body temperature [reviewed in Garami et al. (2020)]. Although rational drug design resulted in “temperature neutral” TRPV1 antagonists (substances that did not block proton activation did not cause hyperthermia either), some of these compounds proved “rat-specific” as they still caused hyperthermia in dogs and primates (Lehto et al., 2008). Nevertheless, with NEO6860 there is a TRPV1 antagonist which does not invoke hyperthermia in humans (Brown et al., 2017). As an interesting twist, the undesirable hyperthermia by TRPV1 antagonists in pain patients might even be useful in patients with surgically-induced hypothermia (Schmidt, 2017).

Although TRPV1 is clearly a heat-activated channel with an activation threshold about 40°C (Caterina et al., 1997), the role of TRPV1 in physiological heat sensation remains a mystery. It was suggested that TRPV1 is really a warmth receptor (Yarmolinsky et al., 2016), though the burn injuries in patients taking TRPV1 antagonists argue otherwise. Species-related differences should

also be taken into consideration. For example, camel TRPV1 is not heat-sensitive (Laursen et al., 2016). Rats have heat-sensitive TRPV1 channels, but mole rats living in burrows underground do not.

But maybe the biggest, and probably most important, mystery of all is the discrepancy between the therapeutic potential of TRPV1 antagonists in preclinical models and clinical studies. In experimental animals, TRPV1 antagonists blocked inflammatory, neuropathic, and cancer pain (Szallasi et al., 2007; Moran et al., 2011; Moran and Szallasi, 2018). However, in patients with migraine and osteoarthritis, TRPV1 inhibition disappointed as therapeutic approach (Mayorga et al., 2017; Arsenault et al., 2018; Vécsei et al., 2019). Likewise, TRPV1 antagonists inhibited evoked cough in experimental animals, but did not show any antitussive activity in chronic cough patients (Khalid et al., 2014; Belvisi et al., 2017).

The explanation of the discrepant preclinical and clinical TRPV1 antagonist efficacies remains to be elucidated. Maybe TRPV1 plays a much less important role in human diseases than in their animal models. Or maybe one size simply does not fit all: one ought to select the patient population that could benefit from the TRPV1 antagonist therapy (targeted approach).

In conclusion, capsaicin has been an invaluable tool in sensory pharmacology to dissect a fundamental population of sensory afferents, and to explore their functions in health and disease. The capsaicin receptor was identified as TRPV1, and a number of selective and potent small molecule antagonists developed. Despite the tremendous progress in our understanding of TRPV1 mechanisms, several “mysteries” remain, ranging from the molecular mechanisms of capsaicin desensitization through the exact role of TRPV1 in thermoregulation and heat sensation to the therapeutic value of TRPV1 antagonists.

AUTHOR CONTRIBUTIONS

All authors listed have made a substantial, direct and intellectual contribution to the work, and approved it for publication.

FUNDING

MJMF was supported by FWF grant P 32534-8.

REFERENCES

- Abrahamsen, B., Zhao, J., Asante, C. O., Cendan, C. M., Marsh, S., Martinez-Barbera, J. P., et al. (2008). The cell and molecular basis of mechanical, cold, and inflammatory pain. *Science* 321, 702–705. doi: 10.1126/science.1156916
- Aghazadeh Tabrizi, M., Baraldi, P. G., Baraldi, S., Gessi, S., Merighi, S., and Borea, P. A. (2017). Medicinal chemistry, pharmacology, and clinical implications of TRPV1 receptor antagonists. *Med. Res. Rev.* 37, 936–983. doi: 10.1002/med.21427
- Amaya, F., Shimosato, G., Nagano, M., Ueda, M., Hashimoto, S., Tanaka, Y., et al. (2004). NGF and GDNF differentially regulate TRPV1 expression that contributes to development of inflammatory thermal hyperalgesia. *Eur. J. Neurosci.* 20, 2303–2310. doi: 10.1111/j.1460-9568.2004.03701.x
- Aneiros, E., Cao, L., Papakosta, M., Stevens, E. B., Phillips, S., and Grimm, C. (2011). The biophysical and molecular basis of TRPV1 proton gating. *EMBO J.* 30, 994–1002. doi: 10.1038/emboj.2011.19
- Arendt-Nielsen, L., Harris, S., Whiteside, G. T., Hummel, M., Knappenberger, T., O’Keefe, S., et al. (2016). A randomized, double-blind, positive-controlled, 3-way cross-over human experimental pain study of a TRPV1 antagonist (V116517) in healthy volunteers and comparison with preclinical profile. *Pain* 157, 2057–2067. doi: 10.1097/j.pain.0000000000000610
- Arsenault, P., Chiche, D., Brown, W., Miller, J., Treister, R., Leff, R., et al. (2018). NEO6860, modality-selective TRPV1 antagonist: a randomized, controlled, proof-of-concept trial in patients with osteoarthritis knee pain. *Pain Rep.* 3:e696. doi: 10.1097/PR9.0000000000000696
- Baral, P., Umans, B. D., Li, L., Wallrapp, A., Bist, M., Kirschbaum, T., et al. (2018). Nociceptor sensory neurons suppress neutrophil and $\gamma\delta$ T cell responses in

- bacterial lung infections and lethal pneumonia. *Nat. Med.* 24, 417–426. doi: 10.1038/nm.4501
- Bates, B., Mitchell, K., Keller, J. M., Chan, C.-C., Swaim, W. D., Yaskovich, R., et al. (2010). Prolonged analgesic response of cornea to topical resiniferatoxin, a potent TRPV1 agonist. *Pain* 149, 522–528. doi: 10.1016/j.pain.2010.03.024
- Behrendt, H.-J., Germann, T., Gillen, C., Hatt, H., and Jostock, R. (2004). Characterization of the mouse cold-menthol receptor TRPM8 and vanilloid receptor type-1 VR1 using a fluorometric imaging plate reader (FLIPR) assay. *Br. J. Pharmacol.* 141, 737–745. doi: 10.1038/sj.bjp.0705652
- Belvisi, M. G., Birrell, M. A., Wortley, M. A., Maher, S. A., Satia, I., Badri, H., et al. (2017). XEN-D0501, a novel transient receptor potential Vanilloid 1 Antagonist, does not reduce cough in patients with refractory cough. *Am. J. Respir. Crit. Care Med.* 196, 1255–1263. doi: 10.1164/rccm.201704-0769OC
- Bevan, S., Quallo, T., and Andersson, D. A. (2014). “TRPV1,” in *Mammalian Transient Receptor Potential (TRP) Cation Channels. Handbook of Experimental Pharmacology*, eds B. Nilius, and V. Flockerzi (Berlin: Springer), Vol. 222, 207–245. doi: 10.1007/978-3-642-54215-2_9
- Bevan, S., and Szolcsányi, J. (1990). Sensory neuron-specific actions of capsaicin: mechanisms and applications. *Trends Pharmacol. Sci.* 11, 330–333. doi: 10.1016/0165-6147(90)90237-3
- Bhave, G., Zhu, W., Wang, H., Brasier, D. J., Oxford, G. S., and Gereau, R. W. (2002). cAMP-dependent protein kinase regulates desensitization of the capsaicin receptor (VR1) by direct phosphorylation. *Neuron* 35, 721–731. doi: 10.1016/s0896-6273(02)00802-4
- Bíró, T., Maurer, M., Modarres, S., Lewin, N. E., Brodie, C., Acs, G., et al. (1998). Characterization of functional vanilloid receptors expressed by mast cells. *Blood* 91, 1332–1340. doi: 10.1182/blood.v91.4.1332
- Blair, H. A. (2018). Capsaicin 8% dermal patch: a review in peripheral neuropathic pain. *Drugs* 78, 1489–1500. doi: 10.1007/s40265-018-0982-7
- Blivis, D., Haspel, G., Mannes, P. Z., O'Donovan, M. J., and Iadarola, M. J. (2017). Identification of a novel spinal nociceptive-motor gate control for Aδ pain stimuli in rats. *eLife* 6:e23584. doi: 10.7554/eLife.23584
- Bölcskei, K., Tékus, V., Dézsi, L., Szolcsányi, J., and Petho, G. (2010). Antinociceptive desensitizing actions of TRPV1 receptor agonists capsaicin, resiniferatoxin and N-oleoyldopamine as measured by determination of the noxious heat and cold thresholds in the rat. *Eur. J. Pain* 14, 480–486. doi: 10.1016/j.ejpain.2009.08.005
- Braga Ferreira, L. G., Faria, J. V., Dos Santos, J. P. S., and Faria, R. X. (2020). Capsaicin: TRPV1-independent mechanisms and novel therapeutic possibilities. *Eur. J. Pharmacol.* 887:173356. doi: 10.1016/j.ejphar.2020.173356
- Brenneis, C., Kistner, K., Puopolo, M., Segal, D., Roberson, D., Sisignano, M., et al. (2013). Phenotyping the function of TRPV1-expressing sensory neurons by targeted axonal silencing. *J. Neurosci.* 33, 315–326. doi: 10.1523/JNEUROSCI.2804-12.2013
- Brito, R., Sheth, S., Mukherjee, D., Rybak, L. P., and Ramkumar, V. (2014). TRPV1: a potential drug target for treating various diseases. *Cells* 3, 517–545. doi: 10.3390/cells3020517
- Brown, W., Leff, R. L., Griffin, A., Hossack, S., Aubray, R., Walker, P., et al. (2017). Safety, pharmacokinetics, and pharmacodynamics study in healthy subjects of oral NEO6860, a modality selective transient receptor potential vanilloid subtype 1 antagonist. *J. Pain* 18, 726–738. doi: 10.1016/j.jpain.2017.01.009
- Btsh, J., Fischer, M. J. M., Stott, K., and McNaughton, P. A. (2013). Mapping the binding site of TRPV1 on AKAP79: implications for inflammatory hyperalgesia. *J. Neurosci.* 33, 9184–9193. doi: 10.1523/JNEUROSCI.4991-12.2013
- Byrnes, N. K., and Hayes, J. E. (2013). Personality factors predict spicy food liking and intake. *Food Qual. Prefer.* 28, 213–221. doi: 10.1016/j.foodqual.2012.09.008
- Cao, E., Liao, M., Cheng, Y., and Julius, D. (2013). TRPV1 structures in distinct conformations reveal activation mechanisms. *Nature* 504, 113–118. doi: 10.1038/nature12823
- Caterina, M. J., Leffler, A., Malmberg, A. B., Martin, W. J., Trafton, J., Petersen-Zeitz, K. R., et al. (2000). Impaired nociception and pain sensation in mice lacking the capsaicin receptor. *Science* 288, 306–313. doi: 10.1126/science.288.5464.306
- Caterina, M. J., Schumacher, M. A., Tominaga, M., Rosen, T. A., Levine, J. D., and Julius, D. (1997). The capsaicin receptor: a heat-activated ion channel in the pain pathway. *Nature* 389, 816–824. doi: 10.1038/39807
- Cavanaugh, D. J., Chesler, A. T., Jackson, A. C., Sigal, Y. M., Yamanaka, H., Grant, R., et al. (2011). Trpv1 reporter mice reveal highly restricted brain distribution and functional expression in arteriolar smooth muscle cells. *J. Neurosci.* 31, 5067–5077. doi: 10.1523/JNEUROSCI.6451-10.2011
- Chaiyasit, K., Khovidhunkit, W., and Wittayalerpanya, S. (2009). Pharmacokinetic and the effect of capsaicin in *Capsicum frutescens* on decreasing plasma glucose level. *J. Med. Assoc. Thai.* 92, 108–113.
- Chu, C., Zavala, K., Fahimi, A., Lee, J., Xue, Q., Eilers, H., et al. (2011). Transcription factors Sp1 and Sp4 regulate TRPV1 gene expression in rat sensory neurons. *Mol. Pain* 7:44. doi: 10.1186/1744-8069-7-44
- Chu, Y., Qiu, P., and Yu, R. (2020). Centipede venom peptides acting on ion channels. *Toxins* 12:230. doi: 10.3390/toxins12040230
- Clapham, D. E. (2003). TRP channels as cellular sensors. *Nature* 426, 517–524. doi: 10.1038/nature02196
- Cosens, D. J., and Manning, A. (1969). Abnormal electroretinogram from a *Drosophila* mutant. *Nature* 224, 285–287. doi: 10.1038/224285a0
- Cruz, F., Guimarães, M., Silva, C., and Reis, M. (1997). Suppression of bladder hyperreflexia by intravesical resiniferatoxin. *Lancet* 350, 640–641. doi: 10.1016/S0140-6736(05)63330-2
- Davis, J. B., Gray, J., Gunthorpe, M. J., Hatcher, J. P., Davey, P. T., Overend, P., et al. (2000). Vanilloid receptor-1 is essential for inflammatory thermal hyperalgesia. *Nature* 405, 183–187. doi: 10.1038/35012076
- Derry, S., and Moore, R. A. (2012). Topical capsaicin (low concentration) for chronic neuropathic pain in adults. *Cochrane Datab. Syst. Rev.* 2012:CD010111. doi: 10.1002/14651858.CD010111
- Dirajlal, S., Pauers, L. E., and Stucky, C. L. (2003). Differential response properties of IB(4)-positive and -negative unmyelinated sensory neurons to protons and capsaicin. *J. Neurophysiol.* 89, 513–524. doi: 10.1152/jn.00371.2002
- Docherty, R. J., Yeats, J. C., Bevan, S., and Boddeke, H. W. (1996). Inhibition of calcineurin inhibits the desensitization of capsaicin-evoked currents in cultured dorsal root ganglion neurones from adult rats. *Pflugers Arch.* 431, 828–837. doi: 10.1007/s004240050074
- Docherty, R. J., Yeats, J. C., and Piper, A. S. (1997). Capsazepine block of voltage-activated calcium channels in adult rat dorsal root ganglion neurones in culture. *Br. J. Pharmacol.* 121, 1461–1467. doi: 10.1038/sj.bjp.0701272
- Donnerer, J., and Lembeck, F. (1982). Analysis of the effects of intravenously injected capsaicin in the rat. *Naunyn Schmiedeberg's Arch. Pharmacol.* 320, 54–57. doi: 10.1007/bf00499072
- Eilers, H., Lee, S.-Y., Hau, C. W., Logvinova, A., and Schumacher, M. A. (2007). The rat vanilloid receptor splice variant VR.5'sv blocks TRPV1 activation. *Neuroreport* 18, 969–973. doi: 10.1097/WNR.0b013e328165d1a2
- Fernandes, E. S., Fernandes, M. A., and Keeble, J. E. (2012). The functions of TRPA1 and TRPV1: moving away from sensory nerves. *Br. J. Pharmacol.* 166, 510–521. doi: 10.1111/j.1476-5381.2012.01851.x
- Fischer, M. J. M., Balasuriya, D., Jeggle, P., Goetze, T. A., McNaughton, P. A., Reeh, P. W., et al. (2014). Direct evidence for functional TRPV1/TRPA1 heteromers. *Pflugers Arch.* 466, 2229–2241. doi: 10.1007/s00424-014-1497-z
- Fischer, M. J. M., Btsh, J., and McNaughton, P. A. (2013). Disrupting sensitization of transient receptor potential vanilloid subtype 1 inhibits inflammatory hyperalgesia. *J. Neurosci.* 33, 7407–7414. doi: 10.1523/JNEUROSCI.3721-12.2013
- Fischer, M. J. M., Mak, S. W. Y., and McNaughton, P. A. (2010). Sensitisation of nociceptors - what are ion channels doing? *Open Pain J.* 3, 82–96. doi: 10.2174/1876386301003010082
- Fischer, M. J. M., and Reeh, P. W. (2007). Sensitization to heat through G-protein-coupled receptor pathways in the isolated sciatic mouse nerve. *Eur. J. Neurosci.* 25, 3570–3575. doi: 10.1111/j.1460-9568.2007.05582.x
- Fischer, M. J. M., Reeh, P. W., and Sauer, S. K. (2003). Proton-induced calcitonin gene-related peptide release from rat sciatic nerve axons, in vitro, involving TRPV1. *Eur. J. Neurosci.* 18, 803–810. doi: 10.1046/j.1460-9568.2003.02811.x
- Gallego-Sandín, S., Rodríguez-García, A., Alonso, M. T., and García-Sancho, J. (2009). The endoplasmic reticulum of dorsal root ganglion neurons contains functional TRPV1 channels. *J. Biol. Chem.* 284, 32591–32601. doi: 10.1074/jbc.M109.019687
- Gao, Y., Cao, E., Julius, D., and Cheng, Y. (2016). TRPV1 structures in nanodiscs reveal mechanisms of ligand and lipid action. *Nature* 534, 347–351. doi: 10.1038/nature17964
- Garami, A., Pakai, E., McDonald, H. A., Reilly, R. M., Gomtsyan, A., Corrigan, J. J., et al. (2018). TRPV1 antagonists that cause hypothermia, instead of hyperthermia, in rodents: compounds' pharmacological profiles, in vivo targets,

- thermoeffectors recruited and implications for drug development. *Acta Physiol.* 223:e13038. doi: 10.1111/apha.13038
- Garami, A., Shimansky, Y. P., Rumbus, Z., Vizin, R. C. L., Farkas, N., Hegyi, J., et al. (2020). Hyperthermia induced by transient receptor potential vanilloid-1 (TRPV1) antagonists in human clinical trials: insights from mathematical modeling and meta-analysis. *Pharmacol. Ther.* 208:107474. doi: 10.1016/j.pharmthera.2020.107474
- Gau, P., Poon, J., Ufret-Vincenty, C., Snelson, C. D., Gordon, S. E., Raible, D. W., et al. (2013). The zebrafish ortholog of TRPV1 is required for heat-induced locomotion. *J. Neurosci.* 33, 5249–5260. doi: 10.1523/JNEUROSCI.5403-12.2013
- Gavva, N. R. (2008). Body-temperature maintenance as the predominant function of the vanilloid receptor TRPV1. *Trends Pharmacol. Sci.* 29, 550–557. doi: 10.1016/j.tips.2008.08.003
- Gavva, N. R., Klionsky, L., Qu, Y., Shi, L., Tamir, R., Edenson, S., et al. (2004). Molecular determinants of vanilloid sensitivity in TRPV1. *J. Biol. Chem.* 279, 20283–20295. doi: 10.1074/jbc.M312577200
- Gavva, N. R., Tamir, R., Qu, Y., Klionsky, L., Zhang, T. J., Immke, D., et al. (2005). AMG 9810 [(E)-3-(4-t-butylphenyl)-N-(2,3-dihydrobenzo[b][1,4]dioxin-6-yl)acrylamide], a novel vanilloid receptor 1 (TRPV1) antagonist with antihyperalgesic properties. *J. Pharmacol. Exp. Ther.* 313, 474–484. doi: 10.1124/jpet.104.079855
- Geron, M., Hazan, A., and Priel, A. (2017). Animal toxins providing insights into TRPV1 activation mechanism. *Toxins* 9:326. doi: 10.3390/toxins9100326
- Gmyrek, D. P. (2013). Wilbur lincoln scoville: the prince of peppers. *Pharm. Hist.* 55, 136–156.
- Gomtsyan, A., McDonald, H. A., Schmidt, R. G., Daanen, J. F., Voight, E. A., Segreti, J. A., et al. (2015). TRPV1 ligands with hyperthermic, hypothermic and no temperature effects in rats. *Temperature* 2, 297–301. doi: 10.1080/23328940.2015.1046013
- Goswami, S. C., Mishra, S. K., Maric, D., Kaszas, K., Gonnella, G. L., Clokie, S. J., et al. (2014). Molecular signatures of mouse TRPV1-lineage neurons revealed by RNA-Seq transcriptome analysis. *J. Pain* 15, 1338–1359. doi: 10.1016/j.jpain.2014.09.010
- Gracheva, E. O., Cordero-Morales, J. F., González-Carcacia, J. A., Ingolia, N. T., Manno, C., Aranguren, C. I., et al. (2011). Ganglion-specific splicing of TRPV1 underlies infrared sensation in vampire bats. *Nature* 476, 88–91. doi: 10.1038/nature10245
- Gracheva, E. O., Ingolia, N. T., Kelly, Y. M., Cordero-Morales, J. F., Holloper, G., Chesler, A. T., et al. (2010). Molecular basis of infrared detection by snakes. *Nature* 464, 1006–1011. doi: 10.1038/nature08943
- Gustorff, B., Poole, C., Kloimstein, H., Hacker, N., and Likar, R. (2013). Treatment of neuropathic pain with the capsaicin 8% patch: quantitative sensory testing (QST) in a prospective observational study identifies potential predictors of response to capsaicin 8% patch treatment. *Scand. J. Pain* 4, 138–145. doi: 10.1016/j.sjpain.2013.04.001
- Han, L., Ma, C., Liu, Q., Weng, H.-J., Cui, Y., Tang, Z., et al. (2013). A subpopulation of nociceptors specifically linked to itch. *Nat. Neurosci.* 16, 174–182. doi: 10.1038/nn.3289
- Han, Y., Li, B., Yin, T.-T., Xu, C., Ombati, R., Luo, L., et al. (2018). Molecular mechanism of the tree shrew's insensitivity to spiciness. *PLoS Biol.* 16:e2004921. doi: 10.1371/journal.pbio.2004921
- Hanack, C., Moroni, M., Lima, W. C., Wende, H., Kirchner, M., Adelfinger, L., et al. (2015). GABA blocks pathological but not acute TRPV1 pain signals. *Cell* 160, 759–770. doi: 10.1016/j.cell.2015.01.022
- Harron, D. W., and Kobinger, W. (1984). Facilitation of the Bezold-Jarisch reflex by central stimulation of alpha 2 adrenoceptors in dogs. *Naunyn Schmiedeberg's Arch. Pharmacol.* 325, 193–197. doi: 10.1007/bf00495942
- Hayes, P., Meadows, H. J., Gunthorpe, M. J., Harries, M. H., Duckworth, D. M., Cairns, W., et al. (2000). Cloning and functional expression of a human orthologue of rat vanilloid receptor-1. *Pain* 88, 205–215. doi: 10.1016/s0304-3959(00)00353-5
- Hazan, A., Kumar, R., Matzner, H., and Priel, A. (2015). The pain receptor TRPV1 displays agonist-dependent activation stoichiometry. *Sci. Rep.* 5:12278. doi: 10.1038/srep12278
- Helliwell, R. J., McLatchie, L. M., Clarke, M., Winter, J., Bevan, S., and McIntyre, P. (1998). Capsaicin sensitivity is associated with the expression of the vanilloid (capsaicin) receptor (VR1) mRNA in adult rat sensory ganglia. *Neurosci. Lett.* 250, 177–180. doi: 10.1016/s0304-3940(98)00475-3
- Hjerling-Leffler, J., AlQatari, M., Ernfors, P., and Koltzenburg, M. (2007). Emergence of functional sensory subtypes as defined by transient receptor potential channel expression. *J. Neurosci.* 27, 2435–2443. doi: 10.1523/JNEUROSCI.5614-06.2007
- Högyes, E. (1878). Beiträge zur physiologischen wirkung der bestandteile des *Capsicum annum*. *Arch. Exp. Pathol. Pharmacol.* 9, 117–130.
- Hökfelt, T., Zhang, X., and Wiesenfeld-Hallin, Z. (1994). Messenger plasticity in primary sensory neurons following axotomy and its functional implications. *Trends Neurosci.* 17, 22–30. doi: 10.1016/0166-2236(94)90031-0
- Holzer, P. (1988). Local effector functions of capsaicin-sensitive sensory nerve endings: involvement of tachykinins, calcitonin gene-related peptide and other neuropeptides. *Neuroscience* 24, 739–768. doi: 10.1016/0306-4522(88)90064-4
- Holzer, P. (1991). Capsaicin: cellular targets, mechanisms of action, and selectivity for thin sensory neurons. *Pharmacol. Rev.* 43, 143–201.
- Hori, S., and Saitoh, O. (2020). Unique high sensitivity to heat of axolotl TRPV1 revealed by the heterologous expression system. *Biochem. Biophys. Res. Commun.* 521, 914–920. doi: 10.1016/j.bbrc.2019.10.203
- Huang, J., Zhang, X., and McNaughton, P. A. (2006). Inflammatory pain: the cellular basis of heat hyperalgesia. *Curr. Neuropharmacol.* 4, 197–206. doi: 10.2174/157015906778019554
- Hwang, S. W., Cho, H., Kwak, J., Lee, S. Y., Kang, C. J., Jung, J., et al. (2000). Direct activation of capsaicin receptors by products of lipoxygenases: endogenous capsaicin-like substances. *Proc. Natl. Acad. Sci. U.S.A.* 97, 6155–6160. doi: 10.1073/pnas.97.11.6155
- Iadarola, M. J., and Gonnella, G. L. (2013). Resiniferatoxin for pain treatment: an interventional approach to personalized pain medicine. *Open Pain J.* 6, 95–107. doi: 10.2174/1876386301306010095
- Jancsó, N., and Jancsó, A. (1949). Desensitization of sensory nerve endings. *Kísérletes Orvostudom.* 2(Suppl. 15), 179–226.
- Jancsó, N., and Jancsó-Gábor, A. (1959). Dauerausschaltung der chemischen schmerzempfindlichkeit durch capsaicin. *Naunyn Schmiedeberg's Arch.* 236, 142–145. doi: 10.1007/BF00259094
- Jancsó, N., Jancsó-Gábor, A., and Szolcsányi, J. (1967). Direct evidence for neurogenic inflammation and its prevention by denervation and by pretreatment with capsaicin. *Br. J. Pharmacol. Chemother.* 31, 138–151. doi: 10.1111/j.1476-5381.1967.tb01984.x
- Jancsó-Gábor, A., Szolcsányi, J., and Jancsó, N. (1970). Irreversible impairment of thermoregulation induced by capsaicin and similar pungent substances in rats and guinea-pigs. *J. Physiol.* 206, 495–507. doi: 10.1113/jphysiol.1970.sp009027
- Jordt, S.-E., and Julius, D. (2002). Molecular basis for species-specific sensitivity to “hot” chili peppers. *Cell* 108, 421–430. doi: 10.1016/s0092-8674(02)00637-2
- Jordt, S. E., Tominaga, M., and Julius, D. (2000). Acid potentiation of the capsaicin receptor determined by a key extracellular site. *Proc. Natl. Acad. Sci. U.S.A.* 97, 8134–8139. doi: 10.1073/pnas.100129497
- Karai, L., Brown, D. C., Mannes, A. J., Connelly, S. T., Brown, J., Gandal, M., et al. (2004). Deletion of vanilloid receptor 1-expressing primary afferent neurons for pain control. *J. Clin. Invest.* 113, 1344–1352. doi: 10.1172/JCI20449
- Karai, L. J., Russell, J. T., Iadarola, M. J., and Oláh, Z. (2004). Vanilloid receptor 1 regulates multiple calcium compartments and contributes to Ca²⁺-induced Ca²⁺ release in sensory neurons. *J. Biol. Chem.* 279, 16377–16387. doi: 10.1074/jbc.M310891200
- Kauer, J. A., and Gibson, H. E. (2009). Hot flash: TRPV channels in the brain. *Trends Neurosci.* 32, 215–224. doi: 10.1016/j.tins.2008.12.006
- Kennedy, W. R., Vanhove, G. F., Lu, S.-P., Tobias, J., Bley, K. R., Walk, D., et al. (2010). A randomized, controlled, open-label study of the long-term effects of NGX-4010, a high-concentration capsaicin patch, on epidermal nerve fiber density and sensory function in healthy volunteers. *J. Pain* 11, 579–587. doi: 10.1016/j.jpain.2009.09.019
- Khalid, S., Murdoch, R., Newlands, A., Smart, K., Kelsall, A., Holt, K., et al. (2014). Transient receptor potential vanilloid 1 (TRPV1) antagonism in patients with refractory chronic cough: a double-blind randomized controlled trial. *J. Allergy Clin. Immunol.* 134, 56–62. doi: 10.1016/j.jaci.2014.01.038
- Kichko, T. I., and Reeh, P. W. (2004). Why cooling is beneficial: non-linear temperature-dependency of stimulated iCGRP release from isolated rat skin. *Pain* 110, 215–219. doi: 10.1016/j.pain.2004.03.033

- Kistner, K., Siklosi, N., Babes, A., Khalil, M., Selescu, T., Zimmermann, K., et al. (2016). Systemic desensitization through TRPA1 channels by capsazepine and mustard oil - a novel strategy against inflammation and pain. *Sci. Rep.* 6:28621. doi: 10.1038/srep28621
- Kobayashi, K., Fukuoaka, T., Obata, K., Yamanaka, H., Dai, Y., Tokunaga, A., et al. (2005). Distinct expression of TRPM8, TRPA1, and TRPV1 mRNAs in rat primary afferent neurons with delta/c-fibers and colocalization with trk receptors. *J. Comp. Neurol.* 493, 596–606. doi: 10.1002/cne.20794
- Laird, J. M., Roza, C., De Felipe, C., Hunt, S. P., and Cervero, F. (2001). Role of central and peripheral tachykinin NK1 receptors in capsaicin-induced pain and hyperalgesia in mice. *Pain* 90, 97–103. doi: 10.1016/s0304-3959(00)00394-8
- Launay, P., Fleig, A., Perraud, A. L., Scharenberg, A. M., Penner, R., and Kinet, J. P. (2002). TRPM4 is a Ca²⁺-activated nonselective cation channel mediating cell membrane depolarization. *Cell* 109, 397–407. doi: 10.1016/s0092-8674(02)00719-5
- Laursen, W. J., Schneider, E. R., Merriman, D. K., Bagriantsev, S. N., and Gracheva, E. O. (2016). Low-cost functional plasticity of TRPV1 supports heat tolerance in squirrels and camels. *Proc. Natl. Acad. Sci. U.S.A.* 113, 11342–11347. doi: 10.1073/pnas.1604269113
- Lawless, H., and Stevens, D. A. (1984). Effects of oral chemical irritation on taste. *Physiol. Behav.* 32, 995–998. doi: 10.1016/0031-9384(84)90291-9
- Lee, B. H., and Zheng, J. (2015). Proton block of proton-activated TRPV1 current. *J. Gen. Physiol.* 146, 147–159. doi: 10.1085/jgp.201511386
- Lee, J., Lee, J., Kim, J., Kim, S. Y., Chun, M. W., Cho, H., et al. (2001). N-(3-Acyloxy-2-benzylpropyl)-N'-(4-hydroxy-3-methoxybenzyl) thiourea derivatives as potent vanilloid receptor agonists and analgesics. *Bioorg. Med. Chem.* 9, 19–32. doi: 10.1016/s0968-0896(00)00216-9
- Lee, M. C., Bond, S., Wheeler, D., Scholtes, I., Armstrong, G., McNaughton, P., et al. (2019). A randomized, double blind, placebo-controlled crossover trial of the influence of the HCN channel blocker ivabradine in a healthy volunteer pain model: an enriched population trial. *Pain* 160, 2554–2565. doi: 10.1097/j.pain.0000000000001638
- Lehto, S. G., Tamir, R., Deng, H., Klionsky, L., Kuang, R., Le, A., et al. (2008). Antihyperalgesic effects of (R,E)-N-(2-hydroxy-2,3-dihydro-1H-inden-4-yl)-3-(2-(piperidin-1-yl)-4-(trifluoromethyl)phenyl)-acrylamide (AMG8562), a novel transient receptor potential vanilloid type 1 modulator that does not cause hyperthermia in rats. *J. Pharmacol. Exp. Ther.* 326, 218–229. doi: 10.1124/jpet.107.132233
- Li, C.-L., Li, K.-C., Wu, D., Chen, Y., Luo, H., Zhao, J.-R., et al. (2016). Somatosensory neuron types identified by high-coverage single-cell RNA-sequencing and functional heterogeneity. *Cell Res.* 26, 83–102. doi: 10.1038/cr.2015.149
- Li, J., Daughters, R. S., Bullis, C., Bengiamin, R., Stucky, M. W., Brennan, J., et al. (1999). The cannabinoid receptor agonist WIN 55,212-2 mesylate blocks the development of hyperalgesia produced by capsaicin in rats. *Pain* 81, 25–33. doi: 10.1016/s0304-3959(98)00263-2
- Li, L., Hasan, R., and Zhang, X. (2014). The basal thermal sensitivity of the TRPV1 ion channel is determined by PKC β II. *J. Neurosci.* 34, 8246–8258. doi: 10.1523/JNEUROSCI.0278-14.2014
- Liao, M., Cao, E., Julius, D., and Cheng, Y. (2013). Structure of the TRPV1 ion channel determined by electron cryo-microscopy. *Nature* 504, 107–112. doi: 10.1038/nature12822
- Lo Vecchio, S., Andersen, H. H., and Arendt-Nielsen, L. (2018). The time course of brief and prolonged topical 8% capsaicin-induced desensitization in healthy volunteers evaluated by quantitative sensory testing and vasomotor imaging. *Exp. Brain Res.* 236, 2231–2244. doi: 10.1007/s00221-018-5299-y
- Luo, L., Wang, Y., Li, B., Xu, L., Kamau, P. M., Zheng, J., et al. (2019). Molecular basis for heat desensitization of TRPV1 ion channels. *Nat. Commun.* 10, 1–12. doi: 10.1038/s41467-019-09965-6
- Magerl, W., Wilk, S. H., and Treede, R. D. (1998). Secondary hyperalgesia and perceptual wind-up following intradermal injection of capsaicin in humans. *Pain* 74, 257–268. doi: 10.1016/s0304-3959(97)00177-2
- Maggi, C. A., Patacchini, R., Santicoli, P., Giuliani, S., Geppetti, P., and Meli, A. (1988). Protective action of ruthenium red toward capsaicin desensitization of sensory fibers. *Neurosci. Lett.* 88, 201–205. doi: 10.1016/0304-3940(88)90126-7
- Maihöfner, C. G., and Heskamp, M.-L. S. (2014). Treatment of peripheral neuropathic pain by topical capsaicin: impact of pre-existing pain in the QUEPP-study. *Eur. J. Pain* 18, 671–679. doi: 10.1002/j.1532-2149.2013.00415.x
- Malek, N., Pajak, A., Kolosowska, N., Kucharczyk, M., and Starowicz, K. (2015). The importance of TRPV1-sensitisation factors for the development of neuropathic pain. *Mol. Cell. Neurosci.* 65, 1–10. doi: 10.1016/j.mcn.2015.02.001
- Mandadi, S., Tominaga, T., Numazaki, M., Murayama, N., Saito, N., Armati, P. J., et al. (2006). Increased sensitivity of desensitized TRPV1 by PMA occurs through PKCepsilon-mediated phosphorylation at S800. *Pain* 123, 106–116. doi: 10.1016/j.pain.2006.02.016
- Manitpitikul, P., Flores, C. M., Moyer, J. A., Romano, G., Shalayda, K., Tatikola, K., et al. (2018). A multiple-dose double-blind randomized study to evaluate the safety, pharmacokinetics, pharmacodynamics and analgesic efficacy of the TRPV1 antagonist JNJ-39439335 (mavatript). *Scand. J. Pain* 18, 151–164. doi: 10.1515/sjpain-2017-0184
- Marshall, N. J., Liang, L., Bodkin, J., Dessapt-Baradez, C., Nandi, M., Collot-Teixeira, S., et al. (2013). A role for TRPV1 in influencing the onset of cardiovascular disease in obesity. *Hypertension* 61, 246–252. doi: 10.1161/HYPERTENSIONAHA.112.201434
- Martini, C., Yassen, A., Olofsen, E., Passier, P., Stoker, M., and Dahan, A. (2012). Pharmacodynamic analysis of the analgesic effect of capsaicin 8% patch (QutenzaTM) in diabetic neuropathic pain patients: detection of distinct response groups. *J. Pain Res.* 5, 51–59. doi: 10.2147/JPR.S30406
- Martins, D., Tavares, I., and Morgado, C. (2014). “Hotheaded”: the role OF TRPV1 in brain functions. *Neuropharmacology* 85, 151–157. doi: 10.1016/j.neuropharm.2014.05.034
- Massaad, C. A., Safieh-Garabedian, B., Poole, S., Atweh, S. F., Jabbur, S. J., and Saadé, N. E. (2004). Involvement of substance P, CGRP and histamine in the hyperalgesia and cytokine upregulation induced by intraplantar injection of capsaicin in rats. *J. Neuroimmunol.* 153, 171–182. doi: 10.1016/j.jneuroim.2004.05.007
- Mayorga, A. J., Flores, C. M., Trudeau, J. J., Moyer, J. A., Shalayda, K., Dale, M., et al. (2017). A randomized study to evaluate the analgesic efficacy of a single dose of the TRPV1 antagonist mavatript in patients with osteoarthritis. *Scand. J. Pain* 17, 134–143. doi: 10.1016/j.sjpain.2017.07.021
- McCoy, E. S., and Zylka, M. J. (2014). Enhanced behavioral responses to cold stimuli following CGRP α sensory neuron ablation are dependent on TRPM8. *Mol. Pain* 10:69. doi: 10.1186/1744-8069-10-69
- Mezey, E., Tóth, Z. E., Cortright, D. N., Arzubi, M. K., Krause, J. E., Elde, R., et al. (2000). Distribution of mRNA for vanilloid receptor subtype 1 (VR1), and VR1-like immunoreactivity, in the central nervous system of the rat and human. *Proc. Natl. Acad. Sci. U.S.A.* 97, 3655–3660. doi: 10.1073/pnas.060496197
- Mishra, S. K., Tisel, S. M., Orestes, P., Bhargava, S. K., and Hoon, M. A. (2011). TRPV1-lineage neurons are required for thermal sensation. *EMBO J.* 30, 582–593. doi: 10.1038/emboj.2010.325
- Mitchell, K., Bates, B. D., Keller, J. M., Lopez, M., Scholl, L., Navarro, J., et al. (2010). Ablation of rat TRPV1-expressing Adelta/C-fibers with resiniferatoxin: analysis of withdrawal behaviors, recovery of function and molecular correlates. *Mol. Pain* 6:94. doi: 10.1186/1744-8069-6-94
- Mitchell, K., Lebovitz, E. E., Keller, J. M., Mannes, A. J., Nemenov, M. I., and Iadarola, M. J. (2014). Nociception and inflammatory hyperalgesia evaluated in rodents using infrared laser stimulation after Trpv1 gene knockout or resiniferatoxin lesion. *Pain* 155, 733–745. doi: 10.1016/j.pain.2014.01.007
- Mohapatra, D. P., and Nau, C. (2005). Regulation of Ca²⁺-dependent desensitization in the vanilloid receptor TRPV1 by calcineurin and cAMP-dependent protein kinase. *J. Biol. Chem.* 280, 13424–13432. doi: 10.1074/jbc.M410917200
- Montell, C., Jones, K., Hafen, E., and Rubin, G. (1985). Rescue of the *Drosophila* phototransduction mutation trp by germline transformation. *Science* 230, 1040–1043. doi: 10.1126/science.3933112
- Moran, M. M., McAleander, M. A., Bíró, T., and Szallasi, A. (2011). Transient receptor potential channels as therapeutic targets. *Nat. Rev. Drug Discov.* 10, 601–620. doi: 10.1038/nrd3456
- Moran, M. M., and Szallasi, A. (2018). Targeting nociceptive transient receptor potential channels to treat chronic pain: current state of the field. *Br. J. Pharmacol.* 175, 2185–2203. doi: 10.1111/bph.14044

- Motter, A. L., and Ahern, G. P. (2008). TRPV1-null mice are protected from diet-induced obesity. *FEBS Lett.* 582, 2257–2262. doi: 10.1016/j.febslet.2008.05.021
- Nagy, I., Friston, D., Valente, J. S., Torres Perez, J. V., and Andreou, A. P. (2014). Pharmacology of the capsaicin receptor, transient receptor potential vanilloid type-1 ion channel. *Prog. Drug Res.* 68, 39–76. doi: 10.1007/978-3-0348-0828-6_2
- NCT00804154 (2020). *Resiniferatoxin to Treat Severe Pain Associated With Advanced Cancer*. ClinicalTrials.gov. Available online at: <https://clinicaltrials.gov/ct2/show/NCT00804154> (accessed November 2, 2020).
- NCT04044742 Sorrento Therapeutics Inc (2020). *A Phase 3 Placebo-controlled Study to Evaluate the Efficacy and Safety of Intra-Articular Administration of Resiniferatoxin Versus Placebo for the Treatment of Moderate to Severe Pain Due to Osteoarthritis of the Knee*. ClinicalTrials.gov. Available online at: <https://clinicaltrials.gov/ct2/show/NCT04044742> (accessed October 29, 2020).
- Nelson, E. K. (1919). The constitution of capsaicin, the pungent principle of capsicum. *J. Am. Chem. Soc.* 41, 1115–1121. doi: 10.1021/ja02228a011
- Nguyen, M. Q., Wu, Y., Bonilla, L. S., von Buchholtz, L. J., and Ryba, N. J. P. (2017). Diversity amongst trigeminal neurons revealed by high throughput single cell sequencing. *PLoS One* 12:e0185543. doi: 10.1371/journal.pone.0185543
- Nishihara, E., Hiyama, T. Y., and Noda, M. (2011). Osmosensitivity of transient receptor potential vanilloid 1 is synergistically enhanced by distinct activating stimuli such as temperature and protons. *PLoS One* 6:e22246. doi: 10.1371/journal.pone.0022246
- Numazaki, M., Tominaga, T., Toyooka, H., and Tominaga, M. (2002). Direct phosphorylation of capsaicin receptor VR1 by protein kinase Cepsilon and identification of two target serine residues. *J. Biol. Chem.* 277, 13375–13378. doi: 10.1074/jbc.C200104200
- Ohkita, M., Saito, S., Imagawa, T., Takahashi, K., Tominaga, M., and Ohta, T. (2012). Molecular cloning and functional characterization of *Xenopus tropicalis* frog transient receptor potential vanilloid 1 reveal its functional evolution for heat, acid, and capsaicin sensitivities in terrestrial vertebrates. *J. Biol. Chem.* 287, 2388–2397. doi: 10.1074/jbc.M111.305698
- Okun, A., DeFelice, M., Eyde, N., Ren, J., Mercado, R., King, T., et al. (2011). Transient inflammation-induced ongoing pain is driven by TRPV1 sensitive afferents. *Mol. Pain* 7:4. doi: 10.1186/1744-8069-7-4
- Olah, Z., Szabo, T., Karai, L., Hough, C., Fields, R. D., Caudle, R. M., et al. (2001). Ligand-induced dynamic membrane changes and cell deletion conferred by vanilloid receptor 1. *J. Biol. Chem.* 276, 11021–11030. doi: 10.1074/jbc.M008392200
- O'Neill, J., Brock, C., Olesen, A. E., Andresen, T., Nilsson, M., and Dickenson, A. H. (2012). Unravelling the mystery of capsaicin: a tool to understand and treat pain. *Pharmacol. Rev.* 64, 939–971. doi: 10.1124/pr.112.006163
- Ono, K., Ye, Y., Viet, C. T., Dang, D., and Schmidt, B. L. (2015). TRPV1 expression level in isolectin B₄-positive neurons contributes to mouse strain difference in cutaneous thermal nociceptive sensitivity. *J. Neurophysiol.* 113, 3345–3355. doi: 10.1152/jn.00973.2014
- Orozco, O. E., Walus, L., Sah, D. W., Pepinsky, R. B., and Sanicola, M. (2001). GFRalpha3 is expressed predominantly in nociceptive sensory neurons. *Eur. J. Neurosci.* 13, 2177–2182. doi: 10.1046/j.0953-816x.2001.01596.x
- Pabbidi, R. M., Yu, S.-Q., Peng, S., Khardori, R., Pauza, M. E., and Premkumar, L. S. (2008). Influence of TRPV1 on diabetes-induced alterations in thermal pain sensitivity. *Mol. Pain* 4:9. doi: 10.1186/1744-8069-4-9
- Palecek, F., Sant'Ambrogio, G., Sant'Ambrogio, F. B., and Mathew, O. P. (1989). Reflex responses to capsaicin: intravenous, aerosol, and intratracheal administration. *J. Appl. Physiol.* 67, 1428–1437. doi: 10.1152/jap.1989.67.4.1428
- Papagianni, A., Siedler, G., Sommer, C., and Üçeyler, N. (2018). Capsaicin 8% patch reversibly reduces A-delta fiber evoked potential amplitudes. *Pain Rep.* 3:e644. doi: 10.1097/PR9.0000000000000644
- Patil, M. J., Salas, M., Bialuhin, S., Boyd, J. T., Jeske, N. A., and Akopian, A. N. (2020). Sensitization of small-diameter sensory neurons is controlled by TRPV1 and TRPA1 association. *FASEB J.* 34, 287–302. doi: 10.1096/fj.201902026R
- Perfumi, M., and Sparapassi, L. (1999). Rat offspring treated prenatally with capsaicin do not show some of the irreversible effects induced by neonatal treatment with neurotoxin. *Pharmacol. Toxicol.* 84, 66–71. doi: 10.1111/j.1600-0773.1999.tb00876.x
- Perry, L., Dickau, R., Zarrillo, S., Holst, I., Pearsall, D. M., Piperno, D. R., et al. (2007). Starch fossils and the domestication and dispersal of chili peppers (*Capsicum* spp. L.) in the Americas. *Science* 315, 986–988. doi: 10.1126/science.1136914
- Pogorzala, L. A., Mishra, S. K., and Hoon, M. A. (2013). The cellular code for mammalian thermosensation. *J. Neurosci.* 33, 5533–5541. doi: 10.1523/JNEUROSCI.5788-12.2013
- Por, E. D., Gomez, R., Akopian, A. N., and Jeske, N. A. (2013). Phosphorylation regulates TRPV1 association with β -arrestin-2. *Biochem. J.* 451, 101–109. doi: 10.1042/BJ20121637
- Premkumar, L. S., and Ahern, G. P. (2000). Induction of vanilloid receptor channel activity by protein kinase C. *Nature* 408, 985–990. doi: 10.1038/35050121
- Price, T. J., and Flores, C. M. (2007). Critical evaluation of the colocalization between calcitonin gene-related peptide, substance P, transient receptor potential vanilloid subfamily type 1 immunoreactivities and isolectin B4 binding in primary afferent neurons of the rat and mouse. *J. Pain* 8, 263–272. doi: 10.1016/j.jpain.2006.09.005
- Ray, P., Torck, A., Quigley, L., Wangzhou, A., Neiman, M., Rao, C., et al. (2018). Comparative transcriptome profiling of the human and mouse dorsal root ganglia: an RNA-seq-based resource for pain and sensory neuroscience research. *Pain* 159, 1325–1345. doi: 10.1097/j.pain.00000000000001217
- Ritter, S., and Dinh, T. T. (1992). Age-related changes in capsaicin-induced degeneration in rat brain. *J. Comp. Neurol.* 318, 103–116. doi: 10.1002/cne.903180108
- Rohacs, T. (2015). Phosphoinositide regulation of TRPV1 revisited. *Pflugers Arch.* 467, 1851–1869. doi: 10.1007/s00424-015-1695-3
- Rolke, R., Baron, R., Maier, C., Tölle, T. R., Treede, R.-D., Beyer, A., et al. (2006). Quantitative sensory testing in the German research network on neuropathic pain (DFNS): standardized protocol and reference values. *Pain* 123, 231–243. doi: 10.1016/j.pain.2006.01.041
- Rosenberger, D. C., Binzen, U., Treede, R.-D., and Greffrath, W. (2020). The capsaicin receptor TRPV1 is the first line defense protecting from acute non damaging heat: a translational approach. *J. Transl. Med.* 18:28. doi: 10.1186/s12967-019-02200-2
- Rozin, P., Mark, M., and Schiller, D. (1981). The role of desensitization to capsaicin in chili pepper ingestion and preference. *Chem. Sens.* 6, 23–31. doi: 10.1093/chemse/6.1.23
- Ryu, S., Liu, B., Yao, J., Fu, Q., and Qin, F. (2007). Uncoupling proton activation of vanilloid receptor TRPV1. *J. Neurosci.* 27, 12797–12807. doi: 10.1523/JNEUROSCI.2324-07.2007
- Sánchez-Moreno, A., Guevara-Hernández, E., Contreras-Cervera, R., Rangel-Yescas, G., Ladrón-de-Guevara, E., Rosenbaum, T., et al. (2018). Irreversible temperature gating in trpv1 sheds light on channel activation. *eLife* 7:e36372. doi: 10.7554/eLife.36372
- Sanz-Salvador, A., Andrés-Borderia, A., Ferrer-Montiel, A., and Planells-Cases, R. (2012). Agonist- and Ca²⁺-dependent desensitization of TRPV1 channel targets the receptor to lysosomes for degradation. *J. Biol. Chem.* 287, 19462–19471. doi: 10.1074/jbc.M111.289751
- Schmelz, M., Schmid, R., Handwerker, H. O., and Torebjörk, H. E. (2000). Encoding of burning pain from capsaicin-treated human skin in two categories of unmyelinated nerve fibres. *Brain* 123(Pt 3), 560–571. doi: 10.1093/brain/123.3.560
- Schmidt, W. K. (2017). Turning up the heat on surgical cold. *Temperature* 4, 97–100. doi: 10.1080/23328940.2017.1319453
- Schwarz, M. G., Namer, B., Reeh, P. W., and Fischer, M. J. M. (2017). TRPA1 and TRPV1 antagonists do not inhibit human acidosis-induced pain. *J. Pain* 18, 526–534. doi: 10.1016/j.jpain.2016.12.011
- Serra, J., Campero, M., Bostock, H., and Ochoa, J. (2004). Two types of C nociceptors in human skin and their behavior in areas of capsaicin-induced secondary hyperalgesia. *J. Neurophysiol.* 91, 2770–2781. doi: 10.1152/jn.00565.2003
- Serra, J., Campero, M., and Ochoa, J. (1998). Flare and hyperalgesia after intradermal capsaicin injection in human skin. *J. Neurophysiol.* 80, 2801–2810. doi: 10.1152/jn.1998.80.6.2801
- Shimizu, I., Iida, T., Horiuchi, N., and Caterina, M. J. (2005). 5-Iodoresiniferatoxin evokes hypothermia in mice and is a partial transient receptor potential

- vanilloid 1 agonist in vitro. *J. Pharmacol. Exp. Ther.* 314, 1378–1385. doi: 10.1124/jpet.105.084277
- Silva, C., Avelino, A., Souto-Moura, C., and Cruz, F. (2001). A light- and electron-microscopic histopathological study of human bladder mucosa after intravesical resiniferatoxin application. *BJU Int.* 88, 355–360. doi: 10.1046/j.1464-410x.2001.02339.x
- Silverman, J. D., and Kruger, L. (1990). Selective neuronal glycoconjugate expression in sensory and autonomic ganglia: relation of lectin reactivity to peptide and enzyme markers. *J. Neurocytol.* 19, 789–801. doi: 10.1007/bf01188046
- Simone, D. A., Baumann, T. K., and LaMotte, R. H. (1989). Dose-dependent pain and mechanical hyperalgesia in humans after intradermal injection of capsaicin. *Pain* 38, 99–107. doi: 10.1016/0304-3959(89)90079-1
- Simone, D. A., Ngeow, J. Y., Putterman, G. J., and LaMotte, R. H. (1987). Hyperalgesia to heat after intradermal injection of capsaicin. *Brain Res.* 418, 201–203. doi: 10.1016/0006-8993(87)90982-6
- Sizer, F., and Harris, N. (1985). The influence of common food additives and temperature on threshold perception of capsaicin. *Chem. Sens.* 10, 279–286. doi: 10.1093/chemse/10.3.279
- Smutzer, G., and Devassy, R. K. (2016). Integrating TRPV1 receptor function with capsaicin psychophysics. *Adv. Pharmacol. Sci.* 2016:1512457. doi: 10.1155/2016/1512457
- Sondermann, J. R., Barry, A. M., Jahn, O., Michel, N., Abdelaziz, R., Kügler, S., et al. (2019). Vt1b promotes TRPV1 sensitization during inflammatory pain. *Pain* 160, 508–527. doi: 10.1097/j.pain.0000000000001418
- Staruschenko, A., Jeske, N. A., and Akopian, A. N. (2010). Contribution of TRPV1-TRPA1 interaction to the single channel properties of the TRPA1 channel. *J. Biol. Chem.* 285, 15167–15177. doi: 10.1074/jbc.M110.106153
- Stevens, D. A., and Lawless, H. T. (1986). Putting out the fire: effects of tastants on oral chemical irritation. *Percept. Psychophys.* 39, 346–350. doi: 10.3758/bf03203002
- Stevens, R. M., Ervin, J., Nezzar, J., Nieves, Y., Guedes, K., Burges, R., et al. (2019). Randomized, double-blind, placebo-controlled trial of intraarticular trans-capsaicin for pain associated with osteoarthritis of the knee. *Arthritis Rheumatol.* 71, 1524–1533. doi: 10.1002/art.40894
- Stueber, T., Eberhardt, M. J., Hadamitzky, C., Jangra, A., Schenk, S., Dick, F., et al. (2016). Quaternary lidocaine derivative QX-314 activates and permeates human TRPV1 and TRPA1 to produce inhibition of sodium channels and cytotoxicity. *Anesthesiology* 124, 1153–1165. doi: 10.1097/ALN.0000000000001050
- Sugiura, T., Tominaga, M., Katsuya, H., and Mizumura, K. (2002). Bradykinin lowers the threshold temperature for heat activation of vanilloid receptor 1. *J. Neurophysiol.* 88, 544–548. doi: 10.1152/jn.2002.88.1.544
- Summers, T., Holec, S., and Burrell, B. D. (2014). Physiological and behavioral evidence of a capsaicin-sensitive TRPV-like channel in the medicinal leech. *J. Exp. Biol.* 217, 4167–4173. doi: 10.1242/jeb.110049
- Sweat, K. G., Broatch, J., Borrer, C., Hagan, K., and Cahill, T. M. (2016). Variability in capsaicinoid content and Scoville heat ratings of commercially grown Jalapeño, Habanero and bhut jolokia peppers. *Food Chem.* 210, 606–612. doi: 10.1016/j.foodchem.2016.04.135
- Szallasi, A. (1995). Autoradiographic visualization and pharmacological characterization of vanilloid (capsaicin) receptors in several species, including man. *Acta Physiol. Scand. Suppl.* 629, 1–68.
- Szallasi, A. (1996). Vanilloid-sensitive neurons: a fundamental subdivision of the peripheral nervous system. *J. Peripher. Nerv. Syst.* 1, 6–18.
- Szallasi, A. (2016). Some like it hot (ever more so in the tropics): a puzzle with no solution. *Temperature* 3, 54–55. doi: 10.1080/23328940.2016.1139964
- Szallasi, A., and Blumberg, P. M. (1989). Resiniferatoxin, a phorbol-related diterpene, acts as an ultrapotent analog of capsaicin, the irritant constituent in red pepper. *Neuroscience* 30, 515–520. doi: 10.1016/0306-4522(89)90269-8
- Szallasi, A., and Blumberg, P. M. (1990). Specific binding of resiniferatoxin, an ultrapotent capsaicin analog, by dorsal root ganglion membranes. *Brain Res.* 524, 106–111. doi: 10.1016/0006-8993(90)90498-z
- Szallasi, A., and Blumberg, P. M. (1999). Vanilloid (Capsaicin) receptors and mechanisms. *Pharmacol. Rev.* 51, 159–212.
- Szallasi, A., Blumberg, P. M., Annicelli, L. L., Krause, J. E., and Cortright, D. N. (1999). The cloned rat vanilloid receptor VR1 mediates both R-type binding and C-type calcium response in dorsal root ganglion neurons. *Mol. Pharmacol.* 56, 581–587. doi: 10.1124/mol.56.3.581
- Szallasi, A., Cortright, D. N., Blum, C. A., and Eid, S. R. (2007). The vanilloid receptor TRPV1: 10 years from channel cloning to antagonist proof-of-concept. *Nat. Rev. Drug Discov.* 6, 357–372. doi: 10.1038/nrd2280
- Szelényi, Z., Hummel, Z., Szolcsányi, J., and Davis, J. B. (2004). Daily body temperature rhythm and heat tolerance in TRPV1 knockout and capsaicin pretreated mice. *Eur. J. Neurosci.* 19, 1421–1424. doi: 10.1111/j.1460-9568.2004.03221.x
- Szolcsányi, J. (1984). “Capsaicin sensitive chemoprotective neural system with dual sensory-afferent function,” in *Antidromic Vasodilatation and Neurogenic Inflammation*, eds L. A. Chalk, J. Szolcsányi, and F. Lembeck (Budapest: Akadémiai Kiadó), 27–56.
- Szolcsányi, J. (2004). Forty years in capsaicin research for sensory pharmacology and physiology. *Neuropeptides* 38, 377–384. doi: 10.1016/j.npep.2004.07.005
- Szolcsányi, J. (2015). Effect of capsaicin on thermoregulation: an update with new aspects. *Temperature* 2, 277–296. doi: 10.1080/23328940.2015.1048928
- Szolcsányi, J., and Jancsó-Gábor, A. (1975). Sensory effects of capsaicin congeners I. Relationship between chemical structure and pain-producing potency of pungent agents. *Arzneimittelforschung* 25, 1877–1881.
- Szolcsányi, J., Jancsó-Gábor, A., and Joo, F. (1975). Functional and fine structural characteristics of the sensory neuron blocking effect of capsaicin. *Naunyn Schmiedeberg's Arch. Pharmacol.* 287, 157–169. doi: 10.1007/bf00510447
- Tamayo, N., Liao, H., Stec, M. M., Wang, X., Chakrabarti, P., Retz, D., et al. (2008). Design and synthesis of peripherally restricted transient receptor potential vanilloid 1 (TRPV1) antagonists. *J. Med. Chem.* 51, 2744–2757. doi: 10.1021/jm7014638
- Tang, Y. H., Lu, R., Li, Y. J., Deng, H. W., and Liu, G. Z. (1997). Protection by capsaicin against attenuated endothelium-dependent vasorelaxation due to lysophosphatidylcholine. *Naunyn Schmiedeberg's Arch. Pharmacol.* 356, 364–367. doi: 10.1007/pl00005063
- Thresh, L. T. (1846). Isolation of capsaicin. *Pharm. J.* 6, 941–947.
- Tian, Q., Hu, J., Xie, C., Mei, K., Pham, C., Mo, X., et al. (2019). Recovery from tachyphylaxis of TRPV1 coincides with recycling to the surface membrane. *Proc. Natl. Acad. Sci. U.S.A.* 116, 5170–5175. doi: 10.1073/pnas.1819635116
- Tominaga, M., Caterina, M. J., Malmberg, A. B., Rosen, T. A., Gilbert, H., Skinner, K., et al. (1998). The cloned capsaicin receptor integrates multiple pain-producing stimuli. *Neuron* 21, 531–543. doi: 10.1016/s0896-6273(00)80564-4
- Turner, H., Fleig, A., Stokes, A., Kinet, J.-P., and Penner, R. (2003). Discrimination of intracellular calcium store subcompartments using TRPV1 (transient receptor potential channel, vanilloid subfamily member 1) release channel activity. *Biochem. J.* 371, 341–350. doi: 10.1042/BJ20021381
- Urban, L., and Dray, A. (1991). Capsazepine, a novel capsaicin antagonist, selectively antagonises the effects of capsaicin in the mouse spinal cord in vitro. *Neurosci. Lett.* 134, 9–11. doi: 10.1016/0304-3940(91)90496-G
- Usoskin, D., Furlan, A., Islam, S., Abdo, H., Lönnberg, P., Lou, D., et al. (2015). Unbiased classification of sensory neuron types by large-scale single-cell RNA sequencing. *Nat. Neurosci.* 18, 145–153. doi: 10.1038/nn.3881
- Utreras, E., Prochazkova, M., Terse, A., Gross, J., Keller, J., Iadarola, M. J., et al. (2013). TGF- β 1 sensitizes TRPV1 through Cdk5 signaling in odontoblast-like cells. *Mol. Pain* 9:24. doi: 10.1186/1744-8069-9-24
- Valenzano, K. J., Grant, E. R., Wu, G., Hachicha, M., Schmid, L., Tafesse, L., et al. (2003). N-(4-tertiarybutylphenyl)-4-(3-chloropyridin-2-yl)tetrahydropyrazine-1(2H)-carboxamide (BCTC), a novel, orally effective vanilloid receptor 1 antagonist with analgesic properties: I. in vitro characterization and pharmacokinetic properties. *J. Pharmacol. Exp. Ther.* 306, 377–386. doi: 10.1124/jpet.102.045674
- Vandewauw, I., De Clercq, K., Mulier, M., Held, K., Pinto, S., Van Ranst, N., et al. (2018). A TRP channel trio mediates acute noxious heat sensing. *Nature* 555, 662–666. doi: 10.1038/nature26137
- Vécsei, L., Lukács, M., Tajti, J., Fülöp, F., Toldi, J., and Edvinsson, L. (2019). The therapeutic impact of new migraine discoveries. *Curr. Med. Chem.* 26, 6261–6281. doi: 10.2174/0929867325666180530114534
- Vellani, V., Mapplebeck, S., Moriondo, A., Davis, J. B., and McNaughton, P. A. (2001). Protein kinase C activation potentiates gating of the vanilloid receptor VR1 by capsaicin, protons, heat and anandamide. *J. Physiol.* 534, 813–825. doi: 10.1111/j.1469-7793.2001.00813.x
- Voets, T., Droogmans, G., Wissenbach, U., Janssens, A., Flockerzi, V., and Nilius, B. (2004). The principle of temperature-dependent gating in cold-

- and heat-sensitive TRP channels. *Nature* 430, 748–754. doi: 10.1038/nature02732
- Vos, M. H., Neelands, T. R., McDonald, H. A., Choi, W., Kroeger, P. E., Puttfarcken, P. S., et al. (2006). TRPV1b overexpression negatively regulates TRPV1 responsiveness to capsaicin, heat and low pH in HEK293 cells. *J. Neurochem.* 99, 1088–1102. doi: 10.1111/j.1471-4159.2006.04145.x
- Wagner, T., Poole, C., and Roth-Daniek, A. (2013). The capsaicin 8% patch for neuropathic pain in clinical practice: a retrospective analysis. *Pain Med.* 14, 1202–1211. doi: 10.1111/pme.12143
- Wang, H., Bolognese, J., Calder, N., Baxendale, J., Kehler, A., Cummings, C., et al. (2008). Effect of morphine and pregabalin compared with diphenhydramine hydrochloride and placebo on hyperalgesia and allodynia induced by intradermal capsaicin in healthy male subjects. *J. Pain* 9, 1088–1095. doi: 10.1016/j.jpain.2008.05.013
- Wang, S., Joseph, J., Ro, J. Y., and Chung, M.-K. (2015). Modality-specific mechanisms of protein kinase C-induced hypersensitivity of TRPV1: S800 is a polymodal sensitization site. *Pain* 156, 931–941. doi: 10.1097/j.pain.0000000000000134
- Wang, S., Wang, S., Asgar, J., Joseph, J., Ro, J. Y., Wei, F., et al. (2017). Ca²⁺ and calpain mediate capsaicin-induced ablation of axonal terminals expressing transient receptor potential vanilloid 1. *J. Biol. Chem.* 292, 8291–8303. doi: 10.1074/jbc.M117.778290
- Wanner, S. P., Garami, A., and Romanovsky, A. A. (2011). Hyperactive when young, hypoactive and overweight when aged: connecting the dots in the story about locomotor activity, body mass, and aging in Trpv1 knockout mice. *Aging* 3, 450–454. doi: 10.18632/aging.100306
- Winning, A. J., Hamilton, R. D., Shea, S. A., and Guz, A. (1986). Respiratory and cardiovascular effects of central and peripheral intravenous injections of capsaicin in man: evidence for pulmonary chemosensitivity. *Clin. Sci.* 71, 519–526. doi: 10.1042/cs0710519
- Witting, N., Svensson, P., Arendt-Nielsen, L., and Jensen, T. S. (2000). Repetitive intradermal capsaicin: differential effect on pain and areas of allodynia and punctate hyperalgesia. *Somatosens. Mot. Res.* 17, 5–12. doi: 10.1080/08990220070256
- Wohlrab, J., Neubert, R. H. H., Heskamp, M.-L., and Michael, J. (2015). Cutaneous drug delivery of capsaicin after in vitro administration of the 8% capsaicin dermal patch system. *Skin Pharmacol. Physiol.* 28, 65–74. doi: 10.1159/000362740
- Wood, J. N., Winter, J., James, I. F., Rang, H. P., Yeats, J., and Bevan, S. (1988). Capsaicin-induced ion fluxes in dorsal root ganglion cells in culture. *J. Neurosci.* 8, 3208–3220. doi: 10.1523/JNEUROSCI.08-09-03208.1988
- Wooten, M., Weng, H.-J., Hartke, T. V., Borzan, J., Klein, A. H., Turnquist, B., et al. (2014). Three functionally distinct classes of C-fibre nociceptors in primates. *Nat. Commun.* 5:4122. doi: 10.1038/ncomms5122
- Xu, X. J., Farkas-Szallasi, T., Lundberg, J. M., Hökfelt, T., Wiesenfeld-Hallin, Z., and Szallasi, A. (1997). Effects of the capsaicin analogue resiniferatoxin on spinal nociceptive mechanisms in the rat: behavioral, electrophysiological and in situ hybridization studies. *Brain Res.* 752, 52–60. doi: 10.1016/s0006-8993(96)01444-8
- Yang, R., Xiong, Z., Liu, C., and Liu, L. (2014). Inhibitory effects of capsaicin on voltage-gated potassium channels by TRPV1-independent pathway. *Cell Mol. Neurobiol.* 34, 565–576. doi: 10.1007/s10571-014-0041-1
- Yarmolinsky, D. A., Peng, Y., Pogorzala, L. A., Rutlin, M., Hoon, M. A., and Zuker, C. S. (2016). Coding and plasticity in the mammalian thermosensory system. *Neuron* 92, 1079–1092. doi: 10.1016/j.neuron.2016.10.021
- Yarnitsky, D., Sprecher, E., Zaslansky, R., and Hemli, J. A. (1995). Heat pain thresholds: normative data and repeatability. *Pain* 60, 329–332. doi: 10.1016/0304-3959(94)00132-x
- Zhang, F., Jara-Oseguera, A., Chang, T.-H., Bae, C., Hanson, S. M., and Swartz, K. J. (2018). Heat activation is intrinsic to the pore domain of TRPV1. *Proc. Natl. Acad. Sci. U.S.A.* 115, E317–E324. doi: 10.1073/pnas.1717192115
- Zhang, X., Huang, J., and McNaughton, P. A. (2005). NGF rapidly increases membrane expression of TRPV1 heat-gated ion channels. *EMBO J.* 24, 4211–4223. doi: 10.1038/sj.emboj.7600893
- Zhao, R., and Tsang, S. Y. (2017). Versatile roles of intracellularly located TRPV1 channel. *J. Cell. Physiol.* 232, 1957–1965. doi: 10.1002/jcp.25704
- Zygmunt, P. M., Petersson, J., Andersson, D. A., Chuang, H., Sörgård, M., Di Marzo, V., et al. (1999). Vanilloid receptors on sensory nerves mediate the vasodilator action of anandamide. *Nature* 400, 452–457. doi: 10.1038/22761

Conflict of Interest: The authors declare that the research was conducted in the absence of any commercial or financial relationships that could be construed as a potential conflict of interest.

Copyright © 2020 Fischer, Ciotu and Szallasi. This is an open-access article distributed under the terms of the Creative Commons Attribution License (CC BY). The use, distribution or reproduction in other forums is permitted, provided the original author(s) and the copyright owner(s) are credited and that the original publication in this journal is cited, in accordance with accepted academic practice. No use, distribution or reproduction is permitted which does not comply with these terms.



Projection Neuron Axon Collaterals in the Dorsal Horn: Placing a New Player in Spinal Cord Pain Processing

Tyler J. Browne^{1,2}, David I. Hughes³, Christopher V. Dayas^{1,2}, Robert J. Callister^{1,2} and Brett A. Graham^{1,2*}

¹School of Biomedical Sciences and Pharmacy, Faculty of Health and Medicine, University of Newcastle, Callaghan, NSW, Australia, ²Hunter Medical Research Institute (HMRI), New Lambton Heights, NSW, Australia, ³Institute of Neuroscience Psychology, College of Medical, Veterinary and Life Sciences, University of Glasgow, Glasgow, United Kingdom

OPEN ACCESS

Edited by:

Istvan Nagy,
Imperial College London,
United Kingdom

Reviewed by:

Tasuku Akiyama,
University of Miami, United States
Renée Morris,
University of New South Wales,
Australia

*Correspondence:

Brett A. Graham
brett.graham@newcastle.edu.au

Specialty section:

This article was submitted to
Integrative Physiology,
a section of the journal
Frontiers in Physiology

Received: 10 May 2020

Accepted: 26 November 2020

Published: 21 December 2020

Citation:

Browne TJ, Hughes DI, Dayas CV,
Callister RJ and Graham BA (2020)
Projection Neuron Axon Collaterals in
the Dorsal Horn: Placing a New
Player in Spinal Cord Pain
Processing.
Front. Physiol. 11:560802.
doi: 10.3389/fphys.2020.560802

The pain experience depends on the relay of nociceptive signals from the spinal cord dorsal horn to higher brain centers. This function is ultimately achieved by the output of a small population of highly specialized neurons called projection neurons (PNs). Like output neurons in other central nervous system (CNS) regions, PNs are invested with a substantial axon collateral system that ramifies extensively within local circuits. These axon collaterals are widely distributed within and between spinal cord segments. Anatomical data on PN axon collaterals have existed since the time of Cajal, however, their function in spinal pain signaling remains unclear and is absent from current models of spinal pain processing. Despite these omissions, some insight on the potential role of PN axon collaterals can be drawn from axon collateral systems of principal or output neurons in other CNS regions, such as the hippocampus, amygdala, olfactory cortex, and ventral horn of the spinal cord. The connectivity and actions of axon collaterals in these systems have been well-defined and used to confirm crucial roles in memory, fear, olfaction, and movement control, respectively. We review this information here and propose a framework for characterizing PN axon collateral function in the dorsal horn. We highlight that experimental approaches traditionally used to delineate axon collateral function in other CNS regions are not easily applied to PNs because of their scarcity relative to spinal interneurons (INs), and the lack of cellular organization in the dorsal horn. Finally, we emphasize how the rapid development of techniques such as viral expression of optogenetic or chemogenetic probes can overcome these challenges and allow characterization of PN axon collateral function. Obtaining detailed information of this type is a necessary first step for incorporation of PN collateral system function into models of spinal sensory processing.

Keywords: pain, spinal cord – spinal cord connection, projection neurons, spinal circuits, sensory processing

ROLE OF PNs IN PAIN SIGNALING

The Dorsal Horn and Ascending Pain Pathway

While it is widely appreciated that acute pain serves important biological functions, persistent or ongoing pain serves no apparent biological purpose, but has far-reaching impacts on patients and society. As for other sensory modalities, such as touch, heat/cold, and itch, we have a good understanding of the anatomy of the pathway over which noxious (or potentially painful) signals generated in skin, muscle, joints, and viscera travels to the brain *via* a series of synaptic connections on neurons located in various CNS regions or “pain nodes.” These nodes are located in anatomically discrete regions and, importantly, pain perception can be dramatically altered depending on the way an incoming sensory signal is processed (or passed on) at these nodes. Much effort has therefore focused on understanding how sensory signals are processed within the different nodes of the ascending pain pathway. This is especially the case for the first central node: i.e., the dorsal horn of the spinal cord. Here, signals carried on peripheral afferents combine with inputs from local interneurons (INs) and descending brainstem centers to determine whether information is relayed to higher brain centers. The reception of this information produces the sensory and emotional components of experience, we call pain (reviewed in more detail in: Todd, 2010; Peirs and Seal, 2016). The relay of nociceptive information from the spinal cord dorsal horn to higher brain centers is ultimately achieved by the output and axon of specialized neurons called projection neurons (PNs). This review focuses on what we believe is an overlooked element in dorsal horn pain processing, namely the role of PN axon collaterals that branch and terminate locally. These collaterals must share PN output with other dorsal horn neurons; however, their impact remains to be determined.

PN Anatomy, Projections, and Synaptic Inputs

As the sole output cell of the dorsal horn, PNs have long been recognized as a vital element in spinal pain processing. Classically, they are considered to reside in laminae I and IV–V of the dorsal horn, with superficial and deep PNs being involved in nociceptive specific signaling or more broadly tuned signals that span innocuous to noxious ranges (wide dynamic range), respectively (Christensen and Perl, 1970; Coghill et al., 1993; Craig, 2003; Werber and Basbaum, 2019). Recent work in rodents, whereby PNs are labeled *via* retrograde tracer injections in the brainstem and thalamus, have provided more detailed information on the location of PN somata in the dorsal horn. PNs are concentrated in lamina I and the lateral spinal nucleus, absent in lamina II, and scattered throughout deeper laminae III–VI (Al-Khater et al., 2008) and lamina X (Krotov et al., 2017). Importantly, PNs are not a frequently encountered cell type in the dorsal horn. They make up <5% of the neurons in laminae I, 1% of the neurons in the superficial

dorsal horn (laminae I–II) and are only sparsely scattered in the deeper laminae (Spike et al., 2003; Polgar et al., 2010; Cameron et al., 2015). Their scarcity alone has made PNs difficult to study, and this has hindered our efforts to understand how they integrate with other dorsal horn circuits (Brown, 1982).

The axons of PNs that transmit cutaneous pain, along with thermal and itch modalities, leave the spinal cord by traveling ventrally, crossing to the contralateral cord within a few segments, and finally ascending in the anterolateral tract (Todd, 2017). Transmission of pain associated with deep structures (e.g., viscera) ascends to the brain in either the anterolateral tract or dorsal column pathways (Willis et al., 1999). Textbook accounts have the axons of PNs terminating in the thalamus before being relayed to somatosensory cortex and limbic structures where the pain percept and its emotional or effective responses are generated. While this holds true for primates, recent work in rodents, however, has provided evidence for extensive PN axon terminals in brain stem centers, such as the nucleus of the solitary tract, caudal ventrolateral medulla, parabrachial nucleus (PBN), and the periaqueductal gray (Al-Khater and Todd, 2009; Cameron et al., 2015).

PN Function in Pain Processing

Our current understanding of how the spinal cord relays nociceptive signals from the dorsal horn to higher brain centers is still heavily influenced by the gate control theory of pain (Figure 1A) published in 1965 (Melzack and Wall, 1965). Although many of the fine details in this theory have since been refined and modified, at its heart is the premise that functional inhibition is critical for appropriate spinal sensory processing and normal pain perception (Yaksh, 1999; Zeilhofer et al., 2012; Mendell, 2014). Specifically, the gate control theory assigned inhibitory INs (iINs) a role in preventing touch inputs from activating pain circuits. More recently, a role for excitatory INs (eINs) in pathological pain has been added where polysynaptic pathways associated with touch information infiltrate nociceptive circuits (Neumann et al., 2008; Takazawa and MacDermott, 2010). Thus, IN networks in the dorsal horn are accepted as a critical factor in shaping output signals that are conveyed to the brain by PNs to produce pain. The final element identified in the original gate control theory is “central control,” where signals arising from the brain itself descend and modify spinal dorsal horn activity. Indeed, several brain structures are now well-established sources of descending input to the spinal dorsal horn (Suzuki et al., 2004; François et al., 2017; Lu et al., 2018). They have the capacity to facilitate or inhibit dorsal horn circuits and alter the gain of pain signaling in this region.

Building on the foundations established in gate control theory, our modern view of spinal sensory circuits in the dorsal horn still includes inhibitory gating mechanisms, with more recent transgenic technologies substantially advancing these views (Figure 1B). For example, termination zones are well-established for small diameter nociceptive primary afferents in the superficial dorsal horn and for large diameter tactile primary afferents in the deep dorsal horn (Peirs and Seal, 2016).

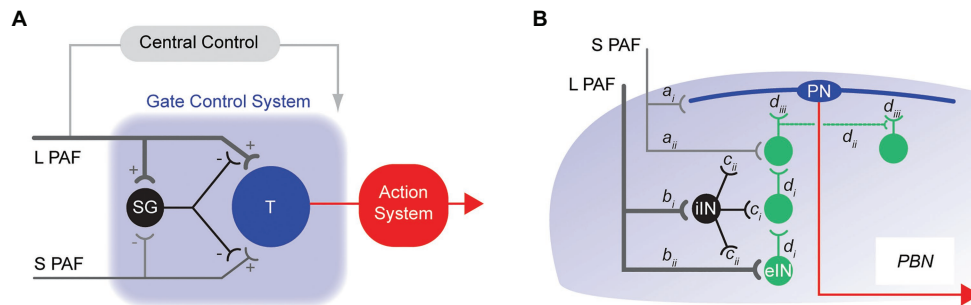


FIGURE 1 | Historical models of spinal pain processing. **(A)**, schematic shows the originally proposed circuitry for the Gate Control Theory of Pain. Touch related sensory information is relayed to the dorsal horn by large fiber (myelinated) primary afferents (L-PAF), whereas nociceptive inputs are relayed by small fiber (unmyelinated) primary afferents (S-PAF). The transmission cell (T) represents the output cell [projection neuron (PN)] of the dorsal horn. An inhibitory interneuron (iIN) is key to the model and is represented as SG. Activation of the SG cell by L-PAF suppresses T cell activation, thereby reducing (gating) pain signaling (i.e., action system). Alternatively, S-PAF activation inhibits SG cell activity, facilitating pain signaling output from the T cell (action system). **(B)**, schematic summarizing more modern views of spinal pain processing circuits. Nociceptive information (S-PAF) is relayed into the superficial dorsal horn and terminates on lamina I PNs (*a_i*) and local interneurons (*a_{ii}*), whereas touch related sensory information (L-PAF) terminates in the deep dorsal horn (*b_i* and *b_{ii}*). Polysynaptic circuits of excitatory interneurons (eINs) (*d_i*) provide a channel for L-PAF input to excite PNs in lamina I (*d_{iii}*). Excitatory interneurons also form polysynaptic networks (*d_{ii}*) that can enhance nociceptive signaling onto lamina I PNs. Populations of iINs also receive sensory signals from the periphery and suppress the activity of nociceptive and touch related circuits via: postsynaptic inhibition of these circuits, and presynaptic inhibition of sensory inputs (*c_i* and *c_{ii}*, respectively). Supra-threshold excitation causes transmission of information along the PN axon (red line) to brainstem and midbrain structures, such as the parabrachial nucleus (PBN).

We now know deep and superficial laminae are linked by polysynaptic circuits of eINs (Brown, 1982; Abraira et al., 2017). This provides a pathway for touch related sensory information to be relayed, or infiltrate, into lamina I and excite lamina I PNs, activating the ascending pain pathway. Populations of eINs have also been shown to form excitatory networks that support reverberating excitation in these circuits. Finally, iINs have been shown to act through a variety of connections to mediate presynaptic and postsynaptic inhibition and thus regulate, or gate, spinal sensory processing. In summary, our current understanding of how nociceptive signals are processed in the dorsal horn is built on the interaction of *three distinct factors* (sensory afferents, dorsal horn INs, and descending brain pathways). Together, the summed activity of these elements determines PN outputs that evoke the pain experience in the brain. We propose PN axon collaterals represent a missing *fourth factor* that must be incorporated into current models of spinal pain processing.

AXON COLLATERALISATION IN THE DORSAL HORN OF THE SPINAL CORD

The anatomy and function of PNs have been studied extensively for over 60 years (Werchberger and Basbaum, 2019) as they play such a key role in channeling highly processed information from the dorsal horn to supraspinal targets. This view is supported by several studies that show a dorsal flow of sensory signals through anatomically and functionally connected dorsal horn IN populations to PNs that can then relay this information to the brain (Cordero-Erausquin et al., 2009; Hachisuka et al., 2018; Smith et al., 2019). The fact that PNs project to readily accessed brainstem centers such as the PBN and periaqueductal

gray has facilitated their identification and study in spinal cord slices through retrograde labeling approaches (Ruscheweyh et al., 2004; Dahlhaus et al., 2005). As a result, we now have some information on the discharge properties (Ruscheweyh et al., 2004), and involvement in certain forms of synaptic plasticity (Ikeda et al., 2006). Few studies have examined PN axon collaterals, even though recent data (see below) show they provide a substrate for pain signals destined for the brain to be shared with, or “copied to” circuitry within the spinal cord. The phenomenon termed efference copy in other systems (Sperry, 1950).

Anatomical Evidence for Axon Collaterals in the Dorsal Horn

Local branches and collaterals arising from the axon of principle (output) neurons are a feature of many CNS regions, including the cortex, cerebellum, and ventral horn of the spinal cord (Figure 2). For dorsal horn PNs, most information we currently have on local axon collaterals comes from electrophysiological studies on identified PNs, where various labels are included in intracellular recording electrodes. Reconstructions of filled PNs have documented axon collaterals in monkey (Beal et al., 1981), cat (Bennett et al., 1981; Brown, 1981; Hylden et al., 1985, 1986; Maxwell and Koerber, 1986; Light et al., 1993), and rat (Luz et al., 2010; Szucs et al., 2010, 2013). Surprisingly, no data are yet available for PN axon collaterals in mouse, despite the increased use of genetically modified mice for pain studies.

Szucs et al. (2010) have provided the most detailed characterization of PN collaterals within lamina I of the rat dorsal horn. They used an *ex vivo* intact spinal cord preparation (lumbosacral enlargement, L1–L6), which allows visualization and identification of presumptive PNs based on their superficial

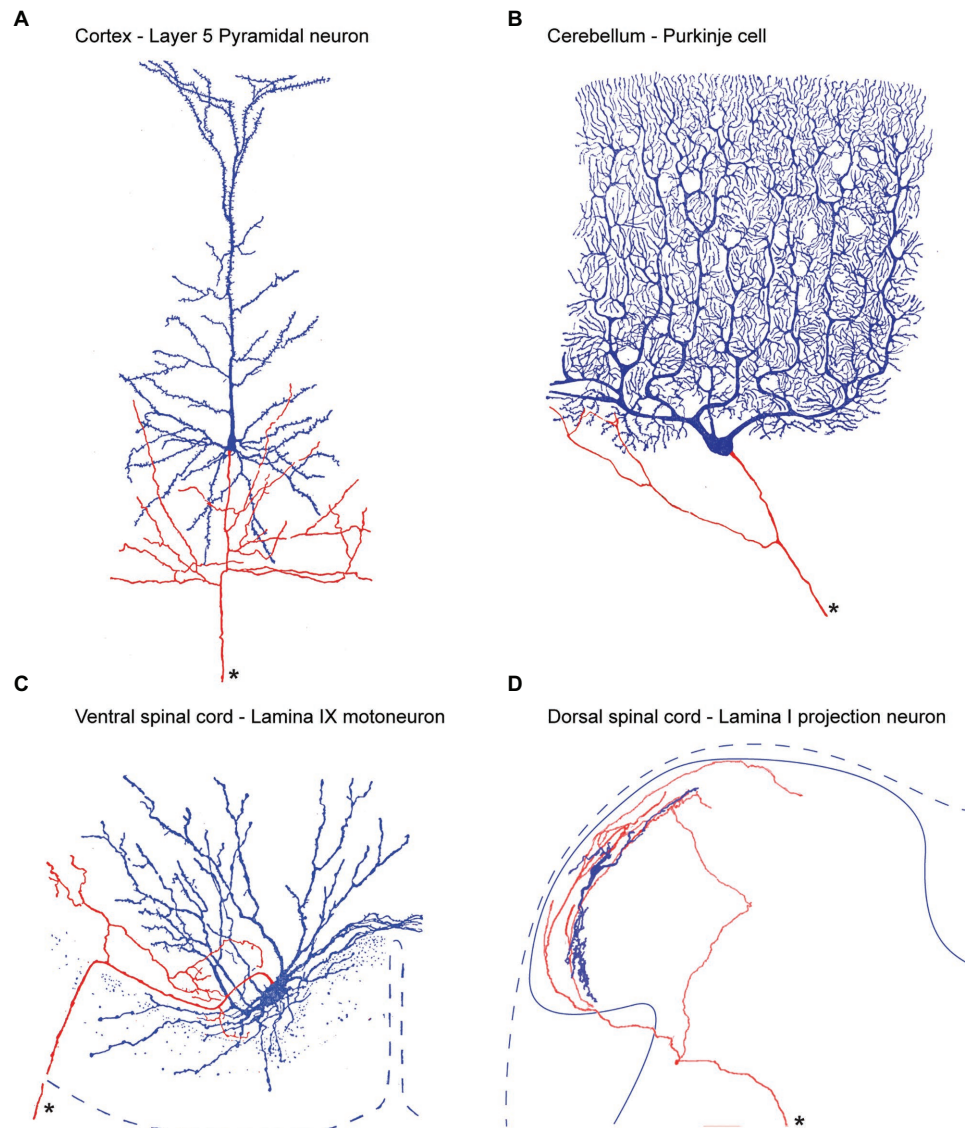


FIGURE 2 | Output neuron axon collateral anatomy throughout the central nervous system. **(A)**, within the cerebral cortex, Layer 5 Pyramidal neurons provide the principle output which can project to regions as distant as the lumbar spinal cord, to neighboring cortical regions, or other brain regions such as the thalamus. In addition, Pyramidal axons branch locally producing an extensive local collateral network (soma and dendrites labeled blue, axon labeled red, and main axon marked by an asterisk). **(B)**, Purkinje cells are the output cells of the cerebellar cortex and send axons to deep cerebellar nuclei. Purkinje cell axons also branch to produce a local collateral network **(C)**, Motoneurons are the output cell of the ventral spinal cord. Their long axons exit the ventral spinal root and innervate skeletal muscle. In addition, motoneuron axons branch within the ventral horn to produce an extensive local collateral network. **(D)**, Lamina I PNs are the output cell of the dorsal spinal cord. Their main axon crosses the midline and ascends to various regions including the PBN, and periaqueductal gray, and thalamus. Lamina I PNs also exhibit an extensive local collateral network. Panels **(A–C)** modified from (Cajal, 1952) and **(D)** is from (Szucs et al., 2010).

location, large size, and the *post hoc* tracing of filled-cell axons tracking to the anterolateral tract. Notably, data using this approach showed PN axon collateral territories were extensive and confined to the ipsilateral cord. PN axon collaterals could be classified into four types according to their course and territory in the dorsal horn. Dorsal collaterals ramified extensively within laminae I–IV of the dorsal horn gray matter and sometimes entered Lissauer's tract. Ventral collaterals projected into the propriospinal and ventral motor territories (Flynn et al., 2011).

Lateral collaterals ran primarily in the rostrocaudal plane for about a spinal segment. Finally, mixed collaterals exhibited combinations of the other three types. Importantly, in all four types, en-passant and terminal synaptic boutons were observed on PN axon collaterals – implying the potential for local (spinal) signaling. The authors concluded that PN axon collaterals likely have an important function in local circuits including intra- and intersegmental spinal cord processing. Furthermore, this widespread distribution positions the ascending signals carried

by PN collaterals to influence the spinal circuits that encode pain, itch, touch, visceral pain, as well as proprioception and motor output.

Neurochemical Phenotype and Function of PN Axon Collaterals

The Todd group (Cameron et al., 2015) showed *via* retrograde labeling and immunohistochemistry that 97% of the synaptic boutons on PN axons in the PBN expressed VGLUT2. This matches the expected excitatory nature of PNs. Presumably, this would also apply to the *en passant* synaptic boutons on PN collaterals within the spinal cord. vGLUT2 is also detected in the majority (>85%) of the output cells in the medullary dorsal horn (Ge et al., 2010; Zhang et al., 2018). Assuming conservation between the spinal and brainstem dorsal horns, these observations further support the likelihood that spinal cord PN collaterals mediate excitatory actions on their immediate, local targets. While the case for glutamate signaling is clear, this work does not exclude the potential for PN terminals to also release neurotransmitters other than glutamate. For example, the same work that confirmed VGLUT2 expression in PN axons also reported some terminals expressed Substance P (~16%). Furthermore, precedent for co-transmission can be found in the ventral horn of the spinal cord, where motoneurons have been shown to utilize multiple neurotransmitters (acetylcholine and glutamate) at synapses in their axon collaterals that excite Renshaw cells (Renshaw, 1946; Callister and Graham, 2010; Lamotte d'Incamps et al., 2017; Callister et al., 2020). Thus, the available anatomical data suggest extensively ramified PN axon collaterals can make excitatory synaptic connections with neurons in the dorsal, intermediate, and ventral horn; however, the functional role of additional transmitters (e.g., peptides) remains to be established.

To the best of our knowledge, there is only one demonstration of a functional synaptic connection made by a PN axon collateral within dorsal horn, albeit from a putative PN in the young rat spinal cord. In this example, Luz et al. (2010) used paired patch clamp electrophysiology and recorded a monosynaptic excitatory connection between two putative PNs. It was not reported if the connection was strong enough to generate a spike in the post-synaptic PN; however, inputs from other lamina I INs were capable of generating spikes in PNs. These data, coupled with the anatomical data presented above, strongly suggest PN axon collaterals have an active role in the dorsal horn of the spinal cord. Substantially, more information will be required; however, before PN axon collateral signaling can be incorporated into models of spinal sensory processing.

AXON COLLATERAL FUNCTION IN OTHER CNS REGIONS

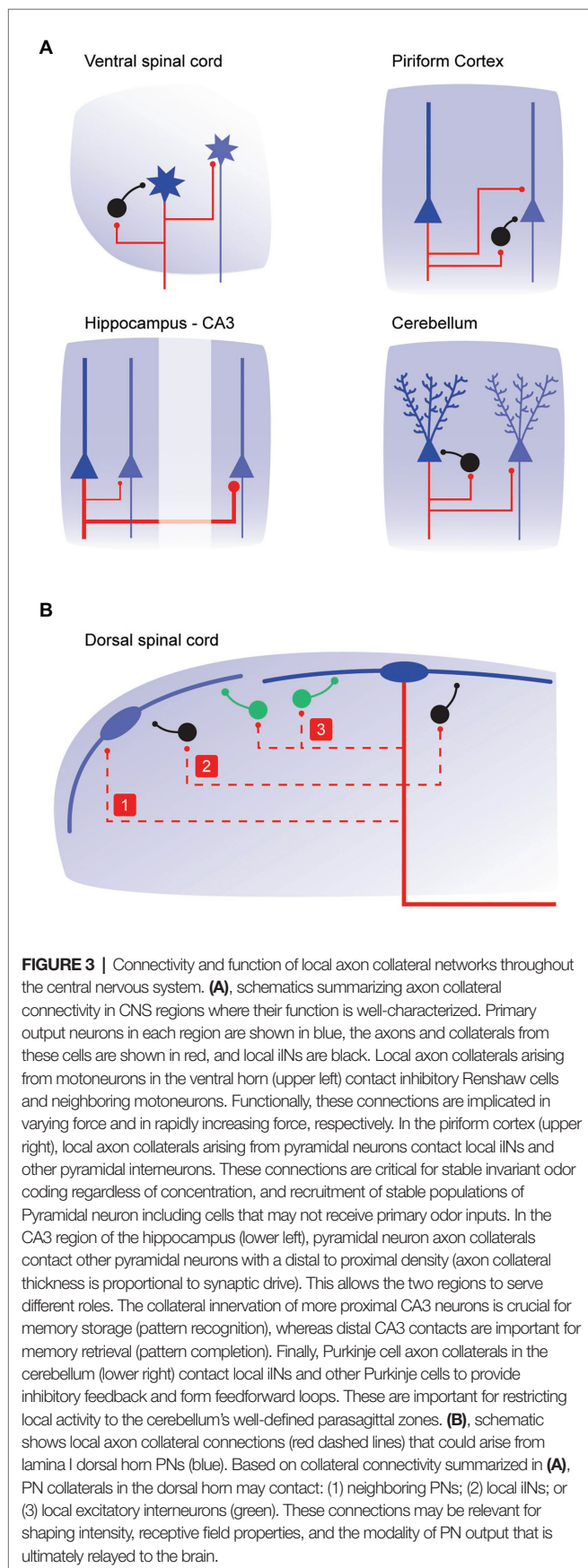
Since the time of Cajal, neuroscientists have found it useful to organize the elements that make up various CNS regions into three components: afferent inputs that bring information to a region, INs that are involved in local processing, and

principal/relay/output or PNs that transmit processed signals. The latter sends out a long axon that carries information to another CNS region or peripheral target. This model also acknowledges a role for local collaterals arising from output neurons (e.g., “the principal or output neuron can also take part in local processing and does so by axon collaterals that ramify extensively among local circuit neurons” Shepherd, 2004).

While the roles of dorsal horn PN axon collaterals remains unknown, the function of such recurrent circuitry has been clarified within other CNS regions. For example, the Schaffer-collateral system in hippocampus, composed of axon collaterals of CA3 pyramidal cells, forms an integral part of the trisynaptic pathway, and the synapses they form onto CA1 pyramidal cells are the most widely studied synaptic connections of any within the central nervous system (Freund and Buzsáki, 1996). In the following section, we discuss some of these PN-derived feedback circuits, and by highlighting common motifs among these examples, provide insight into the potential functions within the spinal dorsal horn.

Our best understood example of axon collateral function in the spinal cord stems from studies of “recurrent inhibition” in the ventral horn of the spinal cord (**Figure 3A**). As early as the 1940s, there was compelling anatomical evidence for the existence of motoneuron axon collaterals. Importantly, these collaterals terminated in the vicinity of other ventral horn cells. The function of this collateral system was initially studied by Birdsey Renshaw in a series of experiments over 1938–1941 (see Callister et al., 2020). Renshaw showed that “reflex” motoneuron activity, initiated by stimulating dorsal roots or dorsal columns, was inhibited by stimulating cut ventral roots (Renshaw, 1941). He proposed that motoneuron axon collaterals produced inhibition in the ventral horn. Eccles subsequently studied the important inhibitory neuron that was underpinning the observation, termed the Renshaw cell (Eccles et al., 1954). It represents one of the first neural circuits ever described in the CNS, and by extension the first to involve axon collateral signaling.

In its simplest form, activation of the motoneuron and its axon collateral, results in the recruitment of the Renshaw cells. In turn, these Renshaw cells then inhibit the homonymous motoneuron pool with glycinergic inhibition. This feedback is not trivial, and evidence has shown that input from one Renshaw cell can cease activity in its coupled motoneuron (Bhumbra et al., 2014). This coupling arrangement has been viewed as a variable gain regulator that allows muscles to produce a wide range of contractile forces (Moore et al., 2015). It is also thought to be important in preventing the runaway excitation of the motoneuron, acting to enable smooth motor control and prevent muscle spasticity such as in *Clostridium Tetani* infection (tetanus). More recently, motoneuron axon collaterals have been shown to target neighboring motoneuron (Spike et al., 2003; Bhumbra and Beato, 2018). Collateral input is to both local (intra-segmental) and more distal (inter-segmental) motoneurons and is thought to play a role in progressively recruiting motor neurons to rapidly increase muscle force. As previously noted, PN collaterals in the dorsal horn are similarly arranged in both inter- and intra-segmental territories.



This suggests they could provide recurrent inhibition to PNs as well as recruiting neighboring PNs. The capacity of the motoneuron circuit to both alter signaling range and rapidly increase the intensity of ventral horn outputs implies PN axon collaterals may help tune the boundaries of sensation and the intensity of pain signals that are ultimately transmitted to the brain.

In the brain, output neurons in the cerebral cortex, hippocampus and amygdala also give rise to extensive local axon collaterals and, in these regions, much is also known about function. In the olfactory (piriform) cortex, axon collaterals form a sparse excitatory network among output “pyramidal” neurons (**Figure 3A**). This connectivity is thought to allow odors to recruit ensembles of pyramidal neurons including cells that do not directly receive an odor input (Franks et al., 2011). Pyramidal neuron collaterals also activate feedforward and feedback inhibition, *via* local iINs. The latter is critical for stable “invariant” odor coding, regardless of changes in odor concentration (Bolding and Franks, 2018). In the basolateral nucleus of the amygdala, principal cell collaterals show spatial selectivity whereby iINs are contacted by terminals on proximal collaterals, and, other principal cells are contacted by those on more distal collaterals (Duvarci and Pare, 2014). This configuration is considered important to prevent runaway excitation within the primary cell, while allowing associative interactions with more distal principal cell populations that underpin associative conditioning (such as fear). In the hippocampus, the Schaffer-collateral system plays a critical role in memory processing (**Figure 3A**). Specifically, graded proximal to distal collateral density along CA3 allows proximal CA3 to perform important roles in responding to novel cues with a tendency to remap and store new memories (i.e., as in pattern recognition). Alternatively, distal CA3 with extensive collaterals is thought to drive memory retrieval functions (pattern completion), especially with degraded or incomplete input patterns (Lee et al., 2015). A similar associative excitatory collateral network has also been described for grid cells in medial entorhinal cortex. This is thought to be important for the correct neural representation of space (Couey et al., 2013). Extending these observations to spinal sensory processing in the dorsal horn, a similar excitatory collateral network connecting PNs, coupled with collateral connectivity to iINs could easily play a role in the reliable representation of sensory signals from the body surface (i.e., receptive fields). Furthermore, in terms of pain signaling, this arrangement would allow for receptive field expansion as observed following tissue damage (**Figure 3B**).

A final example of collateral signaling highlights that these output neuron configurations are not always excitatory. In the cerebellar cortex, the major output neuron, the Purkinje cell, is inhibitory. Various models of cerebellar function have existed for years (Eccles et al., 1967) based on a feedforward circuit with synaptic activity flowing from mossy fibers through granule cells to the Purkinje cell. These neurons have an extensive axon collateral system that is organized preferentially in the parasagittal plane (Watt et al., 2009). Recent advances have allowed detailed functional investigation of Purkinje cell collaterals in adult rodents. Witter et al., 2016,

have shown these collaterals provide inhibitory feedback to several classes of INs and also contact neighboring Purkinje cells (Witter et al., 2016). These important feedback loops are considered important for regulating activity in the cerebellum's well-known parasagittal zones. Thus, even when collaterals arise from inhibitory populations they have been shown to play a role in delineating functional borders and confining excitation.

In summary, there are precedents for axon collaterals playing important roles in the function of various CNS regions *via* either excitation or inhibition (**Figure 3A**). Generally, these output neuron collaterals drive feedback inhibition through local INs or have amplifier and associative functions *via* feedforward excitation. Such data are not yet available for PN axon collaterals, however, insights from other collateral systems throughout the CNS suggest that new information on PN axon collaterals will have a major impact on the way we understand spinal sensory processing (**Figure 3B**).

NEW TECHNIQUES AND A NEW APPROACH TO STUDY PN AXON COLLATERALS

Two major factors have likely hampered our understanding of PN axon collateral signaling in the dorsal horn, compared to the relatively advanced understanding of collateral signaling in other regions. First, the scarcity of PNs in the dorsal horn (~1% of lamina I–II neurons vs. 70–90% principle neurons in cortex, hippocampus, and amygdala) makes them difficult to target with a microelectrode. Second, a definitive genetic characteristic or “signature” that distinguishes PNs from other dorsal horn cells remains to be identified. This contrasts with ventral horn motoneurons, for example, that can be easily identified by location (Lamina IX) and cholinergic markers.

A series of recent technical advances now permit progress in understanding the role PN axon collaterals in spinal sensory processing circuits. Specifically, viral gene transduction with specific trafficking and tropism properties allows gene targeting and protein expression to be directed to neuronal populations according to where their axons ultimately project. This is similar to the classical retrograde labeling approaches that involved injection of tracers, such as HRP, WGA, fast blue, and fluorescent microspheres, into brain regions, such as PBN, periaqueductal gray, thalamus, or rostroventromedial medulla. Application of modern gene targeting and protein expression approaches results in robust expression of fluorescent proteins (e.g., GFP, mCherry, and TdTomato). This allows visualization of dendritic and axonal processes to an extent not possible using classical tracers. Furthermore, multi-labeling experiments using brainbow constructs, a genetic cell-labeling technique that identifies individual cells with unique color hues (Weissman and Pan, 2015), will allow mapping of the relationship between populations of dorsal horn PNs in great detail.

Viral approaches also present an opportunity to express proteins that allow control of PN activity *via* optogenetic or

chemogenetic techniques, both *in vitro* and *in vivo*. These methods are particularly relevant to our efforts to study PN axon collateral function in the dorsal horn. For example, channelrhodopsin-2 assisted circuit mapping (CRACM) could be achieved by selective photostimulation of PNs in acutely prepared tissue slices. The CRACM approach has been used to functionally characterize and map axon collateral connections of semilunar cells (a specific type of principle/output neuron) in piriform cortex. Optogenetic activation of semilunar cells produced recurrent excitation of collaterals that contacted a different population of output cells, termed superficial cells (Choy et al., 2017). CRACM has also been used to study the targets of Purkinje cell axon collaterals in the cerebellum. Notably, optogenetically identified connections contacted other Purkinje cells, molecular layer INs, and Lugaro INs, but *not* Golgi INs (Witter et al., 2016). These results highlight how the optogenetic approach can uncover functional collateral connectivity patterns that would take years to acquire using the low-yield and technically demanding paired patch clamp recording approach.

Transgenic manipulations that silence synaptic function have also been applied while using *in vitro* slice electrophysiology, as well as in anesthetized and freely behaving animals to study local axon collateral function. For example, work in the piriform cortex has used transgenic expression of tetanus toxin light chain (TeLC) to silence pyramidal cell axon collateral synapses while retaining the intrinsic excitability of these cells (Bolding and Franks, 2018). This approach confirmed local collateral signaling that recruited feedback iINs was critical for tuning the local response to concentration-invariant coding of odors. The same approach has also been used to silence the recurrent excitatory circuits of CA3 pyramidal neurons and assess the collateral network's role in epilepsy (Yu et al., 2016). This manipulation reduced kainic acid-induced seizure activity, hippocampal epileptiform oscillatory activity, and cFos expression. This confirmed the long-held view that CA3 pyramidal neurons, and their extensive axon collateral networks, are critical for kainic-acid triggered seizures. These two examples highlight how transgenic targeting of axons and synaptic function allows axon collateral function to be comprehensively studied. Similar approaches in the dorsal horn may help clarify the importance of local PN axon collaterals in sensory experience, although the anatomy of the nociceptive pathway does present some challenges. Specifically, TeLC silencing would prevent local collateral signaling as well as silencing the ascending connections that rely on nociceptive signals to the brain. Thus, it may be difficult to attribute any behavioral phenotype to a specific connection type. Despite this, the proximity of local collateral synapses to the PN cell body, versus the distant projections synapsing in the brain, may be advantageous. This could open a window whereby high local (spinal) TeLC expression achieves local silencing, before significant TeLC expression reaches the more distal brain connections. This delay could allow the direct assessment of PN derived recurrent feedback in the dorsal horn while maintaining normal neuronal excitability and upstream transmission of nociceptive signals.

CONCLUSION AND FUTURE DIRECTIONS

The literature reviewed above provides clear evidence that a local axon collateral system exists in the spinal dorsal horn arising from its output cell, the PN. The only functional information on PN axon collaterals in the dorsal horn comes from a single observation at a connection between two putative PNs in tissue from a young animal. No other functional information is available on these connections. A more advanced understanding of local axon collateral function in other CNS regions suggests “feedforward” excitation of other PNs, and recurrent “feedback” inhibition through connections with iINs is likely to exist. Fortunately, the experiments required to clarify these proposed roles are now possible because of new transgenic and viral techniques that can be applied in the mouse. Accordingly, we suggest the following pressing questions can and need to be answered:

1. Do mouse dorsal horn PNs exhibit branching and local axon collaterals? Anatomical evidence for this and the existence of synaptic specializations has been provided in other species, but not mouse.
2. Do dorsal horn PNs that reside outside laminae I give rise to collateral systems and are they similar? The most detailed characterization, available in rat, only reported on axon collaterals arising from superficial lamina I PNs that could be visualized in an *ex vivo* intact spinal cord preparation.
3. Which type of dorsal horn neuron do PN axon collaterals target? As outlined above, three broad dorsal horn populations include PNs, eINs, and iINs.

As answers to these questions become available it will be possible to incorporate PN axon collateral signaling into

models of spinal sensory processing and thereby include an important new player in these circuits. While it is not yet possible to definitively predict how this information will change our understanding of spinal pain processing, available evidence from other output neurons suggests sharing the ascending “output” pain signal with local spinal pain circuits will be important. This information needs to be first collected under naïve uninjured conditions. Future experiments can then ask whether dysfunctional collateral signaling exists in pain models (both neuropathic and inflammatory). Finally, if this detailed information identifies a discrete post-synaptic arrangement of PN axon collaterals, for example capable of blunting pain signals (such as the Renshaw cell), it will represent an attractive foundation from which to develop targeted, and selective new pain therapies.

AUTHOR CONTRIBUTIONS

All authors contributed equally to all planning, writing and editing associated with this invited submission to a Frontiers Research Topic.

FUNDING

This work was funded by the National Health and Medical Research Council (NHMRC) of Australia (grants 631000, 1043933, 1144638, and 1184974 to BG and RC), the Biotechnology and Biological Sciences Research Council (BB/P007996/1 to DH), and the Hunter Medical Research Institute (grant to BG and RC). TB is supported by a scholarship from Glenn Moss through the Hunter Medical Research Institute.

REFERENCES

- Abraira, V. E., Kuehn, E. D., Chirila, A. M., Springel, M. V., Toliver, A. A., Zimmerman, A. L., et al. (2017). The cellular and synaptic architecture of the mechanosensory dorsal horn. *Cell* 168, 295.e19–310.e19. doi: 10.1016/j.cell.2016.12.010
- Al-Khater, K. M., Kerr, R., and Todd, A. J. (2008). A quantitative study of spinothalamic neurons in laminae I, III, and IV in lumbar and cervical segments of the rat spinal cord. *J. Comp. Neurol.* 511, 1–18. doi: 10.1002/cne.21811
- Al-Khater, K. M., and Todd, A. J. (2009). Collateral projections of neurons in laminae I, III, and IV of rat spinal cord to thalamus, periaqueductal gray matter, and lateral parabrachial area. *J. Comp. Neurol.* 515, 629–646. doi: 10.1002/cne.22081
- Beal, J. A., Penny, J. E., and Bicknell, H. R. (1981). Structural diversity of marginal (lamina I) neurons in the adult monkey (*Macaca mulatta*) lumbosacral spinal cord: a golgi study. *J. Comp. Neurol.* 202, 237–254. doi: 10.1002/cne.902020209
- Bennett, G. J., Abdelmoumene, M., Hayashi, H., Hoffert, M. J., and Dubner, R. (1981). Spinal cord layer I neurons with axon collaterals that generate local arbors. *Brain Res.* 209, 421–426. doi: 10.1016/0006-8993(81)90164-5
- Bhumra, G. S., Bannatyne, B. A., Watanabe, M., Todd, A. J., Maxwell, D. J., Beato, M., et al. (2014). The recurrent case for the rensaw cell. *J. Neurosci.* 34, 12919–12932. doi: 10.1523/JNEUROSCI.0199-14.2014
- Bhumra, G. S., and Beato, M. (2018). Recurrent excitation between motoneurons propagates across segments and is purely glutamatergic. *PLoS Biol.* 16:e2003586. doi: 10.1371/journal.pbio.2003586
- Bolding, K. A., and Franks, K. M. (2018). Recurrent cortical circuits implement concentration-invariant odor coding. *Science* 361:eaat6904. doi: 10.1126/science.aat6904
- Brown, A. G. (1981). The spinocervical tract. *Prog. Neurobiol.* 17, 59–96. doi: 10.1016/0301-0082(81)90004-6
- Brown, A. G. (1982). The dorsal horn of the spinal cord. *Q. J. Exp. Physiol.* 67, 193–212. doi: 10.1113/expphysiol.1982.sp002630
- Cajal, S. R. (1952). *Histologie du système nerveux de l'homme and des vertèbres*. Madrid: Instituto Ramon Y Cajal.
- Callister, R. J., Brichta, A. M., Schaefer, A. T., Graham, B. A., and Stuart, D. G. (2020). Pioneers in CNS inhibition: 2. Charles Sherrington and John Eccles on inhibition in spinal and supraspinal structures. *Brain Res.* 1734:146540. doi: 10.1016/j.brainres.2019.146540
- Callister, R. J., and Graham, B. A. (2010). Early history of glycine receptor biology in mammalian spinal cord circuits. *Front. Mol. Neurosci.* 3:13. doi: 10.3389/fnmol.2010.00013
- Cameron, D., Polgár, E., Gutierrez-Mecinas, M., Gomez-Lima, M., Watanabe, M., and Todd, A. J. (2015). The organisation of spinoparabrachial neurons in the mouse. *Pain* 156, 2061–2071. doi: 10.1097/j.pain.0000000000000270
- Choy, J. M. C., Suzuki, N., Shima, Y., Budisantoso, T., Nelson, S. B., and Bekkers, J. M. (2017). Optogenetic mapping of intracortical circuits originating from semilunar cells in the piriform cortex. *Cereb. Cortex* 27, 589–601. doi: 10.1093/cercor/bhv258
- Christensen, B. N., and Perl, E. R. (1970). Spinal neurons specifically excited by noxious or thermal stimuli: marginal zone of the dorsal horn. *J. Neurophysiol.* 33, 293–307. doi: 10.1152/jn.1970.33.2.293

- Coghil, R. C., Mayer, D. J., and Price, D. D. (1993). Wide dynamic range but not nociceptive-specific neurons encode multidimensional features of prolonged repetitive heat pain. *J. Neurophysiol.* 69, 703–716. doi: 10.1152/jn.1993.69.3.703
- Cordero-Erausquin, M., Allard, S., Dolique, T., Bachand, K., Ribeiro-da-Silva, A., and De Koninck, Y. (2009). Dorsal horn neurons presynaptic to lamina I spinoparabrachial neurons revealed by transynaptic labeling. *J. Comp. Neurol.* 517, 601–615. doi: 10.1002/cne.22179
- Couey, J. J., Witoelar, A., Zhang, S. J., Zheng, K., Ye, J., Dunn, B., et al. (2013). Recurrent inhibitory circuitry as a mechanism for grid formation. *Nat. Neurosci.* 16, 318–324. doi: 10.1038/nn.3310
- Craig, A. D. (2003). Pain mechanisms: labeled lines versus convergence in central processing. *Annu. Rev. Neurosci.* 26, 1–30. doi: 10.1146/annurev.neuro.26.041002.131022
- Dahlhaus, A., Ruscheweyh, R., and Sandkuhler, J. (2005). Synaptic input of rat spinal lamina I projection and unidentified neurones in vitro. *J. Physiol.* 566, 355–368. doi: 10.1113/jphysiol.2005.088567
- Duvarci, S., and Pare, D. (2014). Amygdala microcircuits controlling learned fear. *Neuron* 82, 966–980. doi: 10.1016/j.neuron.2014.04.042
- Eccles, J. C., Fatt, P., and Koketsu, K. (1954). Cholinergic and inhibitory synapses in a pathway from motor-axon collaterals to motoneurons. *J. Physiol.* 126, 524–562. doi: 10.1113/jphysiol.1954.sp005226
- Eccles, J. C., Ito, M., and Szentagothai, J. (1967). *The cerebellum as a neuronal machine*. New York: Springer-Verlag.
- Flynn, J. R., Graham, B. A., Galea, M. P., and Callister, R. J. (2011). The role of propriospinal interneurons in recovery from spinal cord injury. *Neuropharmacology* 60, 809–822. doi: 10.1016/j.neuropharm.2011.01.016
- François, A., Low, S. A., Sypek, E. I., Christensen, A. J., Sotoudeh, C., Beier, K. T., et al. (2017). A brainstem-spinal cord inhibitory circuit for mechanical pain modulation by GABA and enkephalins. *Neuron* 93, 822.e826–839.e826. doi: 10.1016/j.neuron.2017.01.008
- Franks, K. M., Russo, M. J., Sosulski, D. L., Mulligan, A. A., Siegelbaum, S. A., and Axel, R. (2011). Recurrent circuitry dynamically shapes the activation of piriform cortex. *Neuron* 72, 49–56. doi: 10.1016/j.neuron.2011.08.020
- Freund, T. F., and Buzsáki, G. (1996). Interneurons of the hippocampus. *Hippocampus* 6, 347–470. doi: 10.1002/(SICI)1098-1063(1996)6:4<347::AID-HIPO1>3.0.CO;2-I
- Ge, S. N., Ma, Y. F., Hioki, H., Wei, Y. Y., Kaneko, T., Mizuno, N., et al. (2010). Coexpression of VGLUT1 and VGLUT2 in trigeminothalamic projection neurons in the principal sensory trigeminal nucleus of the rat. *J. Comp. Neurol.* 518, 3149–3168. doi: 10.1002/cne.22389
- Hachisuka, J., Omori, Y., Chiang, M. C., Gold, M. S., Koerber, H. R., and Ross, S. E. (2018). Wind-up in lamina I spinoparabrachial neurons: a role for reverberatory circuits. *Pain* 159, 1484–1493. doi: 10.1097/j.pain.0000000000001229
- Hylden, J. L., Hayashi, H., Bennett, G. J., and Dubner, R. (1985). Spinal lamina I neurons projecting to the parabrachial area of the cat midbrain. *Brain Res.* 336, 195–198. doi: 10.1016/0006-8993(85)90436-6
- Hylden, J. L., Hayashi, H., Dubner, R., and Bennett, G. J. (1986). Physiology and morphology of the lamina I spinomesencephalic projection. *J. Comp. Neurol.* 247, 505–515. doi: 10.1002/cne.902470410
- Ikedda, H., Stark, J., Fischer, H., Wagner, M., Drdla, R., Jäger, T., et al. (2006). Synaptic amplifier of inflammatory pain in the spinal dorsal horn. *Science* 312, 1659–1662. doi: 10.1126/science.1127233
- Krotov, V., Tokhtamysh, A., Kopach, O., Dromaretsky, A., Sheremet, Y., Belan, P., et al. (2017). Functional characterization of lamina X neurons in ex-vivo spinal cord preparation. *Front. Cell. Neurosci.* 11:342. doi: 10.3389/fncel.2017.00342
- Lamotte d'Incamps, B., Bhumbra, G. S., Foster, J. D., Beato, M., and Ascher, P. (2017). Segregation of glutamatergic and cholinergic transmission at the mixed motoneuron Renshaw cell synapse. *Sci. Rep.* 7:4037. doi: 10.1038/s41598-017-04266-8
- Lee, H., Wang, C., Deshmukh, S. S., and Knierim, J. J. (2015). Neural population evidence of functional heterogeneity along the CA3 transverse axis: pattern completion versus pattern separation. *Neuron* 87, 1093–1105. doi: 10.1016/j.neuron.2015.07.012
- Light, A. R., Sedivec, M. J., Casale, E. J., and Jones, S. L. (1993). Physiological and morphological characteristics of spinal neurons projecting to the parabrachial region of the cat. *Somatosens. Mot. Res.* 10, 309–325. doi: 10.3109/08990229309028840
- Lu, Y., Doroshenko, M., Lauzadis, J., Kanjiya, M. P., Rebecchi, M. J., Kaczocha, M., et al. (2018). Presynaptic inhibition of primary nociceptive signals to dorsal horn lamina I neurons by dopamine. *J. Neurosci.* 38, 8809–8821. doi: 10.1523/JNEUROSCI.0323-18.2018
- Luz, L. L., Szucs, P., Pinho, R., and Safronov, B. V. (2010). Monosynaptic excitatory inputs to spinal lamina I anterolateral-tract-projecting neurons from neighbouring lamina I neurons. *J. Physiol.* 588, 4489–4505. doi: 10.1113/jphysiol.2010.197012
- Maxwell, D. J., and Koerber, H. R. (1986). Fine structure of collateral axons originating from feline spinocervical tract neurons. *Brain Res.* 363, 199–203. doi: 10.1016/0006-8993(86)90680-3
- Melzack, R., and Wall, P. D. (1965). Pain mechanisms: a new theory. *Science* 150, 971–979. doi: 10.1126/science.150.3699.971
- Mendell, L. M. (2014). Constructing and deconstructing the gate theory of pain. *Pain* 155, 210–216. doi: 10.1016/j.pain.2013.12.010
- Moore, N. J., Bhumbra, G. S., Foster, J. D., and Beato, M. (2015). Synaptic connectivity between rensaw cells and motoneurons in the recurrent inhibitory circuit of the spinal cord. *J. Neurosci.* 35, 13673–13686. doi: 10.1523/JNEUROSCI.2541-15.2015
- Neumann, S., Braz, J. M., Skinner, K., Llewellyn-Smith, I. J., and Basbaum, A. I. (2008). Innocuous, not noxious, input activates PKCgamma interneurons of the spinal dorsal horn via myelinated afferent fibers. *J. Neurosci.* 28, 7936–7944. doi: 10.1523/JNEUROSCI.1259-08.2008
- Peirs, C., and Seal, R. P. (2016). Neural circuits for pain: recent advances and current views. *Science* 354, 578–584. doi: 10.1126/science.aaf8933
- Polgar, E., Wright, L. L., and Todd, A. J. (2010). A quantitative study of brainstem projections from lamina I neurons in the cervical and lumbar enlargement of the rat. *Brain Res.* 1308, 58–67. doi: 10.1016/j.brainres.2009.10.041
- Renshaw, B. (1941). Influence of discharge of motoneurons upon excitation of neighboring motoneurons. *J. Neurophysiol.* 4, 167–183. doi: 10.1152/jn.1941.4.2.167
- Renshaw, B. (1946). Central effects of centripetal impulses in axons of spinal ventral roots. *J. Neurophysiol.* 9, 191–204. doi: 10.1152/jn.1946.9.3.191
- Ruscheweyh, R., Ikeda, H., Heinke, B., and Sandkuhler, J. (2004). Distinctive membrane and discharge properties of rat spinal lamina I projection neurones in vitro. *J. Physiol.* 555, 527–543. doi: 10.1113/jphysiol.2003.054049
- Shepherd, G. M. (2004). *The synaptic organization of the brain*. New York: Oxford University Press.
- Smith, K. M., Browne, T. J., Davis, O. C., Coyle, A., Boyle, K. A., Watanabe, M., et al. (2019). Calretinin positive neurons form an excitatory amplifier network in the spinal cord dorsal horn. *eLife* 8:e49190. doi: 10.7554/eLife.49190
- Sperry, R. W. (1950). Neural basis of the spontaneous optokinetic response produced by visual inversion. *J. Comp. Physiol. Psychol.* 43, 482–489. doi: 10.1037/h0055479
- Spike, R. C., Puskar, Z., Andrew, D., and Todd, A. J. (2003). A quantitative and morphological study of projection neurons in lamina I of the rat lumbar spinal cord. *Eur. J. Neurosci.* 18, 2433–2448. doi: 10.1046/j.1460-9568.2003.02981.x
- Suzuki, R., Rahman, W., Hunt, S. P., and Dickenson, A. H. (2004). Descending facilitatory control of mechanically evoked responses is enhanced in deep dorsal horn neurones following peripheral nerve injury. *Brain Res.* 1019, 68–76. doi: 10.1016/j.brainres.2004.05.108
- Szucs, P., Luz, L. L., Lima, D., and Safronov, B. V. (2010). Local axon collaterals of lamina I projection neurons in the spinal cord of young rats. *J. Comp. Neurol.* 518, 2645–2665. doi: 10.1002/cne.22391
- Szucs, P., Luz, L. L., Pinho, R., Aguiar, P., Antal, Z., Tiong, S. Y., et al. (2013). Axon diversity of lamina I local-circuit neurons in the lumbar spinal cord. *J. Comp. Neurol.* 521, 2719–2741. doi: 10.1002/cne.23311
- Takazawa, T., and MacDermott, A. B. (2010). Synaptic pathways and inhibitory gates in the spinal cord dorsal horn. *Ann. N. Y. Acad. Sci.* 1198, 153–158. doi: 10.1111/j.1749-6632.2010.05501.x
- Todd, A. J. (2010). Neuronal circuitry for pain processing in the dorsal horn. *Nat. Rev. Neurosci.* 11, 823–836. doi: 10.1038/nrn2947
- Todd, A. J. (2017). Identifying functional populations among the interneurons in laminae I–III of the spinal dorsal horn. *Mol. Pain* 13:1744806917693003. doi: 10.1177/1744806917693003
- Watt, A. J., Cuntz, H., Mori, M., Nusser, Z., Sjostrom, P. J., and Häusser, M. (2009). Traveling waves in developing cerebellar cortex mediated by asymmetrical Purkinje cell connectivity. *Nat. Neurosci.* 12, 463–473. doi: 10.1038/nn.2285

- Weissman, T. A., and Pan, Y. A. (2015). Brainbow: new resources and emerging biological applications for multicolor genetic labeling and analysis. *Genetics* 199, 293–306. doi: 10.1534/genetics.114.172510
- Wercberger, R., and Basbaum, A. I. (2019). Spinal cord projection neurons: a superficial, and also deep analysis. *Curr. Opin. Physiol.* 11, 109–115. doi: 10.1016/j.cophys.2019.10.002
- Willis, W. D., Al-Chaer, E. D., Quast, M. J., and Westlund, K. N. (1999). A visceral pain pathway in the dorsal column of the spinal cord. *Proc. Natl. Acad. Sci. U. S. A.* 96, 7675–7679. doi: 10.1073/pnas.96.14.7675
- Witter, L., Rudolph, S., Pressler, R. T., Lahlaf, S. I., and Regehr, W. G. (2016). Purkinje cell collaterals enable output signals from the cerebellar cortex to feed back to purkinje cells and interneurons. *Neuron* 91, 312–319. doi: 10.1016/j.neuron.2016.05.037
- Yaksh, T. L. (1999). Regulation of spinal nociceptive processing: where we went when we wandered onto the path marked by the gate. *Pain* 6, S149–S152. doi: 10.1016/s0304-3959(99)00149-9
- Yu, L. M., Polygalov, D., Wintzer, M. E., Chiang, M. C., and McHugh, T. J. (2016). CA3 synaptic silencing attenuates kainic acid-induced seizures and hippocampal network oscillations. *eNeuro* 3, ENEURO.0003–ENEURO.0016.2016. doi: 10.1523/ENEURO.0003-16.2016
- Zeilhofer, H. U., Wildner, H., and Yevenes, G. E. (2012). Fast synaptic inhibition in spinal sensory processing and pain control. *Physiol. Rev.* 92, 193–235. doi: 10.1152/physrev.00043.2010
- Zhang, C. K., Li, Z. H., Qiao, Y., Zhang, T., Lu, Y. C., Chen, T., et al. (2018). VGLUT1 or VGLUT2 mRNA-positive neurons in spinal trigeminal nucleus provide collateral projections to both the thalamus and the parabrachial nucleus in rats. *Mol. Brain* 11:22. doi: 10.1186/s13041-018-0362-y

Conflict of Interest: The authors declare that the research was conducted in the absence of any commercial or financial relationships that could be construed as a potential conflict of interest.

Copyright © 2020 Browne, Hughes, Dayas, Callister and Graham. This is an open-access article distributed under the terms of the Creative Commons Attribution License (CC BY). The use, distribution or reproduction in other forums is permitted, provided the original author(s) and the copyright owner(s) are credited and that the original publication in this journal is cited, in accordance with accepted academic practice. No use, distribution or reproduction is permitted which does not comply with these terms.



Antinociceptive Effects of Sinomenine Combined With Ligustrazine or Paracetamol in Animal Models of Incisional and Inflammatory Pain

Tianle Gao^{1†}, Tao Li^{2†}, Wei Jiang^{3†}, Weiming Fan^{3†}, Xiao-Jun Xu⁴, Xiaoliang Zhao², Zhenming Yin¹, Huihui Guo¹, Lulu Wang¹, Jun Gao^{5*}, Yanxing Han^{1*}, Jian-Dong Jiang^{1*} and Danqiao Wang^{2*}

OPEN ACCESS

Edited by:

Istvan Nagy,
Imperial College London,
United Kingdom

Reviewed by:

Manuel Ramírez-Sánchez,
University of Jaén, Spain
Merab G. Tsagareli,
Ivane Beritashvili Center for
Experimental Biomedicine, Georgia

*Correspondence:

Jun Gao
gaojpumch@hotmail.com
Yanxing Han
hanyanxing@imm.ac.cn
Jian-Dong Jiang
jiang.jdong@163.com
Danqiao Wang
dq_wang96@163.com

[†]These authors have contributed
equally to this work

Specialty section:

This article was submitted to
Integrative Physiology,
a section of the journal
Frontiers in Physiology

Received: 31 December 2019

Accepted: 25 November 2020

Published: 09 February 2021

Citation:

Gao T, Li T, Jiang W, Fan W, Xu X-J, Zhao X, Yin Z, Guo H, Wang L, Gao J, Han Y, Jiang J-D and Wang D (2021) Antinociceptive Effects of Sinomenine Combined With Ligustrazine or Paracetamol in Animal Models of Incisional and Inflammatory Pain. *Front. Physiol.* 11:523769. doi: 10.3389/fphys.2020.523769

¹ State Key Laboratory of Bioactive Substances and Function of Natural Medicine, Institute of Materia Medica, Chinese Academy of Medical Sciences, Beijing, China, ² Beijing Key Laboratory of Traditional Chinese Medicine Basic Research on Prevention and Treatment of Major Diseases, Experimental Research Center, China Academy of Chinese Medical Sciences, Beijing, China, ³ Zhejiang Zhenyuan Pharmaceutical Co., Ltd, Shaoxing, China, ⁴ Department of Physiology and Pharmacology, Karolinska Institutet, Stockholm, Sweden, ⁵ Department of Neurosurgery, Peking Union Medical College Hospital, Chinese Academy of Medicine Sciences & Peking Union Medical College, Beijing, China

The management of postoperative and inflammatory pain has been a pressing challenge in clinical settings. Sinomenine (SN) is a morphinan derived alkaloid with remarkable analgesic properties in various kinds of pain models. The aim of the current study is to investigate if SN can enhance the effect of ligustrazine hydrochloride (LGZ) or paracetamol (PCM) in animal models of postoperative and inflammatory pain. And to determine if the combined therapeutic efficacies can be explained by pharmacokinetics changes. Pharmacological studies were performed using a rat model of incisional pain, and a mouse model of carrageenan induced inflammatory pain. Pharmacokinetic studies were performed using a microdialysis sampling and HPLC-MS/MS assay method to quantify SN, LGZ, and PCM levels in blood and extracellular fluid in brain. We found that SN plus LGZ or SN plus PCM produced marked synergistic analgesic effects. However, such synergy was subjected to pain modalities, and differed among pain models. Pharmacological discoveries could be partially linked to pharmacokinetic alterations in SN combinations. Though further evaluation is needed, our findings advocate the potential benefits of SN plus LGZ for postoperative pain management, and SN plus PCM for controlling inflammatory pain.

Keywords: neuroimmune interaction, post-operative pain, carrageenan-induced inflammation, drug combinations, pharmacokinetics, microdialysis

INTRODUCTION

Pain generated from operation or inflammation is an important clinical concern. However, current medication is far from satisfactory. Less than half of patients report adequate postoperative pain relief (Chou et al., 2016) following operation, and up to 60% of patients with inflammatory rheumatic diseases experience persistent pain left to be treated (Häuser and Fitzcharles, 2017). Undermanaged pain prevents recovery and induces physical and mental impairments

(Breivik et al., 2006; Langley, 2011). Moreover, when left untreated, the acute pain may undergo a “chronification” process to produce treatment-resistant pain, leading to a tremendous reduction in quality of life (Breivik et al., 2006). Therefore, finding effective analgesic methods has become a pressing challenge.

Traditional Chinese medicine has a long history with rich clinical experience in pain therapy. We turned to this natural resource to search for novel analgesics and discovered sinomenine (SN) as a candidate. SN is a morphinan derived alkaloid purified from the root of the climbing plant *Sinomenium Acutum*. It was traditionally used as herbal medicine for rheumatism and arthritis (Feng et al., 2007; Xu et al., 2008). Clinical studies demonstrated that pain in many types of neuralgia can be relieved by SN (Yamasaki, 1976), suggesting a dual therapeutic role of SN on inflammation and pain. In previous studies, we have demonstrated that SN can alleviate acute pain, neuropathic pain and chronic inflammatory pain arising from rheumatoid arthritis, without introducing tolerance or observable side effects (Gao et al., 2013, 2014, 2015).

During incision or inflammation, a broad range of inflammatory mediators forming an “inflammatory soup” (Boddeke, 2001; Mantyh et al., 2002), and increasing the responsiveness of sensory neurons (Scholz and Woolf, 2002; Woolf and Ma, 2007). As SN has distinct immunoregulative property (Jiang et al., 2020), it may alter the unbalanced neuroimmune interaction and decrease the hyperresponsiveness of sensory neurons in incisional or inflammatory pain states. Indeed, supporting evidences revealed that SN was effective in reducing carrageenan induced inflammatory pain in mice (Gao et al., 2013), and incisional pain in rats (Zhu et al., 2016).

Combining drugs with different mechanisms of actions is usually a beneficial attempt in clinical pain management. Advantage of such combination therapies includes improved analgesia and / or reduced dosages of individual drugs, thus minimizing side effects (Vorobeychik et al., 2011). Recently, we have shown that SN could enhance the analgesic potency of ligustrazine (LGZ, also known as Tetramethylpyrazine, the active substance extracted from plant *Ligusticum chuanxiong Hort*), which is effective on acute inflammatory pain (Liang et al., 2004), and pain after traumatic injury (Gao et al., 2019a). Since SN, LGZ and the widely used painkiller paracetamol (PCM, also known as acetaminophen) are promising non-opioid analgesics. It is worth to determine if SN could generate synergistic interactions with LGZ or PCM against pain induced by incision or inflammation.

Hence, in the present study, we evaluated the antinociceptive effects of SN, LGZ, and PCM from sub-effective to effective levels, as well as examined the pharmacological interactions between SN and LGZ or PCM, using animal models of incisional pain and carrageenan induced inflammatory pain. In addition, we measured pharmacokinetics of SN, LGZ, and PCM in single and combined settings, so that pharmacokinetic and pharmacological studies could be correlated. The aim of this article is to validate: (1) If SN combined with LGZ or PCM could achieve synergy; (2) If efficacies of combinational therapies could be differed between inflammatory pain and incisional pain conditions; and (3) If the

pharmacokinetic properties of individual drug can be influenced by combinational formulas.

MATERIALS AND METHODS

Animals

The animals used were Sprague-Dawley rats, male, weighing 250–300 g (from Harlan, The Netherlands; or Beijing Vital River Laboratory Animal Technology, China), or C57BL/6 mice, male, weighing 20–30 g (from Charles River, Sweden, or Beijing Vital River Laboratory Animal Technology, China). Animals were housed 4 per cage for rats or 5 per cage for mice, at a constant room temperature of 22°C in a 12:12 h light-dark cycle with *ad libitum* access to food and water.

Rat Model of Incisional Pain

We used a rat model of incisional pain that has been reported previously (Brennan et al., 1996). In brief, rats were anesthetized with Domitor (75 mg/kg ketamine + 1 mg/kg medetomidine in 1 ml/kg), and a 1 cm longitudinal incision was made through the skin, fascia and muscle of the plantar aspect of the hind paw. The surgery wound was covered with an antibiotic ointment (Bacitracin Zinc Ointment, Actavis Pharma, Inc., USA), to prevent infections. Mechanical and heat hypersensitivities in the hind paw with incision reached peak value around 24 h after surgery.

For measurement of mechanical hypersensitivity. The rats were placed in plastic cages with a metal mesh floor. After habituation for 1 h, the plantar surface of the hind paw adjacent to the skin incision was stimulated with a set of calibrated von Fray hairs (Stoelting, USA) with increasing force. Each filament was applied 5 times and response threshold was reached when the animal withdrew the paw at least 3 times. The cut-off value was 60 g. Heat hyperalgesia was measured by focusing a radiant heat source (Ugo Basile, Italy) on the plantar surface of hind paw adjacent to the incision. The hind paw withdrawal latency was automatically recorded. The intensity of the stimulation was adjusted and fixed so that the baseline latency for normal animals were around 2 to 6 s and the cut-off value was set at 20 s.

Mouse Model of Carrageenan Induced Inflammatory Pain

As reported in our earlier studies (Hao et al., 1998; Gao et al., 2013), mice were anesthetized with 75 mg/kg ketamine + 1 mg/kg medetomidine, in a volume of 1 ml/kg. λ -carrageenan (20 μ l, 2%, Sigma-Aldrich, Germany) was injected subcutaneously (s.c.) into the plantar surface of one hind paw. Mechanical and heat hypersensitivities of the inflamed hind paw was peaked 24 h after the injection.

The paw-withdrawal threshold to mechanical stimulation in mice was tested using a set of calibrated von Fray hairs (Stoelting, USA), with the cut-off value set at 4 g. For test of heat hyperalgesia, mice were gently restrained and a radiant heat source (Hargreaves' test, Ugo Basile, Italy) was focused on the plantar surface of hind paw. The hind paw withdrawal latency was automatically recorded. The intensity of the stimulation was

adjusted and fixed so that the baseline latency for normal mice were within 2 to 6 s and the cut-off value was set at 15 s.

Pharmacological Study Design

In this study, behavioral studies were performed under intraperitoneal (i.p.) administrations to be consistent (and can be correlated) with our earlier published results (Gao et al., 2013, 2019a). The timeline of pharmacological interventions was illustrated in the **Supplementary Figure 1**. SN/Vehicle was given 60 min prior to the application of LGZ/PCM/Vehicle. Pain behavioral measurement (measurement of mechanical allodynia and heat hyperalgesia) was performed after application of LGZ/PCM/Vehicle, for 240 min. This pharmacological intervention strategy was inherited from our previous study (Gao et al., 2019a), in which we show that the analgesic efficacy of SN combination is optimal when SN was given 60 min prior to the combinational drug. To assess the analgesic effects of SN combinations in incisional pain and inflammatory pain models, animals were randomly assigned to following treatment groups (6–8 rats/mice per group): SN low dose group (SN 10 mg/kg); SN middle dose group (SN 20 mg/kg); SN high dose group (SN 80 mg/kg); LGZ low dose group (LGZ 10 mg/kg); LGZ middle dose group (LGZ 20 mg/kg); LGZ high dose group (LGZ 80 mg/kg); SN+LGZ low dose group (SN 10 mg/kg + LGZ 10 mg/kg); SN+LGZ middle dose group (SN 20 mg/kg + LGZ 10 mg/kg); SN+LGZ high dose group (SN 20 mg/kg + LGZ 20 mg/kg); PCM low dose group (PCM 10 mg/kg); PCM middle dose group (PCM 30 mg/kg); PCM high dose group (PCM 100 mg/kg); SN+PCM low dose group (SN 10 mg/kg + PCM 10 mg/kg); SN+PCM middle dose group (SN 20 mg/kg + PCM 10 mg/kg); SN+PCM high dose group (SN 20 mg/kg + PCM 30 mg/kg); and Vehicle groups (for all separate experiments).

Pharmacokinetic Study Design

Pharmacokinetic studies are performed intravenously (i.v.), to avoid deviations in distribution time (of each drug, from i.p. injection site to blood circulation), so that we can investigate the potential drug-drug interactions in a stable manner. Rats were randomly assigned to 7 treatment groups (6 rats per group): SN group (SN 50 mg/kg); LGZ group (LGZ 50 mg/kg); PCM group (PCM 50 mg/kg); SN+LGZ high dose group (SN 50 mg/kg + LGZ 50 mg/kg); SN+LGZ low dose group (SN 25 mg/kg + LGZ 25 mg/kg); SN+PCM high dose group (SN 50 mg/kg + PCM 50 mg/kg); SN+PCM low dose group (SN 25 mg/kg + PCM 25 mg/kg). In each group, an injection catheter (C19PU, Instech Laboratories, USA) was implanted into the left femoral vein of each rat, 1 day before i.v. drug administration. The i.v. drug administration volume was 0.5 mL/100 g (of rat body weight), and injections were completed within 1 min.

Blood and Brain Microdialysis Surgery and Microdialysate Sampling

After anaesthetization, the blood microdialysis probe (4 mm-effective membrane length and 20 000 molecular weight cut-off, CMA Microdialysis, Sweden) was positioned within the jugular vein toward the right atrium and then perfused with anti-coagulant citrate dextrose (ACD) solution (Sigma-Aldrich,

Germany) consisting of citric acid 3.5 mM, sodium citrate 7.5 mM, and dextrose 13.6 mM. The brain microdialysis probe (4 mm-effective membrane length and 20 000 molecular weight cut-off, CMA Microdialysis, Sweden) was implanted in the corpus striatum zone (AP +0.2 mm, ML 3 mm, and DV 3.5 mm) according to the atlas of rat brain (Paxinos and Watson, 1998), and perfused with Ringer's solution (consisting of NaCl 145.3 mM; KCl 4.01 mM; CaCl₂ 2.97 mM; pH 7.0). During the period of surgery, the body temperature of each rat was maintained at 37°C using a heating pad. Rats were kept in free-moving condition for 1 h prior to the initiation of sample collection for reaching equilibrium. After blank control dialysate samples were collected, animals received corresponding drugs followed by a 6 h dialysate sampling. The dialysates were collected at 20 min intervals at a perfusion rate of 1.5 $\mu\text{L min}^{-1}$ using a CMA120 awake and freely moving system (CMA Microdialysis, Sweden). For all samples, a 10 min delay was added into the sampling procedure to compensate for the dead volume between the active membrane and the sample collection outlet.

Microdialysis Probe Recovery

The concentrations of SN, LGZ, and PCM in blood and brain extracellular fluid (bECF) were calculated from the corresponding dialysate sample according to the following equation:

$$C_{\text{blood or bECF}} = C_d / R_{\text{in vivo}} = (C_d / R_{\text{in vitro}}) \times (D_{\text{in vitro}} / D_{\text{in vivo}})$$

where C_{blood} or C_{bECF} was the measured concentration of each drug in blood or bECF; C_d was the measured concentration of each drug in the dialysate sample; $R_{\text{in vivo}}$ was the recovery of the probe inserted into the rat's blood or brain; $R_{\text{in vitro}}$ was the recovery of the probe immersed in ACD or Ringer's solution containing drug and perfused with drug-free solution; $D_{\text{in vitro}}$ was the delivery of drug calculated by measuring the loss in the compound concentration between the perfusate and the dialysate when the probe was immersed in drug-free solution and perfused with ACD or Ringer's solution containing drug; $D_{\text{in vivo}}$ was the delivery of drug determined in the same way as $D_{\text{in vitro}}$ except that the probe was inserted into the rat blood or brain. In the current study, the $R_{\text{in vivo}}$ of SN, LGZ, and PCM in blood was 21.31, 20.61, and 24.73%, respectively. The $R_{\text{in vivo}}$ of SN, LGZ and PCM in brain was 19.38, 20.11, and 25.33%, respectively.

HPLC-MS/MS Quantification

The quantitative analyses were carried out using the method described earlier (Zhao et al., 2015; Gao et al., 2019b; Li et al., 2019, 2020), in which a HPLC-MS/MS system (AB Sciex LLC, USA) was applied. Reversed-phase separation was performed on an XSelect® HSS T3 column (2.5 μm , 2.1 \times 50 mm, Waters Corp., USA). The mobile phase consisted of (A) water/formic acid (100/0.005, v/v) and (B) methanol/formic acid (100/0.005, v/v). Gradient elution was carried out for 6.0 min at a flow rate of 0.3 mL/min. Gradient conditions were as follows: 0–1.5 min, 15% B; 1.5–3.0 min, 15% B–100% B; 3.0–4.5 min, 100% B; 4.50–4.51 min, 100% B–15% B; 4.51–6.0 min, 15% B. One microliter aliquot of each sample was

injected into the column. The column temperature was kept at 30°C. All samples were kept at 6°C throughout the analysis. Mass spectrometry was performed on an Sciex 6500+ triple quadrupole mass spectrometer equipped with a Turbo V ion source. All compounds were detected in positive electrospray ion mode. Curtain gas (CUR), nebulizer gas (GS1), and turbo-gas (GS2) were set at 20, 55, and 55 psi, respectively. The electrospray voltage was +5.5 kV, and the turbo-ion spray source temperature was 550°C. Nitrogen was employed as the collision gas. The system was operated in multiple reaction monitoring (MRM) mode. Product ion spectrums and fragmentation pattern of SN, LGZ, PCM and naloxone (internal standard) were illustrated in **Supplementary Figure 2**. The precursors and product ions of LGZ, PCM, and SN were 137/80 (CE: 41; DP: 74), 152/110 (CE: 24; DP: 30), and 330/181 (CE: 44; DP: 158), respectively. Ions and fragmentations used in MRM mode for each compound were illustrated in **Supplementary Table 1**. Representative extraction ion chromatograms and retention time of each compound were illustrated in **Supplementary Figure 3**. Data acquisitions were performed using Analyst 1.7 software (Applied Biosystems, USA). Multiquant software (Applied Biosystems, USA) was used to quantify all drugs.

Pharmacokinetic Data Analysis

The blood and bECF pharmacokinetic parameters were estimated by a non-compartmental method using the DAS software package (version 3.0, BioGuider Co., Shanghai, China). The maximal concentration (C_{max}) and time taken to achieve peak concentration (T_{peak}) were observed values with no interpolation. The area under the concentration–time curve up to 6 h (AUC_{0→6h}) was calculated using trapezoidal rule. The t_{1/2} was calculated using the relationship of 0.693/k, where k was the constant elimination rate. The clearance (CL) for i.v. dosing was calculated as dividing the administered dosage by the AUC_{0→6h}. The distribution volume (V_{ss}) for i.v. dosing was calculated as multiplying the CL by the mean residence time (MRT). To assess the extent of brain penetration, the ratio of unbound molecules (SN, LGZ and PCM) in brain / blood (the partition coefficient, K_p) was calculated as AUC_{bECF}/AUC_{blood}.

Preparation of Drug Solutions

For preparation of SN injection solution in pharmacological studies, SN (CAS No. 6080-33-7, Catalog No. 110774, obtained from the National Institute for Food and Drug Control, Beijing, China, purity > 99%) was dissolved in DMSO (CAS No. 67-68-5, Catalog No. 34869, obtained from Sigma-Aldrich, Germany, purity > 99%), then mixed with Cremophor EL oil (CAS No. 61791-12-6, Catalog No. 238470, Sigma-Aldrich, Germany) and saline by vortex mixer (2,500 rpm for 1 min, Bibby Scientific, UK) using the volume rate of 1:4:5. Any further dilution was mixed with saline (CAS No. 7647-14-5, Catalog No. S0817, obtained from Sigma-Aldrich, Germany). Vehicle for SN was the above-mentioned dissolving solution. For preparation of SN injection solution in pharmacokinetic studies, SN (CAS No. 6080-33-7, Catalog No. 9582, obtained from Finetech Industry Limited, China, purity > 99%) was dissolved in saline. For preparation of LGZ injection solution in pharmacological and pharmacokinetic

studies, LGZ (CAS No. 76494-51-4, Catalog No. 3628, obtained from Sinova Inc., USA, purity > 99%) was dissolved in saline. For preparation of PCM injection solution in pharmacological and pharmacokinetic studies, PCM (CAS No. 103-90-2, Catalog No. 1706, obtained from Tocris Cookson Ltd., UK, purity > 99%) was dissolved in saline.

Statistics

All pharmacological experiments were conducted blindly. Data were presented as mean ± SEM, and were analyzed using analysis of variance (ANOVA) followed by Dunn's or Dunnett's multiple comparisons test, and / or Bonferroni's multiple comparisons test. *P* < 0.05 was considered as statistically significant.

RESULTS

Analgesic Effects of SN, LGZ, or PCM on Mechanical and Heat Hypersensitivities in Rat Model of Incisional Pain

Twenty four hours after the incision in the plantar area in the hind paw, rats developed mechanical (**Figure 1A**) and heat (**Figure 1B**) hypersensitivities, which both lasted for 4 days. All pharmacology studies were done between 24 to 48 h after incision while animals exhibit maximum of developed mechanical and heat allodynia.

Single dosages of SN at 80 mg/kg (with analgesia lasted from 30 to 120 min, **Figure 2E**), LGZ at 80 mg/kg (with analgesia lasted from 60 to 180 min, **Figure 2A**), and PCM at 100 mg/kg (with analgesia lasted from 120 to 240 min, **Figure 2I**), but not SN at 10 and 20 mg/kg (**Figure 2E**), LGZ at 10 and 20 mg/kg (**Figure 2A**), or PCM at 10 and 30 mg/kg (**Figure 2I**) produced significant analgesic effects to mechanical stimuli. Similarly, heat hyperalgesia was significantly reversed by i.p. SN at 80 mg/kg (from 30 to 120 min, **Figure 2F**), LGZ at 80 mg/kg (from 60 to 180 min, **Figure 2B**), and PCM at 30 mg/kg (only at 120 min, **Figure 2J**) or 100 mg/kg (from 120 to 240 min, **Figure 2F**), but not by SN at 10 and 20 mg/kg (**Figure 2F**), LGZ at 10 and 20 mg/kg (**Figure 2B**), or PCM at 10 mg/kg (**Figure 2J**).

Combinational Therapy of SN With LGZ or PCM in Rat Model of Incisional Pain

When SN was applied first and then LGZ administrated 60 min after, such combination produced significant analgesic effects for mechanical hypersensitivity from 30 to 180 min in “SN 20 mg/kg + LGZ 20 mg/kg” treatment, and at 60 min in “SN 20 mg/kg + LGZ 10 mg/kg” treatment (**Figure 2C**); Similarly, SN and LGZ combination also significantly alleviated heat hyperalgesia from 30 to 180 min in “SN 20 mg/kg + LGZ 20 mg/kg” treatment, and at 120 min in “SN 20 mg/kg + LGZ 10 mg/kg” treatment (**Figure 2D**). Even though, monotherapies of SN or LGZ at single dosages of 10 or 20 mg/kg failed to produce any analgesia (**Figures 2A,B,E,F**). Unlike SN plus LGZ, SN and PCM combinations (at sub-effective dosages) did not generate significant analgesic effect (**Figures 2G,H**).

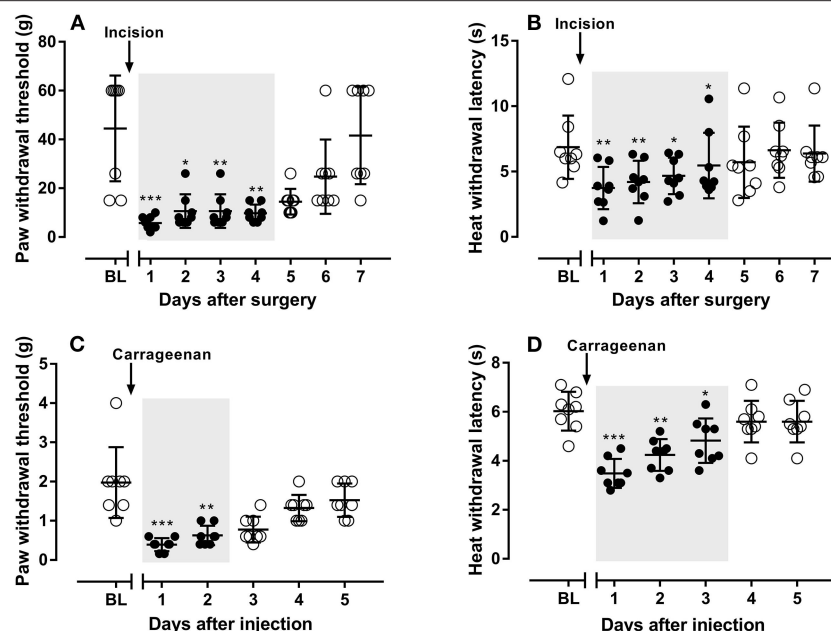


FIGURE 1 | The development of mechanical (A) and heat (B) hypersensitivities in rats after incision in their hand paws, and the development of mechanical (C) and heat (D) hypersensitivities in mice after carrageenan injection in their hand paws. $N = 8$ animals, data were presented as mean \pm SD. * $P < 0.05$, ** $P < 0.01$, *** $P < 0.001$, mechanical (A,C) or heat thresholds (B,D) from Day 1 to 7 in rats (A,B) or from Day 1 to 5 in mice (C,D) were compared with their baseline values, using Dunn's (A,C) or Dunnett's multiple comparisons test (B,D) following ANOVA. Gray shaded areas represent durations that rats or mice experiencing ongoing hypersensitivities.

When 240 min's analgesic effect was compared using Area Under Curve (AUC), "SN 20 mg/kg + LGZ 20 mg/kg" group was significantly greater than "SN 10 mg/kg" group, or "LGZ 10 and 20 mg/kg" groups (Figures 4A,B). In addition, mean of AUCs in group "SN 20 mg/kg + LGZ 20 mg/kg" was higher than that of "SN 80 mg/kg" and "LGZ 80 mg/kg" groups, representing a synergistic effect between SN and LGZ (combined at sub-effective dosages) in incisional pain model. Rats showed no signs of observable side effects including sedation, itching or severe allergy during pharmacological treatment periods.

Analgesic Effects of SN, LGZ, or PCM on Mechanical and Heat Hypersensitivities in Mouse Model of Carrageenan Induced Inflammatory Pain

Similar as reported previously (Gao et al., 2013), 24 h after subcutaneous carrageenan injection (in plantar area of hind paws), mice developed marked mechanical (Figure 1C) and heat (Figure 1D) hypersensitivities, which lasted for 2 and 3 days, respectively. All pharmacology studies were performed between 24 to 48 h after carrageenan injection, while animals exhibit maximum allodynia.

Single dosages of SN at 80 mg/kg (with analgesia lasted from 30 to 240 min, Figure 3E), and LGZ at 80 mg/kg (with analgesia lasted from 60 to 120 min, Figure 3A), but not SN at 10 and 20 mg/kg (Figure 3E), LGZ at 10 and 20 mg/kg (Figure 3A), or PCM at 10, 30, and 100 mg/kg (Figure 3I) produced significant analgesic effects to mechanical stimuli.

Similarly, heat hyperalgesia was significantly reversed by SN at 80 mg/kg (from 30 to 240 min, Figure 3F), LGZ at 80 mg/kg (from 60 to 180 min, Figure 3B), and PCM at 100 mg/kg (from 30 to 60 min, Figure 3J), but not by SN at 10 or 20 mg/kg (Figure 3F), LGZ at 10 or 20 mg/kg (Figure 3B), and PCM at 10 or 30 mg/kg (Figure 3J).

Combinational Therapy of SN With LGZ or PCM in Mouse Model of Carrageenan Induced Inflammatory Pain

When SN was pretreated for 60 min and then combined with LGZ, no significant analgesic effects was produced by "SN 10 mg/kg + LGZ 10 mg/kg", "SN 20 mg/kg + LGZ 10 mg/kg" or "SN 20 mg/kg + LGZ 20 mg/kg" groups (Figures 3C,D). However, "SN 20 mg/kg + PCM 30 mg/kg" treatment generated significant anti-hyperalgesic effects against both mechanical (from 60 to 120 min, Figure 3G) and heat (from 30 to 240 min, Figure 3H) hypersensitivities. In addition, "SN 20 mg/kg + PCM 10 mg/kg" treatment also significantly alleviated heat allodynia (at 30, 60, and 180 min, Figure 3H).

When 240 min's analgesic effect was compared using AUC, "SN 20 mg/kg + PCM 30 mg/kg" group was significantly greater than "SN 10 and 20 mg/kg" group, or "PCM 10 and 30 mg/kg" groups, in heat (Figure 4D) but not in mechanical (Figure 4C) hypersensitivities, showing drug's efficacy is dissociated between two pain modalities. In addition, for heat thresholds, mean of AUC for group "SN 20 mg/kg + PCM 30 mg/kg" group was higher than that of "SN 80 mg/kg" and "PCM 100 mg/kg" groups,

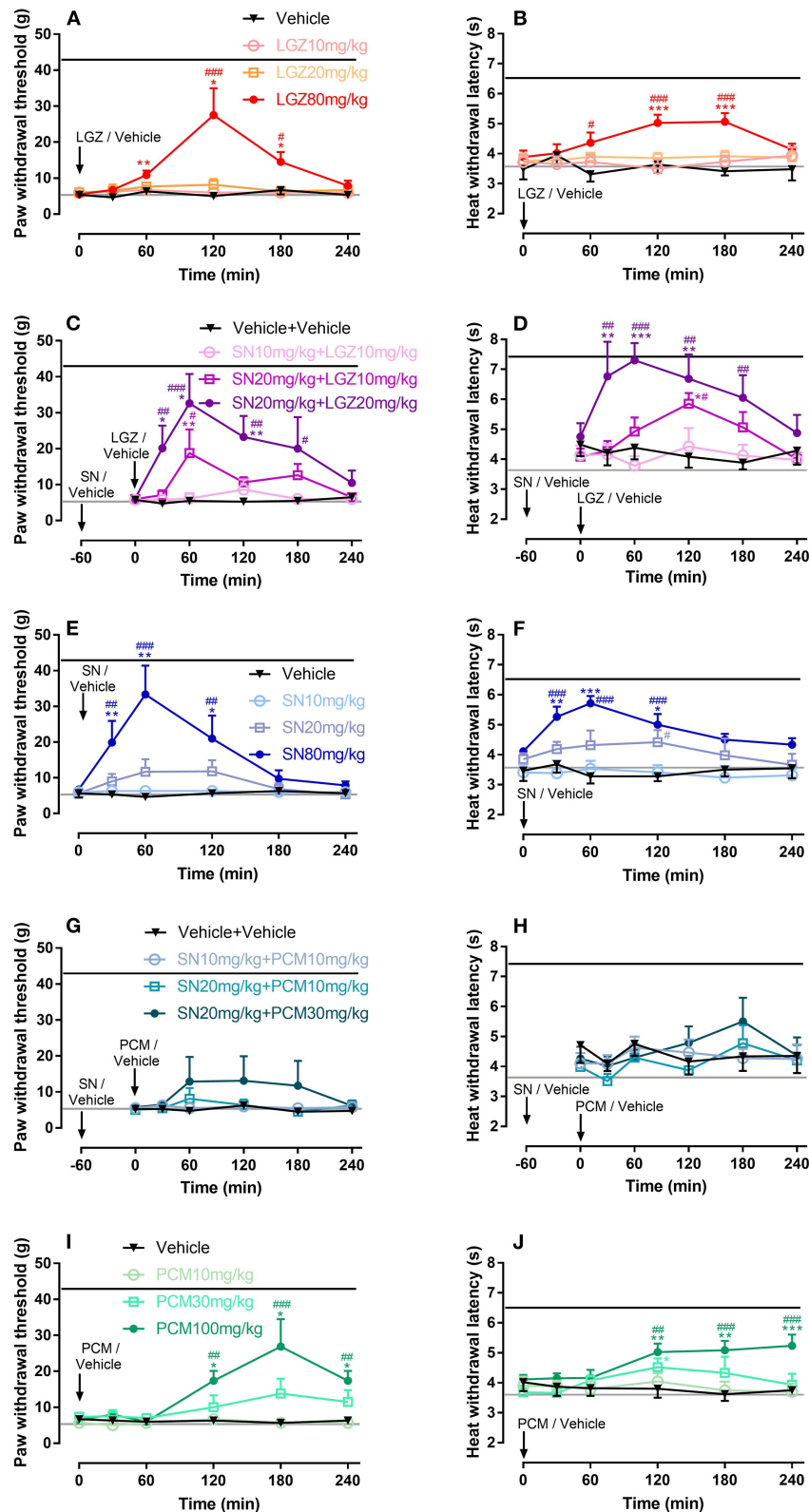


FIGURE 2 | Dose dependent effects of LGZ (A,B), SN (E,F), PCM (I,J); and SN combined with LGZ (C,D) or PCM (G,H) on mechanical and heat hypersensitivities in rats with incisional pain. $N = 6-8$ rats, data were presented as mean \pm SEM. Black or Gray lines represent the average (mechanical / heat) thresholds, before or 1 day after incision, respectively. LGZ was applied at the dosages of 10, 20, and 80 mg/kg (A,B); SN was applied at the dosages of 10, 20, and 80 mg/kg (E,F); PCM was

(Continued)

FIGURE 2 | applied at the dosages 10, 30, and 100 mg/kg (**I,J**); SN (at 10 or 20 mg/kg) were applied 60 min before LGZ (at 10 or 20 mg/kg; **C,D**), or PCM (at 10 or 30 mg/kg; **G,H**) administrations. Mechanical/heat thresholds were measured for 240 min after completion of drug applications. Two Way ANOVA with repeated measures indicated overall significant differences ($P < 0.05$) between the groups (**A–J**). * $P < 0.05$, ** $P < 0.01$, *** $P < 0.001$, post-drug thresholds were compared with pre-drug baselines at 0 min, using Dunn's (**A,C,E,G,I**) or Dunnett's (**B,D,F,H,J**) multiple comparisons test following ANOVA; # $P < 0.05$, ## $P < 0.01$, ### $P < 0.001$, post-drug effects were compared with vehicle treatments at each time points, using Bonferroni's multiple comparisons test following ANOVA.

representing a synergistic effect between SN and PCM (at sub-effective dosages) in carrageenan induced inflammatory pain model (**Figure 4D**). Mice showed no signs of observable side effects including sedation, itching or severe allergy during drug treatment periods.

Effects of LGZ or PCM on the Pharmacokinetic Parameters of SN in Combinational Formulas

After intravenous injection of SN in rats, levels of SN in brain followed same tendency of that in the blood with certain delay (**Figures 5A,B**). T_{max} in brain was 0.33 h. C_{max} in brain was $0.43 \mu\text{g}\cdot\text{mL}^{-1}$ (equivalent to 4.3% of the C_{max} in blood, which was $10.07 \mu\text{g}\cdot\text{mL}^{-1}$; **Table 1**). For $t_{1/2}$, there was no significant difference between brain and blood. However, mean retention time (MRT) in brain extracellular fluid was higher than that in blood ($1.75 \text{ h} > 1.12 \text{ h}$, $P = 0.008$; **Table 1**). In terms of the brain permeability of SN, K_p value is from 0.06 to 0.07 (**Table 1**), indicating poor SN penetration from blood to brain. When combined with LGZ (SN 50 mg/kg + LGZ 50 mg/kg), the parameters (C_{max} , MRT, $t_{1/2}$, and AUC) of SN (at 50 mg/kg), in blood and brain extracellular fluids remained stable. Even in low dose SN and LGZ combination (SN 25 mg/kg + LGZ 25 mg/kg), the parameters (MRT, $t_{1/2}$ clearance, and K_p value) of SN remained stable. These facts indicating LGZ does not influence the pharmacokinetic properties of SN in the blood and in extracellular fluids of brain, when combined.

In SN and PCM combination at 50 mg/kg (**Figures 5E,F**), $t_{1/2}$ of SN in the extracellular fluids of brain or blood was not significantly altered; In blood (**Table 1**), SN's clearance increased significantly ($P < 0.05$), while C_{max} and AUC ($14.80 \mu\text{g}\cdot\text{mL}^{-1} \rightarrow 9.28 \mu\text{g}\cdot\text{mL}^{-1}$) decreased significantly ($P < 0.05$), correlated with respective changes in concentration curves (**Figure 5E**) and AUCs (**Supplementary Figure 4E**); However, SN's C_{max} and AUC in extracellular fluids of brain remained steady. In addition, SN's K_p value was increased ($0.07 \rightarrow 0.12$, $P < 0.01$; **Table 1**).

Effects of SN on the Pharmacokinetic Parameters of LGZ or PCM in Combinational Formulas

After intravenous injection, LGZ appeared rapidly in blood (**Figure 5C**) and extracellular fluids of the brain (**Figure 5D**). LGZ concentration reached peak in brain at the period of 0–20 min (**Figure 5D**). C_{max} in brain ($39.16 \mu\text{g}\cdot\text{mL}^{-1}$) was about 78% of the C_{max} in blood ($50.04 \mu\text{g}\cdot\text{mL}^{-1}$; $P < 0.05$; **Table 2**). MRT and $t_{1/2}$ remained steady in brain extracellular fluids and in blood. K_p value for LGZ was from 0.60 to 0.69 (**Table 2**), representing good blood-brain permeability. After combined with SN (at 50 mg/kg), parameters of LGZ (C_{max} , clearance, $t_{1/2}$,

MRT, AUC and K_p) in blood and brain were not significantly altered, showing that SN does not affect the pharmacokinetics of LGZ in the blood and brain when combined.

After intravenous injection of PCM, the levels of PCM in brain followed the same propensity of that in the blood with certain delay (**Figures 5G,H**). In brain (**Table 2**), T_{max} was about 0.56 h, and C_{max} was $7.24 \mu\text{g}\cdot\text{mL}^{-1}$, which was about 44% of the C_{max} in blood ($16.53 \mu\text{g}\cdot\text{mL}^{-1}$). No significant change for PCM's $t_{1/2}$ was observed in blood or brain. The K_p value for PCM is from 0.47 to 0.54 (**Table 2**), revealing PCM has a moderate the blood-brain permeability. After the combination with SN (at 50 mg/kg), the parameters of PCM (C_{max} , MRT, $t_{1/2}$, AUC, and K_p) in blood and brain were not significantly changed. Albeit, a tendency of increased blood PCM concentrations in the "SN 50 mg/kg + PCM 50 mg/kg" group (compared with PCM 50 mg/kg group) could be seen (from the respective concentration curves, **Figure 5G**; and AUCs, **Supplementary Figure 4G**).

DISCUSSION

Current analgesics against postoperative or inflammatory pain are restricted by incomplete efficacy, and some potent agents such as opioids are limited by side effects (Chou et al., 2016; Häuser and Fitzcharles, 2017). Synergistic interactions of drug combinations might provide superior analgesia with fewer adverse outcomes than monotherapy by targeting of multiple mechanisms (Gilron et al., 2013). In such regard, we used SN in combinational formulas and demonstrated that therapies of SN plus LGZ or SN plus PCM in sub-effective concentrations, produced synergistic analgesia, while avoided opioid-related adverse effects. Indeed, the observed synergism is expected and could be explained by different mechanisms of anti-hyperalgesic actions. Intriguingly, however, we discovered that the synergistic interaction was subjected to the pain models and differed between mechanical and heat modalities. Pharmacokinetics of SN in blood was influenced by coadministration of PCM but not LGZ, which could partially explain the pharmacological discoveries. Topics related to the study results are discussed below.

Synergistic Effects of SN Plus LGZ on Incisional Pain and SN Plus PCM on Carrageenan Induced Heat Hyperalgesia

A pathological change in the nociceptive system induced by incision or inflammation could generate persistent alterations in nociceptors that drive hypersensitivity. SN plus LGZ or PCM might restore the nociceptor to its normal state by their synergistic anti-hyperalgesic mechanisms.

In incisional pain condition, the development of primary hyperalgesia was found to be mediated by sensitizations

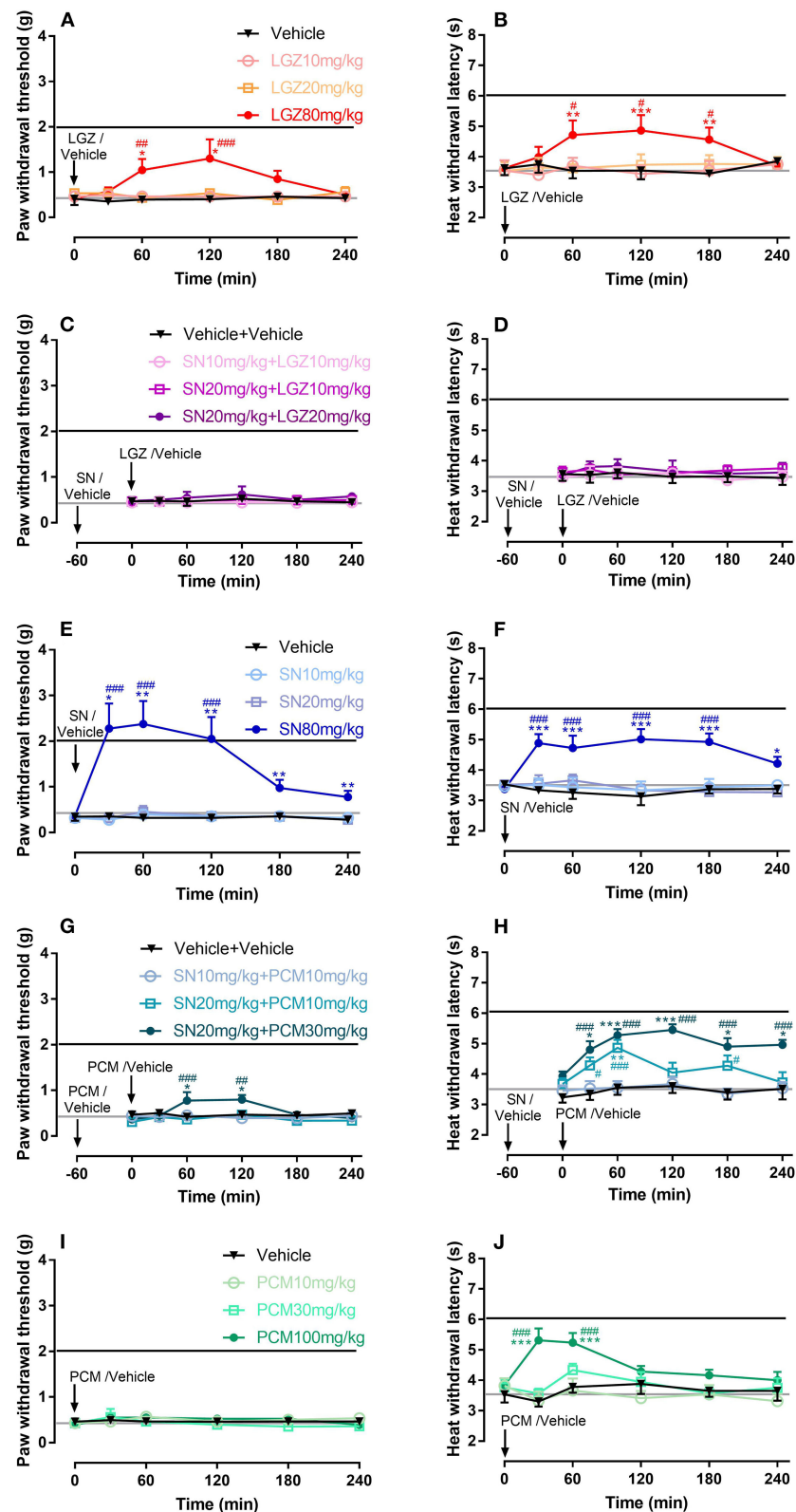
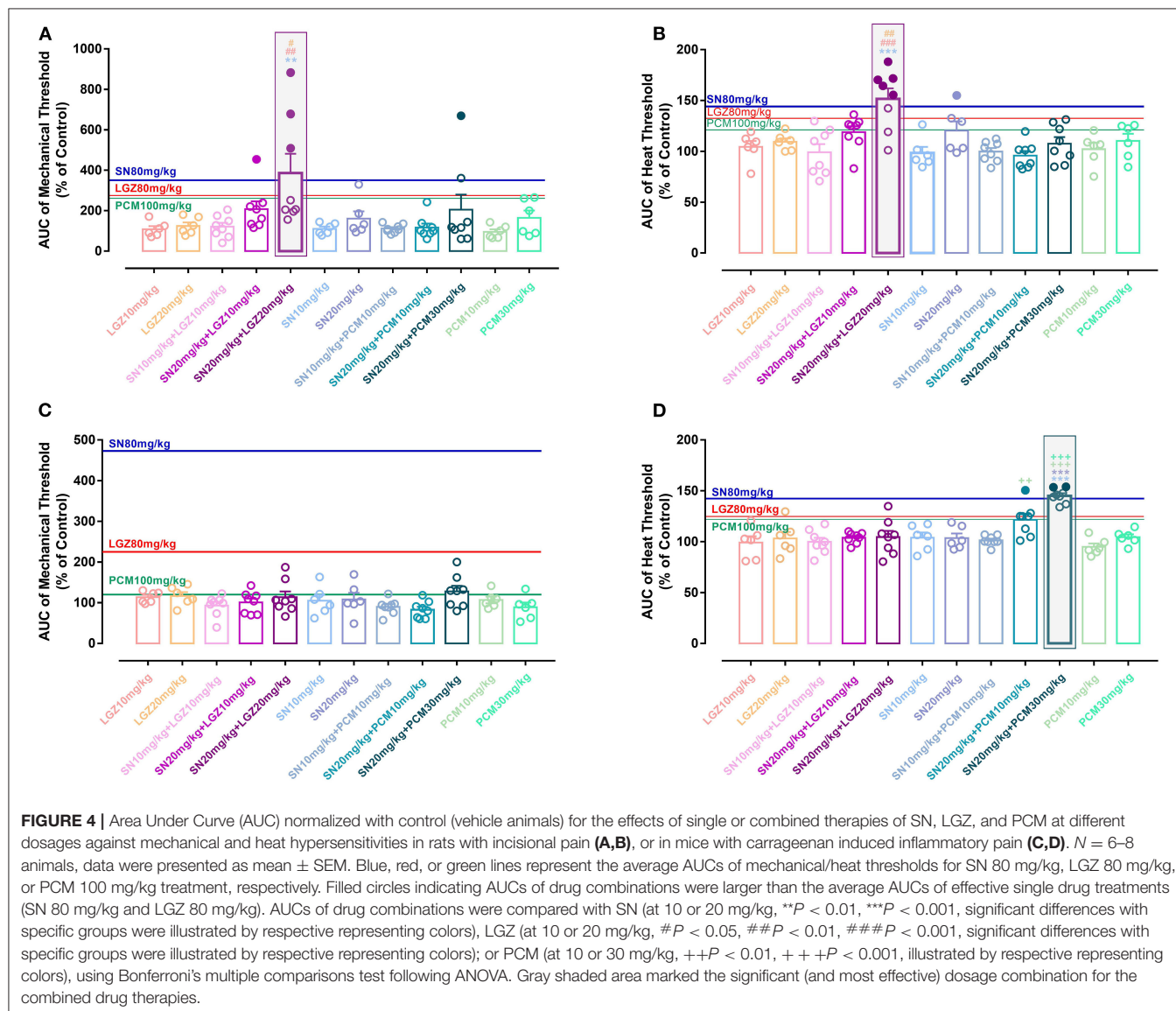


FIGURE 3 | Dose dependent effects of LGZ (A,B), SN (E,F), PCM (I,J); and SN combined with LGZ (C,D) or PCM (G,H) on mechanical and heat hypersensitivities in mice with carrageenan induced inflammatory pain. $N = 6-8$ mice, data were presented as mean \pm SEM. Black or Gray lines represent the average (mechanical/heat) thresholds before or 1 day after carrageenan injection, respectively. LGZ was applied at the dosages of 10, 20, and 80 mg/kg (A,B); SN was applied at the dosages of (Continued)

FIGURE 3 | 10, 20, and 80 mg/kg (E,F); PCM was applied at the dosages 10, 30, and 100 mg/kg (I,J); SN (at 10 or 20 mg/kg) were applied 60 min before LGZ (at 10 or 20 mg/kg; C,D), or PCM (at 10 or 30 mg/kg; G,H) administrations. Mechanical/heat thresholds were measured for 240 min after completion of drug applications. Two Way ANOVA with repeated measures indicated overall significant differences ($P < 0.05$) between the groups (A,B,E,F,G,H,J). $*P < 0.05$, $**P < 0.01$, $***P < 0.001$, post-drug thresholds were compared with pre-drug baselines at 0 min, using Dunn's (A,C,E,G,I) or Dunnett's (B,D,F,H,J) multiple comparisons test following ANOVA; # $P < 0.05$, ## $P < 0.01$, ### $P < 0.001$, post-drug effects were compared with controls (vehicle treatments) at each time points, using Bonferroni's multiple comparisons test following ANOVA.



of primary afferents and dorsal horn neurons (Brennan et al., 2005), and activation of NMDA receptors (Woolf and Thompson, 1991). The analgesic effect of the NMDA receptor antagonist ketamine, can be enhanced by Ligustrazine (Liu et al., 2018). Taking consideration that resembling dextromethorphan (Yamasaki, 1976), SN may also work as a weak NMDA antagonist (Qian et al., 2007, Gao et al., 2007), it is possible that synergy between LGZ and SN on incisional pain is dependent on NMDA receptor system inhibition.

In inflammatory pain condition, changes in the chemical milieu induces excessive prostaglandins, that sensitize the nociceptors (Woolf and Ma, 2007). PCM is generally considered to be a weak inhibitor of prostaglandins (Graham and Scott, 2005). In like manner, SN can systemically suppress the generation of prostaglandins, both *in vitro* and *in vivo* (Liu et al., 1994; Qian et al., 2007). Therefore, it is possible that synergism of SN plus PCM arises from mutual inhibition on the prostaglandin synthesis. Besides, SN also showed capability of reducing various

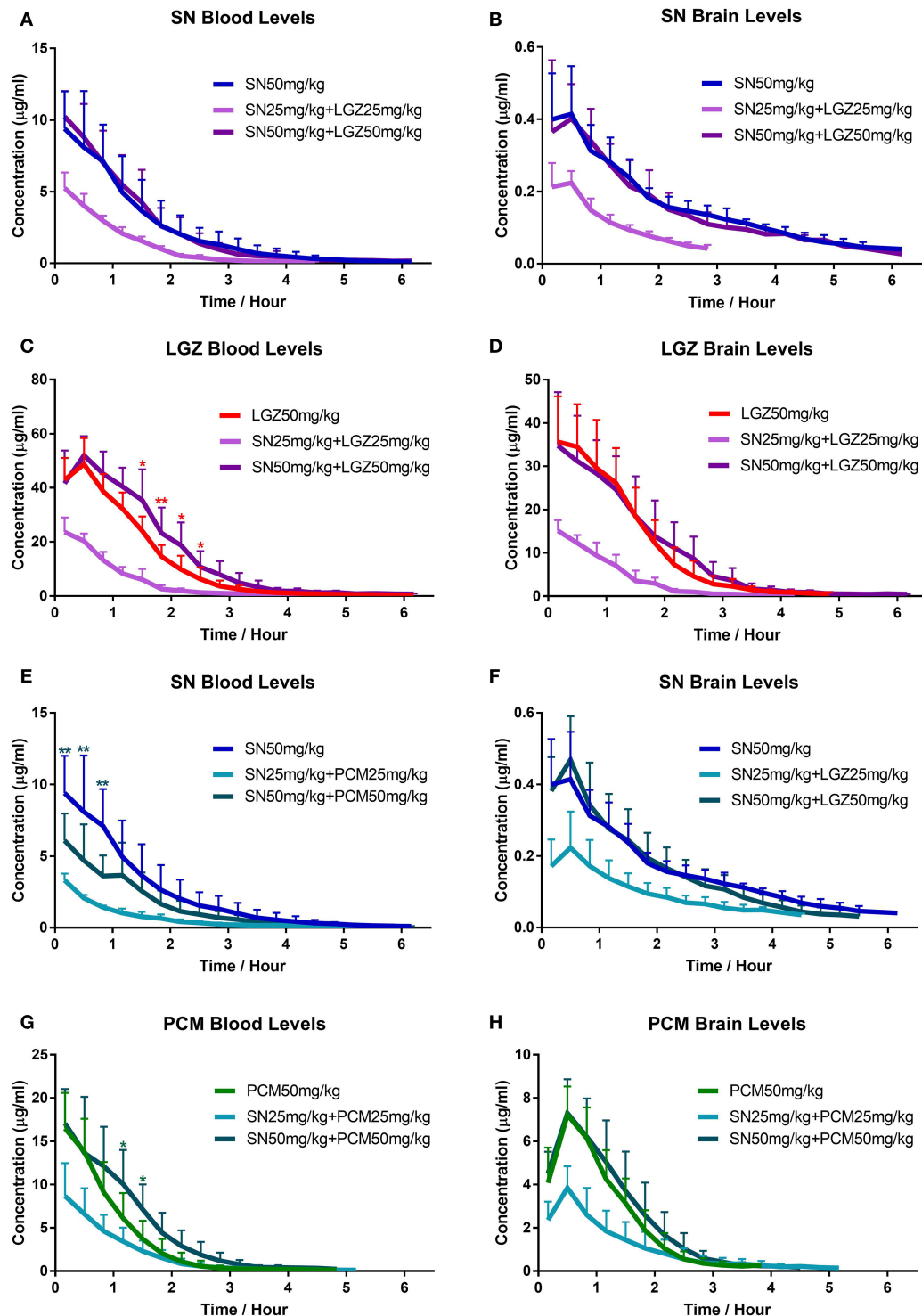


FIGURE 5 | Investigation of pharmacokinetics changes of SN, LGZ, and PCM in combined formulas. Drug concentrations of SN, LGZ, and PCM in blood (A,C,E,G) and striatum of the brain (B,D,F,H) were monitored continuously in collected samples (using microdialysis), after intravenous injection of SN, LGZ, and PCM at 50 mg/kg or SN combine with LGZ/PCM at 50 or 25 mg/kg, in rats. $N = 6$ rats for each group. Data was presented as mean \pm SD. Two Way ANOVA indicated significant differences between the groups (A–H). * $P < 0.05$, ** $P < 0.01$, drug concentrations of different groups were compared at each time points using Bonferroni's multiple comparisons test following ANOVA (significant differences with specific groups were illustrated by respective representing colors).

TABLE 1 | Effects of LGZ or PCM on the pharmacokinetic parameters of SN in blood and extracellular fluid of rat brain tissue.

PK parameter	SN levels				
	SN (50 mg·kg ⁻¹)	SN + LGZ (50 mg·kg ⁻¹ + 50 mg·kg ⁻¹)	SN + LGZ (25 mg·kg ⁻¹ + 25 mg·kg ⁻¹)	SN + PCM (50 mg·kg ⁻¹ + 50 mg·kg ⁻¹)	SN + PCM (25 mg·kg ⁻¹ + 25 mg·kg ⁻¹)
BLOOD					
AUC _{0-t} (h·μg·mL ⁻¹)	14.80 ± 6.13	15.19 ± 4.45	6.25 ± 1.02**	7.72 ± 3.02*	3.72 ± 0.58**
AUC _{0-∞} (h·μg·mL ⁻¹)	15.01 ± 6.20	15.42 ± 4.50	6.36 ± 1.04**	7.84 ± 3.07*	3.84 ± 0.6**
MRT (h)	1.12 ± 0.28	1.05 ± 0.16	0.87 ± 0.08	1.13 ± 0.14	0.98 ± 0.24
t _{1/2} (h)	0.94 ± 0.26	0.97 ± 0.30	0.80 ± 0.17	0.87 ± 0.21	0.96 ± 0.21
V _z (L·kg ⁻¹)	5.30 ± 2.45	4.64 ± 1.31	4.56 ± 0.94	7.60 ± 2.95	9.01 ± 1.49**
CL _z (L·h ⁻¹ ·kg ⁻¹)	3.75 ± 1.31	3.46 ± 0.90	4.01 ± 0.59	6.35 ± 2.61*	6.65 ± 1.11**
C _{max} (μg·mL ⁻¹)	10.07 ± 2.75	10.38 ± 1.60	5.26 ± 1.09**	6.11 ± 1.91*	3.32 ± 0.46**
BRAIN					
AUC _{0-t} (h·μg·mL ⁻¹)	0.91 ± 0.17##	0.77 ± 0.25##	0.32 ± 0.04***##	0.89 ± 0.29##	0.41 ± 0.13***##
AUC _{0-∞} (h·μg·mL ⁻¹)	0.99 ± 0.15##	0.89 ± 0.26##	0.39 ± 0.05***##	0.93 ± 0.32##	0.48 ± 0.13***##
MRT (h)	1.75 ± 0.37##	1.42 ± 0.39	1.05 ± 0.05***##	1.60 ± 0.08##	1.47 ± 0.39#
t _{1/2} (h)	1.14 ± 0.27	1.22 ± 0.19	1.18 ± 0.34	1.09 ± 0.34	1.35 ± 0.34
T _{max} (h)	0.33 ± 0.18	0.33 ± 0.18	0.39 ± 0.17	0.50 ± 0.00	0.37 ± 0.18
C _{max} (μg·mL ⁻¹)	0.43 ± 0.13##	0.45 ± 0.14##	0.24 ± 0.05***##	0.47 ± 0.12##	0.23 ± 0.09***##
BRAIN-TO-BLOOD AUC RATIOS					
K _p	0.07 ± 0.03	0.06 ± 0.02	0.06 ± 0.01	0.12 ± 0.01**	0.11 ± 0.03**

N = 6 rats, data presented as Mean ± SD. **P* < 0.05, ***P* < 0.01, Parameters of SN in SN+LGZ or SN+PCM groups were compared with those in the SN group, respectively; #*P* < 0.05, ##*P* < 0.01, parameters of extracellular fluid of rat brain tissue were compared with that of blood tissue, respectively.

key inflammatory mediators other than prostaglandins (Liu et al., 1994; Wang et al., 2005; Chacur et al., 2010). While the antinociceptive effect of paracetamol was thought to be dependent on spinal serotonergic systems (Tjølsen et al., 1991). Thus, synergy between SN and PCM (in inflammatory pain), might also be achieved based on their complementary mechanisms.

The Inversed Result When Comparing SN Plus PCM vs. SN Plus LGZ Between the Incisional and the Inflammatory Model

In the present study synergy between SN and LGZ was lost in carrageenan induced inflammatory pain condition, while synergy between SN and PCM was lost in incisional pain condition. This inversed result indicates nociceptive system was differentially affected by SN combinations in two pain scenarios.

Surgical damage to peripheral nerve fibers is a key element for incisional pain. However, acute inflammatory pain is mainly mediated through the local inflammatory mediators, and has less “central component.” Studies have shown that both LGZ (Gao et al., 2008; Wang et al., 2016) and SN (Gao et al., 2013, 2014), but not PCM, were effective against pain following various types of nerve injuries. In addition, we have seen a pronounced “central effect,” such as inhibition of the increased spontaneous neuronal activation, and suppression of the enlarged peripheral receptive field of dorsal horn neurons (Coderre et al., 1993), being produced by SN plus LGZ against chronic pain (Gao et al., 2019a). These facts support the rationale why SN combined with LGZ but not PCM could generate synergistic effect on

incisional pain. On the other hand, in inflammatory pain conditions, it is possible that SN and LGZ combination could not sufficiently “silence” the peripheral nociceptors sensitized by the “inflammatory soup,” as the SN and PCM combination did.

In addition, the differing effects of SN combinations on carrageenan induced heat hyperalgesia could be partially linked to the pharmacokinetics changes induced by drug interaction, that SN and PCM when combinedly used, might result in a reduction of SN blood concentration and a probable increase in PCM concentration. As SN showed broad analgesic characteristics especially on incisional pain and neuropathic pain (Gao et al., 2013; Zhu et al., 2016), while PCM has an analgesic profile more reserved to inflammatory pain. It is reasonable to postulate that the pharmacokinetic change induced by SN and PCM combination, drives a shift in the analgesic potency toward a better cure for inflammatory pain (than incisional pain).

Dissociation of Mechanical and Heat Pain Modalities in Response to PCM or SN Plus PCM on in Carrageenan Induced Inflammatory Pain Condition

Hypersensitivities to mechanical and heat stimuli are predominately mediated by A-fiber and C-fiber nociceptors. In primate, A-fiber nociceptors are divided into type I A mechano-heat (AMH) units and type II AMH units (Djoughri and Lawson, 2004). Type I AMHs are noxious mechano-sensors, which predominately comprised of Aδ fibers with a few moderate pressure receptors (Aβ fibers). Type II AMHs are noxious heat-sensors, comprised of thinly myelinated Aδ fibers (Djoughri

TABLE 2 | Effects of SN on the pharmacokinetic parameters of LGZ or PCM in blood and extracellular fluid of rat brain tissue.

PK parameter	LGZ levels			PCM levels		
	LGZ (50 mg·kg ⁻¹)	LGZ + SN (50 mg·kg ⁻¹ + 50 mg·kg ⁻¹)	LGZ + SN (25 mg·kg ⁻¹ + 25 mg·kg ⁻¹)	PCM (50 mg·kg ⁻¹)	PCM + SN (50 mg·kg ⁻¹ + 50 mg·kg ⁻¹)	PCM + SN (25 mg·kg ⁻¹ + 25 mg·kg ⁻¹)
BLOOD						
AUC _{0-t} (h·μg·mL ⁻¹)	76.73 ± 14.27	94.94 ± 18.75	26.87 ± 5.83**	18.06 ± 5.94	23.78 ± 9.08	9.96 ± 3.7*
AUC _{0-∞} (h·μg·mL ⁻¹)	78.02 ± 14.06	96.24 ± 19.02	27.9 ± 5.89**	18.2 ± 6.01	24.08 ± 9.18	10.08 ± 3.71*
MRT (h)	1.04 ± 0.11	1.21 ± 0.22	0.78 ± 0.14**	0.70 ± 0.17	0.92 ± 0.16*	0.87 ± 0.37
t _{1/2} (h)	1.36 ± 0.30	1.40 ± 0.27	1.29 ± 0.43	0.73 ± 0.22	0.85 ± 0.31	0.77 ± 0.32
V _z (L·kg ⁻¹)	1.48 ± 0.58	1.07 ± 0.27	1.71 ± 0.56	2.91 ± 0.28	2.84 ± 1.38	3.05 ± 1.70
CL _z (L·h ⁻¹ ·kg ⁻¹)	0.66 ± 0.13	0.54 ± 0.10	0.93 ± 0.20*	3.03 ± 1.07	2.37 ± 0.98	2.81 ± 1.09
C _{max} (μg·mL ⁻¹)	50.04 ± 8.83	51.99 ± 7.08	23.63 ± 5.37**	16.53 ± 4.1	17.12 ± 4.08	8.66 ± 3.82**
BRAIN						
AUC _{0-t} (h·μg·mL ⁻¹)	53.81 ± 17.72 [#]	57.81 ± 22.38 [#]	16.38 ± 4.25*** [#]	9.3 ± 2.22 [#]	10.81 ± 3.90 [#]	5.01 ± 2.14 [#]
AUC _{0-∞} (h·μg·mL ⁻¹)	54.57 ± 18.11 [#]	58.42 ± 22.6 [#]	16.82 ± 4.18*** [#]	9.43 ± 2.27 [#]	10.95 ± 3.96 [#]	5.08 ± 2.17 [#]
MRT (h)	1.03 ± 0.12	1.18 ± 0.17	0.85 ± 0.06*	0.99 ± 0.14 [#]	1.09 ± 0.14	1.09 ± 0.35
t _{1/2} (h)	1.06 ± 0.13	1.19 ± 0.43	1.19 ± 0.36	0.50 ± 0.11	0.59 ± 0.07	0.58 ± 0.19
T _{max} (h)	0.28 ± 0.17	0.17 ± 0.00	0.17 ± 0.00	0.56 ± 0.14	0.50 ± 0.00	0.50 ± 0.00
C _{max} (μg·mL ⁻¹)	38.14 ± 9.21 [#]	34.73 ± 12.37 [#]	15.1 ± 2.45*** [#]	7.24 ± 1.31 [#]	7.29 ± 1.57 [#]	3.85 ± 1.00*** [#]
BRAIN-TO-BLOOD AUC RATIOS						
K _p	0.69 ± 0.16	0.60 ± 0.17	0.62 ± 0.11	0.54 ± 0.14	0.47 ± 0.1	0.54 ± 0.28

N = 6 rats, data presented as Mean ± SD. **P* < 0.05, ***P* < 0.01, Parameters of LGZ/PCM in SN+LGZ or SN+PCM groups were compared with those in the LGZ/PCM group, respectively; [#]*P* < 0.05, ****P* < 0.01, parameters of extracellular fluid of rat brain tissue were compared with those of blood tissue, respectively.

and Lawson, 2004; Woolf and Ma, 2007). Unmyelinated C-fiber nociceptors do not appear to play a major role in mechanical pain, but are heat specific nociceptors. The detection of heat and mechanical pain modalities are also mediated by specific ion channels and receptors which are localized in mature nociceptors (Woolf and Ma, 2007). For instance, heat sensitivity is mediated by multiple TRP channels—TRPV1, TRPV2, TRPV3, and TRPV4 (Dhaka et al., 2006). Looked from their threshold, TRPV1 (activated by temperature >42°C) and TRPV2 (activated by temperature >52°C) overlapped with heat pain (Caterina et al., 1999). On the other hand, mechanical sensitivity is recently revealed to be depending on activation of Piezo channels (Coste et al., 2012).

Interestingly, in mice with carrageenan induced inflammatory pain, we found PCM monotherapy reduced heat but not mechanical hypersensitivity. In addition, SN and PCM combination also only worked on heat hyperalgesia. Thus, a dissociation between mechanical and heat pain modalities has been seen in response to PCM analgesics. An explanation of this dissociation is the activities of Type I AMHs (noxious mechanosensors) that accounting for the establishment of mechanical allodynia after inflammation might be not sufficiently suppressed by PCM analgesics. While on the hand, Type II AMHs (noxious heat-sensors) and C fibers with the heat responsive receptors TRPV1 and TRPV2 (Caterina et al., 1999), which are “sleeping nociceptors” that becoming “wake” in the presence of inflammation (Woolf and Ma, 2007), could be more sensitive to PCM analgesics. Cellular and molecular mechanisms accounting for this dissociation of drug's effects are still await elucidation.

However, such phenomenon is not unique. The dissociations between different pain modalities could be also found in acute nociceptive pain or incisional pain models under physiological modulation of pain associated receptors (Pogatzki-Zahn et al., 2005; Kayser et al., 2007).

Pharmacokinetic Changes Induced by SN and PCM Combination

SN could induce a concentration dependent lowering effect on the transepithelial electrical resistance of Caco-2 cell monolayers, which was completely reversible (Lu et al., 2010), suggesting SN may altering the membrane transportation in blood brain barrier (increase the transportation of co-administered compounds). On contrary, PCM may reduce the transportation of co-administered molecules such as imatinib (Nassar et al., 2009). It is reasonable to expect that SN plus LGZ or PCM could generate drug-drug interactions that modulate the exposure of each drug in blood and brain. In this study, we were able to reveal that, when SN was combined with LGZ, pharmacokinetic properties of each drug were not altered. However, when SN was combined with PCM, the blood SN concentrations were decreased and there was a tendency of increase in blood PCM concentrations. The reduction of SN blood levels by coadministration of PCM indicates that PCM (and its metabolites) possibly increased expression of transporter proteins (Slitt et al., 2003), especially p-glycoprotein which actively excretes SN (Tsai and Wu, 2003). PCM might also enhance SN's elimination pathway from the kidney by glomerular filtration/active tubular secretion, or facilitate SN's

metabolism thorough activating specific metabolic enzymes such as cytochrome P450, though further investigation is still needed to confirm the exact mechanism.

Safety Concerns for SN Based Drug Combinations

At lethal dose (oral around 1,000 mg/kg in rats), SN can produce apparent sedation, which was soon exacerbated by an increased reflex excitability or seizure, followed by general muscular weakness and reduction in respiration, leading to fatal asphyxia (Yamasaki, 1976). In previous study, when SN was applied at the dosages larger than 80 mg/kg (oral or i.p.), only minor sedation in locomotion (without any sign of respiratory inhibition) could be seen (Gao et al., 2013). In the present study, we have not observed any sign of side effects in SN applied at 10, 20, and 80 mg/kg or in combinational formulas with LGZ or PCM. Taking consideration that repeated administration of SN did not generate tolerance, but increased the baseline thresholds in animals with chronic pain (Gao et al., 2014), the effective combinations used in this study could be safely used for long-terms.

Systemic opioids are widely used pre-/post-surgery (Chou et al., 2016), even at the risk of inducing tolerance/addiction, and eliciting delayed hyperalgesia and allodynia (Revat et al., 2002; Pergolizzi et al., 2011). We have proved that the analgesic efficacies of SN (including SN plus LGZ) could not be blocked by the opioid receptor antagonist Naloxone (Gao et al., 2015, 2019a). Therefore, combination of SN and LGZ could be useful in clinical settings as an opioid alternative medicine for controlling postoperative pain.

CONCLUSIONS

Efforts to develop novel analgesics that surpass the limitation of current treatments have not been successful. Therefore, combination therapy remains an important beneficial strategy. In the current study, we have demonstrated that at sub-effective doses, combined therapy of SN with LGZ significantly reduced mechanical and heat hypersensitivities induced by incision, and combined therapy of SN with PCM was effective against carrageenan induced heat hyperalgesia, without generating observable side effects. The pharmacological discoveries could be partially explained by pharmacokinetic alterations in SN

combinations. Although further clinical validation is still needed, these observed synergies advocate the potential benefits of using SN plus LGZ for postoperative pain management, and using SN plus PCM for controlling inflammatory pain.

DATA AVAILABILITY STATEMENT

HPLC-MS/MS data were uploaded to FigShare; doi: 10.6084/m9.figshare.11545581.

ETHICS STATEMENT

The animal study was reviewed and approved by Stockholm Ethical Committee, Research Ethics Committee at China Academy of Chinese Medical Sciences.

AUTHOR CONTRIBUTIONS

JG, YH, DW, J-DJ, and TG initiated the study and decided the research goal. TG, TL, DW, and JG have major contributions for accomplishing research study. JG, TG, TL, and DW analyzed research data. All authors were involved in establishing the research protocol, preparing the manuscript, and approved the final version of the manuscript.

FUNDING

This study was supported by Fundamental Research Funds for the Central Universities (3332018086), CAMS Innovation Fund for Medical Sciences (2017-I2M-B&R-07, 2019-I2M-5-055, 2020-I2M-1-003, 2017-I2M-B&R-09, 2016-I2M-1-011), The Drug Innovation Major Project (2018ZX09711001-011-003), National Natural Science Foundation (81503278), Fundamental Research Funds for the Central public welfare research institutes (ZZ2019008, ZZ14-YQ-041, ZZ13-YQ-078), and Stiftelsen Olle Engkvist Byggmastre Foundation (2014-12-22, to TG).

SUPPLEMENTARY MATERIAL

The Supplementary Material for this article can be found online at: <https://www.frontiersin.org/articles/10.3389/fphys.2020.523769/full#supplementary-material>

REFERENCES

- Boddeke, E. W. (2001). Involvement of chemokines in pain. *Eur. J. Pharmacol.* 429, 115–119. doi: 10.1016/S0014-2999(01)01311-5
- Brevik, H., Collet, B., Ventafridda, V., Cohen, R., and Gallacher, D. (2006). Survey of chronic pain in Europe: prevalence, impact on daily life, and treatment. *Eur. J. Pain* 10, 287–333. doi: 10.1016/j.ejpain.2005.06.009
- Brennan, T. J., Vandermeulen, E. P., and Gebhart, G. F. (1996). Characterization of a rat model of incisional pain. *Pain* 64, 493–501. doi: 10.1016/0304-3959(95)01441-1
- Brennan, T. J., Zahn, P. K., and Pogatzki-Zahn, E. M. (2005). Mechanisms of Incisional pain. *Anesthesiol. Clin. North Am.* 23, 1–20. doi: 10.1016/j.atc.2004.11.009
- Caterina, M. J., Rosen, T. A., Tominaga, M., Brake, A. J., and Julius, D. (1999). A capsaicin-receptor homologue with a high threshold for noxious heat. *Nature* 398, 436–441. doi: 10.1038/18906
- Chacur, M., Matos, R. J., Alves, A. S., Rodrigues, A. C., Gutierrez, V., Cury, Y., et al. (2010). Participation of neuronal nitric oxide synthase in experimental neuropathic pain induced by sciatic nerve transection. *Braz. J. Med. Biol. Res.* 43, 367–376. doi: 10.1590/S0100-879X2010007500019
- Chou, R., Gordon, B. D., de Leon-Casasola, A. O., Rosenberg, M. J., Bickler, S., Brennan, T., et al. (2016). Management of Postoperative pain: a clinical practice guideline from the American Pain Society, the American Society of Regional Anesthesia and Pain Medicine, and the American Society of Anesthesiologists' Committee on Regional Anesthesia, Executive Committee, and Administrative Council. *J. Pain* 17, 131–157. doi: 10.1016/j.jpain.2015.12.008

- Coderre, T. J., Katz, J., Vaccarino, A. L., and Melzack, R. (1993). Contribution of central neuroplasticity to pathological pain: review of clinical and experimental evidence. *Pain* 52, 259–285. doi: 10.1016/0304-3959(93)90161-H
- Coste, B., Xiao, B., Santos, J. S., Syeda, R., Grandl, J., Spencer, K. S., et al. (2012). Piezo proteins are pore-forming subunits of mechanically activated channels. *Nature* 483, 176–181. doi: 10.1038/nature10812
- Dhaka, A., Viswanath, V., and Patapoutian, A. (2006). TRP ion channels and temperature sensation. *Annu. Rev. Neurosci.* 29, 135–161. doi: 10.1146/annurev.neuro.29.051605.112958
- Djouhri, L., and Lawson, S. N. (2004). Abeta-fiber nociceptive primary afferent neurons: a review of incidence and properties in relation to other afferent A-fiber neurons in mammals. *Brain Res. Rev.* 46, 131–145. doi: 10.1016/j.brainresrev.2004.07.015
- Feng, H., Yamaki, K., Takano, H., Inoue, K., Yanagisawa, R., and Yoshino, S. (2007). Effect of sinomenine on collagen-induced arthritis in mice. *Autoimmunity* 40, 532–539. doi: 10.1080/08916930701615159
- Gao, T., Hao, J., Wiesenfeld-Hallin, Z., Wang, D.-Q., and Xu, X.-J. (2013). Analgesic effect of sinomenine in rodents after inflammation and nerve injury. *Eur. J. Pharmacol.* 721, 5–11. doi: 10.1016/j.ejphar.2013.09.062
- Gao, T., Li, T., Jiang, W., Fan, W., and Jiang, J.-D. (2019b). Exploratory study data for determining the adverse effects of sinomenine plus gabapentin or ligustrazine hydrochloride and the pharmacokinetic insights of sinomenine in plasma and CNS tissue. *Data Brief* 27:104633. doi: 10.1016/j.dib.2019.104633
- Gao, T., Shi, T., Wang, D.-Q., Wiesenfeld-Hallin, Z., and Xu, X.-J. (2014). Repeated sinomenine administration alleviates chronic neuropathic pain-like behaviours in rodents without producing tolerance. *Scand. J. Pain* 5, 249–255. doi: 10.1016/j.sjpain.2014.05.006
- Gao, T., Shi, T., Wiesenfeld-Hallin, Z., Li, T., Jiang, J.-D., and Xu, X.-J. (2019a). Sinomenine facilitates the efficacy of gabapentin or ligustrazine hydrochloride in animal models of neuropathic pain. *Eur. J. Pharmacol.* 854, 101–108. doi: 10.1016/j.ejphar.2019.03.061
- Gao, T., Shi, T., Wiesenfeld-Hallin, Z., Svensson, C. I., and Xu, X.-J. (2015). Sinomenine alleviates mechanical hypersensitivity in mice with experimentally-induced rheumatoid arthritis. *Scand. J. Pain* 7, 9–14. doi: 10.1016/j.sjpain.2014.12.003
- Gao, X., Kim, K. H., Chuang, M. J., and Chung, K. (2007). Reactive oxygen species (ROS) are involved in enhancement of NMDA-receptor phosphorylation in animal models of pain. *Pain* 131, 262–271. doi: 10.1016/j.pain.2007.01.011
- Gao, Y., Xu, C., Liang, S., Zhang, A., Mu, S., Wang, Y., et al. (2008). Effect of tetramethylpyrazine on primary afferent transmission mediated by P2X3 receptor in neuropathic pain states. *Brain Res. Bull.* 77, 27–32. doi: 10.1016/j.brainresbull.2008.02.026
- Gilron, I., Jensen, T. S., and Dickenson, A. H. (2013). Combination pharmacotherapy for management of chronic pain: from bench to bedside. *Lancet Neurol.* 12, 1084–1095. doi: 10.1016/S1474-4422(13)70193-5
- Graham, G. G., and Scott, K. F. (2005). Mechanism of action of paracetamol. *Am. J. Ther.* 12, 46–55. doi: 10.1097/00045391-200501000-00008
- Hao, J.-X., Xu, I.-S., Wiesenfeld-Hallin, Z., and Xu, X.-J. (1998). Anti-hyperalgesic and anti-allodynic effects of intrathecal nociceptin/orphanin FQ in rats after spinal cord injury, peripheral nerve injury and inflammation. *Pain* 76, 385–393. doi: 10.1016/S0304-3959(98)00071-2
- Häuser, W., and Fitzcharles, M.-A. (2017). Opioids for RA: a clinical dilemma. *Nat. Rev. Rheumatol.* 13, 521–522. doi: 10.1038/nrrheum.2017.123
- Jiang, W., Fan, W., Gao, T., Li, T., Yin, Z., Guo, H., et al. (2020). Analgesic mechanism of sinomenine against chronic pain. *Pain Res. Manag.* 2020:1876862. doi: 10.1155/2020/1876862
- Kayser, V., Elfassi, I. E., Aubel, B., Melfort, M., Julius, D., Gingrich, J. A., et al. (2007). Mechanical, thermal and formalin-induced nociception is differentially altered in 5-HT1A-/-, 5-HT1B-/-, 5-HT2A-/-, 5-HT3A-/- and 5-HTT-/- knock-out male mice. *Pain* 130, 235–248. doi: 10.1016/j.pain.2006.11.015
- Langley, P. C. (2011). The prevalence, correlates and treatment of pain in the European Union. *Curr. Med. Res. Opin.* 27, 463–480. doi: 10.1185/03007995.2010.542136
- Li, T., Zhao, X., Gao, T., Jiao, Y., Gao, W., Liu, Y., et al. (2020). Microdialysis sampling and HPLC-MS/MS quantification of sinomenine, ligustrazine, gabapentin, paracetamol, pregabalin and amitriptyline in rat blood and brain extracellular fluid. *Acta Pharm. Sin.* 55, 2198–2206. doi: 10.16438/j.0513-4870.2020-0537
- Li, T., Zhao, X., Nie, Y., Jiao, Y., Liu, Y., Zhang, M., et al. (2019). UHPLC quantification and brain permeability study of sinomenine and ligustrazine in CQM after single intravenous administration. *Acta Pharm. Sin.* 54, 2308–2315. doi: 10.16438/j.0513-4870.2019-0515
- Liang, S.-D., Gao, Y., Xu, C.-S., Xu, B.-H., and Mu, S.-N. (2004). Effect of tetramethylpyrazine on acute nociception mediated by signaling of P2X receptor activation in rat. *Brain Res.* 995, 247–252. doi: 10.1016/j.brainres.2003.09.070
- Liu, C., Li, Z., Huang, Z., Zhang, K., Hu, C., Zuo, Z., et al. (2018). Ligustrazine enhances the hypnotic and analgesic effect of ketamine in mice. *Biol. Pharm. Bull.* 41, 690–696. doi: 10.1248/bpb.b17-00869
- Liu, L., Riese, J., Resch, K., and Kaever, V. (1994). Impairment of macrophage eicosanoid and nitric oxide production by an alkaloid from *Sinomenium acutum*. *Arzneimittelforschung* 44, 1123–1126.
- Lu, Z., Chen, W., Viljoen, A., and Hamman, J. H. (2010). Effect of sinomenine on the *in vitro* intestinal epithelial transport of selected compounds. *Phytother. Res.* 24, 211–218. doi: 10.1002/ptr.2914
- Mantyh, P. W., Clohisy, D. R., Koltzenburg, M., and Hunt, S. P. (2002). Molecular mechanisms of cancer pain. *Nat. Rev. Cancer* 2, 201–209. doi: 10.1038/nrc747
- Nassar, I., Pasupati, T., Judson, J. P., and Segarra, I. (2009). Reduced exposure of imatinib after coadministration with acetaminophen in mice. *Indian J. Pharmacol.* 41, 167–172. doi: 10.4103/0253-7613.56071
- Paxinos, G., and Watson, C. (1998). *The Rat Brain in Stereotaxic Coordinate*, 4th Edn. New York, NY: Academic Press.
- Pergolizzi, J., Alegre, C., Blake, D., Alén, J. C., Caporali, R., Casser, H. R., et al. (2011). Current considerations for the treatment of severe chronic pain: the potential for Tapentadol. *Pain Pract.* 12, 290–306. doi: 10.1111/j.1533-2500.2011.00487.x
- Pogatzki-Zahn, E. M., Shimizu, I., Caterina, M., and Raja, S. N. (2005). Heat hyperalgesia after incision requires TRPV1 and is distinct from pure inflammatory pain. *Pain* 115, 296–307. doi: 10.1016/j.pain.2005.03.010
- Qian, L., Xu, Z., Zhang, W., Wilson, B., Hong, J. S., and Flood, P. M. (2007). Sinomenine, a natural dextrorotatory morphinan analog, is anti-inflammatory and neuroprotective through inhibition of microglial NADPH oxidase. *J. Neuroinflamm.* 4:23. doi: 10.1186/1742-2094-4-23
- Revat, C., Laulin, J. P., Corcuff, J. B., Célérier, E., Pain, L., and Simonnet, G. (2002). Fentanyl enhancement of carrageenan-induced long-lasting hyperalgesia in rats: prevention by the N-methyl-D-aspartate receptor antagonist ketamine. *Anesthesiology* 96, 381–391. doi: 10.1097/0000542-200202000-00025
- Scholz, J., and Woolf, C. J. (2002). Can we conquer pain? *Nat. Neurosci.* 5, 1062–1067. doi: 10.1038/nn942
- Slitt, A. L., Cherrington, N. J., Maher, J. M., and Klaassen, C. D. (2003). Induction of multidrug resistance protein 3 in rat liver is associated with altered vectorial excretion of acetaminophen metabolites. *Drug Metab. Dispos. Biol. Fate Chem.* 31, 1176–1186. doi: 10.1124/dmd.31.9.1176
- Tjølsen, A., Lund, A., and Hole, K. (1991). Antinociceptive effect of paracetamol in rats is partly dependent on spinal serotonergic systems. *Eur. J. Pharmacol.* 193, 193–201. doi: 10.1016/0014-2999(91)90036-P
- Tsai, T. H., and Wu, J. W. (2003). Regulation of hepatobiliary excretion of sinomenine by P-glycoprotein in Sprague-Dawley rats. *Life Sci.* 72, 2413–2426. doi: 10.1016/S0024-3205(03)00118-8
- Vorobeychik, Y., Gordin, V., Mao, J., and Chen, L. (2011). Combination therapy for neuropathic pain: a review of current evidence. *CNS Drugs* 25, 1023–1034. doi: 10.2165/11596280-000000000-00000
- Wang, S., Li, A., and Guo, S. (2016). Ligustrazine attenuates neuropathic pain by inhibition of JAK/STAT3 pathway in a rat model of chronic constriction injury. *Pharmazie* 71, 408–412. doi: 10.1691/ph.2016.6546
- Wang, Y., Fang, Y., Huang, W., Zhou, X., Wang, M., Zhong, B., et al. (2005). Effect of sinomenine on cytokine expression of macrophages and synoviocytes in adjuvant arthritis rats. *J. Ethnopharmacol.* 98, 37–43. doi: 10.1016/j.jep.2004.12.022
- Woolf, C. J., and Ma, Q. (2007). Nociceptors—noxious stimulus detectors. *Neuron* 55, 353–364. doi: 10.1016/j.neuron.2007.07.016
- Woolf, C. J., and Thompson, S. W. (1991). The induction and maintenance of central sensitization is dependent on N-methyl-D-aspartic acid receptor

- activation: implications for the treatment of post-injury pain hypersensitivity states. *Pain* 44, 293–299. doi: 10.1016/0304-3959(91)90100-C
- Xu, M., Liu, L., Qi, C., Deng, B., and Cai, X. (2008). Sinomenine versus NSAIDs for the treatment of rheumatoid arthritis: a systemic review and meta-analysis. *Planta. Med.* 74, 1423–1429. doi: 10.1055/s-2008-1081346
- Yamasaki, H. (1976). Pharmacology of sinomenine, an anti-rheumatic alkaloid from sinomenium. *Acta Med. Okayama* 30, 1–19.
- Zhao, X.-L., Li, T., Liu, Y., Zhang, M.-Y., Chen, Y., Cui, Y., et al. (2015). Pharmacokinetic analysis of sinomenine based on automatic blood sampling system and HPLC-QQQ-MS. *Chin. J. Exp. Trad. Med. Formulae* 21:14. doi: 10.13422/j.cnki.syfjx.2015140066
- Zhu, Q., Sun, Y., Mao, L., Liu, C., Jiang, B., Zhang, W., et al. (2016). Antinociceptive effects of sinomenine in a rat model of postoperative pain. *Br. J. Pharmacol.* 173, 1693–1702. doi: 10.1111/bph.13470

Conflict of Interest: WJ and WF were employed by the company Zhejiang Zhenyuan Pharmaceutical Co., Ltd.

The remaining authors declare that the research was conducted in the absence of any commercial or financial relationships that could be construed as a potential conflict of interest.

Copyright © 2021 Gao, Li, Jiang, Fan, Xu, Zhao, Yin, Guo, Wang, Gao, Han, Jiang and Wang. This is an open-access article distributed under the terms of the Creative Commons Attribution License (CC BY). The use, distribution or reproduction in other forums is permitted, provided the original author(s) and the copyright owner(s) are credited and that the original publication in this journal is cited, in accordance with accepted academic practice. No use, distribution or reproduction is permitted which does not comply with these terms.



Performance of the Surgical Pleth Index and Analgesia Nociception Index in Healthy Volunteers and Parturients

Byung-Moon Choi^{1†}, Hangsik Shin^{2†}, Joo-Hyun Lee³, Ji-Yeon Bang¹, Eun-Kyung Lee⁴ and Gyu-Jeong Noh^{1,5*}

¹ Department of Anesthesiology and Pain Medicine, Asan Medical Center, University of Ulsan College of Medicine, Seoul, South Korea, ² Department of Biomedical Engineering, College of Engineering, Chonnam National University, Yeosu, South Korea, ³ Department of Anesthesiology and Pain Medicine, International St. Mary's Hospital, Catholic Kwandong University, Incheon, South Korea, ⁴ Department of Statistics, Ewha Womans University, Seoul, South Korea, ⁵ Department of Clinical Pharmacology and Therapeutics, Asan Medical Center, University of Ulsan College of Medicine, Seoul, South Korea

OPEN ACCESS

Edited by:

Istvan Nagy,
Imperial College London,
United Kingdom

Reviewed by:

Aisah Anisah Aubdool,
Queen Mary University of London,
United Kingdom
Antonio Longo,
University of Catania, Italy

*Correspondence:

Gyu-Jeong Noh
nohgy@amc.seoul.kr
orcid.org/0000-0002-1964-9294

[†] These authors have contributed
equally to this work and share first
authorship

Specialty section:

This article was submitted to
Integrative Physiology,
a section of the journal
Frontiers in Physiology

Received: 29 April 2020

Accepted: 08 February 2021

Published: 08 March 2021

Citation:

Choi B-M, Shin H, Lee J-H,
Bang J-Y, Lee E-K and Noh G-J
(2021) Performance of the Surgical
Pleth Index and Analgesia
Nociception Index in Healthy
Volunteers and Parturients.
Front. Physiol. 12:554026.
doi: 10.3389/fphys.2021.554026

Various commercially available nociception devices have been developed to quantify intraoperative pain. The Surgical Pleth Index (SPI) and Analgesia Nociception Index (ANI) are among the analgesic indices that have been widely used for the evaluation of surgical patients. This study aimed to evaluate the clinical performance of the SPI and ANI in conscious healthy volunteers and parturients. Ten healthy volunteers and 10 parturients participated in this study. An algometer was used to induce bone pain in the volunteers until they rated their pain as five on the numerical rating scale (NRS); this procedure was repeated during the administration of remifentanyl or normal saline. The study comprised two periods, and the volunteers were infused with different solutions in each period: normal saline during one period and remifentanyl during the other in a randomized order. The parturients' SPI and ANI data were collected for 2 min when they rated their pain levels as 0, 5, and 7 on the NRS, respectively. Both the SPI and ANI values differed significantly between NRS 0 and NRS 5 ($P < 0.001$) in the volunteers, irrespective of the solution administered (remifentanyl or normal saline). At NRS 5, the SPI showed similar values, irrespective of remifentanyl administration, while the ANI showed significantly lower values on remifentanyl administration ($P = 0.028$). The SPI and ANI values at NRS 5 and NRS 7 did not differ significantly in the parturients ($P = 0.101$ for SPI, $P = 0.687$ for ANI). Thus, the SPI and ANI were effective indices for detecting pain in healthy volunteers and parturients.

Keywords: index, pain quantification, volunteers, parturient, physiologic change

INTRODUCTION

Various commercially available nociception devices have been developed for the quantification of intraoperative pain (Ledowski, 2019). These devices possess distinct algorithms that detect the changes in the autonomic nervous system in response to surgical stress (Ledowski, 2019). The performance of analgesic indices such as the Surgical Pleth Index (SPI, GE

Healthcare, Milwaukee, WI, United States) and Analgesia Nociception Index (ANI; MetroDoloris™, Loos, France) has been widely evaluated mainly in surgical patients (Gruenewald et al., 2015; Ledowski et al., 2016; Chanques et al., 2017). The SPI evaluates peripheral vasoconstriction and cardiac autonomic tone using two variables, i.e., the heartbeat interval (HBI) and photoplethysmographic amplitude (PPGA). The equation for calculating the SPI value is as follows: $SPI = 100 - (0.7 \times PPGAnorm + 0.3 \times HBInorm)$, where PPGAnorm and HBInorm stand for the normalized PPGA and HBI, respectively (Ledowski, 2019). The value of the SPI can lie between 0 and 100 and approaches zero with the activation of the sympathetic nerves. The ANI calculates the area under the curve of the high-frequency spectrum of heart rate variability (HRV) and presents it as a value ranging from 0 to 100 (Ledowski, 2019). The ANI value approaches 100 as the parasympathetic nerves are activated. The SPI and ANI should reflect the degree of pain as accurately as possible if they are to be used as meaningful quantitative surrogate measures of pain. If the intensity of the pain felt by the patient is the same, irrespective of analgesic administration, analgesic indices that show similar values for measurements performed in conditions with and without analgesic administration will be more useful. This is because pain management is performed according to the pain score in actual clinical practice [e.g., numerical rating scale (NRS)], which is calculated according to the rating provided by the patient. A recent meta-analysis showed that SPI-guided anesthesia reduced opioid consumption (Won et al., 2018). ANI scores >50 had a high negative predictive value for moderate or severe pain (Boselli et al., 2014). However, studies evaluating the performance of these indices in conscious healthy volunteers are scarce (Yan et al., 2017). The advantage of volunteer-based studies is that they permit the application of numerous methods that cannot be easily used in patient-based studies. Therefore, the performance of these indices should be evaluated using well-controlled volunteer studies.

Another useful study design for accurately assessing the clinical performance of nociception indices entails enrolling participants who feel pain over a wide spectrum of intensity within the same environment. Parturients feel different degrees of pain depending on the cycle of uterine contraction (Labor and Maguire, 2008). The neurophysiology of labor pain can be characterized into two stages. Pain during the first stage of labor is mostly caused by the stimulation of the uterine chemoreceptors, which respond to stretching caused by uterine contractions (Labor and Maguire, 2008). The second stage of labor is associated with a more somatic component resulting from the stretching of the vagina and traction on the uterine ligaments and pelvic organs (Labor and Maguire, 2008). The characteristics of labor pain enable the observation of various changes in pain that occur over time within an individual, which can be useful for evaluating the performance of analgesic indices. Thus, we evaluated the performances of the SPI and ANI in conscious healthy volunteers and parturients.

MATERIALS AND METHODS

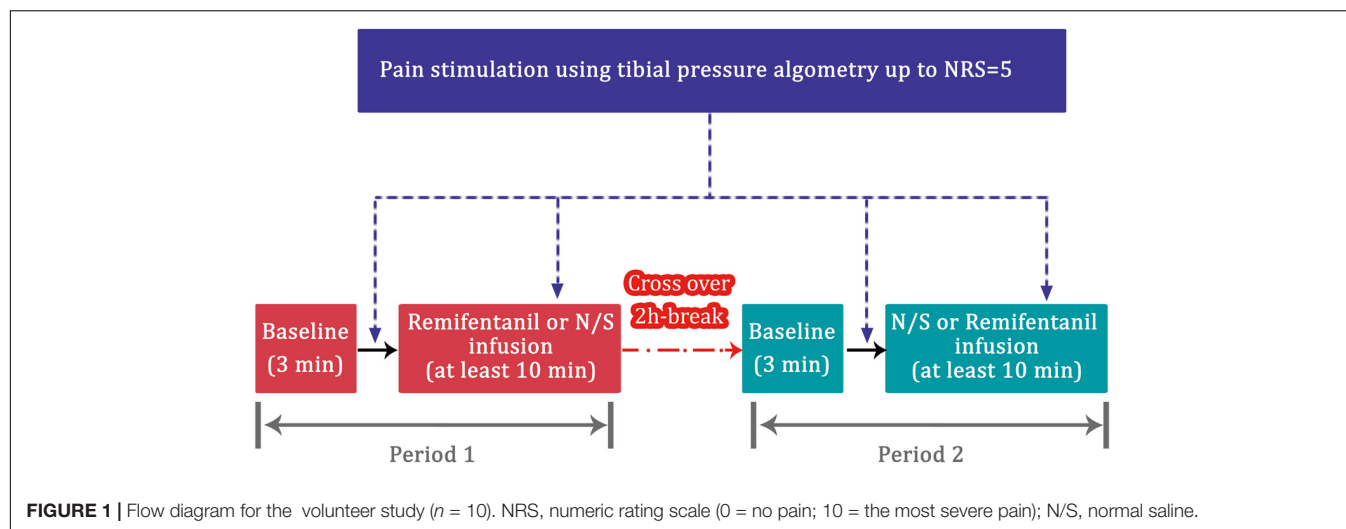
Study Design and Procedure for Volunteers

The volunteer-based study incorporated a randomized, two-period, cross-over design. The study protocol was approved by the institutional review board of Asan Medical Center (approval number: 2014-0309) and registered with an international clinical research information system (¹ KCT0001808, date of registration: February 11, 2016). All methods were performed in accordance with the relevant guidelines and regulations of the institution. Ten healthy young volunteers were enrolled after obtaining informed written consent. The exclusion criteria included autonomic nervous system disorders, arrhythmia, use of sedatives, history of neurosurgery, psychiatric diseases, epilepsy, pregnancy, and any neuromuscular disease evoking spontaneous pain.

All volunteers were monitored using electrocardiography (ECG) and pulse oximetry in the operating room. A reusable SPI sensor (Carescape® B850; GE Healthcare, Milwaukee, WI, United States) was placed on the index finger of one arm. The ANI values were obtained using the ANI electrodes in V1 and V5 ECG positions and were continuously displayed on a stand-alone ANI monitor (MetroDoloris, Lille, France). The SPI and ANI values were recorded on a laptop for offline analysis. The study comprised two periods (**Figure 1**). The volunteers were allowed to acclimatize to the surroundings for at least 10 min in the supine position in a quiet operating room, after which the baseline data (without pain) were collected for 3 min. A painful algometric stimulus was applied with an algometer composed of a piston with a pressure area of 1 cm², and control components were fixed over the anterior tibial bone 15 cm distal to the patella bone. The force driving the piston was manually increased by 25 or 30 N every 10 s until the volunteer rated their pain as five on the NRS. The pressure was maintained for 1 min after reaching an NRS score of 5. The volunteers were allowed to rest for 15 min after the first pain stimulation. The first painful algometric stimulus was applied without any infusion, and the second stimulus was applied at least 10 min after achieving a pseudo-steady state between the blood and brain during the infusion of normal saline or remifentanyl. The administration time was set to at least 10 min based on the results of a previous study. The amount of remifentanyl required to effectively suppress the noxious stimulus of endotracheal intubation was 135 µg (Park et al., 2018). The administration time of remifentanyl was set to at least 10 min after accounting for the target effect-site concentration and the volunteer's weight because the painful algometric stimulus was required after administration of at least this dose or more. The infusion of the target effect-site concentration (3 ng/mL) of remifentanyl or normal saline was controlled using the Minto model (Asan Pump, version 2.1.3, Bionet Co., Ltd., Seoul, South Korea, ², last

¹<http://cris.nih.go.kr>

²<http://www.fit4nm.org/download>



accessed: June 24, 2014) (Minto et al., 1997). The target concentration was set to 3 ng/mL was based on the results of our previous study. An effect-site concentration of remifentanyl 9.11 ng/mL was associated with a 50% probability of occurrence of muscle rigidity (Choe et al., 2017). According to the results of the pharmacodynamic model constructed in the previous study (Choe et al., 2017), the target concentration was set to 3 ng/mL because muscle rigidity may occur when the concentration of remifentanyl exceeds 4 ng/mL. The two study periods were separated by a washout interval of 2 h to avoid carryover effects. The same procedure was repeated once again, but the drug to be administered was changed. The volunteers were infused with different solutions in each period: normal saline in one period and remifentanyl in the other in random order. Simple randomization was performed using a computer-generated allocation sequence. Volunteer randomization was conducted by a coordinator who was not involved in this study.

Study Design and Procedure for Parturients

The protocol of parturient-based observational study was approved by the institutional review board of Asan Medical Center (approval number: 2014-0318) and registered at an international clinical research information system (see text footnote 1, KCT0001793, date of registration: February 01, 2016). All procedures were performed in accordance with the relevant guidelines and regulations of the institution. Ten women admitted for labor and delivery, who had elected to have natural childbirth were enrolled after obtaining informed written consent. The parturients were fully informed about the study protocols. Parturients with clinically significant cardiovascular, respiratory, or endocrine diseases, medications that could affect the heart rate or arrhythmia were excluded. Data collection for the ANI and SPI was performed in the labor ward prior to epidural catheter insertion. According to the standard of care, ECG monitoring was not performed

during the data collection periods. SPI and ANI data were collected for 2 min when the parturient rated their pain as 0 (no pain), 5 (moderate pain), and 7 (severe pain) on the NRS, respectively.

Statistical Analysis

This was not a confirmation study, and the sample size was not calculated owing to its exploratory nature. The sample size was also not calculated by other studies that evaluated the performance of SPI and ANI for this reason (Le Guen et al., 2012; Yan et al., 2017). The sample size was determined within the range in which the clinical trial was practically possible after considering various circumstances. Instead, we decided to assess the validity of the sample size by calculating the power based on the results. Statistical analysis was performed using SigmaStat 3.5 for Windows (Systat Software, Inc., Chicago, IL, United States) and GraphPad Prism 8.2.0 (GraphPad Software, Inc., La Jolla, CA, United States). The means of the SPI and ANI values obtained during baseline measurement in each volunteer were compared with the maximum and minimum values, respectively, obtained within 2 min after establishing the NRS 5 scores. The SPI and ANI data acquired during the three sequences in the volunteers [baseline (NRS 0), first pain stimulation (NRS 5), and second pain stimulation (NRS 5[±])] were compared using the one-way repeated measures ANOVA. The effect of these sequences was considered in the analyses. The mean values of SPI and ANI measured at NRS 0 in the parturients were compared with the maximum and minimum values, respectively, within 2 min after establishing the NRS 5 and NRS 7 scores. The SPI and ANI data obtained during the three sequences in the parturients (NRS 0, NRS 5, and NRS 7) were compared using the one-way repeated measures ANOVA. Data were expressed as mean \pm standard deviation (SD) for normally distributed continuous variables, median (25–75%) for non-normally distributed continuous variables, and counts and percentages for categorical variables. P -values < 0.05 were considered statistically significant.

RESULTS

Volunteers

Sixty sets each of SPI and ANI measurements obtained from the 10 volunteers were analyzed. The volunteers' characteristics are presented in **Table 1**. Algometric forces needed to induce bone pain and heart rate during the study periods are summarized in **Table 2**. The forces needed to obtain NRS 5 were higher during remifentanyl infusion compared with those at the first algometric stimulation in the absence of any medication. The placebo effect was not observed during the normal saline infusion period. After algometric stimulation, the heart rates tended to be higher than those at baseline, and this increase in the heart rate was more prominent after the application of a greater algometric force during the remifentanyl period (**Table 2**). The changes in the SPI and ANI values are presented in **Figure 2**. Significant differences were observed between the SPI and ANI values at NRS 0 and NRS 5, irrespective of the infusion of remifentanyl or normal saline ($P < 0.001$). The SPI values were similar for NRS 5, irrespective of remifentanyl administration, whereas the ANI values were lower for NRS 5 during remifentanyl administration ($P = 0.028$).

Parturients

A total of 16 parturients were enrolled in this study. Six parturients dropped out from the study due to withdrawal of consent ($n = 1$), failure to collect data due to childbirth ($n = 3$), and change to cesarean section ($n = 2$). Thirty sets of SPI and ANI data, each obtained from 10 parturients, were used for the analysis. The characteristics of the parturients are shown in **Table 1**. The changes in the SPI and ANI with respect to the NRS scores are shown in **Figure 3**. Both indices exhibited good distinction depending on the presence of pain (NRS 0 vs. NRS 5 or 7) but did not differ significantly between NRS 5 and NRS 7 (SPI: 47.2 ± 10.7 at NRS 5 and 51.5 ± 11.4 at NRS 7, $P = 0.101$; ANI: 55.5 ± 12.9 at NRS 5 and 54.1 ± 10.7 at NRS 7, $P = 0.687$).

DISCUSSION

The SPI and ANI differed significantly depending on the presence of pain as assessed by the NRS in both volunteers and parturients. The SPI values for NRS 5 were similar, irrespective of remifentanyl administration at the target effect-site concentration of $3 \mu\text{g/mL}$ in volunteers, whereas the ANI values decreased with remifentanyl administration. Neither index was able to distinguish between NRS 5 and 7 scores in parturients.

The results of our volunteer study showed that the SPI may be more appropriate for assessing pain under the influence of remifentanyl from the perspective of its utility in accurately reflecting the degree of pain experienced by the patient. Pain is defined as an unpleasant sensory and emotional experience associated with actual or potential tissue damage or described in terms of such damage (Williams and Craig, 2016). Pain management is mainly based on the subjective evaluation of the patient's complaint. The NRS for pain is mainly used in

TABLE 1 | Characteristics of the study participants.

	Volunteers ($n = 10$)	Parturients ($n = 10$)
Male/female	7/3	0/10
Age, years	22.6 ± 1.5	30.7 ± 4.0
Height, cm	$178.4 (167.6\text{--}179.8)$	160.3 ± 4.1
Weight, kg	67.2 ± 10.7	66.7 ± 11.7
Gestational age, weeks	–	$38.5 (38.0\text{--}39.0)$
Mean infusion rate of remifentanyl, $\mu\text{g/kg/min}$	0.19 ± 0.02	–

Data are expressed as the mean \pm SD, median (25–75%), or count as appropriate.

*The mean infusion rate was calculated as follows:

$$\text{Mean infusion rate} = \frac{\text{Total dose administered during study period}}{\text{Body weight} \times \text{infusion duration}}.$$

clinical practice, and an appropriate analgesic is administered based on the NRS score. For example, according to our hospital's standards, surgical patients received tramadol 50 mg or pethidine 25 mg if their NRS score was more than four or seven, respectively (Jung et al., 2016). In other words, the NRS score determines the need for the type of rescue analgesic and its administration. Since the pain corresponding to the NRS score of five is inevitably different for each patient, an analgesic index that reflects the patient-determined NRS score is necessary in clinical settings. In the current volunteer study, the algometric force corresponding to five points on the NRS was higher when remifentanyl was administered (**Table 2**), which can be interpreted as a logical result, because analgesics were administered in this situation. Pain can only be managed with the NRS score based on the patient's response in actual clinical practice because it is impossible to know the actual intensity of pain corresponding to the algometric force. In fact, even if the pain is very severe, rescue analgesics are not administered unless the patient consent to it. Therefore, it is helpful for the quantitative analgesic index to be well-matched with the NRS score, irrespective of analgesic administration. Moreover, the ANI may have good responsiveness to opioids according to our results, although no study has evaluated the performance of opioid responsiveness for these indices to the best of our knowledge. Based on the results of this study, the ANI may be likely to overestimate pain in the presence of remifentanyl administration. This difference between the two indices may be partly explained by the difference in their algorithms. The SPI value is determined by two variables, i.e., PPGA and HBI (Huiku et al., 2007). The weight of PPGA is approximately twice as great as that of the HBI. In contrast, the ANI value is based only on the HRV and is calculated as the surface of the filtered R-R interval obtained from ECG (Jeanne et al., 2009). Remifentanyl has been shown to blunt the response of HRV to noxious stimuli (Luginbuhl et al., 2007), while the PPGA response was little affected by remifentanyl (Struys et al., 2007). Hence, the SPI seems to be more precise than the ANI in reflecting pain, even with the infusion of remifentanyl.

TABLE 2 | Algometric forces needed to induce bone pain and heart rate in the volunteers.

	Normal saline			Remifentanyl		
	NRS 0	NRS 5	NRS 5*	NRS 0	NRS 5	NRS 5*
Algometric force, N	0	108.5 ± 55.0 [†]	112.5 ± 53.0 [†]	0	98.0 ± 41.0 [†]	173.5 ± 55.4 ^{†‡}
HR, bpm	66.1 (59.8–71.6)	68.6 (58.7–71.5)	71.9 (60.9–75.2) [†]	62.6 ± 7.3	65.7 ± 8.9	78.2 ± 17.0 ^{†‡}
RRI, ms	902.0 ± 104.3	895.2 ± 103.4	869.6 ± 87.7	963.3 ± 88.8	918.3 ± 98.9	784.9 ± 154.2 ^{†‡}

Data are expressed as the mean ± SD or median (25–75%) as appropriate. One volunteer (ID8) showed frequent premature atrial contraction on electrocardiography and was excluded from the HR and RRI analyses. NRS, numerical rating scale for pain; NRS 0, baseline; NRS 5, first algometric stimulation in the absence of any medication; NRS 5*, second algometric stimulation during infusion of normal saline or remifentanyl; HR, heart rate; BPM, beats per minute; RRI, R-R intervals. Three sequences in the volunteers (NRS 0, NRS 5, and NRS 5*) were compared using the one-way repeated measures analysis of variance (ANOVA) followed by a post hoc Holm–Sidak test or Friedman repeated ANOVA by rank followed by a post hoc Tukey's test. [†]*P* < 0.05 vs. NRS 0, [‡]*P* < 0.05 vs. NRS 5.

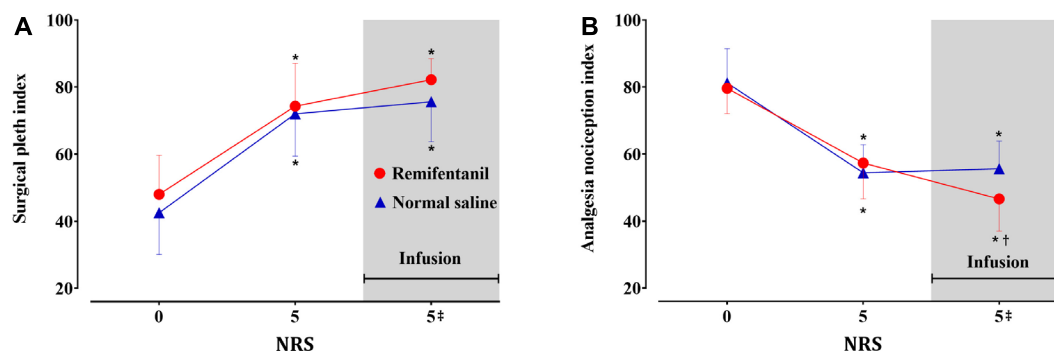


FIGURE 2 | Surgical Pleth Index (A) and Analgesia Nociception Index (B) values in the volunteers (*n* = 10). Data are expressed as mean with the error bars representing standard deviation. Numerical rating scale for pain (NRS) 0: baseline, 5: first algometric stimulation in the absence of medication, 5*: second algometric stimulation during infusion of remifentanyl (red circle) or normal saline (blue triangle). Three sequences (NRS 0, 5, and 5*) were compared using the one-way repeated measures analysis of variance (ANOVA) followed by a post hoc Holm–Sidak test. **P* < 0.05 vs. baseline, [†]*P* < 0.05 vs. NRS 5.

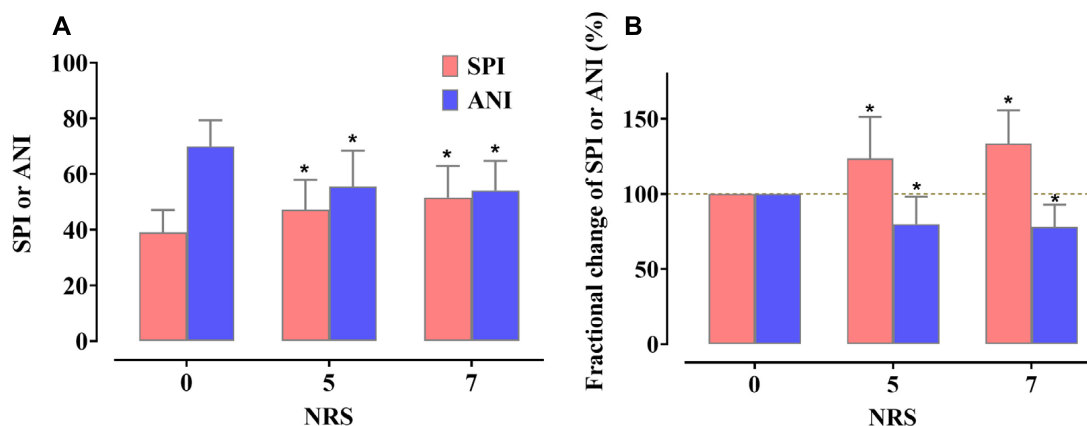


FIGURE 3 | Actual value changes (A) and fractional changes (B) in the Surgical Pleth Index (SPI) and Analgesia Nociception Index (ANI) according to the change in the numerical rating scale (NRS) values. Data are expressed as the mean, with the error bars representing standard deviation. Three sequences (NRS 0, 5, and 7) were compared using the one-way repeated measures analysis of variance (ANOVA) followed by a post hoc Holm–Sidak test. **P* < 0.05 vs. NRS 0.

In the parturient study, neither index was able to successfully distinguish between moderate (NRS 5) and severe pain (NRS 7), which is in line with the results from previous studies: Choi et al. (2018) reported that SPI could not distinguish between moderate ($3 \leq \text{NRS} < 7$) and severe ($7 \leq \text{NRS} < 10$) postoperative pain, while ANI showed only a weak association with the NRS score in patients receiving sevoflurane during general anesthesia

(Ledowski et al., 2013). However, other studies have reported that these indices could distinguish between varying degrees of pain (Le Guen et al., 2012; Boselli et al., 2013; Thee et al., 2015), with ANI showing a negative linear relationship with the visual analog scale in parturients (Le Guen et al., 2012). These conflicting results may be attributed in part to the difference in the study settings, including the type of anesthesia, opioid

administration method, and pain assessment method. The type of sedative-hypnotic and opioid used during anesthesia may also affect these results (Boselli and Jeanne, 2014). Moreover, considering that studies with a larger sample size are better suited to distinguishing between pains of various intensities, the difference in the number of observations used for the analysis may have led to the difference in the results. Studies have suggested that nociception monitoring indices, such as the “traffic light scale,” may provide simpler information (Ledowski, 2019), which may be more meaningful than an inaccurate value between 0 and 100, when trying to determine the need for analgesic administration. From this perspective, the inability to distinguish between moderate and severe pain may not be critical drawbacks of SPI and ANI.

The HRV analysis may be an indicator of autonomic nervous system activity in response to pain stimulation. However, our study did not include an HRV analysis because the accuracy of HRV measurement was not guaranteed for the following reasons. First, the control of respiratory rate is important for accurate HRV analysis, especially high-frequency analysis (Bernardi et al., 2000); however, the respiratory rate could not be controlled in our study since it involved extreme conditions such as pain stimulation, thereby limiting the reliability of HRV. Moreover, in our study, data on baseline, pain stimuli, and drug infusion were obtained in 2-min sessions, which is shorter than the minimum 5-min measurement time recommended by the Taskforce of the European Society of Cardiology and Northern American Society of Pacing and Electrophysiology for HRV analysis (Camm et al., 1996). Previous studies have investigated whether ultra-short-term HRV (i.e., HRV obtained from ECG performed for less than 5 min) could be used as a substitute for the 5-min HRV; however, a recent review on ultra-short-term HRV studies suggested that the available studies have failed to provide a clear basis for validating ultra-short-term HRV (Pecchia et al., 2018), as the three studies that analyzed the effectiveness of ultra-short-term HRV have reported varying results (Esco and Flatt, 2014; Baek et al., 2015; Munoz et al., 2015). For example, the three studies suggested different time intervals of 10, 30, and 60 s, respectively, for the minimum time required for the analysis of the root mean square of the successive difference between the RR interval (RRI) (RMSSD) analysis, which cannot be accepted as generalizable results. Moreover, frequency domain or non-linear analysis are even more ill-equipped to verify the accuracy of ultra-short-term HRV. The most important limitation of using ultra-short-term HRV in our study lay in the experimental conditions. The pain stimuli or drug infusion performed in this study may be directly involved in autonomic nervous system activity, which is thought to be distinct from the resting state in HRV analysis. This also means that the results may be dependent on the length of the HRV analysis interval; thus, the application of ultra-short-term HRV must be confirmed for use in stimulus-application situations such as the ones used in the current study. However, all existing studies on ultra-short-term HRV have been performed in the resting condition and have failed to verify HRV under conditions of physical stress and drug infusion.

Our study had the following limitations. First, the number of observations in the volunteer group was relatively small compared to those used in previous patient-based studies. It is difficult to ignore the possibility of some form of distortion if the analysis is conducted with a small sample. According to the central limit theorem, replacing a given population with mean and SD with a sufficiently large random sample from the population results in a sample mean with an approximately normal distribution. If the sample size is large enough (typically $n > 30$), this theorem holds true whether the source population is normal or skewed (Kwak and Kim, 2017). The theorem holds true even for samples smaller than 30 if the population is normal. The distribution of SPI and ANI measured at each evaluation point passed the normality test for the volunteer and parturient investigations. The changes in the values of SPI and ANI induced by algometric forces were also consistent, and thus, the SD was not sufficiently large when considering the mean value (see Figure 2). The results of the power analysis for verifying the suitability of the sample size of the comparison groups based on the study's results are summarized in the supplementary materials (Supplementary Table 1). Although the sample sizes were small, all comparisons between the groups that showed statistically significant results had powers of 0.85 or more. A future study involving a sufficiently larger study population would be useful to validate the results of the current study. Second, pain was assessed only at one point (NRS 5) in the volunteer study. A more detailed result using multiple pain intensity points would have been useful; however, it is unethical to cause pain beyond NRS 5 (moderate pain) in conscious healthy volunteers.

In conclusion, both the SPI and ANI were found to be effective in distinguishing the intensity of pain in healthy volunteers and parturients. The SPI showed similar values for perceived pain intensity, irrespective of remifentanyl administration and would probably be more useful than the ANI to determine treatment based on pain assessment in clinical practice. Neither of these indices was able to distinguish between NRS 5 and 7 scores in parturients.

DATA AVAILABILITY STATEMENT

The raw data supporting the conclusions of this article will be made available by the authors, without undue reservation.

ETHICS STATEMENT

The study protocol for volunteers was approved by the institutional review board of Asan Medical Center (approval number: 2014–0309) and registered at an international clinical research information system (<http://cris.nih.go.kr>, KCT0001808, date of registration: February 11, 2016). The patients/participants provided their written informed consent to participate in this study. The protocol of parturient-based observational study was approved by the institutional review board of Asan Medical Center (approval number: 2014–0318) and registered at an international clinical research information system (see text footnote 1, KCT0001793, date of registration: February 01, 2016).

AUTHOR CONTRIBUTIONS

J-YB, B-MC, and G-JN collected the data and designed the protocol. HS, J-HL, E-KL, and B-MC performed the data analysis. B-MC, HS, and G-JN interpreted the results. All authors contributed to the writing of the manuscript, provided critical revisions, and approved the final version.

FUNDING

This work was supported by the Ministry of Trade, Industry and Energy, South Korea (grant number 10047988).

REFERENCES

- Baek, H. J., Cho, C.-H., Cho, J., and Woo, J.-M. (2015). Reliability of ultra-short-term analysis as a surrogate of standard 5-min analysis of heart rate variability. *Telemed. e-Health* 21, 404–414. doi: 10.1089/tmj.2014.0104
- Bernardi, L., Wdowczyk-Szulc, J., Valenti, C., Castoldi, S., Passino, C., Spadacini, G., et al. (2000). Effects of controlled breathing, mental activity and mental stress with or without verbalization on heart rate variability. *J. Am. Coll. Cardiol.* 35, 1462–1469. doi: 10.1016/s0735-1097(00)00595-7
- Boselli, E., Bouvet, L., Begou, G., Dabouz, R., Davidson, J., Deloste, J. Y., et al. (2014). Prediction of immediate postoperative pain using the analgesia/nociception index: a prospective observational study. *Br. J. Anaesth.* 112, 715–721. doi: 10.1093/bja/aet407
- Boselli, E., Daniela-Ionescu, M., Begou, G., Bouvet, L., Dabouz, R., Magnin, C., et al. (2013). Prospective observational study of the non-invasive assessment of immediate postoperative pain using the analgesia/nociception index (ANI). *Br. J. Anaesth.* 111, 453–459. doi: 10.1093/bja/aet110
- Boselli, E., and Jeanne, M. (2014). Analgesia/nociception index for the assessment of acute postoperative pain. *Br. J. Anaesth.* 112, 936–937. doi: 10.1093/bja/aeu116
- Camm, A. J., Malik, M., Bigger, J. T., Breithardt, G., Cerutti, S., Cohen, R. J., et al. (1996). Heart rate variability: standards of measurement, physiological interpretation and clinical use. Task Force of the European Society of Cardiology and the North American Society of Pacing and Electrophysiology. *Circulation* 93, 1043–1065. doi: 10.1161/01.cir.93.5.1043
- Chanques, G., Tarri, T., Ride, A., Prades, A., De Jong, A., Carr, J., et al. (2017). Analgesia nociception index for the assessment of pain in critically ill patients: a diagnostic accuracy study. *Br. J. Anaesth.* 119, 812–820. doi: 10.1093/bja/aex210
- Choe, S., Choi, B. M., Lee, Y. H., Lee, S. H., Lee, E. K., Kim, K. S., et al. (2017). Response surface modelling of the pharmacodynamic interaction between propofol and remifentanyl in patients undergoing anaesthesia. *Clin. Exp. Pharmacol. Physiol.* 44, 30–40. doi: 10.1111/1440-1681.12677
- Choi, B. M., Park, C., Lee, Y. H., Shin, H., Lee, S. H., Jeong, S., et al. (2018). Development of a new analgesic index using nasal photoplethysmography. *Anaesthesia* 73, 1123–1130. doi: 10.1111/anae.14327
- Esco, M. R., and Flatt, A. A. (2014). Ultra-short-term heart rate variability indexes at rest and post-exercise in athletes: evaluating the agreement with accepted recommendations. *J. Sports Sci. Med.* 13:535.
- Gruenewald, M., Herz, J., Schoenherr, T., Thee, C., Steinfath, M., and Bein, B. (2015). Measurement of the nociceptive balance by Analgesia Nociception Index and Surgical Pleth Index during sevoflurane-remifentanyl anesthesia. *Minerva Anesthesiol.* 81, 480–489.
- Huiku, M., Uutela, K., Van Gils, M., Korhonen, I., Kymäläinen, M., Meriläinen, P., et al. (2007). Assessment of surgical stress during general anaesthesia. *Br. J. Anaesth.* 98, 447–455. doi: 10.1093/bja/aem004
- Jeanne, M., Logier, R., De Jonckheere, J., and Tavernier, B. (2009). Validation of a graphic measurement of heart rate variability to assess analgesia/nociception

ACKNOWLEDGMENTS

We wish to thank Joon Seo Lim from the Scientific Publications Team at Asan Medical Center for his editorial assistance in preparing this manuscript.

SUPPLEMENTARY MATERIAL

The Supplementary Material for this article can be found online at: <https://www.frontiersin.org/articles/10.3389/fphys.2021.554026/full#supplementary-material>

Supplementary Table 1 | Power calculation to verify the suitability of the sample size of the comparison groups based on the study's results.

- balance during general anesthesia. *Conf. Proc. IEEE Eng. Med. Biol. Soc.* 2009, 1840–1843.
- Jung, K. W., Kang, H. W., Park, C. H., Choi, B. H., Bang, J. Y., Lee, S. H., et al. (2016). Comparison of the analgesic effect of patient-controlled oxycodone and fentanyl for pain management in patients undergoing colorectal surgery. *Clin. Exp. Pharmacol. Physiol.* 43, 745–752. doi: 10.1111/1440-1681.12586
- Kwak, S. G., and Kim, J. H. (2017). Central limit theorem: the cornerstone of modern statistics. *Korean J. Anesthesiol.* 70, 144–156. doi: 10.4097/kjae.2017.70.2.144
- Labor, S., and Maguire, S. (2008). The pain of labour. *Rev. Pain* 2, 15–19.
- Le Guen, M., Jeanne, M., Sievert, K., Al Moubarik, M., Chazot, T., Laloe, P. A., et al. (2012). The Analgesia Nociception Index: a pilot study to evaluation of a new pain parameter during labor. *Int. J. Obstet. Anesth.* 21, 146–151. doi: 10.1016/j.ijoa.2012.01.001
- Ledowski, T. (2019). Objective monitoring of nociception: a review of current commercial solutions. *Br. J. Anaesth.* 123, e312–e321.
- Ledowski, T., Burke, J., and Hruby, J. (2016). Surgical pleth index: prediction of postoperative pain and influence of arousal. *Br. J. Anaesth.* 117, 371–374. doi: 10.1093/bja/aew226
- Ledowski, T., Tiong, W. S., Lee, C., Wong, B., Fiori, T., and Parker, N. (2013). Analgesia nociception index: evaluation as a new parameter for acute postoperative pain. *Br. J. Anaesth.* 111, 627–629. doi: 10.1093/bja/aet111
- Luginbuhl, M., Ypparila-Wolters, H., Rufenacht, M., Petersen-Felix, S., and Korhonen, I. (2007). Heart rate variability does not discriminate between different levels of haemodynamic responsiveness during surgical anaesthesia. *Br. J. Anaesth.* 98, 728–736. doi: 10.1093/bja/aem085
- Minto, C. F., Schnider, T. W., Egan, T. D., Youngs, E., Lemmens, H. J., Gambus, P. L., et al. (1997). Influence of age and gender on the pharmacokinetics and pharmacodynamics of remifentanyl. I. Model development. *Anesthesiology* 86, 10–23. doi: 10.1097/0000542-199701000-00004
- Munoz, M. L., Van Roon, A., Riese, H., Thio, C., Oostenbroek, E., Westrik, I., et al. (2015). Validity of (ultra-) short recordings for heart rate variability measurements. *PLoS One* 10:e0138921. doi: 10.1371/journal.pone.0138921
- Park, J. H., Kim, D. H., Yoo, S. K., Lim, H. J., Lee, J. W., Ahn, W. S., et al. (2018). The analgesic potency dose of remifentanyl to minimize stress response induced by intubation and measurement uncertainty of Surgical Pleth Index. *Minerva Anesthesiol.* 84, 546–555.
- Pecchia, L., Castaldo, R., Montesinos, L., and Melillo, P. (2018). Are ultra-short heart rate variability features good surrogates of short-term ones? State-of-the-art review and recommendations. *Healthcare Technol. Lett.* 5, 94–100. doi: 10.1049/htl.2017.0090
- Struys, M. M., Vanpeteghem, C., Huiku, M., Uutela, K., Blyært, N. B., and Mortier, E. P. (2007). Changes in a surgical stress index in response to standardized pain stimuli during propofol-remifentanyl infusion. *Br. J. Anaesth.* 99, 359–367. doi: 10.1093/bja/aem173

- Thee, C., Ilies, C., Gruenewald, M., Kleinschmidt, A., Steinfath, M., and Bein, B. (2015). Reliability of the surgical Pleth index for assessment of postoperative pain: a pilot study. *Eur. J. Anaesthesiol.* 32, 44–48. doi: 10.1097/eja.0000000000000095
- Williams, A. C. C., and Craig, K. D. (2016). Updating the definition of pain. *Pain* 157, 2420–2423. doi: 10.1097/j.pain.0000000000000613
- Won, Y. J., Lim, B. G., Kim, Y. S., Lee, M., and Kim, H. (2018). Usefulness of surgical pleth index-guided analgesia during general anesthesia: a systematic review and meta-analysis of randomized controlled trials. *J. Int. Med. Res.* 46, 4386–4398. doi: 10.1177/0300060518796749
- Yan, Q., An, H. Y., and Feng, Y. (2017). Pain assessment in conscious healthy volunteers: a crossover study evaluating the analgesia/nociception index. *Br. J. Anaesth.* 118, 635–636. doi: 10.1093/bja/aex061
- Conflict of Interest:** The authors declare that the research was conducted in the absence of any commercial or financial relationships that could be construed as a potential conflict of interest.

Copyright © 2021 Choi, Shin, Lee, Bang, Lee and Noh. This is an open-access article distributed under the terms of the Creative Commons Attribution License (CC BY). The use, distribution or reproduction in other forums is permitted, provided the original author(s) and the copyright owner(s) are credited and that the original publication in this journal is cited, in accordance with accepted academic practice. No use, distribution or reproduction is permitted which does not comply with these terms.

Advantages of publishing in Frontiers



OPEN ACCESS

Articles are free to read
for greatest visibility
and readership



FAST PUBLICATION

Around 90 days
from submission
to decision



HIGH QUALITY PEER-REVIEW

Rigorous, collaborative,
and constructive
peer-review



TRANSPARENT PEER-REVIEW

Editors and reviewers
acknowledged by name
on published articles

Frontiers

Avenue du Tribunal-Fédéral 34
1005 Lausanne | Switzerland

Visit us: www.frontiersin.org

Contact us: frontiersin.org/about/contact



REPRODUCIBILITY OF RESEARCH

Support open data
and methods to enhance
research reproducibility



DIGITAL PUBLISHING

Articles designed
for optimal readership
across devices



FOLLOW US

@frontiersin



IMPACT METRICS

Advanced article metrics
track visibility across
digital media



EXTENSIVE PROMOTION

Marketing
and promotion
of impactful research



LOOP RESEARCH NETWORK

Our network
increases your
article's readership